

Expediting the Discovery and Potential Translation of
Theranostic Agents for Alzheimer's Disease

By

Richard Anthony McClure

Dissertation

Submitted to the Faculty of the
Graduate School of Vanderbilt University
in partial fulfillment of the requirements

for the degree of

DOCTOR OF PHILOSOPHY

in

Neuroscience

December, 2015

Nashville, Tennessee

Approved:

Manus J. Donahue, Ph.D.

John C. Gore, Ph.D.

Wellington Pham, Ph.D.

Danny G. Winder, Ph.D.

Copyright © 2015 by Richard Anthony McClure

All Rights Reserved.

DEDICATION

This work is whole-heartedly dedicated to my mother and father Robin L. & Richard C. McClure. The unconditional love and support you two provide have been and will continue to be the impetus behind my conviction to seize every opportunity presented to me in life.

ACKNOWLEDGEMENTS

I would like to sincerely thank all of the people who made this dissertation possible including all of the wonderful faculty and administrative staff in the Vanderbilt Institute of Imaging Science (VUIIS) and Department of Neuroscience at Vanderbilt University in Nashville Tennessee. In particular, I would like to thank the distinguished faculty which served on my thesis committee. Dr. John Gore of the VUIIS for taking a special interest in my professional development and for providing me with the astonishing resources required for the completion of this work. Dr. Manus Donahue for his numerous contributions to my grant writing endeavors as well as his sustained interest in my thesis work. Dr. Danny Winder for volunteering to be the chair of my graduate thesis committee and for completing all of the responsibilities of this position with the utmost professionalism. And lastly my thesis advisor, Dr. Wellington Pham, for bolstering my scientific prowess over the last three years and solidifying my life-long fascination with the scientific method.

I would also like to thank the Vanderbilt Medical Scientist Training Program (MSTP) and National Institutes of Health for providing me the grant funding with which this work was completed. The numerous travel grants made available throughout my graduate school training were integral to my assimilation into the scientific community and permitted my travel to high-profile forums at which I could share my work with other experts in the field of Alzheimer's disease. Additionally, a training grant generously awarded by the National Institute of Biomedical Imaging and Bioengineering proved an invaluable resource as my work expanded. Lastly, I would like to thank the Vanderbilt Research Core facilities for their numerous scientific vouchers and internally submitted grant mechanisms which permitted the timely completion of my research aims. In particular, I would like to thank Rey Redha formerly of the Vanderbilt High-throughput Screening core for his scientific contributions to my work and for his expert guidance.

Additionally, I would like to thank my friends and colleagues across the Vanderbilt Medical School campus for their continued support and willingness to consult on my academic endeavors at any time. Specifically, I wish to state my sincere appreciation for all of my fellow members of the Vanderbilt MSTP class of 2017 and wish them the best in their future endeavors. In my personal life, the constant support, enthusiasm, and smile of my best friend and greatest love

Victoria Elliott have always kept me motivated and reminded me of why I must continue to strive for excellence. To my brother, I hope to inspire you to great success in the future and continue to make you proud.

TABLE OF CONTENTS

DEDICATION	iii
ACKNOWLEDGEMENTS	iv
LIST OF TABLES	x
LIST OF FIGURES.....	xi
Chapter 1 MEMORY CIRCUITS IN HEALTH AND ALZHEIMER'S DISEASE.....	1
1.1 HIPPOCAMPUS ARCHITECTURE & MEMORY CIRCUITS.....	2
1.2 PATHOLOGICAL CHANGES ASSOCIATED WITH NORMAL AGING	6
1.3 NEUROPATHOLOGICAL CHANGES ASSOCIATED WITH ALZHEIMER'S DISEASE	13
1.3.1 Tau Deposition in AD.....	16
1.3.2 Amyloid Deposition in AD.....	17
Chapter 2 CLINICAL SUBTYPES & SYMPTOMS OF ALZHEIMER'S DISEASE.....	23
2.1 SPORADIC & EARLY-ONSET SUBTYPES OF ALZHEIMER'S DISEASE.....	23
2.2 CLINICAL FEATURES OF ALZHEIMER'S DISEASE	27
2.2.1 Language Dysfunction in Alzheimer's Disease.....	29
2.2.2 Impairments in Visuospatial Skills in Alzheimer's Disease	29
2.2.3 Disturbances in Executive Function and Judgement in Alzheimer's Disease	30
2.2.4 Miscellaneous Signs and Symptoms of Alzheimer's Disease.....	31
2.2.5 Atypical Presentations of Alzheimer's Disease.....	32
2.3 CURRENT CLINICAL DIAGNOSTIC STRATEGIES	34
2.3.1 History of Clinical Guidelines	34
2.3.2 Diagnostic Criteria.....	36
2.3.3 Differential Diagnosis.....	49
2.3.4 Clinical Evaluation Strategy	56

Chapter 3	EPIDEMIOLOGY OF ALZHEIMER'S DISEASE	61
3.1	CURRENT & PROJECTED ESTIMATES OF DISEASE BURDEN	61
3.2	POTENTIAL BENEFIT OF ALZHEIMER'S DISEASE TREATMENT DEVELOPMENT	67
Chapter 4	CURRENT SYMPTOMATIC MANAGEMENT OF ALZHEIMER'S DISEASE.....	73
4.1	ACETYLCHOLINE SYNTHESIS & RECYCLING	74
4.2	CHOLINERGIC SYSTEM NEUROANATOMY & ROLE IN MEMORY	79
4.3	CHOLINERGIC CHANGES IN ALZHEIMER'S DISEASE	85
4.4	CURRENT ALZHEIMER'S DISEASE THERAPEUTIC GUIDELINES.....	88
4.5	USE OF MEMENTINE IN ALZHEIMER'S DISEASE	94
Chapter 5	MOLECULAR ETIOLOGY OF ALZHEIMER'S DISEASE	98
5.1	AMYLOID PROCESSING	99
5.2	GENETIC EVIDENCE SUPPORTING AMYLOID-CENTRIC HYPOTHESES OF AD	101
5.2.1	Down's Syndrome & AD	102
5.2.2	APP Mutations as Support for Amyloid-centric Hypotheses of AD	105
5.2.3	PSEN Mutations as Support for Amyloid-centric Hypotheses of AD	107
5.2.4	APOE4 Support of Amyloid-centric Hypothesis of Sporadic AD Pathogenesis.....	111
5.3	TRANSGENIC MOUSE MODELS AS SUPPORT FOR AMYLOID-CENTRIC HYPOTHESES OF ALZHEIMER'S DISEASE.....	119
5.4	MECHANISMS OF A β NEUROTOXICITY AT THE SYNAPSE.....	121
5.5	TAU AS A MOLECULAR MEDIATOR OF A β NEUROTOXICITY	126
5.5.1	Plausible Mechanisms of A β -induced Tau Dysregulation:	130
5.5.2	Mechanisms of Tau-induced Neurodegeneration	133
5.6	NEUROINFLAMMATION & ALZHEIMER'S DISEASE	135
Chapter 6	BIOMARKERS FOR ALZHEIMER'S DISEASE.....	143
6.1	AMYLOID IMAGING	146
6.2	TAU IMAGING.....	151
6.3	MEASUREMENTS OF AMYLOID IN CEREBROSPINAL FLUID.....	155
6.4	MEASUREMENTS OF AMYLOID IN THE PLASMA	156
6.5	MEASUREMENTS OF TAU IN CEREBROSPINAL FLUID	158
6.6	MRI-MEDIATED IMAGING OF NEURODEGENERATION.....	160
6.7	CURRENT PERSPECTIVE ON AD IMAGING.....	161

Chapter 7	THE UNTESTED AMYLOID-CASCADE HYPOTHESIS	163
7.1	CONFOUNDS UNDERLYING THE FAILURE OF ALZHEIMER'S DISEASE IN CLINICAL TRIALS.....	163
7.2	LESSONS GARNERED FROM ALZHEIMER'S DISEASE CLINICAL TRIALS	165
Chapter 8	INTRODUCTION TO SPECIFIC AIMS	166
Chapter 9	THESIS AIM 1	167
9.1	AIM 1: HIGH-THROUGHPUT SCREENING FOR A β -BINDING MOLECULES	167
9.1.1	Barriers to the Development of AD Diagnostics:	167
9.1.2	Barriers to the Development of AD Therapeutics:	174
9.1.3	Research Strategy and Significance of Work	177
9.2	AIM 1 EXPERIMENTAL METHODS	182
9.3	AIM 1 EXPERIMENTAL RESULTS	190
9.3.1	Results: Validation of HATCO Assay-mediated Screening for Novel A β -binding Compounds	190
9.3.2	Results: HATCO Assay-mediated Screening of a Primary Library for Novel A β -binding Compounds.....	194
9.4	Results: Translation of the HATCO Assay to a 96-well Plate Platform.....	199
9.4.1	Results: Translation of the HATCO assay to a 384-well Plate Platform	204
9.4.2	Results: Large-Scale HTS for A β -binding Compounds Using the HATCO Assay	214
9.4.3	Results: Cross-screening of 15 Hit Compounds	219
9.4.4	Results: Experimental Determination of A β -binding Affinity of Confirmed and Cross-screened Hits	228
9.4.5	Result: Corroboration of PMZ's Regional Retention with A β Plaque Distribution in the Brain Using MALDI-IMS	237
9.4.6	Result: Confirmation of PMZ BBB Penetration and A β -dependent Retention in the Brain Using HPLC.....	240
9.5	DISCUSSION & SIGNIFICANCE OF WORK.....	244
Chapter 10	THESIS AIM 2	250
10.1	AIM 2: EVALUATING THE THERAPEUTIC EFFICACY OF A β CLEARANCE	250
10.2	AIM 2 EXPERIMENTAL METHODS	260
10.3	AIM 2 EXPERIMENTAL RESULTS	277
10.3.1	Result: FMeC1 Aerosol Crosses the Blood Brain Barrier and Binds to A β	277
10.3.2	Result: Enhanced Bioavailability of FMeC1 in the Brain by Atomization Versus I.V. Injection	280
10.3.3	Result: Bio-distribution of Inhaled FMeC1 Differs from I.V. Injection	283
10.3.4	Result: Bioavailability of Aerosolized Curcumin in the Serum Exceeds that of I.V. Injected Doses	287

10.3.5	Result: Curcumin Perturbs A β Fibrillation in vitro	292
10.3.6	Result: Inhaled Curcumin Perturbs A β Fibrillation and Reduces A β -plaque Burden in vivo.....	294
10.3.7	Result: Prophylactically Inhaled Curcumin Prevents Dystrophic Neurite Formation	297
10.3.8	Result: Prophylactically Inhaled Curcumin Prevents the Development of Working & Spatial Memory Deficits in 5XFAD Mice	300
10.3.9	Result: Inhaled Curcumin Associated with Negligible Local & System Toxicity.....	306
10.4	SIGNIFICANCE & DISCUSSION OF WORK.....	310
10.4.1	Significance & Discussion of Aerosol-mediated Delivery.....	310
10.4.2	Significance and Discussion of Prophylactic Curcumin Trial.....	318
Chapter 11	THESIS AIM 3	325
11.1	AIM 3: DIAGNOSTIC READOUTS FOR THE EVALUATION OF THERAPUETIC RESPONSE	325
11.2	AIM 3 EXPERIMENTAL METHODS	331
11.3	AIM 3 EXPERIMENTAL RESULTS	338
11.3.1	Result: ¹⁸ F-labeled COX2 Probe Does Not Penetrate the BBB.....	338
11.3.2	Result: ¹⁸ F-labeled IGF1R Probe Does Not Penetrate the BBB	340
11.3.3	Results: Plasma A β Measurements in Non-treated 5XFAD and Wild Type Mice	342
11.3.4	Results: PMZ Perturbs A β ₄₂ Aggregation In-vitro.....	343
11.3.5	Results: Chronic I.V. Administration of PMZ Reduces A β Plaque Burden in 5XFAD Mice	346
11.3.6	Results: Chronic I.V. Administration of PMZ Improves Working & Spatial Memory in 5XFAD Mice	349
11.3.7	Results: Promethazine Therapy Transiently Shifts A β Peptide Levels in Plasma Specimens.....	353
11.4	DISCUSSION & SIGNIFICANCE OF WORK.....	355
REFERENCES	367

LIST OF TABLES

Table 2-1. DSM-5 Criteria for Major Neurocognitive Disorder.....	47
Table 2-2. NIA-AA Core Clinical Criteria for Probable AD	47
Table 2-3. NIA-AA Core Clinical Criteria for Possible AD	48
Table 2-4. IWG Definitions & Core Clinical Criteria.....	48
Table 2-5. Dementia versus Delirium	60
Table 9-1. Ideal Characteristics of a Candidate Precursor Molecule for AI Radiotracer Development	171
Table 9-2. Molecular Attributes Compatible with Blood Brain Barrier Penetration	195
Table 9-3. Assay Utility as a Function of Excitation Parameters (96-well Plate Format)	203
Table 9-4. Fluorescence Readout as a Function of Incubation Time	203
Table 9-5. HATCO Assay Fluorescent Signal as a Function of 5XFAD Lysate Concentration	209
Table 9-6. Automated HATCO Assay Z-Prime Variables.....	213
Table 9-7. Loading Homogeneity Achieved Via Automated HATCO Assay Pipetting Protocol.....	216
Table 9-8. Full Library Screen Hit List With Percent Inhibition.....	218
Table 9-9. False-positive Library Identified Via 2-Phase Cross-screening of HATCO assay-identified Hits	220
Table 9-10. Confirmed & Cross-screened A β -binding Molecules Identified Via HATCO-mediated HTS	223
Table 9-11. IC ₅₀ Values of HATCO-Identified Hits.....	229
Table 9-12. MALDI-IMS Signals Corresponding to A β -peptide Species	239
Table 10-1. Molecular Targets of Curcumin	254
Table 10-2. Pharmacokinetic Parameters of P.O., I.V. and Aerosol-mediated Curcumin Delivery	291
Table 10-3. Complete Blood Count Analysis Following Curcumin Administration	307
Table 10-4. Metabolic Panel Following Curcumin Administration.....	307
Table 11-1. Pre- and Post-Treatment A β Peptide Levels in 5XFAD Plasma.....	354

LIST OF FIGURES

Figure 1-1. Wiring Diagram of Hippocampal Trisynaptic Loop	5
Figure 2-1. The Amyloid Cascade Hypothesis.	25
Figure 2-2. Diagram Representing the Relationship Between Several Terms About AD.	26
Figure 3-1. Public Health Impact of Deaths from Alzheimer’s Disease.	65
Figure 3-2. Projected Impact of Disease-modifying Treatment for AD	70
Figure 4-1. Schematic Representation of a Hypothetical Cholinergic Synapse.	76
Figure 5-1. Presynaptic and Postsynaptic Regulation of Synaptic Transmission by A β -protein	125
Figure 5-2. Schematic Representation of Normal Dynamic Equilibrium of Tau	128
Figure 5-3. Inflammasome Activation Cascade.....	138
Figure 5-4. Pathomechanistic Sequelae of Microglia Activation.	140
Figure 6-1 Comparison of Clinical, Cognitive, Structural, Metabolic, and Biochemical Changes as a Function of Estimated Years from Expected Symptom Onset.....	145
Figure 9-1. Chemical Structures of PET Probes for Amyloid Imaging and Known Histochemical Stains.	179
Figure 9-2. HATCO Assay Rationale.	181
Figure 9-3. 5XFAD Lysate Modulates Thioflavin Fluorescence.	191
Figure 9-4. Known A β -binding Molecule Resveratrol Attenuates A β -specific Thioflavin Fluorescence at 485 nm in a Dose-dependent Manner.	193
Figure 9-5. Initial Screening Library	195
Figure 9-6. HATCO Assay-mediate, High-throughput Screening of Structurally Diverse Compound Libraries for A β plaque-binding Capacity.	198
Figure 9-7. Thioflavin Optimally Excited by 410 nm Excitation Source in the Presence of 5XFAD Lysate.	201
Figure 9-8. A β -specific Thioflavin Fluorescence at 485 nm is attenuated by DMSO in a Dose-dependent Manner.	206
Figure 9-9. Thioflavin Fluorescence is Attenuated in Proportion to the Dilution Factor Applied to the Lysate Constituent of the HATCO Assay.....	210

Figure 9-10. Preliminary Automation of the HATCO Assay’s Plate Loading Protocol Results in the Generation of Outliers.....	213
Figure 9-11. Two Distinct Absorbance Profiles Characterize False-positive Hit Compounds.	222
Figure 9-12. Cross-screening Excludes Chromophores with Confounding Spectroscopic Profiles.	227
Figure 9-13 MALDI-IMS Protocol for Promethazine.	234
Figure 9-14. Validation of Promethazine Imaging using MALDI-IMS.....	236
Figure 9-15. Differential Retention of Promethazine as a Function of A β Plaque Burden.....	239
Figure 9-16. HPLC Determination of BBB Penetration and Differential Retention of (S)-promethazine in 5XFAD Mouse Model.	242
Figure 9-17. Non-targeted Compounds are Rapidly Cleared from the Brain.	243
Figure 10-1. Curcumin (A) and its perfluoro analogs, FMeC1 (B)	259
Figure 10-2. Atomizer Design and Aerosol Delivery System	263
Figure 10-3. Actual (A) and Graphical Rendering (B) of Y-maze layout.....	275
Figure 10-4. Internalization and A β -dependent Retention of Aerosolized FMeC1 in the Brain.	279
Figure 10-5. Internalization and A β -dependent Retention of Aerosolized FMeC1 in the Brain.	282
Figure 10-6. Biodistribution of FMeC1 by IV and Atomization.	286
Figure 10-7. Validation of Curcumin Plasma Quantification Method.	288
Figure 10-8. Bioavailability of Curcumin Following I.V., P.O, and Aerosol-mediated Dosing Paradigms.	291
Figure 10-9. Curcumin Inhibits Aggregation of A β ₄₂ Monomers.....	293
Figure 10-10. A β Plaque Burden is Reduced Via Chronic Curcumin Inhalation.	296
Figure 10-11. Ultrastructural Analysis of Neurite Diameter in the CA3 Hippocampal Region of Treated and Non-treated 6 month 5XFAD Mice	299
Figure 10-12. Curcumin Nebulization Prevents the Development of Working Memory Deficits in 5XFAD Mice:	302
Figure 10-13. Curcumin Nebulization Prevents the Development of Deficits in Hippocampus-mediated Spatial Memory in 5XFAD Mice.....	303
Figure 10-14. Y-Maze Paradigm Controls:	305
Figure 10-15. No Evidence of Pulmonary Toxicity Associated with Acute or Chronic Inhalation of Curcumin.	309

Figure 10-16. Anatomical Diagram of the Olfactory Epithelium, Bulb, and Tract.	316
Figure 10-17. General organization of the olfactory region.	317
Figure 11-1. Calibration Curve for Quantification of Plasma A β ₄₀ (A) and A β ₄₂ (B) by ELISA.	337
Figure 11-2. PET Imaging of COX-2 in 5XFAD Mice.	339
Figure 11-3. PET-mediated Imaging of IGF-1R Impaired by Poor Blood Brain Barrier Penetration.	341
Figure 11-4. PMZ Inhibits Aggregation of A β ₄₂ Monomers In-vitro.	345
Figure 11-5. Chronic Treatment with Promethazine Reduces Amyloid Plaque Burden.	347
Figure 11-6. Promethazine Attenuates A β -mediated Neuro-inflammation without Effecting APP Expression.	348
Figure 11-7. 2 Month PMZ Treatment Opposes the Development of Memory Deficits in 5XFAD mice:.....	352

CHAPTER 1 MEMORY CIRCUITS IN HEALTH AND ALZHEIMER'S DISEASE

Perhaps to a greater degree than in any other organ system found in the mammalian body, comprehending the etiology of a particular lesion within the CNS requires an understanding of its paradoxically modular yet distributive nature. Science has only begun to identify the neurobiological substrates and circuits which mediate specific domains of cognition and the determination of the complex manner in which these systems interact is arguably one of the greatest challenges left in modern science. Put plainly, our current understanding of the neurobiological processes which sub-serve normal cognition is at best, incomplete. Historically, this state of unknowing has been of central consequence to those who study AD, as a fundamental tenant of deciphering the pathophysiologic mechanism of a particular disease is a working knowledge of how the system it affects operates in the absence of pathology. In the context of AD research, without a complete understanding of how memories are acquired, encoded, and stored, it becomes a daunting task to explain how AD pathogenic lesions produce a particular clinical phenotype. Compounding this issue, AD, as we define it currently, is a heterogeneous neurodegenerative entity with respect to symptomology, pathophysiology, and possibly etiology.

The purpose of this introductory chapter is to orient the reader to the background in which AD is studied. This task, at a minimum, requires a detailed explanation of the intrinsic and extrinsic circuits of the hippocampus in order to facilitate comprehension of the etiology of memory deficits in AD. Furthermore, in order to appropriately interpret the generalized pathogenic changes observed in this disease, one must first be familiar with changes occurring as a consequence of normal aging. Only given this background can a precise neuroanatomical description of the cardinal features of AD pathogenicity, namely neuron loss, neurofibrillary tangles (NFTs) density, and amyloid- β ($A\beta$) plaque deposition, be appropriately discussed. Of note, all subsequent chapters will reference the neuroanatomical description of AD pathology described in this section to provide context for additional descriptions of AD clinical deficits, pathogenic subtypes, proposed molecular etiology, and treatment approaches.

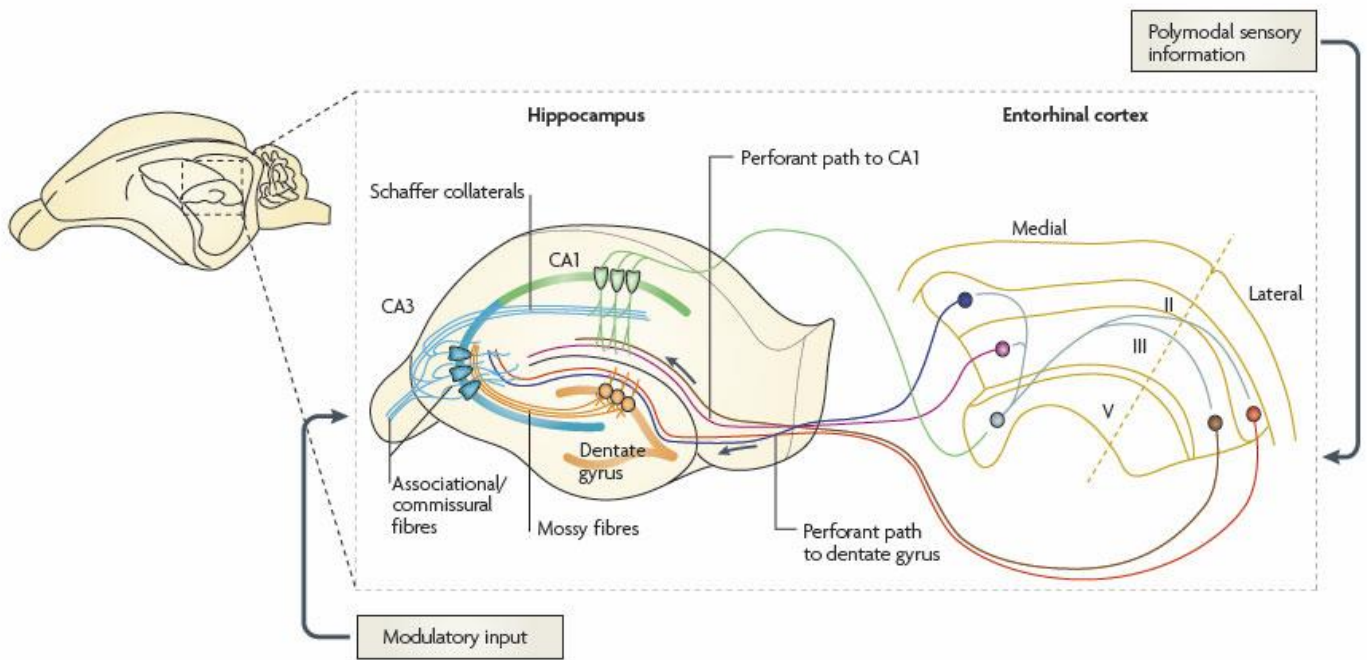
1.1 HIPPOCAMPUS ARCHITECTURE & MEMORY CIRCUITS

Ever since Scoville & Milner's initial report of selective memory deficits in humans following its removal, the hippocampal region has been defined as central to our memory capacity.⁽¹⁾ Following the general trend in neuroscience however, even within the narrow scope of memory, the role of the hippocampus is further constrained to both a temporal window and selective domain of memory processing. With respect to a temporal constraint to hippocampal function, evidence comes from human studies indicating that immediate memory, the ability to recognize items just brought into consciousness, is intact in patients with hippocampal lesions.⁽²⁾ Dated memories that have already been consolidated into long-term memory, such as memories of one's childhood, are similarly exempt from deficits attributable to lesions of the hippocampus.⁽³⁾ Analyzed as a whole, these findings have led the field to theorize that the hippocampus plays a temporally constrained role in memory consolidation, the process occurring between the initial formation of memories and their final repository in the cortex.⁽⁴⁾ Interestingly, the duration of critical hippocampal involvement in memory formation may depend on mediation from adjacent areas of the temporal cortex, as damage to these regions produces a more temporally extensive form of memory loss.^(5,6) While early investigators quickly elucidated these temporal restrictions on hippocampal involvement in memory, they failed to recognize the specific pattern of memory deficits unique to hippocampal lesions until sometime later. Indeed it was not until 1980, that strong evidence supporting the notion that the cognitive domain of memory was not globally dependent on the hippocampus was published. Since that time, we now recognize that the hippocampus plays a critical role only in declarative memory.⁽⁷⁾ Composed of episodic and semantic memory subtypes, the declarative domain of memory defines our ability to consciously recollect events of the past. Its complement, procedural or non-declarative memory, involves the acquisition of skills and biases that can be expressed unconsciously through alternations in performance. Not dependent on hippocampal function, instead, procedural memory is principally mediated by the neo-striatum and cerebellum.^(8,9) Thus, it is now clear that there are several independent yet interconnected memory systems in the brain that sub-serve specific domains of memory. In fact, in addition to the procedural and declarative memories subdivisions already described, robust evidence now supports the existence of an emotional memory system mediated in part by the amygdala and a working memory system sub-served by various cortical regions.^(8,10) The discovery of these regionally distinct memory systems can be credited largely to work done in animal

models through which we are beginning to characterize the neural circuitry and information processing mechanisms that mediate each of the unique domains of memory.

With respect to the generalized anatomy and processing mechanism of the hippocampal memory system, work done predominately in animal models supports what has been termed the classic tri-synaptic model of hippocampal synaptic transmission (Figure 1-1). While not included in this simplified model, extensive work confirms that the origin of afferent information for the hippocampus is derived from virtually every neocortical association area.^(11, 12) Of significance however, these neocortical afferent sources of information do not directly converge at the hippocampus. Instead, the association cortices project to one or more subdivisions of the parahippocampal region; comprised of the perirhinal, postrhinal, and entorhinal cortices.⁽¹³⁾ Each of these parahippocampal subdivisions are highly interconnected and send efferent projections to the CA1 and CA3 sectors of the hippocampus, the dentate gyrus, and subiculum.⁽¹⁴⁾ While each subdivision of the parahippocampal cortex plays an important role in memory, the efferent projections originating in the entorhinal cortex, termed the perforant pathway, constitute the major cortical afferent source for the hippocampus and dentate gyrus and therefore warrant a more precise description. Additionally, as summarized in detail in subsequent sections, this source of cortical afferent information to the hippocampus is specifically perturbed in AD and constitutes the first connection defined in the classic tri-synaptic model of synaptic transmission in the hippocampus.⁽¹⁵⁾ Notably, this collection of efferent projections originates from pyramidal and stellate cells contained in entorhinal layers II and III and to a lesser extent deep layers V and VI, and received its name as a consequence of its projection through the subiculum on its way to the dentate gyrus and hippocampal sectors CA1/CA3.⁽¹⁶⁾ More precisely, it terminates along the outer dendritic branches of the subicular and hippocampal pyramids, and on the outer two-thirds of the dendritic fields of the dentate gyrus granule cells.⁽¹⁷⁾ As described in further detail below, the perforant pathway initiates a multi-synaptic excitatory sequence of intrinsic hippocampal circuits that terminate in the CA1 field and the subiculum.⁽¹⁸⁾ Of functional significance, there appears to be a dichotomy with respect to the laminar origin and terminal distribution of perforant pathway fibers. Axons originating from cell bodies in layers II and VI appear to project selectively to the dentate gyrus, whereas layers III and V project to CA1 and the subiculum in what is termed the temporoammonic pathway. Critically, in addition to its general role in the acquisition of spatial memories, the temporoammonic branch (TA-CA1) of the perforant path has been shown to mediate spatial memory consolidation.⁽¹⁹⁾ Returning to our reference of the tri-synaptic loop of hippocampal synaptic transmission, granule cells in the dentate gyrus fire on CA3 pyramidal neurons via unmyelinated

efferent axons termed mossy fibers. More precisely, these predominantly glutamatergic axons emerge from the basal portions of the granule cells and pass through the polymorphic cell layer of the dentate gyrus before entering the stratum lucidum of CA3.⁽²⁰⁾ Completing the tri-synaptic circuit, hippocampal CA3 pyramidal neurons synapse next on CA1 neurons via Schaffer collaterals.⁽¹⁵⁾ In reality, the afferent signals reaching the hippocampus via the perforant pathway are processed by a broad network of highly convergent/divergent connections which are hypothesized to mediate memory consolidation in a plasticity-dependent manner.⁽²¹⁾ However, as information processing in hippocampus has not been completely elucidated, this tri-synaptic model of hippocampal transmission summarizes the major intrinsic pathways well. The output of these intrinsic hippocampal circuits is conveyed predominately via efferent projections from pyramidal cells in CA1 and the subiculum to a variety of locations in the brain including the: thalamus, hypothalamus, basal forebrain, amygdala, and association cortices.⁽²²⁾ Again, as described in subsequent sections, these efferent pathways are of particular interest when considering the etiology of memory deficits in AD. As the majority of studies have utilized animal models to do this, a brief discussion of the efficacy of employing animal models to study hippocampal-dependent memory is warranted.



Nature Reviews | Neuroscience

Figure 1-1. Wiring Diagram of Hippocampal Trisynaptic Loop

The wiring diagram of the hippocampus is traditionally presented as a tri-synaptic loop. The major input is carried by axons of the perforant path, which convey polymodal sensory information from neurons in layer II of the entorhinal cortex to the dentate gyrus. Perforant path axons make excitatory synaptic contact with the dendrites of granule cells: axons from the lateral and medial entorhinal cortices innervate the outer and middle third of the dendritic tree, respectively. Granule cells project, through their axons (the mossy fibers), to the proximal apical dendrites of CA3 pyramidal cells which, in turn, project to ipsilateral CA1 pyramidal cells through Schaffer collaterals and to contralateral CA3 and CA1 pyramidal cells through commissural connections. In addition to the sequential trisynaptic circuit, there is also a dense associative network interconnecting CA3 cells on the same side. CA3 pyramidal cells are also innervated by a direct input from layer II cells of the entorhinal cortex (not shown). The distal apical dendrites of CA1 pyramidal neurons receive a direct input from layer III cells of the entorhinal cortex. There is also substantial modulatory input to hippocampal neurons. The three major subfields have an elegant laminar organization in which the cell bodies are tightly packed in an interlocking C-shaped arrangement, with afferent fibers terminating on selective regions of the dendritic tree. The hippocampus is also home to a rich diversity of inhibitory neurons that are not shown in the figure. Reproduced with Permissions from Nature Reviews Neuroscience.⁽²³⁾

1.2 PATHOLOGICAL CHANGES ASSOCIATED WITH NORMAL AGING

From a neuropathological point of view, neurofibrillary tangles (NFT), senile plaques (SP), and neuronal/ synaptic loss are the major pathologic features associated with AD. NFTs are comprised of paired helical filaments (PHFs), which are aggregations of a hyper-phosphorylated microtubule-associated protein known as tau. These lesions are intracellularly localized. By comparison, A β plaques are extracellular aggregations comprised of aberrantly cleaved A β peptides. While these histological abnormalities are well established cardinal features of AD pathogenesis, they are not unique to AD, being present in a number of brain disorders and even in normal aging. In fact, at the gross level, the pathophysiology of AD manifests itself in many of the same ways as normal aging, especially with respect to cortical atrophy. Even today, a common misconception about normal ageing is that significant cell loss and dramatic changes in neuronal morphology occur diffusely and with no appreciable regional restrictions. Under this misconception, a multitude of studies have investigated the relationship between cortical atrophy in cognitively normal elderly and patients with AD. Rationally assuming that increased atrophy must underlie the clinical deficits observed in AD, early studies operated under the assumption that brain atrophy must be more severe and regionally restricted in AD than in cognitively normal elderly. Operating under this assumption, several studies have investigated the possibility of meaningful trends existing between brain weights of cognitively normal elderly as compared to individuals with AD.⁽²⁴⁻²⁶⁾ Unexpectedly, even in the largest of these studies, significant differences in brain weight are not detected between AD and aged-matched controls; although a non-significant trend towards more severe atrophy in AD is observed.^(25, 26) From this negative finding, several points of insight can be garnered. Most contributory to the lack of a discernable difference observed in brain weight between AD and cognitively intact elderly, human brain weights in the elderly are characterized by a high degree of inter-individual variability. Furthermore, while brain weight can decrease by nearly 10% in AD patients, the brains of cognitively normal elderly also undergo a significant degree of atrophy.⁽²⁴⁾ In fact, simply as a consequence of normal aging, brain volume/weight declines with age at a rate of around 2-5% per decade after age 40.^(27, 28) Not only does this individually-variable rate of atrophy in cognitively normal subjects compound the intrinsic variability in brain mass present at baseline, it is not constant, with reports suggesting that the rate of neurodegeneration increases over the age of 70 in an unpredictable fashion.^(27, 28) Still, even if AD brains differed in mass from those of cognitively normal elderly subjects, it is

unlikely this finding would harbor diagnostic utility. This is because without knowing what neuronal systems and cell populations underlie the reductions in brain mass, the extent of AD pathology alone is unlikely to correlate robustly with symptom severity. At the most fundamental level this is because the brain is functionally compartmentalized. Highly integrated neuronal networks, capable of robust plasticity, sub-serve very specific functions which when perturbed evoke an equally unique behavioral phenotype. Thus, the severity and nature of a particular functional deficit is always a reflection of two variables: (i) the extent of neuropathology and (ii) the specific neuroanatomical location and nature of that neuropathology. Put differently, since the pathological features of AD are also present in normal aging, it is not sufficient to know the extent of AD pathology in the whole brain. Instead, one must privity to both the severity of the pathology and its anatomical/cellular targets in the brain in order to robustly correlate pathology to functional deficits. The differential in functional deficits associated with atrophy due to AD and normal aging perfectly illustrates this point. While the first variable, the extent of cortical atrophy averaged over the whole brain appears similar in normal aging and AD. The second variable, the neuroanatomical pattern characteristic of each neurodegenerative process is not assessed when considering total brain weight. For example, a reduction in total brain weight could be explained by neuronal apoptosis, loss of non-neuronal cell-types, degeneration of white matter tracks or any number of equally plausible processes. For this reason, the degree of cortical atrophy across the whole brain fails to correlate robustly with symptom severity in either AD or cognitively normal elderly. Here also, we have our answer to the question, “why does the neurodegeneration associated with AD produce more profound clinical deficits compared to the process of normal aging if the degree of cortical atrophy is not significantly different between the two etiologies?” Only when averaged over the whole brain is cortical atrophy equivalent between AD and normal ageing. In reality, the two pathophysiological processes display unique patterns of neurodegeneration and impact each region of the brain to a different degree.

Keen to correlate the degree of cortical atrophy with a precise neuroanatomical region of the brain in order to explain function deficits, beginning in 1955, pioneer neuroanatomist H. Brody began quantifying neuron loss across the human life span.⁽²⁹⁾ Subsequently followed by a large volume of studies, science became falsely convinced of a ubiquitous 10-60% decline in neuronal density from early adulthood to late old age occurring as a consequence of normal aging within the human cerebral cortex.^(24, 29-32) Perplexingly, just as in AD, robust neurodegeneration attributable to the normal aging process was reported to occur to a varying degree in different regions of the brain. While these early studies would later be corrected as described below, profound neuron loss in the range of 18-57%, 15-51%, and 14-29% were

attributed to normal aging in regions such as the temporal association cortices^(29, 31, 33, 34), frontal association cortices^(30, 31, 34, 35), and subiculum^(30, 34), respectively. Especially relevant to the topic of memory impairment, later studies would go on to demonstrate an equally profound 19-43% loss in hippocampal neurons in normally ageing humans.⁽³⁶⁾ Indicative of the technical difficulties inherent in quantifying neuronal degeneration, the precise mechanism by which neuronal density declined in normal aging was not unanimously agreed upon. While the majority of studies supported the hypothesis that neuronal density decreased due to the loss of gray matter, others emphasized that reductions in white matter pathways is also contributory. Still others hypothesized, in defiance of the popular paradigm, that robust neuronal death was not characteristic of normal aging, and that instead reductions in brain volume/mass represented shrinkage of cell bodies or reductions in neuropil. In fact, not until the advent of new stereological principles in the 1980's did investigators begin to uncover the systematic confounds which led to this uncertainty. Employing these more precise methodologies, modern investigators uncovered that early reports of severe neuronal loss as a consequence of normal ageing were confounded by various technical and methodological issues, such as tissue processing and sampling design.⁽³⁷⁾ Instead, the resulting conclusion of these studies was that in humans^(38, 39), non-human primates,^(40, 41) and rodents^(42, 43), significant cell death in the hippocampus and neocortex is not characteristic of normal ageing. In fact, a ~30% reduction in neuron number in layer 8A of the prefrontal cortex (PFC), is one of the only reductions in neuron number attributable to normal ageing that has been corroborated using modern methodologies.⁽⁴⁴⁾ Lending further credibility to this finding, the same report states that neighboring regions of the PFC exhibit conservation of neuron number, and that the neural degeneration in layer 8A of the PFC correlates with impaired performance on a working memory test.⁽⁴⁴⁾

Similar to early reports of a decline in neuronal density with ageing, early investigations of dendritic branching incorrectly suggested massive deterioration in the human entorhinal cortex and hippocampus.^(45, 46) These experiments too, however, were plagued by experimental confounds such as the selection of a heterogeneous study population including both healthy and demented individuals. Subsequent investigations, which were more precisely controlled for the participants' mental status and which applied stereological controls, have found that normal aged individuals exhibit no significant reduction in dendritic branching as a consequence of ageing. In fact, perhaps counterintuitively, dendritic branching and length appears to be greater in aged individuals as compared to younger adults in specific regions of the brain.^(47, 48) Interestingly, some investigators suggest that the observed increases in dendritic branching are largely accounted for by the lengthening and branching (apical dendrites) or lengthening only (basal dendrites) of terminal

dendritic segments.⁽⁴⁷⁾ Mechanistically, these data suggest a model of robust plasticity in which the aging cortex contains regressing/apoptotic and surviving/arborizing neurons, with the latter group predominating even in the aging adult brain. Highlighting only those studies which characterize dendritic branching in regions of particular significance to AD, extensive dendritic branching in layer II of the parahippocampal gyrus, the origin of the perforant pathway, is now well-established in the literature.^(47, 48) Additionally, increased dendritic extent in the dentate gyrus of old compared with middle-aged humans has now been reported.^(49, 50) Lastly, the human hippocampus and subiculum exhibit no change in dendritic branching with age.⁽⁵⁰⁻⁵²⁾ Corroborating these findings in humans, modern studies of dendritic extent in other animal models have, in general, confirmed that there is no regression of dendrites with age. For example in rats, no significant reductions in dendritic length of hippocampal granule cells or CA1 neurons between young (3 months), middle-aged (12–20 months) and aged (27–30 months) rats have been observed.⁽⁵³⁻⁵⁵⁾ Consistent with the studies above which suggest the morphology of PFC neurons is uniquely sensitive to age-related neurodegenerative processes, age-dependent reductions in both apical and basal dendritic branching of PFC neurons have been reported in the medial PFC in humans and rats.^(26, 56, 57) In summary, extensive research in both animal models and human subjects strongly alludes to the conclusion that PFC neurons are more vulnerable to the neurodegenerative processes of ageing than their hippocampal counterparts, although this is not to say more subtle changes to neuronal morphology are completely absent in the regions of the brain which sub-serve memory. To the contrary, while the CA1 region of the hippocampus⁽⁵⁵⁾ and dentate gyrus^(58, 59) demonstrate no significant difference in spine density in humans and rats, in the subiculum of non-human primates, significant reductions in spine density with age have been observed in monkeys between the ages of 7 and 28 years of age.⁽⁶⁰⁾

Summarizing the changes associated with normal aging, at worst, the brains of intellectually preserved elderly individuals are characterized by mild brain atrophy with functionally significant reductions in neuron number and dendritic density predominantly restricted to the cells of the PFC. While this unique pattern of neurodegeneration differentiates normal aging from the neuropathological profile of AD described below, it also raises a new question. Namely, “what neurodegenerative processes, if not neuronal/dendritic reductions, account for the commonly observed phenomenon of age-associated memory impairment (AAMI)?”

Compared to their younger counterparts, it is now well-established that aged humans exhibit a distinct pattern of memory impairment in the domains of episodic memory and working memory.^(61, 62) Given the evidence of robust age-

dependent reductions in PFC neurons in the elderly discussed above, it is not surprising that deficits in working memory are observed in this population. One way these age-dependent deficits in working memory have been demonstrated empirically is by evaluating performance on the delayed non-matching-to-sample (DNMS) task. While humans display significant reduction in performance on this task⁽⁶³⁾, they are not the only species to exhibit deficits in working memory with advancing age, as aged rats⁽⁶⁴⁾ and non-human primates^(65, 66) also show time-dependent deficits on the DNMS task. However, deficits in working memory are not the only behavioral sequela of PFC neurodegeneration. In addition to its involvement in working memory, the PFC is also considered to be the neural substrate of executive function. One way to measure executive function is with the Wisconsin card sorting task (WCST). Unsurprisingly, aged humans are impaired on the WCST and make more perseverative errors.⁽⁶⁷⁾ As with working memory impairment, adaptations of the WCST for animal models have demonstrated deficits in executive function are also seen in non-human models.⁽⁶⁸⁾ Notably, unlike deficits in spatial and episodic memory observed in AAMI, impairment in working memory and executive function are not surprising given that the morphology of neurons in the PFC is more susceptible to age-related neurodegenerative processes.

Whereas the PFC is necessary for working memory^(69, 70) and executive function⁽⁷¹⁾, the remaining deficits associated with AAMI, namely impairment in episodic and spatial memory tasks, are hippocampus-dependent. Perplexingly, despite the lack of overt neurodegeneration in the hippocampus, performance on episodic memory tasks declines with age in humans.^(61, 62) In addition, aged humans⁽⁷²⁾, monkeys^(73, 74), dogs^(75, 76), rats^(77, 78) and mice⁽⁷⁹⁾ all show deficits on tasks designed to test spatial navigation. Until recently, the neurobiological substrate of these observed deficits was a mystery given the absence of overt neuron death or alterations in dendritic density associated with increased age. As it turns out, the mechanism behind age-associated behavioral impairments attributable to hippocampal-dysfunction are far more subtle and result from region-specific changes in dendritic morphology, cellular connectivity, Ca²⁺ dysregulation, gene expression and other factors which affect plasticity. With respect to dendritic morphology and cellular connectivity, electron microscopic investigation at the perforant path–granule cell synapse showed that aged rats have a 27% decrease in synapse number in the middle molecular layer of the dentate gyrus compared with young rats.⁽⁸⁰⁻⁸²⁾ The specificity of this synapse loss in the dentate gyrus is astonishingly constrained, as age-related synaptic loss involves axospinous, but not axodendritic, junctions.⁽⁸²⁾ Moreover, these alternations in synaptic connectivity are both functionally significant and regionally constrained, as spatial memory deficits correlate robustly with a reduction in perforated synapses at the medial

perforant path–granule cell synapse.⁽⁸³⁾ Notably, the alternations in cell-to-cell interactions observed in the dentate gyrus are not observed for Schaffer collateral–CA1 synapses, as the total synapse number remains the same across different age groups.⁽⁸⁴⁾ Instead, it is believed that age-related dysfunction in CA1 pyramidal cells is related to profound reductions in the post-synaptic density area of these perforated synapses. Supporting this conclusion, electrophysiological data demonstrates that the amplitude of the field EPSP recorded in area CA1 of aged rats is reduced compared to younger rats. Taken together, these findings support the idea that many hippocampal perforated synapses become non-functional or silent in aged learning-impaired. While this loss of functional synapses might contribute significantly to cognitive decline during normal ageing, it is not the only change associated with ageing in the hippocampus. In addition to the changes in cell-to-cell interactions described, the biophysical properties of hippocampal neurons are also dramatically altered by age. For example, numerous studies have demonstrated an increase in Ca^{2+} conductance in aged hippocampal CA1 neurons, perhaps due to an increased density of L-type Ca^{2+} channels.⁽⁸⁵⁾ While reductions in synapse number could perturb the cooperativity of active synapses and lead to network dysfunction, dysregulation of Ca^{2+} homeostasis undoubtedly contributes to restrictions in plasticity that may contribute to the observed deficits in spatial and episodic memory seen in the elderly. The best evidence of this summary comes from experiments which demonstrate that aged rats exhibit deficits in LTP, a process universally acknowledged as crucial to memory formation in the hippocampus. Convincingly, the functional consequences of altered morphology, biophysical properties and synaptic connections of aged neurons on plasticity and LTP are robust; with aged rats demonstrate deficits in both phases of LTP. As described earlier, LTP can be divided into an induction phase and a maintenance phase. The induction phase involves the temporal association of presynaptic glutamate release with postsynaptic depolarization, resulting in the ejection of Mg^{2+} from NMDA receptors and a consequent increase in intracellular Ca^{2+} .⁽²¹⁾⁸¹ Considering this phase of LTP's dependence on appropriate Ca^{2+} regulation and the cooperativity of afferent input, it is mechanistically apparently why LTP induction is perturbed in the hippocampus of aged animals. Less intuitively however, normal aging also impairs the maintenance phase of LTP. In this second phase of LTP, changes in gene expression and the insertion/relocation of AMPA receptors into the post-synaptic membrane insures the continued expression of increased synaptic efficacy after induction. As stated, it is known that the maintenance phase of LTP requires gene expression and de novo protein synthesis. This protein synthesis is facilitated via the expression of immediate early genes (IEGs) such as *cfos*. Functionally, IEGs can be grouped into two classes: inducible transcription factors (*c-jun*, *c-fos*, and *zif2*) and effector proteins.⁽⁸⁶⁾ After *c-jun* and *c-fos* mRNA are translated

into protein, their protein products can form a heterodimer called the activator protein 1 (AP1) complex. Critically, AP1 is a transcription factor that promotes the expression of late-response genes, some of which are important for the growth of new synapses or the modification of synaptic structure.⁽⁸⁷⁾ Relating this pathway of LTP maintenance to age-related alternations in plasticity which may affect cognition, although hippocampal pyramidal cell expression of IEGs do not differ significantly across age groups, elderly animals transcribe less IEG mRNA as compared to younger controls.⁽⁸⁸⁾ This consequently may lead to dysregulation of other genes that depend on the AP1 transcription factor, resulting in the deficits in LTP observed in aged animals. Interpreted as a whole, these studies suggest that age-related changes in key excitatory synaptic connections, even in the absence of significant circuit degeneration, perturb neuronal function in the hippocampus to a degree sufficient to impair LTP; one of the principal neuronal phenomenon underlying memory formation.

In summary, once thought to be exclusively a consequence of massive cell loss and the deterioration of dendritic branching, animals experience an age-dependent decline in cognitive function.^(45, 46) Clinically referred to as AAMI, these age-related deficits in episodic, spatial, and working memory in addition to perturbations in executive function have now been mechanistically linked to subtle neuronal changes in the PFC and hippocampus. Without question, of the brain regions affected by ageing, the hippocampus and the PFC appear to be particularly vulnerable. However, alluding to the complexity of the pathogenic processes which underlie age-related neurodegeneration, the impact of ageing on neuronal function in each of these regions differs dramatically. With respect to the PFC, the morphology of these neurons appear more susceptible to age-related change, as these neurons exhibit a decrease in dendritic branching across animal models.^(26, 55-57) Additionally, in stark contrast to initial reports of wide-spread neuronal decline in the aging brain, evidence now suggests that regionally constrained losses in cell number (area 8A in monkeys) occurs naturally with age, and that this decline in cell density is correlated with working memory deficits.⁽⁴⁴⁾ Although there is also evidence of Ca²⁺ dysregulation in aged PFC neurons⁽⁸⁹⁾, the functional consequences of this are not yet known and are far better characterized in the hippocampus. In this second vulnerable brain region, more is known about the impact of ageing on neuronal function. Specifically, dysregulation in Ca²⁺ homeostasis⁽⁸⁵⁾ and changes in synaptic connectivity⁽⁸²⁾ are hypothesized to perturb plasticity and gene expression resulting in an alteration of the hippocampal neuronal circuitry which sub-serve memory. Notably, although the age-related neurological changes described are of sufficient severity to perturb neuronal function in these two brain regions, like the clinically observed deficits associated with AAMI, these

neuronal changes tend to be subtle when compared with the alterations that are observed in age-associated disorders such as Alzheimer's disease. However mild by comparison, a robust understanding of the precise mechanistic underpinnings of AAMI is critical for the study of AD, as understanding age-related changes in cognition sets a background against which it is possible to assess the effects of pathological disease states.

1.3 NEUROPATHOLOGICAL CHANGES ASSOCIATED WITH ALZHEIMER'S DISEASE

As justification for why an understanding of age-related neurodegeneration is fundamental to assessing the pathological changes in AD, one must look no further than the now dated theories of AD pathogenesis developed in the eighties and nineties. During this time period, a considerable portion of the scientific community favored the hypothesis that AD simply exemplified exaggerated aging rather than a truly distinct disease process.⁽⁹⁰⁾ As in the preliminary assessments of brain changes associated with ageing, initial attempts to distinguish between normal aging and AD pathology applied stereological methods for quantitative assessment of neuronal numbers to determine if specific patterns in neuron loss existed between these two etiologies of cognitive impairment. Logically, since memory impairment is a cardinal clinical manifestation of both AAMI and AD pathology, neuroanatomists first focused on the neuronal substrates of memory formation in the brain; the entorhinal cortex, hippocampus and subiculum. In addition to sub-serving the cognitive functions most perturbed by AD, these regions of interest also non-coincidentally are the first to develop the histopathological hallmarks of AD; A β plaques and NFTs. Unlike in normal aging in which preliminary findings of robust neuronal loss were later proven false, the neuronal loss reported in AD has been more or less consistent since its initial discovery. For example, in one of the earliest studies of neuron loss attributable to AD, a 52% and 31% decline in the number of neurons in the subiculum and hilus of the dentate gyrus represent the two most significant findings, respectively.⁽⁹¹⁾ While these studies are notable for being among the first to quantitatively measure neuron loss in AD, later studies which contrasted AD patients with age-matched controls, were those which truly marked the downfall of the theory that AD and normal aging represent the same pathological process. Chronologically, M.J. West and colleagues were the first to present well-controlled evidence of differences in hippocampal neuron loss between AD and cognitively normal elderly. Chief among their 1994 discoveries was the finding of a robust 31% decrease in CA1 hippocampal neuron

number in individuals with AD as compared to both youthful and aged subjects (AD= 4.4×10^6 CA1 neurons versus 14.08×10^6 in normal ageing group).⁽³⁹⁾ In contrast to the finding of reduced CA1 neurons in AD, almost no neuron loss attributable to ageing was measured in this region. Later studies would go on to characterize the rate of hippocampal/entorhinal atrophy between AD and cognitively normal controls only to discover that AD patients demonstrate a greater annual percentage volume change in both the entorhinal cortex (6.8 +/- 4.3%) and hippocampus (5.9 +/- 2.4%) when compared to controls.^(92, 93) From these findings, the authors concluded that the neurodegenerative processes associated with normal ageing and with Alzheimer's disease are qualitatively different.⁽³⁹⁾ The independent corroboration of this groups findings would subsequently confirm this conclusion and disprove the hypothesis that AD and accelerated aging are synonymous terms for the same pathological process.^(39, 94-96)

Now pathologically distinct from normal aging in the literature, the specific pattern of neuron loss in AD was quickly elucidated by further quantitative stereological studies. As stated, the first of these confirmatory studies recapitulated the finding of severe neurodegeneration in regions of the brain sub-serving memory, with estimated neuronal losses of 31-68%, 22-47%, and 14-25%, for pyramidal CA1 neurons, the subiculum, and the hilus of the hippocampus, respectively.^(39, 94, 96, 97) Equally critical, a subset of these studies also demonstrated that the extent of neuronal loss progresses with the pathological severity of AD. For example, Braak stage IV AD patients exhibit a 33% reduction in pyramidal CA1 neurons while a 51% decline in this same neuron population was measured in Braak stage V AD patients.⁽⁹⁶⁾ Of additional significance, neuron loss is not homogenously distributed even within a particular brain region, a finding once again indicative of the selective vulnerability of particular neuronal populations to the unique pathological processes underlying AD. Case in point, comparison of AD and non-demented age-matched controls reveals a 48% decline in the overall neuronal content of the entorhinal cortex. However, the vast majority of this neuron loss in the entorhinal cortex, up to 90%, is secondary to the specific loss of neurons in layer II.⁽⁹⁸⁾ While neuron loss in the structures discussed to this point are certainly fundamental to the clinically observed deficits in memory associated with AD, cell loss in other key brain regions, like the Nucleus basalis of Meynert (NBM), is unquestionably contributory as well. In this region, investigators report a devastating 42-89% reduction in cholinergic neurons.^(99, 100) A component of the highly integrated basal forebrain cholinergic pathways, strong evidence suggests that this system makes key contributions to normal cognitive processes and that disruption of this system in AD has serious consequences for attention, learning and memory. In fact, as described in subsequent chapters, evidence of cholinergic dysfunction contributing to deficits in

memory observed in AD is so great, modulation of this neurotransmitter system currently represents the gold-standard in AD palliative treatment. However the ineffectiveness of these treatments clinically may be an indication of other regions of substantial neuronal degeneration in AD. With respect to neocortical brain regions, two areas of robust neuronal insult have been described; the PFC and superior temporal sulcus. The later of these two brain regions exhibits a greater than 50% reduction in neuron content in severe AD.⁽¹⁰¹⁾ Similar to the entorhinal cortex and hippocampus, the former demonstrates a selectively vulnerable cell population, with an astonishing 90% reduction in PFC pyramidal neurons.⁽¹⁰²⁾ Lastly, while subcortical structures like the substantia nigra are general spared from severe neuron loss in AD⁽¹⁰³⁾, the amygdala⁽¹⁰⁴⁾ and Edinger-Westphal nucleus⁽¹⁰⁵⁾ both exhibit robust degeneration, 51-56% and 67% respectively. Notably, while these quantitative assessments demonstrating an extensive neuronal loss during the progression of AD have been instrumental in defining AD as a unique pathophysiological process, questions still remain regarding the nature of this neuron loss. While the majority of studies support the conclusion that apoptotic cell death underlies the majority of neuron loss observed in AD^(106, 107), other mechanisms of neurodegeneration such as necrosis cannot be ruled out in light of evidence of abnormal oxidative stress and advanced glycation-end products.⁽¹⁰⁸⁾

Beyond distinguishing AD as a unique pathophysiological entity, when interpreted within the context of hippocampal-mediated memory pathways, the patterns of neuron loss in AD also provide a mechanistic understanding of the cognitive dysfunction observed in AD. As discussed, the input and output pathways of the hippocampal formation are formed by axons that arise from specific and discrete cell populations. Summarizing the afferent/efferent pathways relevant to memory formation, cortical input from sensory association and limbic cortices to the hippocampus arises from projection neurons in layers II and III of the entorhinal cortex. The axons of these neurons in the entorhinal cortex constitute the performant pathway and serve as the major cortical afferent source for the hippocampus/dentate gyrus. As these are precisely the neurons lost in AD brains, with layers V & VI unaffected, it is clear to see that afferent input into the hippocampus is very likely perturbed in AD. In the absence of pathology, afferent signals from the performant pathway are then processed via intrinsic hippocampal circuitry. Once processed via a mechanism not yet completely elucidated, hippocampal output to the cortex arises principally via the CA1 pyramidal neurons and from projection neurons originating in the subiculum. Mirroring the specificity of AD lesions with respect to afferent hippocampal pathways, CA1 pyramidal neurons and the subiculum are robustly degenerated as a consequence of AD pathology. Thus, both the principal afferent and efferent pathways to the hippocampus are selectively perturbed in AD. Generalizing for the

sake of clarity, the functional ramification of this finding is analogous to a bi-lateral hippocampal lesion, with hippocampal tissues intact, but unable to facilitate memory consolidation in isolation.

1.3.1 Tau Deposition in AD

While neuronal loss represents the first cardinal pathological feature of AD and partially explains the clinical deficits observed in AD, it is obviously far too ubiquitous among neurodegenerative disorders to be considered a pathognomonic feature of AD. Instead, a fundamental distinction between other neurodegenerative pathologies and AD is that the pathophysiology of the latter is characterized by a distinct topographical distribution of two pathognomonic neurobiological lesions; A β plaques and neurofibrillary tangles (NFTs). In summary of this topographical distribution of NFTs, the CA1 fields of the hippocampus, entorhinal cortex and the inferior temporal cortex typically harbor the greatest degree of tauopathy. In contrast, the superior frontal and occipital cortex are relatively spared in AD, even in the tenth and eleventh decades of life.⁽¹⁰⁹⁾ Acknowledging the finding that NFT deposition in the substantia nigra and locus coeruleus are not specific to AD pathology, NFT deposition follows a stepwise topographic distribution pattern that begins in the trans-entorhinal region (Braak stage I) before affecting the entorhinal cortex (Braak stage II), hippocampus and temporo-occipital gyrus (Braak stage III), temporal cortex (Braak stage IV), parietal cortex (Braak stage V) and lastly occipital cortex (Braak stage VI).⁽¹¹⁰⁾ Notably, while this temporal profile of NFT deposition is typical of AD, NFTs are not specific for AD and are indeed found universally in almost every class of brain disease. Exemplifying the ubiquitous nature of NFTs in diseases of the brain, NFT deposition has been found in the brains of individuals who experience: frontotemporal lobar degeneration with tauopathy (FTLD-MAPT), focal cortical dysplasia, myotonic dystrophy, prion diseases, metabolic/storage diseases, some brain tumors, chronic traumatic encephalopathy, viral encephalitis, and other brain diseases.⁽¹¹¹⁻¹¹⁶⁾ Especially with respect to its role in the pathology of AD, the ubiquitous presence of NFTs in human brain disease suggests that NFTs are, at least under some conditions, a secondary response to injury. In support of this interpretation, NFTs are even found, albeit in a topographically restricted manner, in the absence of overt pathology.⁽¹¹⁷⁾ Two independent studies demonstrate this finding, with all individuals over the age of 40 years exhibited at least initial NFT pathology in the brainstem.^(116, 118) On the other hand, others argue that NFTs play a primary role in neurodegeneration, citing that NFT pathology is observed in the human brain long before the formation of A β plaques in patients with AD.^(116, 118, 119) Still, despite likely representing a secondary response to injury rather than the primary

neurodegenerative insult, the density of neuroanatomical localization of NFTs remains one of the most important clinical parameters in AD. This is principally due to the vast literature supporting the conclusion of a robust correlation between neocortical (not necessarily allocortical or subcortical) NFT density and ante-mortem cognitive status. Highlighting the most scientifically rigorous of these studies, many groups have independently demonstrated that the density of NFTs in select cerebral fields significantly correlate with cognitive performance as assessed via behavioral assays such as the MMSE.^(120, 121) In fact, the correlation between NFT deposition and cognitive deficits is so robust that the neuroanatomical distribution of NFTs is predictive of the cognitive domains affected in patients with AD.^(96, 101, 122) For example, the trend for AD pathology to manifest itself as disturbances in memory clinically has been linked to the deposition of NFTs in the anatomical substrates of memory in the medial temporal lobe. Similarly, deficits in domains associated with mid-to-late stages AD such as executive function, visuospatial capacities, and speech manifest themselves in synchrony with the development of NFTs in the neocortical brain regions sub-serving these constituents of cognition. In summary, regardless of its role as an initiating factor or secondary sequela of AD pathogenesis, NFT load is unequivocally related to cognitive impairment. This relationship is so robust, that amongst the thousands of cases and dozens of studies conducted worldwide, never has there been a report of a documented individual with “end-stage” neocortical NFT pathology who lacked ante-mortem cognitive impairment.^(123, 124)

Beyond this clinical relevance, the neuroanatomical distribution of NFTs has also been shown to correlate with the prototypical pattern of neuron loss observed in AD.^(96, 101, 122) However, a subset of studies have indicate that more neurons disappear in brains of AD subjects than can be explained directly by the number of NFTs observed at autopsy.⁽¹⁰¹⁾ One hypothesis to explain this discordance is that NFTs are removed or reabsorbed from the brain over the course of AD pathogenesis.⁽¹⁰²⁾ While reports of such “ghost tangles” have been made, the cumulative body of evidence is more supportive of neuronal shrinkage and/or non-NFT-mediated cell death mechanisms to explain this observation.

1.3.2 Amyloid Deposition in AD

Despite neuron loss and NFT deposition being cardinal features of AD and more closely related to symptomatic progression, to date, the unequivocal diagnosis of AD rests predominately on the histopathological confirmation of A β senile plaques in the brain.⁽¹²⁵⁾ As discussed, this is in part due to the fact that NFTs and neuron loss are universally common lesions and therefore lack the specificity necessary to differentiate AD from other etiologies of dementia. In this

regard, NFTs and neuron loss resemble many of the additional changes that may also occur in the brains of AD patients including: amyloid angiopathy, age-related brain atrophy, synaptic pathology, white matter rarefaction, granulovacuolar degeneration, and neuroinflammation.⁽¹²⁶⁻¹²⁸⁾ In contrast to all of these lesions described, A β plaques are unique to AD by definition. However their use in defining criteria for the morphological diagnosis of AD is considerably complicated by two other issues; the phenotypical heterogeneity of A β plaques and science's incomplete understanding of their formation. In the current paradigm, amyloid plaques are hypothesized to undergo gradual growth in the interstitial space of the brain via continual extracellular deposition of A β peptides at "seeding sites". These growing plaques encroach progressively on the axons and dendritic processes of neighboring neurons, eventually leading to neuronal death.⁽¹²⁹⁾ While the research behind this assertion is robust and very likely true for a subset of amyloid deposits in AD, its validity may be comprised due to its failure to acknowledge the multiple subtypes of amyloid deposits in AD brains. For instance, deposits of A β peptide frequently, but not always, aggregate at the center of a cluster of dystrophic neurites. Termed, neuritic plaques, this subset of senile plaques are considered to be the most closely associated with neuronal injury. In support of this conclusion, studies have demonstrating greater synapse loss and glial activation around this subset of lesions.⁽¹³⁰⁻¹³²⁾ For this reason, the confirmation of neuritic plaques in the brain at autopsy serves as the keystone of guidelines for the neuropathological assessment of AD. However the pathological significance of the second class of A β plaques, named non-neuritic or diffuse plaques, cannot be underestimated. Speaking generally, this is a morphologically diverse subset of A β -peptide-containing lesions which includes deposits of A β -peptide not in close association with dystrophic neurites. In contrast to their neuritic counterparts, diffuse amyloid plaques lack associated inflammatory cells and are not closely associated with neuron degeneration.⁽¹³²⁾ Recent studies also indicate diffuse plaques originate via an independent mechanism. Instead of a gradual extracellular deposition of A β at seeding sites, diffuse plaques are hypothesized to be the result of leaks of amyloid from compromised blood vessels at focal sites of blood-brain-barrier breaches.⁽¹²⁹⁾ Troublesomely, while the various subtypes of A β plaques have been recognized for decades at the histochemical level, the majority of AD researchers continue to publish under the false assumption that A β plaques can be referred to as a homogenous unit. For those researchers who do make the effort to distinguish between A β plaque types, the issue is further complicating by the inconsistent use of nomenclature pervasive in the literature. Using diffuse plaques as an example, similar lesions are also referred to as cotton wool plaques, amyloid lakes, and sub-pial bands. It is important to emphasize that this issue is not purely semantic. As discussed, not only do neuritic and diffuse plaques differ in their

correlation with cognitive deficits, they may also arise as a consequence of completely distinct pathological processes. While the significance of the latter point is still unknown, the failure to distinguish between morphological plaque types certainly has led to the overemphasis that A β plaque deposition does not correlate with disease severity. To the contrary, when morphological subtypes of A β plaques are considered, progression to clinical dementia is associated with a higher proportion of more “mature” plaque subtypes. For example, in one study comparing plaque morphology between pre-clinical and end-stage AD, 53% of all amyloid deposition was classified as diffuse plaque in the pre-clinical group as compared to 31% in the end-stage cohort.⁽¹³³⁾ Even in the absence of a direct correlation between A β plaques and symptom severity, a strong association between AD genetic risk factors and A β plaque formation is clearly established in the literature.⁽¹³⁴⁾ All high-penetrance AD genetic risk alleles (APOE4, Trisomy 21, APP mutations/duplications, PSEN1/2 mutations) have been linked with increased A β deposition and formation of the putative toxic subtypes of A β peptide species. Given that genetic factors confer approximately 70% of an individual’s risk for AD, these findings carry strong mechanistic implications and support the idea that A β plaques represent a temporally upstream feature of AD pathogenesis.^(134, 135)

Despite inconsistencies in nomenclature and the general failure of the field to recognize the various subtypes of A β plaques, the topographical pattern of A β deposition in the brain has been well-characterized. In stark contrast to the pattern observed for NFTs, the topographical pattern of A β deposition is markedly different. A β plaques appear first in the neo-cortex (phase I) and expand in an anterograde fashion into allocortex (phase II). Next, A β deposition becomes robust in the diencephalic nuclei, striatum and cholinergic nuclei (phase III) before spreading to the brainstem nuclei (phase IV) and finally cerebellum (phase V).⁽¹³⁶⁾ Translating this 5 phase system to pay homage to the 3 stage system used by Braak & Braak, stage A is defined by the presence of neuritic A β plaques in the basal portions of the frontal and temporal cortices.⁽¹¹⁰⁾ Of particular significance with respect to the clinical correlation of A β deposition with memory deficits, during this stage no evidence of amyloid is present in the hippocampus although the pre-subiculum and entorhinal cortex demonstrate evidence of diffuse plaques. Similarly, primary sensory and motor brain regions are completely spared, with the only notable exception to this rule being the olfactory cortex.⁽¹³⁷⁾ By stage B of the Braak & Braak system, a moderate density of A β plaques is found ubiquitously in the isocortex with the notable exceptions of primary sensory and motor areas. During this stage of AD the hippocampal formation is only mildly involved, with sparse A β deposition mostly restricted to the pyramidal cell layers of the subiculum and sector CA1. The unique exception to this description is the

presence of two rows of densely packed amyloid deposits in the molecular layers of the subiculum and fascia dentata. In comparison to CA1, sectors CA2 and CA4 contain relatively few plaques regardless of AD severity. Although A β plaque deposition in the hippocampus worsens with disease progression, the final Braak & Braak stage, stage C, is defined by A β deposition in the primary sensory/motor areas.⁽¹³⁸⁾ Alluding to the possibility of a subpopulation of vulnerable cell types, A β deposition also follows a unique laminar distribution in the cortex across all stages.⁽¹³⁸⁾ Briefly, the external glial layer remains virtually completely devoid of amyloid deposits while layers II and III display sparse A β plaque distribution. Similarly, the myelin rich layers IV and Vb of the isocortex fail to demonstrate a propensity to facilitate amyloid aggregation. Instead, robust A β plaque deposition is loosely restricted to a laminar distribution in layers I, Va, and VI.⁽¹¹⁰⁾

In summary, A β deposition follows a topographically and temporally distinct pattern in AD which distinguishes it from other etiologies of memory impairment. Furthermore, A β deposition appears uniquely restricted to particular layers in specific brain regions. In light of this differential in pathological involvement between brain regions and laminar distribution of NFTs and A β , some investigators have concluded that the pathological changes in Alzheimer disease must extend along connecting fibers. Indeed, as described in other sections, the pathological regions of interest in AD are connected by well-defined groups of neurons. Notably however, the validity of this theory will likely remain untested until the molecular etiology of AD has been completely elucidated. Still, the invariable and severe involvement of the olfactory areas of the brain in AD is in striking contrast to the minimal changes in the somatosensory and primary visual areas. While this finding has various explanations, it raises the possibility that the olfactory pathway may be initially involved in AD pathogenesis and facilitate disease progression as a consequence of its highly integrated nature into the brain's memory circuitry. A more common interpretation of this finding is that A β plaque deposition and even NFT are inconsequential to AD progression and instead represents an epiphenomenon of aging.⁽¹³⁹⁻¹⁴²⁾

Without a doubt one of the longest and most hotly contested controversies in modern science, critics of A β -centric definitions of AD commonly cite four general arguments.⁽¹⁴³⁾ The first of these assertions, stems from reports of cognitively normal individuals with "advanced AD pathology" at autopsy. The second, much weaker argument points to the fact that individuals presenting with cognitive impairment similar to AD but who lack AD pathological changes at autopsy have been reported. Summarizing these first two assertions in a more generalizable manner, the degree of A β pathology corresponds poorly to the clinically observed severity of cognitive impairment. Despite being converse examples of one another, both of these assertions are partially addressed via the implementation of a more complete

definition of “advanced AD pathology”. While it is true that A β plaques in the absence of other neurodegenerative changes are not a sufficient substrate for severe dementia, this definition of “advanced AD pathological change” is incomplete. More precisely, the classification of widespread A β plaque deposition as advanced AD pathology without regard for the numbers and distribution of NFTs is incorrect. Instead, advanced AD pathology should be characterized by all three cardinal features of AD pathology; namely neuron loss, NFT deposition, and A β plaque density. In congruence with this holistic definition of AD pathology, the most recently published guidelines for the pathological confirmation of AD present criteria for both NFTs and A β plaques and even include a distinction between total A β plaque load and neuritic plaque load.⁽¹⁴⁴⁾ Thus, the response to the first assertion is that A β plaques, in the absence of NFTs and neuron loss, do not represent the same pathophysiological process which underlies AD. This retort in part emphasizes the point made earlier with respect to the morphological variability of A β plaques. All aggregations of A β are not equivalent. This is certainly not to say that the failure of A β plaque load to correlate robustly with disease severity is attributable solely to oversights in differentiating between diffuse and neuritic plaques, although the latter do correlate better with disease severity.⁽¹⁴⁵⁾ Instead, as discussed at length in subsequent chapters, the key point here is that A β peptides, and as a consequence A β plaques, are tremendously diverse. A collection of A β peptides of heterogeneous length, amino- and carboxyl-termini, and post-translational modification have been identified. Not only are do each of these peptides differ with respect to their contributions to direct and indirect neurotoxicity, they assemble at different rates and exist in vivo in a variety of different assembly states spanning from small oligomers to protofibrils and plaque aggregates. In short, the simplistic conceptualization of A β plaques and NFTs used by critics of A β -centric models does not adequately reflect the complexity of biological changes in the brains of AD patients. Because critics often subscribe to this simplistic model, some groups argue that A β plaques and NFTs are actually neuro-protective rather than cytotoxic. These groups contend that because A β deposits and NFTs are present in normal aging, albeit to a reduced degree, there must be some beneficial and adaptive aspects to their formation. While the vast literature contending this argument is reviewed in subsequent chapters, the major failure of this third fundamental critique of AD pathology is its failure to recognize the complexity of AD pathophysiology. The immense number of peptides and higher-order aggregates derived from the APP and MAPT genes very likely result in combinations of end-products which may simultaneously be neuro-protective and cytotoxic.⁽¹²⁴⁾ For those critics who do not contest the pathogenicity of A β plaques and NFTs, the fourth and probably largest point of criticism directed towards A β -centric models of AD stems from the failure of amyloid-centric therapies in randomized

clinical trials. This topic is of such prominence, it is addressed fully in subsequent chapters. Speaking generally however, experts in the field agree that the failure of anti-amyloid clinical therapeutic trials does not threaten the validity of A β -centric models of AD pathogenesis because they have yet to appropriately test the hypothesis. Virtually all studies to date have been plagued with experimental confounds, most embarrassingly with some trials drawing negative conclusions only to discover the therapies tested failed to even cross the blood brain barrier. Oversights of this nature in combination with inhomogeneous cohort selection, the late timing of therapy, and a variety of other confounds discussed elsewhere summarize why clinical trials have failed to provide definitive answers as to the direct role of A β plaques or NFTs in the cognitive impairment associated with AD.

CHAPTER 2 CLINICAL SUBTYPES & SYMPTOMS OF ALZHEIMER'S DISEASE

2.1 SPORADIC & EARLY-ONSET SUBTYPES OF ALZHEIMER'S DISEASE

Experts have long recognized two forms of AD: (i) the sporadic variant and (ii) familial AD (FAD) (Figure 2-1). Unfortunately for the field, alternative terminologies have been loosely applied to each of these AD forms in a manner which can be misleading. Most troublingly, the sporadic variant of AD is colloquially referred to as late-onset AD, a term which ignores the existence of early-onset forms of sporadic AD. Furthermore, the classification of FAD can be subdivided based on the development of symptoms and inheritance pattern (Figure 2-2). By definition, the term FAD implies the inheritance of genetic risk factors which has led to the presentation of AD in at least three generations. However because the vast majority of FAD patients develop symptoms before the age of 60-65, this term is commonly used in lieu of the more precise term early-onset FAD (EOFAD). Just as with sporadic AD, not all forms of FAD result in an early-onset presentation. Thus, use of the term FAD to denote only cases of EOFAD inadvertently ignores cases of late-onset FAD (LOFAD). Furthermore, for the subset of LOFAD cases which harbor an autosomal dominant genetic component, the term autosomal dominant AD (ADAD) is correctly employed. Logically, the autosomal dominantly-inherited form of AD which results in early symptom onset is termed autosomal dominant early-onset AD (ADEOAD). Though it may seem academic, this variable nosology is of significance when considering the challenge of identifying individuals that should undergo predictive genetic testing, as the probability of a positive hit will vary depending on the subpopulation tested. For example, using the stringent criteria of symptom onset before age 61, the prevalence of EOAD is 41.2 per 100,000 persons. If instead we were interested in applying genetic screening to individuals with ADEOAD, defined as the occurrence of EOAD in at least three generations, then the expected prevalence would be closer to 5.3 individuals per 100,000.⁽¹⁴⁶⁾ While the topic of genetic screening certainly underlines the importance of understanding of AD nosology, this point can be similarly made for the construction of cohorts for AD therapeutic clinical trials.

Most importantly for the purposes of this work, an appropriate understanding of AD nosology is critical when interpreting the origin and generalizability of amyloid-centric hypothesis of AD. Put in the simplest terms, the distinction

between sporadic AD and FAD is of significance because evidence suggests that the pathologic etiologies of these two forms of AD are distinct. As reviewed at length in subsequent sections, all known cases of FAD arise secondary to mutations in three genes relevant to the production of A β peptides. As a consequence, although myriads of other possible mechanisms for sporadic AD exist and data suggests that disturbances in A β production alone are likely insufficient to incite disease, A β is considered a central mediator of sporadic AD pathophysiology. Still, it is important to recognize that all studies to date suggest that the amyloid cascade theory plays a more important role in EOFAD than it does in sporadic AD.⁽¹⁴⁷⁻¹⁵⁰⁾ Moreover, while this genetic evidence strongly implies the etiology of EOFAD involves the overproduction of A β peptides, the pathogenesis of sporadic AD appears more dependent on the perturbation of both A β production and clearance. From this etiological distinction, one critical point must be made. For decades, the vast majority of AD research has been conducted in preclinical mouse models which carry etiological construct validity only for EOFAD. While it is certainly reasonable to assume that the pathophysiological processes underlying sporadic AD may mimic those observed in EOFAD to an undetermined degree, it is also essential to recognize this experimental confound. This point is of no higher significance when considering the development of therapeutic strategies for sporadic AD. Among the greatest criticisms of A β -centric hypotheses to date, all A β -centric therapies have failed to robustly combat the progression of AD. While the reasons for these failures are discussed at length in the appropriately titled section, it is worth mentioning here that pathophysiological differences between EOFAD and sporadic AD may be contributory, with sporadic AD representing a far more complex disease. Therefore, in order to efficaciously combat the multi-factorial nature of sporadic AD pathology, it is very likely that the most effective therapies will need to target multiple-levels of AD pathophysiology.

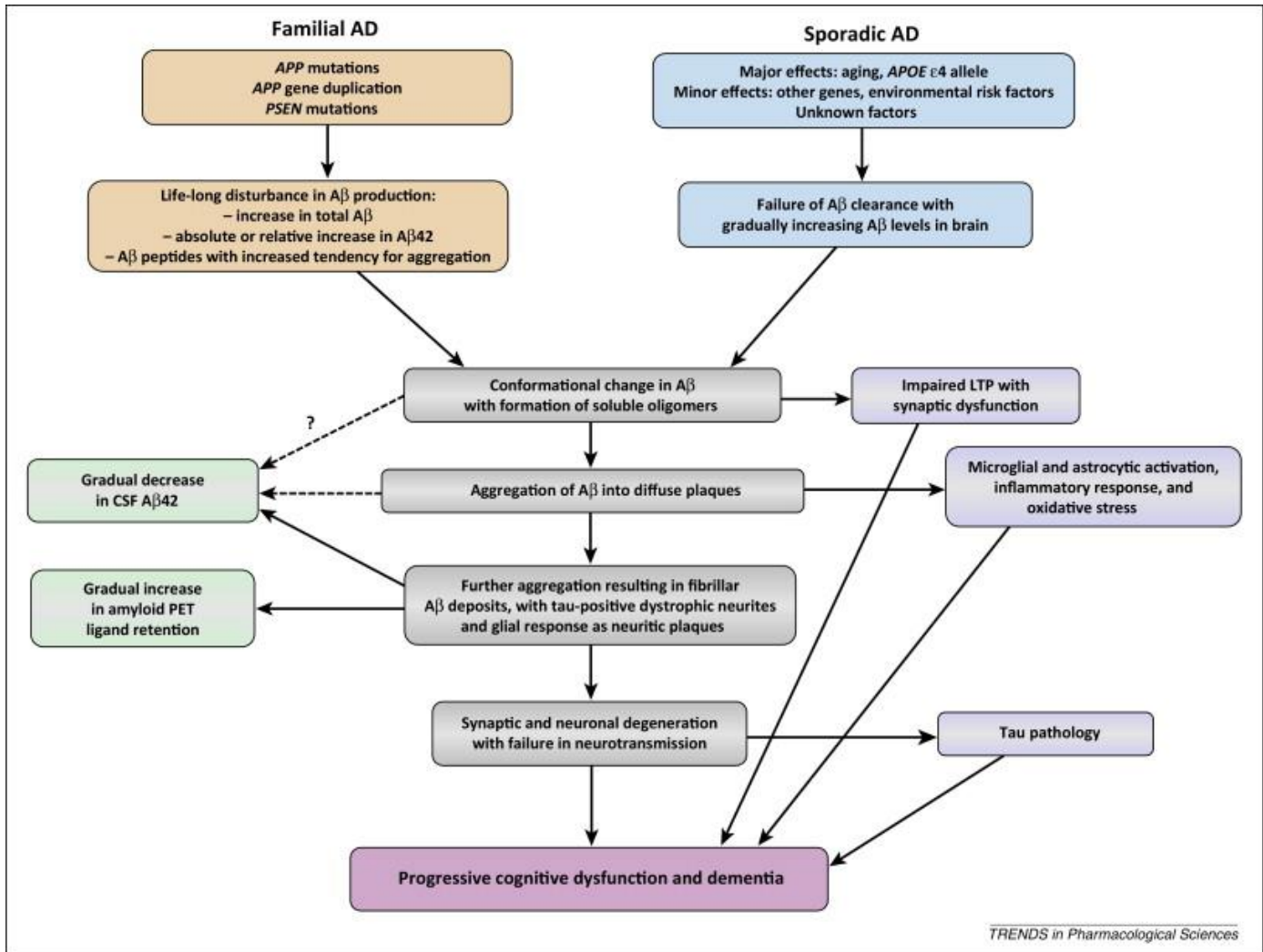


Figure 2-1. The Amyloid Cascade Hypothesis.

This is the lead hypothesis for Alzheimer's disease (AD) pathogenesis, which posits that the central event is an imbalance between β -amyloid ($A\beta$) production and clearance. In familial AD, genetic alterations cause a life-long disturbance in $A\beta$ production or generate $A\beta$ peptides that are more prone to aggregation. In sporadic AD, advanced age and possession of the apolipoprotein E (*ApoE*) $\epsilon 4$ allele have major effects on the risk for developing AD. The common denominator in the pathogenesis is a conformational change in $A\beta$, which makes it prone to aggregation, with the initial formation of soluble oligomers, followed by larger fibrils that accumulate into diffuse plaques and, at a later stage, neuritic plaques. Cognitive impairment is believed to be due to $A\beta$ oligomers inhibiting hippocampal long-term potentiation and impaired synaptic function, as well as an inflammatory response, oxidative stress, and synaptic and neuronal degeneration with neurotransmitter deficits. Tau pathology with tangle formation is regarded a downstream event that contributes to cognitive symptoms. Abbreviations: APP, amyloid precursor protein; CSF, cerebrospinal fluid; LTP, long-term potentiation; PET, positron emission tomography; PSEN, presenilin. Reproduced with Permissions from TRENDS in Pharmacological Sciences.⁽¹⁵¹⁾

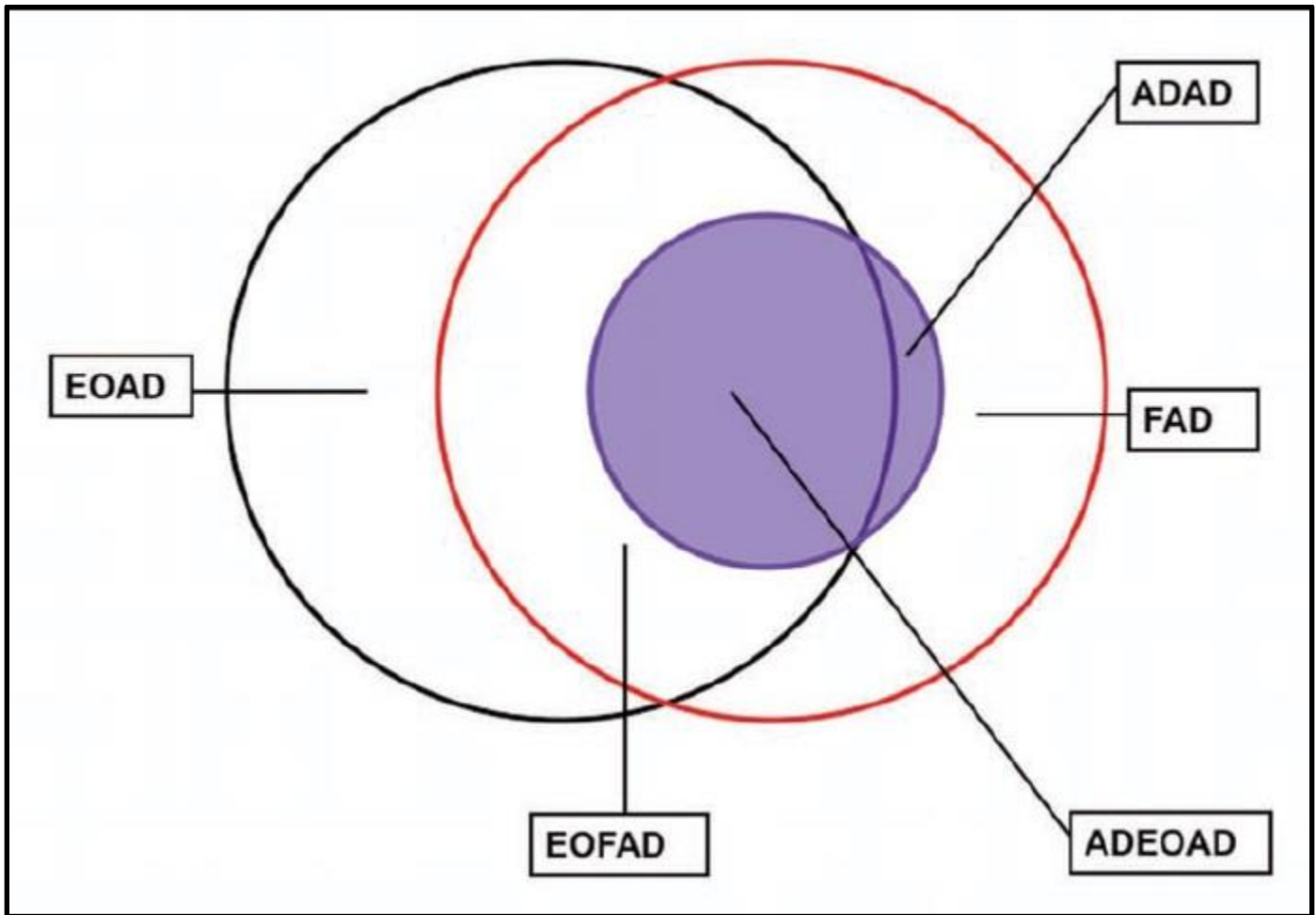


Figure 2-2. Diagram Representing the Relationship Between Several Terms About AD.

Red circle: familial AD (FAD); black circle: early-onset AD (EOAD); blue circle and shadow; autosomal dominant AD (ADAD). The area surrounded by red and black lines represents early onset familial AD (EOFAD). The region encircled by blue and black lines represents the autosomal dominant form of early-onset AD (ADEOAD). Reproduced with Permissions from the Canadian Journal of Neurological Sciences.⁽¹⁵²⁾

2.2 CLINICAL FEATURES OF ALZHEIMER'S DISEASE

Alzheimer's disease (AD) is a neurodegenerative subtype of dementia characterized symptomatically by a progressive decline in cognitive function which leads to severe morbidity and ultimately death. Such is the devastating nature of AD burden that the reported mean survival after diagnosis of AD ranges from only 3-8 years.⁽¹⁵³⁻¹⁵⁷⁾ Interestingly, although the phenotypic heterogeneity of AD is cited as one of the largest impediments to its study, the early deficits in memory which typify AD are largely constrained to explicit memory faculties until late in the disease course. One of the two main subdivisions of long-term memory in humans, explicit memory refers to knowledge that can be consciously recalled (in contrast to implicit memory which cannot be consciously recalled). Thought to be principally supported by mesial temporal and neocortical structures in the brain, explicit memory can be further subdivided into episodic, spatial, autobiographical, and semantic forms of memory^(158, 159) Here again, the clinical presentation of AD exhibits a temporal bias for the development of early deficits in episodic memories before impairment is observed in the semantic memory subcategory of explicit memory.⁽¹⁶⁰⁾ Loosely defined as those memories involving the storage and recollection of life-events, episodic memory is characterized by a subjective sense of time, an egocentric focus, and autoegetic consciousness, or the ability to mentally place oneself in the past.⁽¹⁶¹⁻¹⁶³⁾ The neuronal substrate of episodic memory is believed to include both mesial and neocortical brain regions while semantic memory, the recall of non-biographical knowledge such as the name of objects, vocabulary, and concepts, is not believed to be associated with mesial brain structures.⁽¹⁶⁴⁾ As further demonstration of the brain structure-dependent specificity of early AD memory impairments, within the domain of explicit memory, recall deficits in AD are further biased towards those memories which have not been well consolidated. By dividing explicit memory into immediate recall, memory for recent events, and memory of distant events, it can be demonstrated that AD patients typically exhibit the most profound deficits when recalling recent events.^(1, 165) Strikingly, the recall of this particular temporal subset of memory has been found to be highly dependent on brain structures such as the hippocampus, entorhinal cortex, and related structures in the mesial temporal lobe; precisely the brain regions affected earliest in AD.^(1, 165-167) In contrast to memory of recent events, forms of explicit memory not dependent on the hippocampus and other mesial temporal lobe structures such as immediate memory (encoded in the sensory association areas and prefrontal cortices) and memories which have been consolidated

for many years and are thus retrievable via non-hippocampus mediated mechanisms are spared early on in the AD course. Thus, as a consequence of its bias for recently encoded memories of the episodic subtype of explicit memory, the early memory deficit observed clinically in the majority of AD patients is most precisely described as an anterograde long-term amnesia. Of note, the technical qualifier “long-term” in this description is misleading, as “long-term memories” include those memories which can fail over the course of a few minutes. Instead of denoting an absolute time interval the distinction between long-term and short-term memory systems are best stratified by two fundamental characteristics, temporal decay and chunk capacity limits, with only short-term memories exhibiting both these phenomenon.⁽¹⁶⁸⁾

Precisely due to the confusion these technical definitions impose, clinicians prefer the term “recent memory impairment” when characterizing the early memory impairment of AD. Although highly variable among patients, this “recent memory impairment” typically manifests itself as the first notable symptom of AD and for this reason is the most frequently cited chief complaint of newly presenting AD patients. As AD progresses, the memory impairment initially constrained to recent episodic memories as described progresses slowly to encompass deficits in semantic memory. As a consequence of AD’s tendency to spare the subcortical systems supporting implicit memory and motor learning, deficits in these domains are typically only noted very late in the disease course. Without exception, the clinical course of memory impairment in AD is progressive, although the magnitude of an individual’s cognitive decline is highly unpredictable. Attempts to characterize the standard rate of accrument with respect to memory deficits in AD have largely focused on behavioral measurement tools such as the Mini-Mental Status Examination (MMSE) and Clinical Dementia Rating Scale. In studies tracking probable AD patient cohorts over 2-4 years, studies have reported on average a decline of 3-3.5 points on the MMSE each year.⁽¹⁶⁹⁻¹⁷²⁾ Additionally, in a rapidly progressing subset of individuals suffering from AD, totaling less than <10% of all AD patients, cognitive decline can be very rapid, with a loss of 5-6 points annually on the MMSE.⁽¹⁷³⁾

However, it should be noted that the reliability of cognitive memory examinations are routinely found to be limited in their ability to assess cognitive decline in AD. For example, when the MMSE is administered to probable AD patient cohorts, studies have found that only 15.8% to 65% of patients exhibit a significant decline on their MMSE performance after a 2-3 year follow-up, with significance defined as a loss of >3 points; a single standard deviation in these studies.^{(169,}

¹⁷²⁾ Despite the problems in reliability when employing behavioral metrics of cognitive performance, such studies have demonstrated that the rate of cognitive decline in AD may be associated with age of onset. Perhaps counterintuitively, an older age of onset of AD has been associated with a milder clinical progression as compared to patients diagnosed at a

younger age.⁽¹⁷⁴⁾ Regardless of the age onset, patients presenting with early neuropsychiatric symptoms including psychosis, agitation and aggression coincide highly with those patients whose cognitive decline progresses more rapidly.⁽¹⁷⁵⁾

2.2.1 Language Dysfunction in Alzheimer's Disease

However, despite the constrained nature of AD's presenting memory impairment to recent episodic memories and the correlation this specific deficit shares with regions of the brain most heavily affected in the disease's pathogenesis, it is imperative to recognize that the course of AD is highly heterogeneous. In fact, although memory impairment is the most common presenting symptom in the majority of patients presenting with AD, language dysfunction is quite commonly the first initial symptom recognized by patients.⁽¹⁷⁶⁾ Early deficits in language are most commonly constrained to word-finding difficulties, circumlocution, increasingly restricted vocabulary in spontaneous speech, and anomia on confrontational naming tests which may progress to include agrammatism, paraphasic errors, impoverished speech content, and impaired comprehension. Interestingly, accruing deficits in language are related to the progressive development of deficits in semantic memory. As evidence of this correlation between language dysfunction and semantic memory in AD, studies have demonstrated that patients with AD perform significantly worse on category fluency tests (which rely more heavily on semantic memory) as compared to letter fluency tests.⁽¹⁷⁷⁻¹⁷⁹⁾ Notably, the ability to repeat phrases is highly conserved in AD patients until very late in the disease course.⁽¹⁷⁷⁾

2.2.2 Impairments in Visuospatial Skills in Alzheimer's Disease

Yet another prominent deficit in a subset of patients with early-stage AD is impairments in visuospatial skills. Impairments in the visuospatial domain manifest themselves insidiously, with patients commonly describing difficulties in navigating unfamiliar places or an increasing frequency to misplace items.⁽¹⁸⁰⁻¹⁸²⁾ However, as with the impairments in memory and language, AD progression can commonly lead to patients suffering from difficulties navigating within familiar terrains such as their own neighborhood. As the disease course progresses even further, clinically detectable visual agnosia, the inability to recognize objects, or prosopagnosia, the inability to recognize faces, become a concern. In the very late stages of AD, reports of severe visuospatial deficits such as hemi-spatial neglect have been reported in AD patient populations.^(183, 184)

2.2.3 Disturbances in Executive Function and Judgement in Alzheimer's Disease

Beyond deficits in memory, language, and visuospatial skills, subtle changes in executive function and judgement can also accompany the early deficits observed in AD. Clinically, impairments in executive function are typically first detected by family members due to the insidious onset of symptoms and nature of the impairment. AD patients typically display poor insight and a reduced ability for abstract reasoning upon examination, however the most commonly identified impairments include a lack of motivation or apathetic demeanor as compared to baseline.⁽¹⁸⁵⁾ Indeed, as with the other deficits described in AD, impairment in executive function and errors in judgement inexorably progresses with the disease course. As impairment worsens, poor judgement and an inability to plan may manifest as symptoms, often to the degree that patients are no longer able to complete everyday tasks.⁽¹⁸⁶⁾ Notably, the importance of monitoring the accrual of deficits in executive function is paramount in the assessment of AD patients for two distinct reasons. Firstly, AD patients with severe impairments in judgement may present clinically with anosognosia, or a reduced insight into their own deficits. Thus, if not appropriately noted in the clinical assessment of AD, patients may tend to underestimate their deficits and offer alibis in response to the cognitive dissonance generated by their perceived state of health and what is relayed to them by the physician. Secondly, the severity of impairments in judgement and executive function are correlated with the pattern of associated AD neuropsychiatric symptoms. For example, patients with relatively preserved insight are predisposed to being depressed, while conversely, judgement impaired individuals are more likely to be agitated, disinhibited, and exhibit psychotic features.⁽¹⁸⁶⁻¹⁸⁸⁾

These neuropsychiatric symptoms, more typical in middle to late stage AD, are extremely common and typically lead to greater functional impairment than do the amnesic symptoms of AD.^(189, 190) This is true not only for AD, but for dementias as a whole, with approximately 61-92% of demented patients accruing neuropsychiatric symptoms at some point in their disease course.^(189, 191-194) As with other dementias, the spectrum of neuropsychiatric symptoms observed in AD includes: agitation, aggression, delusions, hallucinations, wandering, depression, and disturbances in sleep.^(195, 196) With respect to symptom onset, personality changes such as apathy, social disengagement, and disinhibition are the most common early manifestations. Sleep disturbances are also highly prevalent, even in early AD, afflicting 25-35% of patients, and can be worsened by typical AD therapies such as acetylcholinesterase esterase inhibitors.^(197, 198) Additionally, 20-45% of AD patients may develop Sundown Syndrome, the psychological propensity to develop

increased confusion, agitation, restlessness, and a generally more severe neuropsychiatric profile in the evening.^(199, 200) More characteristic of middle-stage AD, unlike many other symptoms of AD, the severity of Sundown Syndrome typically attenuates as the disease progresses.⁽²⁰¹⁾ Similar to the well-defined pattern of recent memory impairment observed in AD, the neuropsychiatric symptoms in AD are, in some ways, also useful in differentiating AD from other forms of dementia. Studies demonstrate that the percentage of patients with mild to severe AD who experience delusions is somewhere between the range of 30-34% while only 7% of AD patients report hallucinations.^(193, 202) In a long-term follow up study including 456 patients with mild to moderate AD, 70% of patients reported at least one delusional episode over a 4.5 year time period. As only 33% of patients reported visual hallucinations in this cohort, the literature seems definitive on the typical pattern of neuropsychiatric deficits observed in AD.⁽²⁰²⁾ In short, delusions are most commonly observed in AD, while a patient presenting with the symptoms of memory loss and visual hallucinations, particularly early in the disease course, is more concerning for Dementia with Lewy Bodies. Predictably, the presence of either delusions or hallucinations in AD is correlated with increased risk for severe cognitive impairment, functional decline, and death.⁽²⁰²⁻²⁰⁴⁾ Furthermore, delusions, hallucinations, depression or aggression is highly correlated with patient placement institutionalization and nursing home placement and thus greater socioeconomic burden.^(190, 202, 205, 206) From the perspective of family members, delusions of the paranoid subtype in particular generate significant emotional trauma.⁽²⁰⁴⁾ For example, AD patients may rationalize that their personal objects have been stolen or that someone is trying to harm them. Paranoid delusions in AD can even progress to the stage that they develop Capgras syndrome, the belief that their loved ones have been replaced by imposters. Inappropriate sexual behavior, especially towards caregivers, is yet another neuropsychiatric manifestation of AD and in dementia as a whole, with a reported prevalence of 15-25% of all demented patients.⁽²⁰⁷⁻²¹⁰⁾ Tragically, the neuropsychiatric symptoms and changes in personality observed in AD are progressive and often resistant to therapeutic intervention.

2.2.4 Miscellaneous Signs and Symptoms of Alzheimer's Disease

While the magnitude of morbidity associated with neuropsychiatric symptoms in AD is very high, less stigmatized symptoms such as dyspraxia are also major contributors to dependency in middle to late-stage AD.⁽²¹¹⁾ Defined as an impaired ability to perform coordinated movements, clinical dyspraxia in AD first manifests as a difficulty performing complex multi-step activities. As a consequence of its insidious onset, dyspraxia is best evaluated in a newly

presenting AD patient via ideomotor tasks as opposed to patient history.⁽²¹²⁾ Asking the patient to pantomime the use of an everyday tool, such as a toothbrush or comb for example, has been demonstrated to elicit mild dyspraxia in AD patients before it manifests clinically.^(213, 214) Interestingly, the tendency of AD patients to utilize their body parts as objects may actually stem from an inability to retrieve information about the appropriate holding posture for items.⁽²¹³⁾ Notably, dyspraxia typically manifests only after the emergence of cognitive and language deficits in AD, with damage to the anterior cingulate cortex in particular being correlated with the more debilitating ideomotor and dressing dyspraxia symptoms.^(212, 214) It is important to distinguish dyspraxia from pyramidal and extrapyramidal motor signs such as myoclonus, incontinence, and seizures. While these symptoms do occur in AD, they are restricted to late-stage disease, with seizures occurring in 9-16% of AD patients.⁽²¹⁵⁻²¹⁹⁾ In fact, the presence of clinically apparent motor dysfunction in early to middle stages of cognitive impairment is justification for consideration of an alternative diagnosis.⁽²²⁰⁾ However as mentioned, AD is a phenotypically heterogeneous disease of variable course and unpredictable symptomatology. Thus, atypical symptoms or even distinct presentations of AD are well reported.

2.2.5 Atypical Presentations of Alzheimer's Disease

For example, in AD patients with an uncommonly prominent involvement of the parietal lobes bilaterally, dyspraxia, visuospatial disorientation, and dysgraphia may outweigh language impairment and memory deficits with respect to symptom severity earliest in the disease course.^(221, 222) Interestingly, the development on language and auditory-verbal short term memory deficits in this variant presentation of AD later in the disease course is believed to represent the spread of neuropathology from the parietal cortices to encompass the peri-Sylvian language regions of the brain.⁽²²²⁾ A second atypical presentation of AD is characterized by early and robust posterior cortical atrophy, specifically with deficits in the dorsal visual stream contained in the lateral occipital and parieto-occipital cortices.^(221, 223-227) As opposed to early deficits in memory, this syndrome manifests primarily with progressive cortical visual impairment that is most commonly experienced symptomatically as difficulty reading or driving.^(221, 228) Acalculia (an impairment in performing simple mathematics), alexia (difficulty reading), and anomia (difficulty recalling the names of everyday objects) are also common presenting symptoms.^(229, 230) Clinically, the visuospatial variant of AD may present similar to Balint syndrome, containing elements of simultanagnosia (the inability to integrate a visual scene despite sufficient acuity to resolve the individual elements composing it), optic ataxia (the inability visually guide a limb towards a target), and ocular apraxia

(the inability to direct gaze accurately between targets).⁽²³¹⁾ Visual agnosia, apraxia, prosopagnosia, and visual field neglect comprise the remaining constellation of symptoms associated with this atypical presentation of AD.^(182, 228, 231, 232) Compounding the difficulties associated with correctly diagnosing the visuospatial variant of AD, common alternative pathologies such as Dementia with Lewy Bodies, frontotemporal lobar degeneration, and prior disease can mimic this presentation.^(224, 230) In addition to the visuospatial variant of AD, a frontal variant has also been ubiquitously reported in the literature, with prominent deficits in executive function overshadowing the more typical impairments in memory.^(233, 234) Although considered an atypical presentation, one study found that in a cohort of 100 mild AD patients, 88 exhibited more significant impairment in executive function as compared to 56 who were classified as predominately memory impaired.⁽²³³⁾ Thus, variants of AD may not be as rare as previously thought and more troublingly, both variants have been linked with a more rapid clinical progression.^(233, 234)

Further muddling the clinical presentation of AD, Alzheimer pathology can frequently co-exist with other neurodegenerative processes, most commonly vascular dementia. In fact, the coincidence of AD and vascular dementia is so high patients are more likely to possess a combined pathology as compared to either disease process in isolation.⁽²³⁵⁾ Independent reports of autopsy studies reveal that approximately one-third of all patient brains with vascular dementia contain AD-like pathology, with almost all AD patients demonstrating either cerebral amyloid angiopathy, microvascular degeneration, or periventricular white matter lesions.⁽²³⁶⁾ Typically, the cognitive deficits of vascular dementia are highly specific and subdivided into cortical and subcortical syndromes. Expectedly, the brain regions harboring the most abundant pathology dictate the nature of the impairment. For example, vascular dementia in the medial frontal cortex principally presents with executive dysfunction and apathy, medial temporal localization typically elicits anterograde amnesia. Similarly, vascular dementia involving the left parietal cortex presents with aphasia, apraxia, or agnosia while right parietal involvement produces symptoms such as anosognosia, asomatognosia, confusion, and agitation.⁽²³⁷⁾ With respect to subcortical pathology, deficits in personality, mood, urologic disease, and motor signs may be common.^(238, 239) As many of these symptoms overlap with those observed in AD, the comorbidity of AD with other neurological diseases such as vascular dementia significantly blurs the classical symptomology associated with AD.

Similarly, although more frequent in patients with frontotemporal lobar degeneration (FTLD), approximately one-third of patients with primary progressive aphasia (PPA) also have signs of AD pathology at autopsy.^(221, 240-243) A pathologically heterogeneous disorder, PPA is characterized by progressive language difficulty with relative sparing of

memory and cognitive function early on in the disease course.⁽¹⁷⁶⁾ Notably, AD with PPA typically presents with the logopenic variant, characterized by word-finding pauses in the absence of major grammar or comprehension deficits.^(176, 244-246) However, less commonly, cases of AD with non-fluent or semantic variants of PPA have been reported.^(221, 243) As with most comorbid conditions in medicine, the clinical course and symptomology of either pathology can be modified unpredictably by the other neurodegenerative condition resulting in significant diagnostic uncertainty.⁽²⁴⁷⁾

2.3 CURRENT CLINICAL DIAGNOSTIC STRATEGIES

2.3.1 History of Clinical Guidelines

With such a broad symptomology, unpredictable onset, and variable progression, compounded by the possibility of co-morbid or atypical presentations, reliably establishing a clinical diagnosis of AD remains one of the fundamental problems in geriatric medicine. Of note, a definitive diagnosis of AD requires histopathological analysis of patient brain tissue to confirm presence of A β plaques.^(110, 248) As this approach is only practically implemented post-mortem, experts in the field of AD have sought to establish core clinical criteria with strong diagnostic sensitivity and specificity to facilitate the assignment of a diagnosis of probable or possible AD. The first of these diagnostic recommendations for AD was published in July 1984 by the National Institute of Neurological and Communicative Disorders and Stroke (NINCDS) in collaboration with the National Institute of Aging and Alzheimer's Association (ADRDA). The resulting NINCDS-ADRDA criteria remained largely unmodified for 27 years. In a review of 13 independent studies measuring the diagnostic accuracy of the NINCDS-ADRDA diagnostic criteria for probable AD, a mean sensitivity and specificity of 81% and 70% have been reported, respectively.⁽²⁴⁹⁾ However, these parameters varied greatly between studies, with sensitivity ranging from 49-100% and specificity from 47-100%.⁽²⁴⁹⁾ With respect to the clinical criteria for possible AD, reported sensitivities range from 85-96% while specificity ranges from 32-61% depending on the study.⁽²⁴⁹⁾ Interpretation of this summary provides two pieces of insight. First, the clinical accuracy for diagnosing either probably or possible AD based on clinical examination alone is unacceptably low despite some authors suggesting these values are acceptable. However, consideration of these mean sensitivity and specificity values in the context of AD incidence, estimated to have reached 469,000 people over the age of 65 in 2014, reveals the inadequacy of the NINCDS-ADRDA criteria as the lone diagnostic determinant for AD.⁽²⁵⁰⁾ Even ignoring the unreasonably broad ranges for sensitivity/specificity, the reality of

these values means that almost 90,000 AD patients would not receive the correct diagnosis while over 140,000 individuals would be told they have some other condition. Extrapolating these figures out to 2050, when the incidence of AD is projected to double, and these seemingly reasonable sensitivity/specificity values become much less acceptable.⁽²⁵⁰⁾ Secondly, reports which boast a reasonably high sensitivity for the clinical diagnostic accuracy of the NINCDS-ADRDA criteria are often those which report very low specificity and visa-versa. This trend emphasizes the subjectivity intrinsic to diagnoses made solely on clinical criteria, and reveals the need of objective biomarkers to aid in the diagnosis of AD. To the field's credit, this is precisely the conclusion that was reached when then NINCDS-ADRDA clinical criteria for AD were revised by the National Institute for Ageing-Alzheimer's Association (NIA-AA) in 2011. Here, two principal changes to the NINCDS-ADRDA recommendations were made, (i) preclinical stages of AD were acknowledged and (ii) imaging and biomarker technologies were incorporated to assist in the diagnosis of AD. Briefly, the NIA-AA recommendations note 3 distinct stages of AD: preclinical AD, MCI due to AD, and dementia due to AD. Importantly, clinical diagnostic criteria are only provided for the last of these stages. However, preclinical AD is defined in the guidelines as patients without overt cognitive impairment but with evidence of an underlying AD pathology as assessed by biomarker studies. Very likely, the inclusion of a preclinical stage of AD was incorporated to reinforce the paradigm that AD associated brain changes may occur up to 20 years prior to symptom onset.⁽²⁵¹⁻²⁵³⁾ In contrast to preclinical AD, in which patients have yet to develop signs of cognitive impairment, individuals receiving a diagnosis of MCI due to AD under the NIA-AA guidelines must exhibit measurable cognitive decline. Similar to the preclinical AD stage, the NIA-AA guidelines stress the need for further biomarker validation before the definition of MCI due to AD can be utilized clinically. Once biomarkers have been reliably validated however, the NIA-AA guidelines recommend biomarker screening for AD pathophysiology in all MCI patients to facilitate risk stratification for progression to full dementia. These recommendations stem from studies suggesting that 10-15% of patients presenting with MCI will progress to AD within 1 year of visiting their physician.^(254, 255) More concerning, approximately half of patients with MCI will progress to dementia within 4-5 years.⁽²⁵⁴⁾ Placed in the context of 10-20% of all U.S. citizens over the age of 65 suffering from MCI, it is clear to see why risk stratification in such a large population is warranted.

The second major evolution in the diagnosis of AD made by the NIA-AA guidelines is the inclusion of biomarkers in the assessment of AD. While not yet clinically recommended, the NIA-AA defines two major categories of AD biomarkers: biomarkers of A β pathology and biomarkers of neurodegeneration. As a consequence of the

incorporation of these technologies, the diagnostic bins of probable and possible AD were expanded to include: pathophysiologically proved AD, probable AD, probable AD with AD pathophysiological process, possible AD, possible AD with AD pathophysiological process, and dementia unlikely due to AD. The diagnoses of probable/possible AD with AD pathophysiological process were intended only for research purposes, and differ from probable/possible AD diagnoses only in that they require biomarker evidence of an A β pathophysiology. Four arguments were outlined for the exclusion of biomarkers in the diagnosis of AD in the clinical setting: (1) the core clinical criteria alone were projected to provide good diagnostic accuracy, (2) limited research has been done to characterize the benefit of incorporating biomarkers in AD diagnosis clinically, (3) biomarker tests are highly variable between clinical sites or (4) unavailable in community hospital settings. However, in the recommendations and indeed in the field as a whole, the eventuality of biomarker incorporation in the clinical diagnosis of AD is widely accepted.⁽¹⁴⁴⁾

Although the 2011 NIA-AA recommendations do not remedy the innate limitations associated with an exclusionary clinical diagnosis of AD, they do update the NINCDS-ADRDA recommendations in several meaningful ways. Perhaps most relevant to improving the diagnostic accuracy of the core clinical criteria, the new guidelines incorporate additional exclusion criteria into the diagnosis of AD based on advances in the characterization of similarly presenting dementias such as Dementia with Lewy bodies, vascular dementia, behavior variant frontotemporal dementia, and primary progressive aphasia.⁽²⁵⁶⁻²⁶⁰⁾ More generally, the NIA-AA recommendations also help to acknowledge the heterogeneous nature of AD symptomology, by highlighting the relatively high prevalence of non-amnesic presentations of AD. Similarly, the NIA-AA recommendations do away with proposed age cutoffs for AD, noting that AD pathology before 40 or after age 90 is essentially the same pathophysiological process despite clinical-pathological correlations becoming lost in these populations. Lastly, the recommendations update the diagnostic algorithm to include information on now well-established genetic risk factors for AD such as mutations in APP, the presenilin family, and APOE.⁽¹⁴⁴⁾

2.3.2 Diagnostic Criteria

As described, in an effort to improve diagnostic accuracy with respect to detecting new onset AD, revisions have been made to both the NINCDS-ADRDA criteria and DSM-IV to yield the NIA-AA criteria and DSM-V, respectively. Additionally, the IWG has published its own criteria for the diagnoses of AD. In general, all these guidelines are quite similar, focusing on cognitive decline which must affect a patient's independence or ability to function in everyday life.

Each set of guidelines also require states of delirium and other medical causes of cognitive dysfunction to be ruled out clinically before assigning a diagnosis of AD. All have additionally expanded the domains of cognitive function from their predecessors in an effort to account for the heterogeneous symptomology of AD. In fact, one of the largest differences between the DMS-V, IWG, and NIA-AA criteria lies in their nomenclature. Still, of the three sets of diagnostic criteria, those outlined by the DSM-V are by far the least specific for AD. For example, severely limiting its applicability in the research setting, a major short-coming of the DSM-V criteria is its failure to incorporate biomarker or genetic testing into the clinical assessment. More troublingly, the DSM-V does not specifically assign a diagnosis of AD or address pre-symptomatic manifestations of AD. Still, considerable changes have been made from previous versions in an effort to conform to new-age paradigms of AD. Most strikingly, the classification “Delirium, Dementia, Amnestic, and Other Cognitive Disorders” in the DSM-IV is now referred to as “Neurocognitive Disorders” in the DSM-V. In addition to seeking harmonization with the NIA-AA criteria, this new classification scheme was introduced to distinguish diseases like AD from psychiatric disorders that have cognitive impairment as a symptom rather than a defining feature, such as schizophrenia or depression. Within the classification of neurocognitive disorders exist three main diagnoses: mild neurocognitive disorder (NCD), major NCD, and delirium. In contrast to the DSM-IV guidelines which required deficits in memory and impairment one or more of the following: aphasia (language problems), apraxia (impaired motor ability), agnosia (failure to recognize known objects), or deterioration in executive function, the DSM-V does not require memory impairment for the diagnosis of major NCD. Instead, as outlined in Table 2-1, the diagnosis of major NCD is defined as impairment in two or more cognitive domains that is accompanied by a loss of independence. However, according to the DSM-V, to assign a specific etiology of Alzheimer's to either mild or major NCD requires “clear evidence of decline in memory and learning”. Furthermore limiting the utility of the DSM-V, especially in the research setting, is its failure to capture pre-symptomatic stages of AD. Despite the DMS-V’s criteria for mild NCD being virtually identical to those for "mild cognitive impairment (MCI) due to Alzheimer's disease" as outlined in the NIA-AA diagnostic guidelines, preclinical/asymptomatic AD is not addressed. Thus, only two sets of research criteria for Alzheimer’s disease (AD) are now available: one published by an International Working Group (IWG) in 2007 and a second published by the NIA-AA in 2011. Unlike the DSM-V, both the IWG and NIA-AA guidelines cover the AD clinical spectrum from pre-symptomatic pathology through the development of MCI and eventually dementia. While the IWG criteria and NIA-AA recommendations both address asymptomatic and symptomatic stages of AD, each differs in its approach and

terminology. At the heart of the differences in each respective guidelines approach to classification, lies a difference in the definition of the term AD. In line with more traditional approaches to AD diagnosis, the term AD as used by the IWG refers only to the symptomatic stage of the disease. In contrast, the newer NIA-AA criteria refer to AD as a pathological process, whether asymptotic or symptomatic. Within the domain of symptomatic AD, one of the principal differences between these two sets of guidelines lies in the cognitive criteria required for diagnosis. More stringent in this respect, the 2007 IWG criteria for AD require objectively measured impairment on an episodic memory test. In contrast, the NIA-AA guidelines openly accept both objective and subjective reports of cognitive impairment, as well as deficits in non-memory domains of cognition. Later revisions to the IWG criteria in 2010 would accommodate non-amnesic presentations of AD by assigning subjects with non-memory impairments the diagnosis of atypical AD; but only if presenting with a well-defined syndrome such as: primary progressive non-fluent/logopenic aphasia, frontal variant of AD, or posterior cortical atrophy.⁽²⁶¹⁾ Moreover, currently on the IWG criteria require a positive AD biomarker for the assignment of a diagnosis of AD. Despite these differences between the NIA-AA and IWG guidelines with respect to symptomatic AD, the major advantage of both guidelines as compared to the DSM-V is the recognition of preclinical stages of the disease and the incorporation of biomarkers. Again, terminology differs between both sets of guidelines, with the IWG defining three stages of AD: preclinical AD, prodromal AD, and AD dementia. By comparison the NIA-AA uses a slightly more graded approach, with 3 stages of preclinical AD being followed by the diagnosis of “MCI due to AD” and lastly the diagnosis of AD itself. While the IWG’s criteria for prodromal AD are almost precisely concordant with the NIA-AA’s definition of MCI due to AD, both focusing on objective evidence of cognitive impairment with the preservation of independence, important differences exist when considering the domain of asymptomatic AD.⁽²⁶¹⁻²⁶³⁾ Here, the most important distinctions between the IWG and NIA-AA guidelines stem from their differing utilization of AD-specific and nonspecific biomarkers. Notably, both guidelines utilize essentially the same biomarkers, consisting of: CSF measurements of $A\beta_{42}$ /tau, amyloid imaging methodologies, measures of hippocampal atrophy as assessed by MRI, and evidence of hypo-perfusion/hypo-metabolism as assessed by PET/SPECT imaging. No substantial differences in AD specific biomarkers exist between guidelines, with CSF tau, CSF $A\beta_{42}$, and amyloid imaging methods termed pathophysiological markers and amyloid markers by the IWG and NIA-AA respectively. Similarly, the remaining non-AD specific biomarkers are referred to as topographical markers by the IWG and as neural injury markers by the NIA-AA. Semantic differences between

guidelines considered, perhaps the most relevant difference is the degree of validation for each set of criteria in the literature.

As briefly addressed, when considering only symptomatic AD patients of typical presentation, the DSM-V, IWG, and NIA-AA are in agreement with respect to diagnostic criteria. Given this fact, it is not surprising that the diagnostic accuracy of each set of guidelines appears to be more or less comparable. Although studies of the DSM-V criteria's reliability for major cognitive disorder have not yet been published, previous studies investigating the reliability of DSM-III-R's definition suggest moderate performance (kappa .51-.73).⁽²⁶⁴⁻²⁶⁷⁾ Similarly, no reports of the DSM-V's diagnostic sensitivity/specificity have been reported, however traditionally reports suggest that these parameters have improved with each new generation of the DSM. As evidence, as part of the 1994 Canadian Study of Health and Aging the relative percentage of subjects with AD dementia was evaluated using the DSM-III, DSM-III-R, and DSM-IV in a population of 10,263 individuals. The relative proportion of subjects with AD dementia was 29.1 percent when the DSM-III criteria were used, 17.3 percent with the DSM-III-R criteria, and 13.7 percent with the DSM-IV criteria.⁽²⁶⁸⁾ With respect to sensitivity and specificity, reports for the DSM-III-R are again most abundant. In autopsy confirmed studies, the sensitivity of these dated guidelines lies somewhere in the range of 51-76%, while reported specificities range anywhere from 80-97%.^(269, 270) Information regarding the diagnostic accuracy of the IWG criteria is also scarce, especially when the 2010 adaptations are considered. In the limited studies to date, sensitivity and specificity vary broadly, with ranges of 68%-95% and 86-93% being reported, respectively.^(271, 272) Of particular interest, one of these studies compared the specificity of the IWG criteria for AD in non-demented individuals as well as in a population of mixed dementias included in the differential of AD. Predictably, a reported specificity of 95% was obtained when distinguishing AD from non-demented patients. Optimistically, the results of this study suggest that the IWGs proposed incorporation of biomarkers into the diagnosis of AD can considerably raise specificity, as objective memory tests alone resulted in a specificity of only 86%. However, under the more realistic clinical scenario of attempting to distinguish AD patients in a mixed dementia cohort, specificity dropped considerably to 49%.⁽²⁷¹⁾ While the specificity of the IWG criteria when applied to a mixed dementia cohort is humbling, when contrasted to the 33% specificity when objective memory tests are used in isolation, the incorporation of biomarkers once again becomes supportable. On the hand, sensitivity when applying the IWG guidelines was only 86% compared to 93% for episodic memory tests alone. All data considered, the IWG guidelines appear to yield robust improvements in specificity when applied to non-demented patient cohorts as compared

to conventional diagnostic strategies. In the context of mixed dementia cohorts however, a reasonable specificity of 77% can only be obtained when the requirement that both pathological and topographical biomarkers be positive is implemented. Consistent with the theme however, the application of such stringent criteria affects negatively on sensitivity (48% if requiring both pathological and topographical biomarkers to be positive). In summary, the DSM-V and IWG criteria both appear to fulfill their aim of providing improving diagnostic accuracy for AD; although considerable uncertainty will preside over their true reliability until robust trials are conducted. Here, the NIA-AA criteria demonstrate an advantage, as substantial effort has gone into validating these set of guidelines despite its chronologically delayed publication in 2011. As summarized in Table 2-2, the NIA-AA criteria for probable and possible AD distinguish themselves from the NINCDS-ADRDA, IWG, and DSM-V guidelines via the inclusion of stringent exclusion criteria designed to improve the diagnostic specificity for AD.⁽²⁷³⁾ For example, a patient who meets the core clinical criteria for probable AD but demonstrates evidence of non-AD etiologies, such as cerebrovascular disease or FTLD, would be clinically downgraded from probable to possible AD. Similarly, atypical onset or progressions are grounds for demotion to a diagnosis of possible AD despite the core clinical criteria for probable AD being met.⁽¹⁴⁴⁾ With respect to diagnostic accuracy, in a mixed cohort of 157 patients with pathologically confirmed AD or FTLD, the NIA-AA criteria had a marginal sensitivity of 65.6% for probable and 79.5% for possible AD. The reported specificity of the NIA-AA diagnostic guidelines in the same study were 95.2% and 94% for probable and possible, AD respectively.⁽²⁷⁴⁾ Notably, the high specificity in this study is likely due to the increasingly stringent exclusion criteria adopted by the NIA-AA criteria. Of particular importance, raters in this study were provided only with anonymized clinical data with which they evaluated each patient against the NIA-AA criteria. Raters were not allowed patient interaction nor did they collect the pertinent clinical information themselves. Instead, this was done by a specialist cognitive group.⁽²⁷⁴⁾ While these features were likely necessary for completion of the study, it is important to recognize the ideal nature of this clinical scenario when extrapolating these findings to real-world patient populations. Additional studies which more accurately measure the NIA-AA criteria in typical clinical environments will undoubtedly be necessary.

Other studies have focused on evaluating the NIA-AA criteria with specific focus on the proposed incorporation of biomarkers as modifiers to the diagnosis of probable AD.^(275, 276) Recently, patient data obtained from the Alzheimer Disease Neuroimaging Initiative (ADNI), an ongoing, longitudinal, multi-center study designed to develop clinical, imaging, genetic, and biochemical biomarkers for the early detection and tracking of AD, was used to evaluate the NIA-

AA criteria. Two-hundred and eleven individuals with clinical data, PET or CSF amyloid biomarkers, and MRI or FDG-PET biomarkers for neuronal injury were selected in the final cohort. When using a requirement that subjects have a positive amyloid biomarker and single neuronal injury marker having an AD pattern, 87% (48% for both neuronal injury biomarkers) of the subjects could be categorized as “high probability” for AD according the NIA-AA criteria. However, in this supposedly pure cohort of AD, 10% of patients demonstrated no positive amyloid biomarkers (CSF or PIB-PET) and thus would receive a diagnosis of “dementia unlikely due to AD”.⁽²⁷⁶⁾ While these findings suggest that incorporation into the NIA-AA criteria does stratify a large proportion of subjects with AD, an appreciable minority of clinically categorized AD patients may also be excluded from the diagnosis of AD. Perhaps most troublingly, the study reveals a significant degree of inconsistency in biomarkers on a per-patient basis. For instance, in 37% of patients with confirmed AD pathology as assessed by CSF or PIB-PET, one biomarker for neuronal injury is positive while the other is negative.⁽²⁷⁶⁾ While reported under the context of evaluating the NIA-AA criteria, such findings undermine the diagnostic accuracy of biomarkers as a whole and therefore reflect poorly on the IWG criteria as well. Furthermore, inconsistencies in biomarker readout become even more troubling when they are weighted more heavily in the diagnostic assessment; such as in the evaluation of MCI where clinical symptoms are less pronounced.

Given that 10-15% of amnesic MCI patients progress to AD annually, one of the principal goals of the IWG and NIA-AA has been to generate guidelines capable of predicting the relative risk for convergence to AD among mixed MCI populations.⁽²⁵⁴⁾ Defined as a state of circumscribed anterograde long-term memory impairment with preserved general cognitive and social functioning, each set of guidelines take a distinct approach to the topic of mild cognitive impairment (MCI). Again differentiating itself from the other two sets of guidelines, the DSM-V does not attempt to assign an AD-specific pathological process to the clinical syndrome of MCI, which it classifies under the division “mild neurocognitive deficit”. Thus, the DSM-V criteria does not aid in risk stratification for progression to AD in cohorts of MCI patients. For this reason, no studies on the predictive value of the DSM-V are available. Instead, studies have focused on the degree of diagnostic concordance between the DSM-IV guidelines as compared to those recommended in the DSM-V. For example, in a cohort of 234 individuals with MCI, 85% received a concordant diagnosis of MCI using the DSM-IV and mild NCD using the DSM-V. Raising concern however, 40% of the subjects classified by the DSM-IV as mildly cognitively impaired were diagnosed with major NCD with operationalization of the DSM-V criteria.⁽²⁷⁷⁾ In summary, while the DSM-V performs similarly to previous versions when assessing for dementia (major NCD), these guidelines have a

tendency to over-report dementia in MCI cohorts. Moreover, as the DSM-V does not currently directly address the issue, only the IWG and NIA-AA criteria exist to aid researchers in discriminating between AD and non-AD causes of MCI. While numerous studies have investigated the predictive value of individual biomarkers in patient populations with MCI, fewer have operationalized either the IWG or NIA-AA guidelines in attempt to evaluate their diagnostic accuracy. In one of the best studies today with respect to patient sample size, 138 AD patients, 145 non-demented subjects, 78 patients with other dementias and 91 patients with mild cognitive impairment (MCI) were evaluated using the IWG guidelines. To accomplish this aim, the study operationalized the IWG criteria by combining clinical evaluation with objective episodic memory tests (MMSE & Visual Association Test). Additionally, the IWG's recommendation for "topographical biomarkers" was operationalized via MRI via assignment of a dichotomized medial temporal lobe atrophy (MTA) score. Similarly, dichotomized CSF profiles based on beta-amyloid1-42, tau, and phosphorylated tau at threonine 181 levels were used as "pathological biomarkers" in the study. The report details the positive (the probability of a person who has the disease testing positive divided by the probability of a person who does not have the disease testing positive) and negative (the probability of a person who has the disease testing negative divided by the probability of a person who does not have the disease testing negative) likelihood ratios obtained when applying the IWG criteria for prodromal AD in a MCI population.⁽²⁷⁸⁾ To the credit of the IWG, the new criteria predicted progression from MCI to AD better than objective memory tests alone (+LR=2.44, -LR=.33, +LR=1.75, -LR=.37, respectively). These likelihood ratios correspond to 69% specificity and 77% sensitivity for the IWG criteria, compared to 54% specificity and 80% sensitivity for objective memory tests alone. While these values again support the conclusion that the IWG criteria represent a major improvement in AD diagnostics, it should be noted that most studies of the IWG guidelines lack robust sample sizes; included the one discussed (N=62 MCI patients).

Providentially, larger studies investigating the diagnostic utility of the NIA-AA criteria in MCI populations are available for review.⁽²⁷⁹⁻²⁸²⁾ In congruence with its strategies in both preclinical AD and AD dementia, the NIA guidelines leverage biomarkers to stratify the diagnostic certainty associated with the "diagnosis of MCI due to AD". For example, a patient meeting the core clinical criteria for MCI due to AD but exhibiting negative "amyloid" and "neural injury" biomarkers would be assigned the qualified diagnosis "MCI unlikely due to AD". By comparison, a patient with MCI symptoms and a positive biomarker in either subdivision would be given the diagnosis of "MCI due to AD of intermediate likelihood". Logically, a patient with positive amyloid and neuronal injury biomarkers would be assigned the diagnosis of

“MCI due to AD of high certainty” under the NIA-AA guidelines.⁽²⁶³⁾ In summary of the work that has been done to validate the NIA-AA criteria for MCI due to AD, the vast majority of studies demonstrate increasing clinical severity and higher conversion rates to AD in the subgroups of higher diagnostic certainty.⁽²⁷⁹⁻²⁸¹⁾ For example, reports suggest that 4-14% of “MCI due to AD of low certainty” patients will progress to AD as compared to 50-80% of patients fulfilling the criteria for “MCI due to AD of high certainty”.^(279, 282)

With respect to a comparison of the relative sensitivity/specificity between the IWG and NIA-AA guidelines, a single study in a modestly sized cohort has been performed. Speaking generally, the IWG criteria for prodromal AD were found to be more sensitive but less specific as compared to the NIA-AA guidelines for the diagnosis of “MCI due to AD of intermediate likelihood”. Using the IWG criteria for prodromal AD, cognitive impairment plus positivity in at least one biomarker, a robust sensitivity of 100% was obtained.⁽²⁸⁰⁾ Expectedly however, a high degree of false positives were suffered as a consequence of this high sensitivity, with the IWG criteria for prodromal AD only achieving 36% specificity.⁽²⁸⁰⁾ By way of comparison, a specificity of 97% and sensitivity of 50% was obtained when the NIA-AA diagnostic criteria for “MCI due to AD of intermediate certainty” were employed. Predictably, when the NIA-AA criteria for “MCI due to AD of high certainty” were employed, requiring positivity in both divisions of biomarkers, specificity ranged from 45-69% while sensitivity improved to between 79-93% depending on the combination of biomarkers employed.⁽²⁸⁰⁾ Reviewing the data, it is clear that while the incorporation of a single biomarker for AD increases diagnostic sensitivity robustly, without a confirmatory marker, a high degree of false positives are to be expected. Using a dual-biomarker requirement, one to demonstrate neuronal injury and a second to demonstrate specific amyloid pathology, specificity is improved while sensitivity is reduced. Again, the predominant limitation hindering the incorporation of biomarkers into the clinical diagnostic setting seems to be the high degree of discordance between biomarkers of neuronal injury and AD specific pathology. Several explanations exist for this lack of concordance, especially in minimally symptomatic cohorts. Patients with positive AD pathology biomarkers but negative neuronal injury markers might not yet exhibit sufficient neurodegeneration to elicit symptoms. Conversely, patients with neuronal injury yet negative AD pathology biomarkers may harbor a neurodegenerative process distinct from AD or the heterogeneous nature of AD pathology may be too broad to be captured by only one test. Alternatively, the current generation of biomarkers may simply not be sensitive enough to faithfully detect AD pathology or neuronal injury early in the disease process. Further research and the development of second generation biomarkers will undoubtedly be necessary to overcome these

limitations. Notably this sentiment is echoed by the organizations that develop these guidelines, as both the IWG and NIA-AA limit the scope of biomarkers to the research setting.

As early-detection represents a key goal of AD research, other studies have evaluated the proposed preclinical definitions of AD formulated by the NIA-AA. By definition, preclinical AD refers to the stage of AD in which the molecular pathology of AD is already present in the brain but is not yet clinically expressed. Thus, preclinical AD criteria seek to stratify asymptomatic and cognitively normal individuals into groups which are predictive of clinical progression to AD. As stated in the NIA-AA's report, preclinical AD is defined by biomarker or genetic data and until further validation, is restricted to use in research. Despite this lack of clinical implementation, the preclinical guidelines formulated by the NIA-AA are arguably more important to the future of AD research than the clinically implemented criteria for probable/possible AD. This is because preclinical AD definitions are widely implemented in the recruitment of patients for early intervention strategies and for longitudinal study of people at risk. Again representing the most well studied preclinical AD criteria to date, the NIA-AA describe three stages of preclinical AD. Stage 1 is characterized by abnormal levels of A β which can be demonstrated by PET amyloid imaging or CSF A β levels. Stage 2 represents abnormal levels of A β in addition to brain neurodegeneration as evidenced by brain atrophy on structural MRI, abnormalities on [¹⁸F] fluorodeoxyglucose (FDG) PET, or elevated levels of CSF tau. Stage 3 includes the features of stage 2 as well as subtle cognitive changes. The order of the NIA-AA stages is meant to imply that the risk for cognitive impairment due to AD increases progressively across successive stages.⁽²⁸³⁾ In the first large study investigating the predictive value of the NIA-AA preclinical AD classifications, of the 296 initially normal subjects studied, 10% progressed to a diagnosis of mild cognitive impairment or dementia (27 amnesic MCI, 2 non-amnesic MCI, and 2 non-AD dementias) within 1 year. The proportion of subjects who progressed to MCI or dementia increased with advancing stage (stage 0, 5%; stage 1, 11%; stage 2, 21%; stage 3, 43%; test for trend, $p < 0.001$).⁽²⁸⁴⁾ Validating these findings, an independent group has reported that in initially cognitively normal cohorts 11%, 26%, and 56% of stage 1, 2, and 3 of preclinical AD patients, respectively, progress to symptomatic AD. Moreover, compared to individuals classed as normal at the beginning of the study, participants with preclinical AD as defined by the NIA-AA had an increased risk of death after adjustment for covariates (hazard ratio 6.2, 95% CI).⁽²⁸⁵⁾ Thus, in two independent studies, preclinical AD as defined by the NIA-AA guidelines may correlate with an increased risk of conversion to MCI or dementia.^(284, 285) Not surprisingly, the NIA-AA is not alone in their attempts to generate clinically predictive stages of preclinical AD. Indeed as

stated, due to the irreversible nature of neuronal damage, most researchers have focused on accurately diagnosing AD prior to the onset of symptoms as opposed to developing methods to confirm symptomatic pathology. While the NIA-AA definitions for preclinical AD have been the focus of many preliminary studies, organizations like the IWG have generated similar definitions of preclinical AD that also merit introduction. In comparison to the 3 stage model employed by the NIA-AA, the IWG distinguish between two patient groups. The first diagnosis, “asymptomatic at risk for AD”, refers to cognitively normal individuals with evidence of AD molecular pathology by laboratory or imaging biomarkers.⁽²⁸⁶⁾ As a consequence of being virtually equivalent to NIA-AA stage 1 preclinical AD criteria, not all subjects receiving a clinical assignment of “asymptomatic at risk for AD” are predicted to progress to AD. Rather than being predictive, these diagnostic categories are instead designed to highlight individuals at increased risk for progression to symptomatic AD. In contrast, the second IWG preclinical AD group termed “Pre-symptomatic AD”, refers to cognitively normal and asymptomatic carriers of a dominantly inherited gene mutation that causes AD. In contrast to all NIA-AA and IWG definitions of preclinical AD, individuals within the “Pre-symptomatic AD” group are certain to develop in individuals over the course of a normal lifespan.⁽²⁸⁶⁾

While the studies discussed focused on the predictive value of the NIA-AA criteria for preclinical AD, other groups have focused on the operationalization of the NIA-AA guidelines. In one such study, a group of 42 clinically diagnosed AD subjects were used to generate imaging biomarker thresholds for amyloid burden (PIB-PET) and neurodegeneration (hippocampal volume MRI) which facilitated a diagnostic sensitivity of 90%. Additionally, a control group of 450 cognitively normal adults was used to characterize the cognitive performance of their population-based sample. Using their established thresholds, the 450 cognitively normal adults were then stratified according to the NIA-AA guidelines for preclinical AD. In the cognitively normal cohort scoring in the bottom 10th percentile, 43% were classified as having no sign of AD/cognitive impairment. Of the remaining patients demonstrating subtle cognitive deficits, 16% were classified as stage 1, 12% stage 2, and 3% stage 3.⁽²⁷⁵⁾ Overall, only 3% of the population-based sample was unable to be classified using the NIA-AA guidelines operationalized with the group’s amyloid and cognitive performance thresholds. However, these figures include an additional classification group. Termed suspected non-AD pathophysiology (SNAP), this classification includes patients with normal amyloid PET imaging but abnormal neurodegeneration marker studies. Still, the study concludes that 97% of a population-based cohort is capable of being

stratified into NIA-AA stages of preclinical AD, suggesting the guidelines are generalizable enough to representative patient populations.

Summarizing the current state of diagnostic guidelines for AD, updated consensus criteria for the clinical diagnosis of AD include: the revised NICDS-ADRDA guidelines recommended by the NIA-AA, the DSM-V, and the IWG-2 criteria for AD. While these guidelines are good representations of AD diagnostic criteria as a whole, they by no means reflect the full complement of AD diagnostic criteria. Groups like the European Federation of Neurological Societies, European Neurological Societies, and Canadian Consensus on the Diagnosis and Treatment of Dementia have also published their own sets of guidelines, although they are generally similar to those discussed.^(287, 288) For example, all these updated diagnostic criteria for AD acknowledge the phenotypical heterogeneity of AD by generating specific guidelines for the identification of typical, atypical, and mixed forms of AD. Furthermore a subset of these guidelines, like those published by the IWG and NIA-AA, include criteria for preclinical states of AD and incorporate biomarkers into the diagnostic algorithm of AD in an effort to increase diagnostic accuracy. While the incorporation of biomarkers is arguably one of the greatest advancements made by modern diagnostic criteria, it also represents its greatest shortcoming as to date, no guidelines have published standards for each biomarker.^(271, 279) This in part may contribute to the widely ranging sensitivity/specificity data available for the current diagnostic guidelines for AD. Beyond the lack of biomarker standardization, our lack of knowledge with respect to the pathologic course of AD is also contributory to deficits in diagnostic accuracy. This is particularly true when attempting to identify AD in the preclinical stage, where there isn't even a consensus on whether there is a single sequence of events in the pathological cascade. At present, the limited cross-sectional and long-term follow up studies do not provide adequate data from which to draw a conclusion. Without question more work is warranted, as early diagnosis of AD and its distinction from other dementing disorders is crucial to implement effective treatment strategies and management of AD patients.

Table 2-1. DSM-5 Criteria for Major Neurocognitive Disorder

DSM-5 Criteria for Major Neurocognitive Disorder	
<ol style="list-style-type: none"> 1.) Evidence of significant cognitive decline from a previous level of performance in one or more cognitive domains <ol style="list-style-type: none"> a. Learning & memory b. Language c. Executive Function d. Complex attention e. Perceptual-motor f. Social cognition 2.) Cognitive deficits interfere with independence in everyday activities. At a minimum, assistance should be required with complex instrumental activities of daily living, such as paying bills or managing medications. 3.) Cognitive deficits do not occur exclusively in the context of a delirium 4.) The cognitive deficits are not better explained by another mental disorder 	

Table 2-2. NIA-AA Core Clinical Criteria for Probable AD

NIA-AA Core Clinical Criteria for Probable AD	
Neuropsychiatric Symptoms that:	
<ol style="list-style-type: none"> 1.) Interfere with ability to function at work or at usual activities 2.) Are not explained by delirium or major psychiatric disorder 3.) Cognitive impairment established by history-taking from the patient AND a knowledgeable informant in addition to objective bedside mental status examination 4.) Cognitive Impairment involving a minimum of two domains <ol style="list-style-type: none"> a. Impaired ability to acquire and remember new information b. Impaired reasoning and handling of complex tasks, poor judgment c. Impaired visuospatial abilities d. Impaired language functions e. Changes in personality, behavior, or comporment 5.) Insidious onset 6.) Clear-cut history of worsening symptoms 7.) Initial and most prominent deficits are in one of the following: <ol style="list-style-type: none"> a. Amnestic presentation: recent memory impairment b. Non-amnestic presentation: <ol style="list-style-type: none"> i. language impairment with prominent word-finding deficits ii. Visuospatial impairment with visual cognitive deficits iii. Dysexecutive presentation with prominent impairment of reasoning, judgment, or problem solving 8.) No evidence of substantial: <ol style="list-style-type: none"> a. Concomitant cerebrovascular disease b. Core features of Dementia with Lewy bodies c. Features of behavioral variant of frontotemporal dementia d. Features of semantic or nonfluent/agrammatic variants of primary progressive aphasia e. Other concurrent, active, neurological or non-neurological disease process or medication 	

Table 2-3. NIA-AA Core Clinical Criteria for Possible AD

NIA-AA Core Clinical Criteria for Possible AD	
I.	Atypical course – The core clinical criteria above are met in terms of the nature of the cognitive deficits, but there is either a sudden onset of cognitive impairment or insufficient historical detail or objective documentation of progressive decline.
II.	Etiologically mixed presentation – All of the core clinical criteria for AD dementia are met but the individual also has evidence of concomitant cerebrovascular disease, features of dementia with Lewy bodies other than the dementia itself, or evidence for another neurologic or medical comorbidity or medication that could have a substantial effect on cognition.

Table 2-4. IWG Definitions & Core Clinical Criteria

IWG Definitions & Core Clinical Criteria
<p>Mild cognitive impairment Variably defined but includes subjective memory or cognitive symptoms or both, objective memory or cognitive impairment or both, and generally unaffected activities of daily living; affected people do not meet currently accepted dementia or AD diagnostic criteria</p>
<p>Amnesic mild cognitive impairment A more specified term describing a subtype of mild cognitive impairment, in which there are subjective memory symptoms and objective memory impairment; other cognitive domains and activities of daily living are generally unaffected; affected people do not meet currently accepted dementia or AD diagnostic criteria</p>
<p>Preclinical AD The long asymptomatic period between the first brain lesions and the first appearance of symptoms and which concerns normal individuals that later fulfil AD diagnostic criteria</p>
<p>Prodromal AD The symptomatic prodementia phase of AD, generally included in the mild cognitive impairment category; this phase is characterized by symptoms not severe enough to meet currently accepted diagnostic criteria for AD</p>
<p>AD dementia The phase of AD where symptoms are sufficiently severe to meet currently accepted dementia and AD diagnostic criteria</p>

2.3.3 *Differential Diagnosis*

While refined diagnostic criteria, the inclusion of biomarker technology, and the undeniable increase in AD awareness within the medical, research, and public forums are all causes of celebration within the AD community, these trends likely represent a double-edged sword. This is because as the heterogeneity of AD presentations becomes increasingly well recognized, alternative medical conditions included in the differential diagnosis of AD may be increasingly overshadowed. In fact, in a meta-analysis of 39 studies describing 5620 individuals with dementia-like symptoms, 9% were found to have a non-dementia etiology.⁽²⁸⁹⁾ The sobering message of such findings is made clear when considering that unlike AD, a large proportion of these non-dementia causes of cognitive impairment have robust medical treatments.

While AD is by far the most likely cause of dementia, representing between 60-80% of cases, a number of alternative forms of dementia may closely mimic the presentation of AD.⁽²⁹⁰⁾ Furthermore, less than 50% of all cases of AD dementia reflect an AD pathophysiological process in isolation. Instead, in the majority of cases of dementia due to AD, the pathophysiological hallmarks of AD coincide with patterns of neurodegeneration associated with other forms of dementia. Termed, “mixed dementias”, AD with vascular dementia, AD with DLB, and AD with vascular dementia and DLB constitute the most frequently encountered dual-etiology of dementia, in that order. In addition to being the most common form of comorbid dementia with respect to AD, vascular dementia (VaD) is also the second most common independent form of dementia after AD, representing 10-20 percent of cases in North America and Europe.^(291, 292) Like AD, both incidence and prevalence demonstrate a robust positive correlation with advancing age.⁽²⁹³⁾ Worthy of note however, differences in screening methods and a lack of standardized diagnostic criteria have led to substantial variability in the reported prevalence and incidence of VaD. In fact, no standardized clinical criteria for VaD have been widely-adopted and some investigators have suggested that VaD should not be classified as a dementia at all due to the lack of early presenting memory deficits.⁽²⁹⁴⁻²⁹⁶⁾ Still, studies estimate VaD prevalence to be between 1.2 - 4.2 percent of individuals and report age-adjusted incident rates of 6 to 12 cases per 1000 person years in individuals over the age of 65 and 70 years, respectively.^(291, 297) Thus, as a consequence of its high incidence/prevalence, differentiating VaD from AD represents a common clinical dilemma. At the foundation of the difficulties associated with accurately diagnosing, and estimating the relative health burden of VaD, is the fact that cerebrovascular disease is itself a heterogeneous disorder.

Thus, like FTD discussed later, VaD represents a heterogeneous clinical syndrome rather than a distinct etiology of dementia. Instead, VaD encompasses all pathophysiologic processes attributable to cerebrovascular disease which in some form ultimately manifest as deficits in cognition. However, this is not to say that the pathophysiology of VaD is completely unknown. To the contrary, researchers have discovered that at least three common pathological entities are thought to underlie the deficits observed in VaD.⁽²³⁶⁾ The first and most injurious of these pathological entities involves the infarction of large, principally cortical, but occasionally subcortical, arteries. The second etiology involves infarction of small arteries to form lacunes. Exclusively subcortical, these small arteries include branches of the large arteries emanating off the circle of Willis, and middle cerebral, and basilar arteries.^(298, 299) The sequela of this small-vessel disease is very common, with incidence rates in of micro-infarcts ranging from 26 - 52 individuals per 100,000 population in community-based cohorts.⁽³⁰⁰⁻³⁰²⁾ Furthermore, estimates of the frequency of one or more detectable micro-infarcts range from 16% to 46% in unselected elderly persons dying of all causes, with micro-infarcts being detected in 33% of cognitively normal elderly dying of all causes.⁽³⁰³⁾ Completing the triad of known pathogenic processes underlying VaD, chronic subcortical ischemia can lead to the development of cognitive deficits in the setting of small-vessel disease not sufficiently localized to produce overt micro-infarction. Most commonly, this chronic subcortical ischemia occurs in the distribution of small arteries in the periventricular white matter and affects each constituent of the CNS depending on their selective vulnerability. Put differently, chronic ischemia leads to a pattern of neurodegeneration determined by the specific vulnerability of each cell population; with preliminary losses in neuronal tissues being followed by the death/degeneration of oligodendrocytes, myelinated axons, astrocytes, and endothelial cells.⁽³⁰⁴⁾ Mechanistically, the term micro-infarcts is somewhat miss-leading, as embolization in the small penetrating arteries that perfuse the periventricular white matter or non-cortical gray matter has yet to be pathologically confirmed. Instead, small vessel disease is most commonly attributable to lipohyalinosis or microatheroma formation secondary to chronic hypertension; as evidenced by the decreasing prevalence of these lesions in the setting of properly managed hypertension.^(305, 306) This mechanistic distinction is of significance when ascribing the underlying etiology of observed micro-infarcts to either VaD or AD, as the latter can mimic the former due its high coincidence with cerebral amyloid angiopathy (CAA), the accumulation of amyloid in cerebral vessels. Not only can AD with CAA mimic lacunar pathology, but extensive CAA in AD can also mimic the ischemic white matter damage typically associated with VaD by diffusely narrowing the penetrating cortical vessels with amyloid deposits.^(307, 308) Given the already diverse pathology of VaD, it is not surprising that the clinical

manifestations of vascular dementia (VaD) are diverse and thus overlap tremendously with AD. Also as expected, the pattern of cognitive deficits is highly dependent on the brain regions burdened by pathology. Though pathologically diverse, investigators currently recognize two clinical of VaD.

With respect to prevalence in the United States, the second most common pure neurodegenerative dementia after AD is likely dementia with Lewy bodies (DLB). This statement is only conjecture however, as accurately reporting the epidemiological impact of DLB is limited by medicine's current inability to accurately diagnose DLB clinically or even differentiate its etiology from other dementias. Although the symptomology of DLB can be similar to AD in many ways, a majority of individuals with DLB are more likely to present with prominent visual hallucinations, parkinsonism, cognitive fluctuations, dysautonomia, sleep disorders, and neuroleptic sensitivity. Unlike typical AD, these features, as well as early visuospatial impairment, may even occur in the absence of significant memory impairment. Notably, these symptomatic differences between AD and DLB reflect the contrasting etiologies of the diseases' and correlate with the differential sites of neurodegeneration in the brain associated with each condition. For example, the tendency for DLB patients to present with parkinsonian movement features earlier in the disease course as compared to AD, reflects the predisposition for alpha-synuclein aggregation in the substantia nigra in DLB. Interestingly, these aggregates of alpha-synuclein, referred to as Lewy Bodies, are not unique to DLB but are also found in Parkinson's disease. However, while people with DLB and PD both have Lewy bodies, the onset of the disease is marked by motor impairment in PD and cognitive impairment in DLB. However, especially in late-stage PD, dementia is common, although the incidence of dementia due to PD is about one-tenth that of AD. Troublingly, the differentiation of Parkinson disease dementia and DLB is so arbitrary; a "one-year rule" which has been shown not to correlate with pathological etiology is still employed.^(309, 310) Generally speaking, this "one-year rule" holds that in PDD, dementia occurs in the setting of well-established parkinsonism, while in DLB, dementia usually occurs concomitantly with or before the development of parkinsonian signs. Thus, if parkinsonism is present for more than one year before the onset of dementia, it is officially classified as PDD. Contributing to the diagnostic uncertainty which plagues dementia in general, dementia due to PD may result from a mix of AD and DLB pathological processes as Lewy bodies, A β plaques, and neurofibrillary tangles are all observed in PD brains. Thus, with even the pathological lesions not cleanly segregated between forms of dementia, it is not surprising that distinguishing between phenotypes of dementia clinically remains one of the paramount challenges in medicine.

Denoting more of a heterogeneous group of clinical syndromes than a specific neurodegenerative disease, the definition of frontotemporal lobar dementia (FTD) has evolved over time and currently serves as an umbrella term for three clinical presentations: behavioral variant FTD (bvFTD) and two forms of primary progressive aphasia (PPA), specifically, the non-fluent and semantic variants. Poetically alluding to the clinical similarities of AD and FTD, Alois Alzheimer characterized the first reported case of PPA and dubbed the disorder Pick disease due to the distinctive round, silver-staining inclusions he termed Pick bodies upon histological examination of the patient's brain tissue.⁽³¹¹⁾ Subsequent clinic-pathological studies determined that many patients diagnosed clinically with Pick disease did not have Pick neuropathology at autopsy, and thus Pick disease now designates a pathological diagnosis, rather than a clinical syndrome. Further reflecting the lack of correlation between the clinical syndromes of FTD and underlying pathophysiology, the distinct term frontotemporal lobar degeneration (FTLD) denotes the distinct pathological processes which underlie the clinical syndromes of FTD. Three main histological subtypes of FTLD have been characterized: FTLD-tau, FTLD-TDP, and FTLD-FUS. FTLD-tau is characterized by tau positive inclusions often referred to as Pick-bodies while FTLD-TDP is characterized by ubiquitin and TDP-43 positive, tau negative, FUS negative inclusions. Lastly, FTLD-FUS is characterized by fused in sarcoma RNA-binding protein (FUS) positive cytoplasmic inclusions, intra-nuclear inclusions, and neuritic threads. While the relative prevalence of each of these FTLD subtypes is not well-studied, one report suggests that FTLD-TDP represents 48.5% of FTD cases while FTLD lacking distinctive histopathological features (18.2%) and Pick disease (15.2%) constitute the next two most common neuropathological diagnoses.⁽³¹²⁾ Notably, these lesions display a characteristic pattern of distribution in the cortex, medulla, hippocampus, and motor cells of the spinal cord and XIIth cranial nerve in each of the clinical syndromes of FTD. Again, as in AD and DLB, the initial presenting symptoms of the three FTD variants reflect the pattern of neurodegeneration with respect to brain regions. For example, neuroimaging studies have correlated increasing tissue atrophy in the right ventromedial superior frontal gyrus, right subgenual cingulate gyrus of the ventromedial prefrontal cortex, and right dorsal ACC and left premotor cortex, with worsening apathy, disinhibition and aberrant motor behavior, respectively.^(313, 314) Thus, in the case of bvFTD, which typically presents with disinhibition, apathy/less of empathy, hyper-orality, and compulsive/ritualistic behaviors, the afore mentioned brain regions are most robustly affected. With respect to its contribution to the diagnostic uncertainty surrounding AD, patients with early-onset AD are frequently misdiagnosed with bvFTD and vice versa. This is principally due to AD patients often performing poorly on measures of executive function. Still, symptomatic differences exist, with

AD patients often retaining social cognitive faculties until late in the disease process and having more robust deficits in episodic memory and visuospatial skills than do patients with bvFTD. Although important in differentiating bvFTD from AD, these subtle differences in clinical presentation become of even greater importance when considering the differential of AD versus PPA. Characterized by the insidious onset and gradual progression of aphasia, PPA manifests itself symptomatically as deficits in word finding, word usage, word comprehension, or sentence construction, the only notable clinic difference between PPA and a typically presenting AD patient is the absence of memory impairment in PPA.⁽²⁴⁴⁾ In the context of atypical presentations of AD in which clinically detectable deficits in language outweigh observed deficits in memory impairment, it is easy to see why FTD syndromes constitute a major source of misdiagnosed cases of AD. Further muddling the differentiation of AD versus FTD, although characterized by isolated language impairment early in the disease course other cognitive faculties are frequently reduced in FTD as the disease progresses. Like bvFTD and all other forms of neurodegeneration discussed, the symptoms of PPA correlate best with neurodegeneration to specific brain regions, in the case of FTD the language-dominant hemisphere of the brain, as opposed to with a specific underlying pathophysiologic process. At a group level, three clinical variants of PPA have been described and have been loosely affiliated, with limited clinical value, to different underlying neuropathologies. The first of these clinical PPA variants, termed non-fluent PPA, is most commonly associated with the FTLT-tau pathophysiology.⁽²⁴¹⁾ In contrast, FTLT-TDP pathology most commonly underlies the semantic variant of PPA.⁽²³⁴⁾ Lastly, the logopenic variant of PPA, most typically associated with AD pathology, is characterized by impaired single-word retrieval and repetition with errors in speech and naming but with spared single-word comprehension, object knowledge, motor speech, and absence of agrammatism.⁽²³⁴⁾ Interestingly, though mimicking AD pathology in most ways, hemispheric asymmetry distribution of neurofibrillary tangles distinguishes the logopenic variant PPA from typical AD.^(240, 315) While differences in NFT distribution are not yet clinically utilized to distinguish between logopenic PPA and AD, the symptoms of all FTLT typically manifest earlier in life as compared to AD, with the average age of onset for FTLT and AD being 60 and 65 years old, respectively. Similarly, reports have concluded that FTD progresses more rapidly than AD.⁽³¹⁶⁾ Not surprisingly, this 5 year differential in age of onset nor subtle differences in initial presentation have proven sufficient to reliably distinguish between AD and FTD syndromes and thus, a strong push towards the development of biomarkers for both diseases has been a priority in both fields over the past two-decades. The significance of this clinical dilemma carries ever more significance when considering that the differential between AD and FTD is not purely academic, with current guidelines advising against the

use of cholinesterase inhibitors in FTD. Importantly however, treatment trials with any form of medications, including cholinesterase inhibitors, are not reasonable in the context of robust diagnostic uncertainty. For this reason, questions surrounding the therapeutic management of different forms of dementia are highly prevalent among clinical forums.

As a consequence of their long incubation periods and inexorable progression, prion diseases represent yet another class of dementia causing conditions included in the differential of AD. Representing more than 90% of all cases of prion disease, Creutzfeldt-Jakob disease manifests itself symptomatically as impairments in memory and coordination as well as changes in behavior. Pathologically, human prion diseases such as CJD are associated with common neuropathological features including: neuronal loss (especially in cortical layers III-V), proliferation of glial cells, absence of an inflammatory response, and the presence of small vacuoles (20-30 microns) within the neuropil which produce a spongiform appearance. As in all human prion diseases, these profound neuropathological changes are the result of an accumulation of aberrantly folded proteins. Unlike their non-pathogenic counterparts, prion proteins exhibit multiple structurally diverse conformations, of which at least one is transmissible to other prion proteins.⁽³¹⁷⁾ Like AD patients, the brains of CJD patients may display appear atrophic and exhibit signs of ventricular enlargement. However as with other forms of dementia, the pattern of atrophy is in some ways distinct when compared to AD. Atrophy in CJD may include the deep gray structures: the caudate, putamen, and thalamus, but in contrast to AD typically spares the hippocampus. Conversely, robust cerebellar degeneration is not typical of AD, yet is atrophy of the folia due to loss of gray matter is common in CJD. Although variants of CJD have been defined, sporadic CJD represents 85-95% of cases and is associated with two cardinal clinical manifestations, namely a rapidly progressive mental deterioration with frequent behavioral abnormalities and myoclonus.^(318, 319) Notably, while myoclonus and a rapidly progressive course are not typical of AD, the diverse range of presentations of AD and CJD, coupled with the possibility of atypical presentations for AD, currently generates significant diagnostic uncertainty when distinguishing between the two etiologies.^(320, 321) For example, one study found that 58% of AD patients also meet clinical criteria for CJD. Critics of these types of studies might argue that sensitive and specific biomarkers for CJD should alleviate this diagnostic uncertainty. However, in this same study, approximately 10% of AD patients (2/19) presented with diagnostically significant levels of 14-3-3 protein, a biomarker for CJD, in their CSF.⁽³²⁰⁾ Thus, neither clinical criteria nor biomarker studies are currently sufficient to distinguish between AD and CJD in all cases. In addition to its similar symptomology, Creutzfeldt-Jakob disease afflicts a similar patient demographic as AD, with a typical age of onset between 57 and 62 and rarely reported cases of disease in

young adults or individuals over the age of 80.^(319, 322-325) Despite the symptomatic and demographic overlap between AD and CJD, clinically, this dilemma is rarely played out, as the incidence of sporadic Creutzfeldt-Jakob disease is approximately one case per 1,000,000 population per year. Unfortunately there is no effective treatment for CJD, with death usually occurring within one year of symptom onset with a median disease duration of six months.^(317, 326, 327)

As a consequence of its treatable nature, normal pressure hydrocephalus (NPH) in particular represents an essential consideration in the diagnostic workup of AD. Manifesting itself clinically as the classical triad of difficulty walking, memory loss and urinary incontinence, dementia attributable to normal pressure hydrocephalus is caused by chronically sustained local elevations in CSF pressure at the periventricular white matter secondary to impaired reabsorption. Produced by the choroid plexus in the lateral ventricles, CSF flows next to the third and fourth ventricles before reaching the basal cisterns, tentorium, and subarachnoid space over the cerebral convexities to the area of the sagittal sinus. Under normal conditions, CSF is absorbed into the systemic circulation primarily across the arachnoid villi into the venous channels of the sagittal sinus. As stated, impaired absorption of CSF across the arachnoid villi is the suspected mechanism of most cases of secondary NPH. Most commonly, this is due to intra-ventricular/subarachnoid hemorrhage or prior acute or chronic meningitis of any etiology. However, Paget disease, mucopolysaccharidosis of the meninges and Achondroplasia all constitute other rarely reported causes of NPH. These conditions impair reabsorption of CSF by inciting inflammation and subsequent fibrosis of the arachnoid granulations, although alternative mechanisms have been proposed. Nevertheless, in approximately half of all patients, leptomeningeal biopsy reveals evidence of arachnoid fibrosis.^(328, 329) Decreased CSF resorption leads to gradual accumulation of CSF within the ventricular system, which manifests as increased local pressure. While increased pressure is not measured on lumbar puncture, a pressure effect is nonetheless believed to occur locally on periventricular white matter tracts, producing the observed dilatation of the lateral ventricles which is pathognomonic for NPH. With respect to differentiating NPH from AD, while both classically present with cognitive deficits, gait abnormalities and urinary incontinence are more typical of NPH. However, when considering the prevalence of gait abnormalities in the elderly demographic most at risk for AD, reported by one study to be as high as 56% of individuals over the age of 70, gait abnormalities may frequently coexist with AD.⁽³³⁰⁾ Similarly, urinary incontinence from other causes such as prostatism or stress incontinence may frequently coexist with AD due to its high prevalence in elderly populations. In one study investigating the prevalence of urinary incontinence in the patient demographic older than 70 years of age, 12 percent of men and 36 percent of women were reported to exhibit

clinically observable symptoms.⁽³³¹⁾ Again reflecting the differences in the underlying neuronal insult between AD and NPH, prominent dementia, especially when it includes cortical features (aphasia, apraxia), strongly suggests AD as an alternative or comorbid diagnosis in a patient with suspected NPH. A guideline undoubtedly justified by the restricted nature of CSF elevations, and thus neuronal insult, to the periventricular white matter in NPH as opposed to the cortical neurodegeneration typical of AD. However, further compounding the diagnostic uncertainty when distinguishing between AD and NPH, as with virtually all forms of dementia, NPH can coexist with other dementias, and in particular AD.^(328, 332-334) In studies of patients with strong clinical and laboratory evidence of NPH, biopsies carried out at the time of shunting reveal AD pathology in 20 to 61 percent.^(328, 333-337) Two series have found that the degree of AD pathology correlated with the degree of cognitive impairment.^(334, 336) Uniquely, normal pressure hydrocephalus can often be corrected with surgical installation of a shunt to drain excess CSF, making it one of the few treatable etiologies of dementia. Critically, distinguishing between NPH, AD, and NPH with AD may carry implications for the response to treatment, as NPH patients with underlying AD typically demonstrate no improvement following CSF shunting.

2.3.4 Clinical Evaluation Strategy

Both NIA-AA and equally used DSM-V clinical criteria highlight the importance of the history of present illness when assessing a presenting patient for AD. Throughout the clinical interview, careful observation to the patient's attention, speed of responses, and ability to provide relevant information can be crucial in raising diagnostic suspicion. Critical information to garner during the interview includes the patient's age, education level, pre-morbid function, medical history, and current prescriptions. Additionally, more so than in other illnesses input from family members is an indispensable asset to the physician. Using either guideline, diagnostic suspicion for AD arises principally on documentation of significant impairment in more than one cognitive domain. Notably, a "significant impairment", must represent a change from the patient's baseline and be of sufficient severity to impair his/her independence. In the DMS-V, the cognitive domains are segregated into: learning and memory, language, executive function, complex attention, perceptual-motor, and social cognition. Translated to a complete assessment of mental status in the clinic, physicians should note deficits in: level of consciousness, attention, memory, language, visual spatial perception, executive function, mood and thought content, praxis, and calculations. Level of consciousness or arousal is typically subjectively evaluated and patients can be stratified into alert, attentive, sleepy, or unresponsive. Assessment of attention is critical, as a deficit in

this domain can confound additional testing. Deficits in attention can be elucidated either in the course of the clinical interview or via testing through exams such as the digit span test.^(338, 339) Here the examiner recites numerical digits at a rate of one per second and asks the patient to repeat back the number sequence. Regardless of age or education level, cognitively normal individuals can recite a 5-9 numerical sequence.⁽³⁴⁰⁾ If more subtle deficits in attention are suspected, increasingly complex attentional tasks such as the trail-making test, symbol-copying tasks, and letter-cancellation tasks can be employed.^(338, 341-343) Evaluation of memory in a suspected AD patient should, at minimum, distinguish between impairments in immediate/working memory, recent memory, and retrieval of remote memories. While the digit span test used to assess attention is sufficient to probe working memory, tests of recent memory involve asking the patient to remember 3-4 words and then recite those words 5-10 minutes into the interview once their attention has been shifted. The proctor may issue categorical cues to aid in the retrieval of words, with cognitively intact individuals being capable of recalling 3-8 words.⁽³⁴⁰⁾ Prompting the patient to recall the names of past presidents or recall important historical events is suitable for preliminary probing of long-term memory. Predictably, language deficits are most often noticed during the clinical interview and perceived deficits can be probed via a variety of tests. Commonly, deficits in categorical fluency can be assessed by asking the patient to recite at least 15 words in a particular category (i.e. animals) within a minute, while letter fluency can be assessed by asking patients to recite the same number of words beginning with a particular letter (commonly “F”).⁽¹⁷⁹⁾ In contrast to the necessity of objective behavioral tasks for the evaluation of deficits in memory, it is generally agreed upon that information garnered during the clinical interview is the most appropriate method for documenting impairment in executive function. If not relayed as a problem by the patient, executive function can be probed by asking the patient to describe their probable course of action during an imagined emergency.⁽³⁴²⁾ Alternatively, standardized tests for the 5 domains of executive function including: working memory (serial reverse tasks), verbal fluency (categorical/letter fluency tests), motor programming (Luria fist-edge palm test), response inhibition (go/no go tests), and ability to divide attention (Wisconsin Card Sorting Test) are available.⁽³⁴³⁻³⁴⁵⁾ Clinical evaluation of affect should focus firstly on any abnormal intrusions, preoccupations, perseverations, delusions, or hallucinations as these neuropsychological symptoms best differentiate AD from non-AD causes of dementia.^(190, 193) Additionally, evaluation for depression both in the clinical interview and via standardized batteries such as the Beck Depression Inventory, Geriatric Depression Scale, or Neuropsychiatric Inventory is high yield as up to 40% of AD patients are estimated to harbor an underlying depression.⁽¹⁸⁷⁾ Visuospatial abnormalities can be suggested via patient report of misplacing items with

increased frequency or difficulty navigating unfamiliar terrain. Neurological assessment typically differentiates between perceptual and constructional visuospatial functions. Perceptual function is probed by prompting the patient to draw copies of geometric visual stimuli such as overlapping pentagons.^(182, 340) In contrast, constructional visuospatial function is assessed most commonly via building/assembly tasks with patients asking to construct structures from blocks.⁽³⁴⁰⁾ The evaluation of praxis, defined as impairment in the performance of learned motor activities in the absence of primary motor/spatial deficits, manifests symptomatically as difficulty dressing, feeding, or bathing during the clinical interview. Asking the patient to demonstrate these everyday yet complex learned movements is an ideal way to elucidate deficits during the preliminary evaluation of AD. Lastly, deficits in mathematical calculation are rapidly assessed via the “serial sevens test”, in which patients are asked to sequentially subtract 7 from 100 and recite the difference. Of note, this test must be evaluated in the context of patient’s education level, attention, and anxiety in order to be of diagnostic significance. Two or more deficits in these domains, in the setting of an insidious onset and in the absence of alternative etiologies, should generally prompt the physician to conduct a detailed cognitive and neurological physical evaluation for AD.

In clinical practice, routine independent testing of each of these cognitive domains is impractical. Thus, perceived deficits obtained from the patient history is most often coupled with standardized neuropsychological batteries, most commonly the Mini-Mental State Examination (MMSE), to test for the presence or progression of AD.^(346, 347) Encompassing a broad range of cognitive abilities including: orientation, recall, attention, calculation, language manipulation, and constructional praxis, the MMSE takes minutes complete making it highly compatible with clinical implementation.⁽³⁴⁶⁾ Based on a maximum score of 30 points, a score of less than 24 points is suggestive of dementia or delirium, although the exam is easily confounded by age, education, as well as language, motor, and visual impairments.⁽³⁴⁸⁾ Improvements in the interpretation of the MMSE have been reported, with age-specific norms as well as studies of MMSE scores as a function of education being reported.⁽³⁴⁹⁾ Still, in a large community population study of 18,056 individuals, a reported sensitivity and specificity of the MMSE for accurately detecting dementia was 87%, and 82% respectively.⁽³⁴⁹⁾ Especially when utilized to evaluate the possibility of AD, in addition to a patients overall score, the pattern of point deductions in the MMSE can be of significance. Especially early in the disease course, the cognitive domain of memory may be the only faculty affected. As the MMSE contains two tasks that evaluate memory, the three object naming and delayed recall tests, a patient with mild AD might score zero points on these exams and present with a

“normal” score of 27. Thus, a failure to look specifically for common deficits in the MMSE may contribute to false-negatives, especially in early-stage AD.

Further limiting the diagnostic utility of the MMSE with respect to tracking progression of AD as opposed to establishing a new diagnosis, changes of 2 or less points on the MMSE may represent measurement error, regression to the mean, or a practice effect and are thus of uncertain diagnostic significance.⁽³⁵⁰⁾ Instead, the Clinical Dementia Rating (CDR) scale, designed specifically to measure the severity of AD in a longitudinal manner, is the preferred cognitive test. Conducted as a semi-structured interview with the patient and/or caregiver, impairments in the domains of memory, orientation, judgement, community affairs, home and hobbies, as well as personal care are assessed. The severity of AD is binned as absent, questionable, mild, moderate, or severe. Although designed for implementation in clinical trials and longitudinal studies of AD, the CDR is increasingly utilized in clinical decision making models to assess a patient’s ability to live independently. For example, the CDR can be an objective tool in assessing whether an AD patient’s symptoms are severe enough to warrant placement in a skilled nursing facility or if his/her driver’s license should be revoked. Despite CDR examinations taking upwards of 3 hours to complete, studies have reported strong validity and an inter-rater reliability of 62-83% in well-controlled settings.⁽³⁵¹⁻³⁵³⁾

Physical examination in a patient with suspected AD focuses primarily on ruling out an atypical presentation of a medical illness and a detailed neurological assessment which seeks to identify focal neurological deficits. Specifically, focal sensory-motor neurological deficits suggestive of prior stroke, signs of Parkinson’s disease such as cogwheel rigidity, tremors, gait abnormalities, and abnormal eye movements should be assessed to help exclude alternative diagnoses. Noted specifically in both NIA-AA and DSM-V criteria, the exclusion of delirium is a fundamental component of AD diagnosis. Differentiating between dementia and delirium relies heavily on patient history and repeated assessment of his/her cognitive faculties (Table 2-5). From these longitudinal assessments, dementia and delirium can often be distinguished based on symptom onset, course, duration, and presence or absence of changes in perception or sleep.⁽³⁵⁴⁾ However, especially in the absence of a complete longitudinal history, this exclusion can be difficult. To alleviate this diagnostic burden, the Confusion Assessment Method and Memorial Delirium Assessment scale have been developed and are well validated in their ability to detect delirium.⁽³⁵⁴⁾ In general, both methods require an acute onset of changes or fluctuations in the mental status and attention in the patient, as well as an altered level of consciousness or disorganized

thinking. With an appropriate H&P decreasing the likelihood of alternative forms of dementia, additional laboratory tests can help exclude atypical presentations of common medical illnesses.

Table 2-5. Dementia versus Delirium

Dementia versus Delirium⁽³⁵⁴⁾		
Features	Delirium	Dementia
Onset	Acute	Insidious
Course	Fluctuating	Stable Decline
Duration	Hours to Weeks	Months to Years
Perception	Hallucinations	Normal
Sleep/Wake	Disrupted	Fragmented
Attention	Fluctuates	Normal

CHAPTER 3 EPIDEMIOLOGY OF ALZHEIMER'S DISEASE

3.1 CURRENT & PROJECTED ESTIMATES OF DISEASE BURDEN

Representing the most common cause of senile dementia, Alzheimer's disease (AD) is a neurodegenerative disorder of age-dependent onset characterized by an inexorable and progressive perturbation of cognitive function which invariably leads to a loss of independence and ultimately death. In an effort to convey the magnitude of this disease's current and future impact on global health, it is best to systematically analyze each component of this introductory statement. Firstly, elaborating on the reference made to AD's unrivaled prevalence, as of 2014 AD accounts for 60–80% of all cases of senile dementia.⁽²⁹⁰⁾ To place this statistic in perspective, more than 5 million Americans suffer from this disease while more than 36 million individuals are estimated to be afflicted worldwide.⁽³⁵⁵⁾ Looking forward to the future, conservative projections estimate that an astonishing 66 million people will be living with AD by 2030. With the prevalence of AD continuing to double approximately every 20 years, this forecasts the worldwide health burden attributable to AD at 115 million individuals by the year 2050.⁽³⁵⁵⁾ Expectedly, this relatively short doubling rate for AD prevalence is suggestive of an equally astonishing incidence, with just under half a million Americans developing AD in 2014 alone. Like projections for AD prevalence, future rates of AD incidence are exceptionally morbid. Assuming a historical perspective for the sake of clarity, the incidence of AD in 2000 was estimated at 411,000 new cases. A decade later, this statistic had risen by 10% to an annual incidence of 454,000 new cases in 2010.⁽²⁵⁰⁾ However by 2050, an estimated 959,000 new cases of AD are projected to be reported in the U.S. alone, a 130% increase from the year 2000. Similarly, barring the development of medical breakthroughs to prevent AD, U.S. AD prevalence is expected to triple from the current 5 million cases to nearly 14-16 million cases by 2050.⁽³⁵⁶⁾ As alluded to by the “age-dependent” qualifier used in the introductory sentence, the estimates of AD prevalence and incidence described above are both disproportionately comprised of elderly individuals. Breaking the 500,000 new cases of AD in 2014 down by age, only 59,000 of these cases afflict individuals below the age 75 as compared to the 172,000 and 238,000 cases involving individuals below and over the age of 85, respectively.⁽²⁵⁰⁾ Similar trends in AD prevalence are observed with 1 in 9 individuals over the age of 65 and 1 in 3 individuals over the age of 85 having AD in the U.S.⁽³⁵⁶⁾ In the face of such

jarring epidemiological statistics, the intuitive question becomes “what factors drive the projected increases in AD incidence and prevalence?” While a variety of variables have been identified, the predominant answer in the field references the phenomenon of demographic aging occurring both in the U.S. and worldwide. Generally speaking, this term refers the rising proportion of individuals over the age of 65 in the population. Speaking to the specific case of the U.S., two variables predominantly explain this increase in the elderly population; aging of the baby boomers and extended life expectancy.

Inarguably one of the great achievements of mankind, the average adult lifespan continues to extend within the context of ever improving medical technologies. Over 5 decades ago, average life expectancy was 65 in developed regions and only 42 years in less developed regions of the globe. Today, the average adult can expect to live to 78 years of age in the developed world and 68 years of age in more rural regions.⁽³⁵⁷⁾ Importantly, review of this data suggests the gap between more modern nations and the less developed world is narrowing, which explains why demographic aging is occurring more quickly in these rural countries. Forecasting life expectancy into the year 2050, the average citizen will live to be 83 and 75 years of age in the developed and developing world, respectively.⁽³⁵⁷⁾ While these numbers are interesting they do not directly convey the relevance of an ageing population to AD. To accomplish this, we need to analyze these data in a slightly different manner. Recalling that the average age of onset is between 60-65 years of age, this specific population of elderly individuals represents the main demographic at risk for AD. Assuming no prophylactic treatment options are discovered for AD, the proportion of at risk individuals in this elderly population who will go on to develop AD is unlikely to change significantly. Thus, both the prevalence and incidence of AD are expected to increase proportionally to the number of individuals in the at risk elderly demographic. When looking at the figures for individuals over the age of 65 worldwide, this number has risen from 202 million in 1950 to over 841 million in 2013. Projecting these trends to the year 2050, 1.6 billion people or 32% of the projected world population will be at highest risk for AD.⁽³⁵⁷⁾ Of equal importance, 80% of these individuals will live in less developed regions.⁽³⁵⁷⁾ Of significance, these statistics indicate that any future diagnostic/therapeutic option must not be prohibitively expensive or methodologically complex in order to adequately address the epidemic of AD worldwide.

While longer life-expectancies represent a global phenomenon, the elderly population spike in the U.S. has a second contributing factor of significance; the aging of the baby boomer generation. Describing those individuals born

between 1946 and 1964, during the post-world war II era, over 78.3 million Americans were born over this time period. During this pan-demographic period of prolific reproduction, the number of annual births in the U.S. exceeded 2 children per 100 women for the first time in decades. Relating this to AD epidemiology, as of 2011, the first individuals of this generation have reached age 65, AD's typical age of onset.⁽³⁵⁸⁾ As a consequence of the full cohort of baby-boomers reaching AD's age of onset, the future health burden of AD is daunting with its prevalence projected to reach 65.7 million people by 2030. However, the impact of the baby-boomers does not end here, as their children, termed the millennium generation, will also produce a less dramatic "echo baby boom". While the implications of these projections are admittedly abstract, cumulatively they convey the message that while AD represents a significant public health concern currently, its associated disease burden will reach epidemic proportions in the coming decades.

Having communicated the message that AD represents an increasingly common global health threat, we next focus on statistics which convey the humanitarian and economic cost associated with AD. In congruence with other subtypes of dementia, mortality is often secondary to terminal-stage complications related to advanced patient debilitation. Thus, dehydration, malnutrition, and infection are among the most common causes of mortality in patients suffering from AD, with pneumonia reported to be the most frequently identified cause of death.⁽³⁵⁹⁻³⁶³⁾ Notably, while the World Health Organization defines cause of death as "the disease or injury which initiated the train of events leading directly to death", the tendency within the medical community to report more acute sequela of AD as the primary cause of death carries with it the unfortunate consequence of under-representing the true mortality of AD.⁽³⁶⁴⁾ In fact, one report indicates that the sensitivity of death certificates for reporting AD-related mortality may be as low as 28%.⁽³⁶⁰⁾ Despite this tendency for mortality statistics to substantially underestimate the prevalence of dementing illnesses, according to the National Center for Health Statistics of the Centers of Disease Control and Prevention (CDC), 83,494 people died from AD in 2010; a statistic cementing AD firmly as the sixth-leading cause of death in the United States.⁽³⁶⁵⁾ Again emphasizing AD's age-dependent onset, it rises to the fifth-leading cause of death for those age 65 and older.¹⁴⁵ In an effort to reflect the degree to which under-reporting of AD on death certificates might have, we need to look at the number of individuals who die with AD as a comorbid condition. In 2014 this number is estimated to be 600,000 individuals in the U.S. alone, or put another way, one-third of every senior citizen over the age of 65.⁽³⁶⁶⁾ While the true number of deaths attributable to AD likely falls somewhere between the range of 83,000 and 600,000, there is no doubt

surrounding AD's contribution to premature death in the elderly. Regardless of the cause of death, among people age 70, 61% of those with AD are expected to die before age 80. To provide context to this statistic, simply compare it to the 30% percent of people without AD who die before age 80 in this age demographic.⁽³⁶⁷⁾ In light of these statistics, it becomes clear why AD is a world health priority when compared to less common causes of death. However, the finding that the mortality rate attributable to AD is rising while that of other top ten disease fall, demonstrates the unique public health threat posed AD (Figure 3-1). A testament to the impact translational research can have on human disease, between 2000 and 2010 the number of deaths attributable to heart disease, the number one cause of death in the U.S., decreased by 16%. Similarly, deaths attributable to prostate and breast cancer decreased by 8% and 2%, respectively. Assuming a global health perspective, the number of deaths attributable to HIV declined by 42%.⁽²⁹⁰⁾ Clearly, advances in medicine made possible by translation research are having a profound impact on virtually all top ten causes of death. As NIH funding is projected to reach 586 million dollars for the 2015 fiscal year, a substantial amount of resources have gone in to decreasing the mortality attributable to AD. Disappointingly, the total number of deaths attributable to AD increased by 68% across the 2000 to 2010 decade.⁽³⁶⁶⁾ The purpose of these statistics is to drive home the introductory sentence's final phrase; that AD invariably ends with patient death. However this is not the greatest health burden associable to AD.

Foreshadowed by the phrase "invariably leads to a loss of independence", the true disease burden associated with AD stems from its progressively debilitating clinical course. The statistic which best captures this concept is termed disability-adjusted life-years (DALY) and reflects the sum of the number of years of life lost due to the disease as well as the number of healthy years of life lost secondary to disability. Similar to the mortality data, the magnitude of this statistic has risen for AD to a greater degree than for any other medical condition. Using DALYs as a measure of disease burden, AD rose from the 25th most burdensome disease to the 12th from 1990 to 2010.⁽³⁶⁸⁾

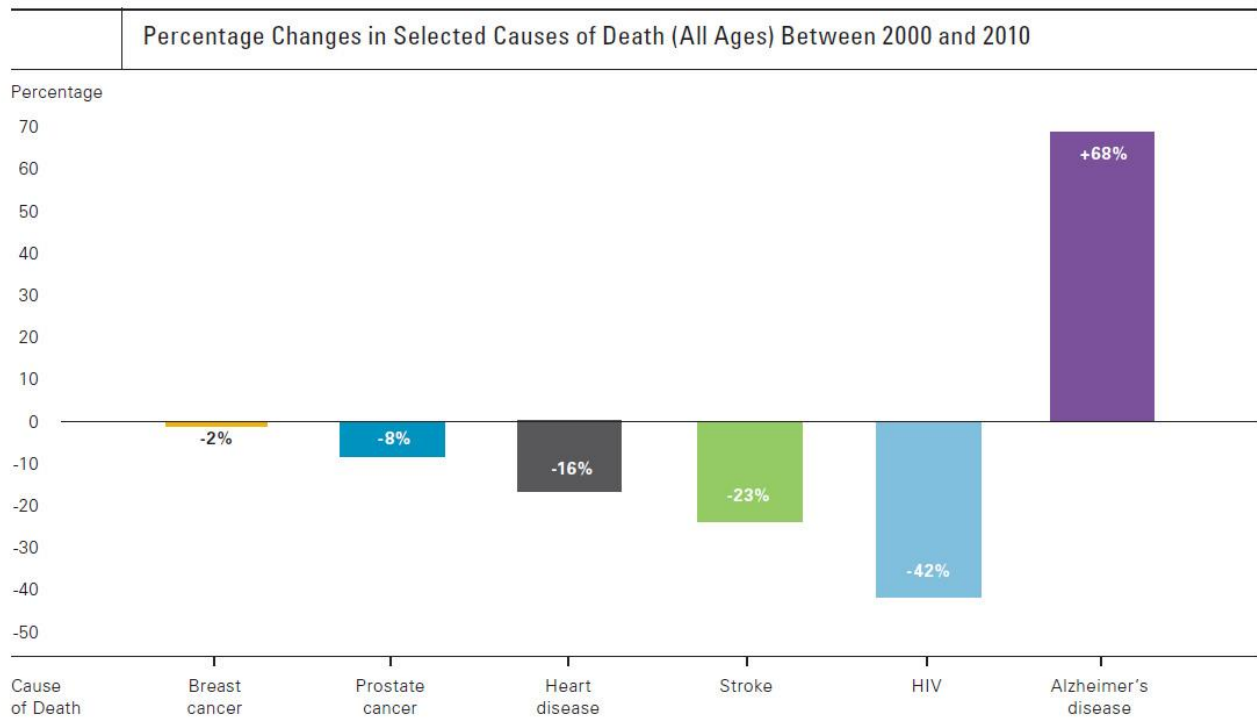


Figure 3-1. Public Health Impact of Deaths from Alzheimer's Disease.

As the population of the United States ages, Alzheimer's is becoming a more common cause of death. While deaths from other major causes have decreased significantly, deaths from Alzheimer's disease have increased significantly. Between 2000 and 2010, deaths attributed to Alzheimer's disease increased 68 percent, while those attributed to the number one cause of death, heart disease, and decreased 16 percent. Reproduced with Permissions from the Alzheimer's Association.⁽²⁹⁰⁾

Increases in both the number of years of life lost and the number of years lived with disability underlie this unrivaled jump in ranking. Importantly, this data confirms that AD contributes significantly to poor health and disability in the U.S. and that AD disease burden is increasing at an unrivaled pace each decade. Predictably, while mortality weighs heavily when considering the humanitarian cost of AD, fiscally, the number of years lived with disability is most contributory to the astronomical cost of healthcare for AD patients. A staggering 214 billion dollars in medical costs for all individuals with dementia was paid in 2014.^(144, 273) Though contributory, the high prevalence of AD is not the main factor driving this cost. Instead, this monetary burden is derived as a consequence of AD being a progressive disease that robs the patient of his/her independence. Individuals affected with AD live an average 4-8 years once diagnosed, but some can live as long as 20 years.⁽²⁹⁰⁾ While the course duration of AD is variable, patients consistently become totally dependent on caretakers for all essential daily living tasks. Aside from losing the ability to feed and bathe themselves, AD patients also frequently develop other behavioral symptoms such as depression and wandering which places them at high risk for institutionalization. To appreciate this, simply compare the average Medicaid payment for a Medicare beneficiary without AD (\$561) to that of one with AD (\$10,771).⁽²⁹⁰⁾ Notably these figures only address the cost directly associated with AD and neglect the cost accrued by patients as a consequence of having AD as a comorbid condition. While this cost is difficult to tabulate, data does demonstrate that AD patients with comorbid conditions can exhibit a 6-50% increase in their number of hospital stays. Taking the specific case of coronary artery disease as an example, total Medicare payments for a non-AD patient with this condition are estimated at \$16,768 annually as compared to \$27,033 for a similar patient with AD.⁽²⁹⁰⁾ Incredibly, even if the annual increase in cost attributable to AD for each of these conditions could be added to the \$214 billion statistic mentioned earlier, this would still not account for even 50% of AD's total economic burden.

As with all diseases that impair one's ability to remain self-sufficient, the greatest cost attributable to AD stems from the 17.7 billion hours spent by friends and family caring for their debilitated loved ones.⁽²⁹⁰⁾ This is due in part to the fact that 85% of all care provided to older adults in the U.S. comes not from trained medical professionals, but family members.⁽³⁶⁹⁾ The second contributing factor stems from AD being a disease which "progressively perturbs cognitive function". There are two components here that deserve attention, the fact that AD is progressive and that it selectively impairs cognition. With respect to the second factor, patients with AD or any form of dementia for that matter require an

exorbitant amount of care to maintain a meaningful quality of life. For example, 54% of AD patients require assistance getting into bed while 40% require help dressing themselves. Furthermore, as a consequence of AD being an “inexorably progressive” disease, the average duration of caregiving is substantially longer for AD than for non-AD elderly.⁽³⁶⁹⁾ Not surprisingly, the economic impact of this unpaid care is tremendous, with 54% of caregivers admitting to having to take time off work and 15% needing to take a leave of absence. Best estimates place the total cost of this unpaid caregiving at \$220.2 billion in 2013 alone.⁽³⁷⁰⁾ Thus, the value of informal care is at least equal to the direct medical and long-term care costs of AD & dementia. Again however, this statistic is misleading, as caregivers have also been shown to be less satisfied in life, become sick more frequently, and report increased levels of stress.⁽³⁷¹⁻³⁷³⁾

In summary, AD is a neurodegenerative disorder of age-dependent onset characterized by an inexorable and progressive perturbation of cognitive function which invariably leads to a loss of independence and ultimately death. As emphasized in the body of this chapter, each component of this description is of significance when tabulating the economic and humanitarian costs associated with AD. It is under this context that we study AD, and in view of the growing socioeconomic catastrophe and worldwide health problems associated with AD, the impetus to develop new diagnostic and treatment strategies for AD has never been greater.

3.2 POTENTIAL BENEFIT OF ALZHEIMER’S DISEASE TREATMENT DEVELOPMENT

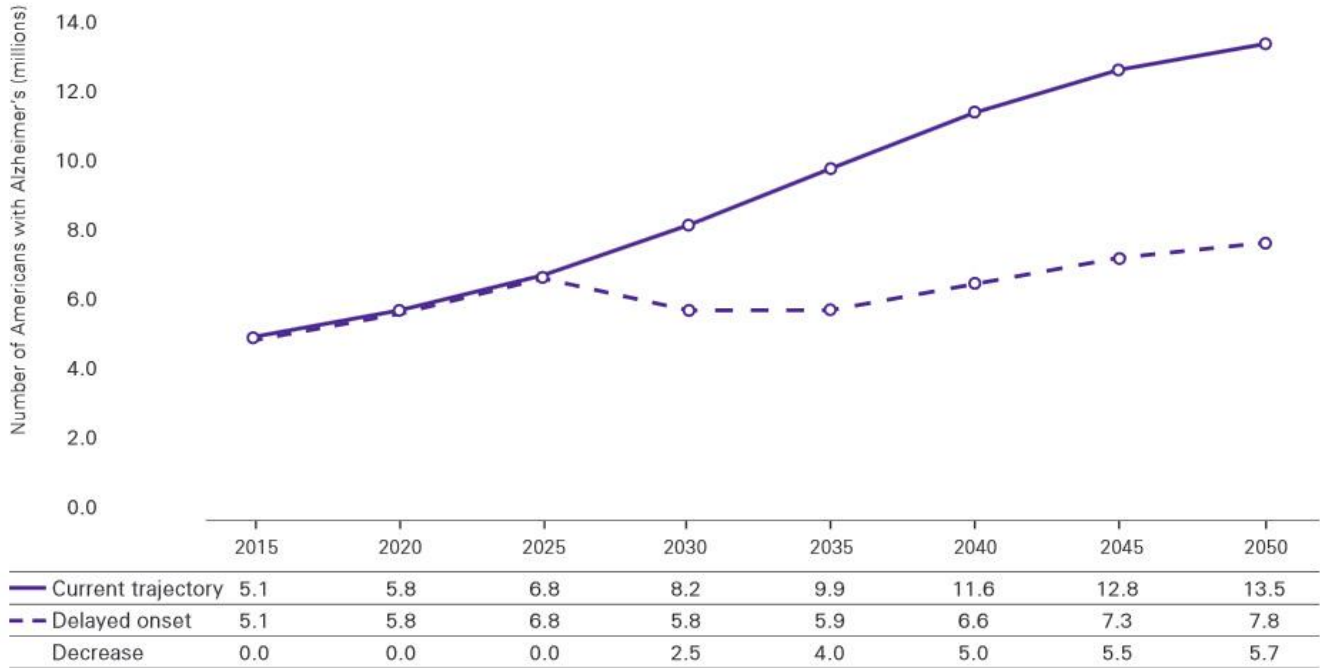
As emphasized in the entirety of this work, there is currently no available disease-modifying therapeutics for AD. Defined as a therapy that addresses the underlying pathogenic etiology of AD symptoms, the lack of such a treatment makes AD unique among the top ten causes of death in the United States. Unlike all of these other conditions, today, medicine is without a way to prevent, cure, or even slow AD progression. Instead, as described in subsequent sections in detail, the five current-generation medications approved by the U.S. Food and Drug Administration for the treatment of AD only provide temporary symptomatic relief in a subset of patients. Put plainly, these drugs do not alter the disease course of AD and as a consequence, as alluded to in the previous section, billions of dollars and millions of American lives are lost. Bluntly, without an effective disease-modifying treatment, the socioeconomic and public health consequences of AD will cripple the nation. Recognizing this, in 2011 the National Alzheimer’s Project Act (NAPA) was signed into law and tasked with the development of a national plan to address the growing threat of AD. Only a year later,

the National Plan to Address Alzheimer's Disease was published. This document calls for additional research dollars and sets scientific benchmarks with the aim of "preventing and effectively treating AD by 2025". As we have no alternative, the purpose of this section is to emphasize the potential impact of a disease-modifying therapeutic for AD. To do this, we will contrast real-world estimations of AD burden with that of a hypothetical U.S. nation with access to a disease-modifying therapy by the NAPA's 2025 deadline.⁽³⁷⁴⁾

For the purposes of this discussion, we will assume the hypothetical treatment is both effective in delaying the onset of AD by 5 years and universally accessible within the United States. Using conservative projections, the number of Americans affected by AD in 2030 is projected to be around 8.2 million people. Now, assuming universal access to a disease-modifying treatment by 2025, the projected number of AD cases in the U.S. drops to 5.8 million (Figure 3-2). Thus, in just 5 years the implementation, a disease-modifying treatment can reduce AD prevalence by approximately a third. Of course, the benefits of such a treatment are compounded as a function of time. For example, 40% of the 9.9 million Americans who would be expected to have developed AD by 2035 would be living normal lives in a U.S. nation with access to a disease-modifying treatment. Of course, and a consequence of AD's age-dependent onset, the demographic most benefited are those individuals over the age of 65. Instead of 11% of all individuals over the age of 65 having AD in 2030, only 8% would be afflicted if AD onset could be delayed by 5 years. These same statistics are 16% without a disease-modifying treatment and 9% by the year 2050, again emphasizing the time-dependent growth in therapeutic benefit associated with a preventative approach to AD. In fact, one of the only negative side-effects associated with a treatment which delays AD progression is that for a brief time, the proportion of those living with severe AD would increase. This is because a delay in onset would prevent people from moving into the mild stage of the disease, but have no effect on those who already had the condition before the treatment became available. Using population statistics to illustrate this point, with a delay in AD onset of 5 years beginning in 2025, 53% of patients with AD in 2030 would be classified as end-stage. If the current AD trajectory remains unaltered, this percentage would only be 41%. Of course, this trend is only temporary and by 2050 the introduction of treatment would actually decrease the proportion of patients with end-stage AD from 48% to 46%. Additionally, a 5 year delay in onset would also decrease the total number of individuals in each stage of AD such that in 2050, 3.6 million individuals would have severe-stage AD compared with the 6.5 million people under the current disease trajectory. Still, it is important to recognize the point that a disease-modifying treatment

is unlikely to alter the disease course of patients with moderate to severe AD. This is because it highlights the following point; the longer the delay in disease-modifying treatment development the more individuals progressing to disease stages which can no longer be altered.⁽³⁷⁴⁾

Impact of a Treatment That Delays Onset by Five Years on the Number of Americans Age 65 and Older Living with Alzheimer’s Disease, 2015-2050



*Totals may not add due to rounding.

Figure 3-2. Projected Impact of Disease-modifying Treatment for AD

A treatment introduced in 2025 that delays the onset of Alzheimer’s by five years would reduce the number of individuals affected by the disease immediately. In 2030, the total number of Americans age 65 and older living with Alzheimer’s would decrease from 8.2 million to 5.8 million. In 2035, 4 million Americans — approximately 40 percent of the 9.9 million Americans who would be expected to have Alzheimer’s — would be living without it. In 2050, total prevalence would be 7.8 million, meaning 5.7 million Americans — or 42 percent of the 13.5 million who would be expected to have Alzheimer’s barring a treatment breakthrough — would not have Alzheimer’s disease. A treatment introduced in 2025 that delays the onset of Alzheimer’s by five years would also reduce the proportion of the U.S. population age 65 and older who have the condition. In 2030, 8 percent of older adults would be living with Alzheimer’s disease instead of 11 percent. In 2050, only 9 percent of older adults would have Alzheimer’s instead of 16 percent. Reproduced with Permissions from the Alzheimer’s Association.⁽²⁹⁰⁾

Time is of the essence too when considering the economic threat posed by AD. As with prevalence, a treatment in 2025 that delays symptom onset by 5 years would reduce the total cost of AD care immediately. Unaltered, the annual treatment cost for AD in the U.S. is projected at \$451 billion for the 2030 fiscal year. Delaying symptoms just 5 years shifts this projected cost to \$368 billion, an \$83 billion dollar savings in just half a decade of implementation. With more time for the benefits to accrue, by 2050, total costs to all payers would decrease by one-third from \$1.101 trillion under the current disease trajectory to \$734 billion. Of special significance to the well-being of the U.S. healthcare system, 40% of this \$367 billion savings would be accounted for by Medicare cost reductions. Employing a Medicare specific example, introduction of a disease-modifying therapeutic would produce a savings of \$67 billion in the 2035 fiscal year alone. Similar benefits are expected for Medicaid, with \$1 billion saved in the first year alone, and a savings of \$38 billion by 2035. Tallying the cumulative savings for federal and state governments from 2026-2035 reveals an astonishing \$535 billion differential in cost. However, significant savings are not restricted to the public sector. To the contrary, AD patients and their family members would spend \$2 billion less on care by 2026, and \$44 billion less by 2035, if an effective disease-modifying treatment was discovered. Again summing the cumulative savings in the decade following the implementation of our hypothetical therapeutic in 2025, total savings for all payers would reach a staggering \$935 billion. While these statistics are of significance because they serve as the principal impetus behind the recent increases in government research funding for AD, the truth of the matter is that the current state of healthcare cannot be maintained if disease-modifying treatments for AD are not developed soon. One statistic, the estimated \$3.2 trillion in government spending to care for AD and other dementias over the 2026-2035 decade, is sufficient to convey this point.⁽³⁷⁴⁾

In summary, it is of fundamental importance to the well-being of society that AD research be appropriately funded so that a disease modifying treatment can be discovered. At the \$2 billion a year investment suggested by the NAPA for AD research, even summing all research spending between now and 2025, the federal government would recoup their funding in the first three years after a disease-modifying treatment became available.^{8,9} The American legislature has taken positive steps in this regard, but further support is needed. So too, measures to insure government funding is being spent on clinically feasible therapies is critical. As of 2015, the American Congress passed the Alzheimer's Accountability Act, requiring the National Institutes of Health to submit a review of AD research investments and the progress being made towards a treatment.¹⁰ Still, more can be done by politicians and scientists alike. Specifically, scientists need to advocate

for newly developed AD therapies with increased scrutiny. As reviewed in subsequent sections, historically AD clinical trials have been initiated without proper attention to study design or the clinical feasibility of the therapy they are designed to evaluate. Not only does this epitomize a misallocation of public funding, but more significantly, if left unchecked, improper evaluation of potential AD therapeutics may lead to the dismissal of agents with true clinical efficacy.

CHAPTER 4 CURRENT SYMPTOMATIC MANAGEMENT OF ALZHEIMER'S DISEASE

Of all the statistics presented to justify the need for further AD research, the most alarming from a public health perspective must be the fact that AD remains the only top ten cause of death in the U.S. without a disease-modifying treatment. Put more plainly, no treatment options which halt or even retard the progression of AD pathology have been successfully implemented clinically. Instead, the mainstay of AD treatment remains symptomatic management, with emphasis placed on the treatment of behavioral disturbances, environmental manipulations to support function, and counseling with respect to safety issues. However, management of even common medical problems can be more complex in patients with dementia.⁽³⁷⁵⁾ Particularly in AD, but generalizable to dementia as a whole, patients have a decreased ability to make decisions, adhere to treatment plans (including medication compliance), and report adverse effects of therapy.^(376, 377) Likely as a consequence of these issues, patients with advanced stages of dementia appear to have diminished survival when faced with acute illnesses.⁽³⁷⁸⁾ In a study that adjusted for length bias, a random sample of 10,263 subjects ages 65 and older from the Canadian Study of Health and Aging were screened for dementia and followed for five years.⁽¹⁵⁷⁾ The adjusted median survival for patients with probable and possible AD was 3.1 and 3.5 years, respectively. In this chapter, the current treatment paradigm for AD will be reviewed with an emphasis on pharmaceutical interventions targeting the cholinergic system. By way of introduction, the synthesis and recycling of Ach in the CNS will be reviewed in addition to the neuroanatomy of the major cholinergic pathways in the brain and their role in memory. Building on this understanding of the cholinergic system's role in memory, the perturbations in cholinergic signaling in AD will be summarized. From this point, a mechanistic review of the major pharmaceutical interventions for AD, namely acetylcholinesterase inhibitors will be presented. The rational, mechanism of action and usage guidelines for the only non-AchE targeting drug used in AD, Memantine, are also summarized. Lastly, data evaluating the efficacy of these therapies in accordance with current guidelines will be reviewed.

4.1 ACETYLCHOLINE SYNTHESIS & RECYCLING

Originally identified in cardiac tissue by Henry Hallet Dale in 1915, Acetylcholine (Ach) was the first neurotransmitter recognized by science after Otto Loewi characterized its function in the Vagus nerve. Acetylcholine (Ach) is a polyatomic cation synthesized via the conjugation of choline and acetyl-CoA by the enzyme choline acetyltransferase. As is the case for all proteins at the synaptic terminal, the enzyme responsible for the synthesis of Ach, choline acetyltransferase (CAT), is produced at the cholinergic cell body and transported down the axon. Importantly, the enzyme kinetics of CAT is not saturated under normal physiological conditions and therefore increased expression of this enzyme is unlikely to modulate cholinergic neurotransmission. Instead, the availability of choline and acetyl-CoA are the rate-limiting steps in Ach synthesis. As described in Figure 4-1, the majority of choline in the synaptic terminal is recycled from the synaptic cleft. Additionally, two independent pathways have been established for the production of choline. First, phospholipase D cleaves the phosphoester bond towards the choline head-group forming free choline and the membrane bound phosphatidic acid. By the second mechanism, phosphatidylcholine is degraded into its glycerol backbone and fatty acid constituents by the sequential actions of phospholipases A and B. Phospholipase A1/2 removes the acyl chain from the C1 position of phosphatidylcholine, forming a free fatty acid and lysophosphatidylcholine. Phospholipase B then removes the C2 acyl residue to form glycerol-3-phosphocholine and a fatty acid. Finally, glycerol-3-phosphocholine is hydrolyzed to glycerol-3-phosphate and free choline. By either mechanism, free choline is then covalently linked with an activated acetyl unit from acetyl-CoA to form Ach in a reaction catalyzed by choline-acetyl transferase. Similarly, a variety of metabolic pathways cause mitochondrial release of acetyl-CoA to rise proportionally with neuronal activity, insuring adequate substrate supply for CAT. Interestingly, while the substrate abundance is the rate limiting step for Ach synthesis, studies indicate that consuming an enriched choline diet does not modulate cholinergic transmission. One explanation of this finding is that increased choline availability peripherally is not translated to the CNS. Once synthesized, the large majority of Ach is immediately packaged into approximately 100 micron vesicular compartments by the vesicular Ach transporter. Only a small fraction of Ach remains in the cytosol of the synaptic cleft and the functional significance of this pool is not completely elucidated. Importantly, no pharmacological agents capable of modifying the function of the vesicular Ach hydrogen-Ach antiporter have been identified. While Ach neurotransmission is generally facilitated via the traditional calcium-dependent mechanisms, it is important to recognize

Ach also serves as a potent neuromodulator. Regardless of its release mechanism, Ach elicits its physiological response via two broad classes of cholinergic receptors: nicotinic and muscarinic Ach receptors. Speaking generally, these two classes of Ach receptors differ in their synaptic localization, structure, and mechanism of action. With respect to localization, nicotinic receptors are predominately restricted to the post-synaptic membrane while their muscarinic counterparts are found both pre- and post-synaptically. Shifting our attention to structure, neuronal nicotinic receptors are selectively-permeable ion channels while muscarinic

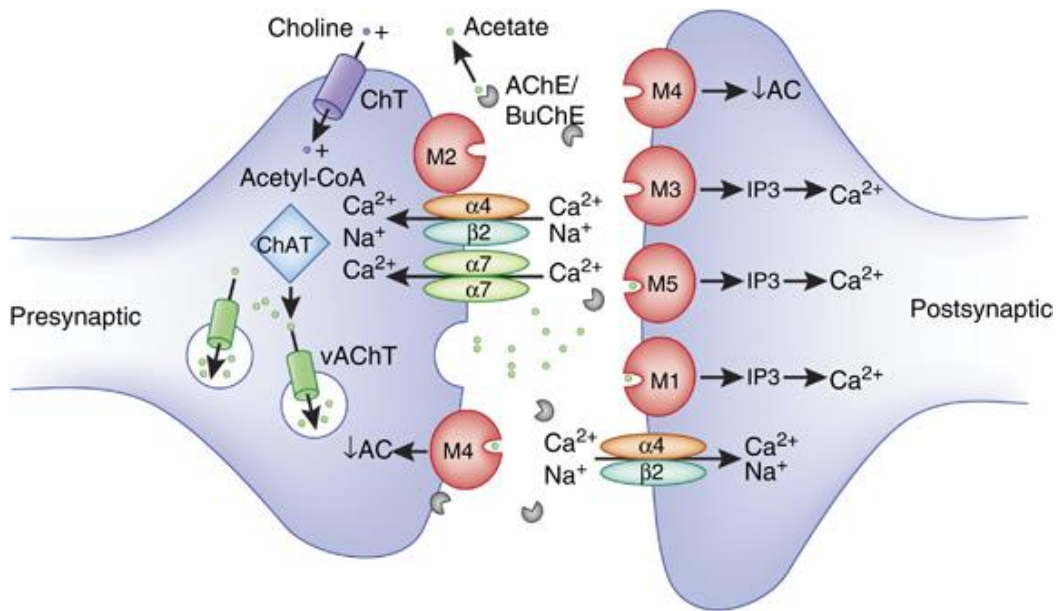


Figure 4-1. Schematic Representation of a Hypothetical Cholinergic Synapse.

mAChR subtypes have diverse synaptic localization patterns and function pre- and post-synaptically to modulate neurotransmitter release and postsynaptic excitability, respectively. For instance, the M_2 and M_4 mAChRs serve as autoreceptors on cholinergic terminals to suppress Ach release and inhibit cholinergic neurotransmission at select synapses in the central nervous system (left neuron). The mAChRs located on non-cholinergic neurons act as heteroreceptors controlling the release of other neurotransmitters, such as DA (not shown). M_1 , M_3 , M_5 , but also M_4 mAChRs that are located postsynaptically facilitate slow cholinergic synaptic neurotransmission relative to nAChR subtypes. The α_7 and $\alpha_4\beta_2$ nAChR subtypes mediate fast synaptic transmission and also use-dependent changes required for neuronal plasticity. These nAChR subtypes can have both pre- and postsynaptic localization. The endogenous ligand of these cholinergic receptors, Ach, is synthesized in cholinergic neurons (left neuron) by the enzyme ChAT through the transfer of acetyl-CoA onto choline. Choline uptake is mediated by presynaptic high-affinity choline transporters (ChT). After synthesis, Ach is packaged into synaptic vesicles by the vesicular Ach transporter (vAChT). After neuronal activation-mediated release into the synaptic cleft, Ach can bind to pre- and postsynaptic receptors, or it can be inactivated through hydrolysis by the AchE enzymes, a process that can be inhibited by different substances (eg, organophosphates, AchE inhibitors) to increase synaptic Ach levels. Once Ach is hydrolyzed, choline is transported through the ChTs into the presynaptic terminal, where it is again synthesized into Ach. Reproduced with Permissions from Nature Neuropsychopharmacology.⁽³⁷⁹⁾

receptors are classified as G protein coupled receptors (GPCRs). In more detail, nicotinic receptors are comprised of 5 polypeptide subunits. Whereas the nicotinic receptor localized to the neuromuscular junction is composed of four different species of subunit (2 α , β , γ , δ), the neuronal nicotinic receptor is composed of only two subunit types (2 α and 3 β). The 5 polypeptide subunits assume a conformation such that a funnel-shaped internal ion channel is formed in the center of the protein complex. Relating this structure to function, nicotinic receptors facilitate post-synaptic membrane depolarization as a consequence of ligand-binding. Of importance to pharmaceutical development, the binding surface on the nicotinic receptor appears to be primarily on the alpha subunits. As stated, the structure of muscarinic receptors is distinct from nicotinic receptors as this class of Ach receptor is classified as a GPCR. The muscarinic receptor is composed of a single polypeptide as compared to the 5 polypeptide subunits described for nicotinic Ach receptors. Seven regions of the single polypeptide which comprises muscarinic receptors are made up of 20-25 amino acids arranged in an α helix. As a consequence of this secondary structure, each of these regions of the protein is markedly hydrophobic and thus spans the cell membrane. Critically, the fifth internal loop and the carboxyl-terminal tail of the muscarinic receptor are believed to be the site of interaction with G proteins. Similarly, the site of agonist binding is a circular pocket formed by the upper portions of the seven membrane-spanning regions. As with all GPCRs, the biochemical responses to stimulation of muscarinic receptors involve the receptor occupancy causing an altered conformation of an associated GTP-binding protein. G protein is made up of the three subunits α , β and γ . In response to the altered conformation of the muscarinic receptor, the alpha subunit of the G protein releases bound guanosine diphosphate (GDP) and simultaneously binds guanosine triphosphate (GTP). The binding of GTP "activates" the G protein and leads to dissociation of the alpha subunit from the trimeric complex. Now free, the alpha subunit can interact with effector systems to mediate specific responses. Again speaking generally, three principal effector systems are employed by muscarinic Ach receptors: inhibition of adenylyate cyclase, stimulation of phospholipase C, and activation of potassium ion channels. The inherent catalytic activity of the G protein hydrolyzes the GTP back to GDP. This hydrolysis results in a conformational change in the alpha subunit which causes it to again associate with the β and γ subunits, terminating the action of the G protein. Thus, the rate of GTP hydrolysis dictates the length of time the muscarinic receptor remains activated, not the period of time in which Ach is bound to the receptor.

Regardless of receptor class however, following dissociation from the receptor, Ach is rapidly hydrolyzed by the enzyme acetylcholinesterase (AChE). AChE is a serine esterase with a catalytic triad consisting of Ser200, His440, and Glu237, a domain similar to that found in serine proteases trypsin and chymotrypsin. The enzyme is located on the surface of the post-synaptic membrane and linked by a GPI anchor. Importantly, AChE has one of the highest catalysis rates known in biology, 2.5×10^4 molecules per second, and breaks Ach down into its choline and acetate constituents. The products choline and acetate are inactive molecules and are reabsorbed by the synapse and recycled to replenish acetylcholine containing vesicles for subsequent chemical transmission. As with the synthetic enzyme for Ach, choline acetyltransferase, AChE is synthesized in the neuronal cell body and distributed throughout the neuron by axoplasmic transport. Unlike all other proteins described in this process, irreversible and reversible classes of AChE inhibitors have been developed. Furthermore, drugs that inhibit Ach breakdown are effective in altering cholinergic neurotransmission in the CNS. Mechanistically, this is because in the absence of AChE activity, Ach molecules accumulate in the synaptic space where they can stimulate either class of Ach receptor continuously. In fact, the irreversible inhibition of AChE by isopropylfluoroesters modulate cholinergic neurotransmission so much, they can be incompatible with life. Two notable examples of this class of AChE inhibitors are organophosphates such as dichlorodiphenyltrichloroethane (DDT) used widely as an insecticide and Sarin nerve gas used in biological warfare. The mechanism of action of these irreversible inhibitors of AChE is that they carbamylate the AChE, rendering both the acetyl and choline binding domains inactive. As evidenced by their use in biochemical warfare, irreversible inhibitors of AChE are too difficult to calibrate in the clinical setting. Instead, reversible AChE inhibitors are employed to transiently increase Ach levels in diseases and conditions where an increased Ach level is desired. As described in detail later, one such condition is AD, with patients routinely demonstrating a variety of perturbations in cholinergic function. Four cholinesterase inhibitors, Tacrine, Donepezil, Rivastigmine, and Galantamine are currently approved for use in AD by the US Food and Drug Administration (FDA). Tacrine, the first cholinesterase inhibitor approved, is essentially no longer used due to hepatic toxicity and severe, predominantly gastrointestinal side effects.

4.2 CHOLINERGIC SYSTEM NEUROANATOMY & ROLE IN MEMORY

Widely distributed in the CNS, Ach has been implicated in a variety of physiological functions including: cerebral cortical development, cortical activity, regulation of cerebral blood flow, sleep-wake cycles, and most relevantly to AD, modulation of cognitive performance on learning and memory tasks. In fact, the discovery that cholinergic neurons in the basal forebrain degenerate in AD has been one of the most potent catalysts behind the relentless investigation of cholinergic contributions to learning and memory. Today, substantial evidence garnered from both human and animal models strongly implicates that the central cholinergic pathways are vital components to the neuronal circuitry underlying learning, memory and cognition. In fact, by 1982 this assertion was so well-established in the literature, that Raymond Bartus and colleagues proposed “the cholinergic hypothesis of geriatric memory dysfunction”.⁽³⁸⁰⁾ According to this hypothesis, the deterioration of cognitive function associated with AD dementia in the elderly is attributable to a decline in basal forebrain cholinergic neurotransmission. Predictably, the same studies that support the notion that cholinergic pathways are of central importance to learning and memory are cited by supporters of this hypothesis and thus warrant brief review. Historically, pharmacological manipulations and lesion studies represent the two traditional approaches used to study the role of cholinergic systems in learning and memory. To interpret these studies, it is first necessary to review the neuroanatomy of the cholinergic pathways which constitute the primary sources of cholinergic innervations to the limbic and cortical brain structures. Note, while this section will detail specific pathways, it is important to recognize that Ach is released from neurons projecting to a broad range of cortical and subcortical sites.

In general, two sets of cholinergic projections can be distinguished; the magnocellular basal forebrain cholinergic system and the brainstem cholinergic system.^(381, 382) Of highest significance to learning and memory, the basal forebrain system is comprised of efferent and afferent projections from cholinergic neurons originating in the nucleus basalis of Meynert (nBM) and the medial septal nucleus (MSn), as well as the vertical and horizontal limbs of the diagonal band of Broca. The cholinergic neurons comprising these structures send predominantly cholinergic projections to a broad range of sites in the neocortex as well as limbic cortices such as cingulate cortex, entorhinal cortex and hippocampus, and other structures including the basolateral amygdala and the olfactory bulb.⁽³⁸¹⁾ More specifically, axons emanating from the MS innervate predominantly the hippocampus and entorhinal cortex (in addition to the vertical limb of the diagonal band of Broca), whereas vertical/horizontal limbs of the diagonal band of Broca project primarily into the anterior cingulate cortex

and olfactory bulb, respectively. Of significance to AD research and Ach's role in learning and memory, the entorhinal cortex, one of the first regions affected by AD pathology, receives some of the densest cholinergic innervation of all cortical structures.⁽³⁸¹⁾ Of less significance to learning and memory but still warranting description, the brainstem cholinergic system includes neurons located in the pedunclopontine tegmental nucleus and laterodorsal pontine tegmentum and provides cholinergic input primarily to the thalamus and basal ganglia, but also to a minor degree the cortex. To summarize the key neuroanatomical substrates of cholinergic influence in learning and memory, the basal forebrain cholinergic system constitutes the major source of afferent Ach-based input to the cortex and hippocampus. Specifically, the horizontal limb of the diagonal band of Broca in conjunction with the nBM provide the majority of cholinergic input to the neocortex while the MS and vertical limb of the diagonal band of Broca project to the entorhinal cortex and hippocampus proper.

While the precise mechanism by which Ach influences the neuronal circuitry facilitating learning and memory is not universally agreed upon for all memory systems, Ach is known to modulate the responsivity of individual neurons via a variety of mechanisms. These effects include depolarization⁽³⁸³⁾, reductions in spike frequency accommodation⁽³⁸⁴⁾, enhancement of long-term potentiation⁽³⁸⁵⁾, presynaptic inhibition of glutamatergic and GABAergic synaptic transmission.^(386, 387) As explained above, two classes of Ach-responsive receptors mediate these effects. Of the five subtypes of muscarinic receptors in the central nervous system, the M1 receptor is located predominantly at post-synaptic sites and is functionally related to the M3 and M5 receptors. The M1 receptor mediates the post-synaptic effects induced via activation of muscarinic receptors including depolarization and suppression of spike-frequency accommodation.⁽³⁸⁸⁾ M2 receptors on the other hand are located at both pre- and post-synaptic sites and are functionally related to the M4 receptor subtype.⁽³⁸⁹⁾ Interestingly, the cholinergic modulation of glutamatergic synaptic transmission via activation of muscarinic receptors on glutamatergic terminals appears to involve the M4 subtype of receptor.^(388, 390) The second class of Ach-responsive receptors, nicotinic receptors, demonstrates an even more diverse range of receptor properties, as well as a temporally and spatially restricted expression pattern. Focusing specifically on the role of nicotinic Ach receptors in the hippocampus, this class of receptor is expressed primarily by interneurons, where evidence suggests they play a role in gating neuronal firing.⁽³⁹¹⁾ With respect to spatial expression of particular subtypes of nicotinic receptors, alpha4beta2 (type I) receptors are sensitive to low concentrations of Ach⁽³⁹²⁾ (0.1–1 μ M) and have been described on the soma and

dendrites of CA1 interneurons of mice.^(393, 394) Alpha4beta2 (type II) receptors are less sensitive than their type I counterparts⁽³⁹²⁾, and have been identified on the axonal segments of CA1 interneurons where their activation by low concentrations of Ach can induce release of GABA without triggering an action potential.⁽³⁹³⁾ While Alpha3beta3beta2 receptors are found on the axons of pyramidal associated interneurons, little is known about their role in neurotransmission.⁽³⁹¹⁾ In contrast Alpha7 nicotinic Ach receptors are well characterized even in the context of AD and display faster dynamics, a high calcium permeability, and are activated by the Ach precursor choline.⁽³⁹¹⁾ Alpha7 nicotinic Ach receptors are found on the somata⁽³⁹⁴⁾ and dendrites⁽³⁹⁵⁾ of hippocampal neurons where they can regulate calcium responses, as well as on the axon terminal where they enhance transmitter release.⁽³⁹⁶⁾ As this description of Ach receptor expression illustrates, the cholinergic pathways of the brain are well-suited to modulate neuronal activity in key memory regions of the brain such as the hippocampus.

With this neuroanatomical description of cholinergic circuitry in mind, it follows logically that the previously mentioned lesion studies focused predominately on the magnocellular basal forebrain cholinergic system when attempting to investigate the role of Ach in memory. And indeed, studies support the role of Ach-signaling in learning and memory. At the most basic level, pharmacological studies have demonstrated that high doses of anti-muscarinic agents such as atropine and scopolamine can disrupt both the acquisition and recall of learned behaviors.^(397, 398) In contrast, the enhancement of central cholinergic tone via administration of AchE inhibitors can, under specific circumstances, enhance performance in learning and memory tasks.⁽³⁹⁹⁾ Importantly these findings have been recapitulated in animal models, providing an experimental avenue through which to investigate Ach's role in cognition.⁽³⁹⁷⁾ For example, robust experimental evidence confirms that depletion of cholinergic input to either the PFC or parahippocampus disrupts working memory. Interestingly however, deficits in working memory associated with each of these cholinergic lesions are distinct from one another. To summarize the relevant animal studies, loss of cholinergic input to the parahippocampal region results in working memory deficits exclusively for non-familiar stimuli while similar lesions in the PFC impair memory for trial-unique stimuli.^(400, 401) Translation of this work into humans reveals even greater insight, as muscarinic blockade does not impair performance on short-term memory tasks such as the digit span.⁽⁴⁰²⁾ These results have been interpreted to suggest that the familiar stimuli used in this paradigm (numbers) are already sufficiently established synaptic connections and therefore have a reduced need for cholinergic neuro-modulation. Distilling these findings into a

commentary on Ach's role in working memory, cholinergic modulation of working memory seems more influential for novel stimuli than for familiar ones.⁽⁴⁰³⁾ While these studies help elucidate the role of Ach in working memory, studies of people who smoke have led to the understanding that cholinergic input modulates attention.⁽⁴⁰⁴⁾ For example, smokers deprived of nicotine are impaired on attention demanding tasks and their performance can be rescued to baseline levels via the administration of nicotine. Additionally, nicotine has been shown to boost visual attention performance in non-smokers.⁽⁴⁰⁵⁾ Cholinergic depletion studies further underscore the importance of Ach in attentional processing. For instance, selective cholinergic deafferentation of the cortex via pharmacological ablation of the nBM in rats has been demonstrated to produce selective deficits in an attention demanding task.⁽⁴⁰⁶⁾ Given the robust evidence supporting Ach's role in attentional processing, investigators have partially elucidated the relevant physiological processes. In short, evidence suggests that Ach potentiates afferent projections while suppressing intrinsic projections, thereby allowing for greater processing of extrinsic stimuli.⁽⁴⁰⁷⁾ Akin to the brain region specific relationship between cholinergic innervation and working memory performance for familiar/non-familiar objects, in attention each Ach receptor class plays a unique role. To summarize, nicotinic receptors are critical for the amplification of afferent signals while the suppression of intrinsic synapses likely depends on the muscarinic class of Ach receptors.⁽⁴⁰⁸⁾

Finally, and perhaps of greatest relevance to AD because the brain regions involved, a wealth of evidence supports a functional link between Ach-mediated neuro-modulation and spatial/episodic memory. Currently, Ach is hypothesized to support the formation of new memories in two ways. The first, as just described, is to increase the extent that afferent signals influence cortical activity while simultaneously decreasing the extent to which intrinsic signals influence activity. Described more generally, Ach's modulation of attention facilitates memory formation because the fidelity of a memory is fundamentally limited by how effectively the relevant information was processed at encoding. The second way Ach may modulate spatial/episodic memory formation is by enhancing the physiological phenomena that support the encoding of new memories; specifically the induction of LTP and theta oscillation amplitude.^(386, 408) In slightly more detail, independent pharmacological manipulation of the alpha4beta2 and alpha7 receptors have revealed that both are capable of inducing LTP but that the alpha7 receptors, in particular, induce a more stable form of LTP.⁽⁴⁰⁹⁾ As mentioned, the second physiological phenomena modulated by Ach is termed the Theta rhythm, a prominent oscillatory rhythm observed in local field potentials of hippocampal neurons when stimuli are presented during memory

tests to humans.^(410, 411) With respect to the evidence supporting its role in learning, the amplitude of theta is predictive of improved memory encoding. In humans for example, the amplitude of intra-cranially recorded theta oscillations during encoding in a free recall task was significantly greater for subsequently recalled words than for forgotten words.⁽⁴¹²⁾ Mechanistically, this may be a consequence of LTP induction demonstrating a dependence on theta phase. In the simplest model, LTP is preferentially induced during the peak of theta in the local field potential whereas LTD is preferentially induced during the trough of theta in the local field potential.⁽⁴¹³⁾ However in addition to this modulation of neuroplasticity, it has been suggested that theta may drive the formation of the spatial tuning pattern observed in hippocampal place cells and entorhinal grid cells. As discussed, the hippocampus and medial EC play crucial roles in navigation; as lesions of either region lead to deficits on spatial memory tasks.⁽⁴¹⁴⁾ Today, we now know a little about how the position of an animal is neutrally encoded in these temporal lobe structures. Cells in the pyramidal cell layers of hippocampal regions CA1 and CA3, for example, preferentially fire in distinct sub-regions of testing enclosures, and as such have been termed “place cells”. Located in the entorhinal cortex, grid cells received their name after the discovery that they fire action potentials in a pattern which marks the vertices of a grid in the shape of an equilateral triangle.⁽⁴¹⁵⁾ Although the precise mechanism by which Ach contributes to the tuning of place cells and grid cells is not clearly understood, a promising hypothesis is that the spatial tuning of such cells is affected by cholinergic modulation through an intermediary: theta rhythms. Happily, models detailing how theta rhythm might relate to spatial memory formation are more refined. Referred to in the literature as the oscillatory interference model, this model holds that grid cells fire when the sum of at least two oscillators cross an arbitrary threshold.⁽⁴⁰³⁾ Importantly, the frequency of each oscillator is determined by the speed of the animal when heading in a preferred direction (e.g., north). Additionally, the frequency of each oscillator increases proportionally with the speed of the animal. Lastly, if the animal travels in a direction orthogonal to the preferred heading (e.g. west), the oscillator returns back to a baseline frequency presumed to lie in the theta frequency range. When two such velocity controlled oscillators that differ in their preferred direction by an integer multiple of 60° are summed and thresholded, the interference pattern closely resembles the spatial tuning pattern of entorhinal grid cells.⁽⁴⁰³⁾ Relating this theoretical model back to behavior, it is predicted that grid cell tuning should then require an intact theta rhythm. And indeed, studies suggest that MS inactivation both significantly reduces the amplitude of theta oscillations and significantly decreased the spatial tuning of grid cells.⁽⁴¹⁶⁾ Provided the additional insight that Theta rhythm is principally modulated by cholinergic and GABAergic inputs from the MS via the fornix, models of

network theta rhythm oscillations suggest how theta may serve as an intermediary between cholinergic regulation and episodic and spatial memory function.⁽⁴⁰³⁾

In summary, Ach plays an important role in cognitive function, as shown by pharmacological manipulations that impact working memory, attention, episodic memory, and spatial memory function. However, it is important to note that our ability to draw conclusions from the studies discussed are not completely devoid of confounds. Specifically relevant in the case of lesion studies is the fact that cholinergic neurons are always intermingled with populations of non-cholinergic cells. In addition to their cholinergic projections, the brain regions constituting the basal forebrain cholinergic system also contain many non-cholinergic neurons, such as GABAergic interneurons that make connections with cholinergic neurons.⁽⁴¹⁷⁾ Importantly, the synaptic connections of these non-cholinergic neurons are not restricted to inter-cholinergic neuronal circuits. Instead, GABAergic innervation from basal forebrain structures also project to the hippocampus.⁽⁴¹⁸⁾ In light of studies which indicate that the degree of cholinergic dysfunction doesn't necessarily predict the severity of cognitive dysfunction, it is possible that perturbations of non-cholinergic may contribute to memory deficits observed when cholinergic signaling is disturbed. As an example of one such study, stereotactic obliteration of the nBM results in robust memory impairment which can be ameliorated via the administration of Physostigmine.⁽⁴¹⁹⁾ While this study generates what appears to be clear association between cholinergic function and memory performance, as discussed, a cholinergic neuron specific lesion in the nBM is virtually impossible. Proponents of Ach's central role in memory formation will argue that in the context of physostigmine-induced amelioration of lesion-induced memory deficits, this fact is academic. However, subsequent studies have demonstrated an important dissociation between a lesion's ability to produce memory deficits and the extent to which it perturbs cortical cholinergic tone. Put differently, under certain experimental procedures, a lesion of the nBM which reduces cholinergic tone by 44% does not produce as robust deficits in conditional learning as does a lesion which only decreases cholinergic tone by 27%.⁽⁴²⁰⁾ The conclusion reached by these studies is that damage to non-cholinergic cells in the vicinity of the nBM must contribute to the observed perturbations in memory. Thus, while it is unanimously agreed that loss of predominantly cholinergic basal forebrain structures impair learning and memory in humans and animal models, the mechanism by which this occurs and the relative importance of Ach in these processes is still yet to be elucidated. Here, the evidence reviewed falls short as a consequence of the pharmacological approach they employ. As highlighted in the introduction to this section, it is

important to note that nearly the entire neuro-axis is innervated by cholinergic neurons.⁽⁴²¹⁾ It is also the case that muscarinic receptors are found in virtually every region of the CNS.^(422, 423) In the context of such ubiquitous Ach receptor expression in the brain, systemically administered cholinergic agents undoubtedly influence behavior by their effects at a variety of targets in the CNS. Furthermore, the sensitivity of these cholinergic based processes underlying cognitive performance would be predicted to vary as a function of the behavioral task probed. As will be discussed in the subsequent section, the very same regions of cholinergic input which have been studied in the context of learning and memory exhibit significant cell death in AD. However, it remains to be fully established if the cholinergic neurodegeneration represents the pivotal functional determinant of the cognitive symptoms observed in AD. Therefore, the subsequent section will emphasize the ways in which AD pathology extends beyond cholinergic signaling dysfunction in an effort to highlight the need for disease-modifying therapies.

4.3 CHOLINERGIC CHANGES IN ALZHEIMER'S DISEASE

Without question, long-standing evidence suggests that cholinergic signaling contribute significantly to learning and memory. Even as early as the 1970's, the systematic scientific investigation of brains of patients with Alzheimer's disease revealed deficits in key pathways associated with Ach neurotransmission. Among the earliest and most influential of these discoveries is that the morphology of cholinergic cells in the basal forebrain are especially susceptible to the pathogenic changes of AD and are thus among the groups of neurons that degenerate robustly.⁽⁴²⁴⁻⁴²⁶⁾ However, the specific functional consequences of this neuron loss remains uncharacterized, as there is no direct evidence that damage to these neurons is responsible for cognitive decline in AD. Still, decreases in the activity of choline acetyltransferase (ChAT) in the cortex and hippocampus are amongst the most consistent and severe neurochemical abnormalities found in AD. For example, a 30-90% decline in ChAT activity is typical in AD brains while in-situ hybridization studies demonstrate a 50% decrease in ChAT mRNA levels in the temporal, frontal and parietal lobes.^(424, 425, 427, 428) However as discussed, ChAT is not rate-limiting for Ach synthesis and thus the purported decrease in ChAT activity is mechanistically unlikely to be a causal factor of AD cognitive symptoms. Instead, the majority of experts favor the hypothesis that changes in ChAT activity and expression simply reflect the degeneration of basal forebrain cholinergic neurons. Supporting this hypothesis, the decline in ChAT activity in the nBM is correlated with the decline in cholinergic

neuron number.⁽⁴²⁹⁾ Also in congruence with this hypothesis, ChAT activity in the neocortex of patients with dominantly inherited olivopontocerebellar atrophy, a condition for which cognitive deficits are not a major symptomatic feature, is reduced to as great an extent as in AD patients.⁽⁴³⁰⁾ This finding in particular raises the question of whether impaired cholinergic function, especially in the cortex, contributes to cognitive decline in AD at all. However, in discordance with the hypothesis that cholinergic dysfunction does not underlie cognitive deficits in AD, ChAT activity in the hippocampus of AD patients is significantly reduced while individuals with olivopontocerebellar atrophy demonstrate no hippocampal cholinergic deficit.⁽⁴³⁰⁾ In contrast to the first finding, this latter discovery raises the possibility that some aspects of cognitive impairment in AD are indeed associated with dysfunction of the cholinergic neuropathways, in this specific case the septo-hippocampal projections. Still, the finding that ChAT levels are decreased only in end-stage AD while patients with MCI or even mild AD display no significant deviation in this marker of cholinergic tone with respect to baseline severely undermines the “cholinergic hypothesis of AD”.^(431, 432) Complicating the matter, for numerous reasons the pharmacological studies which support the role of Ach in learning and memory are not generalizable to AD. Chief among them, even if cholinergic degeneration was the sole pathological feature of AD, because both muscarinic and nicotinic transmission would be impaired, muscarinic receptor antagonists would not be expected to recapitulate the full spectrum of AD pathology. Additionally, the muscarinic antagonists used in these studies produce an acute blockade of cholinergic receptors that are primarily post-synaptic. In contrast to all these characteristics of cholinergic antagonist models of cognitive function, AD is a chronic, slowly progressing, and irreversible disorder that involves, in addition to the noted changes in presynaptic cholinergic function, substantial pathology of many other neurotransmitter systems. A prime example of this ultimate point is the reduction of excitatory neurotransmitters secondary to the selective loss of cortical pyramidal neurons believed to support normal cognition. Similar to the manner in which neuron loss in the basal forebrain underlies deficits in cholinergic signaling, early degeneration of cortical pyramidal neuron in AD impairs uptake of D-aspartate, a putative excitatory amino acid, as well as contributes to observed deficits in glutamate concentrations in the brain of AD patients.⁽⁴³³⁻⁴³⁵⁾ While these changes may occur as a consequence of perturbation in cholinergic signaling, other neurotransmitter systems without direct cholinergic innervations are similarly perturbed in AD. Depending on the stage of disease, neurotransmission facilitated via the serotonergic raphe nuclei, the noradrenergic locus coeruleus⁽⁴³⁶⁾, as well as g-aminobutyric acid (GABA)^(433, 437) and somatostatin^(438, 439) producing interneurons are also disturbed in the neurodegenerative process of AD. Evidence that these distinctions between AD pathology and cholinergic models of AD

cognitive deficits are of significance comes from studies which demonstrate patterns in regional cerebral in AD patients are markedly different from those obtained from young normal subjects given scopolamine to induce memory impairments.⁽⁴⁴⁰⁾

To summarize, while cholinergic models do strongly implicate a robust modulatory role for Ach in learning and memory, there is a lack of evidence which directly links perturbations in Ach signaling with the cognitive deficits observed in AD. This is not to say cholinergic dysfunction does not contribute, as it almost certainly does. However, while cholinergic deafferentation does induce deficits in cognition, it fails to produce the typical longitudinal decline observed in AD.⁽⁴⁴¹⁾ This hints at the fact that dysregulation of Ach neurotransmission is only part of a more complex etiology underlying the memory deficits observed in AD. The hypothesis that cholinergic dysregulation underlies the etiology of AD is even weaker, as loss of Ach-producing neurons fails to induce other pathognomonic lesions of AD such as NFTs and A β plaques. Additionally, markers of cholinergic tone are not severely altered until late in the disease process. These data cumulatively suggest that cholinergic dysfunction is a downstream consequence of some inciting neuropathology. Therefore, a modernized theory of the role of Ach-based signaling in AD extends beyond the involvement of the isolated neurotransmitter system itself and instead investigates the interactions between the cholinergic system and the pathological hallmarks of AD. Here the evidence is convincing, as all cardinal features of AD pathology demonstrate significant correlations with deficits in Ach-mediated neurotransmission and occur either in sync or before them. For example, many studies indicate that the density of senile plaques correlates negatively with ChAT activity in the brains of AD patients.^(442, 443) Albeit to less robust degree, similar correlations have been found for NFTs and cholinergic neuron degeneration in most cortical areas of the brain.^(428, 444, 445) While the mechanistic underpinnings of these correlations are the focus of subsequent sections exploring the molecular pathogenesis of AD, the finding of significance with respect to present day AD therapy is the finding that decreases in ChAT activity and the extent of cholinergic neuron loss in the nBM both correlate with the severity of dementia in AD.^(432, 444) Importantly, these early discoveries of a marked cholinergic deficit in the brains of patients with AD subsequently led to the study of therapeutically augmenting cholinergic activity. Yet, as just discussed, there are several critical points concerning the use of these drugs in AD. In an effort to highlight the validity of these concerns, modern guidelines for the treatment of AD using pharmaceuticals which target the basal forebrain cholinergic pathways will be reviewed. Additionally, data reflecting the real-life clinical efficacy of these drugs will be summarized by highlighting data collected during randomized control studies.

4.4 CURRENT ALZHEIMER'S DISEASE THERAPEUTIC GUIDELINES

To date, the main target of cholinergic therapy continues to be the use of compounds with anticholinesterase activity. This practice comes as a consequence of studies which indicate augmentation of Ach-mediated neurotransmission at other points in its synthesis/degradation pathways is not clinically impactful. Despite reductions in ChAT being the most consistent cholinergic abnormality in the brains of AD patients, investigators rationally ignored this potential drug target recognizing that this enzyme is not rate-limiting in the synthesis of Ach. As discussed previously, the availability of precursors for this enzyme, namely choline and Acetyl-CoA, dictate the rate at which Ach is synthesized in cholinergic neurons. Unfortunately, despite being appropriately grounded in cholinergic physiology, supplementation of choline containing compounds fails to produce improvements in psychological test measures. Notably, this is not due to an inability to raise plasma choline levels, as a 30 gram per day dose of lecithin increased plasma levels of choline 3-fold while a similar treatment with choline chloride produced a doubling of this Ach precursor in the blood.^(446, 447) Clearly, cholinergic precursor loading strategies must in some way fail to induce enzymatic activity. Most likely, increased plasma levels of choline do not necessarily translate to increased substrate availability in the brain. While strategies aimed at increasing cholinergic signaling at the presynaptic neuron have largely failed to modulate behavior, treatments aimed at eliciting a response at the post-synaptic neuron by employing cholinergic receptor agonists have demonstrated limited efficacy. For example, in one study employing a selective muscarinic receptor agonist in a cohort of 343 individuals with mild to moderate AD, a significant treatment effect on behavior was observed at high doses (225 mg per day for 6 months).⁽⁴⁴⁸⁾ Impressively, dose-dependent reductions in vocal outbursts, suspiciousness, delusions, agitation, and hallucinations were noted. End-point analysis also demonstrated improvements in treated cohort's memory, social behavior, mood, self-care, and overall function in daily living as assessed by the Nurses' Observational Scale for Geriatric Patients. Thus, unlike cholinergic precursor loading strategies, pharmacological manipulation of muscarinic signaling pathways may harbor therapeutic efficacy. However, one characteristic of this approach severely limits its clinical applicability; its heinous side-effect profile. In the high-dose arm of the study described for example, 52% of patients discontinued treatment because of adverse events. These dose-dependent adverse events were predominantly gastrointestinal in nature, with 76% of patients experiencing severe nausea and 52% having at least one episode of emesis in the high dose arm of the study. More severe adverse events such as syncope were also reported in 12.6% of patients on

the high dose regiment.⁽⁴⁴⁸⁾ To summarize these findings, cholinergic precursor loading strategies are associated with a negligible side effect profile but also fail to demonstrate clinical efficacy. By contrast, muscarinic agonists demonstrate reasonable therapeutic efficacy, but are clinically impractical as a consequence of their association with adverse events. As it so happens, cholinesterase inhibitors, which increase cholinergic transmission by inhibiting cholinesterase at the synaptic cleft, have a more favorable side effect profile and are of modest benefit in patients with AD. For this reason, of the four drugs currently utilized for the symptomatic treatment AD, three: Donepezil, Rivastigmine, and Galatamine are inhibitors of AchE activity.

Principally due to the inconsistencies associated with their efficacy, universal guidelines for the clinical utilization of AchE inhibitors in AD patients are not available. Instead, prescription of these drugs is based on the individual physician's preference and clinical evaluation. Generally speaking however, the clinical application of AchE inhibitors is guided by the results of extensive randomized control clinical trials. Important variables that have been addressed include: the degree of benefit associated with AchE therapy, the optimal duration of therapy, and the cost-effectiveness of treatment. Beginning with efficacy studies, the average benefit attributable to AchE inhibitor-based intervention in patients with dementia is characterized by small improvements in cognition and activities of daily living.^(449, 450) To illustrate this point, one group performed a meta-analysis of 14 studies measuring changes in cognitive outcome associated with AchE therapy by means of the 70 point AD assessment cognitive subscale. Irrespective of the specific AchE inhibitor employed in any given study, the treated AD patients displayed a 1.5-3.9 point improvement. At the surface these results favor the utilization of AchE inhibitors in AD patients. However, a methodological assessment of these studies reveals considerable flaws, like multiple testing without correction for multiplicity or exclusion of patients after randomization. As a consequence, the major conclusion reached by the referenced meta-analysis is not that AchE inhibitors are a valid therapy for AD, but that the scientific basis for their utilization is questionable.⁽⁴⁵⁰⁾ Importantly similar studies are in congruence with this conclusion. For example, in a second meta-analysis of 29 randomized, placebo-controlled trials, patients on AchE inhibitors improved 0.1 standard deviations on behavioral measures of daily life activities compared with placebo. Placed in a more accessible context, this effect would be similar to preventing a two months per year decline in a typical AD patient.⁽⁴⁵¹⁾ A separate meta-analysis presents the clinical utility of AchE inhibitors in a slightly different manner, concluding that 12 AD patients would require treatment for one to exhibit minimal improvement while one of the 12 patients would develop a treatment-related adverse event.⁽⁴⁵²⁾ Compounding the

complexity associated with interpreting such studies is the fact that the vast majority of the studies included in these meta-analyses were industry sponsored. In an effort to summarize findings devoid of this conflict of interest, in one of the only studies assessing AchE inhibitors not sponsored by the pharmaceutical industry to date, no significant benefit of Donepezil compared to placebo for the two primary endpoints, entry into institutional care and progression of disability, were found.⁽⁴⁵³⁾ Thus, with respect to the degree of benefit associated with therapeutic management of AD using AchE inhibitors, at best this approach yields very modest improvement in cognitive function while at worst its unwarranted utilization in AD generates unnecessary adverse events. Unfortunately, treatment response to AchE is unpredictable and evidence suggests that the response to AchE inhibitors may be quite variable, with as many as 30-50% of patients showing no observable benefit.^(454, 455) The counter-argument to this point stems from research indicating that up to 20% of patients show a greater than average response to AchE inhibitor therapy, exhibiting a clinically relevant >7 point improvement on the AD assessment cognitive subscale.^(456, 457) Yet another subpopulation of AD patients may actually get worse when started at AchE inhibitor therapy.^(458, 459) Taken together, these findings reinforce the importance of making clinical decisions on a per patient basis in a manner which takes into account each individual's clinical response and side-effect profile.

That said, a treatment trial with a cholinesterase inhibitor is typically employed for patients with mild to moderate cognitive impairment (MMSE 10 to 26). In a typical 8-week treatment trial, AchE inhibitors are prescribed at the maximum tolerated dose and a benefit/risk analysis is made by the patients' care team and family. Logically, treatment is continued if improvements are noted upon bedside testing and stopped if no improvement is noticed. As suggested at the beginning of this paragraph, randomized controlled trials investigating the efficacy of AchE inhibitors in mild to moderate AD show more consistent findings in favor of their use at this particular stage of the disease. While AchE inhibitors can be prescribed indefinitely, a significant degree of discord in the literature exists as to whether they are effective in advanced-stage AD. Notably, this issue is particularly relevant with respect to treatment duration, as physicians must decide when to taper patients off their AchE inhibitor regiment. As an example of the uncertainty which still surrounds AchE inhibitor use in end-stage AD, in a study of 208 nursing home residents, 70 percent of whom had a MMSE score <20 at baseline, therapeutic use of Donepezil was associated with improved clinical dementia rating (CDR) and MMSE scores at six months compared with placebo-treated patients. However, there was no difference between groups when assessed using the Neuropsychiatric inventory.⁽⁴⁶⁰⁾ In a similar study of 243 community-dwelling patients with severe AD

(MMSE score 1 to 12), the cognitive function of patients prescribed Donepezil improved when assessed via the Severe Impairment Battery (SIB), Clinician's Interview-based Impression of Change, and MMSE, but not others (activities of daily living, neuropsychiatric inventory, caregiver burden, resource utilization).⁽⁴⁶¹⁾ Other studies offer more convincing support for the use of AchE inhibitors in severe AD, with one study of 216 nursing home patients with severe AD (MMSE 1-10) reporting improvements in cognitive ability as assessed by the SIB.⁽⁴⁶²⁾ To summarize the therapeutic window of AchE inhibitors in AD, these drugs likely provide symptomatic relief in mild to moderate AD with symptomatic benefits lost with disease progression over time despite continued treatment.⁽⁴⁶²⁻⁴⁶⁴⁾ Seeking to extend the therapeutic window of AchE inhibitors, some investigators have looked into the efficacy of high-dose regimens of AchE inhibitors in moderate to severe AD. Such groups hypothesize that the loss of initial therapeutic benefit over time may be mitigated by higher doses of a cholinesterase inhibitor. And indeed there are studies which suggest that current dosing regimens have not maximized the therapeutic potential of AchE inhibition. In more detail, the currently approved doses of 5 and 10 mg/d of Donepezil have been associated with 20% to 30% inhibition of cortical AchE activity, respectively.^(465, 466) Recognizing the opportunity for improvement, a Japanese team placed 61 AD patients who had been receiving a stable dose of Donepezil 5 mg/d on an increased dosing regimen of 10 mg/d for 24 weeks. Over this time period, treatment with high-dose AchE inhibitor was more effective in preventing deterioration in severe AD as measured using the Revised Hasegawa Dementia Scale and Mini-Mental State Examination (MMSE).⁽⁴⁶⁷⁾ Inspiringly, these findings have been recapitulated to some degree in a much larger cohort and scientifically robust manner. In this double-blinded study conducted across 219 sites across the globe, 1371 patients were randomly assigned to either remain on their standard-dose of Donepezil (10 mg) or increase to a 23 mg/day regimen.⁽⁴⁶⁸⁾ Co-primary effectiveness measures were changes in cognition and global functioning, as assessed using least squares mean changes from baseline (LSM [SE] Δ) scores on the Severe Impairment Battery (SIB; cognition) and the Clinician's Interview-Based Impression of Change Plus Caregiver Input scale (CIBIC+; global function rating) overall change score (mean [SD]). After 24 weeks of treatment, the LSM (SE) Δ in SIB score was significantly greater with Donepezil 23 mg/d than with Donepezil 10 mg/d (+2.6 [0.58] vs +0.4 [0.66], respectively; difference, 2.2; $P < 0.001$). Consistent with other studies in its inconsistency, the between-treatment difference in CIBIC+ score was non-significant (4.23 [1.07] vs 4.29 [1.07]).⁽⁴⁶⁸⁾ Still, the authors conclude that in moderate to severe AD, higher doses of Donepezil are associated with greater benefits in cognition compared with standard-doses. In post hoc analysis, the authors go on to note that patients with more advanced AD appear to benefit

from high-dose regimens of Donepezil more so than their less severely demented counterparts. However clearly, as recognized by the investigators of all studies referenced, this observation requires additional work to be validated.

As a direct consequence of the uncertainty surrounding the clinical efficacy of AchE inhibitors, as evidenced by the studies just described, data on the cost-effectiveness of current AD treatments is especially challenging to interpret. Nevertheless, available treatments for AD need to be evaluated in order to determine whether the clinical benefits justify their additional costs. Critically, data on this issue has demonstrated a profound ability to impact clinical practice, as data suggesting AchE inhibitors lose efficacy in late-stage AD patients has led to recommendations in the UK suggesting the restriction of treatment, on cost-effectiveness grounds, for patients with moderate to severe cognitive decline. In an effort to steer policy makers into the appropriate choice, numerous investigators have generated models of cost-effectiveness for AchE inhibitor treatment in virtually all stages of AD. However, the major limitation of these types of studies is that the magnitude of cost offset and of the effect of Ach Inhibitor therapy on health-related quality of life depends heavily on the model's assumptions about the duration of the drug effect, where we just learned internally consistent and controlled data are lacking.⁽⁴⁶⁹⁾ In an effort to limit the impact of this confound, the best constructed studies estimate the duration of drug effect from randomized controlled clinical trials. For example, employing efficacy data from 2 phase III clinical trials of Rivastigmine in this manner, one group has generated a hazard model of disease progression to estimate long-term differences in cognitive functioning between patients receiving Rivastigmine and patients receiving no treatment.⁽⁴⁷⁰⁾ At the conclusion of their study, AchE inhibitor therapy was estimated to delay the transition to more severe stages of AD by up to 188 days for patients with mild AD after 2 years of treatment. For patients with mild-to-moderate and moderate disease, the delay in AD progression attributable to AchE inhibitor therapy was estimated to be 106 and 44 days, respectively. Combining these estimates with data on health-cost obtained from other cross-section studies, the authors report an estimated average daily cost savings ranging from a low of \$0.71 (Canadian dollars) per patient per day after 6 months of treatment to a high of Can \$4.93 (Canadian dollars) per patient per day after 2 years. Placing this data into context, this study and others suggest that on average, treatment with AchE inhibitors yields savings in the direct cost of caring for AD patients that exceed the cost of the drug after 2 years of treatment.⁽⁴⁷⁰⁾ More recent studies have leveraged the advantage of improved literature on the topic of therapeutic efficacy for AchE inhibitors and generally agree with the assessment of early studies, suggesting that after 2 years of treatment in patients with mild AD, incremental cost-effectiveness for direct medical costs is around 20,353 euro/QALY.⁽⁴⁷¹⁾ Therefore, although not definitive, simulations of

cost-effectiveness suggest that health benefits and cost savings justify the use of AchE inhibitors when used to treat mild to moderately severe AD. However, largely in congruence with data of treatment efficacy in late-stage AD, these same studies also indicate that both benefits and savings may be greatest when treatment is started while patients are still in the mild stages of AD. And of course, other studies employing only slightly different methods have reached the opposite conclusion that benefits are below minimally relevant thresholds even in patients with mild AD.

And so, once again, the AD literature is split with respect to the efficacy of AchE inhibitors, be it in mild or advanced stage AD. As a consequence, the appropriate duration of AchE inhibitor therapy in the clinic is also unguided by studies of robust scientific merit. Based only on the relative abundance of conclusions, it is generally agreed upon in the field that AchE inhibitors offer the most therapeutic benefit when initiated early. While a definitive conclusion on the therapeutic value of AchE inhibitors in AD undoubtedly requires more attention, a comparison of these efficacy studies with others performed in patient populations with differing subtypes of dementia reveals a few additional points of interest. First, to date, the vast majority of trials have not provided support for the use of AchE inhibitors in preventing progression of mild cognitive impairment to dementia.⁽⁴⁷²⁻⁴⁷⁵⁾ At first glance, these findings seem to be contradictory to the conclusion that early intervention is the most appropriate treatment interval for cholinergic therapeutics. However instead, this finding may simply reflect differences in the pathogenesis underlying cognitive deficits in MCI as compared to AD. Alternatively, the failure of cholinergic modulators to influence the progression of MCI highlights another open question in the field. Namely, whether AchE inhibitors can induce negative feedback on cholinergic tone, thereby themselves compounding cholinergic decline.^(476, 477) In congruence with the first hypothesis, all subtypes of dementia demonstrate a unique therapeutic response to AchE inhibitor therapy. In summary of the relevant findings, similar benefits are seen with AchE inhibitors in patients with vascular dementia as compared to AD.^(478, 479) In contrast however, cholinesterase inhibitors appear to show greater efficacy in patients with diffuse Lewy body dementia and no efficacy in Huntington disease.^(480, 481) Importantly, these results hint at the existence of distinct etiologies underlying cognitive deficits observed in each disease, each with their own varying susceptibility to the modulatory effects of cholinergic input and as a consequence therapy. Relating this theory to disease back to AD pathology, in general, traditional pharmacological replacement strategies are unlikely to succeed in AD because so many neurochemically distinct systems degenerate, and because structures such as the hippocampus and cortex, which are among the presumed postsynaptic targets for cholinergic drugs, are themselves damaged in this condition. As stated, for these reasons most experts agree

that more fertile grounds for cholinergic based therapies exist in more mildly impaired, more neurologically intact populations.⁽⁴⁰³⁾ An extension of this expert opinion is that research programs aimed at identifying the etiology of the degenerative processes and preventing their progression by various means may be more fruitful long-term strategies.

4.5 USE OF MEMENTINE IN ALZHEIMER'S DISEASE

As a comprehensive understanding of the molecular pathogenesis is still lacking, opinions vary widely with respect to viable drug targets that will influence the etiology of the degenerative processes in AD. Put differently, there is very little consensus as to which pathological abnormalities lies upstream in the pathogenesis of AD and as a consequence, it is difficult to predict which degenerative processes should be of highest therapeutic interest. As stated, numerous lines of evidence suggest that deficits in cholinergic signaling can induce cognitive dysfunction, a finding which has been used to justify the use of AchE inhibitors in AD. However, the mild degree and inconsistent nature of improvements in cognition attributable to cholinergic therapy seemingly confirm the presence of contributory degenerative processes. Further, there is no evidence to suggest that AchE inhibitor therapies perturb the degeneration of cholinergic neurons in the basal forebrain system. Instead this treatment approach simply supplements cholinergic tone to compensate for accruing deficits in cholinergic signaling secondary to loss of nBM projections. Thus, not only do AchE inhibitor therapies fail to qualify as disease modifying treatments, they also fail to prevent the progression of the degenerative process they posit as central to the cognitive deficits in AD. In congruence with the hypothesis that preventing the progression of degenerative processes may prove more fruitful with respect to the long-term treatment of AD, investigators have leveraged the N-methyl-D-aspartate (NMDA) receptor antagonist Memantine (Namenda/Axura in Europe).

Mechanistically unique among the currently quartet of FDA approved drugs for the treatment of AD, Memantine (Namenda/Axura in Europe), is an N-methyl-D-aspartate (NMDA) receptor antagonist devoid of any direct effect on cholinergic signaling. Instead, it is purported to prevent cognitive decline via a neuro-protective mechanism. As discussed, NMDA receptors are highly integrated into the neural circuitry of the hippocampus and cortex, which under physiological conditions; serve as the principal neuronal substrates of learning and memory in the brain. Notably, glutamate is the

principal activator of NMDA receptors as well as the principal excitatory neurotransmitter used by these cortical and hippocampal memory systems. Therefore, succinctly, the rationale behind use of an NMDA receptor antagonist in AD stems from the fact that excessive NMDA stimulation can lead to glutamatergic excito-toxicity. Synthesizing this background information into a mechanistic hypothesis, the purported utility of Memantine in AD is the retardation of neuron loss in the hippocampus and cortex secondary to glutamatergic excito-toxicity. In addition, by shifting glutamatergic signaling closer to baseline, the physiologic function of remaining neurons could be restored, resulting in symptomatic improvement.⁽⁴⁸²⁾ While the literature behind this rationale is by far the most widely recognized, it is important to note that other properties of Memantine may also be relevant to its efficacy in AD. For instance, two of the properties most likely to be contributory to improvements in cognition include its ability to enhance LTP⁽⁴⁸³⁾ and decrease tau hyper-phosphorylation.⁽⁴⁸⁴⁾ Regardless of the significance of these additional mechanisms, efficacy data suggests that Memantine is of modest benefit in patients with moderate to severe AD; a finding which distinguishes it further from AchE inhibitor-based therapies which demonstrate highest efficacy in early-stage disease. Exemplifying this evidence, in a 28-week study of 252 moderately to severely impaired AD patients (MMSE scores of 3-14); Memantine therapy significantly reduced cognitive deterioration on multiple scales of clinical efficacy as compared to placebo.⁽⁴⁸⁵⁾ Similarly, the addition of Memantine to AchE inhibitor regimens in a cohort of 295 patients with moderate to severe AD proved more effective at maintaining MMSE scores as compared to treatment with just AchE inhibitors alone.⁽⁴⁸⁶⁾ Of course, publications which dispute these findings are available for review, some of which suggesting that the continuation of AchE inhibitor therapy may be of higher therapeutic value than the addition of Memantine.⁽⁴⁸⁷⁾ In this discordant study however, only patients who had already received Donepezil for more than 3 months were recruited. Significantly, this recruiting method represents an experimental confound by generating a survivorship bias in which those patients whom Donepezil had an unfavorable side-effect profile or failed to improve cognition could never be recruited.⁽⁴⁸⁸⁾ Thus, in congruence with the majority opinion, Memantine was approved by the FDA in October 2003 for use in patients with moderate to severe AD, making it the only currently approved drug with demonstrated efficacy in late-stage AD.

Fortunately with respect to its clinical use, this drug is also unique in that it carries a negligible side-effect profile. In fact, in some studies, the incidence of adverse events for patients on Memantine was even lower than for placebo.^(485, 489) Importantly this minimal side-effect profile has been used to argue in favor of its use earlier in the AD course. However, with respect to Memantine efficacy early in disease progression, there is little, if any, evidence to

support its use in patients with milder AD. In a systematic review of data pooled from three unpublished studies of Memantine treatment in mild to moderate AD, intention to treat analysis indicated a very small but statistically significant beneficial effect for Memantine at six months on cognition (<1 point on the 70-point ADAS-Cog) but no effect on behavior or activities of daily living. While this result admittedly presents a mixed conclusion, a subsequent review of three additional trials including 431 patients with mild AD (MMSE 20 to 23) failed to recapitulate even a small degree of impact on cognitive function, finding no substantial benefit with Memantine.⁽⁴⁹⁰⁾ Additional studies are clearly needed, but the current consensus in the field is that the prescription of Memantine should be restricted to advanced disease. Notably this restriction to late-stage AD means that Memantine is typically employed as a combination therapy rather than a monotherapy, as patients are typically already on a regiment of AchE inhibitors by the time they reach the advanced stages of AD. Predictably, the literature on the addition of Memantine to an established regiment of AchE inhibitor is mixed. In 322 patients with moderate to severe AD (MMSE 5 to 14), treatment with Memantine plus Donepezil resulted in significantly better outcomes than placebo plus Donepezil on measures of cognition, activities of daily living (ADLs), global outcome, and behavior.⁽⁴⁸⁹⁾ However in an equally powered study, no significant benefits of the combination of Memantine and Donepezil over Donepezil alone were noted.⁽⁴⁸⁶⁾ Given these inconsistencies even in advanced-stage AD, it is not surprisingly that in a cohort of 433 mild to moderate AD patients, addition of Memantine to a regiment of AchE inhibitor produced no significant improvement.⁽⁴⁹¹⁾ And so again, the only consistent finding with respect to the efficacy of combination therapy with Memantine as compared to monotherapy with AchE inhibitors alone is that if combination therapy does provide a modest benefit, it is likely only observable in more advanced stage disease.

Condensing all of the data presented on the topic of modern treatments for AD into a practical algorithm for disease management.⁽⁴⁹²⁾ Pharmacologic therapy using AchE inhibitors should be initiated upon diagnosis of AD, as these drugs exhibit their maximum clinical impact early in the disease course. As a consequence, all of the currently available cholinesterase inhibitors (Donepezil, Galantamine, and Rivastigmine) are indicated for mild-to-moderate AD and are of equal therapeutic potency. Patient or caregiver preference, ease of use, tolerability, and cost should dictate which of these drugs are used. Treatment should be individualized; with patients being switched from one AchE inhibitor to another if the initial agent is poorly tolerated or ineffective. Especially in early-stage disease, the literature supports the conclusion that these drugs improve cognitive function, global clinical status and patients' ability to perform activities of daily living. Additionally, there is also evidence for reduction in emergence of behavioral symptoms with AchE inhibitor therapy. As

patients progress to more severe stages of AD, Memantine may be introduced on top of the patients existing AchE inhibitor regimen without worry of side effects. Most critically, clinicians must regularly monitor symptoms and behaviors, manage comorbidities, assess function, and educate caregivers on how to obtain access to relevant information and support. As emphasized by this summary, the main targets of cholinergic therapy continue to be the use of drugs with anticholinesterase activity despite their inability to overcome the cognitive deficits associated with the cholinergic hypo function seen in AD. Today, it has become evident that dysfunction of the cholinergic projection system is mainly a later stage event in the development of AD. While there is in fact phenotypic dysregulation of cholinergic signaling in early AD, no frank loss of neurons early in the basal forebrain system are appreciated. Correlating nicely with these pathogenic features, AchE inhibitor therapy appears more useful early rather than late in the course of AD. Looking forward, compounds need to be developed not only to enhance cholinergic activity, but preferably to slow or prevent the degenerative processes underlying the eventual extensive loss of CBF neurons in AD. Of course, the ultimate goal must be the discovery and clinical evaluation of disease-modifying treatments.

CHAPTER 5 MOLECULAR ETIOLOGY OF ALZHEIMER'S DISEASE

For well over two decades, the amyloid cascade hypothesis of AD has dominated with respect to its influence on research conducted in academia and the pharmaceutical industry. Distilled to its simplest form, this hypothesis synthesizes histopathological and genetic data, and posits that the deposition of the amyloid- β ($A\beta$) peptide in the brain parenchyma initiates a sequence of events that ultimately lead to AD dementia. An extension of this hypothesis is that the NFTs, cell loss, vascular damage, and dementia associated with AD pathology are a downstream consequence of $A\beta$ -pathology.⁽⁴⁹³⁾ Two seminal events in AD research are predominantly responsible for the generation of this cornerstone hypothesis: (i) the characterization of $A\beta$ plaques by Alois Alzheimer in 1907 in the first described case of AD⁽³¹¹⁾ and (ii) the discovery that AD could be inherited in an autosomal dominant fashion.⁽⁴⁹⁴⁾ Amazingly, the influence of Alois Alzheimer's initial characterization of AD is still readily observed today, as the neuropathological hallmark of AD remains the amyloid plaque and identification of these lesions is required for pathological confirmation of AD in all generations of published guidelines.⁽¹²⁵⁾ Since the discovery that aberrantly cleaved $A\beta$ -peptide was the primary constituent of these lesions, $A\beta$ plaques have been posited as central to AD pathogenesis.⁽⁴⁹⁵⁾ Admittedly this discovery in no way constitutes scientific evidence of a central role for $A\beta$ plaques in the pathogenesis of AD. Nevertheless, this early discovery inarguably placed $A\beta$ plaques at the center of attention with respect to AD pathology, where it has remained since. The fact remains however that this initial discovery does nothing to exclude the possibility that $A\beta$ plaques may simply represent a downstream consequence of some inciting etiology. In discordance with this possibility however, a seemingly irrefutable amount of genetic evidence supports a central role for $A\beta$ peptides in the pathogenesis of at least some forms AD. This data, as well as work done in humans, animal models, and in vitro is the focus of this chapter. However in addition to providing the mechanistic underpinnings underlying $A\beta$ -centric models of AD, this section will also provide the necessary background to address the most commonly levied criticisms of this model. Though expanded on later, it warrants mentioning here that the failure of $A\beta$ -targeted therapies in clinical trials has caused some in the field to question the role of amyloid- β and amyloid deposition in AD. While the primary focus of this chapter will be evidence supporting $A\beta$'s central role in AD pathogenesis, subsequent sections will address these criticisms directly.

5.1 AMYLOID PROCESSING

Before the evidence for and against A β -centric hypotheses of AD pathogenesis can be appropriately presented, a generalized review of the physiological processes behind the production and clearance of the A β peptide is warranted. As early as the 1980's, researchers intent on purifying amyloid plaques discovered they were comprised principally of A β peptides 40-42 amino acids in length that aggregated as oligomers.⁽⁴⁹⁶⁾ Later, gene cloning and cDNA analysis of the monomer A β proteins would lead to the discovery that this peptide family was derived from the proteolytic cleavage of a larger precursor which was subsequently named the amyloid precursor protein (APP).⁽⁴⁹⁷⁾ The *APP* gene contains 18 exons and gives rise to at least eight APP protein isoforms by alternative splicing of exons 7, 8, and 15.⁽⁴⁹⁸⁾ Of note, the APP isoforms mainly expressed in neurons always contain exon 15 and are more amyloidogenic than the non-neuronal forms. The longest APP isoform is a single transmembrane-spanning polypeptide of 770 amino acid residues with a long extracellular N-terminal segment and a short C-terminal tail.⁽⁴⁹⁹⁾ However the AP isoform most commonly expressed in neurons occurs as a result of alternative splicing of exon 7. This generates one polypeptide of 695 amino acids in length whereas alternative splicing of exon 8 results in a polypeptide of 751 amino acids which is also expressed in the brain, but more commonly in non-neuronal tissues.⁽⁵⁰⁰⁾ Structurally, APP is a membrane bound cell-receptor which contains the A β peptide sequence in the extracellular domain.⁽⁴⁹⁹⁾ Unfortunately, the function of APP is still poorly characterized. In-vitro studies suggest that secreted APP can function as an autocrine factor by stimulating cell proliferation and adhesion.^(501, 502) Similarly, APP secretion has been shown to support nerve growth factor-induced neurite outgrowth in PC12 cell culture.⁽⁵⁰³⁾ Still other studies have implied a role for APP in signal transduction⁽⁵⁰⁴⁾ or in the regulation of transcription via interactions with other proteins such as Fe 65 and histone acetyltransferase Tip60.⁽⁵⁰⁵⁾ Fortuitously, more is known about the proteolytic cleavage pathways of APP and their down-stream end-products. Simplified for the sake of clarity, proteolytic processing of APP can occur via an amyloidgenic (pathogenic) or non-amyloidgenic (benign) pathways. Importantly, determination of APP's cleavage fate occurs following transport to the cell membrane in a process chaperoned by the intracellular adaptor protein sorting nexin 17 (SNX17).⁽⁵⁰⁶⁾ Once embedded in the plasma membrane, the initial proteolytic cleavage of APP by α - or β - secretase commits the process to a benign or amyloidgenic product, respectively.¹⁹ In more detail, cleavage of APP by α -secretase, a membrane-bound constituent of the disintegrin and metalloprotease (ADAM) family of proteins, releases a soluble fragment termed sAPP α into the extracellular space.⁽⁵⁰⁷⁾

Additionally, this generates a C-terminal fragment C-83, 83 amino acids in length which is abruptly cleaved by γ -secretase at a cleavage site embedded in the intramembrane space. Of great significance when discussing the genetic evidence supporting amyloid-centric models of AD, the γ -secretase enzyme, though not fully characterized, consists at minimum of four individual proteins: presenilin, nicastrin, anterior pharynx-defective 1 (APH01), and presenilin enhancer 2 (PEN-2).^(508, 509) As a result of γ -secretase mediated intramembranous cleavage, two subsequent fragments are generated from C-83; the APP intracellular domain (AICD) which is released in the cytosol and p3 which are released into the extracellular space. Of note, amyloidgenic processing of APP also results in the cytosolic release of AICD. However, as alluded to by its name, the end result of amyloidgenic processing of APP is the production of A β peptides in lieu of the p3 fragment. To explain how this difference in end-products arises, it is critical to note that the first proteolytic cleavage of APP in the amyloidgenic pathway is mediated by β -secretase or β -site APP converting enzyme (BACE). Like its counterpart α -secretase, this enzyme also cleaves APP at a portion of the peptide contained in the extracellular space. However, the β -site (between residues 671 and 672 of APP) is 18 amino acids closer to the *N*-terminal of the protein as compared to the α -site, resulting in the release of a much shorter soluble APP- β (sAPP β) fragment and longer C-terminal fragment.^(510, 511) Further differentiating β -secretase from its non-amyloidgenic counterpart, cleavage of APP by BACE occurs in the endosomal-lysosomal compartment as opposed to the cell membrane.⁽⁵¹²⁾ Analogous to the C-83 fragment produced in non-amyloidgenic APP processing, the C-terminal fragment of 99 amino acid residues (C-99) generated following β -secretase cleavage remains membrane bound until cleaved by γ -secretase. Cleavage of C-99 by γ -secretase occurs in the vicinity of residue 712 and as stated, results in the release of cytosolic AICD peptide and A β peptide.

Of importance, commitment of APP to the non-amyloidgenic pathway secondary to α -secretase cleavage nullifies the possibility of amyloidgenic processing because the α -site of APP is situated between that of β - and γ -secretases.⁽⁵¹³⁾ Put slightly differently, cleavage of APP by α -secretase results in a C-terminal fragment which is too short to generate A β peptides upon subsequent cleavage by γ -secretase. While this competitive model of α - and β -secretase cleavage of APP makes sense intuitively, a consensus as to whether a physiological imbalance of these pathways contributes to the pathology of AD has not been reached. Arguing against such a hypothesis, inhibition of α -secretase does not increase BACE1 activity *in vitro*.⁽⁵¹⁴⁾ However, this does not exclude the possibility that disruption of non-amyloidgenic processing contributes to AD pathophysiology, to the contrary, a strong body of evidence now suggests that non-

amyloidogenic cleavage of APP is imperative to the maintenance of neuronal growth and function. For example, sAPP α has been shown to have neurotrophic and neuro-protective properties, promoting neurite expansion, synapse production and cell adhesion among various other functions. Additionally, evidence suggests that AICD has a role in modulating p53 expression, activating caspase 3, and maintaining cellular actin dynamics.⁽⁵¹⁵⁻⁵¹⁷⁾ Still, the underlying difference between the two cleavage pathways of APP is the release of A β and p3 fragments. To date, the shorter p3 bi-product of APP cleavage has no known function. As loss of p3 function is seemingly benign, the significance of its generation instead lies in its inability to form stable oligomeric intermediates like those of A β .⁽⁵¹⁸⁾ Like several other proteins associated with neurodegeneration, A β peptides have the ability to self-associate, and can form an array of different assemblies ranging from dimers all the way to aggregates of fibrils.^(519, 520) Importantly, each A β peptide species has its own relative propensity to self-aggregate. In this regard, accumulation of A β_{40} is of minimal concern. In contrast, as a consequence of its two extra hydrophobic residues, alanine and isoleucine, A β_{42} demonstrates a remarkable propensity to self-aggregate, even at low concentrations. Rationally, it was assumed that A β toxicity is mediated by fibrils similar to those present in amyloid plaques. In part due to the poor correlation between A β plaque distribution and neurodegenerative changes however, this assumption has been challenged with more recent data suggesting that non-fibrillar, water-soluble oligomeric assemblies of A β may be the primary toxic species of A β .⁽⁵²¹⁻⁵²³⁾ Of note, the term A β peptide is used here and in the literature to represent a range of peptide products of APP cleavage ranging from 38-42 amino acid residues. Although all are products of γ -secretase cleavage, it is critical to note that each may harbor a unique pathogenicity, a hypothesis which will be explored in full detail below. Before this however, we return to the topic of seminal findings which sparked the creation of amyloid-centric hypothesis of AD.

5.2 GENETIC EVIDENCE SUPPORTING AMYLOID-CENTRIC HYPOTHESES OF AD

As noted in this chapter's introduction, the emergence of amyloid centric hypotheses of AD can be credited in large part to genetic discoveries linking perturbations in APP processing to the development of AD. These findings, to be outlined in this section, are of special significance because they were among the original sources of evidence cited by the authors of the very first iteration of the amyloid cascade hypothesis.⁽⁴⁹³⁾ In homage to its significance in this regard, work highlighting the similarities in AD and Down's syndrome (DS) pathogenesis will be presented first. Next, leveraging the

outline of APP processing provided above, mutations in APP which promote the AD phenotype in humans and animal models will be reviewed. Continuing with this theme, genetic variations in β - and γ -secretase which promote the amyloidgenic cleavage of APP will be summarized. Lastly, the relatively recent discovery in APOE and its effect on the development of AD pathology will be highlighted.

5.2.1 *Down's Syndrome & AD*

Cited by J. Hardy and G. Higgins in their original description of the amyloid cascade hypothesis in 1992, parallels between the pathology of AD and DS were among the strongest lines of evidence supporting a role for APP processing in the pathogenesis of AD.⁽⁴⁹³⁾ Briefly, DS is a condition in which a person inherits an extra full-length or partial copy of the 21st human chromosome resulting in a broad range of disabilities. Of particular relevance to AD however, studies suggest that approximately 75% of DS patients over the age of 65 have AD.^(524, 525) This represents a 6-fold increase in AD prevalence in DS patients as compared to the normal population. Alarming, autopsy studies reveal that by age 31, $A\beta_{42}$ deposits are universal in the brains of individuals with Down's syndrome.⁽⁵²⁶⁾ Furthermore, this rapid accrual of amyloid in the brain has been shown to be detectable in DS patients as young as 12 years of age.⁽⁵²⁶⁾ Just as in sporadic AD, the brains of DS patients exhibit $A\beta$ deposition in blood vessel walls and as extracellular deposits. In general, especially with respect to $A\beta$ plaque distribution, the neuropathology of DS is quite similar to AD. In fact, only a few differences between DS and AD with respect to amyloid neuropathology have been noted. The first comes from PET-imaging studies which leverage amyloid-specific tracers. This work suggests there may be regional differences in the pathological progression of DS and AD, with early accumulation of amyloid in the frontal cortex in DS rather than in the temporal cortex.⁽⁵²⁷⁾ Additionally, less robust progression of neuronal loss in DS compared with AD has been reported. Perhaps contributing to these differences however, these studies note that the brains of DS patients start out with fewer neurons, suggesting a lower brain "reserve" to compensate for accruing pathology, especially in the frontal and temporal cortices.⁽⁵²⁸⁾ Lastly, as noted earlier, amyloid pathology occurs decades earlier in DS as compared to sporadic AD patients, suggesting that if a shared neuropathological etiology exists, it is accelerated in DS.^(527, 529) In an attempt to describe how these findings led to the initial proposition of the amyloid cascade hypothesis, consider the following historical context. Operating under the assumption that the high prevalence of AD in DS is secondary to a shared pathogenic mechanism, initial linkage studies mainly targeted chromosome 21. The general hypothesis of these studies was that in DS, AD is

caused by over-representation of a gene on chromosome 21 as a result of the trisomy 21, while in AD a mutation in that same gene leads to the production of an abnormal protein or to the overproduction of a normal protein. In congruence with this hypothesis, later studies conducted in early-onset AD families would reveal linkage to genetic markers in the region 21q11.2-21q21.⁽⁵³⁰⁾ Serendipitously, at approximately the same time APP was characterized and localized to the same chromosomal region.⁽⁴⁹⁷⁾

In support of the concept of a conserved neuropathological etiology between AD in DS and AD, the key neuropathological features in the former closely mirror those described in the sporadic variant of AD. Beyond similarities in the regional distribution of A β plaques, patients with DS also accumulate NFTs slightly later, with the hippocampus, entorhinal cortex, and neocortex being among the most highly affected regions, just like in AD.⁽⁵³¹⁾ One point that confirms amyloid pathology is exacerbated by the DS phenotype is the finding that both A β and NFT densities are increased in DS as compared to AD.⁽⁵³²⁾ Other similarities between AD and DS neuropathology include increased build-up of plaque-associated proteins, microglial activation, astrogliosis, inflammation, and oxidative stress.⁽⁵³³⁻⁵³⁵⁾ This large degree of overlap in the neuropathology of DS and AD strongly supports that some common pathogenic mechanisms may exist. This point is of critical significance because unlike AD, the molecular etiology of DS is well-established to be secondary to partial or complete trisomy 21. Because chromosome 21 includes the gene for APP, the molecular etiology of DS directly promotes amyloid-centric hypothesis of AD pathogenesis. The argument goes as follows. Since patients with DS are at elevated risk for developing AD of a very early onset, the molecular etiology of DS must accelerate a key pathological mechanism of AD. As the molecular etiology of DS is characterized by an increase in the number of genetic copies of APP, perturbations in APP processing to generate A β peptides must be central to the pathogenesis of AD. However this is not the only finding in DS patients which promotes an amyloid-centric model of AD pathogenesis. Assuming a shared neuropathological etiology of AD in DS patients and the general public, the finding that NFTs accumulate later in DS as compared to A β plaques strongly supports amyloid-centric hypotheses of AD over models which favor tau. Furthermore, the finding that NFTs and A β plaques are both increased in DS patients implies there may be a link between A β deposition and NFT formation. If this were not the case, A β plaque density would be expected to increase as a consequence of increased availability of the APP substrate, but no effect on NFT density would be predicted. Of course, *APP* is not the only gene triplicated in DS and therefore it is very likely that one or more of the roughly 635 genes on chromosome 21 (according to European Bioinformatics Institute) may also play a role in producing the AD

phenotype. Highlighting the importance of APP though, in a DS patient with only partial trisomy 21 (missing *APP* and several other genes), there was no dementia or AD pathology at autopsy.⁽⁵³⁶⁾ On the basis of this case study and the findings summarized above, in the opinion of many investigators, perturbations in APP processing must play some role in the development of AD pathology in DS.

While much of the data summarized to this point is significant in that it partially inspired the generation of the amyloid cascade hypothesis, it is important to note that these early findings do not fully represent the insight garnered from the parallel study of AD and DS. Motivated by the similarities between AD and DS pathology already described, many groups have leveraged mouse models of DS in order to characterize the pathophysiological processes underlying AD. The most widely used mouse model for studying DS to date, the Ts65Dn mouse model, is trisomic for 88/161 of the ortholog protein coding genes on human chromosome 21.⁽⁵³⁷⁾ Lending credibility to this approach, the phenotype of Ts65Dn mice is remarkably similar to changes observed in AD, characterized by a progressive deterioration of working memory, cholinergic deficit in the basal forebrain, and neuroinflammation.⁽⁵³⁸⁾ However, one limitation that severely limits the utility of DS mouse models for researching AD and potentially undermines the classical amyloid cascade hypothesis is its failure to replicate the pathological hallmarks of AD; NFTs and A β plaques.⁽⁵³⁹⁾ Three potential interpretations of this deficiency have been proposed from an amyloid-centric perspective.⁽⁵⁴⁰⁾ First, the current generations of DS mouse models differ genetically from human DS patients in two ways. First, mouse models like Ts65Dn lack trisomy for a number of genes located on human chromosome 21 which demonstrate functional features that are of compelling relevance to AD. Take for example astrocyte-derived growth factor S100 β . Considered a component of the neuro-inflammatory response, in addition to the promotion of neurite degeneration, this protein has been implicated in the formation of neuritic plaques.⁽⁵⁴¹⁾ Secondly, the Ts65Dn mouse model is also trisomic for a small centromeric segment of mouse chromosome 17 that is not orthologous to human chromosome 21. Of the 50 genes contained in this segment, several code for dynein light chains whose increased dosage could influence endosomal transport and thus alter APP processing.⁽⁵⁴²⁾ Lastly, the ability of A β peptide to aggregate is increased in humans as compared to DS mice as a consequence of a three amino acid difference in the A β sequence.⁽⁵⁴⁰⁾ Thus, the lack of A β plaques in DS mouse models, and as a consequence NFTs, may be interpreted not as a failure of the amyloid cascade hypothesis but as a consequence the deficiencies in mouse models with respect to their similarity to human DS. Of significance, the lack of pathological AD hallmark lesions in AD has not limited the utility the DS models but has instead been leveraged to investigate A β -

independent mechanisms of neurodegeneration. Of highest relevance to the cognitive deficits observed in AD, DS mouse models have provided a powerful tool for studying the neurodegenerative mechanisms underlying the loss of cholinergic neuron populations in the basal forebrain. Briefly, in mouse models of DS, APP overexpression results in endosomal enlargement and dysfunction. Exemplifying an A β -independent mechanism which still supports the amyloid cascade hypothesis, endosome enlargement has been shown to be mediated specifically by the β -cleaved carboxyl-terminal fragment (β -CTF) of APP.⁽⁵⁴³⁾ Not surprisingly given the role of endosomes in cellular transport, DS mouse models also exhibit deficits in the retrograde transport of nerve growth factor (NGF) and brain-derived neurotrophic factor (BDNF) signaling. The hypothesis derived from these findings is that failure in growth factor support secondary to impaired endosomal transport is central to the neurodegeneration of basal forebrain cholinergic neurons.⁽⁵⁴⁴⁾ Lending credibility to this work, reductions in the high-affinity NGF receptor, trkA, are observed in basal forebrain cholinergic neurons of Ts65Dn mice, DS patients, and individuals with AD.⁽⁵⁴⁵⁾ In summary, although animal models of DS do not produce plaques and tangles, this does not exclude the possibility that the pathogenic mechanisms underlying DS deficits may contribute to cell loss downstream from these pathological changes. Indeed, the exploration of similarities and differences between DS and AD animal models may point to important aspects of underlying biochemical and structural changes that drive the development of AD.

5.2.2 APP Mutations as Support for Amyloid-centric Hypotheses of AD

As reviewed in a previous chapter, a subset of early-onset forms of AD are inherited in an autosomal dominant fashion and as a consequence are classified as Familial variants of AD (FAD). Still among the strongest lines of evidence supporting amyloid centric hypotheses of AD pathogenesis to date, mutations of the APP gene are robustly linked to early-onset variants of AD.^(494, 546) In addition to the DS literature just presented, yet another discovery made in a distinct neuropathology spurred the discovery of APP mutations in AD. Published in 1990, a Glu693Gln mutation in APP was found in families suffering from hereditary cerebral hemorrhage with amyloidosis of the Dutch type (HCHWA-D).⁽⁵⁴⁷⁾ A rare autosomal dominant disorder found in a few families in the Netherlands, HCHWA-D is characterized by recurrent cerebral hemorrhages secondary to excessive deposition of A β in the walls of blood vessels in the brain.⁽⁵⁴⁸⁾ Though the

degree to which the pathogenic processes underlying HCHWA-D are represented in AD is still under investigation, this discovery did demonstrate that mutations in APP can incite A β deposition. Encouraged by this finding, later studies would perform mutation analysis of APP in early-onset AD families to yield the evidence to be summarized in the following paragraphs.

Notable for being among the first mutations in APP ever discovered, sequence analysis of exons 16 and 17, which encode the A β peptide sequence, revealed a Val717Ile mutation in APP in families with early-onset AD.⁽⁴⁹⁴⁾ Underlining the causative nature of this mutation, the APP Val717Ile mutation is the most prevalent mutation in APP and has been found in several families of unique ethnic backgrounds. Since this discovery, the number of published pathogenic APP mutations has skyrocketed from just 7 as of 1998, to somewhere around 50 today.^(512, 549) As a general rule, the vast majority of pathogenic APP mutations occur in exons 16 and 17 at or near the proteolytic cleavage sites of α -, β -, and γ -secretases. Interestingly, while the vast majority of these mutations are autosomal dominant, two recessive APP mutations, A673V, and E693D, have also been reported in cohorts of early-onset AD families.^(550, 551) These recessive mutations aside, APP mutations exhibit close to a 100% penetrance.⁽⁵⁵²⁾ Significantly, three main groups of APP mutations have been identified: (i) mutations near the beta APP cleaving enzyme 1 (β ACE1) site, (ii) mutations near the gamma APP cleaving enzyme site, and (iii) mutations in the mid-domain of the A β region.⁽⁵⁵³⁾ Critically, the presence of these point mutations in APP suggests, at least for the familial variant of AD, increased amyloid production and as a consequence deposition is the causative factor underlying the disease pathogenesis of AD. Disappointingly the precise mechanism by which each APP mutation influences A β production is not clearly understood. The Swedish mutation APP 670/671 produces, in transfected fibroblast cell lines compared to the wild type cells, elevated levels of the soluble A β peptide, which, in normal conditions, is rapidly cleared.^(554, 555) In contrast, mutations in APP 717 produce a more than two-fold increase in A β_{42-43} , the longer and more insoluble forms of the A β peptide that rapidly aggregate to form amyloid deposits.⁽⁵⁵⁶⁾ Still other mechanisms of uncertain validity have been proposed including: mutations that inhibit the breakdown of the COOH-terminal fragment of APP that contains A β , mutations that alter anchoring of APP in the cell membrane, or mutations which stabilize A β -containing amyloidogenic fragments within lysosomes.^(494, 546, 557, 558) As qualified in the introduction to this section, the apparent causality described between mutations in APP and the development of early-onset forms of AD does not necessarily carry relevance to sporadic forms. That said, a pathogenic missense mutation at codon 665 of APP has been reported in late-onset AD.⁽⁵⁵⁹⁾ Most convincingly, the finding that

mutations in APP which reduce the production of amyloidogenic proteins by 40% are protective against the development of sporadic AD suggests A β -dependent mechanisms of neurodegeneration must be of significance in this variant in addition to inherited forms of the disease.⁽⁵⁶⁰⁾ Others argue that genetic variations in the APP promotor may be closer associated with the development of sporadic AD than are polymorphisms in the gene itself. For example, variant screening in the APP promotor revealed a microsatellite sequence in the first intron of *APP* which showed weak association with AD.⁽⁵⁶¹⁾ More likely, epigenetic modifications of APP in concert with alternative splicing may contribute to the development of sporadic AD.⁽⁵⁶²⁾ Importantly, epigenetic modulation of APP processing provides a mechanism by which environmental exposures can represent an etiologic factor in the pathogenesis of AD. Undoubtedly, more work is warranted in this area. In the interim, the data summarized above solidifies A β overproduction as the etiologic cause of FAD and strongly supports amyloid centric hypothesis of AD. Notably however, APP mutations account for only 5-10% of early-onset forms of AD.^(512, 552) By far the more prevalent etiology, mutations in the presenilin (PSEN) family of proteins are believed to cause up to 80% of familial early-onset AD cases.⁽⁵¹²⁾

5.2.3 *PSEN Mutations as Support for Amyloid-centric Hypotheses of AD*

As described, the vast majority of early-onset AD families do not have mutations in the *APP* gene. Hypothesizing that additional AD loci might exist to explain the remaining cases, in 1992, a locus on the long arm of chromosome 14 was detected by linkage analysis.⁽⁵⁶³⁾ Approximately 3 years later, a gene named *PSEN1* was identified and isolated by a positional cloning strategy.⁽⁵⁶⁴⁾ Remarkably, a second gene, *PSEN2*, was found secondary to its homology to *PSEN1* and mapped to 1q31–q42 later that same year.⁽⁵⁶⁵⁾ Each gene consists of a total of 13 exons, of which exons 3–12 comprise the coding sequence while the others encode the untranslated regions.⁽⁵⁶⁶⁾ Significantly, these genes code for two highly homologous (67% identity) multi-spanning transmembrane proteins termed presenilin 1 and 2 (PS1 and PS2).⁽⁵¹²⁾ With respect to structure, PS1 is comprised of 467 amino acid residues while PS2 is 448 amino acids in length. Both are highly conserved across species and primarily localized to the endoplasmic reticulum, Golgi apparatus, and nuclear envelope.⁽⁵⁶⁷⁾ Furthermore, each presenilin peptide includes eight transmembrane domains and a hydrophilic intracellular loop region. Physiologic endoproteolytic cleavage generates stable N- and C-terminal fragments of each presenilin, and though the

function of this cleavage is still unclear, this fragmented form is the predominant presenilin derivative in the mammalian brain.⁽⁵⁶⁸⁾ With respect to hypotheses of presenilin physiological function, PS1 may play a role in developmental morphogenesis⁽⁵⁶⁹⁾ while the C-terminal fragment of PS2 has been shown to inhibit apoptosis.⁽⁵⁷⁰⁾ The significance of these proteins in FAD however is credited to their involvement in the proteolytic processing of APP. As briefly described, γ -secretase is in fact a complex of at least four distinct proteins: APH-1, nicastrin and PEN-2, and PS1 or 2. Of significance, these constituent proteins are heavily modified by proteolysis during assembly and maturation of the γ -secretase complex. In fact, autocatalytic cleavage of presenilin into its N- and C-terminal fragments is required to endow the complex catalytic activity. In more detail, APH-1 is required for proteolytic activity and is believed to initiate the assembly of premature protein components.⁽⁵⁷¹⁾ Nicastrin on the other hand is credited for maintaining the stability of the assembled γ -secretase complex and for regulating its intracellular trafficking.⁽⁵⁷²⁾ In a similar vein, PEN-2 facilitates the stabilization of the γ -complex after presenilin proteolysis has generated the activated N- and C-terminal fragments.⁽⁵⁷³⁾ Perhaps providing a mechanism by which APP metabolism can be altered without alterations in its purported catalytic activity, PEN-2 associates with the γ -secretase complex via binding of the transmembrane domain of PS1/2.⁽⁵⁷⁴⁾ Lastly, and of highest relevance to the genetics of AD, PS1 and PS2 sub-serve proteolytic processing of specific proteins such as APP and NOTCH by either serving as the catalytic component of the γ -secretase complex (aspartyl protease) or at least serving as a cofactor.⁽⁵⁷⁵⁻⁵⁷⁷⁾ As evidence of their critical role in mediating γ -secretase activity, it has been recently demonstrated that γ -secretase inhibitors bind selectively and specifically to presenilin heterodimers.⁽⁵⁷⁸⁾ Still, when considering an amyloid dependent etiology for sporadic AD, it is important to note that PS1/2 are not unique in their ability to modulate APP metabolism. To the contrary, the other constituent proteins of γ -secretase each act as a key regulator for presenilin-mediated γ -secretase cleavage of C-99 by forming a functional complex with PS1 and PS2. Emphasizing the importance of these regulatory proteins, Nicastrin has been shown to modulate A β production by binding to the carboxy-terminal of derivatives of APP.⁽⁵⁷⁹⁾ Further, missense mutations in a conserved hydrophilic domain of nicastrin increase A β_{42} and A β_{40} peptide secretion while deletion in this domain inhibits A β production.⁽⁵⁷⁹⁾ Thus, while PSEN mutations are unquestionably the etiological cause of the majority of familial early-onset AD cases, there is a danger of oversimplifying A β -related pathways when adapting genetic mutations to support A β -centric hypotheses in sporadic AD. Almost surely, pan-dysregulation across a variety of cell systems contributes to the development of AD in

the general population. Therefore, when considering the following evidence, bear in mind that genetic etiologies are posed as causative only in FAD and are only used to support a central role of A β in sporadic AD.

Incredibly, the more than 120 mutations discovered in PSEN1 and 8 in PSEN2 are thought to underlie up to 80% of familial early-onset AD cases.⁽⁵¹²⁾ Of the pathogenic mutations noted in PSEN1, most are missense mutations while two are nucleotide insertions⁽⁵⁸⁰⁾ and one is a trinucleotide deletion.⁽⁵⁸¹⁾ In contrast to APP mutations, PSEN mutations are scattered over the entire coding region of the gene, with some clustering in exons 5 and 8 corresponding to the second transmembrane domain and the N-terminal portion of the sixth hydrophilic loop, respectively.⁽⁵⁸²⁾ Of interest, these mutations are predominantly located in the highly conserved transmembrane domains. Just as in APP, the molecular mechanisms by which mutant *PS1* exerts its pathogenic effect are not fully elucidated. A favored hypothesis in the field is that mutant PS1 modulates γ -secretase activity by virtue of its altered catalytic properties, resulting in the production of more pathogenic forms of A β peptide. In congruence, in vivo experiments demonstrate that mutant PS1 proteins influence the γ -secretase-mediated processing of APP at the A β C-terminus in a manner which increases the A β_{42} to A β_{40} ratio.^(583, 584) Additionally mutant PS1 increases the levels of A β_{42} in the endoplasmic reticulum and Golgi compartments.⁽⁵⁸⁵⁾ Interpreting this data, wild-type presenilin generates A β_{40} , considered to be less neurotoxic even though it is present in amyloid plaques.⁽⁵⁸⁶⁾ The mutant presenilins discussed on the other hand, direct APP processing towards the production of the more amyloidogenic and neurotoxic A β_{42} peptide.^(556, 587) Importantly, studies demonstrate that A β_{42} -containing fibrils exhibit binding affinity for A β_{40} , providing a mechanism by which low concentrations of A β_{42} could effectively recruit less amyloidogenic species into plaque depositions.⁽⁵⁸⁸⁾

Reiterating, this data is of significance because it laid the foundation for the formation of the A β cascade hypothesis and still serves as one of the fundamental lines of evidence supporting a causal role for amyloid accumulation in the pathogenesis of AD. Just as in studies of DS and APP however, modern discoveries have augmented the proposed mechanisms by which A β peptides induce pathogenesis. With respect to genetic studies of PSEN1/2, a novel splice-site mutation in intron 8 of *PSEN1* was associated with a peculiar form of AD which may partially account for the low correlation between A β plaque deposition and the severity of cognitive impairment. In more detail, the neuropathological features of this variant of AD exhibit diffuse senile plaques of a unique morphology. In contrast to the neuropathology of traditional AD, the predominant plaque type in this variant resembles cotton wool balls without amyloid fibril deposition

in the core or associated dystrophic neurites and inflammatory reactions.⁽⁵⁸⁹⁾ As these patients still develop progressive memory loss, such features suggest that A β deposition is not the key event in the pathogenesis of AD. Instead the rationale goes that the neurotoxic effect of A β ₄₂ must at least partially occur before its extracellular aggregation via a variety of probable mechanisms including but not limited to: disruption of calcium homeostasis, increased production of free radicals, and/or perturbation of intracellular signaling pathways.⁽⁵⁹⁰⁾ While these mechanisms of A β -induced neurodegeneration are explored in full detail in subsequent sections, the point here is that these processes are completely distinct from senile plaque formation and may therefore explain the absence of a strong correlation between AD neuropathology and amyloid plaque distribution. Similarly, it should be noted that alternative mechanisms by which presenilin mutations induce AD neuropathology have been proposed. For example, the discovery of a direct interaction between PS1 and proteins in the catenin family has led to the hypothesis that PSEN1 mutations may increase neuronal apoptosis by altering the stability of β -catenin; a protein notable for this role in cell to cell adhesion mechanisms and as a signaling protein in transcriptional activation pathways. In support of this γ -secretase independent mechanism, β -catenin levels are significantly reduced in AD patients with PSEN1 mutations and loss of β -catenin signaling has been shown to potentiate apoptosis induced by A β proteins in vitro.^(591, 592) With respect to γ -secretase independent mechanisms of AD pathogenesis involving PS2, evidence suggests that phosphorylation of the C-terminal fragment of PS2 inhibits its cleavage by caspase-3, inducing an anti-apoptotic effect.⁽⁵⁷⁰⁾ Thus, alterations in the PS2 phosphorylation might promote the pathogenesis of AD by affecting the susceptibility of neurons to apoptotic stimuli. Of course, many more PSEN-mediated pathogenic mechanisms have been proposed. However, the point in noting γ -secretase independent mechanisms is that it alludes to the complexity underlying pathophysiologic disturbances in APP processing. As discussed, APP and PSEN mutations are noteworthy in that they demonstrate that A β overproduction is the causative etiology behind FAD. Still, mutations in these three genes account for only a third to a half of all autosomal dominant cases of AD, which in turn represent less than 1% of total AD cases.⁽⁵⁹³⁾ As repeatedly suggested, these statistics confirm that the molecular etiology underlying the development of late-onset forms of AD are distinct from those genetically-mediated variants. However, this is not to suggest that genetic mutations have not improved our understanding of the molecular pathogenesis of sporadic AD. As described in subsequent sections, genetic variation in the APOE gene provide some of the most robust evidence supporting modern interpretations of the amyloid-cascade hypothesis.

5.2.4 APOE4 Support of Amyloid-centric Hypothesis of Sporadic AD Pathogenesis

First described by G. Utermann and colleagues in 1979, polymorphisms in apolipoprotein E (ApoE) constitute the most heavily influential genetic risk factor for the development of sporadic AD discovered to date.⁽⁵⁹⁴⁾ Since their initial characterization, three major isoforms of ApoE have been identified which differ in amino acid sequence at two sites, residues 112 and 158.⁽⁵⁹⁵⁾ In more detail, the primary peptide structure of both ApoE2 and ApoE3 are characterized by a cysteine residue at position 112 while an arginine residue resides at this position in the ApoE4 isoform. In contrast, the amino acid sequence of ApoE3 and ApoE4 are similar in that they both contain arginine at the 158 position, while ApoE2 is unique in having a cysteine substituted at this site. Of note, all three isoforms are coded at a single genetic locus on the long arm of chromosome 19 by their three corresponding alleles (ϵ 2, ϵ 3, and ϵ 4).⁽⁵⁹⁶⁾ With respect to prevalence in the United States, the ϵ 3 form is the most common, with about 60% citizens inheriting two copies of this allele.⁽⁵⁹⁷⁾ Consequently, the ϵ 2 and ϵ 4 forms are much less common. An estimated 20-30% percent of individuals in the United States have one or two copies of the ϵ 4 allele while only 2% have two copies of ϵ 4. The remaining 10-20% have one or two copies of ϵ 2.⁽⁵⁹⁷⁾ Lending significance to these population statistics, as stated, many studies have demonstrated an association between the ϵ 4 allele and late-onset familial and sporadic forms of AD. One of the most influential of these studies reported a 20% increased risk in developing AD secondary to heterozygosity for the ϵ 4 allele and an astonishing 90% increase in risk attributable to ϵ 4 homozygosity. Beyond increasing an individual's relative risk of developing AD, this same study also demonstrated that ApoE genotype modulates the mean age of onset. Individuals with a single ApoE4 allele develop AD around age 84 while the mean age of onset for homozygotes is only 68 years of age. Summarizing this work, the ϵ 4 allele influences both the risk of developing AD and its age of onset in a "dose-dependent" fashion. Hauntingly, it was also among the first studies to demonstrate that homozygosity for ApoE4 is virtually sufficient to cause AD by age 80.⁽⁵⁹⁸⁾ Further advancing amyloid-centric hypotheses of AD, apo ϵ 4 allele dosage is highly correlated with increased neuritic plaque density in AD patients.⁽⁵⁹⁹⁾ Critically, this finding has been recapitulated in cognitively normal subjects, with fibrillar A β burden in the brains of cognitively normal individuals increasing in a ϵ 4-dependent manner.⁽⁶⁰⁰⁾ Further alluding to an interaction between ApoE status and A β , the ϵ 4 allele reduces age of onset in early-onset AD families linked to mutations in the APP gene^(601, 602). Of unknown significance, no effect of ApoE status has been detected

in similar cases of AD secondary to mutations in PSEN1.⁽⁶⁰³⁾ In light of these findings, the ϵ 4 allele appears to be a risk factor and not an invariant cause of AD. Considering a molecular mechanism by which ApoE4 exerts its pathogenic effect, this indicates that other environmental or genetic factors operate in concert with the ϵ 4 allele to induce an AD phenotype. Exemplifying this point, in certain ethnic groups, the ApoE4 allele seems to have a weakened or non-existent effect on processing underlying the development of AD.^(604, 605) Thus, an important unanswered question in the field remains what variables influence ApoE function and how do these perturbations contribute to the development of sporadic forms of AD.

Secondary to its association with AD, over the last decade, research into the physiologic function of ApoE has expanded its role in cell biology tremendously. Structurally, it is a plasma glycoprotein comprised of 299 amino acid residues with a combined mass of 34,200 Daltons.⁽⁶⁰⁶⁾ Further characterizing its structure, the N-terminal domain (residues 1–191) is a stable globular structure containing a receptor binding site, while the carboxy-terminal domain (residues 216–299) is helical and facilitates APOE's lipoprotein binding functions.⁽⁶⁰⁷⁾ Peripherally, it is synthesized mainly by the liver, but also by macrophages and monocytes.⁽⁶⁰⁶⁾ Within the CNS, while some reports indicate expression in neurons, more than 95% of ApoE synthesis and secretion has been localized to astrocytes and microglia.⁽⁶⁰⁸⁾ Under the current paradigm, ApoE functions as a ligand in receptor-mediated endocytosis of lipoprotein particles both in the CNS and peripheral nervous system. After receptor-mediated endocytosis of ApoE-containing lipoprotein particles by low-density lipoprotein (LDL) receptor family members, ApoE may be either degraded or recycled back to the cell surface.⁽⁶⁰⁹⁾ Unlike plasma HDL that contains apoA-1 as its major apolipoprotein, the predominant apolipoprotein of HDL in the central nervous system (CNS) is ApoE.⁽⁶¹⁰⁾ In plasma, ApoE proteins are present on lipoproteins in association with other apolipoproteins, whereas in the brain ApoE is predominantly present on distinct high density-like lipoprotein particles.⁽⁶¹¹⁾ However, the role of ApoE containing high density-like lipoprotein particles in lipid and cholesterol homeostasis is not clearly defined in the CNS. What is known is that cholesterol released from ApoE-containing lipoprotein particles is used to support synaptogenesis and the maintenance of synaptic connections.⁽⁶¹²⁾ As a consequence of these findings, the general function of ApoE is hypothesized to involve the mobilization and redistribution of lipids during neuronal growth and after neuronal insult.⁽⁶¹³⁾ Whether ApoE-containing lipoproteins play a major role in supporting synaptogenesis and maintenance of synaptic connections *in vivo* in the uninjured brain has not yet been proven, as several studies have shown that the brain of

ApoE knock-out mice for the most part appear normal in the absence of injury.⁽⁶¹⁴⁾ In addition to these primary functions, reports suggest ApoE may also facilitate a host of other cellular processes including nerve regeneration, immune-regulation, and the activation of several lipolytic enzymes.^(615, 616)

Although perturbations in any of the physiological functions of ApoE may underlie its isoform-specific effect on the risk of developing AD, convincing evidence suggests that the physical interaction of ApoE with A β plays an important role in AD pathogenesis. While this hypothesis will be the main topic of review, it is important to note that other potential mechanisms have not been ruled out. These include the ability of ApoE to modulate tau phosphorylation and neurotoxicity as well as its role in synaptic plasticity and neuroinflammation. Nevertheless, the prevailing hypothesis is generally supportive of the traditional amyloid cascade hypothesis, although it highlights the point that A β peptide aggregation and perturbations in A β clearance play a much larger role in the development of sporadic AD as compared to mechanisms of A β overproduction. Delving deeper into these pathogenic mechanisms, the finding that residues 12–28 of the A β peptide appear to contain the binding site for ApoE, bolsters the hypothesis that a physical interaction between ApoE and A β plays an important role in AD pathogenesis.⁽⁶¹⁷⁾ Similarly, the finding that the efficiency of complex formation between lipidated ApoE and A β follows the order of apoE2 > apoE3 >> apoE4, provides a rationale for the differential in AD rates observed between different ApoE genotypes.⁽⁶¹⁸⁾ The realization that the binding affinity of ApoE isoforms to A β correlates inversely with the risk of developing AD subsequently led to the hypothesis that ApoE isoforms might variably modulate A β production or aggregation. Disappointingly, attempts to experimentally confirm this hypothesis in vitro have produced conflicting results. For example, some studies suggest all three ApoE isoforms promote A β_{40-42} fibrillation, with the apoE4 isoform carrying the greatest potency and ApoE2 the least. In complete discordance however, similar work also suggests that ApoE isoforms decrease A β fibrillogenesis in vitro by interfering with A β nucleation.^(619, 620) As both mechanisms are consistent with the increased amyloid plaque load in subjects with the ApoE ϵ 4 allele, further work will be needed to elucidate if either of these mechanisms contribute to ApoE4's promotion of A β deposition. Cognizant of the fact that the in vivo environment in which ApoE modulates A β in the brain may be very different from the artificial settings described, investigators have generated mouse model knock-outs of ApoE in pursuit of a more physiologically relevant system. In congruence with the hypothesis that ApoE status modulates risk for AD by influencing a central A β -dependent etiology, lack of murine ApoE results in a significant decrease in A β deposition and

consequent lack of amyloid plaques with neuritic dystrophy.^(621, 622) Furthermore, elimination of murine APOE results in a redistribution and alteration in the character of A β deposition in homozygous APP (V717F) transgenic mice. A β deposition in these mice is dramatically reduced in the cortex and dentate gyrus while A β deposition and the number of plaques in the CA1 and CA3 subfields of the hippocampus are markedly increased.^(623, 624) Motivated by the intriguing findings made in ApoE knock-out mice, several lines of transgenic mice have been generated to study the role of human ApoE isoforms in AD pathogenesis. For reasons yet to be deciphered, the expression of human ApoE isoform transgenes in PDAPP mice results in a marked delay in the deposition of A β and formation of neuritic plaques compared to PDAPP mice expressing murine ApoE or no ApoE.^(622, 623) These mice also exhibit isoform-specific differences in A β deposition, with human E4 accelerating plaque formation in a manner similar to its murine analog.^(625, 626) Notably, the studies just described strongly implicate A β as the central pathogenic specie in AD pathogenesis. Still, to date, no in vivo evidence exists to prove that ApoE modulates A β production in a manner which would align its pathogenic mechanism with that of APP and PSEN mutations. For this reason, alternative mechanisms involving the role of ApoE in the clearance of A β have been hypothesized. Summarizing the predominant paradigms in the field, the first hypothesis suggests that ApoE directly and indirectly modulates A β metabolism causing a toxic accumulation of amyloidogenic forms of the peptide over time. The second major theory suggests that ApoE directly interferes with cytoskeletal architecture of neurons via its modulation of tau protein metabolism. Lastly, some investigators suggest that as a consequence of ApoE's role as a key player in lipid homeostasis in the CNS, isoform-specific perturbations in ApoE levels contribute to the development of AD pathology through a variety of non-A β -mediated pathways.

In support of the hypothesis that ApoE modulates A β metabolism, in addition to the effects of ApoE on fibrillogenesis already presented, there is evidence that ApoE4 alters both the transport and clearance of A β in a manner which can facilitate amyloidogenic processes. Inconsistently, studies have demonstrated that lipid-poor and lipid-free apoE4 enhances A β production by inducing LRP1- and ApoER2-mediated endocytosis of APP and β -secretase.^(627, 628) While there is still no convincing data that ApoE isoforms have differential effects on the production of A β in vivo, the literature is more consistent in its assertion that ApoE plays an important role in the metabolism and clearance of A β . Most convincingly, several studies have demonstrated that the endolytic degradation of A β peptides within microglia by neprilysin and related enzymes is dramatically enhanced by ApoE.^(629, 630) Similarly, A β degradation in the extracellular

environment by insulin-degrading enzyme is facilitated by ApoE.⁽⁶²⁹⁾ Supporting the validity of these pathways with respect to the development of sporadic AD, the capacity of ApoE to promote A β degradation is dependent upon the ApoE isoform and its lipidation status. Summarizing the effect of lipidation on ApoE function in this context, enhancement of lipidated ApoE expression via the activation of liver X receptors stimulates A β degradation via the pathways described.⁽⁶²⁹⁾ Transitioning to support for ApoE's role in A β clearance, several studies have demonstrated that human ApoE facilitates the binding and internalization of soluble A β .^(631, 632) Again however, a consensus on isoform-dependent differences in this process has yet to be reached. With respect to general mechanisms through which ApoE might modulates A β transport, reports suggest ApoE-containing lipoprotein particles regulate the cellular uptake of A β by receptor-mediated endocytosis and increase its removal from the brain to the systemic circulation by facilitating transport across the blood-brain-barrier. In support of these both of these mechanisms, a recent study has shown that the brain to blood clearance of lipidated apoE4 in the mouse brain is significantly lower than that mediated by the apoE3 and apoE2 isoforms.⁽⁶³³⁾ Unlike the evidence supporting ApoE's role in the metabolism of A β however, the evidence that apoE4 reduces blood to brain clearance is conflicted, with another study demonstrating no differences in A β clearance from the brain in mice expressing transgenes for either human apoE3 or apoE4.⁽⁶³⁴⁾ Complicating the picture, A β -containing ApoE4 complexes are sequestered from the periphery into brain capillaries to a greater extent than A β bound to apoE2 or apoE3, suggesting that apoE4-mediated blood to brain transport of A β may contribute to the development of AD pathology.⁽⁶³⁵⁾

The second major mechanism by which ApoE might contribute to the development of AD is through direct and indirect interference with the cytoskeletal architecture of neurons via its modulation of tau protein metabolism. As reiterated multiple times, the hyper-phosphorylation of tau and subsequent formation of NFTs is considered a hallmark lesion of AD. Although a complete review of tau's contribution to the etiology of AD is described elsewhere in this work, its relationship with ApoE is discussed here. Fortuitously, work done in both in cell culture and animal models are in accordance with respect to ApoE mediated modulation of tau function. These studies demonstrate that ApoE3 binds tightly to tau through the interaction of its N-terminal domain and the microtubule-binding repeat regions of tau. Perhaps accounting for the isoform-specific variations in AD prevalence, this same work demonstrates that ApoE4 does not interact significantly with tau.⁽⁶³⁶⁾ Since hyper-phosphorylation has been demonstrated to perturb the physiologic function of tau, the finding that ApoE3 binds preferentially to non-phosphorylated tau and can even prevent its phosphorylation

lends further credibility to tau-centric mechanisms of ApoE-mediated pathogenesis. One major limitation to this theory worth noting is that no studies localizing ApoE to the neuronal cytosol, where the majority of tau exists, have been published.⁽⁶³⁷⁾ Data suggesting that a fragment of ApoE4 (1–272 amino acids), but not full-length ApoE4 isoform, can escape the secretory pathway, translocate to the cytosolic compartment, and interact with cytoskeletal components such as tau and neurofilament potentially alleviates this limitation, but future work is needed to confirm the physiological relevance of this interaction.⁽⁶³⁸⁾ Seeking a less convoluted mechanism, others have hypothesized the effects of ApoE on tau phosphorylation could be explained by an intracellular signaling pathway induced by ApoE in lieu of a direct interaction between ApoE and tau.^(639, 640) And indeed, when the signaling pathways stimulated by ApoE are examined in primary neuron cultures, ApoE and ApoE-derived peptides induce activation of the ERK1/2 pathway via a mechanism dependent on calcium influx through the NMDA receptor. Similarly, in a process mediated by γ -secretase and G-proteins, ApoE inhibits the c-Jun N-terminal kinase 1/2 pathway.⁽⁶⁴⁰⁾ In summary, ApoE may exert a direct or indirect effect on tau phosphorylation and these processes may or may not contribute to AD pathogenesis. Despite the accumulation of in vitro evidence just described, in vivo studies confirming the physiological relevance of observed ApoE-isoform dependent effects on tau will be critical.

In an effort to present a holistic representation of the field, the last hypothesis reviewed suggests that isoform-specific perturbations in ApoE levels contribute to the development of AD pathology through a variety of non-A β -mediated pathways. Disappointingly, the demonstration ApoE protein levels in the brain parenchyma or CSF vary as a function of ApoE genotype have not been reliably produced in human cohorts.^(619, 641-644) As human studies fail to support the hypothesis that ApoE genotype influences protein expression, proponents of this hypothesis have moved into transgenic mice lines, weakly arguing these models are less confounded by external variables. Still, initial studies characterizing such mice again failed to demonstrate fluctuations in ApoE levels as a consequence of human ApoE2, ApoE3, or ApoE4 isoform expression.⁽⁶⁴⁵⁾ However, several subsequent studies have reported a genotype-dependent difference in ApoE levels with the ApoE2 genotype corresponding to elevated levels of ApoE as compared to ApoE4 expression (E2>E3>E4).^(646, 647) Notably however, these findings are equally well explained by in vitro studies which demonstrate that ApoE4 is degraded more quickly than ApoE2 or ApoE3 in primary mouse astrocyte cultures.⁽⁶⁴⁸⁾ Assuming for the sake of argument that ApoE levels are modulated by genotype, the question of significance remains

“what relevance does this have on the pathophysiological processes of AD?” Here, the hypotheses are better formulated and grounded in data. Recognizing that ApoE is expressed in response to neuronal injury, it has been hypothesized that ApoE is required for the repair of CNS tissues secondary to its role in redistributing lipids and cholesterol for membrane repair and synaptic plasticity.⁽⁶⁴⁹⁾ In congruence with this concept, most in vitro studies have shown that apoE3 augments neurite outgrowth to a greater extent than ApoE4.⁽⁶⁵⁰⁾ Similarly, compared with ApoE3 transgenic mice, ApoE4 carriers exhibit impaired compensatory sprouting, reduced synaptogenesis, and more severe memory impairment following insult to the entorhinal cortex.^(651, 652) Of note, since a link between this mechanism and A β deposition has not been fully described, it neither supports nor undermines amyloid-centric models. In contrast, the finding that ApoE4 exacerbates the neurotoxicity of A β peptides backs these models.⁽⁶⁵³⁾ Of significance, a potential mechanism by which ApoE mediates this feat may be through its influence on neuro-inflammatory processes. This suggestion stems from the finding that ApoE is capable of modulating innate inflammatory response and may have a generalized anti-inflammatory effect.⁽⁶⁵⁴⁾ Consistent with the anti-inflammatory role of ApoE, lack of its expression in mice is associated with the increased induction of cytokines and pro-inflammatory responses in response to A β insult.^(655, 656) Thus, the interaction and subsequent co-deposition of A β with ApoE might serve to compromise the anti-inflammatory function of ApoE by reducing the functionally available pool size of ApoE, eventually leading to chronic neuro-inflammation. In support of this concept, A β has been shown to induce the production of ApoE. The resulting surge in ApoE can apparently then limit A β -driven neuro-inflammation, suggesting the presence of a feedback-style mechanism.^(655, 657) In an effort to investigate if the anti-inflammatory function of ApoE contributes robustly to the development of AD, investigators have looked for isoform-dependent differences. Again in congruence with the proposed pathogenic model, exogenously applied ApoE4 has more robust pro-inflammatory activity than ApoE3 in astrocytes and microglial cells.^(657, 658) Supporting the physiological relevance of this finding to in vivo conditions, following administration of LPS, ApoE4 knock-in mice exhibited a greater inflammatory response as compared with ApoE3 expressing mice.^(659, 660) Taken as a whole, the data reviewed suggests two possible mechanisms through which ApoE might modulate AD risk via modulation of neuro-inflammatory pathways. From the perspective that ApoE4 invokes a pro-inflammatory response, ApoE4 may exacerbate detrimental neuro-inflammation in the development of AD. Assuming an anti-inflammatory role for ApoE4, as a consequence of less effective anti-inflammatory function the ApoE4 genotype might inefficiently prevent pathological neuro-inflammation in

AD. Given the prominent activation of innate inflammatory responses observed in the brains of AD patients, conclusively testing these two opposing hypotheses should represent a central aim of future AD research.

As can be garnered by the high degree of uncertainty which surrounds each of the purported mechanisms by which ApoE status contributes to the pathogenesis of AD, deficits in our knowledge of AD molecular pathophysiology greatly hinders our ability to form conclusions about genetic risk factors. While this chapter is complete in that it addresses each of the causative mutations of AD, a complete review of all susceptibility genes is lacking. This is in part due to the uncertainty which surrounds their contribution to AD pathology. Of these genes, ApoE is inarguably the strongest predictor of genetic susceptibility for sporadic AD. Therefore, a mechanistic understanding of this genetic risk factor may uncover truths about the underlying molecular etiology of AD. As discussed, humans possess three common ApoE alleles: ApoE2, ApoE3, and ApoE4. Each genetic allele exhibits isoform-specific effects on the development of AD, with possession of an ApoE4 allele decreasing the age of onset, ApoE3 being considered neutral, and ApoE2 thought to be protective. Considering all the data on causative and susceptibility genes in AD to date, it seems safe to assume that the amyloid-cascade hypothesis should be considered the conclusive model of early-onset FAD etiology. With respect to the development of sporadic AD however, the controversies surround the pathophysiological role of ApoE highlight the conclusion that this variant is a complex disorder caused by a manifold of factors. Still, given the vast degree of evidence suggesting that the effect of ApoE occurs in a A β -dependent fashion, or at least influences A β production/clearance, it seems likely that familial and sporadic forms of AD might result from essentially the same pathological cascade.⁽⁶⁶¹⁾ Put another way, while a simplistic interpretation of the amyloid cascade hypothesis holds true for genetically-mediated forms of AD, a more inclusive amyloid-centric model of AD pathogenesis is required to fit all variants of sporadic AD. In congruence with this opinion, the genes that cause the autosomal dominant form of AD have not been detected as risk factors in the gene-wide association studies conducted to date. One likely explanation for this finding is that the common genetic variations in these three genes are not sufficient to alter their expression in a manner that increases the risk of AD to a detectable threshold. Instead, as suggested by the vast literature on the topic, the development of sporadic AD is likely dependent on the convergence of multiple pathophysiological cascades which may or may not intersect on the A β pathogenic cascade.

5.3 TRANSGENIC MOUSE MODELS AS SUPPORT FOR AMYLOID-CENTRIC HYPOTHESES OF ALZHEIMER'S DISEASE

The majority of chronic neurodegenerative diseases, including AD, are associated with the accumulation of misfolded proteins into aggregates that contain fibrillar structures. As demonstrated by a review of AD genetics, an increase in A β production, an increase in the ratio of A β 42 to A β 40, or generation of a mutant form of A β with greater amyloidogenic propensity are the main pathogenic mechanisms underlying the rare early-onset forms of autosomal-dominant familial AD. However, determining whether this A β deposition drives the pathogenesis of sporadic AD, is a neutral bystander, or just represents an unsuccessful repair attempt has proven one of the greatest challenges of translation research to date. Analysis of susceptibility genes like ApoE demonstrate that overproduction of A β is unlikely to represent the major pathogenic mechanisms underlying sporadic forms of AD.^(519, 662) Instead, countless data suggests that defects in the clearance A β from the brain by cellular uptake or transport across the blood-brain barrier might underlie many cases of sporadic AD.^(663, 664) In addition, a vast literature exists suggesting that increased A β aggregation influenced by A β binding molecules may also play an important role. Secondary to intrinsic limitations of human genetic studies, animal models of AD have been developed to help analyze pathogenic pathways in more detail. Not surprisingly, the development of a mouse model of AD which recapitulates the pathological and behavioral features of this complex, chronic and progressive disease has proven to be a major challenge. Confident in the validity of amyloid-centric models of AD, the first-generation of AD mouse models focused on recapitulating the deposition of A β peptides into senile plaque-like structures. Naturally, the general approach employed was to overexpress human APP transgenes bearing mutations associated with early-onset familial forms of AD. Demonstrating the utility of this approach, the PDAPP mouse was the first mutant human APP transgenic mouse reported to exhibit A β plaque pathology.⁽⁶⁶⁵⁾ When the pattern of A β deposition in this early mouse lines was analyzed, early plaque pathology was evident in the hippocampus and cortical brain regions between 6 and 12 months of age. Encouragingly, not only did APP-overexpressing transgenic mice display both diffuse and dense core plaques, they also exhibited other cardinal features such as astrogliosis, microgliosis, and dystrophic neurites. Most significantly, APP transgenic mice also exhibited age-dependent cognitive deficits. Critically, this seminal finding demonstrates A β accumulation and deposition in the brain can induce behavioral impairments and in doing so supports amyloid-centric models of AD pathogenesis.^(666, 667) Shortly after the initial characterization of memory deficits in these mice seemingly confirmed the etiological significance of A β plaques, reports of learning and memory deficits

occurring prior to robust A β deposition in the brain were published.^(668, 669) This revelation, in addition to in vitro studies, led to the hypothesis that soluble oligomeric A β species could also induce cognitive dysfunction. Thus, while the first-generation of AD mouse models provided many answers with regard to the relevance of A β deposition in the pathogenesis of AD, they produced many more novel questions. Chief among these conundrums was the failure of A β plaque density to incite other pathological features of AD such as NFT deposition or robust neuron loss. From a more practical standpoint, the rate of A β accumulation in these models was too slow for robust study of AD pathogenic pathways. In recognition of this shortcoming, additional amyloidogenic mutations were introduced in an effort to bolster the pathogenic A β -cascade. Compared to single APP transgenic mice, APP-presenilin transgenic mice rapidly accumulate deposits of A β , with plaques being observed at a much earlier age and in greater densities. At the pinnacle of these efforts, the 5XFAD transgenic mouse model contains a total of five different familial AD mutations resulting in the formation of A β plaques as early as 2 months of age.⁽⁶⁷⁰⁾ Notably, in addition to reducing costs associated with raising animals to the age where they present with AD features, these models better recapitulate the pathological phenotype of sporadic AD. Unlike the majority of single APP transgenic mice, some double transgenic mice, like the 5XFAD mouse line, demonstrate significant neuron loss upon histological examination.⁽⁶⁷⁰⁾ Still, these second generation mouse models represent an incomplete model, as they fail to demonstrate robust NFT formation. To definitively address this issue, mutant tau mice have recently been crossed with APP/PSEN transgenic mouse lines to generate tri-transgenic APP/PSEN/tau mutant mice (3x-Tg-AD) depicting both A β plaque and NFT pathologies.⁽⁶⁷¹⁾ Reaffirming the conclusion that tau hyperphosphorylation is a downstream pathology with respect to A β -mediated neurodegenerative processes, 3x-Tg-AD mice exhibit A β deposits at the same age as in the single mutant APP transgenic mice (6 months of age). However, the quantity and distribution of the NFT pathology (12-15 months) is greatly enhanced in this model compared to the single mutant tau transgenic mice, suggesting overexpression of A β or APP could accelerate downstream tau pathology.⁽⁶⁷²⁾ Thus, in large part due to the characterization of AD mouse models, disturbances in A β production/clearance are believed to lie upstream of NFT formation in the pathogenesis of AD. This contribution to AD research cannot be overstated, as tau-centric models of AD pathogenesis have represented a well-supported alternative to A β -centric models since their inception. Today, as a result of the genetic and evidence from AD mouse models described, instead of completely refuting A β 's role in AD pathogenesis, the vast majority of literature focuses on how disturbances in A β production/clearance initially occur and why these disturbances cause neurodegenerative changes.

5.4 MECHANISMS OF A β NEUROTOXICITY AT THE SYNAPSE

As discussed, more than 3 decades of research on A β has produced a wealth of evidence that its accumulation in brain regions facilitating memory and cognition contributes strongly to the development of AD. As briefly addressed during its introduction, early versions of the amyloid cascade hypothesis of AD posited that amyloid plaques exert their neurodegenerative influence by interacting with surrounding dendrites, axons and glia. This hypothesis stems in part from histological analysis of A β plaques and their surrounding neuronal tissues which reveals that prototypically straight cortical dendrites assume a distorted and curved morphology when adjacent to an A β plaque.⁽⁶⁷³⁾ Subsequent examination of this phenomenon using array tomography in APP transgenic mice would reveal a striking penumbra of excitatory synapse loss and neuritic dystrophy that is greatest immediately adjacent to a plaque and which lessens in a radial fashion. Emphasizing the high degree correlation between these neurodegenerative changes and proximity to A β plaques, synapses become virtually normal approximately 30–50 μ m away from the plaque core edge.^(674, 675) Despite these convincing findings, the discovery that AD mouse models exhibit signs of neurodegeneration prior to robust plaque deposition made it clear that A β -centric models of AD pathogenesis needed to be rethought in order to retain mechanistic plausibility. After an extensive search for potential molecular mediators of neurodegeneration that coincide with the development of cognitive deficits, the discovery of buffer-soluble bioactive oligomers gave rise to the concept that the insoluble amyloid fibrils comprising the plaques might themselves be relatively inactive but instead mediate pathogenicity of smaller, potentially neurotoxic assemblies by serving as reservoirs. From a biophysical perspective, this model appears more viable, as small oligomers collectively provide a much greater surface area for interaction with neurons and glia than do the large, non-diffusible plaques. An additional strength of this reformulated model is that it maintains the validity of decades of research implying A β plaque deposition is a critical pathogenic event in the development of AD, as A β dimers, trimers, tetramers, dodecamers, and higher-order oligomers have been found in cell culture media⁽⁶⁷⁶⁾, in APP transgenic mouse brains⁽⁶⁷⁷⁾ and in AD brain tissue⁽⁶⁷⁸⁾ Exemplifying the smooth transition from A β plaque centric models to A β oligomer-mediated hypotheses of toxicity, later studies would demonstrate that the penumbra of synaptic loss described in the local environment near A β plaques is reactive to antibodies specific for A β oligomers.^(674, 675) Several findings strongly undermine the possibility that this finding is coincidental. For one, synthetic A β oligomers and soluble A β oligomers isolated from cell culture media or AD brain extracts acutely impair synaptic functions when added to hippocampal slices

or slice cultures.^(678, 679) Furthermore, when biochemically isolated soluble oligomers and insoluble amyloid plaque cores are transplanted into wild-type mouse brain slices, only soluble oligomers potently blocked LTP. Even more convincingly, when these seemingly inert amyloid cores are first dissolved in harsh solvents to release their constituent oligomers before application to wild-type brain slices, they too potently impair LTP.⁽⁶⁷⁸⁾ Such morphological analyses suggest that plaques induce synaptic and neuritic deficits at least in part by acting as local reservoirs of diffusible oligomers. Further promoting the validity of this model, reports have even suggested mechanisms by which the equilibrium between plaques and oligomers can be pathologically modulated. In this context, it has been found that lipids can convert inert A β amyloid fibrils into neurotoxic protofibrils that can subsequently impair learning in mice.⁽⁶⁸⁰⁾ Taken together, these and other experimental approaches suggest that plaques may confer local neurotoxicity because they are in equilibrium with surrounding oligomers and protofibrils. Beyond shifting attention away from A β plaques, research conducted in APP transgenic models also demonstrates that synaptic transmission is commonly perturbed by soluble A β oligomers via a variety of mechanisms. This point is critical, as it highlights the error in concluding that A β is non-contributory to the pathogenesis of AD when interpreting the finding that APP transgenic mice do not universally exhibit neuron loss. While it is true cell bodies are not significantly decreased in all models, the substantial neuritic dystrophy and synapse loss present in these models are clear signs of a neuronal degenerative process. As for synaptic perturbations being of relevance to AD, not only is synaptic loss considered one of the pathological hallmarks of AD, it is best correlate of cognitive decline.^(131, 681) Furthermore, in APP transgenic mouse models, manipulations that prevent or reverse synaptic deficits also prevent or reverse cognitive impairment.^(682, 683) Thus, the assertion made by some that APP transgenic mice do not exhibit pathophysiological relevant signs of neurodegeneration is a complete falsehood.

With respect to mechanisms by which A β elicits neurotoxicity directly, the hypothesis that A β oligomers modulate synaptic function is among the most well-supported in the literature to date. Rephrasing the original amyloid-cascade hypothesis to fit this model, current A β -centric models contend that progressively growing assemblies of A β in the brain result in synaptic dysfunction and consequent dismantling of the neuronal circuits and networks which sub-serve learning and memory, ultimately resulting in the cognitive disturbances characteristic of AD. As evidence of A β modulating synaptic transmission, in vitro and in vivo studies have shown that A β oligomers promote the collapse of glutamatergic dendritic spines in part by reducing the number of surface AMPA and NMDA receptors.⁽⁶⁸⁴⁻⁶⁸⁶⁾ On the other

hand, the production of A β and its secretion into the extracellular space are in turn regulated in part by neuronal activity.⁽⁶⁸⁷⁾ Interestingly, these experimental findings raise the possibility of a feedback loop via which A β peptide concentration can modulate neuronal excitability.⁽⁶⁸⁴⁾ In this paradigm, A β production is enhanced by action potential-dependent synaptic activity, leading to increased levels of extracellular A β at synapses where it may facilitate reductions of excitatory transmission. With respect to AD pathophysiology, elevated levels of A β would be expected to put this negative feedback regulator into overdrive resulting in suppressed excitatory synaptic activity at the postsynaptic level. In addition to this data suggesting A β acts as a negative regulator of neuronal activity post-synaptically, other work suggests that A β could also act as a positive regulator at the presynaptic level. As illustrated by Figure 5-1, in general studies have demonstrated that low concentrations of synthetic A β_{42} (picomolar range) markedly potentiate synaptic transmission, whereas higher concentrations of A β_{42} (low nanomolar range) synaptic depression.⁽⁶⁸⁸⁾ Unlike A β 's post-synaptic effects on synaptic transmission, the potentiating effect of A β at the presynaptic terminal is not dependent on NMDA and AMPA receptor modulation. Instead, presynaptic modulation of synaptic transmission by A β appears to be dependent on $\alpha 7$ -nicotinic Ach receptor (nAChR) activation, as confirmed by the finding that inhibition of this nicotinic receptor subtype decreases A β secretion and blocks A β -induced facilitation.⁽⁶⁸⁹⁾ Given that $\alpha 7$ -nAChR permit influx of Ca²⁺, the current paradigm suggests that A β may be part of a positive feedback loop that increases presynaptic Ca²⁺ levels and A β secretion via direction interaction with $\alpha 7$ -nAChR.⁽⁶⁸⁹⁾ Importantly, in a similar manner to its effects at the post-synaptic neuron, A β -induced presynaptic effects depend on an optimal A β concentration, with higher or lower concentrations potentially impairing synaptic transmission.⁽⁶⁹⁰⁾ Overall, these and other data suggest an apparent bell-shaped relationship between extracellular A β and synaptic transmission in which intermediate levels of A β potentiate presynaptic terminals, low levels reduce presynaptic efficacy, and high levels depress postsynaptic transmission.

While presynaptic and postsynaptic regulation of neurotransmission by A β -peptides is an intriguing phenomenon, these mechanisms are worth reviewing in that they possibly relate A β levels to the neurodegenerative changes and the development of cognitive deficits characteristic of AD. As reviewed, excitatory synaptic transmission is tightly regulated by the number of active NMDA and AMPA at the synapse. This high degree of regulation is necessary as NMDA receptor activation can induce either long-term potentiation (LTP) or long-term depression (LTD) depending on the extent of the resultant [Ca²⁺] rise in the dendritic spines. In more detail, a large transient rise in synaptic Ca²⁺ levels secondary to robust

NMDA receptor activation induces LTP. In contrast, in regions such as the hippocampus, persistent weak synaptic stimulation resulting in mild increases in synaptic Ca^{2+} concentration is sufficient to induce LTD. Once induced, LTD results in the internalization of synaptic NMDA receptors and the activation of peri-synaptic NMDA receptors. Generally speaking, LTP induction promotes the recruitment of AMPA receptors to the post-synaptic membrane resulting in enhanced excitatory post-synaptic potentials and growth of dendritic spines. On the other hand LTD induces spine shrinkage and synaptic loss.⁽⁶⁹¹⁾ These effects of LTD on synaptic density are most relevant to our discussion, as pathologically elevated levels of $\text{A}\beta$ may shift NMDA receptor-dependent signaling cascades towards pathways involved in the induction of LTD.

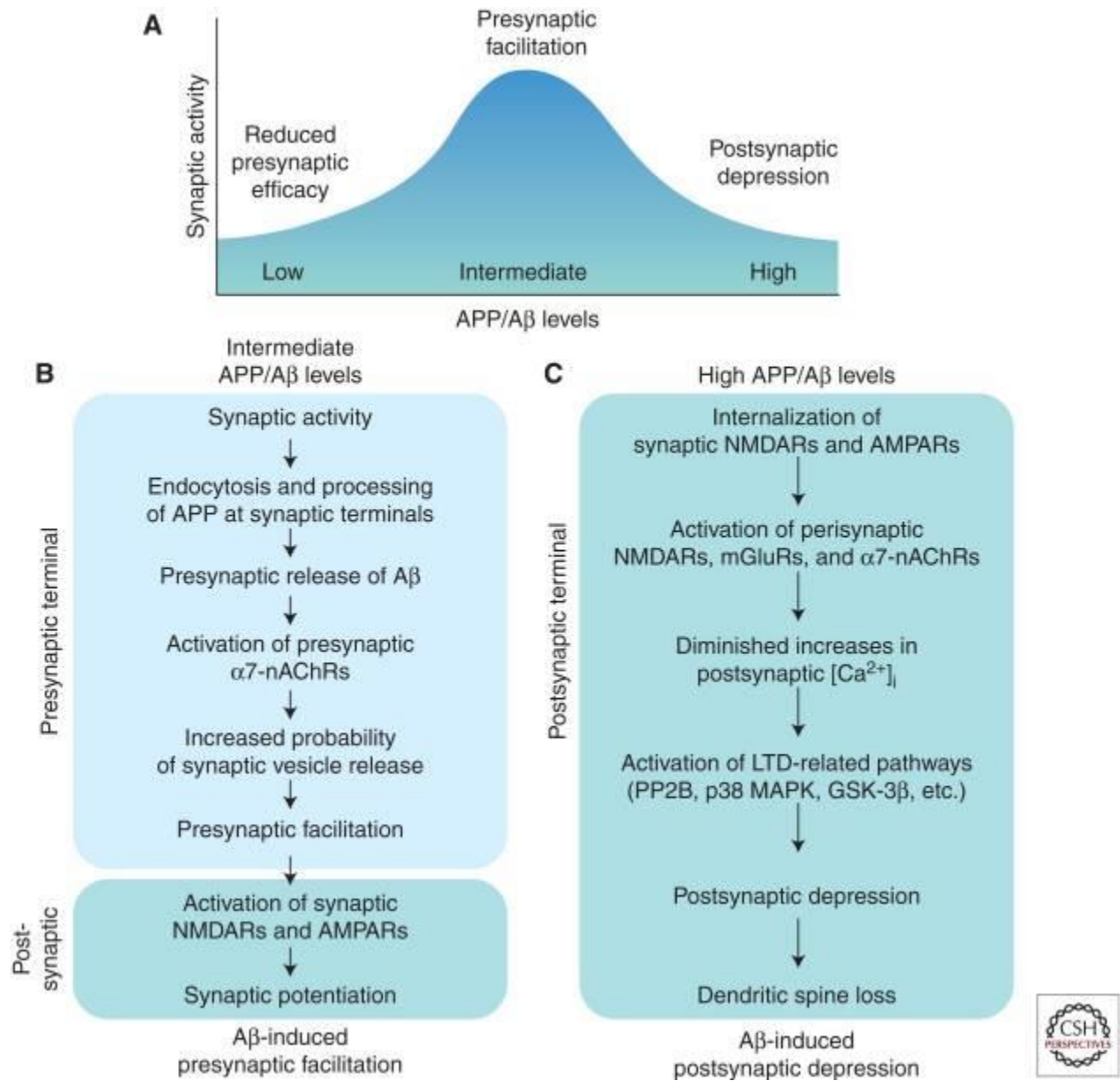


Figure 5-1. Presynaptic and Postsynaptic Regulation of Synaptic Transmission by A β -protein

(A) Hypothetical relationship between A β level and synaptic activity. Intermediate levels of A β enhance synaptic activity presynaptically, whereas abnormally high or low levels of A β impair synaptic activity by inducing postsynaptic depression or reducing presynaptic efficacy, respectively. (B) Within a physiological range, small increases in A β primarily facilitate presynaptic functions, resulting in synaptic potentiation. (C) At abnormally high levels, A β enhances long-term depression (LTD)-related mechanisms, resulting in postsynaptic depression and loss of dendritic spines. Reproduced with Permissions from Cold Spring Harbor Perspectives in Medicine.⁽⁶⁹²⁾

The mechanism by which this is accomplished has not been completely elucidated, but may involve activation of α 7-nAChR⁽⁶⁹³⁾, peri-synaptic activation of NMDA receptors^(679, 686) and downstream effects on calcineurin–STEP–cofilin, p38 MAPK and GSK-3 β signaling pathways.^(686, 694, 695) Importantly, A β -induced LTD-like processes may also underlie A β -induced LTP deficits, as blocking LTD-related signaling cascades prevents A β -dependent inhibition of LTP.⁽⁶⁹⁴⁾

In summary of these findings, various soluble oligomers of A β appear to induce complex patterns of synaptic dysfunction and network disorganization that underlie the intermittent but gradually progressive cognitive manifestations of AD. These oligomeric A β species may be in dynamic equilibrium with insoluble, fibrillar deposits of A β contained within A β plaques and demonstrate the ability to interact with components of neuronal and non-neuronal plasma membranes. Evidence suggests that there are multiple assembly forms of A β peptide that induce neuronal dysfunction through unique mechanisms of action. For this reason, it is unlikely that there are only one or two cognate receptors for neurotoxic forms of A β . Instead, the ever-expanding variety of molecular mediators of A β -protein neurotoxicity has led to the notion that the binding of hydrophobic A β assemblies to cellular membranes triggers multiple effects affecting diverse pathways. In the subsequent section, we explore a selectin of these molecular mediators in an attempt to provide a holistic understanding of AD pathogenesis.

5.5 TAU AS A MOLECULAR MEDIATOR OF A β NEUROTOXICITY

Despite the many criticisms against the amyloid cascade hypothesis, accumulating evidence obtained in in vitro and in vivo models and in patients provides solid experimental support for the hypothesis, and particularly for A β -induced Tau-pathology. More importantly these data position A β as accelerator/initiator and Tau as executor of the pathogenic process, designating their interaction as crucial triggering event in AD. As mentioned earlier, in addition to neuron loss and A β plaque deposition, NFTs containing hyper-phosphorylated tau are a hallmark of AD pathology. However NFTs cannot be considered pathognomonic for AD, as they are present in a number of other disorders including: Pick's disease, progressive supranuclear palsy, corticobasal degeneration, and motor neuron diseases. Still, there is a strong correlation between the severity of cognitive dysfunction and NFT load and localization in the brains of AD patients.⁽⁶⁹⁶⁾ Of note,

there are six major isoforms of human tau derived by alternative mRNA splicing from a single gene on human chromosome. Alternative splicing of exon 10 gives rise to 3-repeat (3R) and 4-repeat (4R) forms, but all forms are expressed in the adult brain. Found mainly in the axonal compartment, to date, the best established functions of tau involve the stabilization of microtubules and the regulation of motor-driven axonal transport.⁽⁶⁹⁷⁾ Importantly, physiologic phosphorylation of tau is critical regulator of these functions as it modulates its association with signaling proteins. As tau's physiologic functions are posited as central to proper neuron function and survival, loss of this protein's influence secondary to hyper-phosphorylation is assumed to contribute greatly to the pathogenesis of AD.^(697, 698) While the precise mechanisms by which tau hyper-phosphorylation occurs in disease is not completely understood, it likely involves disruptions in the balance of protein phosphatase and kinase activities⁽⁶⁹⁹⁾, or structural alterations that result in changes in the availability of specific residues in these enzymes (Figure 5-2).⁽⁷⁰⁰⁾ Tau has as many as 84 putative phosphorylation sites, of which 45 are serines, 35 threonines, and 4 tyrosines. Exemplifying the degree to which physiological tau phosphorylation is deregulated in AD, in filamentous tau extracted from AD patients almost 50 of these residues are phosphorylated in comparison with only nine sites identified in normal human brain tissue.^(701, 702) With respect to its role in AD pathogenesis, tau phosphorylation is believed to contribute to neuronal cell death by decreasing the assembly of tubulin⁽⁷⁰³⁾, disrupting axonal transport⁽⁷⁰⁴⁾, causing reentry of neurons into the cell cycle⁽⁷⁰⁵⁾, and possibly leading to further abnormal tau processing. As stated in the introduction however, current models of AD pathogenesis place tau-mediated neurodegeneration downstream of disruptions in A β production/clearance. Much of the rationale for this stems from the genetic findings already outlined. Unlike mutations in APP and PSEN genes, no AD causing mutations had been identified in the tau gene. Further, in some lines of APP transgenic mice, A β formation causes tau hyper-phosphorylation, whereas tau transgenic mice do not show A β plaque pathology.⁽⁷⁰⁶⁾ Additionally, crossing APP transgenic mice with tau transgenic mice results in a greatly enhanced quantity and distribution of the NFT pathology, without altering A β plaque pathology.⁽⁷⁰⁷⁾ However, dysregulation in tau must play significant role in mediating neurodegeneration in AD, as mutations in the tau gene are linked to familial forms of frontotemporal dementia with parkinsonism.⁽⁷⁰⁸⁾ Integrating these findings, the leading hypothesis with respect to tau's contribution to the neurodegenerative process underlying AD is that tau serves as a molecular mediator of A β -induced neurodegeneration. Importantly, a robust literature supports this hypothesis.

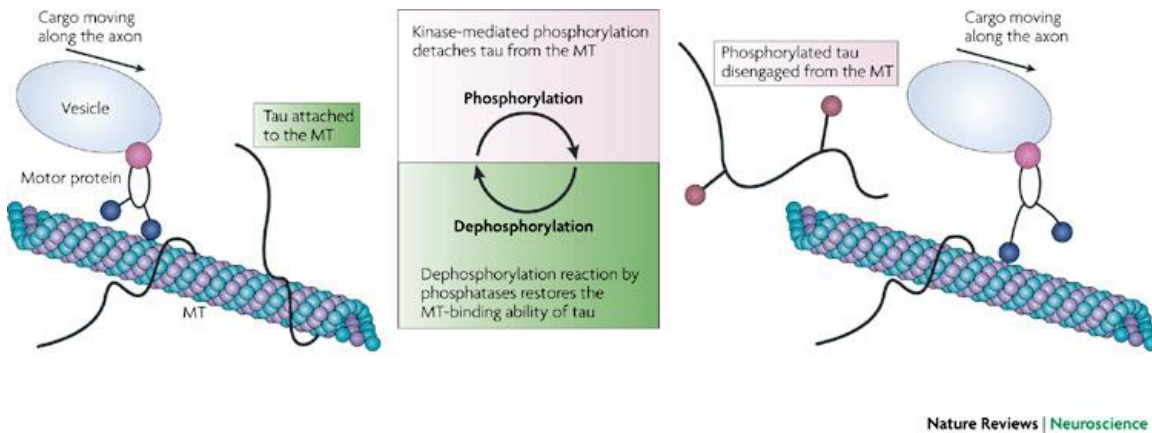


Figure 5-2. Schematic Representation of Normal Dynamic Equilibrium of Tau

A schematic representation of the normal dynamic equilibrium of tau, on and off the MTs, which is primarily determined by the phosphorylation state of tau. Although the presence of tau on the MTs presents a physical obstacle for vesicles and other cargoes that are moving along the axon, MT-bound tau is essential to MT integrity. Thus, relatively frequent cycles of tau–MT binding (promoted by dephosphorylation of tau) and detachment of tau from the MT (promoted by phosphorylation of tau) are needed in order to maintain effective axonal transport. Reproduced with Permissions from Nature Reviews Neuroscience.⁽⁷⁰⁹⁾

Focusing first on the relevant *in vitro* findings, application of synthetic or extracted A β peptides increases tau-phosphorylation and alters its conformation in a GSK3-dependent manner.⁽⁷¹⁰⁻⁷¹²⁾ Importantly, beyond GSK3, several other signaling mechanisms have been implicated in A β induced Tau-alterations in primary neurons. For example, CAMKK2-AMPK kinase- and C-Jun N-terminal kinase-mediated tau phosphorylation have also been reported in cell lines exposed to A β peptides.^(713, 714) Regardless of the primary mechanism, these *in vitro* findings provide compelling evidence that A β induces pathologically relevant alterations in tau. Similarly, experiments conducted in AD transgenic animal models strongly support the hypothesis of A β -induced tau-pathology. Although addressed specifically in another section, it is worth noting here that preliminary characterization of mutant APP or mutant APP/PS1 transgenic mice revealed a lack of NFT deposition, leading to the conclusion that A β -deposition could not induce tau dysregulation. However, subsequent analysis of APP/PSEN transgenic mouse lines with high A β plaque burden consistently revealed the presence of hyper-phosphorylated tau contained within the dystrophic neurites surrounding A β plaques.^(665, 667, 715, 716) The failure of these models to exhibit NFT formation is now ascribed to the low propensity of endogenous mouse tau to form NFTs, as APP/PSEN transgenic rats readily demonstrate NFT formation.^(717, 718) In order to overcome this limitation, a triple-transgenic model expressing human mutated forms of the APP, tau, and presenilin was developed. In congruence with the research described, characterization of this model further reinforced the relationship between A β deposition and NFT pathology, as A β plaque pathology preceded NFT deposition in these mice.^(671, 672) Additionally, anti-A β immunization in combined amyloid and tau transgenic mice reduces attenuates early tau hyper-phosphorylation. Lastly, in tau transgenic mice, injection of pre-aggregated A β peptides into the brain results in the induction of NFTs remote from the injection site, in neurons functionally connected with the site of injection.⁽⁷¹⁹⁾ In summary of these findings, the invariable demonstration of A β -induced tau-alterations in animal models, regardless of the approach employed to upregulate A β , strongly supports the conclusion that A β is an upstream inducer of tau-pathology. Conversely, the consistent failure of tau mouse models to affect or aggravate amyloid pathology seemingly excludes the possibility that A β deposition simply represents a downstream consequence of tau dysregulation, as proposed by some.⁽⁷²⁰⁾

Importantly, dynamic biomarker analysis has confirmed the temporal order in which changes in A β burden, tau-hyper-phosphorylation, and measures of neurodegeneration occur in AD patients. In these studies, measurements of cerebrospinal fluid (CSF) A β levels were used in combination with PET amyloid imaging to monitor the initial presentation and progression of amyloid-specific pathology. Similarly, CSF measurements of total tau and phosphorylated

tau were taken as indicators of NFT burden. Lastly, hypo-metabolism as assessed via fluorodeoxyglucose (FDG) PET and atrophy as measured by structural MRI served as markers of neurodegeneration in these studies. In congruence with the trends observed in animal models, the earliest changes in AD patients were noted in CSF A β ₄₂ levels followed closely by the detection of significant A β plaque burden via PET imaging.^(721, 722) Uniquely, A β pathology was the only biomarker identified which exhibited changes prior to the onset of symptoms. Later, once symptoms had developed, alterations in CSF tau were noted and subsequently followed by measurable brain atrophy.^(136, 721) Thus, the data summarized strongly supports amyloid-centric mechanisms of AD pathogenesis by demonstrating that changes in A β proceed alterations in tau-phosphorylation or neuron degeneration. Those familiar with the field may question the validity of these biomarker studies, pointing out the fact that histopathological data suggests that tau deposition occurs prior to A β plaque formation and in asymptomatic adults.⁽¹¹⁰⁾ Although the referenced data indeed demonstrates that tau-pathology can precede amyloid deposition, subsequent studies have since demonstrated that this tau-pathology is associated with normal aging and that the tau-pathology of AD is markedly increased and progresses more rapidly. Therefore, the proposed effect of A β on tau is to qualitatively transform and accelerate the antecedent subcortical tauopathy associated with normal aging, leading to the neocortical spread NFTs characteristically observed in AD patients.^(577, 722-724) Convinced of this mechanism, the field has since focused its attention on elucidating the mechanisms by which amyloid induces alterations in tau-phosphorylation.

5.5.1 *Plausible Mechanisms of A β -induced Tau Dysregulation:*

Generally speaking, three mechanisms have been proposed to underlie the phenomenon of A β -induced tau-pathology in AD. To be reviewed in more detail below, the first of these mechanisms links the development of tau-pathology to the downstream effects of A β on synaptic function reviewed in a previous section. Alternatively, others suggest that A β -mediated neuro-inflammation results in the perturbation of kinase/phosphatases critical to the physiological phosphorylation of tau. Lastly, recent evidence suggests that A β cross-seeding of tau may induce a transition from “mild” tau-strains to more aggressive tau-strains, thereby triggering a prion-like spreading of tauopathy along neuronal circuitries. While a unifying mechanism of amyloid-induced tau-pathology is yet to be identified, the

significance of these models to our discussion lies in their emphasis of A β -induced acceleration of tau-pathology as a critical mediator of AD pathology.

Since the discovery that extracellular application of A β peptides can induce tau-pathology in tau transgenic mice, researchers have assumed that A β must interact with neurons through association with its membrane or receptors. And indeed, binding of A β to different types of receptors and directly to membranes has been reported. Highlighting some of the most well-established interactions, A β has been shown to interact directly with: alpha7 nicotinic acetylcholine receptors (α 7 nAChR), NMDA and AMPA receptors, the Ephrin-type B2 receptor (EphB2), insulin receptors, the receptor for advanced glycation end products (RAGE), the prion protein receptor (PrP-receptor), the mouse paired immunoglobulin-like receptor (PirB) and its human counterpart the leukocyte immunoglobulin-like receptor (LilrB2).^(675, 725-730) Similarly, reports of A β induced neurotoxicity via association with membranes and their integral proteins have been published.⁽⁷²⁵⁾ Lending pathological relevance to the existence of these interactions, association of A β with a subset of these receptors has been shown to potentiate disturbances in tau-phosphorylation. Taking for example the putative interaction between A β and α 7 nAChR, binding of A β to this nicotinic receptor subtype increases tau-phosphorylation at Ser-202, Thr-181, and Thr-231.⁽⁷²⁶⁾ The observant reader might note that this same interaction was posited to contribute to A β -induced LTD. On that topic, A β assemblies are believed to interact indirectly with NMDA-receptors through the EphB2 receptor.⁽⁷²⁹⁾ As discussed, the general effect of A β on synaptic plasticity is to shift synaptic potentiation (LTP) to synaptic depression (LTD) via modulation of NMDA receptor function. Interestingly, in addition to synaptic degeneration, A β -induced reduction of NMDA-dependent LTP has been linked to increased tau-phosphorylation via a GSK3-mediated pathway in both hippocampal slices and mouse models.^(707, 731, 732) Thus, NMDA receptors may play a role in A β -induced changes in tau via GSK3 β . Synthesizing the reviewed interactions into a model of A β -induced tau dysregulation, increases in A β results in perturbed intra-cellular signaling cascades secondary to direct and indirect interactions between A β and a variety of neuronal receptors/membrane proteins. Dysregulation of these intra-cellular cascades in turn raises intra-cellular Ca²⁺ levels and disrupts the physiological function of phosphatases and protein kinases such as GSK3. This in turn results in the hyper-phosphorylation of tau, leading to its aggregation and deposition in NFTs and associated neurotoxicity.

Interestingly, the ability of A β to induce robust neuro-inflammation stands as a second plausible mechanism through which A β -induced tau hyper-phosphorylation may arise. As reviewed at length in subsequent sections, a variety

of molecular pathways link the deposition of A β with the development of inflammation in the brain, with several authors going so far as to suggest that neuro-inflammation constitutes a better etiological cause of AD than do A β assemblies. Highlighting the significance of inflammatory cascades to the development of tauopathy only, several reports have demonstrated that tau-pathology is dramatically aggravated by acute and chronic inflammatory insults.⁽⁷³³⁾ Interestingly, some data suggests that the correlation between neuro-inflammation and the development of tau-pathology may be mediated by astrocytes and glial cells. For example, antibody-mediated inhibition of the interleukin 1, a potent pro-inflammatory cytokine produced by microglia, attenuates hyper-phosphorylation of tau while potentiation of interleukin 1 β signaling exacerbates tau-pathology.^(733, 734) Additionally, in vitro studies corroborate the conclusion that astrocytes and microglia play a role in A β -induced tau-phosphorylation, as this pathological process is exacerbated in co-cultures with glial cells as compared to in cultures of primary neurons alone.^(735, 736) Importantly, this hypothesis is physiologically plausible as amyloidgenic mouse models of AD invariably exhibit astro- and micro-gliosis, a finding which seemingly confirms that A β pathology results in the activation and recruitment of these cell types to amyloid-burdened regions of the brain.⁽⁷¹⁶⁾

A third hypothesis in the field is that A β assemblies may qualitatively transform antecedent tau-pathology via a cross-seeding mechanism. The consequence of this being the triggering of an accelerated prion-like spreading of tau-pathology along neuronal circuits. Breaking this model into its constituent components, it has been demonstrated that A β peptides can enable initiation and propagation of amyloid plaque formation to remote regions of the brain via a prion-like seeding mechanism.^(737, 738) In this mechanism, a specific subtype of misfolded A β proteins can subsequently act as seeds that structurally induce misfolding of other proteins, causing them to aggregate into pathogenic assemblies ranging from small oligomers to large fibrillar amyloids. Recently, these prion-like spreading properties have been demonstrated for tau, with misfolded tau extracted from brains of transgenic mice being shown to propagate tau-pathology in a seed dependent manner when administered to the brains of tau transgenic mice.⁽⁷³⁹⁻⁷⁴¹⁾ Given the evidence that A β and tau can form soluble complexes in vitro, it is possible that A β species might induce this form of prion-like spreading in tau pathology as well, although such a mechanism has yet to be directly demonstrated.⁽⁷⁴²⁾ Instead, proponents of this theory point to animal studies demonstrating that injection of A β assemblies into the brain can induce tau-aggregation not only at the site of injection, but also in remote regions of the brain functionally connected to the injection site.⁽⁷⁴³⁾ Similarly, in some AD mouse models, NFT deposition is noted in regions of the brain like the hippocampus in the absence of robust

A β deposition. However, the hippocampus very much anatomically and functionally connected to the subiculum, a region of the brain riddled with A β plaque pathology.⁽⁷³²⁾ While support for this hypothesis requires significant bolstering, one strength of this model is that it might explain the spatio- and temporal characteristic spreading of tau across brain regions as described originally by Braak and Braak.⁽¹¹⁰⁾ Furthermore, confirmation of this hypothesis might serve to reconcile the discrepancies observed between histopathological data suggesting that tau-pathology proceeds A β deposition and biomarker data collected in AD patients which supports the converse relationship. Under this model, a pre-existing tauopathy associated with normal aging becomes qualitatively transformed by A β -mediated cross-seeding, resulting in a conformational change in tau which increases its propensity to aggregate and propagate across functionally connected brain circuits. Thus, the pre-existence of tau-pathology may be a requirement for the development of AD, explaining why A β pathology specifically affects neurons with pre-existing tau-pathology (Braak stage I-II), and not nearby neurons.⁽⁷³²⁾

5.5.2 Mechanisms of Tau-induced Neurodegeneration

Although the relative contributions of each of the outlined mechanisms by which tau-pathology is induced in AD are still being investigated, a consensus has more or less been reached in the literature with respect to tau misfolding and fibril formation occurs under pathological conditions.⁽⁷⁴⁴⁻⁷⁴⁶⁾ Based on a variety of evidence, abnormal disengagement of tau from microtubules secondary to hyper-phosphorylation and a concomitant increase in the cytosolic concentration of tau are believed to be the key events that lead to tau-mediated neurodegeneration. Under the current paradigm, tau misfolding is thought to be a stochastic phenomenon that is more likely to occur at higher cytosolic tau concentrations. Additionally, it is believed that the transition from unbound tau to NFTs is a multi-step phenomenon complete with intermediate tau assemblies. In congruence with this idea, the earliest deposits of tau are called ‘pretangles’ and are not stained by Congo red or thioflavin-T.^(747, 748) This finding is of significance, as it indicates that pretangles do not contain β -sheets, and that a structural rearrangement involving the formation of the characteristic pleated β -sheet must occur during the transition from pretangles to PHFs. Importantly, morphometric analysis suggests that in AD, at least 95% of total tau is contained in NFTs located in neuronal processes known as neuropil threads or dystrophic neurites.⁽⁷⁴⁹⁾

Furthermore, while the vast majority of tau is axonally located under physiological conditions, in AD, re-localization of tau to the somatodendritic domain has been observed and may contribute to its neurodegenerative effects.

One obvious mechanism by which tau-mediated neurodegeneration might occur is via the loss of its normal microtubule stabilizing function. Such a disturbance would be expected to compromise axonal transport and in this way contribute to the synaptic dysfunction underlying the observed neuron death characteristic of AD. In support of this model, administration of the microtubule stabilizing drug paclitaxel has been shown to ameliorate the neurodegenerative phenotype in tau transgenic mouse models.^(750, 751) Notably however, if loss of tau's physiological function was the only contributory process to the neurodegenerative changes observed in AD, the density and localization of NFTs would not be expected to robustly correlate with the degree of cognitive impairment. The existence of such a correlation was among the first lines of circumstantial evidence to suggest that toxic gains-of-function by NFTs might play an important part in the progression of AD.⁽⁷⁵²⁾ Though not yet verified, some suggest that the toxic effects of NFTs may be mediated by their large size. In this model, the fibrillary material contained within NFTs serves as a physical barrier which disrupts cellular functions such as axonal transport. In a similar gain-of-function, tangles may sequester larger quantities of other functionally significant proteins.

Although loss of tau function and the toxic gain-of-function acquired by NFTs as they enlarge may contribute to neurodegeneration, to date, the interaction of tau with the tyrosine protein kinase Fyn represents the most well supported hypothesis of tau-mediated synaptic loss. Importantly, studies demonstrate that in addition to its axonal functions, tau also targets Fyn kinase to the dendrite via its amino-terminal projection domain.⁽⁷⁵³⁾ Once at the postsynaptic membrane, Fyn phosphorylates the NR subunit 2 of NMDA receptors to facilitate their interaction with the postsynaptic density protein 95 (PSD-95).⁽⁷⁵⁴⁻⁷⁵⁶⁾ Critically, the ability of NMDA receptors to bind to PSD-95 is essential in the generation of glutamatergic excitotoxicity, an essential component of AD pathophysiology. Evidence emphasizing the significance of this interaction comes from studies which demonstrate disruption of NMDA receptor/PSD-95 complexes prevents excitotoxic damage in cultured neurons and in vivo models.⁽⁷⁵⁷⁾ Given this background information, it is clear how elevated levels of tau might contribute to neurodegeneration. Put simply, dissociation of tau from microtubules secondary to hyper-phosphorylation results in a larger available pool of unbound tau in the somatodendritic compartment capable of increasing Fyn levels at the post-synaptic membrane. As a consequence, the interaction between NMDA receptors and

PSD-95 is increasingly facilitated resulting in enhanced NMDA-mediated excitotoxicity. As stated, a number of experiments support this model. For example, when truncated versions of tau which are incapable of targeting Fyn to the dendritic compartment are expressed in transgenic mouse models, dendritic levels of Fyn are reduced, NMDA receptors become uncoupled from PSD-95, and as a consequence the animals are spared of any signs of tau-induced neurodegeneration.⁽⁷⁵⁸⁾ As a final note, beyond outlining a clear molecular mechanism of tau-induced neurodegeneration, this model also links tau dysregulation to amyloid centric models of AD in that reduction of Fyn in APP transgenic mice prevents A β -induced cognitive deficits while its overexpression increases neurodegeneration.^(759, 760)

5.6 NEUROINFLAMMATION & ALZHEIMER'S DISEASE

As discussed, in vivo evidence suggests that a dynamic equilibrium exists between amyloid plaque deposits, fibrils, oligomers, and monomer peptides. Critically, aggregation of A β peptides changes not only their biophysical characteristics but also dramatically alters their biological activity. This is well evidenced by the finding that oligomeric assemblies of A β are more neurotoxic in cell cultures as compared to A β monomers.⁽⁶⁷⁶⁾ Furthermore, the phase transition from monomeric A β peptide into larger oligomeric, fibrillary, and aggregate species has been shown to facilitate A β 's interaction with a host of receptors that mediate its endocytosis. This is particularly true of constituent receptors of the innate immune system, as toll-like receptors- (TLR) 2, 4, and 6 and their co receptors can all be triggered by assemblies of A β .⁽⁷⁶¹⁾ Similarly, class A scavenger receptors; CD36 and CD47 all promote the phagocytosis of A β .⁽⁷⁶¹⁾ These findings raise an interesting question, "why is it that so many pattern recognition receptors interact with A β species?" Interestingly, some authors now leverage the binding promiscuity of A β to advocate for the hypothesis that neuro-inflammatory cascades triggered by A β could have evolved in cells of the immune system as a host response to microbial challenges.⁽⁷⁶¹⁾ The background rationale for this hypothesis is fascinating and thus warrants review. The origin of this hypothesis can be credited to the observation that the receptors that sense pathogen-associated molecular patterns, such as bacterial lipopolysaccharide and viral surface proteins, are also those triggered by A β aggregates. This led to the speculation that the tertiary structure of misfolded A β assemblies may contain a conserved molecular pattern for which the innate immune system has evolved immunological signaling receptors. In support of this thought process, both bacteria and fungi express surface amyloids.⁽⁷⁶²⁻⁷⁶⁴⁾ Unbeknownst to many in the field, the spectrophotometric dye Congo red, one of two gold-

standard histochemical stains for A β deposits, was originally also used as a stain for bacterial amyloid fibrils. Thus, it is not far-fetched to hypothesize that the detection of amyloid by pattern-recognition receptors of the immune system could have evolved as a host response to microbial challenges. However, in contrast to an immune response to microbes, which is terminated once the stimulating pathogen has been removed, sustained elevations of A β may not allow the resolution of inflammation. Therefore, while many A β -induced inflammatory mediators might initially support the clearance of pathogenic A β and promote cell survival, chronic neuro-inflammation developing in the context of sustained A β might directly compromise neuronal function and survival.⁽⁷⁶⁴⁾

Undeniably, evidence supports the existence of a contributory role for neuro-inflammation in the pathogenesis of AD. In fact, just as with tau, some groups have gone so far as to suggest a neuro-inflammatory etiology of AD which largely denies a pathological significance to the amyloid cascade. With the relatively recent discovery that A β accumulation can begin decades before the onset of clinical symptoms however, a majority in the field have again returned to amyloid-centric models. Generally speaking, these models postulate that assemblies of A β can activate immunologically relevant cell types via a multitude of interactions with their immunological receptors. Most relevantly to the hypothesis that A β -induced neuro-inflammation represents a vestigial response to exogenous pathogens, many of the signal-transduction pathways that are elicited by AD are also activated during a host response to microbes. For example, a key component of the innate immune system's response to viral/microbial pathogens is the activation of a proteolytic cascade that regulates the production of pro-inflammatory cytokines like those in the IL-1 β family.⁽⁷⁶¹⁾ Importantly, these cytokines exist in biologically inert precursor forms until activated by proteolytic cleavage mediated by either caspase-1 or caspase-8.⁽⁷⁶⁵⁾ Activation of these caspases is in turn regulated by a large multi-molecular signaling complex known as an "inflammasome" (Figure 5-3). The sensor molecules of this structure include members of the Nod-like receptor (NLR) or pyrin and HIN domain-containing (PYHIN) families, and have been shown to be sensitive to a range of aggregated molecules including A β .⁽⁷⁶⁶⁾ Supporting a pathophysiological relevance of A β 's interaction with sensor molecules of the inflammasome, brains from patients with AD have a greater abundance of active caspase-1 than do those of age-matched control subjects.⁽⁷⁶⁶⁾ Similarly, APP/PSEN transgenic mice with mutations in NLR, caspase-1, or any other constituent of the inflammasome complex are largely protected for the neurodegenerative effects of A β over-expression.⁽⁷⁶⁶⁾ This effect may be attributed to observed increases in A β clearance and/or a removal of IL-1 β 's negative influence on synaptic

plasticity. While the interaction between $A\beta$ and inflammasomes is one of the best characterized neuro-inflammatory mechanisms underlying AD to date, it is important to note other pro-inflammatory factors may also influence the pathogenesis of AD. As evidence, the CSF of AD patients is enriched in p40, a subunit of IL-23, indicating that the IL-12 and IL-23 signaling pathways are additionally activated in AD.⁽⁷⁶⁷⁾

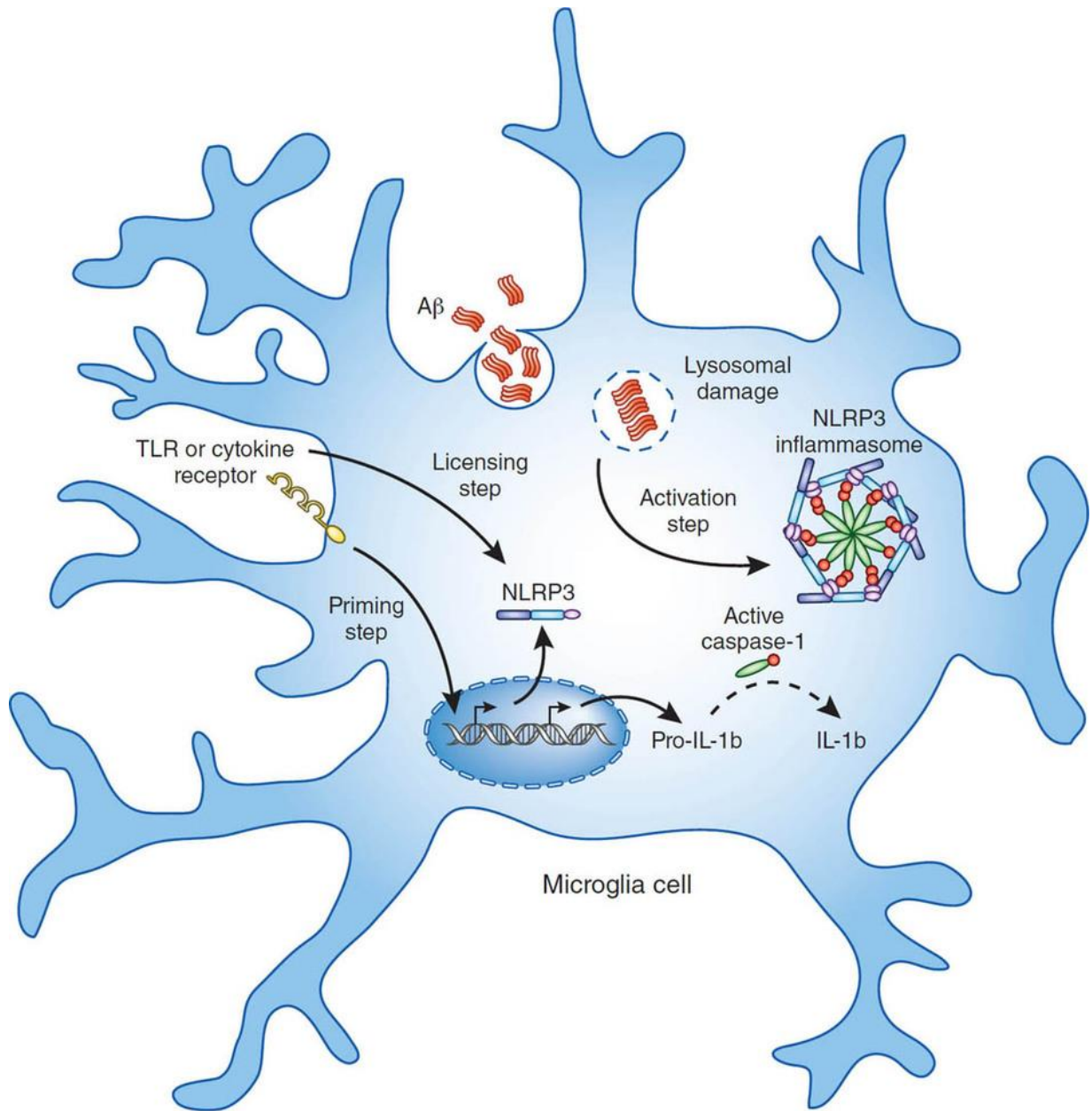


Figure 5-3. Inflammasome Activation Cascade.

The activation of microglia with TLR agonist or cytokines leads to the transcriptional induction of genes encoding components of the NLRP3 inflammasome and pro-IL-1 β (priming step). Additional signals, including deubiquitination of NLRP3, are further required for the activation of NLRP3 (licensing step). A β can induce lysosomal damage that leads to assembly of the NLRP3 inflammasome (activation step) and the activation of caspase-1. Active caspase-1 leads to the processing of IL-1 β and release of the bioactive form of IL-1 β . Reproduced with Permissions from Nature Immunology.⁽⁷⁶¹⁾

Furthermore, studies done in transgenic animal models demonstrate that attenuation of these neuro-inflammatory pathways reduces A β load and abolish deficits in spatial memory. Interestingly, as astrocytes are the principal immune cell type expressing IL-23 receptors, it may be that microglial derived p40 may stimulate the astroglial uptake of A β . Similarly, as discussed, astrocytes may reciprocally modulate the clearance of A β by microglia via the release of lipidated ApoE, a critical mediator of microglial phagocytosis of A β .⁽⁷⁶⁸⁾ Adding to the complexity, the release of small-molecular mediators such as nitric oxide (NO), can also influence the pathogenesis of AD. Indeed, studies demonstrate that during AD the inducible isoform of NO synthase (iNOS) is expressed by neurons and glial cells in response to pro-inflammatory cytokine release.⁽⁷⁶⁹⁾ Aside from NO's ability to directly facilitate neurodegeneration by inhibiting mitochondrial respiration, facilitating axonal and synaptic damage, and inducing neural apoptosis, iNOS can directly nitrate the Tyr 10 residue of A β resulting in its enhanced propensity to self-aggregate. Not only is this nitrated form of A β thus more capable of seeding cores of A β plaques, but studies also demonstrate it is more potent in suppressing synaptic plasticity.⁽⁷⁷⁰⁾ This last finding highlights two key points that need to be addressed in further detail. The first is that mediators of neuro-inflammation have a robust ability to modulate synaptic plasticity and thus are uniquely poised to disrupt the physiological mechanisms which maintain the integrity of neural circuits. The second is that A β production, clearance, and aggregation may be influenced by neuro-inflammatory signals in a manner which magnifies the innate neurotoxicity of A β .

Elaborating on the first point, a well published function of microglia is the maintenance of synaptic integrity. In fact, under physiological conditions the processes of microglia constantly scan dendritic spines and influence the continuous remodeling of neural contacts.⁽⁷⁷¹⁾ As a result of activation by a pro-inflammatory stimulus however, microglial processes retract. Thus, it is hypothesized that loss of neuronal synapse monitoring by microglia during an A β -induced inflammatory response could lead to neuronal changes and disrupt circuits relevant to learning and memory (Figure 5-4). This idea is supported by the finding that several cytokines including IL-1 β ⁽⁷⁷²⁾, IL-18⁽⁷⁷³⁾, and TNF- α ⁽⁷⁷⁴⁾, have been shown to suppress long-term potentiation in the hippocampus.⁽⁷⁷⁵⁾ Moreover, inhibition of inflammasome-mediated responses to A β through selective down-regulation of its NLR constituent prevents the suppression of LTP in APP/PSEN transgenic mice.⁽⁷⁷⁶⁾ However, the induction of neurodegeneration by soluble inflammatory mediators is almost certainly not the exclusive mechanisms by which microglia contribute to the killing of neurons.

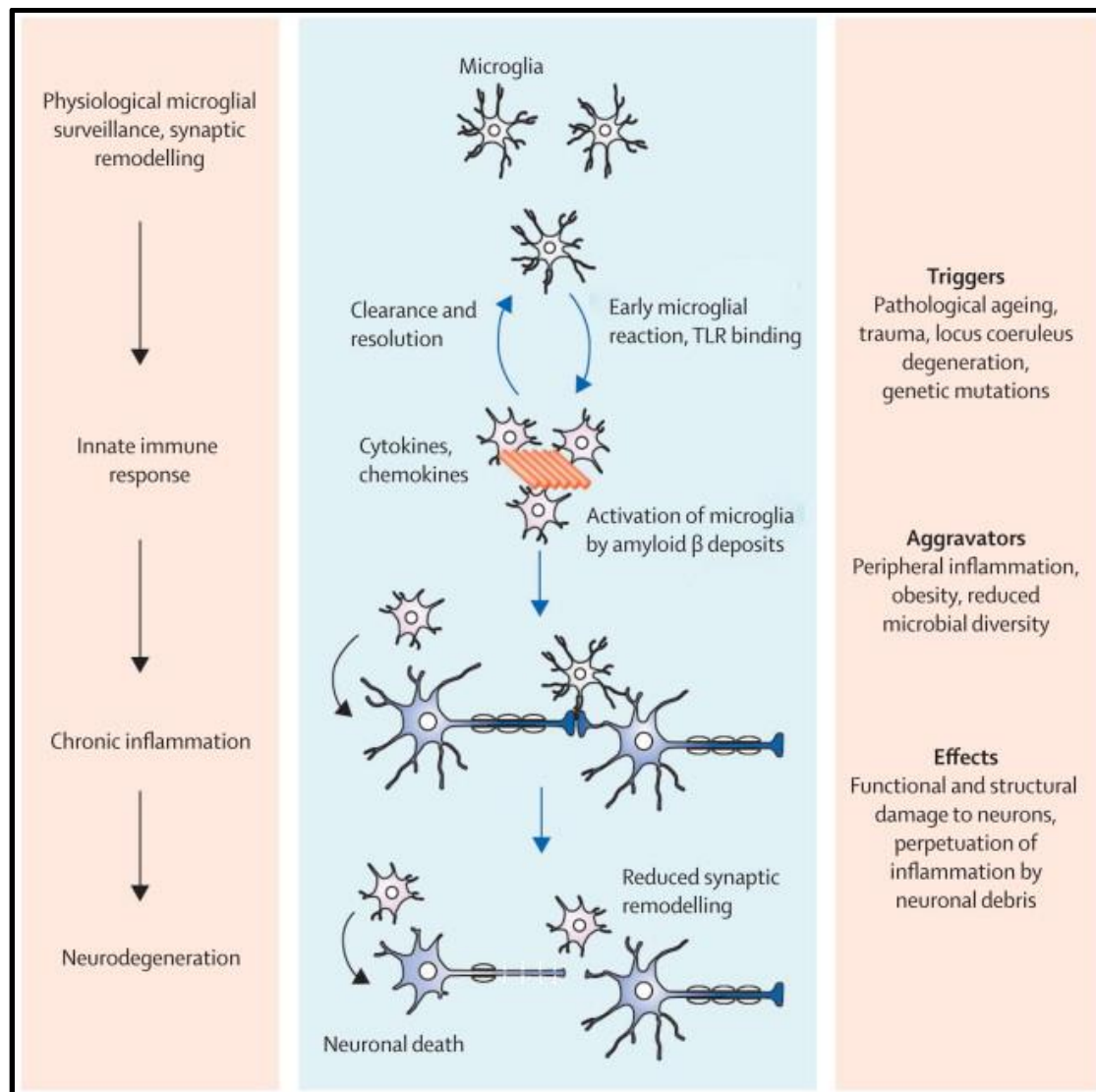


Figure 5-4. Pathomechanistic Sequelae of Microglia Activation.

Physiological functions of microglia, including tissue surveillance and synaptic remodeling, are compromised when microglia sense pathological amyloid β accumulations. Initially, the acute inflammatory response is thought to aid clearance and restore tissue homeostasis. Triggers and aggravators promote sustained exposure and immune activation, which ultimately leads to chronic neuroinflammation. Perpetuation of microglia activation, persistent exposure to proinflammatory cytokines and microglial process retraction cause functional and structural changes that result in neuronal degeneration. TLR=Toll-like receptor. Reproduced with Permissions from Nature Immunology. ⁽⁷⁶¹⁾

For example, it has been found that activated microglia can destroy functional neurons via an A β -dependent phagocytosis.^(777, 778) In this process, A β -induces increased expression of phosphatidylserine on processes of non-apoptotic or necrotic neurons, resulting in their destruction by microglia.

Transitioning to our second point, a third mechanism by which activation of the innate immune system may contribute to the pathophysiology of AD is via their ability to reciprocally influence A β deposition. With respect to the effect on pro-inflammatory mediators on A β production, studies demonstrate that inflammatory processes mediated via migration inhibitory factor-related protein 14 upregulate BACE1, the rate-limiting enzyme of amyloidogenic APP processing. As already discussed, nitration of A β by iNOS enhances the peptide's propensity to aggregate and to form seeding cores of A β plaques. Thus, neuro-inflammatory signals clearly modulate amyloid production and the pathogenicity of certain amyloid species. And yet, these mechanisms neglect one of the principal functions of microglia in the brain, the clearance of cellular debris and aggregated proteins. As discussed, microglia contribute to the clearance of A β by phagocytosis and the release of enzymes like insulin degrading enzyme (IDE) that are able to degrade A β in the extracellular space. Unlikely by coincidence, binding of fibrillar A β to CD36 expressed on the surface of microglia induces the formation of a TLR4-TLR6 heterodimer that results in activation of downstream transcription which reduce IDE levels such as NF-kB.^(779, 780) At the systems level, the phagocytic clearance function of microglia is greatly impaired in response to degeneration of the locus coeruleus, the chief source of norepinephrine in the brain and an early target of AD pathology.^(780, 781) Overall, these pathways suggest that the activation of pro-inflammatory pathways in the brain can maintain a dangerous feed-forward loop secondary to their ability to reciprocally influence A β deposition. Alternatively or in addition, it is logical to assume that sustained activation of microglia might strain the existing cell population ultimately leading to cellular exhaustion and demise. The consequence of this being that microglia which subsequently proliferate will do so in a microenvironment of immunological activation. Under such conditions, microglia develop a more pro-inflammatory gene-expression pattern compared to that of microglia that resided in the affected brain area before such activation. Thus, newly generated microglia might carry a phenotype that increasingly contributes to the maintenance of the chronic inflammatory response that characterizes AD. In addition, there is some evidence that cells of the myeloid lineage are attracted from the periphery to the site of plaque formation and therefore may contribute to AD's observed inflammatory phenotype. In support of this hypothesis, loss of the chemokine receptor CCR2 results in a gene dose–

dependent aggravation of amyloid pathology in Tg2576 mice. Given that CCR2 is a critical mediator of peripheral immune cell recruitment to the CNS, these results suggest that these non-CNS associated cells may somehow modulate A β burden.⁽⁷⁸²⁾

CHAPTER 6 BIOMARKERS FOR ALZHEIMER'S DISEASE

Arguably runner-up only to the lack of disease-modifying treatments, one of the most significant impediments to the management of AD is the inability to definitively diagnose the disease until post-mortem examination. As reviewed in detail, the initial diagnosis of possible/probable AD is presumptive until death. Today, the only tools at the disposal of diagnosticians are clinical evaluation, neuropsychological testing, and the core clinical criteria as laid out in the International Classification of Disease (ICD-10), the Diagnostic and Statistical Manual of Mental Disorders (DSM-V) and the National Institute for Ageing-Alzheimer's Association (NIA-AA). On average, application of these criteria yields a diagnostic accuracy of 80–90% when compared to the histopathological gold standard. However as reviewed in great detail, one of the defining characteristics of AD is the heterogeneity of its clinical presentation. Compounding this issue, the vast majority of AD patients carry co-morbid neurodegenerative process which can alter not only the symptomatic manifestations of the disease but also the pathophysiology of the disease itself. Thus, one of the fundamental goals of AD research has been the validation of reliable biomarkers. According to the National Institutes of Health (NIH) Biomarkers Definitions Working Group, a biomarker is defined as 'a characteristic that is objectively measured and evaluated as an indicator of normal biological processes, pathogenic processes, or pharmacologic responses to a therapeutic intervention.'⁽⁷⁸³⁾ In 1998, the Ronald and Nancy Reagan Research Institute of the Alzheimer's Association and the National Institute of Aging Working Group set up criteria for an ideal AD diagnostic biomarker. These recommendations stated that the biomarker should be (i) able to detect a fundamental feature of Alzheimer's neuropathology, (ii) validated in neuropathologically confirmed AD cases, (iii) characterized by good sensitivity/specificity, (iv) reliable, (v) non-invasive, (vi) technically simple to perform, (vii) and inexpensive.⁽⁷⁸⁴⁾ Once identified, AD biomarkers may be utilized in three distinct applications: (i) as a diagnostic marker to aid in the early diagnosis of AD in clinically representative populations, (ii) as a classificatory marker capable of distinguishing AD from dementia subtypes that have similar clinical presentations, and (iii) as a prognostic marker capable of predicting disease progression with or without therapeutic intervention.⁽⁷⁸⁵⁾ As was highlighted in the review of current AD diagnostic criteria, AD biomarkers are just now coming of age, having a central position in the newly revised criteria for prodromal stages of AD as outlined by the IWG and NIA-AA. Importantly, dynamic biomarker analysis has confirmed the temporal order in which changes in A β burden, tau-

hyper-phosphorylation, and measures of neurodegeneration occur in AD patients (Figure 6-1). In these studies, measurements of cerebrospinal fluid (CSF) A β levels were used in combination with PET amyloid imaging to monitor the initial presentation and progression of amyloid-specific pathology in humans. Similarly, CSF measurements of total tau and phosphorylated tau were taken as indicators of NFT burden. Lastly, hypo-metabolism as assessed via fluorodeoxyglucose (FDG) PET and atrophy as measured by structural MRI served as markers of neurodegeneration in these studies. In congruence with the trends observed in animal models, the earliest changes in AD patients were noted in CSF A β_{42} levels followed closely by the detection of significant A β plaque burden via PET imaging.^(721, 722) Uniquely, A β pathology was the only biomarker identified which exhibited changes prior to the onset of symptoms. Later, once symptoms had developed, alterations in CSF tau were noted and subsequently followed by measurable brain atrophy.^(136, 721) Thus, many in the field have championed A β -targeted diagnostics for the early-detection of AD. As will be discussed however, this approach has proven insufficient with respect to improving diagnostic accuracy; alluding to the need for continued research in this space. Importantly, the development of an imaging technology capable of visualizing and quantifying A β plaques in animal models and in the AD brain is critically important for translational, preclinical and clinical research.

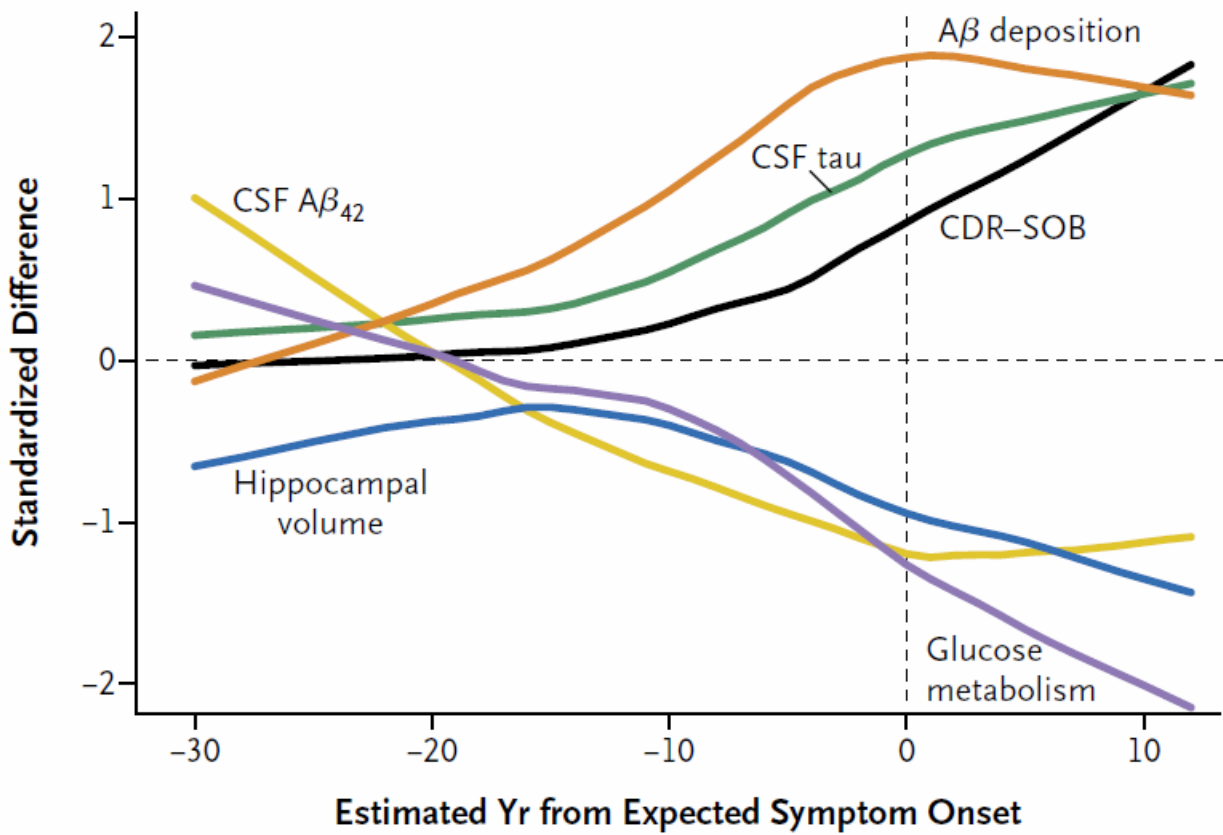


Figure 6-1 Comparison of Clinical, Cognitive, Structural, Metabolic, and Biochemical Changes as a Function of Estimated Years from Expected Symptom Onset.

The normalized differences between mutation carriers and noncarriers are shown versus estimated years from expected symptom onset and plotted with a fitted curve. The order of differences suggests decreasing $A\beta_{42}$ in the CSF (CSF $A\beta_{42}$), followed by fibrillar $A\beta$ deposition, then increased tau in the CSF (CSF tau), followed by hippocampal atrophy and hypometabolism, with cognitive and clinical changes (as measured by the Clinical Dementia Rating-Sum of Boxes [CDR-SOB]) occurring later. Mild dementia (CDR 1) occurred an average of 3.3 years before expected symptom onset. Reproduced with Permissions from Massachusetts Medical Society.⁽⁷⁸⁶⁾

6.1 AMYLOID IMAGING

Of the early diagnostic modalities proposed for AD, PET-mediated amyloid imaging (AI) has emerged as the most promising approach with respect to developing a minimally-invasive yet clinically applicable diagnostic methodology. The first study of amyloid deposition employing PET imaging used an ^{11}C -labeled derivative of the amyloid-binding histological dye Thioflavin-T called Pittsburgh Compound-B (PiB). In this ground-breaking study, increased ligand retention was revealed in the cortical brain regions of AD patients as compared with controls, using cerebellum as a reference region.⁽⁷⁸⁷⁾ Since this discovery, PiB has become the most widely employed and well-validated AI imaging ligand in the world. With respect to the correlation between PIB retention and A β plaque burden *in vivo*, a criteria restricted review of seven primary studies (24 case reports) concluded that sufficient evidence exists to make an association between PIB retention and A β plaque density.⁽⁷⁸⁸⁾ In more detail, binding of the PiB appears specific for β -sheet-folded A β . Therefore, PiB selectively binds to compact plaques and cerebrovascular amyloid angiopathy (CAA). By contrast, diffuse plaques are less prominently labeled and amorphous plaques comprised of loosely aggregated A β are virtually unrecognized by PiB.⁽⁷⁸⁹⁻⁷⁹¹⁾ Interestingly, PiB does not bind to aggregated forms of A β in patients presenting with the arctic *APP* gene (E693G) mutation.⁽⁷⁹²⁾ As these patients still exhibit severe signs of dementia, some have interpreted this lack of fibrillary A β to mean that other forms of A β such as oligomers and protofibrils must be of more importance to the pathologic processes underlying AD. With the exception of the arctic APP mutation however, AD patients consistently exhibit a 50-70% increase in PiB retention compared to aged-matched, cognitively normal adults in regions such as the prefrontal cortex, precuneus, and posterior cingulate.^(787, 793-798) In a review of fifteen studies which cumulatively included 341 AD and 651 cognitively normal subjects, the difference in PIB retention observed in AD dementia subjects and cognitively normal controls was highly significant ($p < 0.001$). Furthermore, this study estimated the diagnostic specificity of PIB to be approximately 76%.⁽⁷⁸⁸⁾ As a prognostic biomarker, within a follow-up period ranging from eight months to three years, 38-82% of mild cognitive impairment (MCI) patients who screened positive for amyloid pathology via PIB imaging converted to AD compared to a mere 7% convergence rate for PIB(-) MCI cohorts.⁽⁷⁹⁹⁻⁸⁰²⁾ Taken as a whole, these data clearly lend support to the notion that PiB-mediated AI can serve as a robust biomarker for AD. On the other hand, some studies indicate that PIB retention correlates poorly with memory deficits in

AD patients and healthy controls.^(794, 803-809) In part, this is not surprising as post-mortem measurements of A β load also fail to correlate robustly with symptom severity. Additionally, according to some investigators, PiB retention may correlate poorly with observed cognitive deficits due to differences in cognitive reserve between subjects.⁽⁸¹⁰⁻⁸¹⁴⁾ Nevertheless, more recent work directly opposes this assertion, finding that AI correlates most robustly with symptom severity when compared to other biomarker options.⁽⁸¹⁵⁾ The source of discrepancy between these studies is difficult to pinpoint, but generally speaking the consensus in the field is that AI demonstrates a reliable correlation with cognitive impairment in pure AD cohorts. Still, this first-generation AI radio-ligand is not without severely limiting characteristics. For example, human subjects with CAA may have positive PiB amyloid PET scans, even in the absence of amyloid plaques.⁽⁸¹⁶⁾ While investigators had hoped these two pathologies could be distinguished based on the differential in their distribution in the brain, this has not proven to be the case.⁽⁸¹⁷⁾ Most practically, the approximately 20 minute half-life of ¹¹C hinders the use of ¹¹C-PiB outside expert research centers, unless there is access to an on-site cyclotron and radiochemistry expertise. Thus, efforts were initiated to make ¹⁸F-labeled tracers, and currently four such amyloid ligands have been developed, which have a half-life of approximately 110 min. Critically, the development of these second generation AI PET ligands enables centralized production and regional distribution to centers having a PET facilities. To date, four radio-labeled ligands have been improved and include ¹⁸F-florbetapir (Amyvid), also called AV-45⁽⁸¹⁸⁾, ¹⁸F-flutemetamol (Vizamyl), ³F-PiB or GE-067⁽⁸¹⁹⁾, ¹⁸F-florbetaben (Neuraseq), also called BAY94-9172 or AV-1⁽⁷⁹⁸⁾, and ¹⁸F-NAV4694, formerly known as AZD4694.⁽⁸²⁰⁾ Summarizing the relevant differences between these compounds and PiB, using these amyloid tracers, a 40–70% increase in cortical ligand retention is found in AD patients as compared to controls. However, some of these second-generation PET-ligands have higher nonspecific white matter binding than ¹¹C-PiB, while others show lower cortical binding in patients with AD.⁽⁸²⁰⁾ Still, cumulatively, the evidence clearly supports the efficacy of PET-mediated imaging of A β plaques as a biomarker of AD and for this reason, the use of PiB and other forms of PET-mediated AI in humans is highly prevalent in the research setting. Unique in having overcome this major hurdle, today the major bottleneck in the advancement of PET-mediated imaging is the identification of novel A β -binding compounds with higher affinity and specificity. As described, PiB is better characterized as a β -pleated-sheet specific ligand than an A β -specific probe. As evidence of this assertion, human subjects with CAA may have positive PiB amyloid PET scans even in the absence of amyloid plaques.⁽¹⁵¹⁾ Furthermore, the distribution of PiB binding does not significantly differ between patients with clinically diagnosed AD and CAA.⁽¹⁵¹⁾ Thus, the development of third-generation PET-

compatible AI ligands is necessary in order to accurately measure the precise constituents of A β burden in the brains of AD individuals. To do this, novel background structures capable of selectively binding to A β plaques and crossing the BBB will be critical.

Inspired in part by positive PET-based imaging studies, significant progress has been made in MRI-mediated detection of A β plaques. Two general approaches for MRI-mediated detection have been reported: i) high-field MRI and ii) A β -specific contrast agents. Critically, these two approaches are fundamentally different in that they make completely contradictory assumptions about the intrinsic contrast properties of A β plaques. Proponents of the first method argue that A β plaques can be delineated from normal tissue secondary to their focal iron content and/or the highly compact nature of fibrillary A β . On the other hand, groups who focus on the development of A β -specific contrast agents are implicitly implying a lack of sufficient intrinsic contrast to facilitate detection. One of the first lines of evidence supporting the assumption that MRI can detect A β plaques came from ex-vivo MR imaging of AD tissues.⁽⁸²¹⁾ Notably, the in vivo application of MRI-mediated AI has suffered secondary to the technological challenge of co-registering planar histology tissue samples with MR images. Importantly, the development of histological radio-frequency coils partially alleviated this limitation in the field, allowing MR images and histology data from the same tissue sample to be directly overlaid and compared without the confound of co-registration between the two imaging modalities.⁽⁸²²⁾ Employing this method, one group has tested the hypothesis that iron found in and around the amyloid plaques is the dominant cause of the hypointensities seen in T2*-weighted images. Interestingly, examination of the relationship between MR contrast due to A β plaque and iron deposition both in human AD and the APP/PS1 model revealed that iron load alone does not account for all A β -generated contrast in mouse models of AD. Instead, the data suggests a duality in the relaxation mechanism, where both high focal iron concentration and highly compact fibrillar A β cause rapid proton transverse magnetization decay. Where as in human tissues iron deposition was found to be the dominant source of R2* relaxation, for APP/PSEN animals the compact and globular nature of A β plaques is likely the major cause of increased transverse proton relaxation rate.⁽⁸²³⁾ Regardless of the contrast mechanism however, investigators employing optimized spin echo acquisition methods have successfully detected histologically confirmed A β plaques with a 40-50-micron diameter at 7-9.4 Tesla.^(824, 825)

With respect to the second approach to MRI-mediated A β imaging, a number of amyloid-specific tracers compatible with MRI have been reported.⁽⁸²⁶⁻⁸²⁸⁾ Towards this aim, two general approaches have been utilized. The first

general method attempts to construct MR-contrast agents which mimic A β species in the hope they will be incorporated into A β assemblies and thus report A β burden. A prime example of this approach can be seen in a novel tracer designed to resemble A β_{40} peptides, a core constituent of A β plaques, which has been labeled with gadolinium to detect A β plaques in conjunction with micro-MRI (μ MRI). Impressively, the numerical density of A β plaques as assessed by μ MRI using this tracer correlates well with immune-histochemical analysis.⁽⁸²⁷⁾ In an extension of this work motivated by the relatively recent paradigm shift from A β plaques to soluble A β species, MR-contrast probes that specifically bind A β oligomers have been developed. In this work, oligomer-specific antibodies are conjugated onto magnetic nanostructures. Again showing great promise, extensive characterization of this A β -oligomer specific contrast agent demonstrates that the complex is stable and facilitates delineation of AD versus wild-type mouse models *ex-vivo*.⁽⁸²⁹⁾ Using similar MRI-based strategies, some groups have semi-quantitatively assessed A β plaque burden in AD mouse models using ^{19}F and ^1H MRI compatible probes.⁽⁸³⁰⁾ The second general approach to MR-probe development is quite recognizable to the trends described in PET-mediated AI. In both fields, the most common approach to the development of MRI-compatible AI probes employs derivation of known A β -binding molecules. Quite commonly, the A β -binding molecule of choice for this endeavor has been curcumin. In one of the first successful modifications of curcumin described, Dr. Tooyama and colleagues developed a novel ^{19}F -containing curcumin derivative named FMeC1. Like naturally curcumin, this compound can exist in equilibrium between keto and enol tautomers, with the enol form being unique in its ability to bind A β aggregates. Importantly, histological analysis of FMeC1-injected mouse brain showed penetration of the compound across the blood-brain barrier and binding to A β plaques in peripherally injected APP transgenic mice. Moreover, the distribution of A β deposits in these mice was in accordance with the region of the brain in which the ^{19}F signal was imaged. Lastly, lending significant clinical translatability to the compound, FMeC1 also exhibited an affinity for senile plaques in human brain sections.⁽⁸²⁶⁾ Utilizing a slightly different approach, another group has conjugated magnetic nanoparticles made of super-paramagnetic iron oxide (SPIO) to curcumin. After injection of this magnetically-labeled curcumin derivative, amyloid plaques could be visualized in *ex vivo* mouse tissue sections via T2*-weighted MRI.⁽⁸³¹⁾ Taken as a whole, the data presented here suggests that MR-mediated AI may represent a powerful diagnostic tool in the future. From a practicality stand point MR is safer and more easily implemented clinically, as it does not require the use of radioisotopes. Despite these advantages however, MR-mediated *in vivo* measurement of A β burden in humans has not been convincingly accomplished.

Arguably, optically-based imaging methodologies offer the most robust platform for *in vivo* detection of A β plaques if not for a few severely limiting characteristics. Chief among them, the signal of optically-based probes in the visible spectrum is highly scattered by native tissues. As a consequence, the vast majority of fluorescence-based imaging methods which have been employed to track A β burden have necessitated the removal of overlying tissues and/or thinning of the skull. Still, several groups have reported fluorescent derivatives of known A β plaque-binding compounds (principally thioflavin and Congo red) to facilitate the optical imaging of AD animal models.⁽⁸³²⁻⁸³⁵⁾ As a result of the light-scattering phenomenon described however, more recently, optically based amyloid imaging approaches have become increasingly focused on near-infrared (NIR) probes in an effort to enhance the resolution of deeper brain structures.^(836, 837) In the first published study in which NIR technology was employed to visualize A β plaques *in vivo*, the fluorescent intensity of the A β -binding dye AOI987 accurately detected the presence of A β plaques in a mouse model of AD.⁽⁸³⁸⁾ In a similar *in vivo* study, the fluorescent signal of the amyloid-binding NIR probe THK-265 demonstrated a progressive increase in proportion to elevated burdens of A β plaque.⁽⁸³⁹⁾ Despite these considerable successes however, NIR fluorescence imaging of A β plaques remains limited by the low number of A β -specific probes and is characterized by poor A β plaque-to-background contrast. Yet, many investigators believe that these obstacles can be circumvented via the development of “smart” fluorophores which, when bound to their target, fluoresce with enhanced quantum efficiency, a shifted spectrum and/or an altered lifetime.⁽⁸⁴⁰⁾ In a similar effort to advance the optical imaging of AD pathology, many groups have capitalized on the intrinsic advantages of fluorescence-lifetime imaging microscopy (FLIM) to improve the optical imaging of AD biomarkers. Using the FLIM approach, investigators can detect weak fluorescent probes in an auto-fluorescent background; a scenario in which traditional measures of fluorescence intensity are not efficacious.⁽⁸⁴¹⁻⁸⁴³⁾ Given that PET-mediated amyloid imaging lacks the sensitivity to detect individual plaques, and despite its limited ability to report A β plaque loads more than several centimeters below the brain’s surface, many investigators predict that optical-based imaging methodologies will provide a powerful and complimentary approach to A β imaging.⁽⁸⁴⁴⁻⁸⁴⁶⁾

In summary, PET-, MR-, and optically-based approaches to AI have all been validated as efficacious approaches to monitor A β burden in the brain. Importantly, each technique has been validated to varying degrees, with PET-based AI unequivocally leading the field with respect to clinic implementation. As will be describe in subsequent sections, a popular alternative to the AI is ELISA-mediated quantification of A β in the CSF and plasma. Importantly, while data

suggests that both reliably report A β plaque load, AI is unique in its ability to characterize the topographical distribution of A β . This advantage will likely be central to the continued use of AI, as future imaging studies will undoubtedly note that the regional profile of A β deposition influences clinical presentation. Lastly, it is important to mention that the diagnostic utility of AI does not rest on the validation of amyloid-centric hypothesis of AD. Regardless of A β 's role in the pathogenesis of AD it remains the pathognomonic lesion of AD. Thus a definitive diagnosis will always require verification of A β deposition up until the point the pathological diagnostic criteria are changed. Seeing as how A β plaques have retained their centralized place in such criteria over the past 3 decades, it is highly unlikely this is to occur. Furthermore, several globally implemented and clinically useful biomarkers do not detect a fundamental feature of disease pathology. For example, prostate-specific antigen (PSA) is arguably an excellent biomarker for prostate cancer despite no evidence of its involvement in the pathophysiology of this particular cancer.

6.2 TAU IMAGING

Predictably, the success of AI mediated via PiB and fluorinated alternatives has spurred efforts worldwide to develop selective tau PET tracers. In the context of an amyloid-centric model, Tau PET tracers are likely to be used as surrogate markers of cognition to predict cognitive decline and disease progression. Clinically, the integration of tau imaging into existing diagnostic algorithms which include AI will improve the specificity of AD diagnosis and perhaps improve early detection.^(275, 284, 847) However in many ways, the development of tau-specific ligands is more difficult than for A β secondary to the unique characteristics of tau. Most limiting, tau aggregates are mostly intra-cellular and therefore any potential tau tracer has to not only cross the blood–brain barrier but also the cell membrane before reaching its target. Furthermore, like assemblies of A β , tau aggregates have several conformations, with the same tau isoform adopting multiple ultrastructural forms.⁽⁸⁴⁸⁾ In more detail, soluble hyper-phosphorylated tau rapidly aggregates into spherical units of nucleation that then assemble linearly and form ribbons of protofibrils with a β -sheet core.⁽⁸⁴⁹⁾ The absence or periodicity of twists within the ribbons of each protofibril enables classification of hyper-phosphorylated tau into straight filaments, paired helical filaments (PHFs) with regular twists (about 80 nm), or irregularly twisted filaments.^(850, 851) In AD, the 3R and 4R isoforms of tau are hyper-phosphorylated and subsequently produce paired helical filaments as the

predominant tau specie and straight filaments as the minor aggregate form. Further complicating the matter, tau aggregates are subject to several post-translational modifications including: phosphorylation, acetylation, glycosylation, nitration, glycation, ubiquitination, and truncation, all of which modulate the ultrastructural conformation of tau-aggregates.⁽⁸⁵²⁾ In addition to this structural heterogeneity, the reported concentrations of PHF-tau^{arc} about 4–20-times lower than those of A β .^(853, 854) Thus, experts argue that a 20–50-times higher in vivo selectivity for PHF-tau as compared to A β might be required in order for a tau ligand to overcome the higher concentrations of A β in the brains of AD patients.⁽⁸⁵⁵⁾

Although limited by its inability to distinguish signal retention secondary to A β plaques or NFTs, 2-(1-(6-[(2-[18 F] fluoroethyl) (methyl) amino]-2-naphthyl) ethylidene) malononitrile (¹⁸F-FDDNP) represents the most thoroughly studied PET-based reporter of tau accumulation in human and mouse models of AD.^(834, 856, 857) Today, elevated ¹⁸F-FDDNP retention has been reported in patients with AD⁽⁸⁵⁸⁾, Down's syndrome⁽⁵²⁷⁾, chronic traumatic encephalopathy⁽⁸⁵⁹⁾, progressive supranuclear palsy⁽⁸⁶⁰⁾, and in prion diseases such as Creutzfeld–Jakob Disease.⁽⁸⁶¹⁾ Despite reports of nanomolar binding affinity for tau, independent experiments demonstrate a very limited dynamic range for ¹⁸F-FDDNP mediated PET secondary in part to low blood brain barrier penetration.⁽⁸⁶²⁻⁸⁶⁴⁾ Following the discovery of FDDNP, ¹⁸F-FSB35 and ¹⁸F-FP-curcumin radiotracers have been reported. However, all of these radio-ligands bind to A β aggregates in addition to NFTs, substantially limiting their value with respect to investigating tau's contributions to AD pathogenesis.^(858, 865, 866) Despite this limitation, ¹⁸F-FDDNP signal increases with cognitive decline and mirrors the classic trajectory of tau deposition.⁽⁸⁶⁷⁾ In pursuit of a tau-selective PET tracer, since 2002 researchers at Tohoku University, Japan, have been screening small molecules that bind a β -sheets. From this work, it has been discovered that a series of quinolone derivatives bind specifically to tau NFTs.⁽⁸⁶⁸⁾ Convincingly, one of the tracers developed from this work, 2-(4-aminophenyl)-6-(2-[18 F] fluoroethoxy) quinoline (¹⁸F-THK523), exhibits high binding affinity for tau fibrils at nanomolar concentrations and a 12-fold selectivity for tau over A β .⁽⁸⁶⁹⁾ Further, assessment in preclinical mouse models demonstrated high in vivo retention in tau transgenic mice and low binding in the brains of transgenic mice overexpressing A β but which lack NFTs, thus demonstrating its selectivity for tau.⁽⁸⁷⁰⁾ When translated into humans, significantly higher ¹⁸F-THK523 retention in temporal, parietal, and orbitofrontal lobes, and in the hippocampi of patients with Alzheimer's disease was noted in comparison with age-matched healthy controls. Disappointingly, high tracer

retention in white matter precluded the assessment of the distribution of tau pathology by visual inspection of the images.⁽⁸⁷¹⁾ Seeking to overcome this limitation two improved 2-arylquinoline derivatives were developed, 6-[(3-[¹⁸F]fluoro-2-hydroxy)propoxy]-2-(4-dimethylaminophenyl)quinolone (¹⁸F-THK5105) and 6-[(3-[¹⁸F]fluoro-2-hydroxy)propoxy]-2-(4-methylaminophenyl)quinolone (¹⁸F-THK5117).⁽⁸⁷²⁾ In preclinical validation, ¹⁸F-THK5105 and ¹⁸F-THK5117 both showed higher binding affinity than ¹⁸F-THK523 to tau-rich brain homogenates.⁽⁸⁷³⁾ Validating these findings, PET studies of ¹⁸F-THK5105 and ¹⁸F-THK5117 showed a robust quantitative separation of patients with Alzheimer's disease from healthy controls in brain regions harboring high tau deposition. Furthermore, the topographic profile of tau deposition as assessed by both of these probes was distinct from A β imaging with PiB highlighting the tau-specificity of the probes.⁽⁸⁷²⁾ In the third iteration of this work, the PET-compatible probe 6-[(3-[¹⁸F]-2-hydroxy)propoxy]-2-(4,-methylaminopyridyl)quinoline (¹⁸F-THK5351) has been described, boasting faster kinetics, lower white matter retention, and higher signal-to-noise ratio than its predecessors.⁽⁸⁷⁴⁾ In a separate yet similar line of work, two novel benzimidazole-pyrimidine derivatives, (*E*)-4-(2-(6-(2-(2-(2-[¹⁸F]fluoroethoxy)ethoxy)ethoxy)pyridin-3-yl)vinyl)-*N*-methyl benzenamine (¹⁸F-T807⁸⁷) and 2-(4-(2-[¹⁸F]fluoroethyl)piperidin-1-yl)benzo(4,5)imidazo(1,2-a)pyrimidine (¹⁸F-T808¹⁸) have demonstrated nanomolar binding affinity and a 25-fold selectivity for PHF-tau over A β .^(869, 875) Retention of these newly developed NFT-tau radio-ligands has been shown to co-localize significantly with tau pathology in experiments employing tau overexpressing mouse models.^(876, 877) Initial human ¹⁸F-T807 PET studies showed cortical retention comparable with the known distribution of PHF-tau in the Alzheimer's disease brain, low retention in white matter, and a strong association with disease severity.⁽⁸⁷⁶⁾ However, despite the tremendous progress described, all current generation selective tau PET tracers have unexplained quandaries.⁽⁸⁷⁸⁾ For example, some investigators suggest that both quinolone and benzimidazole derivatives have substantial retention in the striatal region, a finding inconsistent with neuropathological reports.⁽⁸⁷⁸⁾ Still, in comparison to MRI and optical imaging based approaches, PET-mediated tau imaging represents the closest investigators have come to a clinically applicable method to measuring regional NFT distribution in the brain. In contrast, MR imaging of tau is in its infancy, still relying upon correlations between tau deposition and hippocampal atrophy. Because both tau deposition and brain atrophy both correlate with the severity of cognitive decline in AD patients, many study groups have hypothesized that patterns of gray matter loss as assessed by structural MRI can serve as an approximate *in vivo* surrogate indicator of tau pathology.⁽⁸⁷⁹⁾ Unfortunately, considerably less progress has been made towards the development and characterization of tau-specific MRI probes. Currently, FSB

and [13C]BSB are among the best characterized precursors capable of serving as potential contrast agents for magnetic resonance imaging of tau *in vivo*.⁽⁸⁸⁰⁾ More recently, some evidence has emerged that the MRI probe CR-BSA-(Gd-DTPA) may possess the ability to detect NFTs.⁽⁸⁸¹⁾ These compounds represent derivatives of the AB plaque and NFT staining dye Congo red. Therefore, of the compounds published to date, none are specific to tau-comprised NFTs. Thus, an evaluation of MR imaging of tau as a biomarker of AD awaits the discovery of tau-specific precursors for MRI probes. Similarly, optically-based imaging of tau has largely been limited due to the lack of tau-specific precursor molecules. Interestingly, both FSB and BSB compounds posited for MRI also emit a fluorescent signal when complexed with NFTs making them potential candidates for *in vivo* imaging of tau in AD models.⁽⁸⁶⁵⁾ Indeed, molecules structurally analogous to these probes have been used to image tau deposition in human tissues in an *ex vivo* manner.⁽⁸⁸²⁾ More recently, investigators have shown that fluorescent trimethinine cyanine probes can bind to NFTs with high contrast and selectivity over A β plaques, though none of these methods have been utilized in a non-invasive manner.⁽⁸⁸³⁾ Clearly, more work is needed in this area.

Given the dominance of amyloid-centric hypotheses, it is unsurprising that few precursor molecules for PET-, MRI- and optically-based tau imaging have been thoroughly described. In addition, numerous obstacles, such as the heterogeneous nature of mature NFTs and their high degree of structural similarity with A β plaques, have added to the difficulty of characterizing tau-specific probes.⁽⁸⁸⁴⁾ As probe development progresses, *in vitro* studies to determine the binding characteristics of the probe, including its equilibrium with paired helical filaments, will be needed. Notably, however, dissociation constants (K_d) and binding capacity (B max) determined *in vitro* are difficult to translate to *in vivo* conditions. For this reason, *in vivo* application of potential tau ligands need to be evaluated in animal models of tauopathy prior to clinical implementation.^(719, 834) In this regard, PET-mediated tau is by far the most mature, still significant advances are needed.

6.3 MEASUREMENTS OF AMYLOID IN CEREBROSPINAL FLUID

In most vascularized tissues, the lymphatic system serves as a fundamental pathway for interstitial solute and fluid clearance and is thus critical to both hydrostatic and homeostatic maintenance. Yet, despite its high metabolic rate and the sensitivity of its constituent cells to changes in the extracellular environment, the brain does not have histologically identifiable lymphatic vessels.⁽⁸⁸⁵⁾ This has led many to hypothesize that the cerebrospinal fluid (CSF) of the central nervous system (CNS) may support solute clearance from the brain. Briefly, CSF is formed in the choroid plexi of the lateral ventricles before flowing through the remaining cerebral ventricles and the subarachnoid space to its ultimate sites of reabsorption into the bloodstream. These sites of CSF reabsorption include the arachnoid villi of the dural sinuses, the cranial nerve sheaths, and/or through the nasal lymphatics.⁽⁸⁸⁶⁻⁸⁸⁸⁾ While these mechanisms of CSF production and clearance are well studied, less is known about how interstitial solutes in the brain are cleared to the CSF. To date, the leading hypothesis is that convective bulk flow of interstitial fluid coursing through brain tissue facilitates this process, as no anatomically distinct structures have been identified.^(886, 889, 890) On the basis of *in vivo* two-photon imaging of small fluorescent tracers, some groups have demonstrated that CSF enters the parenchyma along perivascular spaces that surround penetrating arteries and that the brain's interstitial fluid is cleared along paravenous drainage pathways.⁽⁸⁸⁵⁾ Suggesting these findings have relevance to AD, other groups have reported that intra-parenchymal injected A β is cleared along perivascular pathways.⁽⁸⁹¹⁾

Since its potential has been recognized, measurement of A β in CSF has become an important candidate biomarker for AD. Disappointingly however, initial reports on CSF A β showed no clear change in AD patients as compared to controls.^(892, 893) A consistent theme in AD research, the error of these initial reports was that they did not discriminate between A β isoforms. Instead, the ELISA's employed used non-specific antibodies and thus measured total CSF A β levels. Just as in the brain, CSF contains many different A β isoforms of which A β_{40} is the most predominant species, with levels around ten times that of A β_{42} .⁽⁸⁹⁴⁾ Later, as the field became more convinced of the enhanced pathogenicity of A β_{42} , immunoassays with specificity to this isoform began to emerge. The first paper to leverage such an ELISA was published in 1995 and demonstrated a marked reduction in A β_{42} levels in the CSF of patients with AD.⁽⁸⁹⁵⁾ Generally speaking, in AD dementia, the CSF level of A β_{42} is decreased to approximately 50% of the levels in age-matched cognitively normal individuals.⁽⁸⁹⁶⁾ Later studies would confirm that levels of the much more abundant A β_{40} isoform do not change in AD,

suggesting that the failure of initial studies to demonstrate changes in CSF A β were indeed a consequence of this major amyloid specie masking changes that to occur in less predominant A β isoforms. Additionally, the discovery that A β_{40} levels remain constant in AD led to the hypothesis that the ratio of A β_{42} /A β_{40} might improve diagnostic accuracy by normalizing individual variations in total A β production. In support of this idea, many studies have demonstrated that there is a reduction in the CSF A β_{42} :A β_{40} ratio in AD that is more marked than the reduction in A β_{42} alone.⁽⁸⁹⁷⁻⁹⁰⁰⁾ Importantly, though these observations provided evidence that CSF A β could be utilized as a biomarker, the interpretation of why CSF A β_{42} is reduced in AD was not understood. The favored hypothesis has been that aggregation and deposition of A β results in decreased A β clearance secondary to lower rates of diffusion into the extracellular space and CSF. However, other possible explanations include decreased A β production, decreased A β clearance via active export from the brain to the blood, and/or increased proteolytic degradation. The first indication that the lowering of CSF A β_{42} is due to aggregation of the peptide in the brain came in 2003 in a study showing that low levels of A β_{42} in post-mortem ventricular CSF showed an inverse correlation with plaque load in cortical regions.⁽⁹⁰¹⁾ Later, this mechanism would become better established after studies *demonstrated an inverse correlation between global cortical amyloid PET ligand retention and CSF A β_{42} levels.*⁽⁹⁰²⁾ *Since this initial study elucidated the relationship between CSF A β and PET-mediated AI, more than 1000 patients and controls have undergone both amyloid PET and CSF A β_{42} examinations.*^(799, 903-910) *Most subjects (88%) had concordant amyloid biomarker results, with either negative or positive amyloid PET scans or CSF A β_{42} levels. A few had discordant amyloid biomarkers results, with either positive (low) CSF A β_{42} but normal amyloid PET (6.6%), or normal CSF A β_{42} levels but positive amyloid PET scans (5.4%).*⁽¹⁵¹⁾ Cumulatively, these data indicate that the reductions in CSF A β_{42} in patients with AD is due to A β deposition and thus reflects plaque (or fibrillar A β) load in the brain. However, conflicting results have been reported on the association of the CSF A β levels with cognitive/clinical status, raising uncertainty as to how this biomarker should be utilized clinically.^(899, 911-914)

6.4 MEASUREMENTS OF AMYLOID IN THE PLASMA

As reviewed, CSF and PET A β biomarkers accurately predict an underlying AD pathology. However, they represent massively invasive or prohibitively expensive diagnostic tools, respectively. Therefore, in an effort to generate a

cost-effective and non-invasive diagnostic strategy, investigators have rigorously explored the possibility of adapting blood-based biomarkers like plasma A β . Indeed, this approach seems rationale, roughly 50% of radiolabeled albumin injected into the CSF drains to the cervical lymphatics via the cribriform plate, whereas the remainder is cleared to the bloodstream via arachnoid granulations of the dural sinuses.⁽⁹¹⁵⁻⁹¹⁷⁾ Generally speaking, the blood-brain barrier and the blood-CSF barrier regulate the passage of solutes like A β between blood and the central nervous system. Lending credibility to the hypothesis that equilibrium may exist between A β and the CSF/interstitial fluid of the brain, there are a number of receptors that are implicated in the influx and efflux of A β through the blood-brain barrier. For example, influx of A β into the brain may be facilitated by the receptor for advanced glycation end products (RAGE) while efflux appears to be dependent on low-density lipoprotein receptors, low-density lipoprotein receptor-related proteins 1/2, P-glycoprotein, and very-low density lipoprotein receptors.⁽⁹⁰⁰⁻⁹⁰³⁾ Disappointingly however, many studies that have compared plasma A β levels with their CSF counterparts⁽⁹¹⁸⁻⁹²¹⁾ or the binding of PET A β radiotracers^(919, 922) have found no or low correlations. Importantly, there are several physiological factors that might explain the low correlation between plasma and CSF A β /PET amyloid plaque measurements observed in these studies. First, A β species in the CSF and the CNS interstitial fluid originate exclusively in the CNS. In contrast, A β in the plasma is also produced by APP metabolism in skeletal muscle, pancreas, kidney, liver, vascular walls, lung, intestine, skin and several glands.⁽⁹²³⁻⁹²⁵⁾ Additionally, most A β found in the plasma is bound to several proteins such as apolipoprotein A-I, A-IV, E and J, α 2-macroglobulin, complement factors, immunoglobulins, transthyretin, apoferritin and serum amyloid P component.^(924, 926) Moreover, platelets have been shown to release APP and A β in response to activation.⁽⁹²⁷⁾ From a more mechanistic angle, while a sizable fraction of the A β pool in the brain's interstitial fluid is believed to be in equilibrium with the CSF, it is less clear as to what degree these pools of A β contribute to plasma levels of the protein. Compounding all of these variables, plasma levels show a circadian fluctuation that decreases with aging and a strong genetic influence.⁽⁹²⁰⁾ With respect to this genetic modulation of baseline A β levels in the plasma, reports suggest a higher heritability for A β ₄₂ (30-73%) as compared to A β ₄₀ (23-54%) with no effect being demonstrated for ApoE status.^(928, 929) The last, and probably most confounding of all these potential variables are the technical aspects of A β plasma sample collection, storage, and measurement. Highlighting the significance of this last variable, when plasma samples are kept at room temperature for 24 hours a considerable 20% loss in A β pools has been reported.^(920, 930-932) Thus, the take home message of all of these studies is that standardization of sampling is critical to the utility of plasma A β .

Likely in part a result of methodological variations between studies, a wide range of mean plasma A β ₁₋₄₀ (214 to 985 pg/ml)^(903, 933) and A β ₁₋₄₂ (36 to 140 pg/ml)^(903, 924) levels in AD patients have been reported. In a more consistent fashion, studies report an increase of A β ₁₋₄₀ and A β ₁₋₄₂ with an overall decline in A β ₁₋₄₂/A β ₁₋₄₀ with advancing age.^(919, 921) Overall, it is very difficult to develop a consensus on the utility of plasma A β measurements. In the published opinions of the many experts, it appears that plasma A β levels are not useful as a diagnostic classifier in its current form. However, it is essential to note that in the largest, prospective, community-based study to date; lower plasma A β levels were associated with an increased risk of incident AD.⁽⁹³⁴⁾ Thus, given the potential impact a validated plasma A β biomarker might have on the field, the majority of experts in the field encourage further evaluation of plasma A β levels as a biomarker for risk of developing clinical AD.

6.5 MEASUREMENTS OF TAU IN CEREBROSPINAL FLUID

As discussed in multiple chapters of this work, NFT density correlates strongly with the severity of cognitive impairment in AD while discrepancies exist in the literature with respect to A β 's relationship to symptom progression. 46-48. Therefore, logically, measurements of tau in the CSF represent the most frequently used diagnostic tool used by some clinicians in the research setting to assess for the presence of AD pathology. Generally speaking, the literature on the use of CSF tau as a biomarker for AD has reached the consensus opinion that this diagnostic method has robust clinical utility. In most studies, an approximate 300% increase in the total concentration of tau in the CSF of AD patients is noted in comparison to normal controls.⁽⁹³⁵⁾ Given this large differential in CSF tau levels in AD, it is not surprising that the vast majority of studies indicate a significant difference exists between the CSF T-tau levels of AD and healthy controls. Translating these results into the clinical realm, the reported sensitivity of CSF total tau levels is 82% (95% CI = 76–87%) with a specificity of 90% (95% CI = 86–93%).⁽⁹³⁶⁾ Similar results have been reported for phosphorylated-tau, with CSF levels also increased in AD when compared to healthy controls. Although originally hypothesized to be more specific to AD pathology, mean sensitivity and specificity values are not dramatically different from those of total tau CSF measurements, reported at 80% (95% CI = 71–84%) and 83% (95% IC = 75–88%), respectively. Given these values, CSF measurements of phosphorylated-tau are predicted to facilitate the correct diagnosis of AD in 81.8% of cases. Importantly,

in a meta-analysis of the diagnostic accuracy of CSF measurements using different tau epitopes no significant differences were found.^(936, 937) Thus, despite the ambiguity with respect to how tau phosphorylation mechanistically contributes to the development of AD pathology, it is virtually unanimously agreed that tau contributes to AD neurodegeneration.⁽⁹³⁸⁻⁹⁴¹⁾ Despite this consensus, the utility of tau as a biomarker for AD has been questioned due to i) the poor corroboration between A β plaques and tau deposition, ii) reports of neurodegeneration in tau models without NFT formation and iii) its presence in other diseases. NFT deposition follows a stepwise topographic distribution pattern that begins in the trans-entorhinal region (Braak stage I) before affecting the entorhinal cortex (Braak stage II), hippocampus, temporo-occipital gyrus (Braak stage III), temporal cortex (Braak stage IV), parietal cortex (Braak stage V) and occipital cortex (Braak stage VI).^(110, 116, 118) By comparison, the topographical pattern of A β deposition is markedly different, with A β plaques appearing first in the neo-cortex and expanding in an anterograde fashion into allocortex (phase II), diencephalic nuclei, striatum and cholinergic nuclei (phase III), brainstem nuclei (phase IV) and the cerebellum (phase V).⁽¹³⁶⁾ Given the amyloid-centric focus of current AD research, this anatomical separation of NFT from A β plaques must be interpreted before NFT deposition can be rationalized as a biomarker of AD. Further compounding the concerns that surround tau's ability to serve as a biomarker of AD, neurodegenerative changes and cognitive deficits have been observed in the absence of NFTs.⁽⁹⁴²⁻⁹⁴⁶⁾ In a strategy similar to that observed in A β plaque research, some investigators have hypothesized that pre-tangle tau species (monomers/oligomers) underlie tau-mediated dysfunction and toxicity and thus account for studies which report dissociations in NFT density and cognitive symptoms.^(939, 940, 947-950) Regardless of tau's neurotoxic mechanism of action, studies which demonstrate that only 85% of neuronal loss can be explained by NFT formation clearly imply the existence of non-NFT mechanisms which contribute to the neurodegenerative changes observed in AD.⁽¹⁰¹⁾ Lastly, tau expression in multiple neurodegenerative diseases including: AD, frontal-temporal dementia, progressive supra-nuclear palsy, Picks disease and corticobasal degeneration may potentially limit its efficacy as an AD biomarker. However, because NFT and tau morphologies differ between disease models and the elevations of tau in AD are significantly greater than those observed in alternative dementias, the evidence supports the notion that tau retains sufficient specificity to represent a viable biomarker for AD.^(951, 952) Additionally, considerable evidence has emerged which links A β plaque toxicity with tau hyper-phosphorylation providing additional support for its use as an AD biomarker.^(110, 953, 954) For example, crossing mutants that overexpress amyloid precursor protein with tauopathy mouse models results in significant increases in NFT formation and associated tau hyper-phosphorylation.⁽⁹⁴¹⁾ Conversely,

reducing tau expression in A β -producing mouse models protects mice from the cognitive deficits loosely associated with high A β burden in the brain.⁽⁹⁵⁵⁾

6.6 MRI-MEDIATED IMAGING OF NEURODEGENERATION

The two imaging modalities facilitating quantification of brain atrophy in routine clinical use today are computed tomography (CT) and MRI. Of the two, MRI is preferred with respect to structural imaging studies due to its far superior soft tissue resolution.⁽⁹⁵⁶⁾ Today however, the clinical role of structural neuroimaging in AD is the exclusion of pathology that may be causative of cognitive decline.^(144, 956) These alternative causes of dementia include cerebrovascular disease, tumors, subdural hematoma, and other forms of dementia including dementia with Lewy bodies and frontotemporal dementia.^(957, 958) However, as highlighted by its inclusion in the new diagnostic guidelines, the use of MRI to quantify atrophy in medial temporal lobe structures of the brain is slowly gained acceptance as a robust biomarker for AD. While brain atrophy is not specific to AD, studies have revealed atrophy of the MTL is well correlated with changes in cognition and disease progression.⁽⁹⁵⁹⁻⁹⁶¹⁾ More specifically, studies demonstrate that atrophy of the hippocampus and entorhinal cortex is of particular value as a biomarker due to their involvement in the earliest stage of disease and strong correlation with NFT pathology.⁽⁹⁶¹⁻⁹⁶³⁾ Cross-sectional volumetric analysis of medial temporal lobe (MTL) structures can be done qualitatively by visual assessment or in a quantitative fashion employing either manual tracing methods or automated techniques.⁽⁹⁶¹⁾ In addition, voxel-based analysis has also been applied for comparisons between an AD cohorts and cognitively normal control groups.^(961, 962) In studies which employ these methods, hippocampal volume is reduced in MCI patients by 10–15% while in mild and moderate AD a 15–30% and 30–40% reduction is observed, respectively.^(960, 964) The rate of atrophy is also predictive of progression, being 4–6% per year in MCI/AD patients compared to 1–2% in age-matched controls.⁽⁹⁵⁹⁾ Taken as a whole, such studies support the use of MRI-mediated imaging of neurodegenerative changes in the brain as a complimentary biomarker of AD.

Beyond measurements of medial temporal lobe atrophy, an emerging body of literature has highlighted the potential of leveraging other MR imaging technologies to image pathological alterations in gray and white matter structures altered in AD. For example, diffusion weighted imaging (DWI) and diffusion tensor imaging (DTI) have been

employed to quantify white matter changes in areas such as the temporal lobe, hippocampus and corpus callosum in AD patients.^(957, 963) Interestingly, studies employing DTI suggest this modality is capable of assessing microstructural and connective changes in the hippocampus arising secondary to neuronal loss and axonal degeneration.^(965, 966) Alternatively, magnetization transfer imaging (MTI) is able to detect structural damage as a reduction in the magnetization transfer rate. This approach leverages the fact that magnetization transfer rate is influenced by tissue homogeneity, with increasing inhomogeneity secondary to pathological changes such as neuronal loss and gliosis in gray matter, and demyelination and axonal loss in white matter.^(962, 963) Supporting the utility of this approach as a future biomarker for AD, decreased magnetization transfer rate is typical of both white and gray matter brain regions in AD patients.⁽⁹⁶³⁾ However, as neuronal loss occurs relatively late in the disease progress, other groups are attempting to leverage functional imaging methodologies to detect neuronal dysfunction. The assumption made by these groups is that neuronal dysfunction should be reflected as regional changes in cellular metabolic rate. Two general approaches are employed to study this variable; cerebral blood flow/volume measurements or changes in the blood oxygen level dependent (BOLD) effect. In cerebral blood flow and cerebral blood volume experiments, an intravenous paramagnetic contrast such as gadolinium or superparamagnetic iron oxide nanoparticles are injected into the patient and imaged.^(967, 968) In contrast, the BOLD effect utilizes the paramagnetic properties of deoxyhemoglobin. The assumption made by BOLD imaging is that increased neuronal activation induces an increase cerebral blood flow as a consequence of increased metabolic need. This leads to an increase in oxyhemoglobin and a relative decrease in deoxyhemoglobin which results in a relative increase in signal on T2* weighted imaging.^(967, 968) Using either of these approaches, functional imaging in AD patient cohorts reveals decreased hippocampal and parahippocampus activity as well as decreased activity in the frontal and prefrontal regions.⁽⁹⁶⁹⁾ Thus, while volume analysis of the hippocampus and entorhinal cortex volume stands as the current gold-standard MR imaging-method for the detection of AD, future technologies might facilitate early detection before irreversible neuron loss has occurred.

6.7 CURRENT PERSPECTIVE ON AD IMAGING

As summarized, to date most of the progress made towards applying imaging technologies to the study of AD has been amyloid-centric. As the limitations of amyloid imaging become increasingly recognized, interest in alternative

biomarkers has grown substantially. While MR-mediated imaging of structural changes in the brain of AD patients is well studied, much work is needed in the field of tau-imaging to make this potential biomarker clinically impactful. However, considering current epidemiological projections for AD, the refinement of future imaging technologies for the detection of alternative biomarkers, including tau, cannot evolve over decades in a manner similar to amyloid imaging. In the years to come, high-throughput screening approaches similar to those created for A β plaque probe discovery must be adapted in order to expedite the validation of complimentary biomarkers for delivery into clinical trials.⁽⁹⁷⁰⁾ In a continuation of the current trend, the imaging of AD biomarkers such as A β plaques and tau will need to be integrated into a more holistic diagnostic panel in order to best capture the multi-factorial nature of AD.

CHAPTER 7 THE UNTESTED AMYLOID-CASCADE HYPOTHESIS

The rationale for believing that A β is critical to the etiology of AD is simple and compelling. At the foundation of this hypothesis, very high levels of A β accumulate in the brains of patients with AD and all genetic forms of AD are mechanistically linked with increased amyloid deposition. In addition, AD develops in nearly all individuals with Down syndrome, who have a triplication of the APP gene and as a consequence increased substrate for amyloidogenic processing. The ApoE4 polymorphism, which markedly increases the risk for late onset AD, is associated with an increase in amyloid deposits, whereas the ApoE2 polymorphism that diminishes risk for AD is associated with decreased amyloid levels. Lastly, a rare polymorphism in the APP gene which reduces amyloidogenic processing of APP has been shown to be protective for AD. All evidence considered, a primary pathogenic link between A β and AD seems irrefutable. For this reason, A β has remained the primary target for therapeutic intervention in AD, with numerous phase III trials designed to reduce A β levels currently underway or completed. Unfortunately to date, the results of these randomized clinical trials are either negative or inconclusive, leading many to call into question the underlying validity of the amyloid-centric hypotheses. However, despite the enormous investment already made, the failure of most A β -targeted therapies for AD can be associated to inadequacies in trial design as opposed to the invalidity of the underlying therapeutic hypothesis. In truth, this expert opinion should be expanded, as the apparent failure of A β -centric therapies is best interpreted as a failure to appropriately test the underlying amyloid hypothesis. This is an extremely important point, because it suggests that amyloid-centric hypotheses have not been refuted, which would motivate a search for new targets, but rather that trials need to be redesigned in order to confirm their validity.⁽⁹⁷¹⁾ Although a multitude of potential confounds are present in the anti-amyloid therapeutic trials conducted to date, two key points stand above the rest.

7.1 CONFOUNDS UNDERLYING THE FAILURE OF ALZHEIMER'S DISEASE IN CLINICAL TRIALS

The first major shortcoming of anti-amyloid clinical trials has been the lack of appropriate analysis in response to therapy. For example, the vast majority of studies fail to investigate whether amyloid was effectively neutralized, whether an adequate dose was administered to achieve therapeutic response, or whether side effect profiles generated

enrollment/survival biases. Put more generally these clinical trials have failed to adequately characterize the pharmacokinetic profile of each drug in humans. Two double-blind, randomized, placebo-controlled phase 3 trials investigating the therapeutic efficacy of the A β -binding antibody Bapineuzumab epitomize this assertion. After 6 treatments over the course of 78 weeks, no significant difference in primary outcome measures were observed between drug-treated and placebo-treated cohorts.⁽⁹⁷²⁾ The primary outcome measures were scores on the 11-item cognitive subscale of the Alzheimer's Disease Assessment Scale (ADAS-cog11) and the Disability Assessment for Dementia. In an effort to monitor treatment response, AI imaging using PiB was employed in combination with CSF measurements of tau. While the failure of this trial can be interpreted to suggest a failure of anti-amyloid targeted therapies, the lack of clinical efficacy in these studies was later determined to be secondary to poor blood brain barrier penetration and thus an inability to reach therapeutic doses in the brain. Unacceptably, this failure is not isolated to clinical trials of Bapineuzumab. Instead, experts agree that a large majority of anti-amyloid clinical trials have failed to appropriately address the issue of delivering therapeutics across the blood brain barrier (BBB). For example, in one of the largest randomized clinical trials to date, an evaluation of the clinical efficacy of the γ -secretase inhibitor Tarenflurbil yielded negative results. Disappointingly, those in charge of this trial were well aware of the compounds poor bioavailability in the brain, noting that "earlier studies indicated a dose-dependent penetration from plasma to CSF of only .5-1%". Nevertheless, as is the case in far too many studies, the authors note that "low BBB penetration did not deter plans for phase 2/3 study".⁽⁹⁷³⁾ While the investigators may have rationalized proceeding with the trial was warranted on the basis of promising phase 2 results, because of the grand scope of this particular trial, its failure led many experts to begin arguing for a re-evaluation of amyloid-centric hypotheses of AD pathogenesis. Clearly however this trial never even tested the viability of A β as the compound likely never reached concentrations in the brain near the therapeutic threshold of the drug. Investigators at a major pharmaceutical company come to largely the same conclusion—that failed anti-amyloid trials in AD did not achieve sufficient target engagement to truly test the hypothesis that reducing amyloid in the brain would ultimately improve symptoms, or at least stabilize disease progression.⁽⁹⁷⁴⁾ To be fair to these failed anti-amyloid clinical trials, drug delivery across the BBB represents one of the most daunting endeavors in medicinal chemistry. The derivitization of precursor molecules with potent anti-amyloid effects is as much an art as it is a science, requiring immense time, money, and expertise. Therefore, future drug discovery paradigms should incorporate tests for this characteristic in the screening protocols.

7.2 LESSONS GARNERED FROM ALZHEIMER'S DISEASE CLINICAL TRIALS

Despite the negative press generated by the failure of anti-amyloid therapies in clinical trials, we have nonetheless learned some important lessons. Chief among these lessons is the second major limitation of all clinical trials completed to date, the failure to employ a prophylactic approach to AD therapy. The rationale here is even simpler than for the first point. Given the irreversible nature of neuronal death, since AD is indisputably a neurodegenerative process in which symptoms accrue with increased neuronal loss, why then would therapies initiated after substantial neurodegeneration has already occurred be expected to significantly ameliorate symptoms? Put more plainly, once A β has already initiated the series of pathological cascades resulting in neuronal dysfunction and death, reducing A β levels is unlikely an insufficient therapeutic approach. The results of failed clinical trials support this claim, none better than the ill-fated AN1792 active immunization trial. Not surprisingly, this anti-amyloid immunization therapy did not reduce or reverse cognitive deficits and had only a small effect on neurodegenerative phenotypes such as neural loss, gliosis, and accumulation of tau.⁽⁹⁷⁵⁾ However, although the number of patients followed was small secondary to the emergency of a subset of patients with meningoencephalitis making it necessary to halt the trial, AN1792 administration did reverse amyloid deposition.⁽⁹⁷⁵⁾ Again, while critics cite this finding as evidence against the role of A β in the pathogenesis of AD, an alternative model of AD in which amyloid acts as an early step in a more complex neurodegenerative cascade that becomes independent of amyloid as disease progresses is more likely.⁽⁹⁷⁶⁾ In this scenario, even if a drug successfully engages and reduces amyloid levels, clinical improvement will be difficult to achieve once disease becomes sufficiently advanced. This point is critical, because it emphasizes that in order to test amyloid-centric hypotheses of AD correctly, we need to give drugs to the right patients at the right time and then follow them closely. Specifically, trials must recruit patients in whom amyloid-dependent neurodegeneration is still active. Dauntingly, this critical period of therapeutic intervention may be a decade before frank cognitive symptoms emerge, emphasizing the need for improved early-detection methodologies. This feat is not impossible, as current AI methods are already able to note a rise in A β levels in the brains of asymptomatic AD patients.⁽⁷⁸⁹⁾ As these same studies demonstrate that A β levels off as AD symptoms begin to manifest robustly, it is likely that the correct time to test anti-amyloid drugs is in asymptomatic patients identified with AI or cerebrospinal fluid analysis.

CHAPTER 8 INTRODUCTION TO SPECIFIC AIMS

As explicitly communicated by the title, the impetus behind the work presented in this document stems from our inherent passion to expedite the clinical translation of a disease-modifying therapeutic for AD. Towards this goal, we have described a novel HTS technology which facilitates the repurposing of existing compounds with previously undiscovered A β -binding affinity for the purpose of treating AD. Significantly, this contribution also offers the potential of dramatically improving AD diagnostics, by expanding the chemical genetics of A β molecules and thus offering a rich repository of structural motifs off which to base the next generation of AI probes. In addition, we describe the application of an unorthodox drug administration method which alleviates limitations associated with the delivery of potential A β theranostic agents to the brain. Building on this discovery, we employ aerosol-mediated drug delivery to recapitulate the therapeutic benefit of intravenous curcumin administration in a preclinical mouse model of AD, but in a clinically applicable manner. Lastly, we demonstrate the therapeutic application of a completely novel disease-modifying therapeutic for AD, Promethazine. Taken together, we feel these contributions go a long way towards the ultimate goal of contributing to the development of a disease-modifying treatment for AD.

CHAPTER 9 THESIS AIM 1

9.1 AIM 1: HIGH-THROUGHPUT SCREENING FOR A β -BINDING MOLECULES

As described in abundant detail in the introductory chapters, identification of A β plaques in the brain is an essential component to the neuropathological confirmation of AD. The rationale for this diagnostic policy comes largely from the robust genetic and bio-molecular evidence supporting the hypothesis that aggregation of A β assemblies plays a central role in the pathogenesis of AD. Given these two points, it is clear that the targeting of A β species is of stout diagnostic and therapeutic significance. This is in no way a new revelation in the field, as A β assemblies have been of interest since the initial clinical characterization of AD over 100 years ago. As reviewed at length however, to date, only 4 A β -targeted probes for AI imaging have been approved by the U.S. Food and Drug Administration for clinical use. Furthermore, no A β -targeted therapies, considered the leading approach with respect to the development of a disease-modifying treatment for AD, have been clinically implemented. This begs the question, “What factors have limited the clinical implementation of A β -targeted diagnostics and therapeutics?”

9.1.1 Barriers to the Development of AD Diagnostics:

Beginning first with barriers in the field of AD diagnostics, at the most fundamental level, the paucity of AI-compatible probes can be attributed to the inherent complexity associated with designing imaging diagnostic agents for neurodegenerative diseases like AD. Unique to the identification of clinically implementable pharmaceuticals in the brain, drug discovery approaches must simultaneously evaluate a compound's ability to: (i) cross the BBB and (ii) bind specifically to the target of interest. Generally speaking, two approaches to the development of A β -binding molecules which meet these criteria can be employed. Beginning with the dominant method in the field over the last two to three decades, every clinically implemented AI probe to date can credit its development to (i) rational drug design. In more detail, the approaches contained under the umbrella of “rational drug design” can be subdivided into direct and indirect methods. Significantly, these two methods differ in their requirement for structural information of the biological target and are thus differentially suited for the development of AI-imaging probes as for decades, little has been known about

the molecular structure of amyloid assemblies. Critically, when employing a direct drug design paradigm, knowledge of the three-dimensional structure of the biological target is absolutely required. For this reason, direct drug design is more commonly referred to as structure-based drug design. In this approach, candidate drugs that are predicted to bind with high affinity and selectivity to the target may be designed using computer-modeling and the intuition of an expert medicinal chemist. However, no reference structure is available for any A β species of higher order than the fibril form. This is due in part to the fact that in vivo A β peptides exist in a variety of assembly states, making the isolation/characterization of a particular high-order specie challenging. To circumvent this limitation, several groups have attempted study on more homogenous samples of synthetic amyloid fibrils, only to find that conventional structure-elucidating techniques cannot be applied to these samples either. For example, methods such as single crystal X-ray crystallography and solution nuclear magnetic resonance (NMR) cannot be used on A β fibrils since they are insoluble.⁽⁹⁷⁷⁾ As a consequence, until relatively recently, the only aspect of amyloid fibril structure that was firmly established by experimental data is that they contain ribbon-like β -sheets. Since recognizing the inherent limitations of studying A β -structure through conventional means, X-ray fibre diffraction, electron microscopy (EM), solid state NMR, Fourier transform infrared spectroscopy (FTIR) and circular dichroism (CD) have been used to examine amyloid structure. These techniques have yielded considerable information about the morphology of amyloid fibrils and their internal structural conformation, as well as how their constituent components aggregate. Briefly, at the structural level of A β -fibrils, β -sheets run the length of the fibrils and appear to be arranged in a “cross- β ” motif, in which β -strand segments are oriented approximately perpendicular to the long axis of the fibril and are connected by backbone hydrogen bonds that are oriented approximately parallel to the long axis of the fibril.^(978, 979) With respect to the A β fibril assembly process, this mechanism appears to be a nucleation-dependent pathway characterized by a conformational switching from an α -helix or random coil to a β -sheet structure.⁽⁹⁷⁷⁾ Furthermore, along this pathway small oligomeric intermediates and short fibrillar structures (protofibrils) have been identified, a result which only confirms the mechanistic complexity of A β aggregation. The take home point here is that science has yet to obtain an unambiguous structure of the amyloid fibril or higher order amyloid assemblies. Therefore, it is difficult to apply structure-based rational drug design paradigms to the problem of developing agents with bind to A β assemblies.

Fortunately, as alluded to earlier, an alternative strategy which does not require a direct structural

characterization of the biological target is available. This approach is termed indirect rational drug design. Though more informatively referred to as ligand-based design, indirect rational drug design relies on knowledge of other molecules that bind to the biological target of interest. Summarizing the application of this approach to A β -binding drug design, known A β -binding molecules are used to generate a pharmacore model that defines the minimum necessary structural characteristics a molecule must possess in order to bind to A β . Put more generically, a model of the biological target is built based on the knowledge of what binds to it, and this model is then in turn employed to design new molecular entities that interact with the target. Importantly, the reliability of the pharmacore model is dependent on the number and diversity of the known target-binding compounds. In the case of A β -targeted molecules, these reference molecules have traditionally been limited to the histochemical stains thioflavin and Congo Red. As a consequence of this low number of reference compounds available to generate sufficiently robust pharmacore models, a majority of A β -binding studies have instead analyzed quantitative structure-activity relationships (QSAR) in the pursuit of novel A β -specific precursors. In this subdivision of ligand-based drug design, a correlation between the calculated properties of molecules and their experimentally determined biological activity is derived and used to predict the activity of new analogs. Importantly, a major limitation of this approach is that in the absence of a diverse molecular library of target-binding ligands, such as the case with A β , the chemical structure of predicted analogs typically resemble that of the parent compounds. This limitation is particularly detrimental to the development of A β -binding precursors for AI as the reference compounds thioflavin and Congo Red do not possess the structural attributes compatible with BBB permeability. Thus, as a consequence of the limited structural diversity of known A β -binding molecules, the development of A β -targeted ligands for AI can be historically summarized as the struggle to modify the non-BBB permeable A β -binding molecules thioflavin and Congo Red, without sacrificing their target specificity.

To the credit of the field, rational drug design has successfully been leveraged to generate the current generation of AI probes in its entirety. However, as discussed, the paucity of known ligands to A β assemblies coupled with our inability to accurately describe their structure have negatively impacted the ability of either drug design approach with respect to developing an ideal A β -targeting precursor of PET-probe development. Furthermore, while modeling techniques for prediction of binding affinity are reasonably successful, there are many other properties, such as bioavailability, metabolic half-life, and side effects that first must be optimized before a ligand can be translated into

a viable AI agent. As summarized in Table 9-1, a number of groups have developed criteria for candidate PET radiotracers for AI.⁽⁹⁸⁰⁾ Disappointingly, evidence suggests that the current generation of AI probes have yet to be optimized with respect to some of these criteria. For example, with respect to bioavailability in the brain, as suggested by its name, the BBB prevents the uptake of most pharmaceuticals into the brain and has posed the greatest barrier to the development of AI probes. While many investigators make the false assumption that sufficiently small molecules are freely transported across the BBB, in truth close to 98% of all small molecules fail to reach the brain parenchyma when injected into the peripheral circulation.⁽⁹⁸¹⁾ Importantly however the BBB is not impenetrable. Instead, certain small molecule drugs may cross the BBB via lipid-mediated free diffusion providing that the drug has a molecular weight of less than 400 daltons and forms no more than 8 hydrogen bonds.⁽⁹⁸¹⁾ Unfortunately these chemical properties are lacking in the majority of small molecule drugs and completely absent in large molecules. Structurally, the BBB is comprised of two membranes separated by 200 nm of endothelial cytoplasm; the luminal and abluminal membranes of the brain capillary endothelium.⁽⁹⁸²⁾ Owing to the presence of epithelial-like, high resistance tight junctions within the brain capillary endothelium, the intercellular pores that characterize the endothelial barriers of peripheral organs are absent in the endothelial barriers of the brain. Further compounding the exclusive nature of transport of molecules into the brain, there is minimal fluid-phase pinocytosis in the brain capillary endothelium.⁽⁹⁸³⁾ Therefore, the absence of para-cellular or trans-cellular channels within the BBB means that molecules in the circulation may only gain access to brain via two mechanisms: (1) lipid-mediated free diffusion through the BBB or (2) carrier- or receptor-mediated transport through the BBB. The current generation of PET-ligands for AI, including PiB and its derivatives, utilize the first of these two mechanisms of BBB penetration to successfully reach PET-compatible concentrations in the brain. This is no way however implies that these AI imaging probes robustly penetrate the BBB, as one of the principal advantages of PET-mediated imaging is its incredible sensitivity. In reality, the BBB penetration of these probes is quite low in comparison to other PET-imaging agents and likely incompatible with other imaging modalities which lack the sensitivity of PET. To give a sense of where AI-agents fall on the spectrum with respect to BBB penetration, one can compare the brain concentrations achieved by AI-probes with those of other commonly used PET-tracers. A convenient measure of brain tissue radiotracer concentration is the standardized uptake value (SUV), which simply reflects the normalization of radioactivity concentration in the brain to the injected radioactive dose and subject's body

weight. With a peak concentration of 9.3 SUV, the D2/D3 targeted PET-probe Fallypride nicely exemplifies a highly BBB penetrating PET-compatible ligand.⁽⁹⁸⁴⁾ At the other end of the spectrum, with SUVs in the range of 1.3-1.7, PET-probes for translocator protein (TSPO) typify compounds with low BBB penetration.^(985, 986) Even in the most optimistic of studies, the BBB penetration of PET-tracers for AI fall nearer the low end of the spectrum, with a SUV of 4 being published for PiB.⁽⁷⁸⁷⁾ Importantly, the determinants of PET-agent penetration across the BBB are the same as for other small molecules: (i) a molecular weight less than 400 daltons and (ii) the formation of no more than 8 hydrogen bonds when in aqueous solution. With a molecular weight of 256.32 g/mol, PiB and its similarly sized derivatives meet this size restriction. Importantly, the second criteria involving hydrogen bond-formation represents a slightly oversimplified criteria in that it assumes the hydrophobicity of any give compound can be determined by just this variable alone; which is of course untrue. In reality, lipophilicity is the major factor influencing passive brain entry and several molecular features of a radiotracer may govern this characteristic. Experimentally, the most commonly used index of compound lipophilicity is $LogP$, where P is the *n*-octanol/water partition coefficient of the unionized species. The corresponding distribution coefficient for all derived species (ionized and non-ionized) of a particular compound at physiological pH is termed $D_{7.4}$. In the literature, blood-brain barrier penetration is optimal when a molecule is characterized by a $LogP$ values in the range of 1.5-2.7, with the mean value of most CNS penetrating drugs being 2.1.⁽⁹⁸⁷⁾ Similarly, analyses of small drug-like molecules suggested that for better brain permeation, the compound needs to be characterized by a $D_{7.4}$ value greater than 0 and less than 3.^(988, 989) With a $LogP$ of 3.33 and a $LogD_{7.4}$ of 3.31, PiB is again slightly outside the optimum range for ideal BBB penetration.^(787, 980) Taken as a whole, this data highlights the fact that the current generations of AI probes have yet to be optimized with respect to BBB penetrance. Critically, this is because these compounds have been, out of necessity, derivatized from poorly BBB penetrating precursors such as thioflavin and Congo Red.

Table 9-1. Ideal Characteristics of a Candidate Precursor Molecule for AI Radiotracer Development

Ideal Characteristics of a Candidate Precursor Molecule for AI Radiotracer Development
High Affinity for a Specific Amyloid Assembly/Assemblies (Monomers, Oligomers, Protofibrils, Fibrils, Diffuse Plaques, Cored-Neuritic Plaques)
Selectivity for a Specific Amyloid Assembly/Assemblies (Low Non-specific Binding)
Ability to Penetrate the Blood-brain Barrier
Not a Substrate for Efflux Transporters
Lack of Radio-metabolites
Suitable Brain Pharmacokinetics in Relation to Radiolabel Half-life
Amenability to Labeling with ^{18}F at High Specific Radioactivity
Safe for Administration at PET-tracer Doses

While the limitations imposed by ligand-based rational based drug design on BBB permeability have arguably not influenced the clinical application of current-generation AI probes, the specificity of these compounds for A β also remains less than ideal. For example, at tracer concentrations achieved during in vivo imaging scans, PiB labels not only senile plaques, but also diffuse plaques and deposits of A β in the vasculature, a pathology referred to as cerebrovascular amyloid angiopathy (CAA). Furthermore, though to a lesser degree than A β , PiB also demonstrates significant binding to tau-comprised NFTs.⁽⁷⁸⁹⁾ Lastly, PiB is characterized by a relatively high degree of non-specific binding to white matter as demonstrated by in vitro studies employing white matter brain homogenates from AD and cognitively normal individuals.⁽⁹⁹⁰⁾ Undisputedly, the off-target binding of PiB just described constitutes a minor constituent of its overall signal in the brains of AD patients, and thus does not limit its use as a biomarker. Still, the non-specificity of current AI probes like PiB might provide a molecular explanation for the limited diagnostic specificity and dynamic range demonstrated by these compounds in studies evaluating their ability to monitor AD progression.⁽⁷⁸⁹⁾ Most importantly for the purposes of this work, these findings emphasize the limitations imposed on AI probe development when attempting to employ rational based drug design strategies with only a handful of available structures with confirmed A β -binding affinity.

Fortuitously for the field, the second major approach to the development of A β -binding molecules, (ii) high-through screening (HTS) methodologies, represents a complimentary approach to rationale design-based strategies as it does not require a priori knowledge of A β 's structure or a large library of molecules known to bind with it. To the contrary, the primary strength of HTS methods is their ability to identify large numbers of structurally diverse compounds which bind to a particular biological target of interest. However, the implementation of this approach requires a robust, cost-effective, and validated assay; a need that has not been sufficiently met until the publication of the work described herein.⁽⁹⁷⁰⁾ This is not to say that HTS technologies have not been developed for the identification of A β -binding compounds. To the contrary, a vast literature describing multiple, supposedly HTS compatible, methodologies exists in the field. None of these methods are more popular or more routinely implemented than the thioflavin fibrillation assay.^(991, 992) Although the specifics of various protocols vary widely, generally speaking, in this approach thioflavin, a candidate A β -binding compound, and synthetic A β monomers are added together in solution. Due to the inherent propensity for A β peptides to aggregate, within an hour, the A β monomers in solution self-organize into higher order A β assemblies such as

amyloid fibrils. Critically, thioflavin fluorescence increases several orders of magnitude when complexed with structurally mature A β fibrils.⁽⁹⁹³⁾ Thus, in the absence of a compound which inhibits A β assembly, thioflavin emission at 485 nm will increase exponentially over the 1 hour incubation time as the availability of A β fibrils increases.⁽⁹⁹²⁾ By comparison, if the compound added to the initial reaction conditions does in fact bind to A β , it is assumed that this interaction will perturb amyloid aggregation to a degree that can be detected as a significant attenuation in thioflavin emission. Given this brief introduction to the method, several shortcomings of this approach become clear. Most condemningly, all iterations of this approach employ synthetic A β -peptides which fail to recapitulate the tertiary structure of in vivo derived A β assemblies. Without question, all naturally produced amyloid species, including the amyloid fibrils to which thioflavin binds, are polymorphic with respect to their structure at the molecular level.^(994, 995) This finding alone confirms that the amino acid sequence of A β peptides does not completely dictate the tertiary structure of higher-order assemblies.⁽⁹⁹⁶⁾ However, this is not the only line of evidence suggesting that the use of synthetic A β peptides poses a significant confound when screening for A β -binding structures. As further evidence, consider studies on synthetic forms of A β peptide which demonstrate that even within this supposedly homogenous sample, peptide conformation and aggregation behavior are highly dependent on initial solvent conditions.⁽⁹⁹⁷⁾ Most alarmingly, synthetic A β_{42} assemblies demonstrate differences in fundamental biochemical properties such as SDS-stability when compared to their in vivo derived counterparts.⁽⁹⁹⁸⁾ Importantly these structural variations are of functional significance, as differences are noted in the relative toxicity of synthetic and cell-derived A β under the same experimental conditions. For example, natural A β oligomers impair memory and LTP at doses a hundred to thousand times lower than effective doses of synthetic A β oligomers.⁽⁶⁹⁴⁾ Furthermore, when administered to the brain, the pathological effects of synthetic A β oligomers are temporally delayed in comparison to cell-derived A β species.⁽⁹⁹⁹⁻¹⁰⁰¹⁾ Cumulatively, these described differences in structure, rate of aggregation, and toxicity call into question the validity of HTS-mediated approaches dependent on synthetic forms of A β .⁽¹⁰⁰²⁾ It is worth noting that when leveraging HTS to identify A β precursors for translation into PET probes for AI, it may be that only the structural discrepancies between synthetic and naturally produced A β are of significance. However, when considering HTS approaches for the discovery of therapeutic agents, such as small molecule inhibitors of A β -aggregation, observed differences in all domains of structure and function become of supreme relevance. For this reason, we hold that the previous lack of a HTS method which utilizes cell-derived A β assemblies represents a fundamental barrier to the development of a disease-modifying therapeutic for AD.

9.1.2 *Barriers to the Development of AD Therapeutics:*

Compounding the significance of identifying novel A β -compounds via HTS methods, small molecules that bind to A β -assemblies may also serve as therapeutic agents for AD by perturbing A β -aggregation.⁽¹⁰⁰³⁾ Not surprisingly, cognizant of confounds associated with synthetic A β , a variety of technologies to circumvent this limitation have been devised. Most obviously, a strong number of cell-culture based HTS techniques have been proposed. For example, in a novel application of real-time cell monitoring techniques, one group has demonstrated that the therapeutic efficacy of a particular drug can be simply and objectively investigated by assessing A β -induced apoptosis in PC12 cells in the presence or absence of that particular compound.⁽¹⁰⁰⁴⁾ This drug design paradigm is irrefutably the predominant approach in the field, as similar methods have been described employing different biological models including C-elegans and various microbes.^(1005, 1006) Representing the pinnacle of this HTS approach with respect to in vivo translatability, one group has developed a three-dimensional human neural cell culture model of AD.⁽¹⁰⁰⁷⁾ Impressively, the neurons used in this assay dramatically overexpress A β , with a 9-fold and 17-fold increase in A β ₄₀, and A β ₄₂ being measured compared to the control cells, respectively. Further, other key features of AD pathogenesis are recapitulated by this model, including increase in aggregated tau fractions.⁽¹⁰⁰⁷⁾ However, while these systems do circumvent confounds introduced by the use of synthetic A β and appear to harbor considerable construct validity, they are all limited by their inability to confirm A β -binding specificity of a particular compound. Put another way, the readout of these assays in no way reports whether A β -aggregation was perturbed secondary to the amyloid-binding properties of the screened compound or some off target effect. As reviewed at length, the pathophysiologic pathways leading to A β aggregation are incredibly complex and poorly integrated. Thus, hits identified through this screening method might bind A β and prevent its aggregation or elicit its effect via a non-A β -dependent interaction. Notably, it can be argued that this is strength of the approach as it might potentially broaden the biologic targets available to AD researchers. On the other hand, the time investment needed to define the central mechanism of action of any drug identified makes this approach unsuitable for the specific task of A β -targeting small-molecule discovery. More generally, these drug discovery approaches have not been optimized on truly HTS-compatible platforms. As evidence, all of the assays described have been validated only on 96-well plate based platforms not realistically compatible with the screening of very large molecular libraries. Further limiting the clinical

translatability of drugs discovered via these methods, none of these assays characterize the BBB permeability of hit compounds. Importantly, the failure of amyloid-centric therapies to date highlights the significance of this oversight, as millions of dollars have been spent evaluating A β -targeted therapies that never reached therapeutically relevant concentrations in the brain.⁽¹⁰⁰⁸⁾

Our collective failure to recognize the importance of characterizing a compound's BBB permeability, and the consequences of this oversight, are no better illustrated than in the field of AD immunotherapy. Notably, while active immunization strategies have proven successful in preventing and treating diseases that manifest secondary to foreign antigens such as bacteria, viruses and toxins; passive immunization paradigms are favored when targeting diseases that present with "self-antigens". In contrast to active immunization strategies, in which the immune system is primed to generate and sustain an immune response against a novel antigen, the premise of passive immunization is to identify an epitope in the laboratory, generate antibodies *ex vivo* and then directly inject these antibodies into the patient. Although this approach is robust in that it facilitates precise manipulation of the epitope to which the antibodies will be targeted, its disadvantages include the need for continuous dosing across the BBB.⁽⁷⁶¹⁾ Still, treatment of APP transgenic mouse models of AD with monoclonal antibodies against the N-terminus of A β showed significant reductions in CNS amyloid burden and reversed memory deficits in multiple behavioral paradigms prompting further evaluation of this therapeutic approach.⁽¹⁰⁰⁹⁾ The first of these passive immunotherapies to be evaluated in clinical trials was Bapineuzumab, a humanized monoclonal antibody against A β 1-5 capable of binding to both amyloid fibrils and plaques. Disappointingly, patients treated with Bapineuzumab in randomized control trials showed little cognitive improvement and no appreciable modulation of CSF A β levels.^(1010, 1011) Concerned that off target effects on APP might explain the lack of clinical efficacy of A β -targeted antibodies like Bapineuzumab that preceded it, a humanized IgG antibody targeted specifically to A β ₄₀, Ponezumab, was generated. Again however, little to no improvement in cognitive impairment was observed and trials were discontinued.^(1012, 1013) Having excluded the possibility of off-target on APP confounding the results of proceeding clinical trials, investigators rationally considered the possibility that the lack of therapeutic efficacy in the trials might be attributable to its inability to bind more toxic oligomeric species of A β . To address this hypothesis, a humanized antibody to an internal epitope of A β ₁₃₋₂₈ was developed and evaluated in clinical trials. The advantage of this particular immunotherapy is that it demonstrates preferential binding to soluble forms of A β , including the putative cytotoxic

oligomeric species. This time, although dose-dependent increases in plasma and CSF levels of A β were noted in addition to a minor delay in symptom progression, investigation in humans again concluded that passive immunization against A β harbors minimal therapeutic efficacy in moderate AD patients.⁽¹⁰⁰⁸⁾ Critically, beyond all representing attempts to utilize passive immunotherapy to combat AD, a common theme shared across antibody-mediated therapies conducted to date are confounds associated with poor BBB delivery. Now cognizant of this barrier, recent approaches seeking to leverage anti-A β antibodies have begun devising methods to increase BBB permeability. In the less elegant of the two approaches made to date, a modified human IgG isotype with reduced affinity for Fc receptor binding (Crenezumab) has been developed in hopes of reducing the risk of immune cell stimulation.⁽¹⁰¹⁴⁾ In addition to attenuating the risk of vasogenic edema noted in previous studies, this approach seeks to overcome the BBB by facilitating higher dosing of the antibody than previous immunotherapies has allowed. Furthermore, Crenezumab appears to bind to many forms of A β including monomer, oligomer and fibrillary assemblies.⁽¹⁰¹⁴⁾ Given the results of previous A β trials targeted to these A β species coupled with its strong safety profile in Phase I study, Crenezumab is currently under Phase II investigation. However, the approach to circumvent brain bioavailability simply by increasing the delivered dose seems naïve given the fact that approximately 0.1% of injected antibodies cross the BBB, with the rest being metabolized in the liver or excreted through the kidneys.⁽¹⁰¹⁵⁾ Thus, the newest generation of anti-A β antibodies seek to utilize receptor-mediated uptake pathways into the brain in order to troubleshoot the limitations imposed by the BBB. This approach merits investigation, as active transport or transcytosis of proteins from the blood to the CNS can increase brain penetration up to 2–3% of the injected dose.⁽¹⁰¹⁶⁾ Although many groups are attempting to functionalize antibodies in this manner, one example of this approach an A β -targeted IgG antibody fused at the Fc region to a Fab fragment with binding affinity to the transferrin receptor.⁽¹⁰¹⁷⁾ Encouragingly, reports suggest that this bi-functional antibody penetrated the brain parenchyma significantly greater than the anti-Ab monoclonal antibody alone and showed a significantly greater reduction in accumulated A β at equal molar doses.⁽¹⁰¹⁷⁾ Still, results in human studies will be necessary in order to validate these antibody-delivery paradigms, and should they too fail, it would mark yet another setback in the field attributable to attempting to deliver non-BBB permeable drugs to the brain. Thus, to avoid repeating our mistakes, techniques which facilitate characterization of a therapeutic candidate's BBB penetration must be integrated into existing and novel drug discovery paradigms. The take home message of this summary is that decades of chronic under-development of BBB drugs for AD are a major cause of clinical trial drug failures. Put plainly, instead of attempting to modify existing structures which bind A β to be BBB

permeable, a more rapid and cost effective avenue of AD therapy design would be to search for A β aggregation inhibitors with innate CNS bioavailability.

It is important to recognize that although many of these immunotherapeutic approaches have failed to elicit significant improvements in mild to moderate AD patients, the exact cause of failure is not known and thus amyloid-centric hypothesis of AD remain untested in humans. This is the predominant expert opinion in the field, but it is important to note that many individuals, especially those not privy to the literature, have interpreted the limited efficacy of A β -targeted therapies as a failure of the amyloid cascade hypothesis. While it is certainly possible this conclusion might prove valid, it is currently premature. Two interrelated hypotheses have been proposed to explain the lack of success of all amyloid-centric therapies to date: (1) poor uptake of the drug/monoclonal antibody to the CNS across the BBB; and (2) treatment of patients too late in the progression of AD. Critically, the discovery of novel A β -binding compounds may address both of these current limitations in the field. With respect to poor drug uptake the argument is straightforward, by leveraging HTS method which not only evaluate a compound's affinity but also its ability to bypass the BBB, clinical translation into humans should not be restricted by issues of bioavailability. Speaking towards the second point, the topic of treating late stage patients with current mild to moderate cognitive impairment is important to take into account when reviewing the results of any therapeutic trial for AD, not just passive immunotherapy. It has long been thought that during the later stages of AD, the neurodegenerative changes which have occurred are likely permanent and independent of further A β deposition. Therefore, reducing or eliminating A β accumulation at this stage may not be sufficient to overcome the deficits in neuronal function. The alternative to studying treatment in these patients would be to study the efficacy of prophylactic interventions in patients with early MCI or who are cognitively intact. However to do this, robust biomarkers are necessary; biomarkers like those which could be developed through the discovery of novel A β -binding molecules which are not plagued by the limitations of current generation AI probes.

9.1.3 Research Strategy and Significance of Work

Admittedly, the question “What factors have limited the clinical implementation of A β -targeted diagnostics and therapeutics?” is a complicated one. However, a review like the one provided above unquestionably reveals that many of the barriers to the development of AD diagnostics and therapeutics are mutually shared amongst the two applications.

Most detrimentally, both have historically suffered from an inconsistent evaluation of BBB penetration. Moreover, both applications have had to rely on ligand-based rational drug design strategies in the absence of robust HTS methods. While true in the therapeutic domain as well, this is no more apparent than in the molecular structure of current generation AI probes. As depicted in the Figure 9-1, structural comparison of the current AI probes for PET-mediated AI reveals a striking lack of diversity and dependence on known amyloid-binding precursors which exhibit abysmal BBB penetration. Transitioning to the therapeutic domain, given that the prevalence of AD is projected to rise dramatically in the coming decades, there is an increasing urgency to develop novel therapeutics to prevent and/or treat this debilitating disease ⁽¹⁰⁰⁴⁾. The therapeutic translation of amyloid-binding compounds is straightforward, as most interfere with protein misfolding and aggregation. Just as in the diagnostic realm, two approaches are useful in identifying compounds that bind to and interfere with aggregation of A β plaques: (i) rational drug design and (ii) high-throughput screening. As highlighted however, since a range of intermediates along the A β aggregation pathway have been implicated as potentially toxic species and at present, no detailed structural information is available on amyloid fibrils (owing to their short-lived intermediates and insoluble nature), the structure-based drug design approach is not yet feasible. Thus, for the time being, high-throughput screening remains the more promising approach ⁽¹⁰⁰⁴⁾.

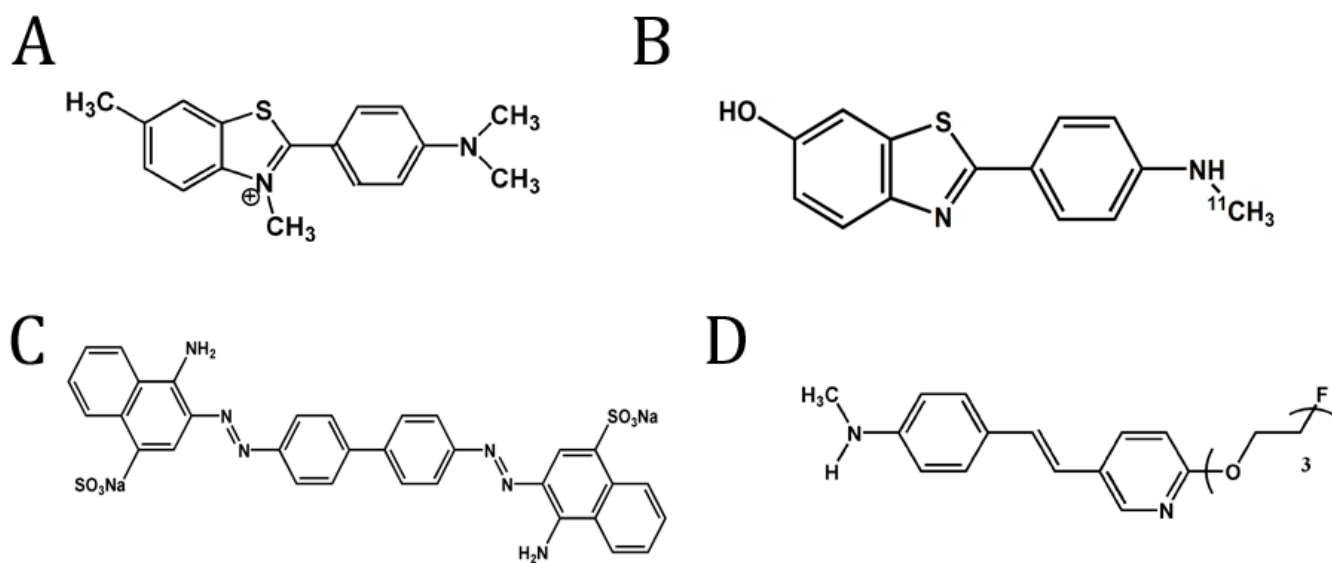


Figure 9-1. Chemical Structures of PET Probes for Amyloid Imaging and Known Histochemical Stains.

Thioflavin. (B) Pittsburgh Compound B. (C) Congo Red. (D) Florbetapir (AV-45)

In light of these shared barriers, the significance of the work discussed herein is that it represents the first HTS approach using an optical platform (HATCO) combined with ex-vivo imaging (MALDI-IMS) to identify A β -binding compounds. The primary goal of this work is to identify orphaned compounds possessing the ability to bind A β -plaques and repurpose them to serve as precursors for novel A β -aggregation inhibitors and diagnostic probes. Importantly, this approach directly addresses the shortcomings of current high-throughput approaches which employ artificial A β derivatives and do not evaluate a molecule's ability to cross the blood brain barrier (BBB). To reach this objective, we hypothesize that a two phase screening approach is necessary. In the first phase, a modified thioflavin-based high-throughput assay is employed to screen for compounds able to specifically bind to A β plaques with modest affinity. Termed the High-throughput Amyloid/Thioflavin Competitive Optical (HATCO) assay, this technique provides a robust means of improving the chance for a biologically meaningful hit in two distinct ways: first by facilitating the rapid screening of large compound libraries, and second by removing the intrinsic limitations associated with a thioflavin-analog-based probe design. Improving on assays which came before it, this assay serves as an excellent starting point in the screening process as it facilitates the screening of thousands of compounds in a matter of minutes in order to produce a manageable library for secondary screening in phase 2. In addition, because our approach utilizes an amyloid-containing lysate derived from the 5XFAD mouse model, the compounds identified in this HTS approach are known to bind to A β assemblies with realistic tertiary structure. For reference, the rationale of the HATCO assay is diagrammatically summarized in Figure 9-2. While this modified HTS approach alone marks a robust improvement from previous techniques, we hypothesize it should be combined with a second screening phase utilizing MALDI-IMS to ensure hit compounds can truly bind to A β and be used in vivo. Notably, MALDI-IMS provides complimentary data unobtainable via independent implementation of the thioflavin-based assay by facilitating the direct analysis of intact tissue and preserving the spatial distribution of molecules within the brain tissue. Put another way, MALDI-IMS-based analysis of thioflavin-discovered hits enables researchers to assess the biological relevance of the molecule's retention pattern in the brain by comparing it with known regions of A β plaque distribution. Of equal importance, it also facilitates confirmation of BBB penetration, meaning that compounds identified via this approach will not compound the barriers to diagnostic and therapeutic development like the known A β -binding precursors used to date.

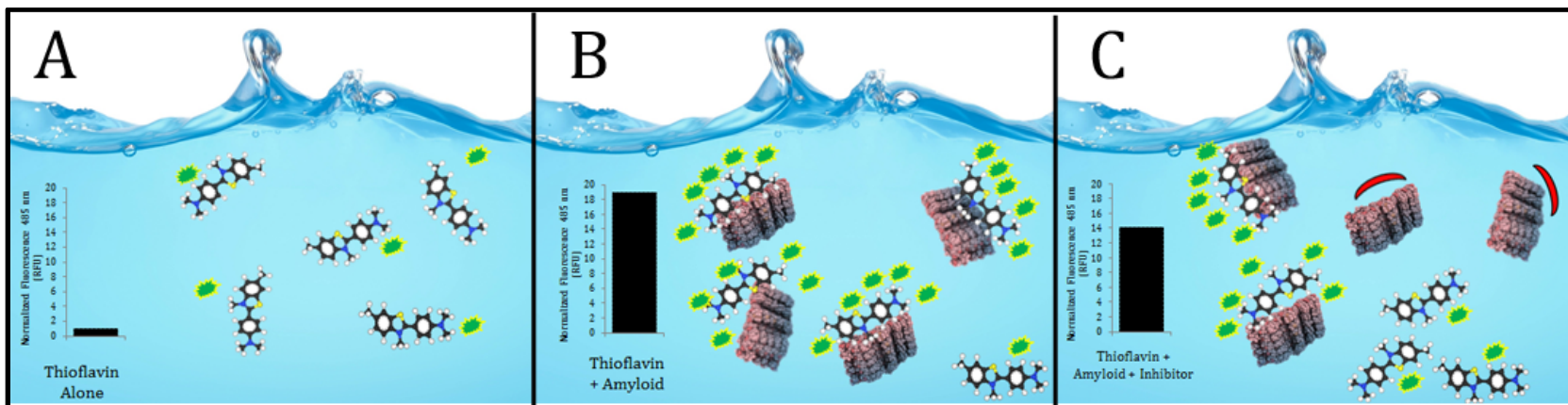


Figure 9-2. HATCO Assay Rationale.

Under aqueous conditions (A), thioflavin (5 molecules depicted) elicits a minimal fluorescent signal at 485 nm (represented by green photons). Arbitrarily establishing this baseline fluorescence as equal to 1 RFU, we can next visualize the effect of adding amyloid species. When assemblies of A β derived from the 5XFAD mouse model are added to a solution of thioflavin (B), fluorescence is increased 19-fold relative to baseline. This is depicted graphically by an increase in the number of photons emitted by the amyloid-bound molecules of thioflavin relative to the unbound species. In the presence of an amyloid binding compound (C), complexes of thioflavin and amyloid are disrupted resulting in an attenuation of thioflavin's fluorescent signal at 485 nm. In this way, a molecule's ability to bind amyloid plaques can be reliably investigated.

Of course, the production of such a robust screening approach requires extensive optimization. In the first aim of this work, initial experiments focused on the feasibility of utilizing an amyloid-containing brain lysate in combination with thioflavin to screen for A β -binding compounds. To sufficiently characterize the optical properties of the assay, this required exquisitely sensitive photometric measurements best supplied by a fluorimeter. On the other hand this approach is not compatible with HTS platforms. Therefore, once the basic principle of the assay had been proven, subsequent work focused on its transition first to a 96-well plate format. Once optimized to this stage, the disadvantages of manual plate loading, most notably the inflation of standard deviation, were recognized. To combat this, subsequent work focuses on the transition of the HATCO assay to a fully automated 384-well platform. Importantly, beyond greatly improving the reproducibility and sensitivity of the assay, this translation also substantially reduced the overall cost of the assay making it an economically feasible means of screening for A β -binding molecules in a high-throughput fashion. In its final optimized form, the HATCO-assay was used to screen a diverse chemical library of nearly 3500 compounds made available via collaboration with the Vanderbilt HTS core. The HATCO assay proved a remarkably specific technique, eliminating 99.8% of screened molecules and highlighting just 7 compounds for future study. To illustrate the advantages of our two-phase approach to HTS, we next selected one of these compounds, PMZ, for further characterization using MALDI-IMS. Impressively, these experiments inarguably demonstrate that PMZ faithfully reports A β plaque burden in the 5XFAD mouse model, making it an ideal candidate precursor for future AI probe development.

9.2 AIM 1 EXPERIMENTAL METHODS

HATCO Reagents:

Thioflavin stock solutions were freshly prepared by dissolving 1.3 mg in 100 mL of deionized water. The solution was vortex, sonicated and passed through a micro-filter after which the concentration was measured using Beer's law (extinction coefficient of 26,620 M⁻¹ cm⁻¹ at 416 nm). The stock solution was stored in darkness using aluminum foil and kept at 4 °C during the assay. Fresh stock solution was prepared for each assay.

Amyloid-enriched 5XFAD lysate was prepared using a two buffer system; a homogenization buffer and a lysate buffer. To prepare a 250 mL stock of homogenization buffer, 21.5 grams of sucrose, 5 mL of 1M Tris, and .5 mL of .5M

EDTA were added to deionized water and mixed thoroughly. The lysate buffer consists of a .5% BSA and .03% Tween 20 in DPBS. Stock homogenization and lysate buffers can be stored at 4 degrees C for up to one year. Immediately prior to use, protease inhibitor must be added to both buffer systems in accordance with manufacturer recommendations. In this work, one Roche cOmplete protease inhibitor tablet was added to every 8 mL of buffer stock.

Production of amyloid-containing 5XFAD lysate is best performed no more than 3 days prior to running the assay and is accomplished via the following protocol. All animal experiments performed complied with institutional guidelines and were conducted according to the protocol approved by the Vanderbilt Institutional Animal Care and Use Committee. First, brain tissue must be isolated from 5XFAD mice of at least 18 months of age. Of note, the entirety of this procedure is performed on ice to minimize tissue damage. Prior to surgical isolation of the brain, the mouse is anesthetized under 2% isoflurane and cardiac perfusion is performed in order to exsanguinate all tissues. For each mouse, a midline incision spanning from the abdomen to the upper thorax is made allowing retraction of the chest wall. Using a 10cc syringe equipped with a 27 gauge needle, 20 cc of PBS chilled to 4°C is perfused via the now exposed left ventricle. Prior to insertion of the needle, it is critical that the right atria of the heart be lacerated with a scalpel to allow complete exsanguination of all tissues. With this done, surgical isolation of the brain can commence. To begin, the skull is separated from the body by cutting along the cervical vertebrae. Next, surgical scissors are threaded through the remaining cervical vertebrae and fractured along their lateral aspect. Cutting is continued along the lateral aspect of the skull in a posterior to anterior fashion, progressing first through the occipital condyle and paraoccipital process before ending at the most anterior aspect of the zygomatic bone. With this procedure done on both sides of the skull, the resulting cap of bone can be easily removed by grasping its posterior portion with tweezers and pulling lightly. Now completely exposed, the brain can be separated from the skull by severance of the cranial nerves. Once isolated, the brain tissue should be immediately placed in a pre-chilled 1.5 mL wide-bottom Eppendorf tube and placed on ice. Next, 800 µL of homogenization buffer should be added to the sample and thoroughly homogenized using a T-25 basic Ultra-Turrax homogenizer. The resulting concentrated brain lysate is then transferred to a 15 mL polypropylene conical tube and diluted with 4 mL of lysate buffer. For best results, this can be done with 1 mL aliquots so that any lysate sticking to the walls of the Eppendorf tube can be washed with the subsequent volume of lysate buffer. Importantly, use of other plastics and/or glassware is prohibited in this procedure as prolonged exposure to these materials can result in loss of A β content. At this stage, the sample is then

centrifuged at 16,000xG at 4°C for 30 minutes. The resulting supernatant should then be transferred into a new polypropylene storage vessel and either kept at 4°C for immediate use or frozen at -80°C for short-term storage.

Fluorimeter-based HATCO Assay

Fluorescence was measured using excitation/emission parameters at 465/485 nm with 5 nm slits, 0.1 second integration time and at 1-nm intervals using a Photon International fluorimeter. In a typical measurement, thioflavin (50 μ L, 40 μ M) was added to 100 μ L of freshly prepared 5XFAD amyloid lysate (70 mg/mL). Prior to the addition of each of these reagents, each stock solution was vortexed and sonicated to insure a homogenous sampling. The mixture of 5XFAD lysate and thioflavin was then incubated at room temperature for 10 min. After incubation, test compounds (50 μ L) in PBS (50 mM) were added to the mixture. The concentration of the tested compounds was 250 μ M in deionized water. After equilibration for 10 min at room temperature, the fluorescence signal of the sample was measured at an emission λ_{max} of 485 nm. All measurements were performed in triplicate and data are presented as mean with standard deviation.

96-well Plate-based HATCO Assay:

Stock solution preparation and concentrations were accomplished as described above. Fluorescence was measured using excitation/emission parameters at 465/485 nm using the Synergy Neo Multi-mode plate reader system. On a 96-well plate platform, thioflavin (50 μ L, 40 μ M) was added to 100 μ L of freshly prepared and vortexed 5XFAD amyloid lysate (70 mg/mL). The mixture was incubated at 4°C for 30 minutes prior to fluorescence reading. After incubation, test compounds (50 μ L) in PBS (50 mM) were added to the mixture. The concentration of tested compounds in the well was 250 μ M. After equilibration for 10 min at room temperature, the fluorescence signal of the sample was measured at an emission λ_{max} of 485 nm. All measurements were performed in triplicate and data are presented as mean with standard deviation.

384-well Plate-based HATCO Assay:

Stock solution preparation and concentrations were accomplished as described above. To decrease standard deviation between samples secondary to variations in loading, deep-well source plates of thioflavin and 5XFAD lysate were generated using the COMBI liquid handling system. Importantly, prior to loading of the source plates using the COMBI liquid handling system, all reagents must be vortexed for 10 minutes and sonicated for 15 minutes at 4⁰C. For both source plates, a 10 μ L void volume was added in addition to the required reagent. To this void volume, 5 additional μ L of thioflavin or 20 μ L of 5XFAD lysate was added to each well of the 384-well plate to be screened. For example if running a single 384-well plate, 15 μ L of thioflavin and 30 μ L of 5XFAD lysate should be loaded into each respective source plate. Once both thioflavin and lysate source plates have been generated, they should be immediately centrifuged for 10 seconds to eliminate bubbles and subsequently sonicated to insure all protein constituents remain homogenously distributed in solution. Next, the 125 nanoL (10 miliM) of each compound in the library must be shot onto a non-binding black flat-bottom 384-well plate using the ECHO liquid handling system. This plate is referred to as the library plate. In the final phase of the operation, thioflavin and 5XFAD lysate are then robotically pipetted to the library plate. This is done using the Bravo liquid handling system and begins with automated mixing of the 5XFAD source plate via serial aspiration and dispensing of 50% of the total well volume. Once mixed, 20 μ L is aspirated from the source plate and dispensed into the library plate. Each well is again slowly mixed over a 5 minute period to insure a binding equilibrium is reached between the 20 μ L of lysate and 125 nanoL of library compound. In a similar manner to the process described above 5 μ L of thioflavin is mixed and then added from the source plate to the library plate. With each well now containing the full complement of reagents, including 5 μ L thioflavin, 20 μ L of amyloid-containing 5XFAD lysate, and 125 nanoL of library compound, each well is again thoroughly mixed 10x by the automated liquid handling algorithm. Of note, relevant parameters for all of these steps include a 2 μ L post-dispense void volume and automated tip-touch procedure to eliminate the possibility of reagent adhesion to the pipette tips. To facilitate statistic-mediated hit identification, columns 1, 2, 23, and 24 should be loaded with positive (20 μ L 5XFAD lysate (7 mg/mL) 5 μ L Thioflavin (40 μ M) 125 nL DMSO) and negative (20 μ L wild type lysate (7 mg/mL) 5 μ L thioflavin (40 μ M) 125 nL DMSO) controls in a checkerboard fashion. It is critical that positive and negative controls are loaded onto each 384-well plate, as inter-plate analysis is not permitted. Once loaded, fluorescence measurements are provided via the Synergy Neo Multi-mode plate reader system in a similar fashion as described above.

HATCO-Assay Cross-Screening

Following identification of A β -binding compounds via primary screening of large molecular libraries with the HATCO assay, a cross-screening protocol is necessary to exclude false positives. In its finalized 384-well format, this procedure involves two phases. In the first phase of the cross-screening procedure, the absorbance profile of each hit compound is characterized over the 250-900 nm wavelength range. To do this, 20 μ L of each hit compound (10 milliM) were shot onto 384-well clear-bottom polystyrene plates (PerkinElmer) in a triplicate fashion. Absorbance was then measured across the specified wavelengths using the Synergy Neo Multi-Mode Microplate reader (BioTek) with a step size of 10 nm and a 0 millisecond delay. Scatterplots of absorbance as a function of wavelength are then used to qualitatively assess whether the analyzed hit compound significantly absorb at relevant wavelengths. For example, as a reduction in thioflavin emission at 490 nm is the primary indicator of A β -binding potential in the assay, hit compounds absorbing at this wavelength should be considered false positives. To quantitatively cross-screen for false positives secondary to interference of thioflavin absorbance or emission at 410 nm and 490 nm, respectively, a separate experimental design is employed. In this second phase of cross-screening, 125 nL of each hit compound (10 milliM) is plated with 25 μ L of thioflavin (10 μ M) in triplicate fashion. As a control, 25 μ L of 10 μ M thioflavin is plated in the presence of 125 nL of DMSO. Again, the Synergy Neo Multi-Mode Microplate reader (BioTek) is employed to measure thioflavin's emission at 490 nm (excitation 410 nm). Statistical determination of false-positives is accomplished via a Paired 2-tailed Student T-test comparing of the mean fluorescence for the DMSO-treated control wells to that of wells containing thioflavin and the posited hit compound. In this work, a P-value < .05 was used as the threshold statistic for classification as a false positive hit.

Evaluation of A β -binding Affinity Using Concentration Response Curves

After primary screening, confirmatory screening, and cross-screening experiments, the A β -binding affinity of compounds identified via the HATCO assay was quantitatively assessed via the generation of concentration response curves for each molecule. To do this, 750 nL of each hit compound was robotically plated in the presence of 20 μ L of 5XFAD lysate (7 mg/mL) and 5 μ L of thioflavin (40 μ M). Critically, the concentration of the hit compound was varied such that its final

concentration in the well ranged from 15 nM-300 μM. In more detail, this was done by dividing the specified concentration range up according to a 1:3 dilution, resulting in 10 data points per compound. Notably, each hit compounds was plated in duplicate across the entire concentration range on a 384-well plate. Furthermore, plating was done in an automated fashion similar to that described for HATCO-assay mediated HTS on the 384-well plate platform. After 1 week of incubation at 4 °C to facilitate complete equilibration, fluorescence at 485 nm was measured using the Synergy Neo Multi-Mode Microplate reader (BioTek). To facilitate the generation of concentration response curves, fluorescence at each data point was averaged on a compound by compound basis and plotted as a function of concentration. From these plots, the relative Aβ-binding affinity of each compound can be assessed by comparing IC50 values generated via the GraphPad Software package.

Tissue Fixation by Cardiac Perfusion

5XFAD and wild type mice of different ages were obtained from the in-house Vanderbilt breeding facility and housed in a temperature controlled 12-hour light/dark cycle facility. After injection of the tested compounds (25 mg/kg), at a designated time point, including 10 min and 4 h, cardiac perfusion was performed. A sharp incision into the abdomen of the anesthetized mouse was made. This was followed by a longitudinal cut with a scalpel to open the thoracic cavity, which then was stabilized with a retractor. Perfusion began with a 20-gauge syringe containing ice cold PBS (30 ml, pH 7.4) in the left ventricle while the atrium was snipped followed by the injection of paraformaldehyde (PFA) solution (4%). Once the perfusion was completed, the animals were decapitated and the brains were quickly removed and fixed in PFA overnight at 4 °C followed by sucrose precipitation overnight at 4 °C. The brains were then embedded in Cryo-OCT compound (Fisher Scientific) before sectioning. All animal experiments performed complied with institutional guidelines and were conducted according to the protocol approved by the Vanderbilt Institutional Animal Care and Use Committee.

Matrix-assisted Laser Desorption Ionization Imaging Mass Spectroscopy MALDI-IMS:

Analyses of promethazine were performed on an LTQ XL linear ion trap mass spectrometer equipped with a MALDI source (ThermoFisher, Waltham, MA). Fresh frozen mouse brain coronal sections of 12 μm were thaw-mounted onto gold-coated, stainless steel target plates which were kept at room temperature in a vacuum desiccator until analysis. A serial section was obtained on a glass slide and stained using hematoxylin and eosin. The tissue sections were manually coated with matrix (DHB, 30 mg/mL in 50:50 methanol: water with 0.1% trifluoroacetic acid) using a glass nebulizer (thin-layer chromatography reagent sprayer, Kontes Glass Company, Vinland, NJ). The matrix was applied by passing the sprayer across the tissue section several times and allowing the tissue to dry. This process was repeated approximately 20 times to ensure a homogeneous coating of matrix crystals formed on the tissue section while minimizing analyte delocalization. After coating, the target plate was attached to a modified LTQ slide holder and inserted into the instrument. MS/MS spectra for promethazine were acquired over the entire tissue section at 100 μm spatial resolution. An isolation window (1.0 amu) centered on m/z 285 was selected to isolate the precursor ion for PMZ. This was subjected to collisionally activated dissociation (CAD) at collision energy of 27. Main fragment ions were formed at m/z 86 and 198 (likely corresponding to fragmentation at the phenothiazine-N) as well as at m/z 240 (likely corresponding to loss of the dimethylamine moiety).⁽¹⁰¹⁸⁾ Images representative of the distribution of PMZ across the tissue section were generated by plotting the summed intensity of the main fragment ions at m/z 86 and 240 at each pixel using ImageQuest software (Thermo Scientific, Waltham, MA). Analyses of amyloid peptides were performed on a linear MALDI time-of-flight mass spectrometer (Autoflex, Bruker Daltonics, Billerica, MA). The samples on the plate analyzed using the LTQ were washed in sequential steps of 70% ethanol, 100% ethanol, Carnoy's solution (60% ethanol, 30% chloroform, 10% acetic acid), and water to remove the matrix and potential ion suppressant's such as lipids and salts. After reapplying the matrix, three brain sections were imaged in positive ion mode from m/z 2500–7000 at a spatial resolution of 75 μm . Specific ion images were reconstructed in fleximaging software (Bruker Daltonics, Billerica, MA).

Brian Bioavailability Analysis by HPLC:

Whole brains from perfused 5XFAD or wild type mice treated previously with promethazine at different times were collected, weighed, and homogenized in PBS (g tissue/3 mL PBS) using a homogenizer (Tissuemizer Homogenizer, Fisher Scientific, Pittsburg, PA). The homogenized solution was added with 20% acetonitrile and warmed at 70 $^{\circ}\text{C}$ using a

heating block for 10 min to maximize promethazine extraction. During this extraction process, the sample was continuously agitated using a magnetic stir bar. The extract was lyophilized overnight and then reconstituted with HPLC grade acetonitrile. With respect to HPLC parameters, a two mobile phase system was employed on a carbon-18 column. Solution A consisted of .1% TFA in double deionized water. Pure HPLC grade methanol constituted solution B. For HPLC analysis of promethazine content, a temporally varying isocratic strategy was used in which a 20% solution A and 80% solution B gradient was held for the first 5 minutes. For the subsequent 30 minutes, the gradient was inverted to 80% solution A and 20% solution B. Under these conditions, the R-enantiomer of promethazine was reliably eluted at retention time of 15 minutes while the S-enantiomer was characterized by a retention time of 17 minutes. After establishing the detection limit of the instrument and determining a promethazine concentration–response calibration curve, the quantitative amount of promethazine in the brain lysate against the injected dose was analyzed by integrating the area under the curve using EZChrome Elite software (Hitachi). Every retention time peak in the spectrum was collected and analyzed using LC–MS.

MALDI-IMS Imaging Analysis

Each coronal brain slice was manually segmented to create individual ROIs of the hippocampus and isocortex or of the whole coronal section. The Allen mouse brain atlas was used as a reference for the segmentation of these regions and analysis was performed by an outside collaborator. The ROIs were then used to isolate the pixels in the MALDI ion images representing promethazine (m/z 86 + 240) and the pixels within the direct A β 40 images (m/z 4331+/-4). Once the images were segmented, mean signal values were calculated. Next, the pixels within each ROI were segmented into two groups using the k-means clustering algorithm, which represents signal vs. no signal. Experimental data were reported as mean \pm SD. We compared the test groups using the Mann–Whitney t-test using GraphPad software (La Jolla, CA). P values are two-tailed and differences with P- values > 0.05 were considered statistically significant.

9.3 AIM 1 EXPERIMENTAL RESULTS

9.3.1 Results: Validation of HATCO Assay-mediated Screening for Novel A β -binding Compounds

As described, thioflavin is classified as a topologically activated dye. Put simply, this class of compounds possesses substantial conformational freedom while in free solution and as a consequence exhibits a relatively low fluorescence signal. However, upon binding to A β plaques, thioflavin's conformational freedom is dramatically reduced. This increase in structural rigidity decreases the vibrational-rotational processes available to the thioflavin molecule, resulting in a decreased radiation decay rate of thioflavin in both ground and excited states. Cumulatively, these phenomena contribute to the observed increase in thioflavin's fluorescence quantum yield when bound to A β plaque compared to the unbound molecule.⁽⁸³⁵⁾ Although increased thioflavin fluorescence alone is highly indicative of the thioflavin molecule existing in an A β -bound state, secondary validation of this fact is available as a consequence of a characteristic spectral shift in thioflavin's fluorescence signal observed only when thioflavin is bound to A β plaques. As discussed, when not complexed with A β , thioflavin emits a weak fluorescent signal at a λ_{max} of 440–445 nm. However, when bound to A β plaques, thioflavin's fluorescence increases dramatically resulting in a strong fluorescent signal with a characteristically shifted λ_{max} of approximately 485 nm.^(228, 1019) We employed these unique characteristics of thioflavin to develop the HATCO assay for screening compounds for the ability to bind to A β plaques in a high-throughput fashion. Again, in an effort to utilize the most biologically representative A β plaques possible, fresh brain lysates were obtained from 5XFAD mice and analyzed using the Bradford assay to ensure an equal amount of protein was used in each assay trial. To test our hypothesis that A β plaques contained within our 5XFAD lysate are sufficient to modulate thioflavin fluorescence, it was first necessary to optimize the excitation and emission parameters of the assay. To identify the optimal excitation criteria for thioflavin at a 485 nm emission, an excitation scan was performed (Figure 9-3A). Results were largely consistent with the literature in suggesting that an excitation at 410 nm was optimal for stimulating thioflavin fluorescence at 485 nm. Next, an emission scan of A β -containing 5XFAD lysate mixed with thioflavin was performed to directly test the hypothesis that A β -containing 5XFAD lysate could generate an amyloid-specific increase in thioflavin fluorescence at 485 nm. Again, as demonstrated in Figure 9-3B, this hypothesis was confirmed suggesting that the underlying rationale of the HATCO assay was sound.

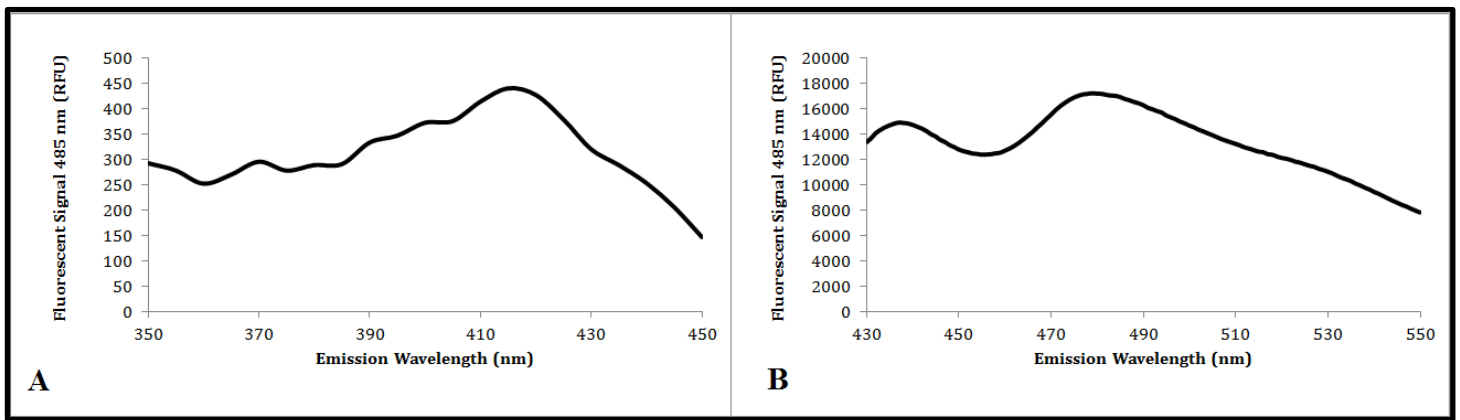


Figure 9-3. 5XFAD Lysate Modulates Thioflavin Fluorescence.

(A) Thioflavin Emission Scan at 485 nm as a Function of Excitation Wavelength. Results indicate an excitation λ_{\max} near 410 nm suggesting this as the optimal excitation wavelength for the HATCO assay. (B) Thioflavin Emission Scan in the Presence of 5XFAD Lysate at 410 nm Excitation. Results demonstrate a robust A β -specific signal at 485 nm, confirming the hypothesis that A β assemblies within 5XFAD lysate can bind thioflavin and modulate its fluorescence signal. Critically, the observed shift in thioflavin's emission λ_{\max} from 465 nm to 485 nm provides strong support for the hypothesis that 5XFAD lysate contains sufficient A β to modulate thioflavin's signal.

With this preliminary characterization of the HATCO assay completed, it was next time to investigate whether the known A β plaque binding molecule Resveratrol would attenuate thioflavin signal at 485 nm as hypothesized. Strongly supporting the ability of the assay to identify A β -binding molecules, thioflavin fluorescence at 485 nm was attenuated 4.4%, 25.9%, and 51% at 100 μ M, 500 μ M, and 2000 μ M concentrations of Resveratrol, respectively (Figure 9-4). Cumulatively, these results suggest that (i) 5XFAD lysate can be used as a source of A β assemblies, and (ii) attenuations in thioflavin fluorescence at 485 nm can serve as a reporter of a compound's ability to bind A β -plaques. Under the working model, as depicted in Figure 9-2, addition of 5XFAD lysate to thioflavin results in the formation of thioflavin-amyloid complexes which increase thioflavin's fluorescent signal at 485 nm. However, in the presence of a compound which can bind to A β species, a fraction of the thioflavin-amyloid complexes are disrupted via a competitive-binding mechanism, resulting in a measurable attenuation of thioflavin's fluorescent signal. With this working model for the assay strongly supported by initial experiments, we next proceeded to screening a small molecular library of compounds for A β -binding potential.

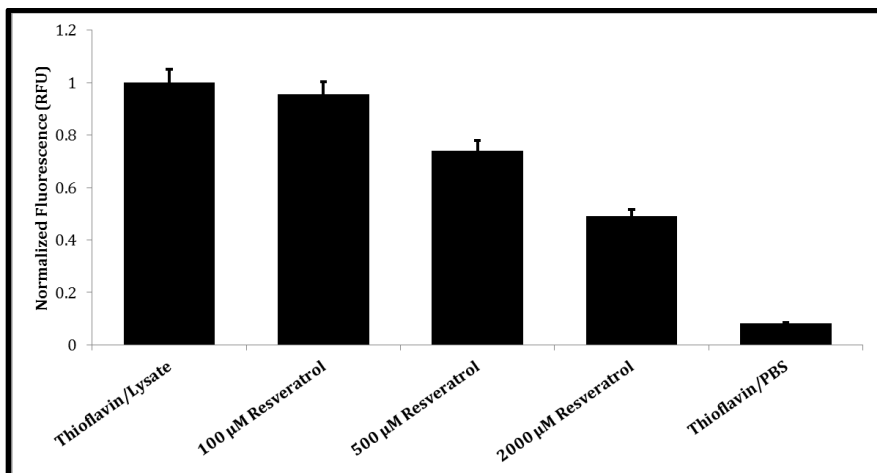


Figure 9-4. Known A β -binding Molecule Resveratrol Attenuates A β -specific Thioflavin Fluorescence at 485 nm in a Dose-dependent Manner.

In accordance with the fluorimeter-based HATCO assay protocol, 100 μ L of 5XFAD lysate was incubated with 50 μ L of the A β -binding agent Resveratrol. Next, 50 μ L of 40 μ M thioflavin was added to solution and fluorescence at 485 nm was measured. In the positive control condition, PBS was substituted for Resveratrol, facilitating optimal thioflavin-amyloid interactions. As a negative control, 5XFAD lysate was emitted from solution. Relative to the positive control condition, 100 μ M, 500 μ M, and 2000 μ M concentrations of Resveratrol significantly reduced thioflavin fluorescence by 4.4%, 25.9%, and 51%, respectively ($P < .01$). Data presented as mean \pm standard deviation.

9.3.2 Results: HATCO Assay-mediated Screening of a Primary Library for Novel A β -binding Compounds

Confident in the ability of our assay to identify A β -binding molecules after demonstrating that Resveratrol attenuates thioflavin fluorescence in a dose-dependent manner, we next characterized the HATCO assay using a small number of non-A β -binding molecules. In addition to these non-A β compounds, several compounds with the potential to bind A β , as predicted by a ligand-based design strategy, were also included in the primary screen (Figure 9-5). Importantly, all compounds included in the primary library were hand-chosen to have a high probability of crossing the BBB. In fact, for virtually all of the compounds screened BBB permeability was already reported in the literature. Regardless, almost all compounds screened met the highly restrictive inclusion criteria listed in Table 9-2. Before performing a specific displacement study, we conducted a series of control experiments intended to (i) assess whether the tested library of compounds emitted or absorbed at wavelengths might confound thioflavin's signal by overlapping with its excitation or emission spectra and (ii) demonstrate the specificity of thioflavin toward A β plaques.

Table 9-2. Molecular Attributes Compatible with Blood Brain Barrier Penetration

Compound Feature	Criteria
Lipophilicity	logP 1.5-2.7
Hydrophobicity	Clogp < 5
Molecular Weight	< 450 g/mol
Hydrogen-bond Donors	< 3
Hydrogen-bond Acceptors	< 7
Rotatable Bonds	< 8
Molecular Charge	Pka 7.5-10.5
Polar Surface Area	< 60-70 Å ²
Aqueous Solubility	< 60 µg/ml

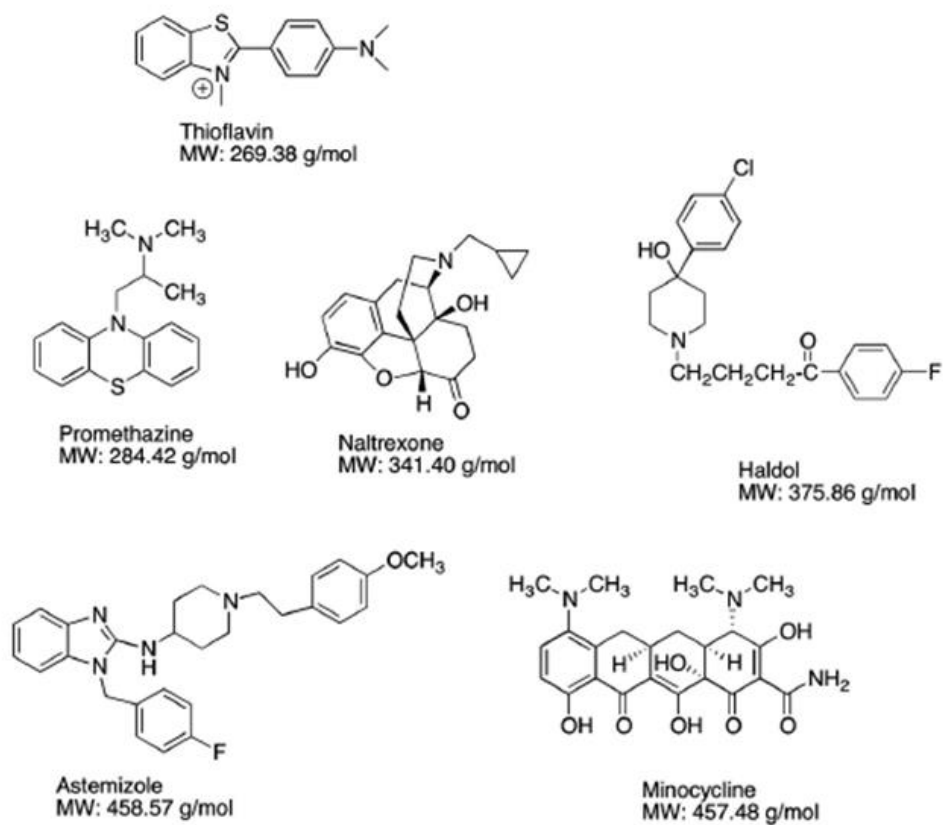


Figure 9-5. Initial Screening Library

Chemical structures and molecular weights of thioflavin and candidate amyloid-binding compounds. Thioflavin and a series of selected compounds comprising a small molecular library were screened for the ability to bind A β plaques using the HATCO assay. Structural diversity was maximized within this library to include benzimidazole, benzylisoquinoline, butyrophenone, tetracycline and phenothiazine motifs contributed by astemizole, naltrexone, haloperidol, minocycline, and promethazine, respectively.

As shown in Figure 9-6A, when the compounds were mixed with thioflavin in the absence of A β plaque, no significant modulation of thioflavin fluorescence is observed. These findings lend strong support to the claim that the compounds tested do not bind to thioflavin directly and are incapable of directly modulating its fluorescence due to overlapping spectra. In support of thioflavin's affinity for A β plaques, mixing thioflavin (10 μ M) with A β plaques (35 mg/mL) contained within the 5XFAD brain lysate resulted in a nearly 19-fold enhancement in thioflavin fluorescence signal compared to a control sample ($P < 0.0001$) in which the same concentration of thioflavin was dissolved in PBS without A β protein. Importantly, the enhanced fluorescence signal of thioflavin observed in the presence of the 5XFAD lysate exhibited a λ_{max} of 485 nm, a characteristic of thioflavin bound to A β plaques. By comparison, the thioflavin mixed with PBS controls emitted most strongly at 440 nm, which is the λ_{max} associated with unbound thioflavin. In a more rigorous demonstration of thioflavin's specificity for 5XFAD-derived A β plaques, we treated the same thioflavin concentration with brain lysate isolated from wild type mice lacking A β plaques. Despite some degree of non-specific binding, a reliable differential in fluorescence signal enhancement was observed between amyloid-containing 5XFAD lysate and amyloid-deficient wild type lysate, which confirmed our hypothesis that thioflavin fluorescence could be used as a reliable reporter to identify A β -binding compounds. Again, spectral analysis of thioflavin's fluorescence in the presence of wild type lysate reveals a λ_{max} of 440 nm as compared to the λ_{max} of 485 nm observed in the 5XFAD trials. This spectral shift confirms the thioflavin fluorescence signal utilized as a reporter in the subsequent HATCO assays reliably reflects the proportion of A β -bound thioflavin. Thus, any observed modulation in thioflavin fluorescence when the compounds are added cannot represent the dissociation of thioflavin from non-A β proteins, as these complexes do not contribute to the measured thioflavin signal at 485 nm (Figure 9-6B)

Next, we tested the ability of the compounds to displace thioflavin for binding to A β plaques. Again, the assumption was that if thioflavin is dissociated from A β plaques by a competitively binding compound, the fluorescence signal of thioflavin would be reduced. 5XFAD brain lysates of normalized concentration were treated with thioflavin in quartz cuvettes and allowed to equilibrate for 10 min before the addition of the tested library compounds. After equilibration, the proportion of thioflavin molecules bound to A β plaques in solution was measured using fluorescence spectroscopy. Among the tested compounds, we found that only promethazine caused a notable reduction (19%) of thioflavin's fluorescence signal ($P < 0.0001$) (Figure 9-6C). Of note, it is improbable that this signal attenuation is

attributable to fluorescence resonance energy transfer (FRET), as promethazine is not a chromophore and is therefore unable to interfere with the excitation states of thioflavin via the FRET mechanism. Still, the control experiments summarized in Figure 9-6A completely exclude this possibility, as they provide no evidence of a direct interaction between promethazine and thioflavin. Taken as a whole, the results strongly indicate that PMZ binds to A β plaques, a result which confirms the utility of the HATCO assay in identifying novel A β -binding molecules.

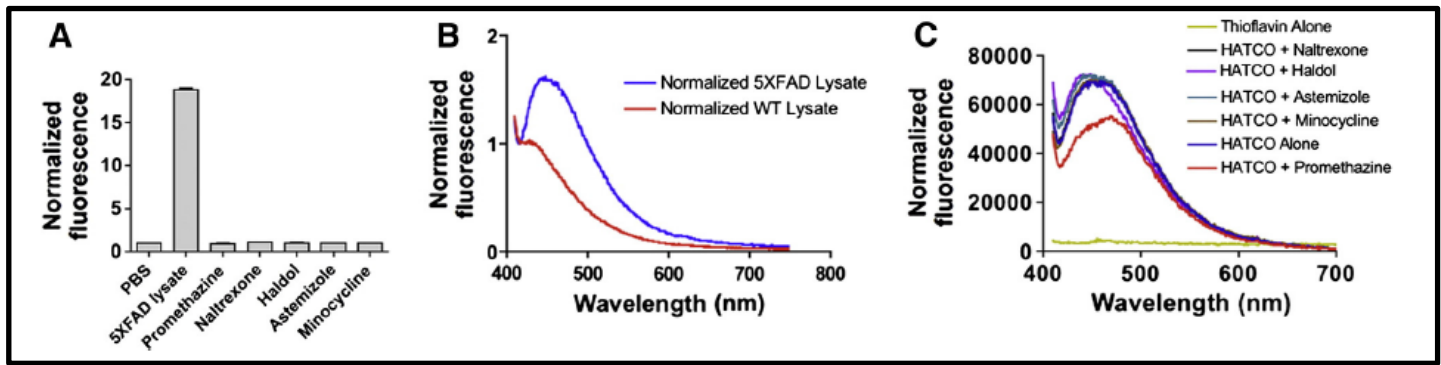


Figure 9-6. HATCO Assay-mEDIATE, High-throughput Screening of Structurally Diverse Compound Libraries for A β plaque-binding Capacity.

(A) Fluorescence signal of thioflavin in the presence of freshly isolated 5XFAD brain lysate, PBS or candidate compounds. The results demonstrate a 19-fold increase in thioflavin fluorescence in the presence of 5XFAD lysate compared to PBS and compound library trials ($P < 0.0001$). Values represent normalized fluorescence with respect to PBS trial \pm S.D. ($n = 3$). (B) Enhancement of thioflavin fluorescence in the presence of 5XFAD lysate compared to wild type lysate. The spectral shift in thioflavin's λ_{max} toward 480 nm in the presence of 5XFAD lysate arises as a consequence of thioflavin-amyloid complexes and validates the reliability and specificity of the thioflavin reporter. Note that the emission maximum of 440 nm in the wild type trials excludes the possibility of the thioflavin signal enhancements representing non-specific binding of thioflavin to endogenous peptides of the brain. Protein concentrations in 5XFAD and wild type lysates were normalized throughout the assays. (C) Increased thioflavin fluorescence secondary to the presence of amyloid-containing 5XFAD lysate is attenuated by the addition of promethazine but not by other candidate compounds. Promethazine reduces thioflavin fluorescence at 480 nm by 15.6% with respect to PBS trials ($P < 0.0001$). The results suggest promethazine may displace thioflavin for amyloid plaques and thus attenuate the fluorescence signal. All measurements were performed in triplicate at candidate compound concentrations.

9.4 Results: Translation of the HATCO Assay to a 96-well Plate Platform

Having leveraged the HATCO assay to identify a new A β -binding molecule, PMZ, the HATCO assay needed to be translated to plate-reader compatible platforms in order to facilitate truly robust HTS. To help facilitate the transition from cuvette-based measurements, the original assay parameters were maintained in the first set of experiments performed on a 96-well plate platform. To reiterate for the sake of clarity, under the positive control condition “HATCO”, 200 μ L of A β -containing 5XFAD lysate was mixed with 50 μ L of thioflavin and an additional 50 μ L of PBS. Interestingly, although fluorimeter-based excitation scans corroborated thioflavin’s λ_{max} at 410 nm, similar experiments performed on the positive control condition in the 96-well plate format revealed three distinct absorption peaks: 375 nm, 410 nm, and 430 nm. Seeking to characterize these excitation parameters in more detail, emission scans were performed on the positive control condition. This data was compared with the emission profile of a control hit condition (HATCO + PMZ), comprised of 200 μ L of A β -containing 5XFAD lysate, 50 μ L of thioflavin, and 50 μ L of PMZ (2000 μ M). In congruence with the standards of the field, a Z-factor was generated for each assay parameter in an attempt to quantify the suitability of the HATCO assay for use in a full-scale, high-throughput screen. Briefly, the Z-factor is defined in terms of four parameters: the means (μ) and standard deviations (σ) of both the positive (p) and negative (n) controls (μ_p , σ_p , and μ_n , σ_n).

$$Z - factor = \frac{3(\sigma_p + \sigma_n)}{|\mu_p - \mu_n|}$$

Breaking down this equation into its constituent components emphasizes the key design considerations of a HTS assay. At the most basic level, there must be a sufficiently robust difference between negative and positive controls. More importantly however, the standard deviation within the positive and negative control conditions must be minimized as this factor is accentuated in the Z-prime calculation by a factor of 3. At its heart, the Z-factor is a measure of statistical effect size. Thus, the utility of Z-factor calculations in the field of HTS is straight-forward. Because large screens are expensive with respect to both time and resources, the Z-factor provides a quantitative means of evaluating the utility of any particular assay. Importantly, guidelines for the interpretation of the Z-factor are well-established in the literature.⁽¹⁰²⁰⁾ Summarizing these interpretive guidelines, a Z-factor can be translated into three categories corresponding to useless, marginal, and excellent assays. A hypothetical ideal assay carries a Z-factor of 1, the maximum Z-factor mathematically

possible, whereas a Z-factor less than 0 indicates that there is too much overlap between positive and negative controls for the assay to be useful. More commonly seen are assays characterized by Z-factors in the range of 0 to 1. In this range, an assay characterized by a Z-factor between 0-.5 is considered marginally useful while a Z-factor above .5 qualifies an assay to be considered excellent. Impressively, a Z-factor of .5 indicates a 12 standard deviation difference between μ_p and μ_n when $\sigma_p = \sigma_n$. This statistic highlights the extreme conservatism which characterizes the field of HTS when evaluating the utility of a newly designed assay. Although these strict criteria eliminate novel assays with extreme prejudice, they are necessary due to the fact that experimenters often compare millions of single measurements of unknown samples to positive and negative controls during the course of a HTS. Therefore, prior to starting a large screen, smaller pilot screens are used to generate a Z-factor for the assay in an effort to help assess the quality of the assay and predict if it will be useful in a high-throughput setting.

To generate a Z-factor for the HATCO assay, a checkerboard pattern was manually pipetted. Significantly, by distributing the positive and negative controls in this manner, edge artifacts or other confounds associated with plating can be assessed. As depicted in Figure 9-7, comparison of the raw fluorescence elicited at each of the three excitation wavelengths reveals that at 375 nm, the A β -specific thioflavin signal at 485 nm is maximized. Despite this trend, excitation at 375 nm or 430 nm failed to increase the differential between positive and hit conditions as compared to the original 410 nm excitation. Furthermore, although excitation at 375 nm increases the magnitude of thioflavin fluorescence at 485 nm as compared to absorbance at 410 nm (28,838 A.U. versus 20231 A.U.), standard deviation also increases at the 375 nm excitation (473 RFU versus 142 RFU). As previously mentioned, when utilizing a Z-factor statistic to assess any assay's utility, increases in standard deviation have the most negative effect on the assays overall performance ranking as this parameter is accentuated in the equation. Thus, although excitation at 410 nm doesn't necessarily represent the λ_{max} of absorption, it does maximize the utility of the HATCO assay by minimizing standard deviation. These notes can be appreciated in Table 9.3. Of highest significance with respect to utilizing the HATCO assay to facilitate true HTS of A β -binding molecules, under the optimized assay condition a Z-factor of .64 was calculated, placing this novel assay in the "excellent" category of high-throughput screening techniques.

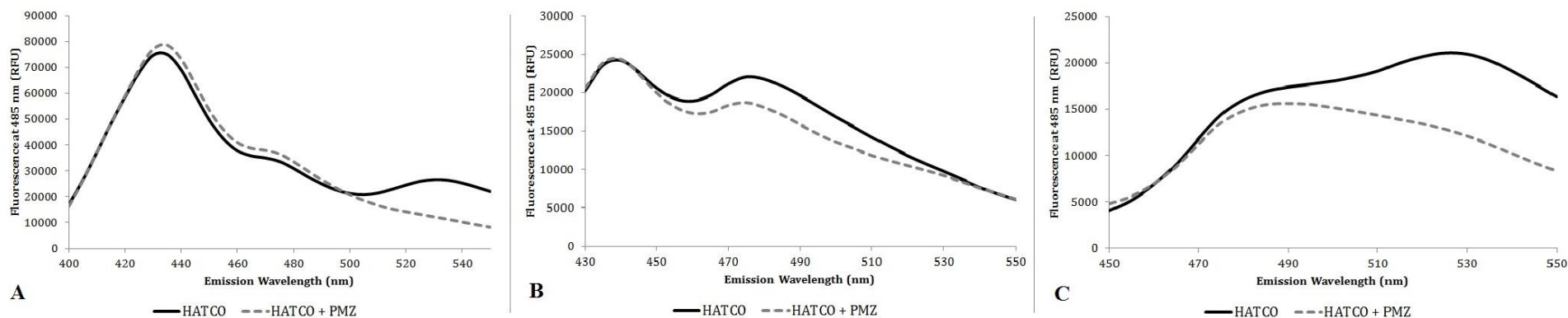


Figure 9-7. Thioflavin Optimally Excited by 410 nm Excitation Source in the Presence of 5XFAD Lysate.

Emission scans of 10 μ M thioflavin in the presence of 70 mg/mL 5XFAD lysate under two conditions were performed in order to optimize the excitation wavelength of the HATCO assay. In the positive control condition (HATCO), PBS was added to thioflavin and 5XFAD lysate containing wells. In the hit condition, these same reagents were allowed to interact in the presence of 200 μ M Promethazine (HATCO + PMZ). As discussed, three peak excitation wavelengths were discovered for thioflavin in the presence of A β assemblies including (A) 375 nm (B) 410 nm and (C) 430 nm. As depicted in subfigures (A) and (C), excitation at 375 nm or 430 nm failed to produce a robust differential in thioflavin fluorescence between the positive control and hit conditions. On the other hand, excitation at 410 nm revealed a robust 25% differential in fluorescence at 485 nm between these two samples. Taken as a whole, the data support the continued use of a 410 nm excitation source when translating the HATCO assay to the 96-well plate format.

In addition to confirming the excitation/emission parameters of the assay and validating its utility as an HTS assay, translation to the 96-well plate format allowed for longitudinal assessment of thioflavin fluorescence in the presence of 5XFAD lysate. This ability proved critical to the development of the assay, as the length of incubation dramatically influenced thioflavin's fluorescence and the differential in signal between positive and hit compounds. As illustrated in Table 9.4, mean signal intensity increases with prolonged incubation time rising on average approximately 2000-3000 A.U. over the course of one week. The trends for standard deviation are not as predictable, with initial measurements of thioflavin fluorescence being widely variable, becoming more internally consistent after 3-7 days of incubation, and then again diverging as a function of time. Importantly, this set of experiments also incorporated the use of non-amyloid-containing brain lysate generated from wild type mice as a negative control condition. The rationale behind the addition of this sample was that it increased the stringency of our negative control to insure that the differential observed between the positive (HATCO) and hit conditions (HATCO + PMZ) truly reflected differences in amyloid-specific thioflavin signal and not non-specific interactions. Impressively, regardless of whether HATCO + PMZ or wild type lysate were utilized as the negative condition, Z-factors again classify this novel HTS technique as an "excellent" assay.

Table 9-3. Assay Utility as a Function of Excitation Parameters (96-well Plate Format)

Assay Utility as a Function of Excitation Parameters (96-well Plate Format)						
Excitation Wavelength (nm)	Emission Wavelength (nm)	Mean Fluorescence HATCO (RFU)	Standard Deviation HATCO (RFU)	Mean Fluorescence HATCO + PMZ (RFU)	Standard Deviation HATCO + PMZ (RFU)	Z-prime
375	485	28838.33	797.8981	33568.67	1141.982	-0.23028
410	485	20231.33	175.499	17058	201.666	0.643436
430	485	13710.5	192.3235	11260.5	352.0668	0.3334

Table 9-4. Fluorescence Readout as a Function of Incubation Time

Fluorescence Readout as a Function of Incubation Time						
Time	HATCO Mean Fluorescence (RFU)	Control Mean Fluorescence (RFU)	Promethazine Mean Fluorescence (RFU)	Z-Prime	P-Value HATCO vs. Control	P-Value HATCO vs. PMZ
T= 0	15942 +/- 556.76	13558 +/- 1126.54	13402 +/- 625.68	-1.12E+00	4.67E-03	2.73E-07
24 hours	15435 +/- 308.41	13300 +/- 301.46	13778 +/- 253.98	1.43E-01	2.02E-05	5.68E-08
72 hours	18430 +/- 162.99	15306 +/- 352.40	16605 +/- 206.10	5.05E-01	1.74E-07	1.08E-07
Day 5	19765 +/- 240.08	16056 +/- 333.09	17753 +/- 186.97	5.36E-01	6.10E-08	3.35E-07
Day 7	19752 +/- 205.55	16026 +/- 345.22	17593 +/- 146.01	5.57E-01	4.67E-08	3.23E-08
Day 10	17778 +/- 419.18	14380 +/- 601.09	15674 +/- 504.13	9.92E-02	4.97E-05	1.19E-03

9.4.1 Results: Translation of the HATCO assay to a 384-well Plate Platform

Having firmly established the excitation/emission parameters of the HATCO assay using both fluorimeter- and plate reader-based methodologies in addition to validating its utility as a HTS assay using the Z-factor statistic, we next sought to translate the technology to a 384-well plate platform. Critically, the translation of the assay to this platform was necessary for three reasons. Most practically, under the original parameters, the total volume of all constituents of the HATCO assay was 300 μL ; double the practical well volume of most 384-well plates. On a related note, the second major limitation of the original assay parameters is that they become cost-prohibitive when attempting to screen large compound libraries. This is mainly because 200 μL of 5XFAD lysate is required per compound screened. Extrapolating these figures, a single 96-well plate requires the sacrifice of 3 transgenic mice; an unreasonable requirement given the high input cost associated with raising 5XFAD mice to 18 months of age. Put another way, under the original HATCO parameters used for both the fluorimeter-based validation and 96-well plate optimization phases of the study, an average of \$60 worth of 5XFAD lysate is needed per compound screened. Placed in the context of compound libraries in excess of 40,000 distinct molecules, it is clear that despite its favorable statistical evaluation the HATCO assay would not be an economically feasible means of identifying $\text{A}\beta$ -binding molecules. The third limitation associated with the fluorimeter- and 96-well plate-based assay conditions is that automated liquid handling systems were not available for automation of every step of the procedure, meaning manual pipetting would be required. In our experience up to this point, we had noted that the average percent error attributable to manual pipetting was approximately 2-3 fold higher than that of the most accurate liquid handling systems available, which carry a coefficient of variation of approximately 2%. Since the Z-prime statistic is acutely sensitive to the magnitude of the positive and negative controls' standard deviation, the automatization of the plating process proved a lucrative means of improving the assays accuracy. Thus, recognizing that any of these limitations would make HTS for $\text{A}\beta$ -binding molecules using the HATCO assay impractical at best, each of these points was methodically addressed in the translation of the assay to the 384-well plate platform.

Out of necessity, the volume restrictions imposed by the 384-well plate were addressed first. Fortuitously, despite necessitating a redesign of the HATCO assay's parameters, the volume restrictions imposed by the 384-well plate platform also partially alleviated concerns associated with 5XFAD lysate consumption. Seizing this opportunity to reduce the cost of the assay, the volume of each constituent was dramatically reduced beyond what was required to facilitate

compatibility with the 384-well plate platform. After exhaustive study, the finalized assay parameters for the positive control condition included 20 μL of 5XFAD lysate, 5 μL of 40 μM thioflavin, and 125 nanoliters of DMSO. Several notable deviations from the original HATCO parameters can be recognized in this description and each deserves further elaboration. Perhaps most obviously, the proportion of amyloid-containing lysate was increased relative to the other assay constituents. This change reflects a desire to insure an abundance of $\text{A}\beta$ -containing lysate in each sample such that thioflavin's fluorescent signal is not dominated by non-specific binding interactions. In addition to this deviation, the astute reader might also note the change from PBS to DMSO as the solvent of choice for library compounds. Several advantages come with this alteration. To begin, all compounds contained within most HTS libraries are dissolved in DMSO due to its: negligible spectral properties, compatibility with biological assays at low concentrations, and reputation as a robust universal solvent. Importantly the ability of DMSO to solvate a great variety of structurally diverse compounds at high concentrations is of supreme importance to the HATCO assay, as μM concentrations of each inhibitor can be achieved via the addition of negligible volumes. Despite these advantages, the use of DMSO to add inhibitor compounds to the assay did represent a significant alteration to the original protocol and was therefore studied in more detail. The major concern surrounding the use of DMSO in the assay is its ability to perturb inter-molecular binding as a consequence of being an amphiphile. To address this concern, the proportion of DMSO was incrementally increased in the positive control condition from 2.5% to 50% of the assays total volume. For example, in the 2.5% total volume condition, 625 nanoliters of DMSO was added to 20 μL of 5XFAD lysate and 5 μL of thioflavin. Similarly for the 50% total volume DMSO condition, 12.5 μL of DMSO was added to the same volumes of $\text{A}\beta$ -containing lysate and thioflavin. As graphically illustrated in Figure 9-8, the addition of DMSO attenuates thioflavin fluorescence at 485 nm in a dose dependent manner. The interpretation of this finding is that the amphiphilic properties of DMSO do indeed perturb amyloid-thioflavin complexes above a threshold concentration. Supporting this conclusion in a more quantitative manner, addition of 625 nL of DMSO (2.5% total volume condition) resulted in less than a 2% reduction in thioflavin fluorescence at 485 nm. By comparison, the corresponding values for the 5%, 10%, 25%, and 50% total volume DMSO conditions were 6.4%, 15%, 31%, and 38%, respectively.

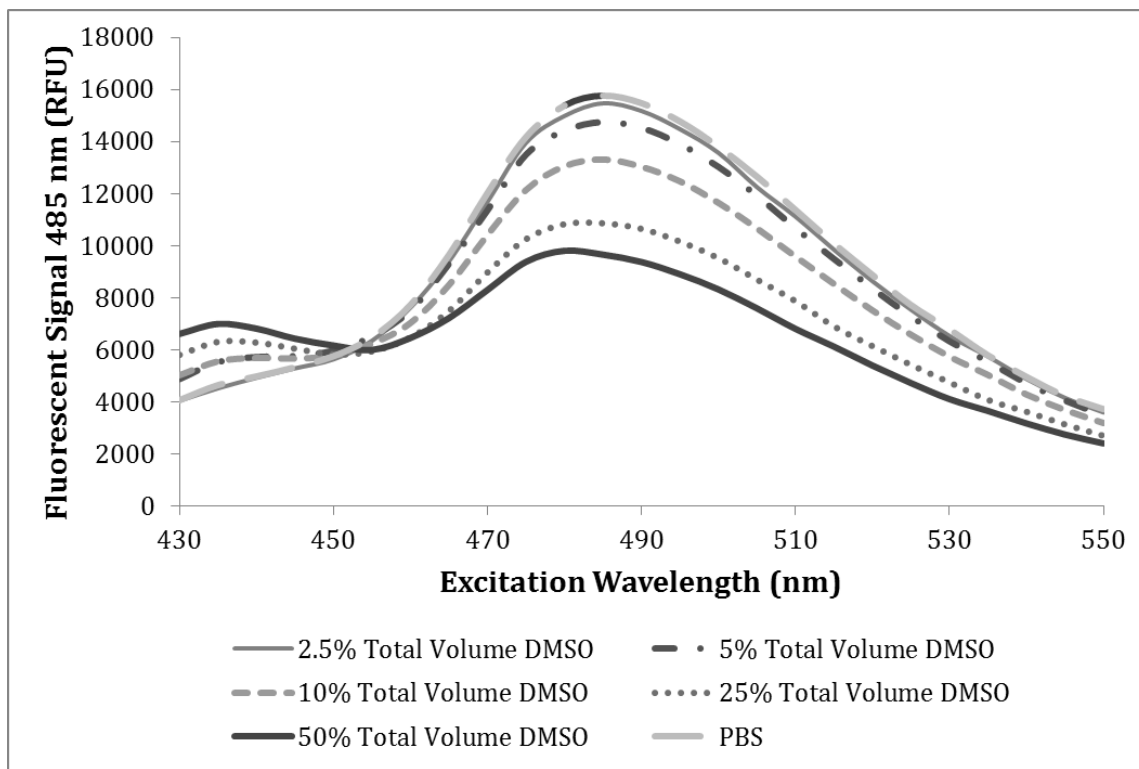


Figure 9-8. $\text{A}\beta$ -specific Thioflavin Fluorescence at 485 nm is attenuated by DMSO in a Dose-dependent Manner.

To test the HATCO assay's tolerance to increasing proportions of DMSO, increasingly large volumes of DMSO were added to 20 μL of 5XFAD lysate and 5 μL of thioflavin. DMSO concentration is presented as the percent of the assays total volume (25 μL). These percentages correspond to the addition of 625 nL, 1.25 μL , 2.5 μL , 6.25 μL , and 12.5 μL of DMSO for the 2.5%, 5%, 10%, 25%, and 50% total volume data points, respectively. For each of these conditions, a fluorescence profile secondary to excitation at 410 nm was collected on the sample across an emission range of 430-550 nm. Results demonstrate a negligible loss of $\text{A}\beta$ -specific thioflavin signal at 485 nm up to 5% total volume of DMSO, with a dose-dependent decrease in signal at increasingly higher concentrations. Cumulatively, the results suggest the HATCO assay is compatible with the use of DMSO as a solvent up to a threshold tolerance of 5% the assay's total volume.

The relevance of this data to the translation of the HATCO assay to the 384-well platform is that it highlights the need to minimize the addition of DMSO to maintain strong signal to noise. Put another way, as the concentration of DMSO increase, the Z-factor of the assay decreases. Under the modified HATCO parameters described for the 384-well platform, this threshold appears to be reached when the volume of DMSO added exceeds 5% of the assay's total volume. It is worth noting that this severe DMSO volume restriction represented a major hurdle to the development of the assay, as the original assay parameters call for candidate inhibitor concentrations of 200 μM . To maintain these inhibitor concentrations while being respectfully cautious of the HATCO assay's newly defined DMSO tolerance; delivery of less than 625 nanoL of solvated compound was required. Fortuitously, DMSO is a potent solvent, allowing Vanderbilt's entire molecular library to be stored at 10 milliM concentrations. This means that only 125 nL of library compound-containing DMSO needs to be added to the assay to achieve screening concentrations (50 μM) of each candidate inhibitor. Of course, the downside to this design is that the consistent delivery of such miniscule volumes is its own unique challenge; one requiring the integration of highly refined liquid handling systems to overcome.

Before the HATCO assay warranted automation however, the high cost associated with the use of 5XFAD lysate needed to be addressed. Notably several experimental avenues were available. One option was to simply enrich the 5XFAD lysate with synthetic A β peptide so that smaller volumes could be utilized. Of course, this approach would have violated our aim identifying compounds which bind to A β -assemblies with correct tertiary structure. Unwilling to sacrifice this critical advantage of our assay, the effect of serially diluting the 5XFAD and wild type lysates was explored. As depicted graphically in Figure 9-9 and numerically in Table 9-6, predictably, dilution of either 5XFAD or wild type derived lysate reduced thioflavin fluorescence at 485 nm in proportion to the dilution factor. Less predictably however, the differential in thioflavin fluorescence between 5XFAD and wild type lysates did not vary with dilution factor. Instead, the ratio of thioflavin fluorescence evoked via 5XFAD and wild type lysates remained constant at around the range of 1.91 to 2.1. Referring back to our Z-factor statistic, this finding indicates that the lower half of the equation, the difference between the positive and negative controls, is not affected by dilution of the lysate constituent of the assay. As the only other determinant of the assay's Z-factor is the sum of the positive and negative controls' standard deviations, if this variable was also comparable between dilutions then the utility of the assay should theoretically be unaffected by dilution of the lysate constituent. And indeed, analysis of Table 9-6 reveals that standard deviation remains comparable across

dilutions factors, reaching a minimum at the 1:10 dilution factor (7 mg/mL). As a consequence of these findings, in particular the trend in standard deviation, a 1:10 dilution of the 5XFAD lysate was employed in the finalized assay parameters. In combination with the ten-fold reduction in volume, the ability to dilute the 5XFAD lysate results in a 100-fold decrease in cost. From an ethical perspective, the optimized assay conditions also substantially reduce the number of 5XFAD sacrificed in order to screen a large molecular library. In fact, under the optimized assay parameters, the sacrifice of a single 5XFAD mouse can facilitate the screening of over 2,000 compounds.

Table 9-5. HATCO Assay Fluorescent Signal as a Function of 5XFAD Lysate Concentration

Sample	Mean	Standard Deviation	Coefficient of Variation
70 mg/mL Wild Type	5276	169.8852554	0.032199631
35 mg/mL Wild Type	4065	101.5036945	0.024970159
17.5 mg/mL Wild Type	2472.666667	18.87679351	0.007634184
7 mg/mL Wild Type	1258.666667	87.55188938	0.069559234
3.5 mg/mL Wild Type	819	35.51056181	0.043358439
70 mg/mL 5XFAD	10158	598.1880975	0.058888373
35 mg/mL 5XFAD	7129.666667	383.6825945	0.053814941
17.5 mg/mL 5XFAD	5197.333333	592.1928177	0.113941666
7 mg/mL 5XFAD	2390	210.2641196	0.087976619
3.5 mg/mL 5XFAD	1567.333333	118.988795	0.075917989

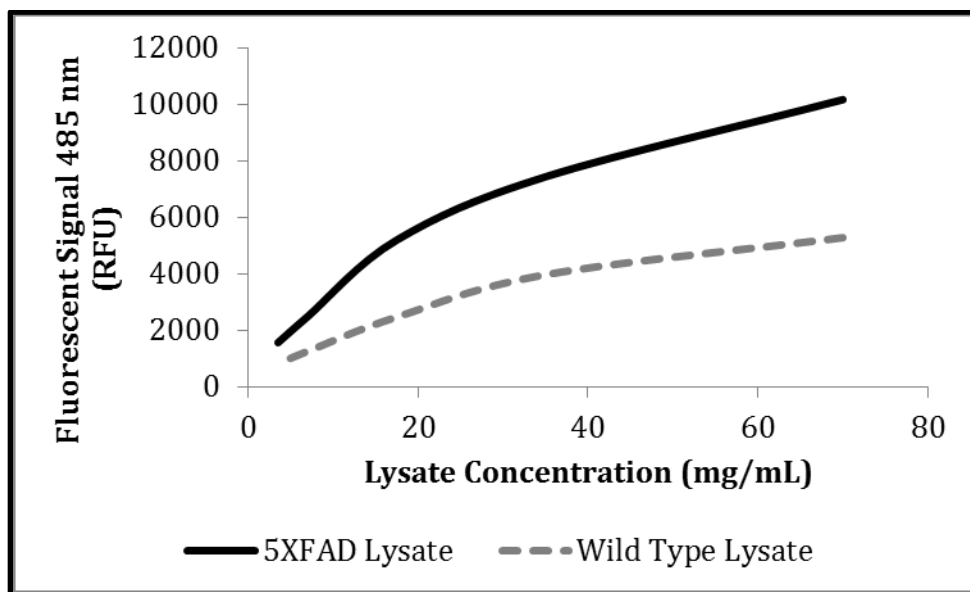


Figure 9-9. Thioflavin Fluorescence is Attenuated in Proportion to the Dilution Factor Applied to the Lysate Constituent of the HATCO Assay.

Under the 384-well plate assay conditions the concentration of 5XFAD and wild type lysates were varied across a protein concentration range of 3.5-70 mg/mL. Results demonstrate that thioflavin signal at 485 nm decreases proportionally with dilution factor. However, both standard deviation and the signal differential between positive and negative controls improved or remained constant with decreasing lysate concentration. Interpreted as a whole, these data suggests that a 1:10 dilution factor can be applied to the lysate component of the HATCO assay to reduce the total cost of the assay without negatively impacting its optimization.

Having alleviated the barriers imposed by volume restrictions of the 384-well plate and high cost of 5XFAD lysate, the penultimate step in validating the HATCO assay involved the automatization of the plate loading procedure. Generally speaking, the aim of this set of experiments was to improve the reproducibility of the assay and thus eliminate false positives/negatives secondary to inappropriate plate loading. After extensive testing, three independent and specialized liquid handling systems were necessary to achieve this aim. The first of these technologies, the BRAVO liquid handling system, is notable for its ability to add multiple reagents in a step-wise fashion. Significantly, this system is unrivaled with respect to the accuracy of its volume dispensing, with a coefficient of variation below 2%. Since pipetting-error is a large contributor to the magnitude of standard deviation and reductions in standard deviation greatly improve the utility of the assay, it was decided that all reagent additions would be accomplished using this system. Inconveniently however, the precision of the BRAVO system comes with a cost as it requires assay constituents to be distributed in a 384-well plate before being re-dispensed. Therefore, as described in more detail in the methods section of this work, source plates for the thioflavin and lysate constituents of the HATCO assay were generated using the second liquid handling system referenced above, a Multidrop Combi Reagent Dispenser. This liquid handling system was selected due its ability to load a 384-well plate with a reagent of choice in a matter of seconds. Naturally, the tradeoff associated with this technology is its relatively poor pipetting accuracy, with a coefficient of variation of approximately 10%. To negate this shortcoming of the Multidrop Combi Reagent Dispenser, this equipment was utilized uniquely for the loading of reagent stock plates from which the BRAVO liquid handling system aspirated reagents. Notably, this approach is only applicable for the lysate and thioflavin components of the assay, as these reagents are added in manageable volumes (microliters). In contrast, the library compounds to be screened must be added to each well in nanoliter volumes. To accomplish this feat with supreme accuracy, the Echo liquid handling system was employed. Unlike the other two liquid handling systems described which employ more traditional transfer methods; this technology utilizes acoustic energy to transfer reagents between 384-well plates. While this approach is ill-suited for the transfer of μL volumes of reagent, it is highly accurate when dispensing volumes in the nanoliter range and is more cost-effective than other methods in that it does not require the use of pipette tips. Most importantly, this liquid handling system is integrated into the Vanderbilt HTS core's compound library storage system, facilitating rapid dispensing of complete compound libraries in a manner of minutes.

Obviously, prior to utilizing this series of automated systems to conduct a large-scale HTS, the assay's reproducibility again required assessment. In a manner similar to previous experiments, a full-checkerboard pattern was generated using only the automated liquid handling systems and scanned for fluorescence at 485 nm. Disappointingly, statistical analysis revealed a Z-score well below 0, indicating that some error during plate loading had occurred. Undeterred, increased scrutiny was applied to the assay's characterization in the hope of identifying confounds that may have been introduced secondary to automation. Importantly, having read the literature, we were aware that extreme outliers in either the positive or negative controls could adversely affect the Z-factor, potentially leading to an apparently unfavorable Z-factor even when the assay would perform well in actual screening.⁽¹⁰²¹⁾ And indeed, as demonstrated by the scatterplot and histograms contained in Figure 9-10, major errors in the assay's plating were noted upon subsequent evaluation. Curiously, over 8% of the wells plated appeared to have significantly reduced fluorescence ($P < .001$) as compared to either positive or negative control conditions. No bias for positive or negative control wells could be noted. Moreover, the distribution of these outliers with respect to their location on the plate also demonstrated no appreciable pattern. Fortuitously, during the course of the work, investigators noticed the presence of droplets on some of the pipette tips utilized by the BRAVO liquid handling system. Confident volume carryover could explain this random distribution of outliers, analysis of the source plates was performed. In congruence with our hypothesis, the wells of the source plate corresponding to the outliers on the checkerboard plate demonstrated differences in residual volume attributable to reagent carryover. To correct this issue, a tip-touch procedure, in which the end of each pipette is touched to the rim of its corresponding well, was employed. Further precautions included the modulation of pipetting speed to insure no bubbles were generated during the mixing or dispensing procedures; as these artifacts might interfere with accurate aspiration. With these changes integrated into the automated plate-loading protocol, the HATCO assay was again characterized using the Z-factor statistic. In this set of experiments, the benefits associated with the removal of human pipetting were realized, as analysis revealed the highest Z-score obtained until that point, .62 (Table 9-7). Predictably, the majority of this improvement could be attributed a reduction in the standard deviation for both positive and negative controls. To summarize this effect, prior to automation, the coefficient of variation for the positive control condition was consistently in the range of 7-10%. Once the liquid handling systems described had been employed, this statistic dropped to a 4% CV; a doubling of plate-loading accuracy. Thus, confident that no further improvements could be made, we proceeded to screen three complete molecular libraries using the optimized HATCO assay.

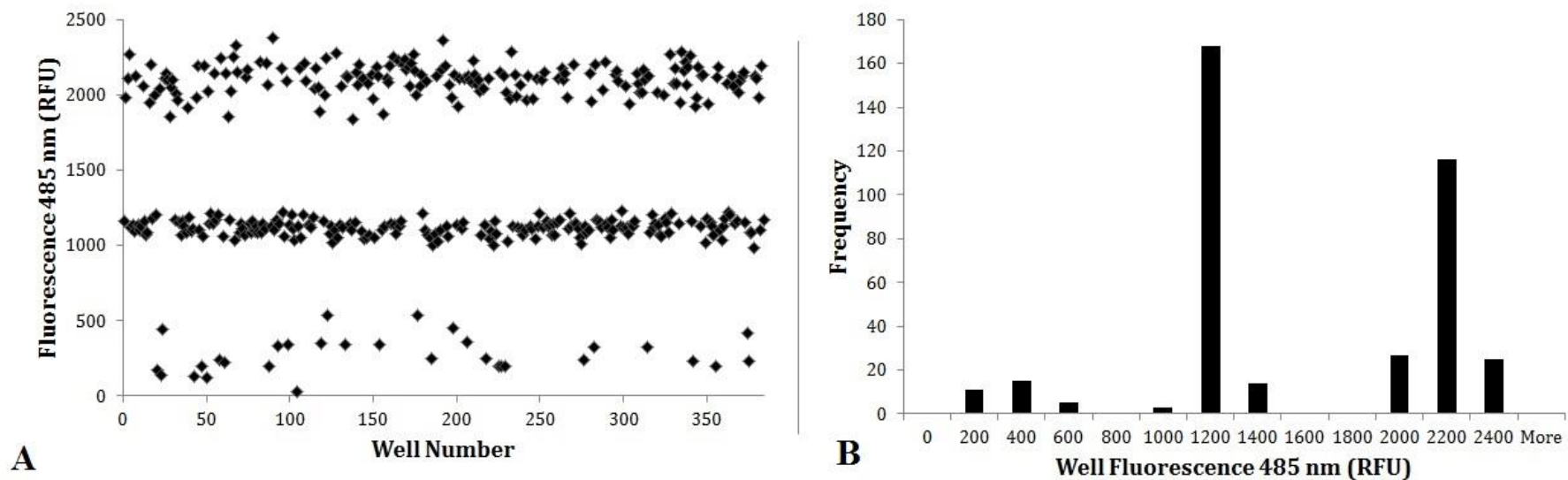


Figure 9-10. Preliminary Automation of the HATCO Assay's Plate Loading Protocol Results in the Generation of Outliers.

(A) Scatterplot of thioflavin fluorescence (485 nm) measured from a 384-well plate loaded with positive and negative control conditions in a checkerboard pattern. (B) Histogram of the same data emphasizing the magnitude of liquid handling error following automation. Results demonstrate three distinct populations: (1) positive controls with a mean fluorescence of 2100 A.U., (2) negative controls with a mean fluorescence of 1200 A.U., and (3) a subgroup of outliers evenly distributed amongst positive and negative control conditions with a fluorescence range of 100-600 A.U. Importantly, this last group represented over 8% of the total wells plated and was responsible for the assays poor performance after automation as assessed by the Z-factor statistic.

Table 9-6. Automated HATCO Assay Z-Prime Variables

	Positive Control (5XFAD Lysate)	Negative Control (Wild Type Lysate)	Percent Coefficient of Variation
Average	2098.73	1069.44	0.04
Standard Deviation	85.02	46.68	0.04

9.4.2 Results: Large-Scale HTS for A β -binding Compounds Using the HATCO Assay

Four large-scale compound libraries were selected with guidance from experts in the Vanderbilt HTS core. The largest of these libraries, the Spectrum Collection, is comprised of 2,000 structurally diverse molecules with a wide range of biological activity. Briefly, the Spectrum Collection contains approximately 50% drug components, 30% natural products, and 20% other bioactive molecules. As one of the principal aims of this work is to expand the chemical genetics of A β -binding compounds, the primary advantage of screening this particular compound library is that its innate chemical diversity can help identify unique A β -binding structural motifs. Furthermore, because over half of the constituent molecules of this library are drug components, there is an increased likelihood of these structural motifs exhibiting unique binding profiles to biological targets. On the other hand, the constituents of this compound library that are classified as natural products or bioactive molecules carry the unique advantage of possibly harboring non-A β -centric therapeutic potential. This possibility is important, as a molecule which harbors mediocre A β -binding potential may prove a more potent therapeutic agent secondary to anti-inflammatory or anti-apoptotic effects. Despite these advantages however, the end goal of our aim to expand the structural diversity of A β -binding molecules is to expedite the development of novel diagnostic and therapeutic agents for AD by repurposing existing compounds with A β -binding affinity. Naturally, compounds with a history of use in human clinical trials are ideal targets for this purpose. For this reason, the NIH Clinical Collections I and II were also screened using the HATCO assay. Importantly, while the cumulative compound library generated by these three collections is robust with respect to both chemical diversity and clinical applicability, the molecules contained are in no way screened for BBB permeability. For this reason, a fourth customized library containing only compounds (200) which exhibit the cardinal structural characteristics of a BBB penetrating molecule was added to the large-scale screen. Thus, in total, nearly 3,500 unique compounds were screened using the HATCO assay; each fulfilling our desired criteria of high translatability, distinct chemical structure, and suitability to cross the BBB to varying degrees.

Screening of all compound libraries was performed as described in the methods section entitled “384-well plate HATCO assay”. Briefly, 125 nL of DMSO was loaded into columns 1, 2, 23, and 24 while columns 3-22 were shot with an equivalent volume of 10mM library compounds. Plating in this manner, eleven 384-well plates were required to

complete the screen. To each of compound containing wells, A β -containing 5XFAD lysate was added in an automated fashion in accordance with the described protocol. Similarly, in the wells located at the outer two columns of each plate, a checkerboard pattern of 5XFAD lysate or wild type lysate was loaded. The specified volume of thioflavin was then simultaneously added to all wells again using the BRAVO liquid handling system. Critically, statistical analysis using the Z-factor revealed a remarkable consistency between plates (Table 9-8); a finding credible to the automation of the assay. More importantly, the Z-factor calculated for all plates was well above the .5 threshold, indicating that hit analysis on each plate could be performed without concern for false-positives secondary to inappropriate plate-loading. In support of this conclusion, both positive and negative controls across all plates demonstrated a coefficient of variation below 4.5%. Hit identification was performed using automated statistical analysis that required the tested library compound to attenuate thioflavin's fluorescent signal by a magnitude in excess of 3-standard deviations. Appropriately, this practice is in accordance with standards in the field of HTS. In addition to this analysis, a preliminary characterization of each compound's relative binding-affinity was generated. This variable was termed "percent inhibition", and was calculated according to the equation:

$$\text{Percent Inhibition} = 100 \times \left(1 - \frac{(\sigma_C - \sigma_N)}{(\sigma_P - \sigma_N)}\right)$$

Where σ_P and σ_N denote the mean fluorescence of measured from positive and negative control wells on the plate, respectively, and σ_C represents the mean signal measured for the compound-containing well. Operating under the hypothesis that A β -binding molecules can reduce thioflavin signal at 485 nm by competitively-binding with amyloid plaques, compounds with a higher percent inhibition are predicted to have a higher binding-affinity for A β assemblies; an assumption confirmed in subsequent experiments.

In a manner which highlights the specificity of our approach, HATCO-mediated screening of nearly 3,500 compounds produced only 42 hits. A complete list of all hit compounds, including the fluorescence measured from the wells that contained them, is provided in Table 9-8.

Table 9-7. Loading Homogeneity Achieved Via Automated HATCO Assay Pipetting Protocol

Loading Homogeneity Achieved Via Automated HATCO Assay Pipetting Protocol											
Plate 1	Plate 2	Plate 3	Plate 4	Plate 5	Plate 6	Plate 7	Plate 8	Plate 9	Plate 10	Plate 11	Plate 12
0.725	.604	.591	.638	.626	.568	.609	.592	.597	.646	.615	.621

In addition, relevant statistics such as the calculated percent inhibition are included for review. Importantly, percent inhibition was appropriately calculated on a plate by plate basis. This is because the mean values for positive and negative controls vary slightly between plates. The relevance of this point to the reader is that a comparison of the raw fluorescence values measured for each individual compound cannot be used to gauge relative binding-affinity. An example of how such analysis could lead to false conclusions is provided by comparison of compounds VU0243418-3 and VU0244402-4. Based only on the raw fluorescence data, it appears as though compound VU0244402-4 binds A β -aggregates with greater affinity than its counterpart VU0243418-3, as thioflavin's signal is weaker in this sample. However, because the mean fluorescence measured from positive control samples located on the plate containing VU0243418-3 was higher (WPH058695), in truth this compound attenuated thioflavin signal to a greater degree than did VU0244402-4. This statistical detail aside, the robust attenuation of A β -specific thioflavin fluorescence at 485 nm by compounds such as VU0656139-1, strongly implies that these compounds are capable of binding to amyloid-assemblies. To confirm these results, a confirmation screen was performed.

In this work, the 42 hit compounds identified in the primary screen were again probed for the ability to bind to A β -assemblies using the HATCO assay. However, in contrast to previous experiments in which only a single well was allocated for each library molecule, each of the hit compounds were plated in duplicate in this study. Of note, this practice is again in congruence with established protocols in the field, as it brings the total number of measurements for each compound into the triplicate range. In a manner which highlights the reliability of the HATCO assay as a primary screening technique, 35 of the 42 originally identified hit compounds again met statistical criteria for classification as an A β -binding molecule. Moreover, the 7 compounds which failed to reach statistical significance when measured in triplicate were those with the lowest percent inhibition. Importantly, while percent inhibition calculated for each hit compound during the primary screen generally corresponded with that measured in the confirmatory screen, as a whole, the magnitude of this statistic decreased. This is most likely attributable to the confirmatory screen being run with a distinct batch of 5XFAD lysate, with slightly varying proportions of A β assemblies. Interested in only the most potent A β -binding molecules, an arbitrary threshold of 50% inhibition was established, with the consequence being that only 15 of the remaining 35 compounds warranted further evaluation. Most urgently, these 15 compounds required cross-screening to confirm their A β -binding potential.

Table 9-8. Full Library Screen Hit List With Percent Inhibition

Plate	Well	VU Number	Fluorescence 485 nm	Percent Inhibition
WPH058692	C16	VU0656139-1	608	97.7863749
WPH058693	B09	VU0243635-2	728	88.8849105
WPH058693	A18	VU0243640-9	840	79.7186701
WPH058695	P11	VU0243421-5	892	76.9811507
WPH058695	K22	VU0243418-3	906	75.8758512
WPH058694	I21	VU0244402-4	894	74.834963
WPH058697	B21	VU0656634-1	930	71.8207283
WPH058693	H20	VU0244454-2	948	70.8797954
WPH058693	P18	VU0244310-2	950	70.7161125
WPH058697	K06	VU0656668-1	954	69.8650369
WPH058693	G18	VU0656769-1	977	68.5063939
WPH058695	I20	VU0518361-2	1001	68.3756045
WPH058693	G03	VU0005325-3	1059	61.7953964
WPH058697	E20	VU0656659-1	1096	58.293863
WPH058692	K22	VU0656169-1	1094	57.9411237
WPH058692	J22	VU0243610-4	1108	56.7933181
WPH058698	C04	VU0424095-2	1142	54.5889053
WPH058696	C19	VU0656568-1	1149	53.9910859
WPH058697	D11	VU0243664-4	1156	53.4046346
WPH058697	O05	VU0243646-4	1157	53.3231474
WPH058695	G15	VU0656445-1	1193	53.2172111
WPH058693	F21	VU0656808-1	1167	52.9565217
WPH058696	C03	VU0254088-3	1164	52.7755267
WPH058699	P16	VU0254343-2	1155	52.4809261
WPH058693	E18	VU0243638-4	1173	52.4654731
WPH058692	G18	VU0656154-1	1166	52.0381235
WPH058701	J06	VU0465285-1	1116	51.840117
WPH058699	L03	VU0254295-4	1188	49.7027098
WPH058700	I21	VU0243360-3	1172	48.5124054
WPH058696	P10	VU0239662-6	1220	48.2374392
WPH058696	A19	VU0254117-5	1228	47.589141
WPH058695	K06	VU0656374-1	1281	46.2696141
WPH058693	E03	VU0243022-2	1301	41.9897698
WPH058700	A19	VU0239546-6	1299	37.8311606
WPH058699	M05	VU0239603-6	1334	37.4112076
WPH058694	F19	VU0656003-1	1373	36.79456
WPH058700	O11	VU0424047-1	1345	33.9623633
WPH058700	A17	VU0424052-1	1358	32.8690076
WPH058700	C13	VU0253939-2	1358	32.8690076
WPH058691	A20	VU0239562-8	1576	32.4070047
WPH058691	A05	VU0243165-3	1737	20.6134829
WPH058691	K17	VU0244461-2	1738	20.5402312

9.4.3 Results: Cross-screening of 15 Hit Compounds

Representing a limitation shared by all colorimetric based technologies including the HATCO assay, compounds with considerable spectroscopic properties can generate false positive readouts. In the specific case of the HATCO assay, two distinct absorbance profiles may theoretically confound our results. These include chromophores which absorb light near or at (i) 410 nm and (ii) 485 nm. Generally speaking, both of these absorbance profiles generate false positives by interfering with thioflavin fluorescence at 485 nm, the primary readout of A β -binding affinity employed by the HATCO assay. Considering first molecules that absorb at 410 nm, these compounds might significantly attenuate thioflavin fluorescence not via competitive-binding for A β -assemblies, but instead by quenching the excitation source. Similarly, chromophores absorbing at the measured emission wavelength of 485 nm pose an equally relevant problem, as these compounds may be attenuating thioflavin fluorescence in a process most analogous to the concept of Forster resonance energy transfer (FRET). In clarification of this mechanism, photons emitted at 485 nm secondary to thioflavin-amyloid complex formation would be immediately quenched by the false-positive library compound. Thus, instead of attenuating thioflavin fluorescence secondary to competitive inhibition, molecules absorbing at/near 485 nm would instead employ thioflavin as a donor chromophore. To exclude either of these possibilities, a two-phase cross-screening protocol was developed for subsequent evaluation of putative hit compounds. The precise methodology of this approach is described in detail under the appropriately titled methods section.

As summarized in Table 9-10, over half of the putative A β -binding compounds which met our most stringent confirmatory criteria harbored spectroscopic properties which confounded the interpretation of their effect on 5XFAD lysate induced thioflavin fluorescence.

Table 9-9. False-positive Library Identified Via 2-Phase Cross-screening of HATCO assay-identified Hits

False-positive Library Identified Via 2-Phase Cross-screening of HATCO assay-identified Hits									
Sample	Positive Control	VU0656668	VU0656634	VU0243421	VU0243418	VU0656769	VU0244310	VU0656445	VU0518361
Mean (RFU)	149.80	85.67	47.00	109.00	111.67	113.67	110.33	93.00	97.33
Standard Deviation (RFU)	10.52	2.08	1.00	8.89	5.51	6.51	0.58	4.36	0.58
%CV	7.02	2.43	2.13	8.15	4.93	5.72	0.52	4.69	0.59
P-value	NA	1.33E-13	5.92E-21	4.93E-08	1.72E-07	5.49E-07	7.19E-08	6.28E-12	5.59E-11
% Signal Decrease	NA	42.81	68.62	27.23	25.45	24.12	26.34	37.92	35.02

Fortuitously, statistical identification of false-positives is easily accomplished via comparison of the mean fluorescent signal of thioflavin at 485 nm in the presence, or in the absence of, each putative A β -binding compound. As can be appreciated from the data, chromophores which falsely generate the signature of an A β -binding molecule exhibit a robust effect on thioflavin fluorescence in the absence of lysate. For this particular set of chromophores, thioflavin fluorescence was reduced via non-competitive binding mechanisms by as little as 24.12% and by as much as 68.62%. Importantly, because the standard deviation within each sample is miniscule relative to the mean (%CV ranging from .52-8.15%), in this work, a simple two-tailed paired student t-test proved an adequate statistical measure. As stated, this quantitative approach to the cross-screening of hit compounds is highly sensitive. The best support for this statement is garnered by review of the relevant P-values, all of which are orders of magnitude below the threshold of .05. Therefore, while the false-hits identified in our screen are characterized by relatively robust spectroscopic confounds and are thus easily identifiable, given the high statistical power of this cross-screening approach it is projected that less optically active molecules would also be correctly rejected from further study. Furthermore, beyond simply identifying false positives, our cross-screening approach also provides a mechanistic rationale for their exclusion. As detailed in the appropriately labeled methods section, this is accomplished via characterization of the unique absorbance profile of each putative hit.

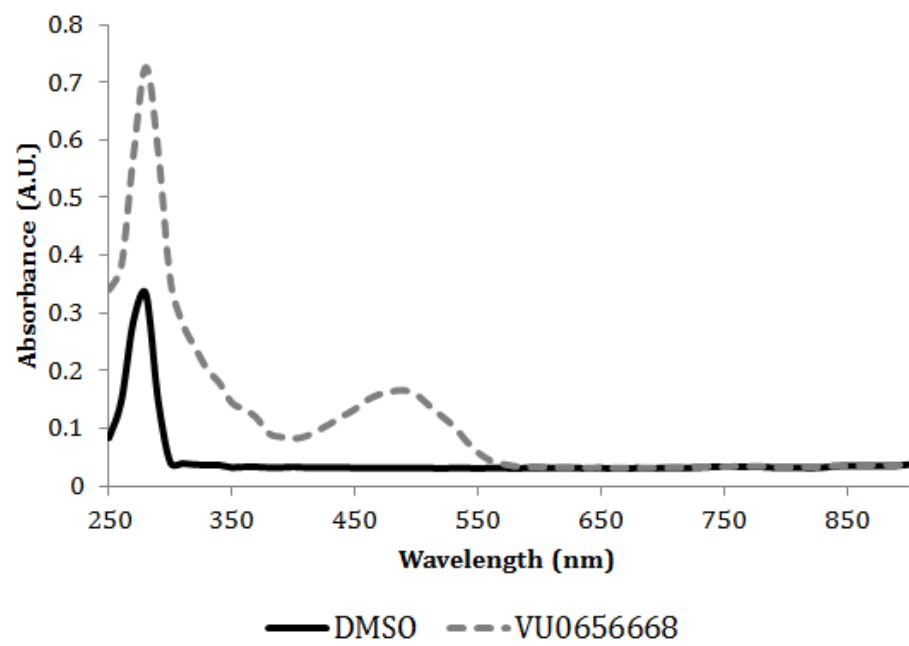
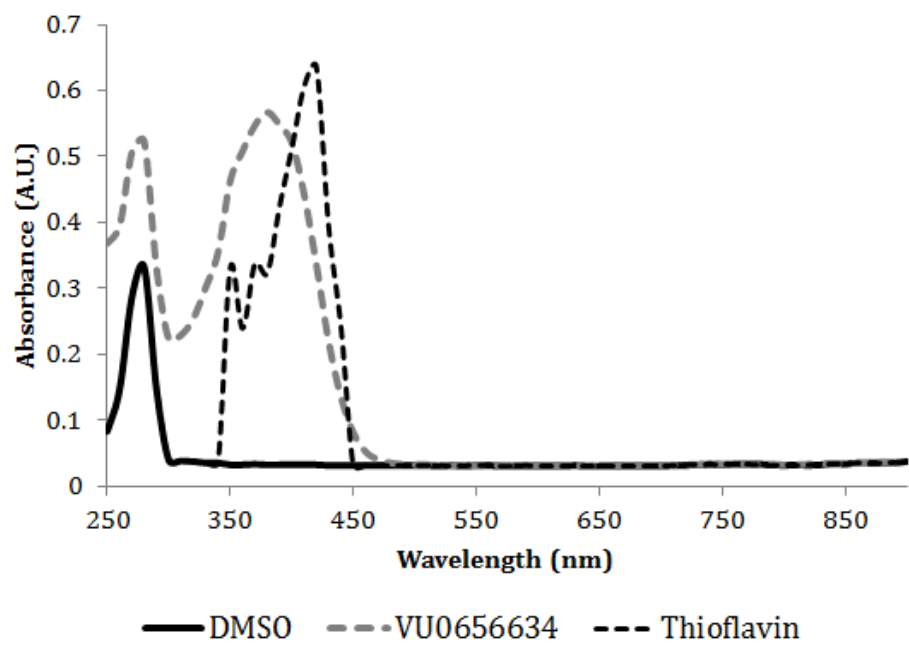
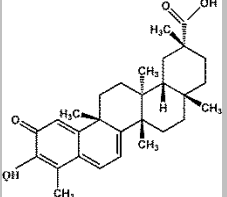
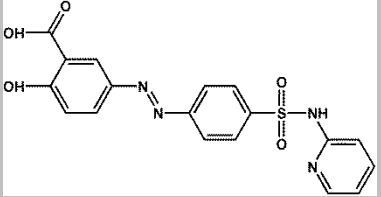
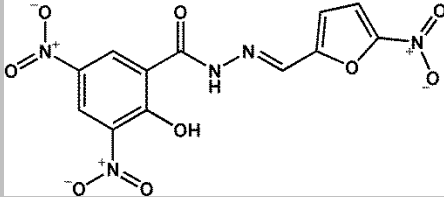
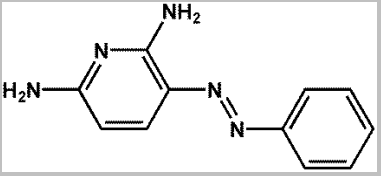
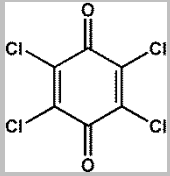
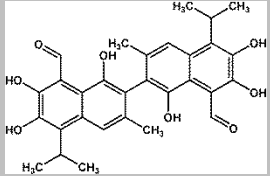
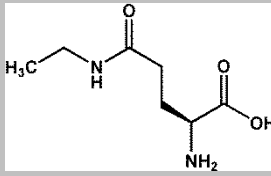


Figure 9-11. Two Distinct Absorbance Profiles Characterize False-positive Hit Compounds.

In congruence with our two-phase cross-screening paradigm, absorbance profiles for each of the 15 candidate A β -binding molecules identified via HATCO-mediated HTS were collected over the 250-900 nm range. For each trial DMSO was used as a control spectra. Notably, absorbance over the 250-350 nm range is confounded by the spectroscopic properties of the 384-well plate. As hypothesized, molecules with one of two distinct absorbance profiles were confirmed as confounding variables in the readout of the HATCO assay. These include chromophores with absorbance at: (i) 410 nm (left) or (ii) 485 nm (right).

Table 9-10. Confirmed & Cross-screened A β -binding Molecules Identified Via HATCO-mediated HTS

Confirmed & Cross-screened A β -binding Molecules Identified Via HATCO-mediated HTS				
Sample	Positive Control	VU0243664	VU0243360	VU0656139
Mean Fluorescence (RFU)	149.80	163.00	148.00	144.50
Standard Deviation (RFU)	10.52	7.55	2.65	6.36
Percent CV	0.07	0.05	0.02	0.04
P-value	NA	0.04	0.77	0.49
Percent Signal Decrease	NA	-8.82	1.20	3.54
Structure				

Confirmed & Cross-screened A β -binding Molecules Identified Via HATCO-mediated HTS (Continued)				
Sample	VU0244402	VU0243635	VU0243640	VU0656658
Mean Fluorescence (RFU)	138.50	148.67	151.00	144.00
Standard Deviation (RFU)	2.12	15.82	7.00	0.00
Percent CV	0.02	0.11	0.05	0.00
P-value	0.14	0.86	0.85	0.45
Percent Signal Decrease	7.54	0.75	-0.80	3.87
Structure				

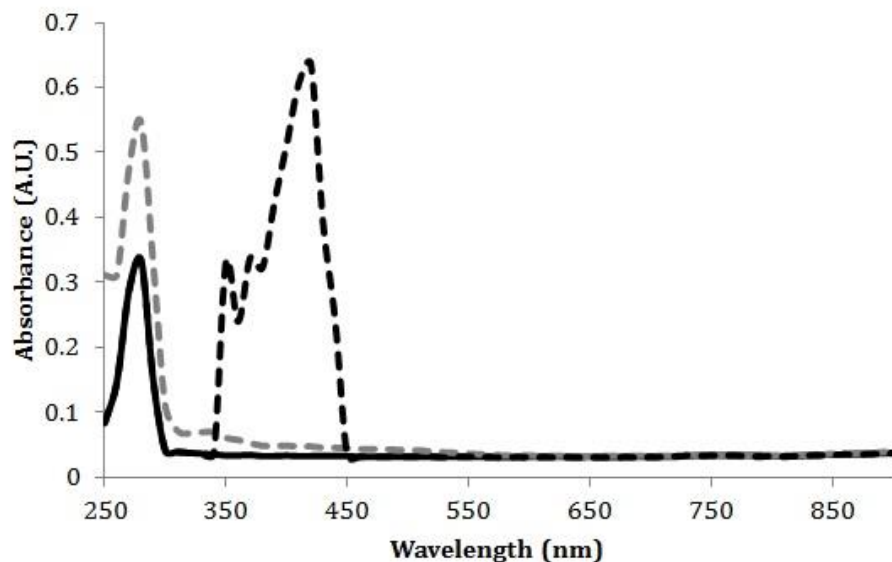
As discussed, two distinct absorbance profiles may theoretically confound the readout of the HATCO assay and thus generate false-positives. These include chromophores with absorbance at (i) 410 nm and (ii) 485 nm. Interestingly, review of the relevant spectroscopic data suggests that both types of chromophores might be contained in our library of false-positives. Taking the absorbance profile of compound VU0656634 for example, as graphically illustrated in Figure 9-11A, this molecule's ability to attenuate thioflavin fluorescence might best be explained by its ability to absorb at 410 nm. Under the proposed mechanism, a considerable portion of the incident light is absorbed by the chromophore, resulting in fewer photons of appropriate energy being available to excite the orbital electrons of thioflavin from their ground state. Despite the coincident trends in the data however, it is worth noting that this scenario was hypothesized to be unlikely prior to data analysis, as the excitation lamps of the plate reader were thought to emit enough incident photons to mask any quenching. Therefore, it is possible that compounds like VU0656634 may attenuate thioflavin fluorescence via mechanisms not yet elucidated. Still, of the 8 compounds classified as false-positives secondary to their ability to attenuate thioflavin fluorescence in the absence of 5XAFD lysate, 3 absorbed uniquely near 410 nm. Less surprisingly, other members of our false-positive library were potent absorbers at 485 nm, the emission wavelength employed by the HATCO assay to identify the dissociation of A β -thioflavin complexes. As expected, even molecules with modest absorption at 485 nm, such as VU0656668, are capable of generating false-positive readouts (Figure 9-11B). Taken as a whole, the data strongly supports the utility of our cross-screening approach for the identification of false-positive hits. Moreover, by employing a two-phase cross-screening paradigm, not only are non-A β -binding chromophores eliminated from future study, but a plausible mechanism underlying their ability to attenuate thioflavin fluorescence is also garnered. Lastly, because both components of this procedure are compatible with HTS methodologies, even if a large fraction of hit compounds identified via HTS with the HATCO assay ultimately end up being false-positives, minimal resources are required to refine the hit library to only those molecules with true A β -binding potential.

Building on this point, because false-positives are readily identifiable, the high incidence of these confounding chromophores in the HATCO assay's hit library actually improves the statistics which characterize its utility. Reviewing the data up to this point, primary screening of 3,500 compounds for A β -binding potential using the HATCO assay resulted in a hit list of 42 compounds. If these results were to be interpreted without further study, this would mean that just over 1% of the library compounds screened bind to A β -plaques. While this information is certainly useful, especially for

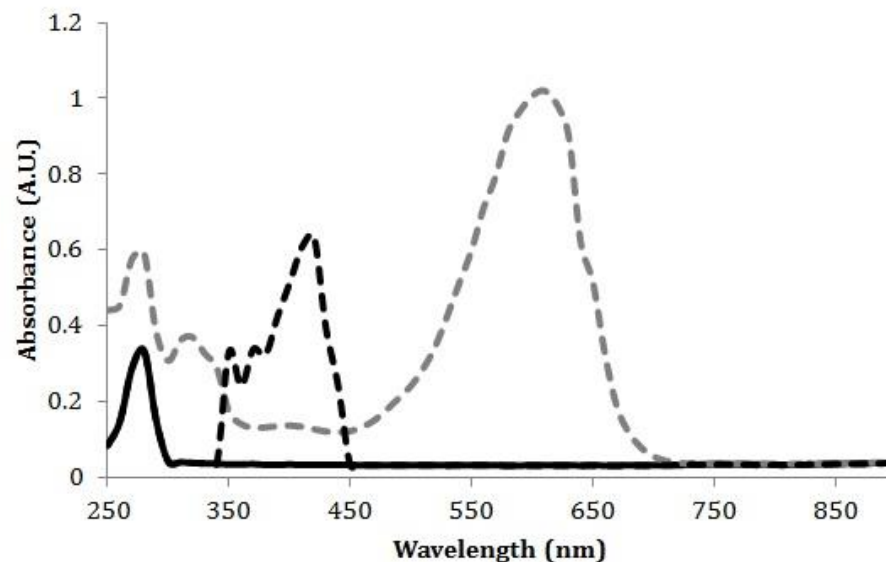
ligand-based rational drug design approaches, the time and expense associated with characterizing each of these molecules is too great to facilitate rapid progress in the field. Therefore, a more refined molecular library of A β -binding molecules is necessary. Confirmatory screening certainly progressed this work towards that aim, reducing the hit library from 42 compounds to 35, an approximate 17% decrease. Still, further refinement was deemed necessary and for this reason, only those compounds which inhibited thioflavin fluorescence by more than 50% were selected for further study. While this threshold is indeed arbitrary, it is grounded in the rationale that only the most potent A β -binding structures warrant further study. Significantly, by instituting this cut-off, the number of hit compounds remaining in the library was decreased from 35 to just 15; representing a nearly 60% refinement. Now just over a third of its original size this library of hit compounds can be further refined via cross-screening for false-positives. As listed in Table 9-11, cross-screening of the remaining 15 candidate hit compounds resulted in a final library of only 7 confirmed and cross-screened hits. Impressively, this places the HATCO assays' exclusion rate at 99.8%, a statistic that characterizes it firmly as an optimally useful screening technique.

Lending further credibility to our hypothesis that chromophores with considerable absorbance at 410 nm and 485 nm represent the major source of false-positives in the assay, none of the cross-screen validated hits exhibited robust absorption at these wavelengths. Instead, the majority of cross-screened hits, such as VU0243640 and VU0656658, exhibited little to no spectroscopic activity (Figure 9-12A). In a manner which emphasizes the precise spectroscopic properties needed to generate a false-positive result, other hit compounds, for example VU0243360, are characterized by robust absorbance profiles at wavelengths compatible with HATCO assay-mediated screening (Figure 9-12B). Notably, the inclusion of such chromophores in our cross-screened and validated hit library is of supreme significance to the utility of the HATCO assay, as it confirms that not all molecules with spectroscopic properties are excluded from study. Elaborating on the significance of this point further, as a consequence of its β -pleated-sheet tertiary structure, molecules which bind assemblies of A β are at an increased likelihood of exhibiting a planar structure. As a consequence of this molecular configuration, such molecules are routinely characterized by the presence of aromatic hydrocarbons. Because this structural motif exhibits a high ring density of π electrons capable of absorbing photons falling within the visible spectrum, molecules containing these structures are routinely fluorescent. Summarizing this point, if the HATCO assay was incompatible with all spectroscopically active molecules, a large fraction of highly relevant structural motifs would

have to be excluded from HATCO-mediated HTS studies. However as this is not the case, the data strongly suggest that the HATCO assay is an ideal HTS technology for the initial identification of A β -binding compounds.



A — DMSO — VU0656658 — Thioflavin



B — DMSO — VU0243421 — Thioflavin

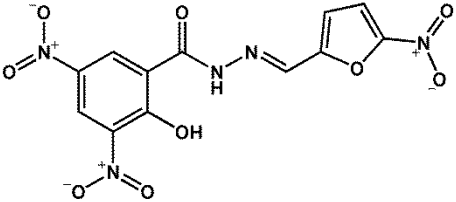
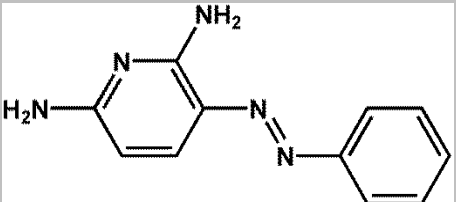
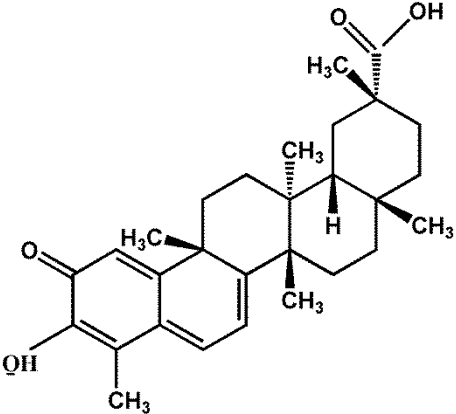
Figure 9-12. Cross-screening Excludes Chromophores with Confounding Spectroscopic Profiles.

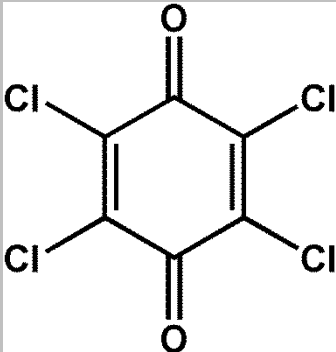
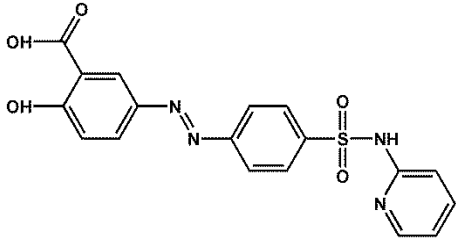
Absorbance profiles for each of the 15 candidate A β -binding molecules identified via HATCO-mediated HTS were collected over the 250-900 nm range. For each trial, DMSO was used as a control spectrum. Notably, absorbance over the 250-350 nm range is confounded by the spectroscopic properties of the 384-well plate, which absorbs robustly between these wavelengths. Following cross-screening, only 7 compounds with confirmed A β -binding potential remained in our hit library. Predictably, compounds with no spectroscopic activity were not eliminated by our absorbance-based operation (left). Significantly however, compounds with robust absorbance profiles also comprised our finalized hit library. In congruence with our hypothesis that false-positives can attenuate thioflavin fluorescence by absorbing at the 410 nm or 485 nm wavelengths, compounds absorbing outside this range were not eliminated by our cross-screening operation. Thus, with the unique exception of molecules that absorb at either of these two wavelengths, all chromophores appear compatible with HATCO assay-mediated assessment of A β -binding potential.

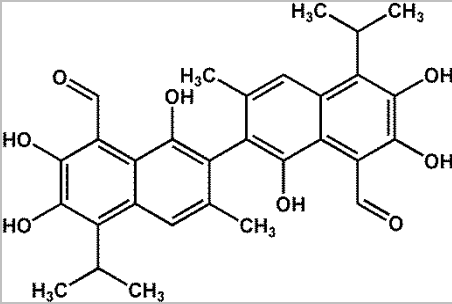
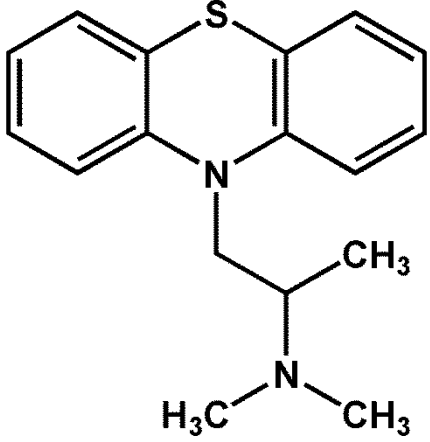
9.4.4 Results: Experimental Determination of A β -binding Affinity of Confirmed and Cross-screened Hits

Seeking to further characterize our hit compounds by quantitatively determining their A β -binding affinity, a protocol routinely used by the Vanderbilt HTS core facilitating the determination of each hit compound's IC₅₀ value was adapted for compatibility with the HATCO assay. While this operation is described in detail in the appropriately labeled methods section, briefly, each hit compound was shot onto a 384-well plate in the presence of 5XFAD lysate and thioflavin over a concentration range of 15 nL- 300 μ L. Following an incubation period designed to permit complete equilibration, fluorescence at 485 nm was measured using an automated plate reader. As expected, plotting of the resultant fluorescence data as a function of concentration in a logarithmic fashion revealed the characteristic sigmoidal curve. From this curve, IC₅₀ values for each compound were calculated using algorithms available in the GraphPad software package. These values are summarized in Table 9-11 and reveal that of all compounds screened using the HATCO assay to date, promethazine exhibits the highest binding affinity for A β assemblies. Importantly, this data provided a strong impetus to continue evaluating promethazine's ability to bind A β -plaques in the second phase of our HTS approach.

Table 9-11. IC50 Values of HATCO-Identified Hits

IC50 Values of HATCO-Identified Hits					
Compound ID	IC50 (μM)	Molecular Structure	Chemical Name	M.W. (g/mol)	CLogP
VU0656139	61.23		2-Hydroxy-3,5-dinitro-benzoic acid (5-nitro-furan-2-ylmethylene)-hydrazide	365.21	2.40
VU0244402	74.29		3-Phenylazo-pyridine-2,6-diamine	213.24	2.05
VU0243664	108.52		2,4a,6a,9,10,12b,14a-Heptamethyl-11-oxo-1,2,3,4,4a,5,6,6a,11,12b,13,14,14a,14b-tetradecahydropicene-2-carbaldehyde	481.69	6.82

VU0243635	90.85		2,3,5,6-Tetrachloro-[1,4]benzoquinone	245.88	3.3
VU0243360	68.07		2-Hydroxy-5-[4-(pyridine-2-ylsulfamoyl)-phenylazo]-benzoic acid	398.39	3.88

VU0243640	84.17		1,6,7,1',6',7'-Hexahydroxy-5,5'-diisopropyl-3,3'-dimethyl-[2,2']binaphthalenyl-8,8'-dicarbaldehyde	518.55	5.36
Promethazine e	53.63		Dimethyl-(1-methyl-2-phenothiazin-10-yl-ethyl)-amine	284.42	4.89

Results: MALDI IMS Ex-Vivo Imaging of Promethazine's Spatial Distribution in the 5XFAD Mouse Brain

Referencing back to the introductory sections of this aim, our research strategy employs a two phase approach to repurposing existing compounds with A β -binding affinity. As demonstrated by the abundance of data presented to this point, the first phase of our approach, HATCO-mediated HTS, provides an excellent methodology for characterizing the A β -binding affinity of molecules in a preliminary manner. However to fully investigate the diagnostic and therapeutic potential of hit compounds identified via the HATCO assay, we believe a more extensive characterization of each compound's BBB permeability and A β -specificity is warranted. Of note, while this protocol is designed to be generalizable to any hit compound detected via HATCO assay-mediated HTS, in this work, phase 2 characterization was restricted to PMZ. As described in the appropriate titled methods section, MALDI-IMS was leveraged for this purpose. Summarizing the general protocol, cohorts of 5XFAD and wild type mice are injected with the putative A β -binding compound via tail-vein injection at a standardized dose of 25 mg/kg. Four hours later, sufficient time for a molecule with no affinity for A β to completely wash out of the brain, each animal is sacrificed. Importantly, prior to tissue harvesting, cardiac perfusion with copious volumes of PBS is performed to avoid confounds associated with drug retention in the microvasculature. As visually depicted in Figure 9-13, following this procedure, the brain tissue is flash frozen, sectioned in the coronal plane, mounted onto gold-plates, coated with a 2,5-dihydroxybenzoic acid (DHB) matrix, and analyzed on the LTQ via pseudo-selected reaction monitoring. Naturally, before settling on this optimized protocol and analyzing the distribution of promethazine in the brains of treated mice, we optimized the MALDI IMS method for promethazine. To do this in a controlled fashion, promethazine was analyzed on a linear ion trap equipped with a MALDI source (Thermo LTQ XL) using DHB as the matrix. Under these experimental conditions, promethazine forms a protonated ion at m/z 285.1 which is subjected to collisionally activated dissociation. Fragmentation occurs at the nitrogen moieties, resulting in three main fragment ions including the phenothiazine ring, a substituted N-propyl phenothiazine, and N,N-dimethylisopropylamine at m/z 198, 240 and 86, respectively. In a manner which highlights the specificity of this analysis, these ions are unique to promethazine and are not observed in the DHB matrix (Figure 9-14A & 9-14B). Moreover, MALDI-IMS of non-treated brain tissues generated virtually no signal at the specified mass to charge ratios, confirming the specificity of our protocol for PMZ (Figure. 9-14C).

With this necessary control confirming our ability to sensitively distinguish PMZ from other ion sources, we next determined whether PMZ accumulates sufficiently in the brain to permit detection. In this set of experiments, 8-month-old 5XFAD (n = 5) and age-matched wild type mice (n = 3) were leveraged to assess the topographical distribution of PMZ in the brain after tail-vein injection of PMZ. To minimize stress to the dosed cohorts of animals, 4 injections resulting in a cumulative dose of 25 mg/kg were administered over an 8 hour period. In addition to improved survivability of the animal, this approach carries the notable advantage of negating the need for pharmacokinetic profiling of each hit compound in the brain. All other experimental details were followed in accordance with the appropriately titled methods section.

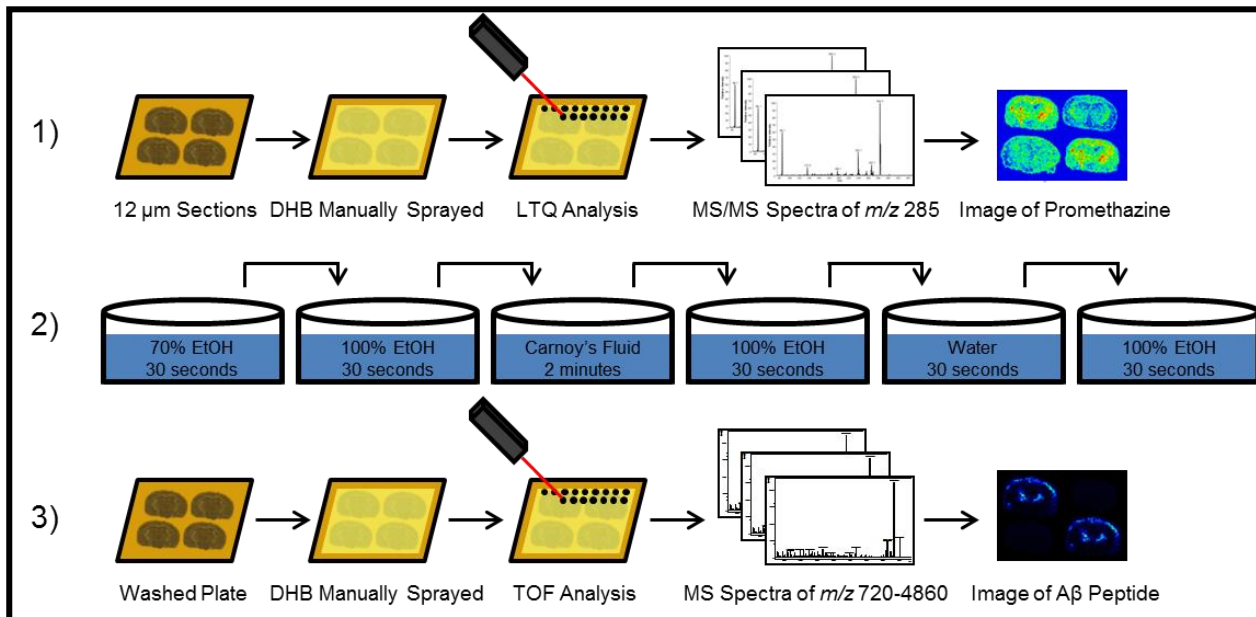


Figure 9-13 MALDI-IMS Protocol for Promethazine.

Snap frozen mouse brains from dosed 5XFAD transgenic mice (2 and 8 months old) and wild-type mice were sectioned into 12 µm thick slices and thaw-mounted onto a MALDI target plate. Matrix (30 mg/mL 2,5-dihydroxybenzoic acid [DHB] in 50:50 methanol:water with 0.1% trifluoroacetic acid) was manually applied using a glass-reagent sprayer. Tissue sections were analyzed (100 µm spatial resolution) for promethazine distribution on a linear ion trap mass spectrometer with a MALDI source (LTQ XL, ThermoFisher). Following drug distribution analysis, the tissues were washed in sequential steps of 70% ethanol, 100% ethanol, Carnoy's solution (60% ethanol, 30% chloroform, 10% acetic acid), 100% ethanol, water, and 100% ethanol to remove the matrix and potential ion suppressants such as lipids and salts. The same matrix was reapplied using a glass-reagent sprayer, and the tissue sections were analyzed (150 µm spatial resolution) for the distribution of amyloid beta peptides using a MALDI TOF/TOF mass spectrometer (UltrafleXtreme, Bruker) in reflectron mode. For peptide identification, matrix was hand-spotted onto a 5XFAD brain and analyzed in LIFT mode on a MALDI TOF/TOF MS (UltrafleXtreme). A total of 35,000 laser shots were summed to enhance the signal-to-noise ratio. Database searching was performed using BioTools (Bruker) and Mascot.

The results of this protocol are illustrated in Figure 9-14C, which shows the detected promethazine signal (m/z 86) on representative brain sections from dosed wild type (top), non-dosed 5XFAD (middle), and dosed 5XFAD (bottom) animals. Again, the lack of measurable signal in the non-dosed cohort confirms that biologically innate molecules do not contribute to what is experimentally assumed to represent PMZ-derived signal. More importantly, while PMZ is detected in the brain tissues of both dosed animals (5XFAD and wild type); there is a qualitatively higher signal from the dosed 5XFAD sections. In data not presented secondary to its redundancy, similar images were obtained for the other two fragment ions (m/z 198 and m/z 240), confirming the molecular specificity of the analysis. Despite their qualitative nature, these findings provided the first experimental support for our hypothesis that MALDI-IMS imaging can expedite the characterization of $A\beta$ -binding molecules discovered via HATCO-mediated HTS. As predicted, phase 2 screening employing MALDI-IMS contributes to the characterization of $A\beta$ -binding molecules in two ways. First, the detection of PMZ signal in the brain inarguably confirms the ability of this molecule to cross the BBB. Secondly, as described in the following section, MALDI-IMS provides complementary data unobtainable via independent implementation of the HATCO assay by facilitating the direct analysis of intact tissue and preserving the spatial distribution of molecules within that tissue. Put plainly, MALDI IMS-based analysis of HATCO discovered hits enables researchers to assess the biological relevance of the molecule's retention pattern in the brain via comparison with known regions of $A\beta$ plaque distribution.

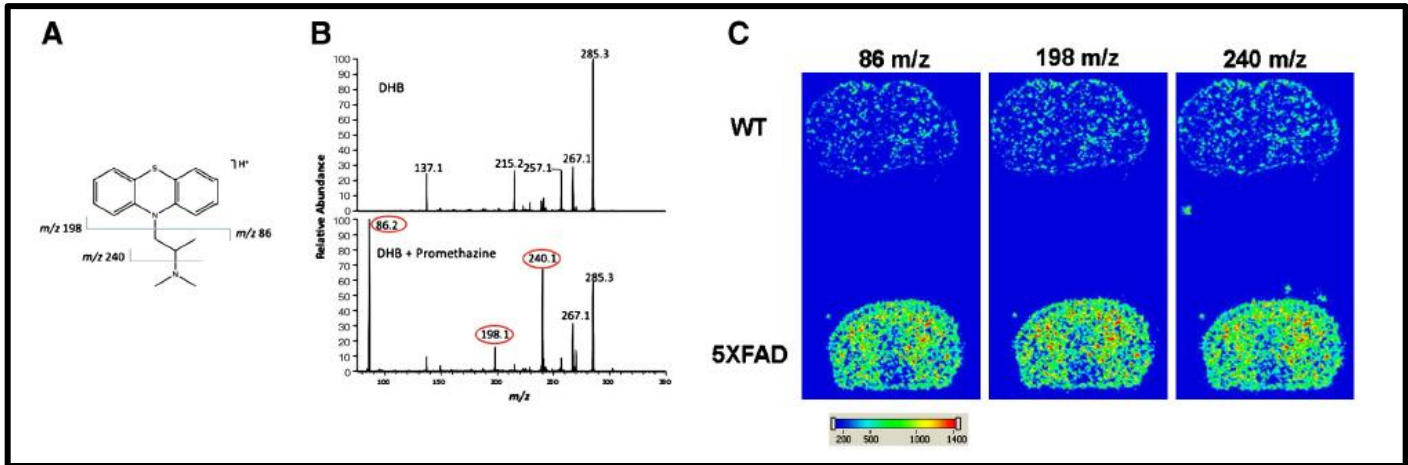


Figure 9-14. Validation of Promethazine Imaging using MALDI-IMS.

(A) Chemical structure of promethazine and its fragmentation pattern under the described experimental conditions. (B) Fragmentation pattern of promethazine generates ions with unique m/z values (red circles) that are distinct from the DHB matrix. (C) Visualization of promethazine retention in 12 μm coronal brain slices of dosed 5XFAD and wild type mice at three ions. Mice were given a cumulative dose of 25 mg/kg of promethazine using four tail vein injections at 2-hour intervals. Four hours after the last injection, cardiac perfusion was performed and the brain tissue harvested. MALDI-IMS analysis reveals enhanced retention of promethazine in amyloid-burdened brain tissue (5XFAD) compared to wild type. Critically, MALDI-IMS of non-treated brain tissues (5XFAD NT) generated virtually no signal at the specified mass to charge ratios, confirming the specificity of our protocol for PMZ. The high degree of corroboration between all three m/z peaks confirms the specificity of this protocol for promethazine.

9.4.5 *Result: Corroboration of PMZ's Regional Retention with A β Plaque Distribution in the Brain Using MALDI-IMS*

As stated, beyond confirming BBB penetration under in vivo conditions, MALDI IMS-based analysis of HATCO discovered hits enables researchers to assess the biological relevance of the molecule's retention pattern in the brain via direct comparison with the topographical distribution of A β -peptide assemblies. At the most basic level, the MALDI-IMS method combines the multichannel (m/z) measurement capability of mass spectrometry with a surface sampling process, enabling us to probe and map the presence of putative A β -binding molecules and A β peptides themselves in brain tissue. Critically, our protocol has been designed such that the same coronal brain sections analyzed for PMZ can be analyzed for individual A β peptides after a series of washes to remove confounding ion sources. After washing, the sample plate was put into a time-of-flight MS (Bruker Autoflex TOF) and analyzed in linear positive ion mode from m/z 2500–7000 to screen for A β -specific signal. As predicted, a number of signals corresponding to amyloid peptides were detected, as shown in Table 9-13 (based on human amyloid precursor protein, Swiss Prot entry number P05067). Interestingly, the resulting image is similar for all amyloid ions detected (data not shown). However, the signal for m/z 4332, corresponding to A β_{1-40} , was the most abundant A β signal detected in the brains of 5XFAD mice, and was thus selected for comparison with PMZ retention in subsequent studies. Critically, the A β_{40} peptide is widely accepted in the field of AD research as a major constituent of mature A β plaques, and it has been shown to possess considerable cytotoxicity.^(1022, 1023) Thus, our study assumes that A β_{40} deposition reasonably reflects the regional A β plaque load in any given region of the brain. For reference, the localization of m/z 4332 is shown in Figure 9-15. A quantitative analysis of this data reveals that the brains of 8-month-old 5XFAD mice exhibit a five-fold increase in amyloid peptide signal as compared to both the 2-month-old 5XFAD animals and age-matched wild type controls. Moreover, the amount of A β peptide in the 2-month-old 5XFAD cohort is not significantly different than that of the 8-month-old wild type mice. Importantly, these results are in congruence with our a priori predictions, as 5XFAD mice do not begin accruing A β plaques until 3 months-of-age. Furthermore, critical analysis of these images reveals the characteristic predilection of A β plaques to accumulate in specific regions of the brain, including the isocortex and hippocampal CA1–CA3 areas. Thus, the data strongly suggests that MALDI-IMS imaging at 4332 m/z reports A β -burden in the brains of 5XFAD mice with high fidelity.

In an effort to demonstrate promethazine's potential efficacy as a reporter of A β plaque burden in the brain, we first quantified the total promethazine generated MALDI-IMS signal in each of the three cohorts. To do this, we employed standard image processing techniques which rely on transformation of the MALDI IMS data into a binary image format to facilitate quantification of the average signal intensity generated by promethazine and the A β ₄₀ peptide. As depicted in Figure 9-15B, MALDI IMS imaging of promethazine in 8-month-old 5XFAD animals revealed a signal intensity nearly 3-fold greater than that of age-matched wild type animals. In contrast, promethazine-dosed wild type mouse brains exhibit virtually no A β ₄₀-generated signal and a minimal signal representing promethazine. This data is consistent with the HPLC data presented in Figure 9-16, which indicates that only residual amounts of promethazine remain in the brain of wild type mice 240 min post-injection. Notably, the signal trends observed in promethazine signal mirror those of direct A β peptide imaging; as signal intensities derived from both promethazine and the A β ₄₀ peptide are similarly elevated in 8-month-old 5XFAD mice compared to age-matched wild type controls. In addition, the level of A β plaque burden assessed by MALDI-IMS imaging of the A β ₄₀ peptide is comparable within experimental groups, a finding which alludes to the possibility of inter-subject comparisons of A β plaque burden using this technique. However, it remained possible that the brain regions responsible for generating the enhanced promethazine signal in the 8-month-old 5XFAD cohort might not be of biological significance with respect to AD pathophysiology. Therefore, we sought to investigate whether regions of known pathological significance, including the isocortex and hippocampal fields possessed promethazine signal differences like those observed in the whole brain analysis. As depicted in Figure 9-15C, quantification of the MALDI IMS signal intensities generated by promethazine within each experimental group supports the conclusion that promethazine is retained as a function of the A β plaque burden in regions of the brain relevant to AD pathophysiology. On average, the promethazine signal measured in the brains of 8-month-old 5XFAD mice is 2-fold greater than that of age-matched controls in both the hippocampus and isocortex (n = 3 per region, P < 0.01). In congruence with our whole brain analysis, no significant differences in promethazine retention were observed between wild type and 2-month-old 5XFAD animals in either of these regions. Considered together, the similarity in mean signal values generated by promethazine and A β ₄₀ in each experimental cohort, in addition to the evidence which illustrates that these trends are observable in biologically relevant brain regions, lends convincing support to the conclusion that promethazine is preferentially retained in the brain in an amyloid dependent manner.

Table 9-12. MALDI-IMS Signals Corresponding to A β -peptide Species

MALDI-IMS Signals Corresponding to A β -peptide Species		
Peptide	[M + H] ⁺ Predicted Average	[M + H] ⁺ Observed Average
A β 1-37	4075.5	4076
A β 1-38	4132.6	4134
A β 1-39	4231.7	4232
A β 1-40	4330.9	4332

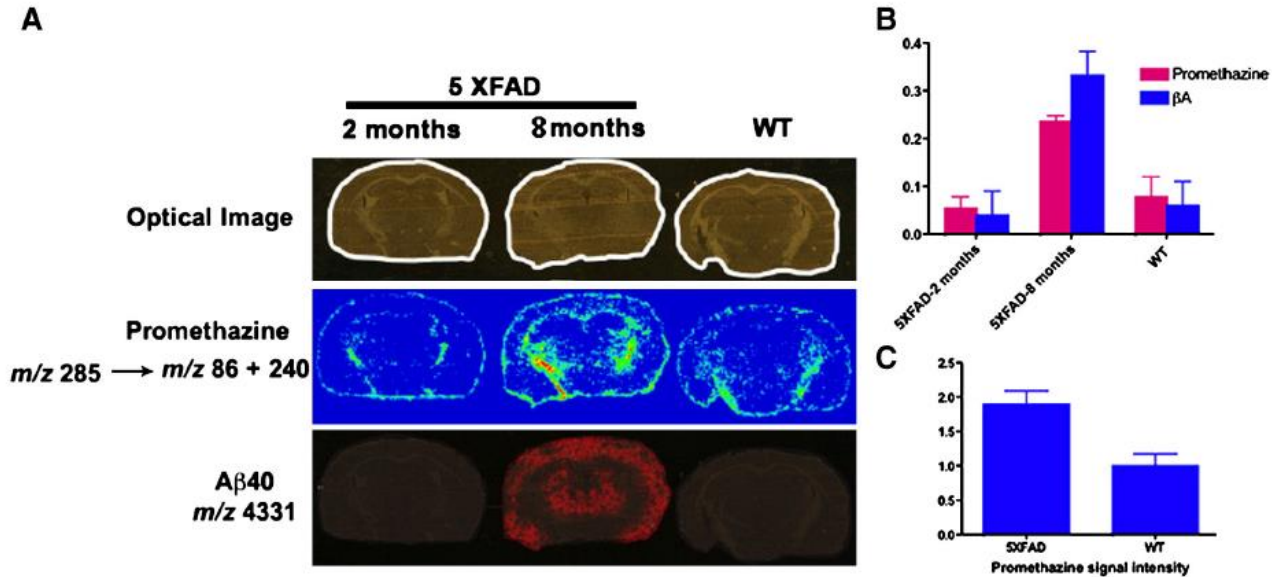


Figure 9-15. Differential Retention of Promethazine as a Function of A β Plaque Burden.

(A) Representative coronal brain slices obtained from promethazine-treated wild type and 5XFAD mice (4 h post injection) were assembled on a gold plate for analysis via MALDI IMS. In the A β 40 imaging panel, the comparable signal intensities in the wild type and 2-month-old 5XFAD cohorts implies that A β plaques are not well developed in 2-month-old 5XFAD mice. Importantly, this finding excludes differences in BBB permeability or brain protein composition between 5XFAD and wild type models as alternative explanations of the differential retention of PMZ observed in the 8-month-old 5XFAD group. The differential signal intensity of PMZ between 2- and 8-month-old 5XFAD mice confirms promethazine's potential to serve as a proxy of A β plaque burden as well as demonstrates its specificity for mature A β plaques. (B) Quantification of total brain promethazine and A β 40-generated MALDI IMS signal in wild type and 5XFAD mice. Signal intensity was calculated as the percentage of pixels exhibiting promethazine-generated MALDI IMS signal above background levels. The mean promethazine-generated MALDI signal obtained from brains of 8-month-old 5XFAD mice was 3-fold greater than that of wild type controls ($n = 3$, $P < 0.01$). Furthermore, no significant differences in promethazine-generated signal were observed between 2-month-old 5XFAD mice and wild type controls ($P = 0.47$). Critically, these trends in promethazine retention between experimental cohorts directly mirror those observed via direct visualization of the A β 40 peptide, thus supporting the conclusion that promethazine retention in the brain is amyloid dependent. (C) Quantification of promethazine-generated MALDI IMS signal in pathologically relevant regions of interest. Overlay of MALDI IMS promethazine images with the Allen mouse brain reference atlas facilitated quantification of the mean promethazine-generated signal intensities within the hippocampus and isocortex. Mean signal values from these regions were then normalized to age-matched wild type controls. Within these regions of interest, promethazine retention was significantly greater in 8-month-old 5XFAD mice compared to wild type controls ($n = 3$, $P = 0.006$). The results suggest that promethazine is retained preferentially in amyloid-burdened brains in regions of the brain known to be susceptible to A β plaque aggregation.

9.4.6 Result: Confirmation of PMZ BBB Penetration and A β -dependent Retention in the Brain Using HPLC

To confirm the results of our second phase of screening (MALDI-IMS) using a gold-standard approach, HPLC analysis of brain homogenates was leveraged. Again, the purpose of this work was to demonstrate that PMZ's harbors the ability to both cross the BBB and be retained in the brain parenchyma in an amyloid-dependent manner. Therefore, in precisely the same manner as for the MALDI-IMS set of experiments, wild-type and 5XFAD mice (n = 3 per group) were injected with promethazine (25 mg/kg) via the tail veins and subsequently perfused. In an effort to better assess the pharmacokinetic profile of PMZ retention in the brain, mice were sacrificed 10 minutes or 4 hours post-injection. Freshly isolated brains were then homogenized to facilitate extraction and quantification of the promethazine contained within the sample via HPLC using a procedure reported by our group previously.⁽¹⁰²⁴⁾ As shown in Figure 9-16, following a brief systemic distribution, we noted pronounced peaks at retention times of 15 and 17 min, which corresponded to (R) and (S) enantiomers, respectively.^(1025, 1026) Of note, the molecular weight of the molecule associated with the peaks at 15 and 17 min match that of promethazine as determined by LC-MS and identically matches the peaks obtained by HPLC analysis of a racemic promethazine solution (data not shown). Among the wild type mice, the peaks corresponding to both (R) - and (S)-promethazine disappeared 4 h post-injection. However, both enantiomers of promethazine remained in amyloid burdened 5XFAD brains 4 h post-injection. Interestingly, retention of the (S)-enantiomer appeared favorable compared to that of the (R) configuration. This may suggest that the (S) configuration of promethazine is principally responsible for binding to A β plaques. Using standardized concentration curves and integration software available from the HPLC system, we calculated that 2% and 0.5% of the original promethazine dose was retained 10 min post-injection in 5XFAD and wild type mice, respectively. Thus, promethazine exhibits a 4-fold higher retention in amyloid-burdened brains at the 10-minute time-point with respect to wild type controls. At the 240-minute time-point, 0.5% of the original dose remained in 5XFAD brains compared to 0.01% retention in the wild type animals. These results represent a significant difference in the retention of promethazine as a function of A β plaque burden in the brains at the 240-minute time-point. Further analysis of this data reveals that the amount of promethazine retained in the brain of wild type mice drops 97% during the 10- to 240-minute time interval, while promethazine retention falls by only 75% in amyloid-burdened 5XFAD brains. We performed a control study to demonstrate the notion that compounds lacking any kind of binding targets in the brain will be virtually 100% cleared an hour after administration. Toward that goal, we injected Cy5.5 succinimide ester dye (2

nmol) into the left ventricle of a mouse and tracked the distribution using an optical imaging system. Immediately after injection, we observed the dye diffused into the brain tissues; however, one hour post-injection, no trace of the material was detected in the brain (Figure 9-16). Thus, the finding that the rate of promethazine clearance in the brain varies in an amyloid-dependent manner is best explained by the ability of the compound to bind to A β assemblies. Taken together, the data is highly congruent with the analysis achieved via phase 2 screening with MALDI-IMS. Namely, that promethazine can penetrate the BBB and is retained in the brain in an amyloid-dependent manner

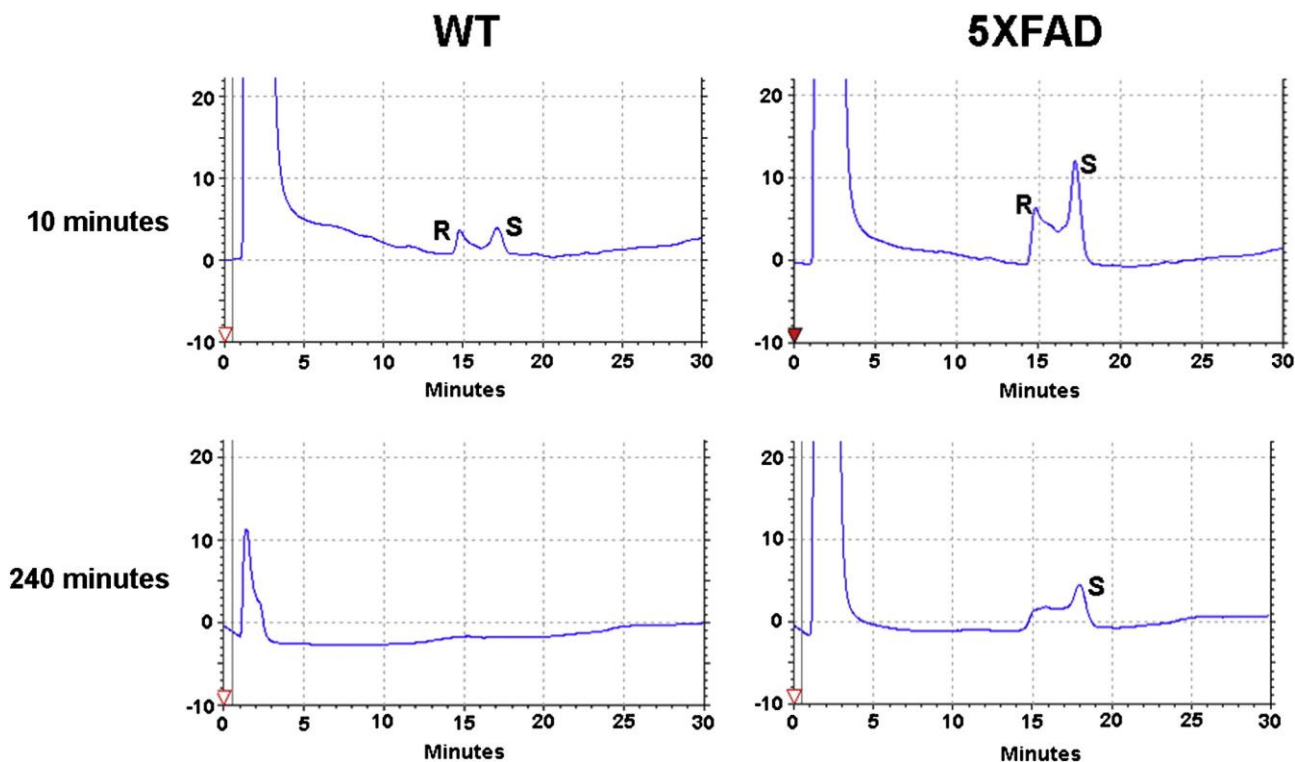


Figure 9-16. HPLC Determination of BBB Penetration and Differential Retention of (S)-promethazine in 5XFAD Mouse Model.

Ten minutes post-injection, detectable levels of promethazine were measured in both wild type (mean = 2.57 μg) and 5XFAD (mean = 9.62 μg) mouse models, thus confirming promethazine's ability to cross the BBB in both models. At this time-point, 0.5% of the original promethazine dose is retained within the brains of wild type mice compared to 2% retention in the 5XFAD model. This is approximately a 4-fold increase in promethazine retention in amyloid-burdened brains. At the 240-minute time-point 0.5% of the original dose retained in 5XFAD brains versus 0.01% in wild type mice. Given that the difference in promethazine retention between wild type and 5XFAD grows over time, it is highly probably the enhanced retention of promethazine in amyloid-burdened brains reflects an affinity of promethazine for A β plaques. Tail vein injection of racemic mixtures of promethazine facilitated the determination of stereo-specific binding. Note that both the (R) - and (S)-promethazine enantiomers are retained at relatively the same level in wild type brains; however, the (S)-version is retained at higher levels 240 min post-injection in the 5XFAD mice. These results support the conclusion that the (S)-promethazine enantiomer may be primarily responsible for A β plaque binding. Further, cardiac perfusion protocol was performed prior to brain extraction/homogenization to avoid confounds associated with promethazine being retained in the micro-vasculature. All measurements were performed in triplicate with each dose equivalent to 25 mg/kg.

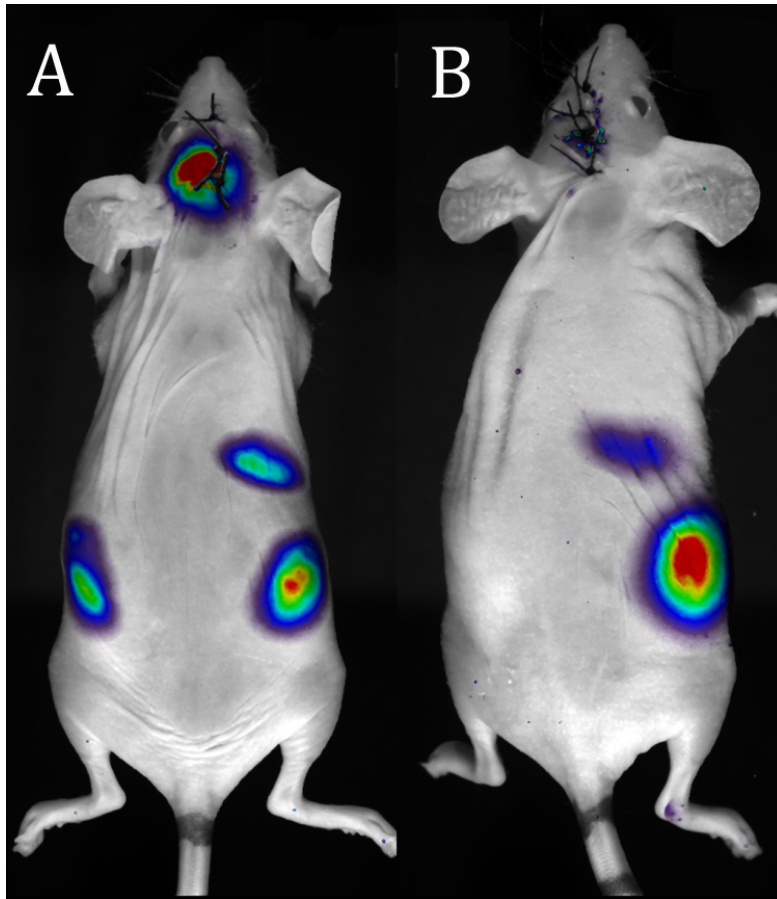


Figure 9-17. Non-targeted Compounds are Rapidly Cleared from the Brain.

Intra-cerebroventricular injection of the Cy5.5 succinimide ester dye (3.0 μL) was performed using a stereotactic surgical instrument. Once anesthetized with isoflurane, the skull was exposed and a small burr hole was generated using a dental drill. The animal was subsequently injected using a Hamilton syringe with a 27-gauge needle at a rate of 0.5 $\mu\text{L}/\text{min}$ into the left lateral ventricle using the coordinates: 1mm caudal to bregma, 1.3 mm lateral to sagittal suture, and 2 mm in depth. After injection, the skin was closed using surgical sutures and the animal was subjected to imaging immediately and 1 hour post-injection. Analysis of the resulting data reveals that compounds lacking binding-affinity for a substrate in the brain are virtually completely cleared within a one hour timeframe.

9.5 DISCUSSION & SIGNIFICANCE OF WORK

As reiterated time and time again, despite the wide-spread application of amyloid-binding contrast agents in AD research trials, the identification of A β -binding molecules capable of crossing the BBB remains a significant bottleneck in the overall effort to detect and treat AD. Prior to our work, the predominant drug design strategy available to science involved the structural manipulation of known amyloid-binding molecules such as thioflavin and Congo Red. However, the efficacy of this approach has proven largely inadequate and has arguably been exhausted. Supporting this claim, only 4 clinically implemented diagnostic probes for AI have been generated in nearly three decades of research. Moreover, no disease-modifying therapeutic has been developed for AD, despite considerable evidence in preclinical models that perturbation of amyloid-aggregation via small molecules represents an ideal therapeutic strategy. Thus, given the costly development and structural limitations intrinsic to ligand-based probe design, the impetus for our work is the passion to find new approaches which facilitate the identification of unorthodox amyloid-binding compounds. In pursuit of this goal, we successfully integrated the unique advantages of assay- and IMS-mediated HTS technologies to describe a robust, reliable, and rational technique for the identification of ideal amyloid-binding compounds. Considering first the HATCO assay component of our research, this particular screening methodology is unique in several aspects. Most importantly, unlike alternative thioflavin-based screening technologies which are traditionally restricted to the 96-well plate format, rigorous troubleshooting has been performed on the HATCO assay to facilitate its translation to the 384-well platform. Most practically, the assay's working volume has been reduced by a factor of 8, from its original total volume of 200 μ L to its final optimized volume of approximately 25 μ L. In a similar manner, the assay's volume requirement for each candidate compound has been substantially reduced in order to facilitate compatibility with widely implemented restrictions imposed by the HTS core. For this parameter, the initial requirement of 50 μ L of library compound was reduced by a factor of 400; optimized down to a volume of just 125 nanoL. Equally critical to the successful translation of the HATCO assay to the 384-well plate format was the incorporation of automated liquid handling systems for plate loading. It is noteworthy that prior to this optimization, the Z-prime statistic for the HATCO assay was abysmally low, with a mean value of .34. As revealed by the data, this is largely attributable to the viscosity of the 5XFAD lysate, which causes it to exhibit a propensity to adhere to the tip of the pipette. In doing so, major deviations in total well volume are

introduced into the plate, which dramatically alter fluorescent signal, increase standard deviation, and consequently reduce the Z-prime statistic. To address this issue, loading techniques practically implemented only with the assistance of liquid handling systems proved to be necessary. Relevant operations to combat the inherent difficulty of loading the 5XFAD lysate included the integration of an automated tip-touch protocol, pre- and post-aspirate volume, as well as reagent specific rates of dispensation. With these parameters optimized, the HATCO assay again reached descriptive statistics of reproducibility compatible with efficacious HTS, with a mean Z-prime of .62 and a %CV under 5% under real-world screening conditions. Placed in context, this seats the HATCO assay among the most robust HTS technologies described for the identification of A β -binding molecules to date, with techniques achieving a Z-prime above .5 being considered exceptionally well optimized. Despite these exceptional statistics, the real-world utility of our technique could have been limited by the high cost associated with harvesting sufficient brain mass to produce the 5XFAD lysate. Fortunately, this concern has been sufficiently addressed via a 10-fold dilution of the original lysate parameters. In fact, under the optimized protocol, the sacrifice of just one 5XFAD mouse is sufficient to screen approximately 2,000 library compounds. Again, this cost-efficiency would be meaningless if the validity or reproducibility of our assay was negatively impacted by this alteration. However this scenario proved not to be the case. To the contrary, in a manner which highlights the reliability of the HATCO assay as a primary screening technique, 35 of the 42 (83.33%) originally identified hit compounds met statistical criteria for classification as an A β -binding molecule in a confirmatory screen. Moreover, the 7 compounds which failed to reach statistical significance when re-screening using the HATCO assay were those with the lowest A β affinity. All attributes considered, the HATCO assay is inarguably well-suited for the screening of vast molecular libraries for A β -binding affinity.

Beyond simply surpassing alternative screening methodologies with respect to speed and efficiency, we argue that the HATCO assay offers unique advantages over its competitors. Most substantially, by utilizing naturally formed amyloid species derived from the 5XFAD mouse model in lieu of in vitro derived alternatives the increasingly recognized confounds associated with synthetic amyloid assemblies can be avoided entirely. Put another way, hits identified via the HATCO assay are predicted to have higher translational validity, as they are targeted to amyloid assemblies with biologically relevant tertiary structures. A second way in which our HTS-based approach to the identification of A β -binding agents optimizes translation validity is via its ability to repurpose orphaned compounds. It should be noted that

orphaned compounds, those drugs that have been rejected for the treatment of non-related diseases, hold a key advantage with respect to translatability, as this tremendously large and heterogeneous group of molecules typically have a history of use in human trials. Moreover, the possibility of identifying an A β -binding molecule with off-target therapeutic benefits is increased by probing libraries of orphaned compounds, as the vast majority of these compounds were designed to harbor biologic activity. With these key advantages in mind, our initial screening experiments focused predominantly on compound libraries enriched with orphaned compounds, such as the NIH clinical collection I and II. However, beyond the potential of identifying A β affinity in abandoned drugs, reliable HTS technologies like the HATCO assay also permit the characterization of natural products with innate and often times pleiotropic therapeutic effects. To leverage this advantage, we screened the Vanderbilt HTS facility's "Spectrum Collection", a compound library comprised of 2,000 biologically active drugs and natural products. As demonstrated in this work, primary screening of the large, structurally diverse molecular libraries described using the HATCO assay can selectively identify compounds possessing affinity for A β -assemblies of correct tertiary structure. In principal, this assay operates by monitoring a compound's ability to dissociate complexes of thioflavin-A β via competitive inhibition. Highlighting the utility of this novel assay, HTS of a 3,500 compound molecular library resulted in just 7 confirmed and cross-screened hits. Put another way, HATCO assay-mediated HTS eliminates 99.8% of molecules tested. Critically, known A β -binding compounds such as resveratrol also register as hits when screened with the assay; a result which supports the validity of our approach. Taken as a whole, the data strongly supports the utility of the HATCO-assay as a primary screening methodology for the identification of novel A β -binding molecules.

Notably however, if we were to limit our drug discovery paradigm to just this assay-mediated HTS, we would risk repeating the mistakes of our predecessors by failing to appropriately characterize the BBB penetrance of our initial hits. As reviewed at length in earlier chapters, the failure to sufficiently characterize the BBB penetrance of putative therapeutic compounds has historically manifested itself as the single most ubiquitous limitation of all AD clinical trials conducted to date. Unwilling to accept this limitation, our approach radically differs from all previously published probe/drug discovery methodologies in that we employ a second phase of screening which provides information regarding a candidate probes performance in an in vivo model of AD. Importantly, this approach obviates the development of unsuitable compounds and thus minimizes the potentially colossal and wasteful investment associated with traditional

probe design strategies. To facilitate this improvement, we utilize the 5XFAD model combined with a robust mass spectrometry imaging capability to both confirm the A β specificity of our hit compounds while simultaneously evaluating their bioavailability across the BBB. As a demonstration of the applicability of this second phase of compound characterization, the hit compound of highest clinical applicability, PMZ, was studied in this manner.

In this work, 5XFAD mice with moderate A β -burden and age-matched wild type controls were used for ex vivo MALDI-IMS analysis of promethazine retention in the brain. Both qualitative and quantitative assessment of the resulting MALDI-IMS images showed a clear and statistically significant signal difference between promethazine treated wild type and 5XFAD mice after intravenous injection of the compound. Impressively, the inter-sample consistency of the promethazine-generated MALDI IMS signal facilitates a 100% accurate discrimination of AD from wild type mouse models using only a simple threshold-based algorithm. When these observed differences in PMZ retention between wild type and 5XFAD mice were quantified using HPLC, we calculated that 2% and 0.5% of the original promethazine dose was retained 10 min post-injection in 5XFAD and wild type mice, respectively. Described in a different manner, promethazine exhibits a 4-fold higher retention in amyloid-burdened brains at the 10-minute time-point with respect to non-amyloid burdened controls. While this result certainly alludes to an amyloid-dependent retention of PMZ in the brains of 5XFAD mice, PMZ levels at later time points were evaluated in order to definitively attribute this differential in PMZ retention to the molecule's putative amyloid-affinity. In a manner congruent with this model, at the 240-minute time-point, 0.5% of the original dose remained in 5XFAD brains compared to just a 0.01% retention in the wild type animals. Further analysis of this data reveals that the amount of promethazine retained in the brain of wild type mice drops 97% during the 10- to 240-minute time interval while promethazine retention falls by only 75% in amyloid-burdened 5XFAD brains. Thus, given the convergent evidence offered by MALDI IMS and corroborating HPLC data, we conclude that promethazine is retained in an amyloid-dependent manner in the brain. In this model, PMZ is retained in the brains of 5XFAD mice secondary to a reduced rate of clearance attributable to its interaction with assemblies of amyloid. Lending feasibility to this hypothesis, regional differences in the retention of promethazine correlate well with the spatial distribution of A β plaques in the brain, a finding which further supports the conclusion that promethazine is capable of binding A β plaques. Taken as a whole, these findings conclusively support the specificity of promethazine for A β

assemblies and allude to its potential utility as a diagnostic probe for assessing the relative degree of A β plaque pathology in AD patients.

Highlighting the potential significance of this finding, successful translation of PMZ into such a probe would facilitate longitudinal assessment of plaque expression levels in response to therapy. Moreover, by revealing subtle differences in A β plaque density and topographic distribution, a PMZ-based diagnostic probe might provide insight into the observed phenotypical variability characteristic of AD. Most critically, because aggregations of A β are detectable decades before the onset of symptoms, the development of a more clinically robust AI agent might expedite the organization of clinical trials designed to investigate the efficacy of prophylactic treatment regimens. In order to facilitate these advances however, a suitable AI probe should prove capable of detecting A β plaque expression patterns well beyond the yes/no strategy employed by the current generation of diagnostic techniques. Instead, third-generation AI probes must progress towards the ability to quantitatively evaluate A β plaque burden in order to facilitate intra-subject longitudinal studies of A β plaque load. As evidenced by the MALDI-IMS data, PMZ fulfills this requirement, as PMZ retention in the brain is highly correlated with A β plaque expression in pathologically relevant regions of interest such as the hippocampus. Fortunately, the chemical structure of promethazine is quite amenable to the development of a [11C] carbon PET imaging probe via N-methylation using [11C]methyl triflate or [11C]methyl iodide.⁽¹⁰²⁷⁾ Of note, we are keenly aware of promethazine's off-target effects and routine use as an anti-histamine medication for the treatment of nausea. Despite the well-established side-effect profile of promethazine and other first-generation antihistamines, a unique aspect of PET imaging probe development is that this technique uses trace amounts of radiolabeled compound well below the threshold required to induce adverse pharmacological effects. Therefore, translation of PMZ into a PET-compatible AI agent is among the group's highest priorities.

While the scientific impact of identifying and translating PMZ into a probe for AI is readily apparent, the discovery of unique amyloid-binding motifs may prove of equal importance to the field. As stated, one of the preliminary goals of this work was to expand the chemical genetics of known A β -binding molecules. To a degree, the identification of PMZ accomplishes this task. Although identified as part of a random screening process, promethazine contains a unique structural scaffold which bears a striking resemblance to that of prototypical amyloid-binding compounds. For instance, while thioflavin exhibits a thiazole backbone, promethazine is supported by a phenothiazine structural motif. While the

two backbone structures are different, they share common features including an N-alkylation extension from the ring system and a dimethyl amine moiety. However, critical structural differences between these compounds also exist. Significantly, some of these differences likely underlie promethazine's ability to cross the BBB. For example, the electronic neutrality of promethazine probably facilitates its penetrance into the CNS, while thioflavin's quaternary amine moiety imparts a positive charge which reduces its lipophilicity and thus negatively impacts its bio-distribution into the brain.⁽¹⁰²⁸⁾

In summary, in this aim, a novel, two-phase HTS approach that facilitates the identification of amyloid-binding compounds was developed. Importantly, this approach differs from conventional probe discovery methodologies in two ways: (i) by utilizing biologically-derived A β -assemblies with pathologically relevant tertiary structure to optimize the translatability of discovered hits and (ii) by extending beyond in vitro binding affinity assays and offering information regarding a candidate probes performance in an in vivo model of AD. To facilitate this second improvement, we utilize the 5XFAD model combined with a robust mass spectrometry imaging capability to assess BBB penetrance and confirm A β -binding specificity. More generally, by successfully marrying the unique advantages of assay- and IMS-mediated HTS technologies, we describe a robust, reliable, and rational technique for the identification of ideal amyloid-binding compounds. Significantly, the discovery of new A β -binding molecules can robustly advance both AD diagnostics and therapeutics. From a diagnostic perspective, the discovery of novel agents with A β -binding affinity will expand and potentially improve upon our current repertoire of amyloid imaging agents. With respect to therapeutic applications, newly discovered A β -binding structural motifs, like the ones described in this work, might possibly be leveraged as A β -aggregation inhibitors to prophylactically prevent the accumulation of A β in the brain. In light of the substantial number of orphaned compounds untested with respect to A β plaque affinity, we anticipate that this combinatorial approach to probe development will enhance the likelihood of getting a hit by facilitating rapid evaluation of untapped molecular libraries. Because of the operational simplicity, high sensitivity, compatibility with high-throughput platforms, it is our hope that the approach outlined in this work will serve to catalyze far-reaching advances in the development and understanding of AD pathophysiology, diagnostics and therapeutics.

CHAPTER 10 THESIS AIM 2

10.1 AIM 2: EVALUATING THE THERAPEUTIC EFFICACY OF A β CLEARANCE

As described at length in the introductory chapters of this work, secondary to decades of experimental support, the vast majority of investigators favor amyloid-centric models of AD pathogenesis. In short, these models hypothesize that perturbations in A β production/clearance lead to neuronal dysfunction and loss secondary to direct and indirect mechanisms. Lending considerable support to this hypothesis, drugs which counteract the pathological changes in A β processing observed in AD have demonstrated robust benefit in preclinical mouse models. For this reason, the predominant therapeutic avenue studied in human clinical trials to date involves the administration of pharmaceutical agents designed to attenuate the production, or bolster the clearance of, A β -assemblies. Disappointingly however, all of these A β -centric therapies have failed to produce robust clinical improvements in patients with established AD. As a result, today AD stands alone as the only top-ten cause of death without a disease-modifying treatment option. As reviewed in earlier chapters at length, several hypotheses for why randomized controlled clinical trials evaluating A β -centric therapies fail have been proposed. Consistently however, two limitations are ubiquitously acknowledged: (i) therapeutic intervention in patients with established AD pathology and (ii) poor delivery of therapeutic agents across the BBB. Significantly, both of these limitations are potentially addressed by the discovery of new A β -binding molecules like those identified in Aim 1 of this work. For example, because accumulation of A β in the brains of AD patients occurs decades before the onset of symptoms or substantial neurodegeneration, the development of improved AI probes may serve to alleviate the barrier imposed by our current inability to test putative treatments prophylactically. Thus, by serving as unique precursors for the development of improved AI technologies, newly identified A β -binding agents can facilitate prophylactic treatment by allowing the construction of non-demented AD cohorts required for such trials. With respect to improving the delivery of therapeutic agents the argument is more straightforward. Newly identified A β -binding molecules with innate BBB permeability can be further screened for anti-A β -aggregation properties and thus be leveraged in a therapeutic manner. However, while preventing A β plaque formation or facilitating their demolition, particularly during the early disease process, inarguably represents a key therapeutic strategy, it is important to recognize the multi-

factorial nature of AD pathogenesis. As described in detail in earlier chapters, non-amyloid-centric mechanisms of AD pathogenesis have been proposed. In fact, modern interpretations of amyloid-centric models suggest that amyloid acts as an early step in a more complex neurodegenerative cascade that becomes independent of amyloid as disease progresses.⁽⁹⁷⁶⁾ Ascribing to this model, it is easy to recognize why therapies targeting only A β have proven ineffective, particularly in the cohorts of moderate to late-stage AD patients typically employed by clinical trials.

Considering all of these points, we hypothesize that an ideal disease-modifying therapeutic for AD should be capable of (i) crossing the BBB (ii) perturbing the aggregation of A β species and (iii) influencing the pathogenesis of AD in a multi-factorial fashion. Evaluating the A β -targeted therapies studied to date according to these guidelines, these drugs fail to satisfactorily meet the first and third criteria listed. Importantly, this is attributable to the fact that the majority of these drugs have been developed via ligand-based rational drug design paradigms, which prioritize the optimization of A β -binding affinity. As described in the context of AI probe development, an alternative to rational drug design is the utilization of HTS technology. As demonstrated in Aim 1, hit compounds discovered via HATCO-mediated HTS exhibit promise with respect to alleviating the limitations plaguing the current generation of A β -aggregation inhibitors. However, as partially addressed in Aim 3 of this work, further research is necessary to evaluate the ability of such novel A β -compounds to perturb AD pathogenesis using preclinical mouse models. More generally, the majority of compounds identified via HTS are unlikely to exhibit the multi-factorial therapeutic profile deemed optimal when considering the treatment of such a complex neurodegenerative disease. Thus, even if these compounds are proven robust inhibitors of A β aggregation, the clinical efficacy of such compounds is likely to be restricted to prophylactic treatment approaches. To summarize, of the drugs developed via rational design- or HTS-based approaches, none satisfactorily fulfill all of the requirements of an ideal disease-modifying therapeutic for AD. Fortunately, a third avenue facilitating the discovery of disease-modifying treatments for AD has been identified in the application of naturally existing compounds. Although generally not held in high esteem by modern medicine, the massive influence natural products have had in modern drug development is undeniable. For example, of the approximately 877 small molecule drugs introduced worldwide between 1981 and 2002, most (61%) can be traced back to their origins in natural products.⁽¹⁰²⁹⁾ To a certain degree this is not surprising, as plant-based drugs may be more suitable, at least in biochemical terms, for medicinal use in humans as compared to exotic synthetic drugs produced through combinatorial chemistry. Importantly, the main advantage of this

approach is that because these repositories of compounds are not artificially designed for a particular target, they typically harbor a manifold of therapeutic mechanisms of action. Unwilling to limit the potential impact of our work by uniquely leveraging HTS approaches to facilitate the development of novel AD drugs; we focused on the naturally occurring turmeric extract curcumin (diferuloylmethane) as a potential theranostic agent for AD.

Interestingly, the hypothesis of a potential therapeutic role of curcumin in dementia originates from epidemiological studies demonstrating a lower prevalence of AD in populations who consume a diet rich in curry; a food product containing substantial curcumin content.⁽¹⁰³⁰⁾ Subsequently, reports conducted in cohorts of healthy elderly individuals suggested that those who consume curry more frequently perform better on cognitive test batteries.⁽¹⁰³¹⁾ Highlighting the multi-factorial nature of curcumin's therapeutic profile, more than a 100 clinical studies have credited this naturally-occurring compound with antioxidant, anti-inflammatory, anti-cancer, anti-viral and anti-bacterial properties. Of historical note, long before modern science defined its therapeutic efficacy; curcumin had been employed by non-allopathic practitioners of medicine for the treatment of a wide array of diseases. In a manner which makes it uniquely suited for therapeutic applications in AD however, curcumin exhibits a robust ability to cross the BBB and disrupt assemblies of A β peptide.⁽¹⁰³²⁾ Moreover, curcumin's effect on A β -metabolism is far more holistic than that of synthetically-derived drugs. For example, in addition to perturbing A β fibril formation in a dose-dependent fashion⁽¹⁰³³⁾, curcumin also destabilizes preformed A β fibrils⁽¹⁰³⁴⁾, inhibits amyloid-genic APP cleavage⁽¹⁰³⁵⁾, prevents A β -induced tau hyper-phosphorylation⁽¹⁰³⁶⁾, and enhances A β uptake from macrophages.⁽¹⁰³⁷⁾ Having thus met the first and exceeded the second criteria of an ideal therapeutic agent, the features which make curcumin uniquely suited to perturb AD pathogenesis are its vast array of "off-target" effects. Accumulating evidence suggests curcumin is a highly pleiotropic molecule, physically interacting with a diverse range of molecular targets including: transcription factors, growth factors and their receptors, cytokines, and enzymes (Table 10-1). Significantly, the pleiotropic nature of curcumin facilitates its modulation of numerous biochemical and molecular cascades which are posited to be of significance to AD pathogenesis. Supporting this notion, the therapeutic effect of curcumin has been well established in AD models. Chief among the non-amyloid-targeted benefits of curcumin are its potent neuroprotective and antioxidant effects; which reports suggest to be greater than that of tocopherol.⁽¹⁰³³⁾ In studies conducted on AD mouse models, low to moderate doses of curcumin succeeded in reducing oxidative damage and increasing microglial reaction near A β deposits. Mechanistically, this

therapeutic benefit is attributable to the anti-oxidant properties of curcumin which serve to decrease $A\beta$ -induced radical oxygen species.⁽¹⁰³⁸⁾

Table 10-1. Molecular Targets of Curcumin

Molecular Targets of Curcumin	
Transcriptional factors	Growth factors
Activating protein-1	Connective tissue growth factor#
β -Catenin	Epidermal growth factor#
CREB-binding protein	Fibroblast growth factor#
Early growth response gene-1	Hepatocyte growth factor#
Electrophile response element	Nerve growth factor#
Hypoxia inducible factor-1	Platelet derived growth factor#
Notch-1	Tissue factor#
Nuclear factor-kappa B	Transforming growth factor-b1#
Nuclear factor 2-related factor	Vascular endothelial growth factor#
Peroxisome proliferator-activated receptor-gamma	Inflammatory cytokines
Signal transducers and activators of transcription-1	Interleukin-1
Signal transducers and activators of transcription-3	Interleukin-2
Signal transducers and activators of transcription-4	Interleukin-5
Signal transducers and activators of transcription-5	Interleukin-6
Wilms' tumor gene 1	Interleukin-8
Enzymes	Interleukin-12
Arylamine N-acetyltransferases-1#	Interleukin-18
ATFase#	Monocyte chemoattractant protein
ATPase#	Migration inhibition protein
Cyclooxygenase-2#	Macrophage inflammatory protein
Desaturase#	Tumor necrosis factor alpha
DNA polymerase#	Receptors
Farnesyl protein transferase#	Androgen receptor#
Glutathione-S-transferase"	Aryl hydrocarbon receptor#
Glutamyl cysteine ligase	Chemokine (C-X-C motif) receptor 4#
Hemeoxygenase-1"	Death receptor-5"
Inducible nitric oxide synthase#	EGF-receptor#
Lipoxygenase#	Endothelial protein C-receptor"
Matrix metalloproteinase#	Estrogen receptor-alpha#
NAD(P)H:quinone oxidoreductase#	Fas receptor"
Ornithine decarboxylase#	Histamine (2)- receptor#
Phospholipase D#	Human epidermal growth factor receptor-2#
Src homology 2 domain-containing tyrosine phosphatase 2"	Interleukin 8-receptor#
Telomerase#	Inositol 1,4,5-triphosphate receptor#
Tissue inhibitor of metalloproteinase-3#	Integrin receptor#
Glutamate-cysteine ligase"	Low density lipoprotein-receptor"
Kinases	Adhesion molecules
Autophosphorylation-activated protein kinase#	Endothelial leukocyte adhesion molecule-1#
Ca ²⁺ -dependent protein kinase#	Intracellular adhesion molecule-1#
EGF receptor-kinase#	Vascular cell adhesion molecule-1#
Extracellular receptor kinase#	Anti-apoptotic proteins
Focal adhesion kinase#	B-cell lymphoma protein 2#

IL-1 receptor-associated kinase#	Bcl-xL#
Janus kinase#	Inhibitory apoptosis protein-1 #
c-jun N-terminal kinase"	Others
Mitogen-activated protein kinase#	Cyclin D1#
Phosphorylase kinase#	DNA fragmentation factor 40-kd subunit"
Protamine kinase#	Heat-shock protein 70"
Protein kinase A#	Multi-drug resistance protein#
Protein kinase B#	Urokinase-type plasminogen activator#
Protein kinase C#	P53"
pp60c-src tyrosine kinase#	
Protein tyrosine kinase#	

Although a variety of groups have confirmed the therapeutic efficacy of curcumin in a multitude of preclinical AD mouse models, the therapeutic potential of curcumin is perhaps best illustrated by a series of studies performed by Bacskai and colleagues. In this work, two-photon microscopy was employed to visually confirm reports that curcumin can cross the BBB, bind to A β deposits, and clear existing plaques in a transgenic mouse model of AD.^(1039, 1040) Importantly, this approach is only viable secondary to curcumin's intrinsic fluorescence emission at 557 nm. Understandably, as these studies highlight the potential of curcumin-mediated measurement of A β burden in the brain, several groups have attempted to functionalize this molecule as a diagnostic agent for AD. As highlighted in the chapter reviewing optically-based diagnostic probes however, while curcumin's fluorescent signal facilitates optical measurement of its A β -binding affinity, it is not compatible with non-invasive assessment of A β burden due the poor tissue penetrance of this particular wavelength. Thus, seeking to translate curcumin's ability to bind A β -assemblies into a clinically relevant diagnostic technique, groups have successfully radiolabeled curcumin derivatives for A β imaging.⁽¹⁰⁴¹⁾ Similarly, we recently developed a perfluoro curcumin analog (FMeC1) for ¹⁹F NMR imaging (Figure 10-1) to facilitate in vivo visualization of the mechanism that enables curcumin to bind to A β .⁽⁸²⁶⁾ Subsequent structural characterization of the FMeC1 compound in physiologically relevant buffer systems revealed the existence of an equilibrium between keto and enol tautomers. In a manner which highlights the A β -specificity of our compound, while FMeC1 exists in the keto form when dissolved in physiological buffers, it displays a shift to the enol structural motif once bound to A β aggregates.⁽⁸²⁶⁾ Seeking to leverage this novel diagnostic agent in vivo, colleagues at the Shiga University of Medical Science in Japan successfully detected FMeC1 in the brain of Tg2576 mice using ¹⁹F MRI. While considered a successful study in that the diagnostic utility of the FMeC1 compound was robustly demonstrated, a less emphasized aspect of this study highlights the principal limitation encountered by investigators seeking to leverage curcumin and its derivatives for theranostic applications in AD; its poor solubility in biologically relevant solvents. In fact, while essential to its ability to permeate the BBB, curcumin's amphiphilic properties require that the compound be dissolved in a combination of buffer solutions which contain excessively high concentrations of detergent. Secondary to the viscous nature of this formulation, bolus administration by intravenous injection has proven lethal in preclinical animal models and is therefore unsuitable for human trials.⁽⁸²⁶⁾ Thus, the delivery of curcumin at therapeutically meaningful doses stands as the major factor limiting the utility of this promising theranostic agent. As employed by our colleagues in Japan, one way to circumvent this limitation is by using a controlled pump to infuse the substance over an extended period; however, enormous uncertainty persists

regarding how these methodological adaptations can be implemented in translational studies without major unforeseen complications. Unable to overlook curcumin's therapeutic potential, our group and others have cumulatively proposed a myriad of methods to successfully deliver curcumin to the brain.⁽¹⁰⁴²⁾

Following what was perceived as the most clinically applicable avenue, historically, investigators have focused on optimizing oral dosing regimens of curcumin. However, a pharmacokinetic evaluation of this dosing strategy reveals it to be grossly inadequate. To start, as indicated by blood plasma levels in various animal models after P.O. dosing, curcumin is poorly absorbed from the gut. Exemplifying this point, in rats receiving a 1g/kg oral dose of curcumin, 75% of the ingested dose was excreted unprocessed in the feces.⁽¹⁰⁴³⁾ In a similar study, plasma and tissue levels of tritium-labeled curcumin administered at doses of 400, 80, and 10 mg were measured as a function of time. While largely in congruence with the previously cited study, this experimental design revealed that the percentage of curcumin absorbed remained constant regardless of the dose administered.⁽¹⁰⁴⁴⁾ Put another way, this study indicates that increasing the dose of curcumin may not necessarily result in higher absorption. The implication of this finding is of supreme clinical importance, as it highlights the folly in employing the obvious strategy of dose escalation to compensate for curcumin's poor P.O. pharmacokinetic profile. To confirm this assertion, one need look no further than dose-escalation trials to determine curcumin's maximum tolerated dose and safety. In one prototypical trial, a standardized powder extract of uniformly milled curcumin (C3 Complex™, Sabinsa Corporation), was administered to 24 healthy volunteers at single doses ranging from 500 to 12,000 mg. Predictably given the pharmacokinetic profile just discussed, no curcumin was detected in the serum of subjects at any of the administered doses.⁽¹⁰⁴⁵⁾ It is worth noting the poor P.O. bioavailability reported in these studies is not uniquely attributable to curcumin's abysmal rate of intestinal uptake. To the contrary, an equally unfavorable aspect of P.O. administration is its immediate delivery of any absorbed curcumin to the liver where it is promptly metabolized. Termed the first-pass effect, this generalizable phenomenon greatly reduces the serum concentration of a susceptible drug before it reaches systemic circulation. Thus, when interpreted as a whole, the literature suggests two interrelated phenomena contribute to the poor bioavailability of curcumin when administered orally (i) poor gastrointestinal uptake and (ii) extensive clearance secondary to first-pass metabolism.

Recognizing the need to deliver curcumin in a manner which bypasses the intrinsic limitations of P.O. administration yet remains clinically applicable; we describe herein a novel approach for delivering curcumin to the brain

via inhalation. In more detail, a curcumin-containing suspension was aerosolized using a center-flow atomizer, diluted with air, and delivered intra-nasally. To demonstrate the robust nature of this dosing methodology, we compared aerosol-mediated delivery of FMeC1 to the gold-standard of I.V. injection. Preliminary data demonstrated that drug delivery using our atomization approach alleviated toxicity concerns and efficiently deposited FMeC1 compound in the brain slightly better than I.V. injection. Excitingly, this result promotes further research into leveraging aerosol-mediated delivery to facilitate the delivery of diagnostic probes for AD across the BBB. Towards this end, we show that delivery of the FMeC1 compound reached concentrations in the brain detectable by ^{19}F NMR. Moreover, plaque-like punctate fluorescence attributable to complexes of the inhaled FMeC1 analog were co-localized to immuno-stained $\text{A}\beta$ plaques in the cortex and hippocampal regions of the 5XFAD mouse brain under fluorescence microscopy. Importantly, this result strongly suggests that $\text{A}\beta$ -targeted compounds like FMeC1 retain their amyloid-specificity when administered via aerosolization. Cumulatively, these findings led us to hypothesize that aerosol-mediated delivery of curcumin might be applied to efficaciously leverage the multi-factorial therapeutic profile of curcumin for the prevention of AD. To test this hypothesis, we characterized the therapeutic effect of aerosol-mediated delivery of a 5 mg/kg dose of curcumin delivered three times a week over the course of 20 week period on 1.5-month old-5XFAD mice. Astonishingly, this prophylactic treatment regimen reduced $\text{A}\beta$ plaque burden in the hippocampus, subiculum, and neocortex by 90.72%, 79.48%, and 68.75% respectively. Further characterization of these treated mice via transmission electron microscopy revealed an equally stunning absence of dystrophic neurites in the CA3 sub-region of the hippocampus. Most importantly from the therapeutic perspective, these observed therapeutic benefits are correlated with improvements in both working and spatial memory as assessed by the Y-maze behavioral assay.

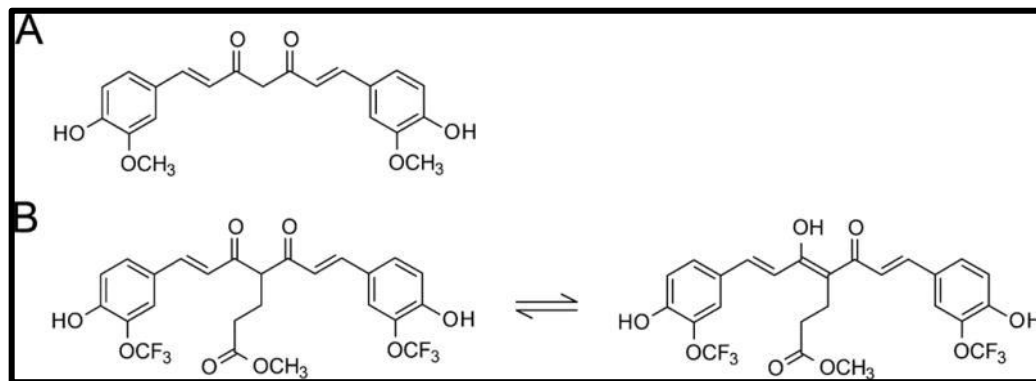


Figure 10-1. Curcumin (A) and its perfluoro analogs, FMeC1 (B)

10.2 AIM 2 EXPERIMENTAL METHODS

Animals

The C57BL/6 and 5XFAD mice (8–12 months old) were maintained at Vanderbilt University under standard conditions, in a 12-hour light/dark cycle and with free access to food and water. The 5XFAD mice overexpress both mutant human APP and PS1 express high APP levels correlating with high burden and accelerated accumulation of the A β as described by Vassar et al.⁽⁶⁷⁰⁾ A colony of 5XFAD transgenic mice obtained from Jackson Laboratories was maintained by crossing 5XFAD mice with a wild-type C57BL/6J strain. The mice were genotyped by a standard polymerase chain reaction using DNA isolated from tail tips with the following primers: PSEN1 forward, 5'-TCATGACTATCCTCCTGGTGG3' and reverse, 5'-CGTTATAGGTTTTAAACACTTCCCC-3'. For APP, forward, 5'-AGGACTGACCACTCGACCAG-3' and reverse, 5'-CGGGGGTCTAGTTCTGCAT-3'. We also genotyped mice for the presence of retinal degeneration Pde6b^{rd1} mutation using forward, 5'-AAGCTAGCTGCAGTAACGCCATTT-3' and reverse, 5'-ACCTGCATGTGAACCCAGTATTCTATC-3'. After polymerase chain reaction amplification, the DNA product of each reaction was analyzed by size fractionation through a 1% agarose gel; with Pde6b mutant = 560 bp, APP transgene = 377 bp and PSEN1 transgene = 608 bp. The 5XFAD mice were maintained as homozygous. Animal experiments were conducted per the guidelines established by Vanderbilt University's Institutional Animal Care and Use Committee.

Inhalation Exposure and Compound Atomization

The atomizer system is comprised of a PVDF fluorinated polymer cross-flow atomizer (Single Pass Atomizer, SPA), an L-shaped conveyer, three inhalation ports, inlets for pressurized gas and liquid and a control unit to regulate aerosol generator air (Figure 10-2). In a typical experiment, an aqueous solution containing FMeC1 was pumped through a capillary the SPA. Because of the rapid flow of air across the capillary tip, the airflow shears FMeC1-containing solution into micron sized particles that are diluted with a stream of air delivered by an adjacent source. Together, these processes generate the FMeC1-containing aerosol, the concentration of which and in some instances its aerodynamic size being controlled by a flow of dilution air through the atomizer at ambient temperature (23–25°C). Delivery of the generated aerosol to cohorts of experimental animals is facilitated via a delivery trumpet assembled within each inhalation chamber.

Similarly, exhaled aerosol is conveyed to an exhaust outlet via escape channels just below the connector cone. In its current configuration, the stainless steel inhalation chamber is fitted with multiple ports and protected septum seals that enable the simultaneous respiratory exposure of three animals. The system can be expanded to accommodate up to five animals.

Before atomization of the test compound airflow was calibrated as a function of pressure to ensure that every experiment ran at a consistent airflow rate of 3 L/min and an operating pressure of 20 psi. The solution to be sprayed consisted of 15 mg of FMeC1 in 30 mL of 1:6 PBS: Tween 20 mixture that was delivered to the SPA atomization via syringe pump (Harvard Apparatus) at a rate of 50 mL/hour (833 μ L/min). The atomization process commenced when compressed air was introduced into the aerosol generator inlet via a pressure regulator. The pressurized air interacted with fluid within the SPA. The resulting aerosol particles of respirable size were then emitted into the exposure apparatus. To reduce aerosol size by evaporation, the aerosol was diluted with additional clean dry air. The resulting mixture was then directed to three nose ports within the reduced volume inhalation chamber via a connector that directs the aerosol flow to each chamber inlet. During animal trials, non-anesthetized mice were placed into a restraining tube which was inserted into the exposure chamber. The animal's snout was secured within the restraint tube by a stainless steel nose cone within the tube to focus delivery of the aerosol to the breathing zone of the animal. The tapered nose cone inside the restraint tube enables the animal to inhale the presented aerosol. As noted above, exhaled air is redirected to a second channel that leads to the system's exhaust. Rebreathing of exhaled air does not occur.

Prior to commencing the inhalation exposure of animals, an analysis of each port's aerosol flow was conducted to ensure the amount of aerosol delivered to each inhalation chamber was identical. In this work, 50-mL condensing tubes were inserted into each outlet port and sealed with parafilm. This configuration ensured that all aerosolized FMeC1 delivered through the outlet port was deposited on the surface of the condensing tube. To assess atomization efficiency, 1 mL of the 0.889 mM FMeC1 solution was aerosolized by the atomizer system. The condensing tubes for each port were then repeatedly rinsed with 1 mL of PBS and assessed for FMeC1 concentration by employing absorbance spectroscopy in combination with Beer's law. To do this, standard solutions of FMeC1 were prepared across a concentration range of .001-.025 μ M and plotted as a function of mean their absorbance at $\lambda=420$. From this data, linear regression was employed to experimentally evaluate the slope of the line of best fit ($R^2 = .99$). Importantly, using this approach, the slope

of the line of best-fit is the product of the molar absorptivity constant and the cuvette path length (1.00cm). Over the course of three atomization trials, no significant difference in aerosol delivery efficiency was detected between outlet ports (mean variance = 0.006 micrograms per 500 micrograms aerosolized), confirming that each inhalation chamber, and thus each animal, would receive identical amounts of the aerosolized product. Additionally, we determined from this data that 7.8% of the volume entering the nebulizer was successfully aerosolized and conveyed to the inhalation chambers. This quantitative data enables us to calculate and normalize equivalent doses to compare probe distribution between respiratory exposed and I.V.-injected animal groups. A representative calculation is included below.

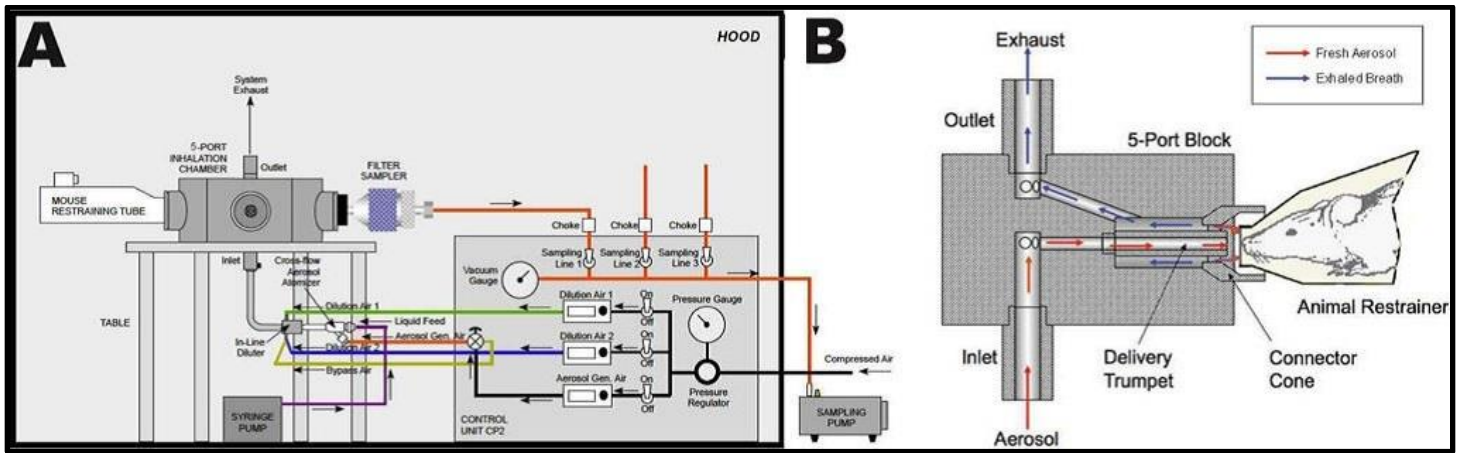


Figure 10-2. Atomizer Design and Aerosol Delivery System

(A) Atomizer schematic. (B) Magnified view of inhalation chamber and nosecone assembly. FMeC1-containing aerosol (red arrows) is conveyed through the inlet while air exhaled by the animal (blue arrows) is directed toward the system exhaust port via outlet channels.

Image analysis of ex vivo fluorescence brain imaging

Monochromatic images of slide-mounted coronal brain slices (n=40 per cohort) were manually segmented to create individual ROIs that encompassed the hippocampus and isocortex using ImageJ software. The Allen mouse brain atlas was used as a reference for the segmentation of the ROIs, and manual tracing was performed by a blinded collaborator. Mean signal intensity at $\lambda = 557$ nm was calculated for each ROI across three cohorts of animals; (i) I.V.-injected 5XFAD mice, (ii) respiratory exposed 5XFAD mice and (iii) respiratory exposed wild-type mice (n=4 per cohort).

Brain perfusion

Following exposure or treatment, deeply anesthetized animals were laid onto ice after which the thoracic cavity was accessed via a sharp transverse incision into the abdomen. This was followed by a series of longitudinal cuts with a scalpel to open the thoracic cavity, which then was stabilized with a retractor. Perfusion was performed with a 25-gauge syringe containing ice-cold PBS (30 mL, pH 7.4) inserted through the left ventricle and injected slowly into the ascending aorta. Upon initiation of perfusion, the right atrium was snipped to facilitate drainage of the systemic venous return. Immediately following PBS perfusion, 30 mL of paraformaldehyde (PFA) (pH 7.4) was perfused. With perfusion completed, the animals were decapitated and their brains quickly harvested and fixed in 4% PFA overnight at 4°C, which was followed by 10% sucrose precipitation overnight at 4°C. The fixed brains were then embedded in Cryo-OCT compound before cryosectioning.

Ex vivo imaging of the brain slides

Excised brain sections were imaged using a fluorescence tomographic imaging system (Visen FMT, PerkinElmer, MA, USA). Using a laser diode, the system scanned the surface of the FMeC1-containing brain tissues in a user-adjustable grid pattern and generated a two-dimensional map of FMeC1 deposition. Laser power and exposure time were kept constant between imaging sessions and were automatically optimized by the system to provide a maximum signal-to-noise ratio while avoiding pixel saturation. Configuration of the system to image FMeC1 fluorescence was accomplished via manual

insertion of excitation (450–490 nm) and emission (560–600 nm) optical filters. Using this imaging system coupled with Maestro 3.1 software (PerkinElmer, MA, USA), monochromatic images of three slides were acquired simultaneously at FMeC1 emission λ_{max} of 557 nm, at an exposure time of 1 msec.

Immunohistochemistry

Midbrain coronal sections (12 μm) were mounted onto charged glass slides, placed in 4% PFA for 10 minutes, transferred to tris buffer for 5 minutes and then allowed to dry before being subjected to a citrate buffer antigen retrieval protocol. Briefly, slide mounted sections were incubated for 40 minutes in a 100°C bath of sodium citrate buffer (10 mM sodium citrate, 0.05% Tween 20, pH 6.0) and allowed to cool for 20 minutes before PBS washing and blocking. Treated sections were then incubated overnight at room temperature with primary antibodies: rabbit anti-A β (1:1000 dilution, Thermo, Pittsburgh, PA, USA). Following PBS washes, the sections were subsequently incubated with secondary biotinylated goat anti-rabbit (1:2000, Thermo, Pittsburgh, PA, USA) for 2 hours at room temperature. The ABC Elite Kit (Vector Laboratories) was used with DAB as a chromogen to visualize the reaction product. The sections were then counterstained with hematoxylin, dehydrated in a series of alcohols, cleared in xylene and then cover-slipped.

FMeC1 Fluorescence Microscopy

To localize the distribution of FMeC1 in the brains of treated mice and corroborate its intrinsic fluorescence signal with that of the fluorescently labeled A β antibodies, dual channel fluorescence microscopy was employed. For all fluorescence imaging, a GFP-BP filter (excitation filter 450–490 nm; dichroic mirror 495 nm; emission filter 510–560 nm) was used to image FMeC1 fluorescence. A Texas Red filter (excitation filter 540–580 nm; dichroic mirror 595 nm; emission filter 600–660 nm) was utilized to visualize the anti-A β antibodies. All images were acquired using a CCD camera and data were analyzed using Nuance 2.6 software.

Co-localization Analysis of A β -antibody and FMeC1 Dual-channel Fluorescence Microscopy

To demonstrate that the A β -specificity of FMeC1 is retained when administered via atomization, coronal sections (n=30) isolated from respiratory exposed 5XFAD mice (n=5) were co-stained with anti-A β antibodies. Fluorescence images of the co-stained sections were acquired in hippocampal and cortical brain regions in the Cy5 channel, thus reflecting A β plaque expression as reported via anti-A β antibodies. Without changing the position of the sample, a second set of images that captured FMeC1 fluorescence were acquired in the GFP channel. To qualitatively demonstrate the co-localization between anti-A β antibody fluorescence and that of FMeC1, line plots of mean pixel intensity as a function of pixel coordinates were generated using ImageJ software for both channels and overlaid. To demonstrate co-localization quantitatively between the FMeC1 and antibody signals, the red and green channels for Cy5 and GFP images were isolated, respectively. The pixels in each monochromatic image set were then segmented into two groups using the k-means clustering algorithm to generate binary images with pixel values that represented signal versus no signal. Quantitative assessment of the degree of co-localization between each processed image set (n=20) was then completed using the JACoP plugin for ImageJ following well-established protocols.⁽¹⁰⁴⁶⁾

Detection and Quantification of FMeC1 in the Brain by NMR Spectroscopy

A 5 mg/kg dose of FMeC1 was administered to 5XFAD mice (n=4) via atomization. One hour after administration, the brain of each animal was removed and processed for FMeC1 extraction using methods previously described.⁽¹⁰²⁴⁾ Briefly, each tissue was weighed before homogenization in 2 mL of PBS, after which 200 μ L of acetonitrile was added to the tissue lysate. The solution was then vortexed for 5 minutes, heated to 50°C for 10 minutes, and vortexed again before being centrifuged at 12,000 g for 1 hour. The supernatant was collected and all PBS/acetonitrile solvent removed via lyophilization. The resulting FMeC1 residue was reconstituted in deuterated chloroform to a total volume of 200 μ L for ¹⁹F NMR analysis using a 300 MHz Bruker NMR spectrometer.

The concentration of FMeC1 was calculated using ¹⁹F NMR spectroscopy. To enhance the detection threshold, 200 μ L of the extracted FMeC1 solution was placed in a 3-mm NMR tube. The ¹⁹F NMR experiment for this sample acquired over a period of 15 hours (31,000 scans), revealed a single peak at -75.96 ppm. To provide accurate and reproducible quantitative results, 0.1 M trifluoroacetic acid (TFA) (-76.55 ppm) served as an external reference. Since

sample material was not a consideration, 600 μ L of the TFA sample was placed in a 5-mm NMR tube and analyzed using the same experimental NMR parameters as the FMeC1 sample; however, it required only a 20-minute scan time. The calculation of FMeC1 concentration involved first adding the processed NMR spectra for both samples. The NMR spectrum for the TFA sample was offset to avoid spectral overlap. The spectra were then integrated by fitting the NMR peaks using either Gaussian and/or Lorentzian line shapes. Once the values were calculated using line fitting techniques, the integral ratios were scaled to compensate for the differences in the number of scans and sample volume.

Tissue Preservation & Thioflavin Staining

Following cardiac-perfusion as described in the corresponding methods section, the extracted brain tissue was fixed first 4% PFA, then in a 10% sucrose/PBS solution for 5 and 2 days, respectively. Immediately after fixation, each brain tissue (N=5 per group) were divided along the sagittal fissure. One hemisphere was then utilized for western blot analysis as described elsewhere while the other hemisphere was utilized for histochemical staining using thioflavin. Sagittal sections (12 μ m) were mounted onto charged glass slides, placed in 4% PFA for 10 minutes, transferred to TRIS buffer for 5 minutes and then allowed to dry before being subjected to a citrate buffer antigen retrieval protocol. Briefly, slide mounted sections were incubated for 40 minutes in a 100^oC bath of sodium citrate buffer (10 mM sodium citrate, 0.05% Tween 20, pH 6.0) and allowed to cool for 20 minutes before PBS washing and blocking. Treated sections were then incubated for 30 minutes at 37^oC with a freshly prepared 1% thioflavin solution which was sonicated and passed through a .2 micron syringe filter prior to use. Following PBS washes, dehydration in a series of alcohols, and clearance in xylene, each slide was then cover-slipped using VECTASHEILD mounting medium (Vector Laboratories Inc., Burlingame CA, USA).

Determination of A β -aggregation Inhibitor Status Via the SensoLyte Assay

To investigate the ability of curcumin to perturb A β monomer aggregation, a commercially available thioflavin T-based aggregation kit with colorimetric readout was employed (AnaSpec). Of the two commercially available versions, the 96-

well plate-based assay employing synthetic A β ₄₂ was chosen due to the increased relevance of this isoform to AD pathogenesis. Generally speaking, all operations were performed in congruence with the protocol provided by the manufacture. Briefly, 1 mL of the proprietary assay buffer, chilled to 4⁰C, was added to .5 mg of A β ₄₂ peptide. Following hydration of the peptide sample (3 minutes), the reconstituted A β peptide was sonicated for 5 minutes at 4⁰C to complete dissolve the peptide and insure that monomerized A β species predominated in solution. Next, this sample was spun at 10,000 rpm for 5 minutes at 4⁰C to remove any precipitated material. With the A β sample prepared, 10 μ L of 2 mM thioflavin was added into each well. Subsequently, 5 μ L of curcumin was added to achieve a final concentration in solution of 200 μ M. Lastly, 85 μ L of A β ₄₂-containing assay buffer was added to each reaction vessel. Immediately upon mixing (Time = 0), fluorescence at 485 nm (excitation 440 nm) was measured. Following this baseline measurement, the 96-well plate was transferred to a 37⁰C incubator to expedite A β fibrillation. Subsequently, fluorescence for each well was measured in 10 minute intervals for 90 minutes. In addition to wells containing test compounds, several control conditions were also included. For example, wells containing only 100 μ L of assay buffer served as “blank” controls. “Vehicle controls” were also included in congruence with the manufacture’s protocol and were comprised of 85 μ L of A β -containing assay buffer, 10 μ L of thioflavin, and 5 μ L of a 20% DMSO solution.

Serum Bioavailability Analysis of Inhaled Curcumin

To confirm systemic uptake of curcumin following nebulization and assess the pharmacokinetics of our administration method, whole blood samples were collected from mice throughout the nebulization process via retro-orbital collection and assessed for curcumin content by HPLC. Whole blood samples were collected just prior to nebulization (T=0) and at 60, 120, and 300 minutes. Whole blood samples were allowed to clot at room temperature for one hour and centrifuged as described to yield serum samples. To facilitate extraction of curcumin, 100 μ L of acetonitrile was added to 100 μ L of serum, vortexed, and centrifuged at 20 xG for 20 minutes to remove any remaining cellular debris. 20 μ L of the resulting sample was then analyzed for curcumin content by HPLC. Briefly, after establishing the detection limit of the instrument at 10 nM and determining a concentration–response calibration curve, the amount of curcumin in the serum was

calculated by integrating the area under the curve using EZChrome Elite software (Hitachi). Notably, every retention time peak in the spectrum was collected and analyzed using LC–MS to verify the compounds identity.

Assessment of A β Plaque Burden by Thioflavin Histochemical Staining

To quantitatively assess the effect of chronic curcumin therapy on A β plaque burden in the brain, sagittal sections (n=50) isolated from nebulized 5XFAD mice and non-treated littermates (N=5 per group) were stained with 1% thioflavin as described. Fluorescence imaging of the hippocampus, subiculum, and neocortex were then acquired in the GFP channel. Automated quantification of A β plaque burden was performed for each slide using a custom image analysis script written in MATLAB (Mathworks, Natick, MA). In more detail, first, uneven background illumination is removed using morphological top-hat filtering. Second, the image contrast was enhanced to highlight plaques by nonlinear mapping. Third, a plaque mask was created using a user-defined spatially varying threshold based on the background illumination, which was then cleaned up using a morphological opening. Finally, manual ROIs were drawn around the hippocampus and subiculum and were selected to avoid histologic artifacts. From the ROI plaque masks, plaque morphologic parameters can be calculated. Plaque density is reported in mm⁻² and is defined as the number of plaques divided by the ROI area.

Lung Toxicity Analysis

To provide a preliminary assessment of pulmonic toxicity potentially attributable with curcumin inhalation, the lung tissue of acutely (N=3) and chronically nebulized (N=3) 6-month old 5XFAD mice were examined by a blinded pathologist. The “acute nebulization” cohort received one standard 5 mg/kg dose of curcumin as previously described and were sacrificed 24 hours post-exposure. In contrast, the “chronic nebulization” cohort received 48 5 mg/kg doses of inhaled curcumin over a 16-week time-period (3 doses/week). Just as in the acute nebulization cohort, mice in the chronically nebulized cohort received their last dose 24 hours prior to sacrifice. Immediately prior to sacrifice, cardiac perfusion was performed under 2% isoflurane as previously described. The trachea and lung tissues were then surgically dissected as a complete

unit, before being inflated with 10% formalin to facilitate observation of alveolar architecture. Briefly, following removal of the rib cage forceps were utilized to separate the trachea and esophagus. Next a 26-gauge syringe containing 10% formalin was used to penetrate the trachea and inflate the lung lobes. The inflated tissues were fixed in 10% formalin for 2 days before serial sectioning/slide mounting at 8 microns. H&E and Masson Tri-chrome staining was performed on each tissue section, with >50 microns between each section to ensure adequate sampling of the lung tissue (N=5 sections/mouse/stain). Both H&E and tri-chrome stained sections from each animal were reviewed by a blinded clinical pathologist for any pathological evidence of toxicity. Images used for quantitative analysis of collagen deposition were captured by traditional light microscopy methods (Visen FMT, PerkinElmer, MA, USA) at 10x & 20x magnification for respiratory bronchioles and lung parenchyma, respectively.

Quantitative analysis of collagen deposition in the respiratory bronchioles (N=20 per animal) and lung parenchyma (N=30 ROI per animal) were performed in ImageJ on Masson's tri-chrome stained lung tissue sections. Briefly, RGB stacks were generated from the original images and a uniform threshold applied to the red channel to facilitate isolation of the signal attributable to collagen. Next, regions of interest were manually drawn by a blinded investigator. Lastly, the area fraction of lung tissue comprised of collagen was calculated as the quotient of red pixels over the total number of pixels in the ROI.

Transmission Electron Microscopy Analysis of Neurite Diameter in Treated & Non-treated 5XFAD Mice

Ultrastructural analysis of neurite diameter in the CA3 hippocampal region of 6 month 5XFAD mice was performed using TEM. Two cohorts of 5XFAD were analyzed. Representing the treatment group, 6-week old 5XFAD mice were chronically administered a 5 mg/kg dose of aerosolized curcumin three times a week for 18 weeks (N=3). As a control, non-treated, sex-matched 6-month old 5XFAD mice were employed (N=2). Once of appropriate age, mice were perfused with 20 mL of a 0.1 M cacodylate/sucrose buffer to wash out extraneous proteins. Subsequently, cardiac perfusion with 2% PFA/2.5% Glutaraldehyde in 0.1M Cacodylate/Sucrose Buffer was employed to fix the tissues for TEM analysis. Brains were next surgically harvested and placed in 2%PFA/2.5% Glutaraldehyde in 0.1M Cacodylate/sucrose buffer for 2 hour at room temperature before being stored for 6 days overnight at 4⁰C. Using a scalpel, the hippocampal region of the brain was excised and subsequently rinsed in 0.1M Cacodylate buffer. The sample was then post-fixed with 1%

osmium tetroxide in 0.1M cacodylate buffer for 1 hour at room temperature, then overnight in refrigerator. After rinsing in 0.1M Cacodylate buffer, the sample was dehydrate through a graded series of ethanol in 15 minute intervals. Over the course of 3 days, the sample was embedded in TEM-compatible epoxy resin and then cut into thick sections (0.5 um) for analysis via light microscopy. This facilitated the identification of the CA3 sub-region, facilitating the shaving of ultrathin sections (70 nm) from the epoxy-embedded sample. Ultrathin sections were next post-stained with uranyl acetate for 15 minutes. These same samples were then subsequently stained with Reynolds lead citrate for 10 minutes. Lastly, each sample was examined by transmission electron microscopy (FEI Tecnai T-12 electron microscope) at 100 KeV.

Western Blot

Treated & Non-treated mice were anesthetized before undergoing brain perfusion with ice cold 1X PBS containing a protease inhibitor cocktail (Roche, Indianapolis, IN) in accordance with previously described methods. Following perfusion, the brain tissue was removed and homogenized in 2 mL of tissue lysate buffer containing protease inhibitor (Sigma-Aldrich, Saint Louis, MO). Brain homogenates were normalized for protein content using BCA assay (Pierce, Rockford, IL) and 20 µg of protein was run on 4-12% Tris-HCL SDS-PAGE gels (Bio-Rad, Hercules, CA). After transfer to polyvinylidene difluoride membrane, blots were incubated with 4G8 anti-A β monoclonal antibodies (Covance, Princeton, NJ) at 1:1000 overnight at 20⁰C. Peroxidase conjugated secondary antibodies (Pierce, Rockford, IL) were applied and immunoblot signals were detected by enhanced chemiluminescence and quantified using the Xenogen IVIS 200 bioluminescent and fluorescent imaging system.

Blood Chemistry Toxicity Analysis

To investigate the potential of systemic toxicity associated with curcumin administration, the blood serum of wild type mice (N=2/group) was analyzed following curcumin dosing via nebulization or tail-vein injection. Chemistry profiles (CPs) and complete blood counts (CBCs) from each treatment group were then compared to non-treated littermates. The I.V. injected cohort received a 5 mg/kg dose of curcumin in the form of a 150 µL bolus injection. Due to curcumin's

insolubility in biological solvents, a 1x PBS buffer containing 20% Tween-20 was used as a solvent for the bolus injection. Nebulization was performed as outlined in the corresponding methods section.

Prior to sample collection, mice were anesthetized using 2.5% isoflurane at 2L/min. Whole blood samples (~250 μ L) were then acquired via cardiocentesis using a 22-gauge needle. Once extracted, the needle was removed and each blood sample aliquoted into EDTA-containing or serum-clot tubes for CBC and CP analysis, respectively. Whole blood samples for CBC analysis were kept at 4⁰C until analysis. In contrast, CP blood samples were allowed to clot at 25⁰C for 1 hour. Following coagulation, serum for CMP analysis was acquired via centrifugation at 3700 G for 20 minutes at 4⁰C. Serum samples for CP analysis were stored at 20⁰C until use.

CBC analysis was performed via an automated hematology instrument. Automated CBC parameters included WBC count, RBC count, HCT, hemoglobin concentration, MCV, MCH, MCHC, and platelet count. Serum samples for CP analysis were transferred into microfuge tubes for clinical chemistry analysis by an automated analyzer.

Y-Maze Behavioral Assay

Y-maze study: In an effort to quantitatively assess the effect of inhaled curcumin on spatial-dependent and working memory in a pre-clinical mouse model of AD, the Y-maze behavioral assay was employed. Briefly, 6-week old 5XFAD mice (N=10) were chronically administered a 5 mg/kg dose of nebulized curcumin three times a week for 18 weeks. Two cohorts consisting of a group of age matched 5XFAD and a group of wild type mice (N= 10 per group) which remained in their home caging and were untreated throughout the study served as controls. Following a one week habituation period in the behavioral testing facility to decrease experimental confounds attributable to the animals' stress, working memory and spatial memory were assessed via Y-maze. All behavioral assays were run during the night cycle and all mice were allowed to habituate to the experimental environment for 3 hours prior to testing.

Working Memory Y-maze Paradigm: In this behavioral assay, spontaneous alteration was tested in a Y-shaped maze with three opaque plastic arms at a 120° angle from each other. In an effort to make each arm distinguishable to the animal, laminated sheets of uniquely patterned paper were fastened to the outside of the maze (Figure 10-3). These patterns

included a “black arm” surrounded completely with black background while a “dotted arm” consisted of alternating black and white vertical bars with a 2.5 cm width. Lastly, the third arm or “dotted arm” contained white circles with a 2 cm diameter on a black background. Prior to behavioral testing, rigorous controls were run on a naïve cohort of animals to insure no intrinsic preference for a particular arm existed. The entire maze was cleaned and dried thoroughly with ethanol both before and after each trial to insure standardized maze conditions. After introduction of the mouse into a standardized arm of the maze, the animal was allowed to freely explore the three arms for 6 minutes with the sequence of arm entries being recorded. The number of arm entries and the number of correct triads were recorded using ANY-maze behavior tracking software in conjunction with a CCD video camera system. Arm entries were logged when all four limbs of the animal crossed a line arbitrarily placed 50% down each of the three maze arms. A quantitative evaluation of working memory performance was made by calculating the percent spontaneous alteration for each animal. Possible confounds associated with differences in locomotion between cohorts were controlled for via comparison of the total number of arm entries.

Spatial-Memory dependent Y-maze Behavioral Assay: One week following completion of the working memory Y-maze behavioral assay, all animal cohorts were then tested in the spatial memory paradigm. To directly assess hippocampal function at the behavioral level, a two-phase Y-maze paradigm was employed. As in the working memory task, each arm of the Y-maze was decorated with spatial cues to increase the salience of each arm. Notably, quantification of the mean number of entries and seconds exploring each arm of the maze in a naïve cohort of animals confirmed no innate preference for any of the arms. Additionally, no differences in the initiative to explore were noted between any of the cohorts suggesting that any observed differences in behavior truly reflect alterations in spatial memory. During the first phase of this paradigm, the mouse was allowed to freely explore 2 of the three arms of the Y-maze for a 6 minute period. The arm which was blocked during this first phase was randomized between animals, and designated as the "novel" arm in the secondary phase of the study. Following the first period of exploration, each mouse was returned to its home cage and left undisturbed for a 30 minute period. Following this period of rest, each mouse was placed into a randomized arm of the maze and allowed to freely explore all three arms of the Y-maze for a 5 minute time interval. To quantitatively assess spatial memory, the proportion of time spent exploring the previously blocked "novel arm" arm was quantified and plotted

as the fraction of overall time spent exploring. All arms of the maze were cleaned with 70% ethanol both prior to and after each trial to insure standardized maze conditions between animals.

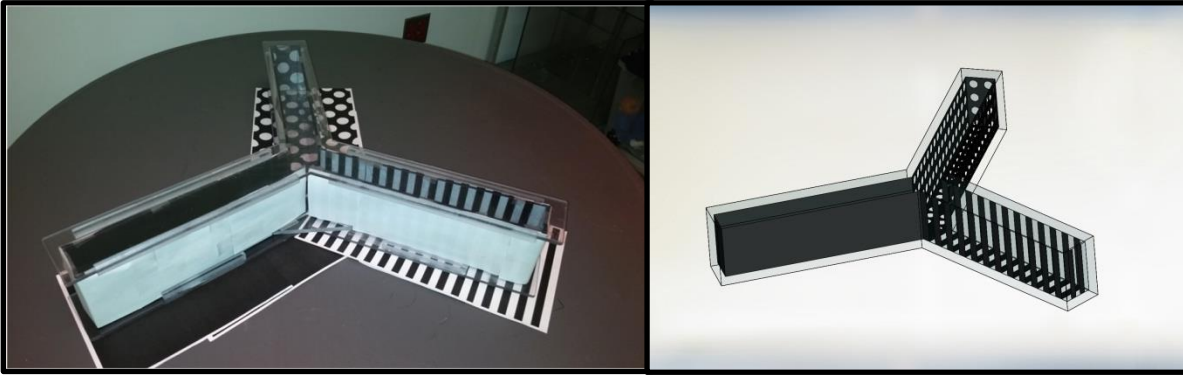


Figure 10-3. Actual (A) and Graphical Rendering (B) of Y-maze layout.

A Y-shaped maze with three opaque plastic arms at a 120° angle from each other was employed for behavioral testing. Laminated sheets of uniquely patterned paper were fastened to the outside of the maze to increase the salience of spatial cues for the mice. These patterns included a “black arm” surrounded completely with black background while a “dotted arm” consisted of alternating black and white vertical bars with a 2.5 cm width. Lastly, the third arm or “dotted arm” contained white circles with a 2 cm diameter on a black background. A CCD mounted camera mounted to the ceiling was used in conjunction with the AnyMaze software package to facilitate behavioral scoring.

Statistical analysis

All values were measured by independent experiments, conducted in triplicate, and represented as the mean \pm standard deviation. Statistical analysis was performed using a 2-tailed Student's t-test conducted with StatView for Windows Ver. 4.5 (Abacus Software) with a $p < 0.05$, which is considered to represent a statistically significant difference.

10.3 AIM 2 EXPERIMENTAL RESULTS

10.3.1 Result: FMeC1 Aerosol Crosses the Blood Brain Barrier and Binds to A β

Two cohorts of awake and alert 8-month-old mice, one comprised of C57BL/6 wild-type controls and a second of 5XFAD mice (n=5, each), were exposed by inhalation to a solution containing FMeC1 at a dose equivalent to a 5 mg/kg injection. One hour after respiratory exposure, trans-cardiac perfusion was performed prior to removal of the animal's brain, which was then processed for histological analysis. FMeC1 accumulation in the brain was assessed via wide-field fluorescence microscopy of FMeC1's intrinsic fluorescence at $\lambda_{\text{max}}=557$ nm. Critically, one hour following exposure via the inhalational route, no fluorescence signal from FMeC1 or anti-A β antibodies was detected in the brains of wild-type mice (Figure 10-4A, E). In contrast, we observed remarkable punctate fluorescence emitted by FMeC1 in the frontotemporal cortex and hippocampus, brain regions known to harbor robust A β plaque deposition in the 5XFAD mouse model (Figure 10-4B, F). Importantly, the signal detected in the 5XFAD mouse brain is distinct from background as auto-fluorescence measured in untreated 5XFAD cohorts is orders of magnitude below the fluorescence observed in the respiratory exposed 5XFAD brain sections. Impressively, fine details of the morphology of individual A β plaques are recognizable in higher magnification images (Figure 10-4C, G). Having demonstrated that respiratory exposed FMeC1 penetrates the BBB efficiently and is retained in the brain of A β -burdened mice, we then worked to confirm the binding specificity of FMeC1 for A β plaques. In this effort, immunohistochemical staining of A β plaques using fluorescent anti-A β antibodies was employed to co-localize the punctate fluorescence of FMeC1 with A β plaques. Here, we employed dual-fluorescence microscopy to image both FMeC1 deposition and A β plaques in the same section, relying on the GFP channel to image FMeC1 deposition and the Cy5 channel to image monoclonal anti-A β antibodies labeled with a near-infrared dye that provided a distinct absorption/emission profile. Of note, a high degree of co-localization was observed between the clusters of FMeC1 fluorescence and the signal emitted from the distinctly labeled anti-A β antibodies in both the hippocampus (Pearson's coefficient = 0.9, n=25) and frontotemporal cortex (Pearson's coefficient = 0.9, n=25) (Figure 10-4D, H). In addition to this quantitative analysis of FMeC1's A β -specificity, a representative line plot through image sets acquired in the GFP and Cy5 channels, for FMeC1 and A β antibodies, respectively, qualitatively demonstrates the high degree of corroboration between FMeC1 deposits and the location of A β plaques (Figure 10-4I). Overall, this data

confirms the ability of atomization technology to deliver A β -targeted diagnostics or therapeutics, such as FMeC1, to the brain. Furthermore, this work confirms that FMeC1 delivered to the brain via the respiratory route penetrates midbrain structures, such as the hippocampus and retains its binding specificity for A β plaques.

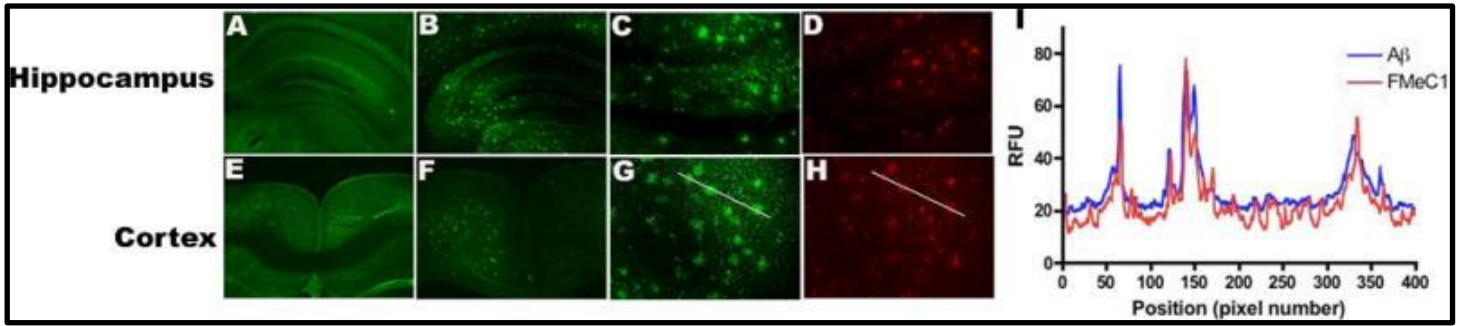


Figure 10-4. Internalization and A β -dependent Retention of Aerosolized FMeC1 in the Brain.

Cohorts of wild-type and 5XFAD mice (n=5, each) were respiratory exposed with a 5 mg/kg dose of FMeC1 and allowed to recover for one hour prior to cardiac perfusion and removal of the brain tissue. Note the absence of a GFP signal associated with deposits of FMeC1 associated with A β plaques in both the hippocampus (A) and isocortex (E) of respiratory exposed wild-type animals. In contrast, the hippocampus (B) and isocortex (F) of respiratory exposed 5XFAD mice show a robust deposition of FMeC1. At 20 \times magnification, the clusters of FMeC1 fluorescence (GFP channel) in the hippocampus (C) of respiratory exposed 5XFAD mice co-localizes profoundly (mean Pearson's coefficient = 0.9, n=25) with anti-A β antibody staining (Cy5 channel) within the same coronal section (D). Similarly impressive co-localization of FMeC1 (G) and anti-A β antibody (H) generated fluorescence was observed in the isocortex (mean Pearson's coefficient = 0.9, n=25). (I) Line plot of pixel intensity as a function of image coordinates along the white line overlaid on subfigures (G) and (H). Peaks in signal intensity in the Cy5 channel (anti-A β antibodies) reflect A β plaque deposits and are highlighted in blue. For all A β plaque deposits, FMeC1 fluorescence intensity is increased in magnitude almost identically to fluorescence changes in the anti-A β antibody channel. Overall, these data confirm that respiratory exposed FMeC1 is delivered to the brain across the BBB, associates with A β plaques and is retained in the brain in an A β -dependent manner.

10.3.2 Result: Enhanced Bioavailability of FMeC1 in the Brain by Atomization Versus I.V. Injection

To compare the biodistribution of FMeC1 in the brain by inhalation versus I.V. injection and assess whether FMeC1 deposition significantly increased in regions that harbor A β plaques, high-throughput ex vivo brain imaging was employed. Briefly, respiratory exposed 5XFAD and wild-type, and I.V. injected 5XFAD cohorts (n=5 per group) were similarly dosed with FMeC1 (5 mg/kg) via their respective administration method. One hour after treatment, all mice were subjected to cardiac perfusion and their major organs promptly removed and processed for sectioning using the protocols we reported in the past.^(970, 1042) In this work, we employed the Visen 3D imaging system (PerkinElmer) to perform high-throughput imaging of multiple slide-mounted brain slices. Using this experimental configuration, the global FMeC1 distribution in each cohort was assessed via fluorescence imaging ($\lambda=557$ nm) of brain slices containing midbrain structures of interest such as the hippocampus. Then, employing NIH ImageJ software, isocortical and hippocampal regions of interest were manually selected by a blinded collaborator and quantitatively evaluated for mean fluorescence intensity. As illustrated in Figure 10-5A, a higher FMeC1-derived fluorescence signal is readily appreciable in the isocortex of 5XFAD mice as compared wild type mice following the administration of FMeC1 either by I.V. or atomization (p=0.02 & p<0.001, respectively). Similarly, the A β -plaque dependency of FMeC1 retention holds in the hippocampus, where both I.V. and respiratory exposed 5XFAD mice demonstrate greater FMeC1 fluorescence signals as compared to respiratory exposed wild-type controls (p=0.002, p=0.002, respectively) (Figure 10-5B). Interestingly, the brains of both I.V. injected and respiratory exposed 5XFAD mice exhibit a similar topographic retention of FMeC1 in A β plaque-laden regions, which alludes strongly to an amyloid dependency with respect to FMeC1 retention in the brain. In contrast, no differences in the FMeC1 signal were detected in non-amyloid-burdened brain regions such as the hypothalamus. As perhaps the best illustration of the amyloid dependency of FMeC1 retention, FMeC1 fluorescence measured from the hippocampus or cortex of respiratory exposed 5XFAD mice was significantly greater than that of the thalamus (n=60, p<0.001) (Figure10-5B). Notably, the result of interregional analysis is markedly different within the wild-type cohort, with no statistically significant differences were noted between any of the analyzed regions. Again, taken as a whole, these results confirm the specificity of respiratory exposed FMeC1 for A β plaque as well as the ability of FMeC1 to report A β plaque load in the brain with regional specificity. Lastly, when comparing the FMeC1 signal

measured in the isocortex of I.V.-injected and respiratory exposed animals, it is interesting to note that a modest, yet statistically insignificant improvement in FMeC1 delivery is achieved by implementing inhalation technology ($p < 0.05$).

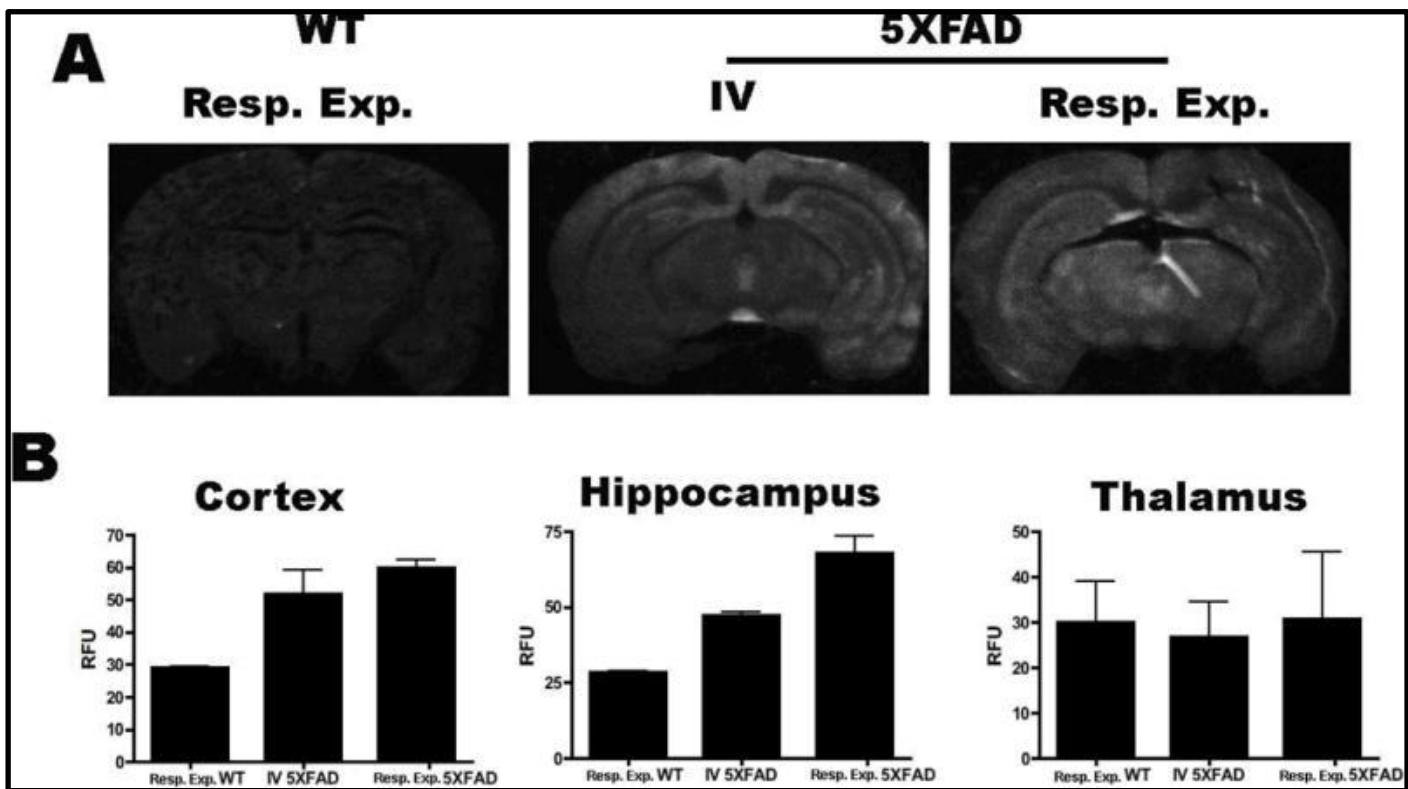


Figure 10-5. Internalization and A β -dependent Retention of Aerosolized FMeC1 in the Brain.

Cohorts of wild-type and 5XFAD mice (n=5, each) were respiratory exposed with a 5 mg/kg dose of FMeC1 and allowed to recover for one hour prior to cardiac perfusion and removal of the brain tissue. Note the absence of a GFP signal associated with deposits of FMeC1 associated with A β plaques in both the hippocampus (A) and isocortex (E) of respiratory exposed wild-type animals. In contrast, the hippocampus (B) and isocortex (F) of respiratory exposed 5XFAD mice show a robust deposition of FMeC1. At 20 \times magnification, the clusters of FMeC1 fluorescence (GFP channel) in the hippocampus (C) of respiratory exposed 5XFAD mice co-localizes profoundly (mean Pearson's coefficient = 0.9, n=25) with anti-A β antibody staining (Cy5 channel) within the same coronal section (D). Similarly impressive co-localization of FMeC1 (G) and anti-A β antibody (H) generated fluorescence was observed in the isocortex (mean Pearson's coefficient = 0.9, n=25). (I) Line plot of pixel intensity as a function of image coordinates along the white line overlaid on subfigures (G) and (H). Peaks in signal intensity in the Cy5 channel (anti-A β antibodies) reflect A β plaque deposits and are highlighted in blue. For all A β plaque deposits, FMeC1 fluorescence intensity is increased in magnitude almost identically to fluorescence changes in the anti-A β antibody channel. Overall, these data confirm that respiratory exposed FMeC1 is delivered to the brain across the BBB, associates with A β plaques and is retained in the brain in an A β -dependent manner.

10.3.3 Result: Bio-distribution of Inhaled FMeC1 Differs from I.V. Injection

To corroborate our ex vivo imaging data, which demonstrated that atomization of an FMeC1-containing aerosol can deliver diagnostic or therapeutic compounds to the brain with an efficacy similar to that of I.V. injection but without associated toxicity, we quantitatively compared the biodistribution of FMeC1 in all major organs following the administration of a 5 mg/kg dose by either administration method. As in previous atomization administration experiments, the awake and alert mice were kept in the inhalation chamber, which was attached to the atomizer via the nosecone. By comparison, I.V. administration of the FMeC1 solution was accomplished via the caudal vein. One hour after I.V. injection or the completion of respiratory dosing, animals were sacrificed and their major organs surgically isolated and processed for FMeC1 extraction using methods previously described. Briefly, liquid-liquid extraction was employed to isolate FMeC1 into an acetonitrile organic layer from individual tissues homogenized in 1.0 mL of PBS. Following additional processing, the acetonitrile-PBS solvent was removed from the FMeC1 via lyophilization. This resulted in an FMeC1 residue that could be reconstituted in 30 μ L of 1:1 acetonitrile: PBS for concentration analysis using a spectrophotometer. While this protocol facilitates the isolation of FMeC1 from each tissue, it also allows the total tissue FMeC1 to be concentrated into a minimal volume, which ensures the sample absorption falls into the linear range of the Beer-Lambert plot for FMeC1. To avoid overestimating the mass of FMeC1 deposited in each organ secondary to absorption by proteins intrinsic to the tissue, each measurement was normalized to similarly processed control samples isolated from untreated 5XFAD mice. Using these techniques, in a comparison of two age-matched 5XFAD mice cohorts (8 months, n=3, each), quantitative analysis of the mass of FMeC1 in the brains of mice injected with a 5 mg/kg bolus (mean = 630 ng FMeC1/g tissue) did not differ significantly from the amount retained in the brains of the respiratory exposed cohort (mean= 567 ng FMeC1/g tissue) (p=0.6) (Figure 10-6A). Interestingly, comparison of the FMeC1 mass retained in the brains of the respiratory exposed 5XFAD cohort with that of a similarly treated cohort of age-matched wild-type mice revealed a greater deposition and retention of FMeC1 in the brain of the 5XFAD cohort (2 ng versus 567 ng FMeC1/brain). Again, this result corroborates our ex vivo imaging studies and suggests an amyloid-dependent retention of FMeC1 in the brains of A β -plaque-expressing 5XFAD animals (p=0.005). Cumulatively, this analysis confirms that respiratory exposed FMeC1 is delivered and preferentially retained in the brains of 5XFAD mice in an A β -dependent manner, and with an efficacy similar to that achieved via I.V. injection.

In addition to confirming that inhalation efficaciously delivers FMeC1 to the brain, our tissue-specific analysis of FMeC1 deposition provided additional insight into the biodistribution pathways employed during atomization. As expected, FMeC1 deposition in the lungs of respiratory exposed cohorts, both 5XFAD ($p=0.009$) and wild-type ($p=0.003$), was significantly greater than that of I.V.-injected animals (Figure 10-6A). Cumulatively, the data suggest that two major pathways are utilized for the delivery of FMeC1 during atomization. First, aerosolized FMeC1 is likely directly transported to the brain following deposition onto the nasal mucosa and is subsequently transported in a retrograde manner along trigeminal and olfactory neurons. Secondly, a fraction of respiratory exposed FMeC1 likely deposits in the lungs and nasal mucosa, and is subsequently conveyed to the blood stream, where it avoids the deleterious effects of first-pass metabolism associated with enteric administration methods. Combined, these biodistribution pathways result in a cumulative deposition of FMeC1 in the brain via atomization which is at least as efficacious as that of I.V. injection. Interestingly, approximately 0.25% of the original 5 mg/kg dose reaches the brain, a figure similar to that reported in previous studies.⁽¹⁰⁴⁷⁾ However, the major advantage of drug administration via atomization is the robust reduction in toxicity, since the system shock associated with bolus injection is avoided. In fact, during the course of this work, the I.V. injection of high doses of curcumin and related analogs produced mortal toxicity in approximately 50% of the mice. Moreover, that systemic toxicity is well reflected in the significantly elevated FMeC1 load measured in the liver ($p=0.01$) and kidneys ($p=0.004$) of I.V.-dosed mice as compared to the respiratory exposed cohorts. By comparison, no toxicity was observed in any mouse dosed using the atomization protocol described in this study; an observation is in line with the previous study reported by Minko et al.⁽¹⁰⁴⁸⁾

To corroborate our biodistribution studies and demonstrate the potential of capitalizing on FMeC1's perfluoro labeling for the detection of amyloid plaques, the concentration of FMeC1 in the brain was calculated using ^{19}F NMR spectroscopy. In that effort, 5XFAD mice ($n=4$) were respiratory exposed with a 5mg/kg dose of FMeC1 and perfused prior to removal of the brain tissues for homogenization. The FMeC1 was then extracted from the homogenized lysate samples and reconstituted in deuterated chloroform to facilitate detection by ^{19}F NMR. The acquisition of a quantitative NMR experiment typically does not require any special pulse sequences or new parameter settings. Nevertheless, attention must be paid to standard parameter settings such as the excitation pulse length and recycle delay. The ^{19}F NMR experiment for this sample was acquired for 15 hours (31,000 scans) and revealed a single peak at -68.33 ppm (Figure 10-

6B). Notably, our ability to detect FMeC1 in the brain following inhalation might prove a major advance with respect to AD diagnostics, as this work represents the first time the compound has been delivered at biologically relevant concentrations in the brain without severe life-threatening toxicity.

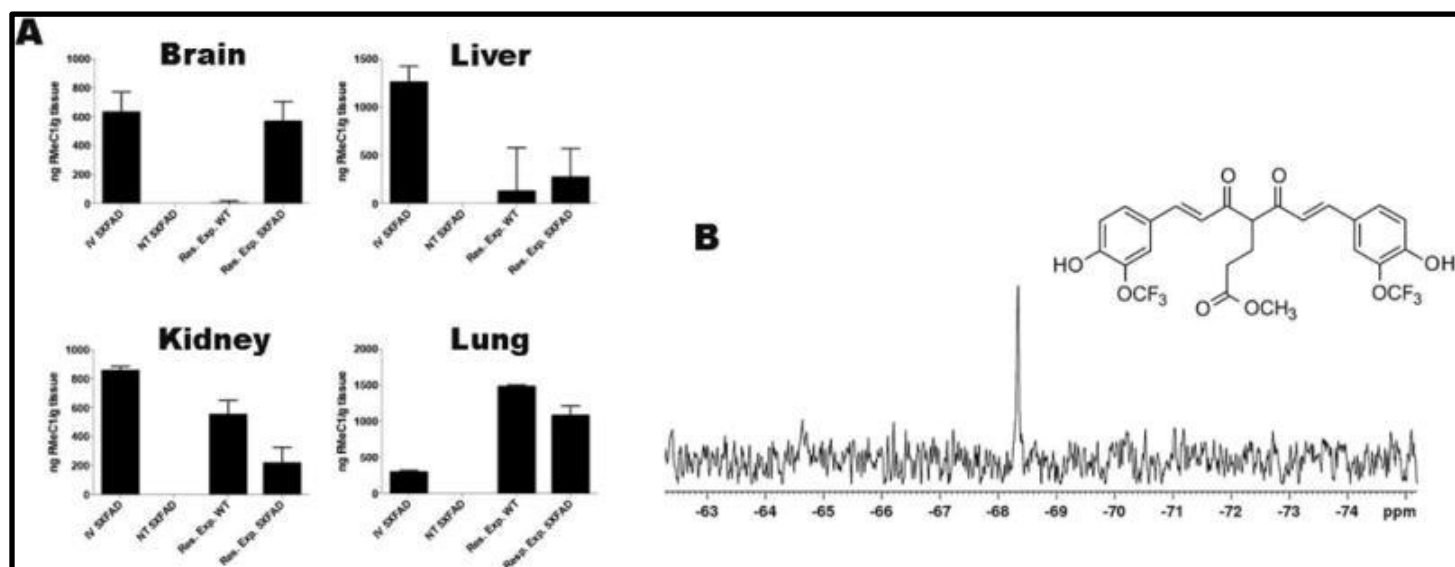


Figure 10-6. Biodistribution of FMeC1 by IV and Atomization.

(A) Equivalent doses of FMeC1 (5 mg/kg) were administered by iv injection or atomization. One hour after dosing, FMeC1 was isolated from each homogenized tissue using liquid-liquid extraction. Total FMeC1 mass was calculated using standard spectrophotometric methods. (A) FMeC1 mass retained in the brain. Respiratory exposed and iv-dosed 5XFAD mice retained significantly greater amounts of FMeC1 compared to untreated 5XFAD controls ($p=0.005$, $p=0.01$, respectively). Correspondingly, respiratory exposed 5XFAD mice retained greater FMeC1 in the brain compared to similarly treated wild-type mice ($p=0.005$). These results confirm the $A\beta$ plaque dependency of FMeC1 retention. (B) FMeC1 mass retained in the liver. The livers of respiratory 5XFAD and wild-type cohorts exhibited no difference in FMeC1 mass compared to untreated controls. The iv-injected mice demonstrated elevated levels of FMeC1 in the liver compared to untreated animals ($p=0.01$). (C) FMeC1 mass retained in the kidney. No significant difference in FMeC1 retention was measured in the kidneys of respiratory exposed and untreated mice. The livers of iv- injected mice showed enhanced FMeC1 retention as compared to untreated cohorts ($p=0.04$). (D). FMeC1 mass retained in the lung. Respiratory exposed 5XFAD and wild-type cohorts retained greater masses of FMeC1 compared to untreated controls ($p=0.009$, $p=0.03$, respectively). (B) Fluorine NMR spectroscopy was used to detect FMeC1 compound extracted from the brains of respiratory route exposed 5XFAD mice.

10.3.4 Result: Bioavailability of Aerosolized Curcumin in the Serum Exceeds that of I.V. Injected Doses

Having demonstrated that aerosol-mediated delivery results in an equivalent or perhaps slightly improved delivery of FMeC1 to the brain as compared to I.V. injection, we sought to apply this dosing approach to the therapeutic delivery of curcumin. To confirm systemic uptake of curcumin following nebulization and assess the pharmacokinetic profile of our administration method, whole blood samples were collected from mice (N = 3) throughout the nebulization process via retro-orbital collection and assessed for curcumin content by HPLC. Similarly, blood was sampled from mice treated with an equivalent dose of curcumin via oral (N = 3) or intravenous routes (N = 3). Whole blood samples were collected just prior to nebulization (T=0) and at 60, 120, and 300 minutes. For the P.O. and I.V. conditions, blood collection also began immediately prior to dosing and thereafter at varying intervals for 9 hours. Once collected, the curcumin from each blood sample was extracted in acetonitrile and analyzed via HPLC. To do this, a concentration–response calibration curve (Figure 10-7A) was constructed for pure curcumin. Using this curve, the amount of curcumin in the serum was calculated by integrating the area under the curve using EZChrome Elite software (Hitachi).

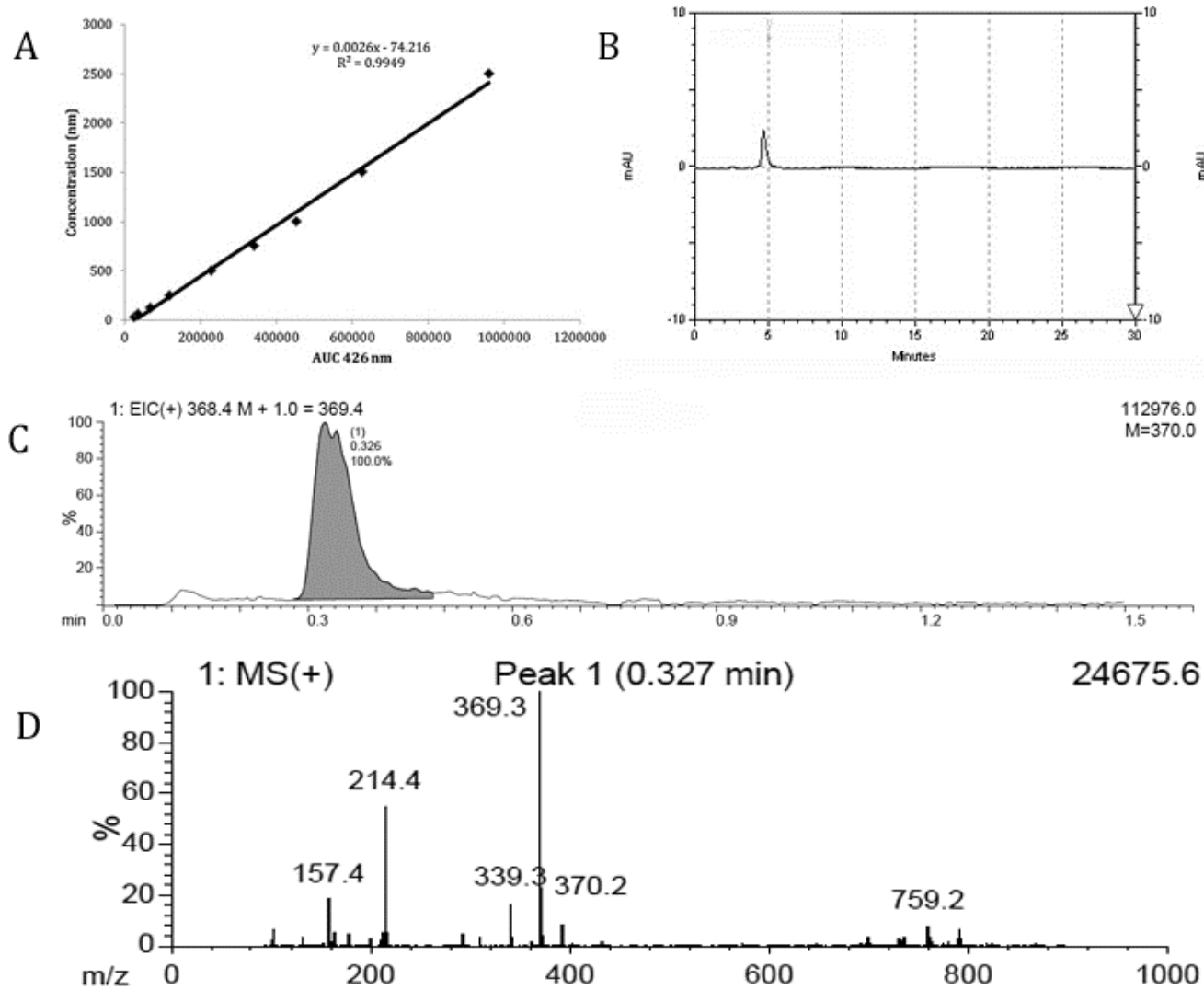


Figure 10-7. Validation of Curcumin Plasma Quantification Method.

To facilitate quantification of plasma curcumin levels achieved via I.V. injection, oral administration, or inhalation, plasma samples were prepared for analysis via HPLC. Briefly, whole blood samples were allowed to clot at room temperature for one hour. To facilitate extraction of curcumin, 100 μ L of acetonitrile was added to 100 μ L of plasma, vortexed, and centrifuged at 20 xG for 20 minutes to remove any remaining cellular debris. 20 μ L of the resulting sample was then analyzed for curcumin content by HPLC. (A) A concentration–response calibration curve for curcumin. (B) HPLC of plasma curcumin extractions revealed a single peak at a retention time of 4.86 seconds. This result precisely matches that achieved when pure curcumin is analyzed. Subsequent analysis of each sample via mass spectrometry of the plasma extracted curcumin samples confirmed the validity of our analysis (C) and (D).

Graphically depicted in Figure 10-8, comparison of the pharmacokinetic profiles of aerosol-, intravenously- and orally-administered curcumin reveal a number of striking differences. First describing the general features of each graph, as expected, I.V. delivery of curcumin results in an immediate spike in plasma concentration which exponential decays secondary to curcumin clearance/uptake by the peripheral organs. Predictably, I.V. injection results in the highest peak plasma concentration of all the administration methods tested, with a mean maximum of 454.96 mcg/mL at 5 minutes post-injection. By comparison, peak plasma levels of curcumin for P.O. and aerosol-mediated dosing achieve only 17.68% and 65.19% of this concentration, respectively. Thus, in congruence with the published literature, gastrointestinal absorption of curcumin in our study is characterized by inefficient yet rapid, occurring in under an hour, transmission to the plasma.⁽¹⁰⁴⁷⁾ In contrast to both P.O. and I.V. administration methods, the concentration of curcumin in the plasma of aerosol-dosed mice increases as a function of time, reaching peak levels after 6 hours of dosing. Once the nebulization process is halted, in this example at the 360 minute time point, plasma curcumin is immediately cleared at a rate similar to that observed in I.V. injected mice (Table 10-2). Importantly, this pharmacokinetic profile matches precisely that predicted for pulmonary absorption of curcumin and thus supports our model that aerosolized curcumin is predominately absorbed via the respiratory epithelium. Moreover, these results mechanistically explain how aerosol-mediated delivery can outperform I.V. injection with respect to drug delivery to the brain. Although peak serum levels of curcumin after I.V. administration are approximately 150% that of aerosol-mediated delivery, these elevated levels are only sustained for a matter of minutes. In fact, only five minutes after peak plasma concentrations are reached, curcumin levels in the blood drop to just 46.89% of their crowning value. Put another way, serum concentrations of curcumin above 400 nM are only sustained for a 5-10 minute period when administered intravenously. Applying this same analysis to aerosol-mediated delivery, it is clear that peak plasma concentrations are sustained for an extended period of time. Again selecting an arbitrary threshold of 400 nM, aerosol-mediated delivery maintains this elevated concentration in the blood for just under 2 hours. The significance of this analysis is that these differences between I.V. and aerosol-mediated delivery are the primary factors underlying the observed trends in absolute bioavailability. As noted in Table 10-2, the absolute bioavailability achieved via inhalation is 2.62 times that of I.V. injection, which by definition represents 100% bioavailability. Of note, the significantly increased bioavailability of curcumin ($P < .001$) following inhalation might be attributable to decreased clearance, continued absorption, or a combination of both factors. In a manner which decreases the likelihood of the first option, the elimination rate constant (K_{elim}), half-life ($T_{1/2}$), and clearance (CL) of curcumin is

nearly identical between administration methods. Thus, the data strongly suggests that increases in bioavailability achieved via inhalation are secondary to the sustained absorption of curcumin from the lung parenchyma into the bloodstream.

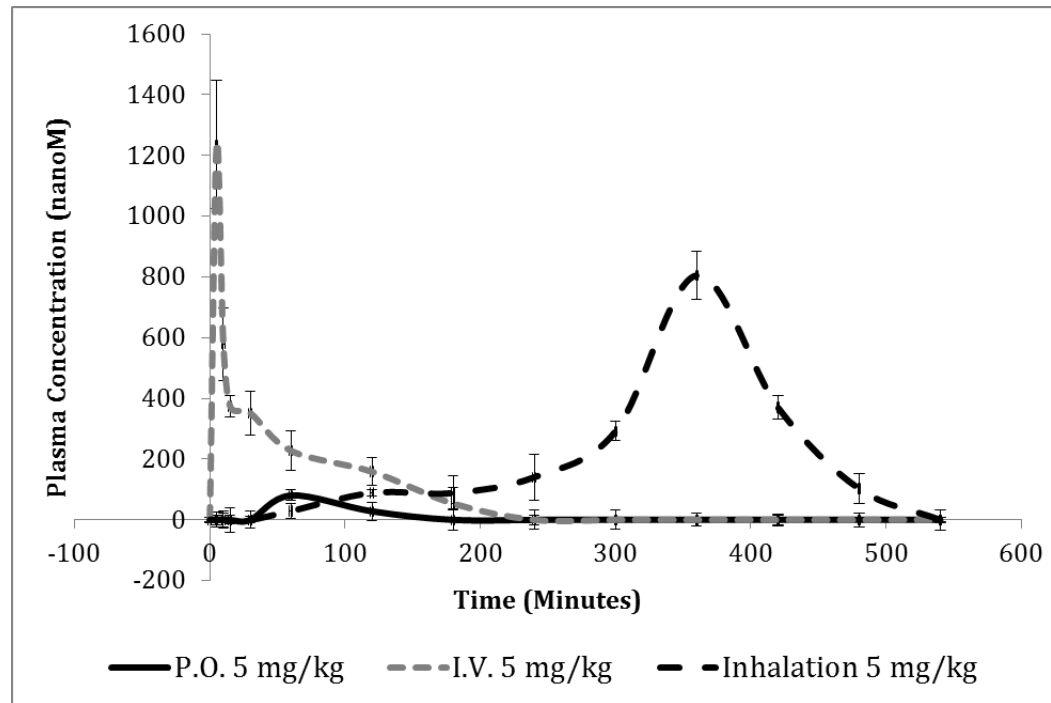


Figure 10-8. Bioavailability of Curcumin Following I.V., P.O., and Aerosol-mediated Dosing Paradigms.

Three cohorts of mice received an equivalent 5 mg/kg dose of curcumin via the administration routes listed. Whole blood samples were collected via retro-orbital bleeding over a 9 hour time window. Samples were next processed for analysis of curcumin content via HPLC. Analysis of the resulting data was plotted as a function of time. Statistical analysis of the area under each curve was utilized to calculate a percent bioavailability for each administration method. Impressively, aerosol-mediated delivery achieved an absolute bioavailability of 262%, supporting our conclusion that this administration method has robust therapeutic potential.

Table 10-2. Pharmacokinetic Parameters of P.O., I.V. and Aerosol-mediated Curcumin Delivery

Pharmacokinetic Parameters of P.O., I.V. and Aerosol-mediated Curcumin Delivery						
Administration Method	C _{max} (mcg/mL)	T _{max} (min)	T _{1/2} (hours)	K _{elim} (hr ⁻¹)	Absolute Bioavailability	CL (mL/hr)
I.V.	454.96	5	0.68	1.026	100%	0.46
Inhalation	296.59	360	0.67	1.031	262.38%	0.39
P.O.	80.45	60	0.66	1.051	12.16%	3.83

10.3.5 Result: Curcumin Perturbs A β Fibrillation in vitro

To investigate the ability of curcumin to perturb A β monomer aggregation, a commercially available thioflavin T-based aggregation kit with colorimetric readout was employed (AnaSpec). Packaged in a 96-well plate-based format, the SensoLyte A β_{42} aggregation kit provides a standard method to measure A β_{42} aggregation using Thioflavin T dye. In principal, the assay employs thioflavin's increased fluorescence in the presence of amyloid fibrils as a reporter of A β peptide aggregation. Importantly, the A β_{42} peptide is pretreated to ensure it is in a monomeric state, allowing increased thioflavin fluorescence to be correlated with A β fibrillation. As demonstrated by Figure 10-9, in the presence of only buffer, thioflavin fluorescence grows steadily as a function of time as A β fibrillation proceeds. At the 40 minute time point, equilibrium between monomeric and higher-order A β species is reached, resulting in the observed plateau in thioflavin fluorescence. The fluorescence curves produced by thioflavin and A β_{42} mixtures in the presence of known A β aggregation inhibitors such as Morin, phenol red, and resveratrol are markedly different. Most significantly, the plateau in thioflavin fluorescence is dramatically reduced under these conditions as compared to the buffer control. A similar yet attenuated trend is observed in the curcumin condition, with the addition of this putative therapeutic to A β -monomers resulting in a 28.46% reduction in thioflavin fluorescence. Interpreted as a whole, the results suggest that curcumin perturbs A β aggregation, albeit to a lesser degree than the control compounds listed, and thus merits further investigation as a potential therapeutic for AD.

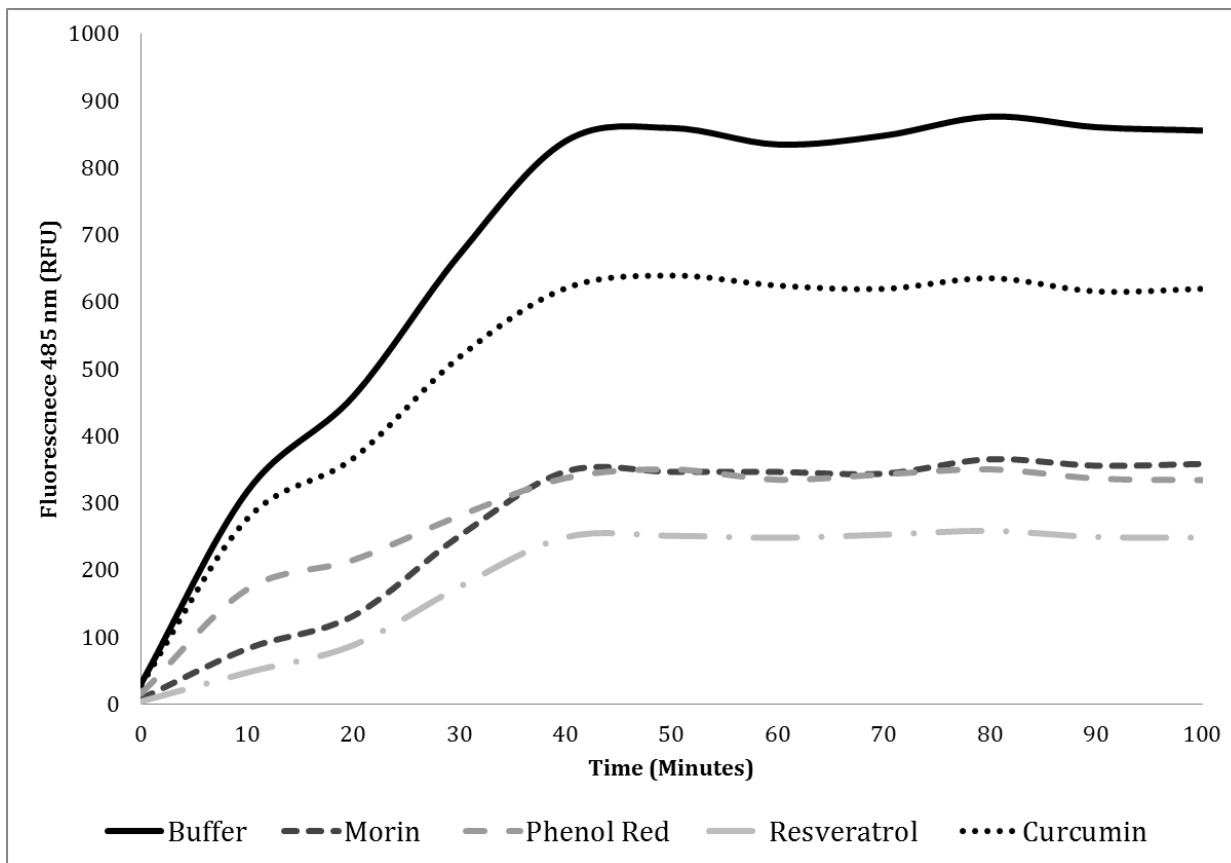


Figure 10-9. Curcumin Inhibits Aggregation of A β ₄₂ Monomers.

A colorimetric assay facilitating the identification of A β aggregation inhibitor activity was used to investigate the ability of curcumin to perturb A β monomer aggregation. Briefly, thioflavin and monomerized A β ₄₂ peptide were incubated in the presence and absence of known and putative A β -aggregation inhibitors. Thioflavin fluorescence at 485 nm serves as a reporter of A β fibrillation, with increasing fluorescent signal representing an increased availability of A β fibrils in solution. As illustrated, in the presence of curcumin, A β -fibril induced increases in thioflavin fluorescence only reached 71.54% of that measured from the positive control condition (buffer only). Interpreting this finding, the data strongly suggests that curcumin perturbs A β aggregation.

10.3.6 Result: Inhaled Curcumin Perturbs A β Fibrillation and Reduces A β -plaque Burden in vivo

Having comprehensively demonstrated the enhanced bioavailability of aerosol-mediated drug delivery, we next evaluated the ability of this administration method to recapitulate curcumin's therapeutic efficacy in a preclinical mouse model of AD. To facilitate this work, A β -plaque burden was assessed in the brains of two distinct cohorts of 6-month-old 5XFAD mice. Constituents of the treated cohort (N=5) received a 5 mg/kg dose of curcumin three times a week by inhalation for 18 weeks beginning at 6 weeks of age while non-treated littermates (N=5) served as controls. Importantly, this design obviates confounds associated with treating too late in the disease process, as detectable A β burden is not seen in 5XFAD mice until 2-3 months of age. To quantitatively assess the effect of chronic curcumin therapy on A β plaque burden, sagittal sections (n=50) isolated from nebulized 5XFAD mice and non-treated littermates (N=5 per group) were stained with 1% thioflavin as described and quantified using a custom plaque segmentation algorithm designed in Matlab. Three pathologically relevant regions of interest were selected for analysis. In support of our hypothesis that inhaled curcumin can reach therapeutically relevant concentrations in the brain parenchyma, analysis of the data reveals that A β plaque burden in the cortex of treated 5XFAD mice is just 31.59% that of non-treated age-matched littermates (Figure 10-10).

Transitioning to more pathologically relevant regions of interest in the brain, automated plaque counting performed in the hippocampus of treated mice revealed that this cohort contained less than 10% of the mean A β burden carried by non-treated littermates. Put differently, prophylactic curcumin treatment administered via inhalation significantly reduced A β number by 90.72% ($P < .001$). Not surprisingly these trends led to statistically significant differences in A β plaque density between treated and non-treated cohorts ($P < .001$). To assess this parameter quantitatively, the total area of A β deposition was divided by the total tissue area in each region of interest and multiplied by 100 to generate a percentage which we termed the plaque fraction. Analysis of this variable in the hippocampus of non-treated mice produced a value of .26%. By comparison, this variable is significantly reduced in treated 5XFAD mice as the area of A β plaque deposition comprises just .05% of the total tissue area ($P < .001$). Most likely, this trend reflects the ability of curcumin to inhibit the aggregation of A β ; as confirmed by our previously presented in vitro findings. In favor of this model, the mean area of each A β plaque in treated 5XFAD mice is significantly reduced as compared to controls, 32.96 μm^2 versus 68.60 μm^2 , respectively ($P < .001$). Interestingly, the area and diameter of the largest hippocampal A β plaques in treated 5XFAD mice were also significantly reduced in size as compared to those measured in the non-treated

cohort ($P < .001$). In more detail, the top 5% of plaques in treated 5XFAD mice were characterized by a mean diameter of 10.8 μm and mean area of 154.76 μm^2 . For comparison, these measurements obtained for these parameters in age-matched non-treated littermates were 8.78 μm and 530.55 μm^2 , respectively. Taken together, these findings suggest that the observed reductions in mean plaque diameter are exclusively a consequence of large diameter plaque loss, as no significant differences in the diameter or area of the smallest fraction of A β plaques were noted between cohorts.

Impressively, similar therapeutic benefits of inhaled curcumin were observed in the subiculum, the main output of the hippocampus and the region harboring the earliest and most profound neuron loss in the 5XFAD mouse model.⁽¹⁰⁴⁹⁾ In this region of pathological interest, A β plaque burden was significantly reduced by a margin of 79.48% compared to non-treated littermates ($P < .001$). In a manner consistent with curcumin's ability to perturb A β aggregation, statistically significant differences ($P < .01$) in mean plaque diameter and area for the largest A β plaques were observed (16.44 μm versus 21.84 μm and 249.29 μm^2 versus 384.50 μm^2 , for treated and non-treated cohorts, respectively). Again, the loss of the largest A β assemblies appears to underlie differences in mean plaque diameter and area between cohorts, with treated 5XFAD mice exhibiting significantly smaller plaques on average as compared to non-treated littermates (9.37 μm versus 10.63 μm and 84.65 μm^2 versus 104.30 μm^2 , respectively). Predictably, these trends resulted in a statistically appreciable difference in plaque fraction between cohorts, with A β assemblies representing 1.27% of tissue area in non-treated mice but just .14% in treated littermates. Of note, no differences in the eccentricity of individual plaques was noted between treated and non-treated cohorts, suggesting that curcumin does not alter the morphology of A β assemblies in addition to reducing their size. Taken together, these results strongly suggest that aerosol-mediated delivery of curcumin reduces A β burden in the brains of 5XFAD mice and thus warrants further evaluation as a disease-modifying therapy for AD.

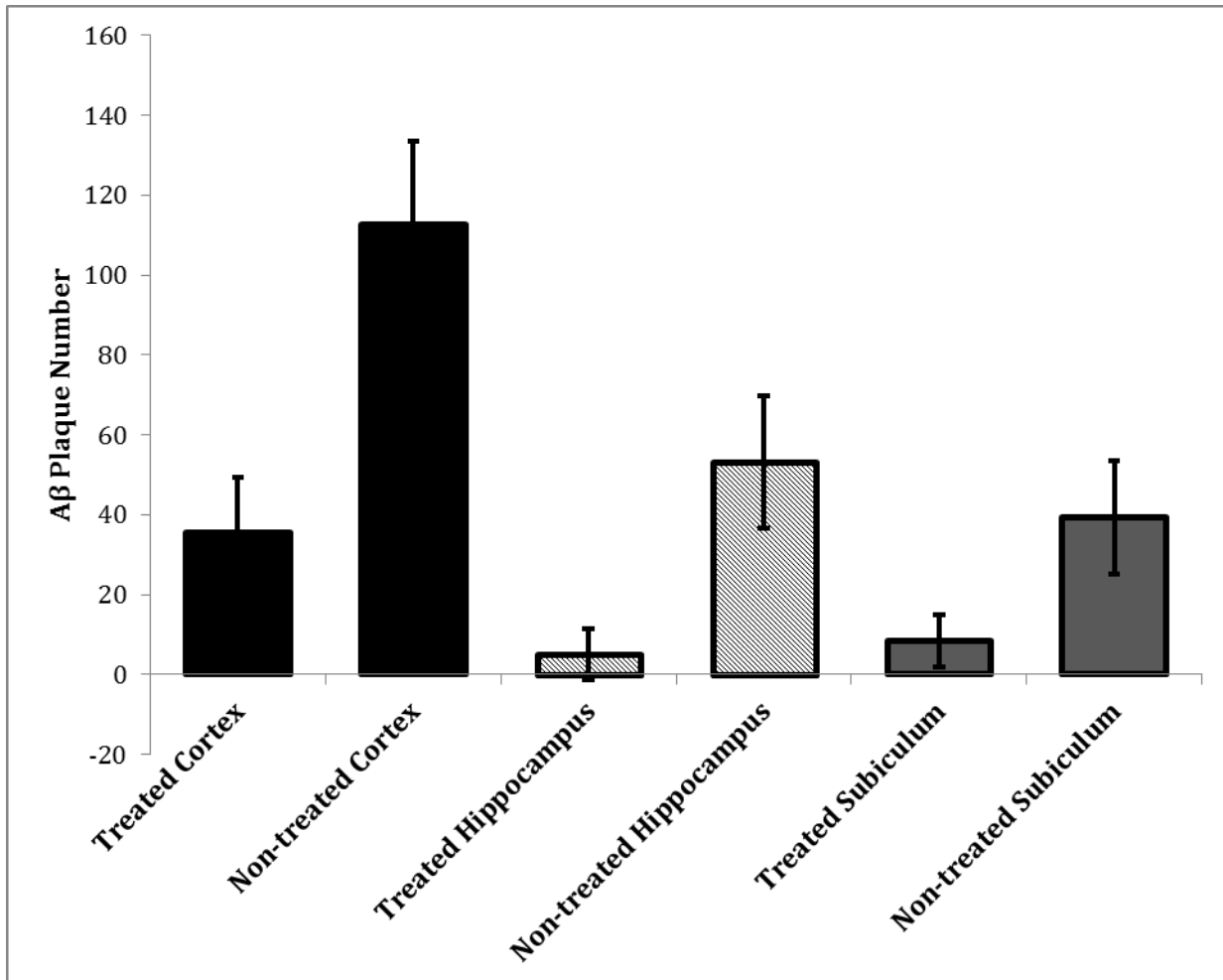


Figure 10-10. Aβ Plaque Burden is Reduced Via Chronic Curcumin Inhalation.

To quantitatively assess the effect of chronic curcumin therapy on Aβ plaque burden in the brain, sagittal sections (n=50) isolated from nebulized 5XFAD mice and non-treated littermates (N=5 per group) were stained with 1% thioflavin. Fluorescence imaging of the hippocampus, subiculum, and neocortex were then acquired. Quantification of Aβ plaque burden was performed in a blinded and automated fashion. As graphically illustrated, 4 months of prophylactic treatment with curcumin significantly reduced Aβ plaque number in the cortex, hippocampus, and subiculum by 68.75%, 90.72%, and 79.48%, respectively. Furthermore, reductions in the mean and maximum plaque diameter were noted in treated 5XFAD mice as compared to non-treated littermates in all regions analyzed. Importantly, these results are congruent with our finding that curcumin inhibits Aβ aggregation in vitro, and highlights the potential utility of inhaled curcumin for the prevention/treatment of AD.

10.3.7 Result: Prophylactically Inhaled Curcumin Prevents Dystrophic Neurite Formation

As described in previous chapters, A β assemblies exert a profound neurotoxic influence at the level of the synapse. Furthermore, as reviewed, a large body of literature suggests that the consequent loss of synaptic function secondary to A β accumulation correlates more robustly with the development of behavioral deficits than do estimates of total A β plaque burden. For these reasons, we investigated whether prophylactic curcumin administration via inhalation influenced the development of dystrophic neurites in the hippocampus. To investigate this key pathological feature of AD, ultrastructural analysis of neurite diameter in the CA3 hippocampal region was performed using TEM. As in related experiments, two cohorts of 5XFAD were analyzed (i) a treatment group comprised of 6-week old 5XFAD mice chronically administered a 5 mg/kg dose of aerosolized curcumin three times a week for 18 weeks (N=3) and (ii) a non-treated control group of sex-matched 6-month old 5XFAD mice (N=2).

Morphologically, dystrophic neurites are identifiable secondary to the accumulation of autophagic/lysosomal vesicles which increase their luminal diameter relative to healthy neurites. As illustrated in (Figure 10-11A/B), numerous swollen neurites in close proximity to A β assemblies are appreciable in the non-treated cohort. Interestingly, qualitative evaluation of the data revealed a virtually complete absence of dystrophic neurites in the brains of treated mice. In the non-treated cohort, dystrophic neurites were always associated with one of two A β -laden structures. The first of these structures is classically recognizable as a mature A β plaque as a consequence of its electron-dense core and the cross-hatched appearance of its surrounding penumbra. The second structure observed to be in proximity to dystrophic neurites were fibrillar A β deposits, identifiable under TEM by their characteristic cross-hatched morphology and lack of an electron-dense core. In an effort to objectively demonstrate the relative prevalence of dystrophic neurites between treated and non-treated cohorts of 5XFAD mice, the circular diameter of neurites within a 200 microns radius of CA3 pyramidal cell bodies were quantified. First considering the data obtained from non-treated 5XFAD mice, two Gaussian-distributed populations of neurites with distinct diameters are immediately identifiable. In congruence with the literature, healthy neurites, those lacking vesicles containing dense amorphous or multi-lamellar cellular debris, are characterized by a mean diameter of .5 microns.⁽¹⁰⁵⁰⁾ By comparison, in a manner faithfully reflecting their swollen morphology, a second population of dystrophic neurites was characterized by a significantly increased mean diameter of 4.5 microns (P < .001). Transitioning to the data obtained from curcumin treated 5XFAD mice, neither A β plaques nor associated populations of

dystrophic neurites could be identified in this cohort. Graphically this is demonstrated by the existence of only a single Gaussian distributed population of neurites with a mean diameter of .5 microns. Critically, the absence of A β plaques in the treated cohort not only corroborates the histochemical staining, but also suggests that beyond reducing A β - plaque load in the brain, prophylactic curcumin treatment also prevents A β plaque-associated neurodegenerative changes in the CA3 region of the hippocampus.

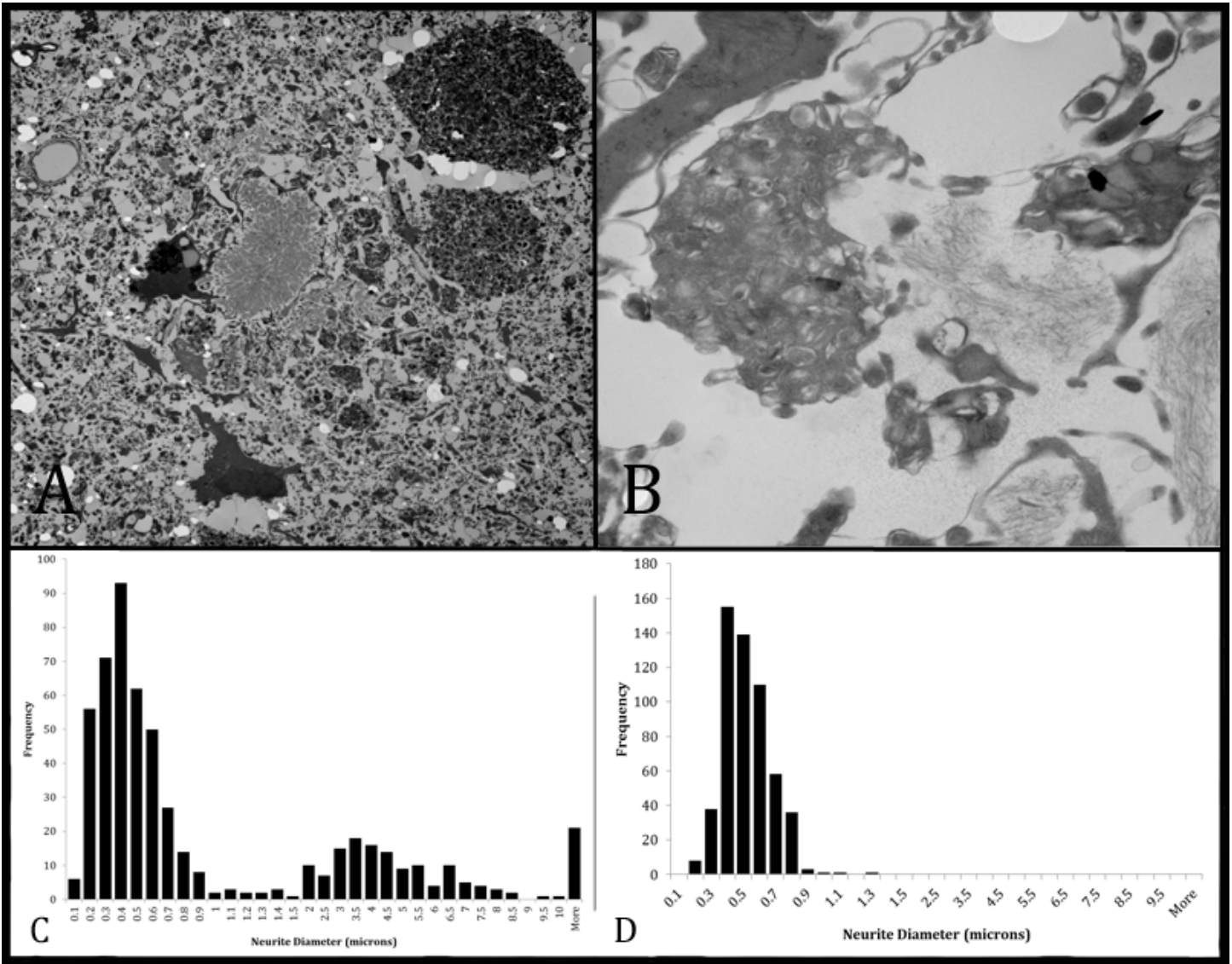


Figure 10-11. Ultrastructural Analysis of Neurite Diameter in the CA3 Hippocampal Region of Treated and Non-treated 6 month 5XFAD Mice

(A) Representative TEM image of a 6-month non-treated 5XFAD mouse illustrating a 5 micron A β plaque (asterisk) and associated neurodegenerative changes. Note that the lumen of each dystrophic neurite (arrow) is swollen relative to healthy neurites due to an abundance of autophagic/lysosomal vesicles containing dense amorphous or multi-lamellar cellular debris. (B) Representative TEM image of dystrophic neurites in close-association with fibrillary A β deposits in the CA3 region of the hippocampus in a 6-month non-treated 5XFAD mouse. (C) Histogram of CA3 pyramidal neurite diameter in non-treated 6 month 5XFAD mice (N = 2). As illustrated in (A/B), numerous swollen neurites in close association with A β plaques or fibrils are appreciable in this cohort. Graphically, this is demonstrated by the presence of a second population of neurites with a mean diameter of 4.5 microns. Notably, this population of dystrophic neurites is clearly distinguishable from the lone population of healthy sized neurites distributed around a mean of .5 microns in the treated cohort (N = 2) (D). Significantly, dystrophic neurites were exclusively observed in the non-treated animals and always in association with either fibrillar deposits or large accumulations of A β . No A β plaques greater than 2 microns or associated populations of dystrophic neurites could be identified in the treated cohort; as demonstrated by the Gaussian distribution of neurite diameters around a mean of .5 microns. Critically, the absence of A β plaque load in the brain, prophylactic curcumin treatment also prevents A β plaque-associated neurodegenerative changes in the CA3 region of the hippocampus.

10.3.8 Result: Prophylactically Inhaled Curcumin Prevents the Development of Working & Spatial Memory Deficits in 5XFAD Mice

Seeking to evaluate whether the observed reductions in A β plaque burden and dystrophic neurite formation correlated with behavioral improvements, the effect of inhaled curcumin on spatial-dependent and working memory was probed using the Y-maze behavioral assay. Briefly, 6-week old 5XFAD mice (N=10) were chronically administered a 5 mg/kg dose of nebulized curcumin three times a week for 18 weeks. Two cohorts consisting of a group of age matched 5XFAD and a group of wild type mice (N= 10 per group) were left untreated throughout the study and thus served as controls. Following a one week habituation period in the behavioral testing facility to decrease experimental confounds attributable to stress, working memory and spatial memory were assessed via two variations of the Y-maze behavioral paradigm. In the working memory paradigm, spontaneous alteration was quantified over a 6 minute trial and reported as percent spontaneous alternation. Importantly, this variable denotes the percentage of time the animal correctly entered all three arms in sequence over the total number of choices made. The interpretation of this parameter according to the literature is as follows. When arriving at the junction of all three arms the animal is presented with the choice to return back to the arm it started in or explore the two novel arms of the maze. Assuming the mouse is motivated to explore novel routes, the subsequent arm entry should be restricted to either of the two unexplored arms. Similarly, in the third entry of the sequence, only one unexplored arm remains and thus, if the working memory of the mouse is intact, this route should be selected. In the Y-maze paradigm employed each “correct” 3-arm sequence increase the overall percent spontaneous alteration. Thus, the greater the percent spontaneous alteration (%SA), the higher functioning the animal is with respect to working memory.

As graphically illustrated in Figure 10-12, statistical comparison of working memory performance in non-treated 5XFAD mice reveals a mean reduction in performance of 22.51% relative (Mean = 53.01% SA) to wild type controls (Mean = 75.51% SA). This result confirms that without therapeutic intervention, the working memory of 5XFAD mice becomes significantly perturbed by 6 months of age when compared to non-amyloid bearing mice (P<.001). In stark contrast to the non-treated 5XFAD cohort, working memory function in 5XFAD mice treated with curcumin via inhalation appear protected from amyloid-induced neurodegeneration. Impressively, 5XFAD mice treated with curcumin exhibit a %SA of 71.15% in the working Y-maze paradigm described. This constitutes an 18.15% improvement over the

age-matched non-treated cohort of 5XFAD mice and confirms a statistically significant therapeutic benefit on working memory ($P < .01$). In fact, as further evidence of curcumin's robust therapeutic impact, %SA measured in the curcumin nebulized 5XFAD cohort did not significantly differ from wild type controls (Mean = 71.15% and 75.51%, respectively). Critically, the mean number of entries for each arm did not significantly vary, confirming no innate preference for any of the arms which might confound these results (Figure 10-14). Taken as a whole, his data strongly supports the conclusion that curcumin delivery via nebulization prevents the acquisition of working memory deficits on the 5XFAD mouse model and confirms the efficacy of this approach for the delivery of therapeutic molecules like curcumin to the brain.

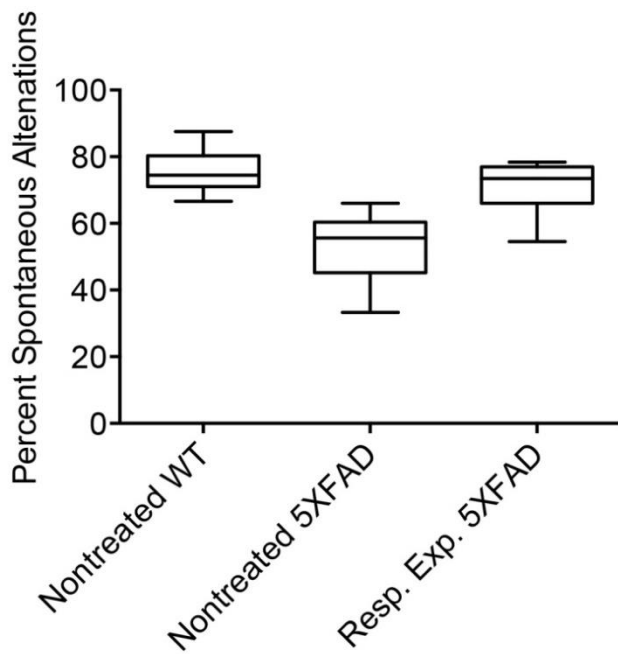


Figure 10-12. Curcumin Nebulization Prevents the Development of Working Memory Deficits in 5XFAD Mice:

(A) Box-whisker plot of percent spontaneous alternation (%SA) in the Y-maze behavioral paradigm. In order to investigate the behavioral sequelae of curcumin's amyloid-clearing properties, we leveraged the Y-maze paradigm to probe whether the acquisition of neurodegeneration induced deficits in working memory could be prevented in the 5XFAD mouse model. Towards this aim, spontaneous alternation in the Y-maze paradigm was evaluated in 6 month-old curcumin nebulized and non-treated 5XFAD cohorts, as well as in non-treated wild type controls (N=10 per cohort). A 5 mg/kg dose of curcumin was administered three times a week via nebulizer at 1 month of age in the 5XFAD treated cohort and continued for 18 months. Following a two week non-treatment period included to alleviate stress confounds associated with routine treatment, working memory was probed during a 6 minute Y-maze trial. Statistical comparison of spontaneous alternation performance in the Y-maze paradigm reveals a mean reduction in performance of 22.51% in non-treated 5XFAD mice (Mean = 53.01%) when compared to wild type controls (Mean = 75.51%). This result confirms that without therapeutic intervention, the working memory of 5XFAD mice becomes significantly perturbed when compared to non-amyloid bearing mice ($P < .001$). In stark contrast to the non-treated 5XFAD cohort, working memory in 5XFAD mice treated with curcumin via nebulization appears to be protected from amyloid-induced neurodegeneration. Impressively, 5XFAD mice treated with curcumin exhibit a %SA of 71.15% in the Y-maze paradigm. This constitutes a 18.15% improvement over the age-matched non-treated cohort of 5XFAD mice and confirms a statistically significant therapeutic benefit on working memory ($P < .01$). In fact, as further evidence of curcumin's robust therapeutic impact, %SA measured in the curcumin nebulized 5XFAD cohort (Mean = 71.15%) did not significantly differ from wild type controls (Mean = 75.51%). Taken as a whole, this data strongly supports the conclusion that curcumin delivery via nebulization prevents the acquisition of working memory deficits on the 5XFAD mouse model and confirms the efficacy of this approach for the delivery of therapeutic molecules like curcumin to the brain.

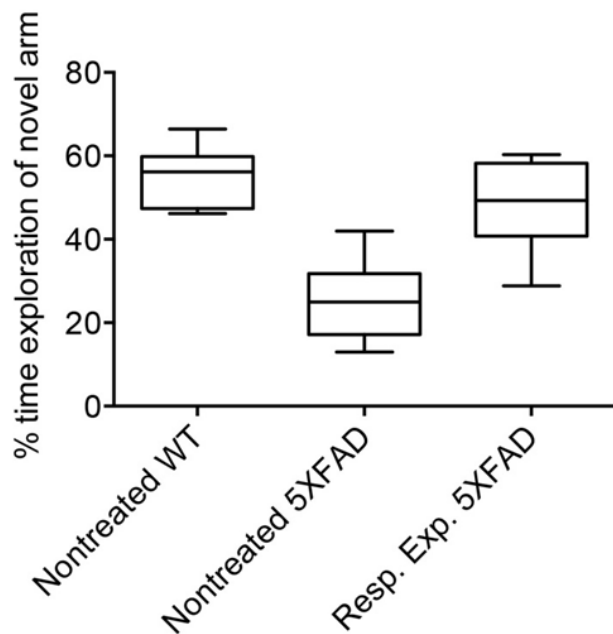


Figure 10-13. Curcumin Nebulization Prevents the Development of Deficits in Hippocampus-mediated Spatial Memory in 5XFAD Mice

Box-whisker plot reporting the time spent exploring the novel arm as a percentage of total exploration time. As an extension of our investigation into the therapeutic efficacy of nebulized curcumin, spatial memory was probed using a two-trial Y-maze behavioral assay. Briefly, during the first trial, a randomized arm of the maze was blocked and the mice were allowed to freely explore the remaining two arms of the Y-maze for 6 minutes. Following the first trial, the animals were returned to their home cage for 30 minutes. During the second trial, spatial memory was probed by recording the percentage of time the animal spent exploring each arm within a 5 minute period. Mice exhibiting normal spatial memory are expected to spend a higher percentage of time exploring the "novel" previously blocked arm while animals with impaired spatially memory are expected to spend equal amounts of time exploring each arm. Within this Y-maze paradigm, wild type mice exhibited profound recognition of Y-maze arms, spending 55.03% in the previously blocked arm. In contrast, untreated 5XFAD mice appeared incapable of recognizing the spatial cues of the maze and thus demonstrated no discernible preference for the "novel arm", spending 25.24% of their time exploring the previously blocked arm. Corroborating the immunohistochemical findings indicating a reduced plaque load in curcumin nebulized 5XFAD mice, this cohort exhibits a robust and significant 22.71% improvement in spatial memory (Mean = 47.95%) when compared to non-treated 5XFAD littermates ($P < .01$). Again, the therapeutic efficacy of the nebulized curcumin was so impressive, that the behavior of treated 5XFAD animals was not statistically different from wild type controls. Notably, these findings confirm that curcumin nebulization improves hippocampal function as assessed by a spatial-memory dependent behavioral assay.

One week following completion of the working memory Y-maze behavioral assay, all animal cohorts were then tested in the spatial memory paradigm. To directly assess hippocampal function at the behavioral level, a two-phase Y-maze paradigm was employed. During the first phase of this procedure, the mouse was allowed to freely explore 2 of the three arms of the Y-maze for a 6 minute period. The arm which was blocked during this first phase was randomized between animals and designated as the "novel" arm in the secondary phase of the study. Following the first period of exploration, each mouse was returned to its home cage and left undisturbed for a 30 minute period. Following this period of rest, each mouse was placed into a randomized arm of the maze and allowed to freely explore all three arms for a 5 minute time interval. To quantitatively assess spatial memory, the proportion of time spent exploring the previously blocked "novel arm" arm was quantified and plotted as the fraction of overall time spent exploring. The interpretation of this paradigm is quite similar to that employed to probe working memory. If spatial memory function is intact, the mouse should remember exploring the original two arms during the first trial and is thus predicted to spend a majority of its time exploring the novel arm. In contrast, animals with impaired spatially memory function are expected to spend equal amounts of time exploring each arm. As presented in Figure 10-13, wild type mice exhibit profound recognition of Y-maze arms, spending 55.03% of their time exploring the previously blocked arm. In contrast, untreated 5XFAD mice appeared incapable of recognizing the spatial cues of the maze and thus demonstrated no discernible preference for the novel arm, spending just 25.24% of their time exploring this region of the maze. Corroborating the immunohistochemical findings indicating a reduced plaque load in curcumin treated 5XFAD mice, this cohort exhibits a robust and significant 22.71% improvement in spatial memory (Mean time spent exploring novel arm = 47.95%) when compared to non-treated 5XFAD littermates ($P < .01$). Again, the therapeutic efficacy of the aerosolized curcumin was so impressive that the behavior of treated 5XFAD animals was not statistically different from wild type controls. Notably, quantification of the mean number of seconds exploring each arm of the maze in a naïve cohort of animals confirmed no innate preference for any of the arms (Figure 10-14C). Additionally, no differences in amount of time spent actively exploring were noted between groups, indicating that the initiative to explore was similar between animals and confirming that observed differences in behavior truly reflect alterations in spatial memory (Figure 10-14A/C).

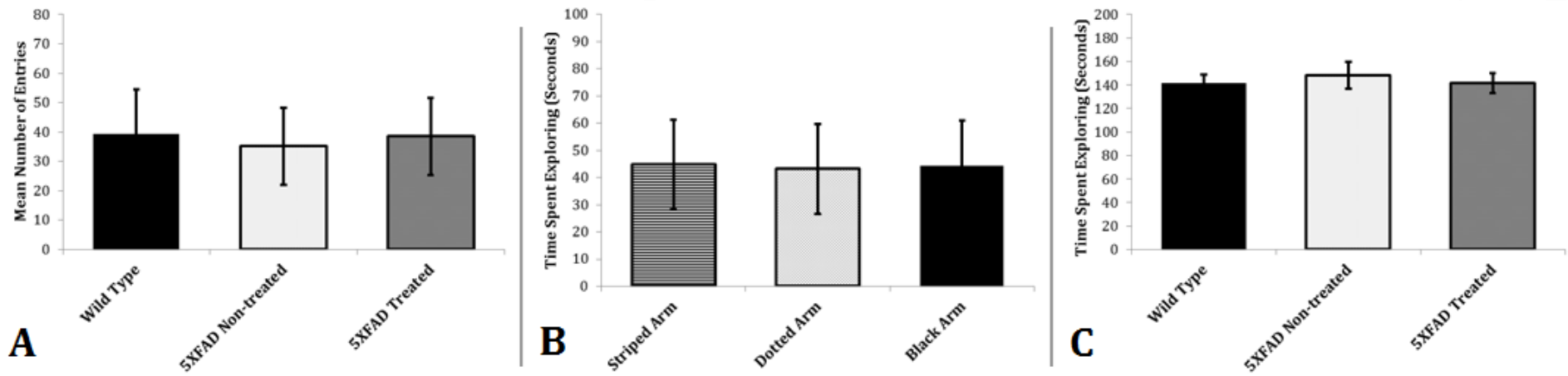


Figure 10-14. Y-Maze Paradigm Controls:

(A) Mean number of arm entries during Y-maze working memory trial. Throughout the 6 minute trial of exploration, the sequence of arm entries made by the animals was automatically recorded using the AnyMaze software package. Analysis of the number of arm entries per arm reveals no innate preference for any of the arms which might confound our behavioral analysis. (B) Mean seconds spent exploring each Y-maze arm. Throughout the 5 minute trial of exploration, the time spent exploring each arm of the maze was automatically recorded using the AnyMaze software package. Analysis of the mean number of seconds spent exploring each arm of the Y-maze confirms no intrinsic bias for a particular arm of the maze. Therefore, the spatial cues used in the behavioral assay were equally salient to the mice. (C) Mean seconds spent exploring in the spatial memory Y-maze trial. In an effort to exclude differences in genotype or treatment side effects from confounding our behavioral data, the mean amount of time spent exploring was quantified using the AnyMaze software package. Notably, no differences in the initiative to explore were noted between wild type and 5XFAD mice. Furthermore, no significant difference in exploration was noted between nebulized 5XFAD mice as compared to their non-treated littermates. Thus, differences in spatial memory observed between cohorts do not reflect confounds imposed by differences in the desire to explore novel arms.

10.3.9 Result: Inhaled Curcumin Associated with Negligible Local & System Toxicity

Having demonstrated the therapeutic efficacy of inhaled curcumin in a preclinical mouse model of AD, the next step in evaluating the clinical applicability of this technique is the exclusion of local and system toxicities. To investigate the potential of systemic toxicity associated with curcumin administration, the blood serum of wild type mice (N=2/group) was analyzed 1 hour after curcumin dosing via inhalation or tail-vein injection. Chemistry profiles (CPs) and complete blood counts (CBCs) from each treatment group were then compared to non-treated littermates (Tables 10-3 & 10-4). Results indicate a negligible systemic toxicity profile for the aerosol-mediated delivery method. In more detail, the normal WBC indicates the lack of a systemic inflammatory response to treatment. Additionally, the ordinary nature of the remaining CBC values indicates a normal hemodynamic state. In contrast, I.V. injection appears to elicit a mild increase in WBC as compared to non-treated controls. Given the experimental observation that these mice fell into severe shock immediately following injection, this result most likely reflects a mobilization of the marginated pool of white blood cells secondary to physiologic stress. Support for this assumption is found in the CP panel, where marked disruptions in the physiological levels of sodium and potassium ions can be noted exclusively in the I.V. injected cohort. In a manner which again supports the absence of systemic toxicity attributable to curcumin dosing via aerosol, no deviation from physiological norms were noted in the metabolic parameters measured in the respiratory exposed cohort.

Table 10-3. Complete Blood Count Analysis Following Curcumin Administration

Complete Blood Count Analysis Following Curcumin Administration (Mean +/- Standard Dev.)			
Test	5 mg/kg Inhaled Curcumin	5 mg/kg Intravenous Curcumin	Non-treated Controls
WBC	6.57 +/- .53	9.43 +/- .47	6 +/- 1.22
HCT	40.025 +/- 4.40	40.15 +/- 6.15	41.55 +/- .93
RBC	9.105 +/- 1.78	6.81 +/- 1.43	9.765 +/- .32
HB	12.35 +/- 2.44	9.3 +/- 2.19	13.05 +/- .50
MCV	43.75 +/- .25	44.1 +/- .14	42.55 +/- 2.33
MCH	13.65 +/- 1.27	13.5 +/- .29	13.35 +/- .92
MCHC	31.25 +/- 1.26	30.7 +/- .70	31.45 +/- .50
RDW	13.275 +/- .36	13.7 +/- 0	14.4 +/- 1.13
RSD	5.825 +/- .33	6.05 +/- .08	6.1 +/- .14
RETIC#	33.1 +/- 9.25	22.9 +/- .84	48.75 +/- 27.12
RETIC%	0.565 +/- .30	0.255 +/- .05	0.495 +/- .26
PLT	737.5 +/- 190.19	994.5 +/- 9.19	1058.5 +/- 9.20
MPV	5.425 +/- .13	5.45 +/- .21	5.65 +/- .21
PDW	42.325 +/- 1.04	42.15 +/- 1.2	41.65 +/- 1.06
PCT	0.4035 +/- .17	0.542 +/- .01	0.5985 +/- .03

Table 10-4. Metabolic Panel Following Curcumin Administration

Metabolic Panel Following Curcumin Administration (Mean +/- Standard Dev.)				
Test	5 mg/kg Inhaled Curcumin	5 mg/kg Intravenous Curcumin	Non-treated Controls	Normal
Na	146.1 +/- 4.14	139.7 +/- 7.19	151 +/- 3.61	142-167 mmol/L
K	5.75 +/- 1.63	3.56 +/- 2.56	6.7 +/- .41	5-9 mmol/L
Cl	116.1 +/- 7.12	122.3 +/- 10.66	108 +/- 7.53	104-120 mmol/L
ALP	50 +/- 20.78	103 +/- 13.38	80 +/- 14.67	44-118 U/L
ALT	88 +/- 40.25	42.5 +/- 36.79	61 +/- 10.62	26-120 U/L
AST	114 +/- 40.25	195.5 +/- 20.42	173 +/- 30.70	69-191 U/L
BUN	35 +/- 2.31	37 +/- 1.85	33 +/- .67	19-34 mg/dL
CREAT	0.5 +/- .02	0.5 +/- .013	0.5 +/- .05	.5-.8 mg/dL

Confident in our preliminary exclusion of severe systemic toxicity, we next sought to evaluate the effect of chronic curcumin inhalation on the respiratory tissues. In our experimental design, H&E and Masson's Tri-chrome stained lung tissues collected from acutely (N=3) and chronically nebulized (N=3) 6-month old 5XFAD mice were compared with age-matched non-treated controls. In more detail, mice in the "acute inhalation" cohort received one standard 5 mg/kg dose of inhaled curcumin while the "chronic inhalation" cohort received 48 similar 5 mg/kg doses over an 18-week time-period (3 doses/week). Notably, in an effort to thoroughly investigate the potential of local toxicity, both a qualitative and quantitative analysis of each slide of lung tissue was performed. To enhance the credibility of our study, the qualitative assessment was performed by a blinded expert pathologist. Summarizing her assessment of the H&E stained sections; both acute and chronically treated mice exhibited an absence of either lymphocytic or neutrophilic interstitial infiltration. Additionally, no distinguishable alveolar thickening was observed in any of the treatment groups when compared to controls. To investigate the possibility of increased eosinophilic matrix around medium to small airways, especially in chronically treated mice, Masson's Tri-chrome staining was employed to highlight connective tissue deposition. Again, a blinded qualitative assessment of the tissues acquired from both acute and chronically nebulized mice revealed average collagen deposition indistinguishable from non-treated controls.

Always pursuing the most objective experimental design possible, the possibility of atypical collagen deposition in the respiratory bronchioles and interstitial pulmonary tissues was further assessed in a semi-quantitative manner using ImageJ software. As depicted in Figure 10-15D, the area lung fraction comprised of connective tissue is consistent between acute and chronically treated mice as compared to non-treated controls in both the respiratory bronchioles and pulmonary interstitium. Collectively, these data strongly suggest that even in the context of an aggressive and chronic treatment regimen, spanning 15% of the animal's average lifespan, inhaled curcumin does not elicit robust pulmonary toxicity.

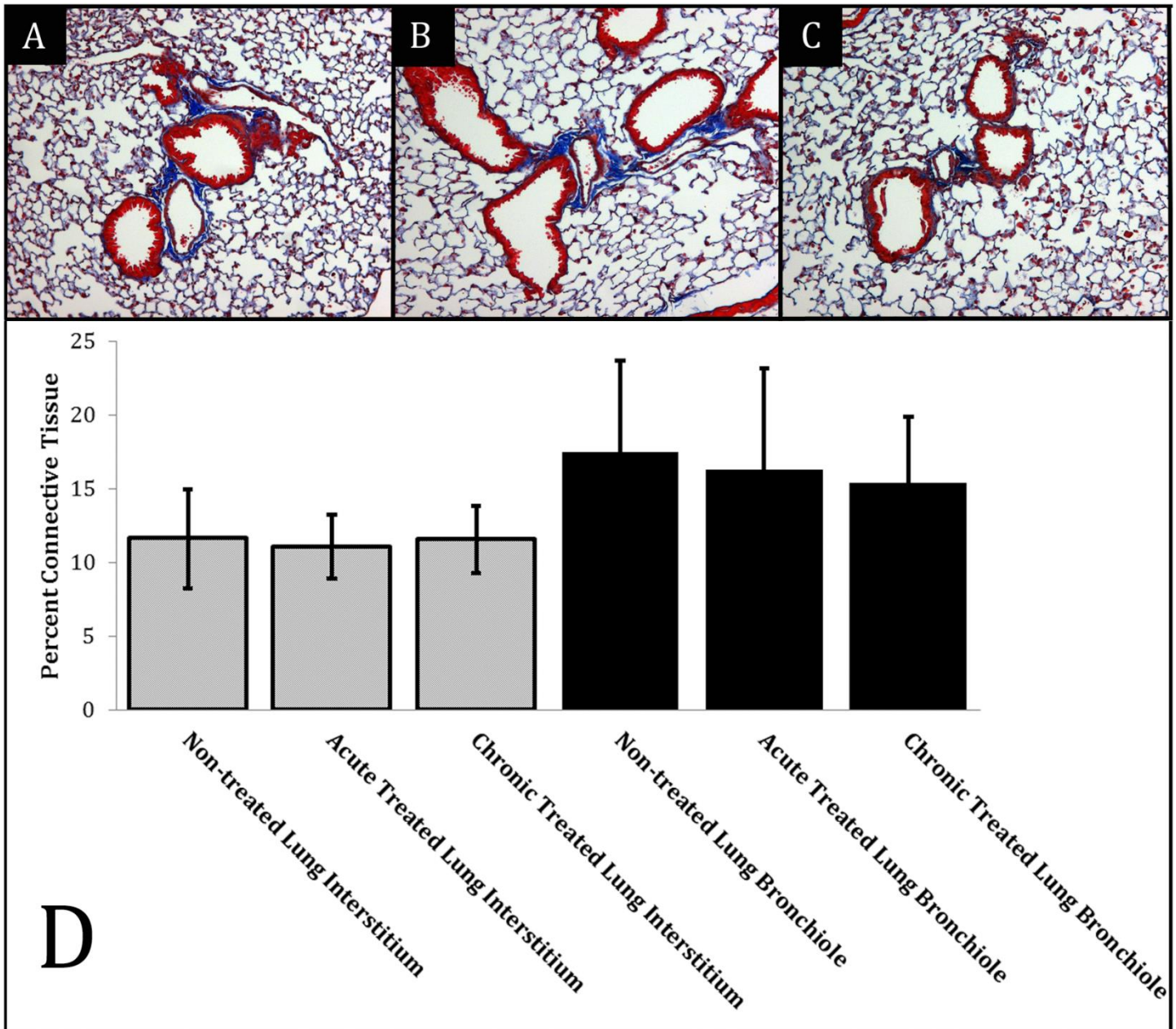


Figure 10-15. No Evidence of Pulmonary Toxicity Associated with Acute or Chronic Inhalation of Curcumin.

Masson's Tri-chrome stained lung tissues collected from acutely (N=3) and chronically nebulized (N=3) 6-month old 5XFAD mice were compared with age-matched non-treated controls. Mice in the "acute inhalation" cohort received one standard 5 mg/kg dose of inhaled curcumin while the "chronic inhalation" cohort received 48 similar 5 mg/kg doses over a 16-week time-period (3 doses/week). A blinded qualitative assessment performed by an expert pathologist on H&E stained sections confirmed the absence of both lymphocytic and neutrophilic interstitial infiltration in either of the curcumin treated cohorts when compared to controls. Additionally, no distinguishable alveolar thickening was observed in any of the treatment groups. To investigate the possibility of increased eosinophilic matrix around medium to small airways, especially in chronically treated mice, Masson's Tri-chrome staining was employed to highlight connective tissue deposition. Again, a blinded qualitative assessment of the tissues acquired from both acute and chronically nebulized mice revealed average collagen deposition indistinguishable from non-treated controls. The possibility of atypical collagen deposition in the respiratory bronchioles and interstitial pulmonary tissues was also assessed in a semi-quantitative manner using ImageJ software. As depicted in subfigure D, the area lung fraction comprised of connective tissue is consistent between acute and chronically treated mice as compared to non-treated controls in both the respiratory bronchioles and pulmonary interstitium. Collectively, these data strongly suggest that even in the context of an aggressive and chronic treatment regimen, spanning 15% of the animal's average lifespan, inhalable curcumin does not elicit robust pulmonary toxicity.

10.4 SIGNIFICANCE & DISCUSSION OF WORK

10.4.1 Significance & Discussion of Aerosol-mediated Delivery

Drug delivery to the brain for imaging or treatment of AD requires a perfect balance of the chemical bioisosteres that enable the compound to be sufficiently hydrophilic enough to traverse the brain's circulation yet maintain sufficient lipophilicity to enable it to cross the BBB. Curcumin is one such compound among a mere handful of known A β -binding agents. However, its strength as an amphiphilic molecule is also its shortcoming. As noted in the literature, polyphenols such as curcumin present a unique challenge with respect to their formulation for in vivo application. With a log p value of 2.9, curcumin is insoluble in any physiological aqueous condition suitable for in vivo application.⁽¹⁰⁵¹⁾ Therefore, it must be dissolved in saline with a high proportion of either methanol or Tween.^(1032, 1047) In congruence with significant mortality associated with I.V. injection of curcumin noted our study, bolus administration of a viscous solution like that used to administer curcumin can be associated with robust toxicity. This incompatibility with I.V. administration methods has proven the most profound limitation associated with the in vivo application of amphiphilic molecules such as curcumin. In fact, all past and ongoing clinical trials seeking to evaluate the therapeutic efficacy of curcumin in AD patients have been forced to employ oral dosing regimens.⁽¹⁰³²⁾ Disappointingly, this approach has likely stained the reputation of one of the most promising theranostic agents for AD discovered in the last two decades, as the compound's bioavailability via this method of administration is nothing short of abysmal.⁽¹⁰³²⁾ To elaborate on this point, one of the principal criticisms leveraged against those in favor of the therapeutic application of curcumin in AD is the failure of this therapeutic intervention to improve cognition in human clinical trials. However, a review of the literature reveals that the dependence on oral dosing in these trials is likely the reason these studies have failed to recapitulate the robust improvements in memory observed in preclinical animal models of AD.^(1032, 1052) In support of this hypothesis, investigators have reported that even following oral doses of 4 grams, the highest curcumin dose utilized in a completed AD-specific human study to date, curcumin does not reach detectable levels in the blood.⁽¹⁰⁵³⁾

Two factors predominantly contribute to the poor systemic bioavailability of curcumin when delivered via oral administration. These features include: (i) poor initial uptake via the intestinal mucosa and (ii) profound first-pass metabolism in the liver. Considering first the barrier posed by intestinal absorption, detailed in vitro studies demonstrate

that exceedingly low levels of curcumin (5-6% ID) are transported from the mucosal membrane to the serosal side of the tissue.^(1044, 1054) In spite of this apparently low rate of transport, early studies noted that anywhere from 30-80% of the added curcumin disappeared from the mucosal side.⁽¹⁰⁵⁵⁾ As less than 3% of the added curcumin was found in the intestinal tissue, these findings led to the hypothesis that curcumin is actively metabolized at the level of the intestinal mucosa.⁽¹⁰⁴⁴⁾ Many years later, this hypothesis was explored in more detail by comparing subcellular fractions of human and rat intestinal tissue with metabolism in the corresponding hepatic fractions.⁽¹⁰⁵⁴⁾ Consistent with the idea of intestinal curcumin metabolism, curcumin glucuronide was identified in intestinal and hepatic microsomes, and curcumin sulfate, tetrahydrocurcumin, and hexahydrocurcumin were found as curcumin metabolites in intestinal and hepatic cytosol isolated from both humans and rats. In a manner which may explain the discrepancies in therapeutic efficacy observed between humans and animal models, the extent of curcumin conjugation was found to be much greater in intestinal fractions isolated from humans compared to those harvested from rats. In fact, the curcumin-reducing ability of cytosol from human intestinal and liver tissue exceeded that observed with the corresponding rat tissue by factors of 18 and 5, respectively.⁽¹⁰⁵⁴⁾ At the molecular level, curcumin was sulfated by human phenol sulfotransferase isoenzymes SULT1A1/SULT1A3 and equine alcohol dehydrogenase catalyzed the reduction of curcumin to hexahydrocurcumin. In a more unique manner, it has been discovered that curcumin-converting microorganisms dominate the intestinal flora.⁽¹⁰⁵⁶⁾ For example, colonies of *Escherichia coli* isolated from human feces were found to contain an enzyme which may contribute to the low bioavailability of orally dosed curcumin. In more detail, this curcumin-converting enzyme, appropriately named “nicotinamide adenine dinucleotide phosphate (NADPH)-dependent curcumin/dihydrocurcumin reductase”, has a molecular mass of about 82 kDa and consists of two identical subunits. The enzyme has a narrow substrate spectrum, and facilitates the microbial metabolism of curcumin via a two-step reduction. First, curcumin is converted NADPH-dependently into an intermediate product, dihydrocurcumin, and then the end product, tetrahydrocurcumin. While the relative contribution of each of these enzymes to the intestinal breakdown of curcumin remains debated, cumulatively, the literature compellingly demonstrates that curcumin undergoes extensive metabolic conjugation and reduction in the gastrointestinal tract and that there is more metabolism in humans’ than in rat intestinal tissue. Importantly, historical precedents undeniably confirm the devastating effect the metabolic pathways described can have on a putative therapeutics bioavailability. For example, the limitations observed in curcumin are highly analogous to the low bioavailability of other drugs such as the oral contraceptive ethinylestradiol, which is thought to be caused by

extensive sulfate conjugation.⁽¹⁰⁵⁷⁾ Unfortunately, this underappreciated literature has failed to be adequately considered in the design of trials evaluating the therapeutic efficacy of this dietary constituent and so human studies continue to publish negative results.⁽¹⁰⁵²⁾

Alarming for those committed to the discovery of a disease-modifying therapeutic for AD, poor intestinal uptake is not the only major shortcoming associated with oral dosing of curcumin however. To the contrary, as previously noted, hepatic clearance of curcumin also significantly contributes to the poor delivery of curcumin to the brain. This is because of a phenomenon termed first-pass effect, in which the entirety of the intestinal tract's venous drainage is immediately filtered by the liver before being allowed to reenter systemic circulation. In humans, substances/drugs absorbed along the gastrointestinal tract anywhere between the lower third of the esophagus to the upper portions of the anal canal are subject to this effect. From an anatomical perspective, this is because the venous drainage of these tissues is sub-served, at least in part, by the superior/inferior mesenteric or splenic veins which feed into the hepatic portal vein.^(1058, 1059) Substances contained in the blood of this vein are then subject to the metabolic machinery of the liver via percolation through sinusoids. In the specific case of curcumin, detailed analysis has demonstrated that the major biliary metabolites include glucuronides of tetrahydrocurcumin and hexahydrocurcumin. In addition, dihydroferulic acid together with traces of ferulic acid have been identified as minor biliary metabolites.⁽¹⁰⁶⁰⁾ The significance of this biotransformation of curcumin is that constitutes a pharmacological deactivation process, in that metabolism generates species that are either devoid of biological activities or less potent than their metabolic precursor. As evidence, in a comparative analysis of the ability of five curcumin metabolites, curcumin sulfate, curcumin glucuronide, tetrahydrocurcumin, hexahydrocurcumin, and hexahydrocurcuminol, to interfere with phorbol ester-induced expression of the enzyme cyclooxygenase-2, none of these species was found to be as potent as their metabolic progenitor.⁽¹⁰⁶¹⁾ Moreover, a multitude of studies have demonstrated that curcumin is a more potent anti-oxidant than its metabolic derivatives.⁽¹⁰⁶²⁾ Most relevantly to AD, studies have confirmed that curcumin, but not its primary metabolic derivative tetrahydrocurcumin, is effective in reducing amyloid plaque burden and tau hyper-phosphorylation.^(1063, 1064)

It is worth noting that an exhaustive amount of effort and resources has been poured into circumventing the poor bioavailability of curcumin associated with P.O. dosing. However, despite more than 40 reports that have attempted to increase the bioavailability of curcumin through a variety of methods such as nanotechnology, encapsulation in

liposomes/cyclodextrin/polylactic-co-glycolic acid or administration with metabolic inhibitors, traditional methods employed to overcome curcumin's poor biodistribution have proven insufficient.⁽¹⁰⁶⁵⁻¹⁰⁶⁹⁾ Thus, the development of administration techniques that better facilitate the delivery of amphiphilic molecules to the brain is of critical importance, as reliance on non-optimized dosing regimens may lead to the premature dismissal of potentially clinically impactful molecules such as curcumin. As emphasized earlier, the clinical utility of curcumin extends beyond AD and therefore, it is indeed in our interest to develop innovative, practical, and translatable administration methodologies that can be used to deliver curcumin to the brain and other targets.⁽¹⁰⁷⁰⁾ Toward that end, we have demonstrated the utility of a novel atomization-based drug administration technology that rivals I.V. injection with respect to delivery of the compound to the brain. Review of the data highlights four key advantages of curcumin delivery by inhalation: (i) effective delivery of the compound to pathologically relevant regions of the brain such as the hippocampus; (ii) avoidance of the glucuronidation and biotransformation attributable to the first-pass effect, (iii) circumvention of the low bioavailability of curcumin associated with its poor absorption/metabolism in the gut and (iv) negligible toxicity.

Considering the first of these three points as a whole, we hypothesize that the improved bioavailability profile of inhaled curcumin is supported via two independent routes of uptake. Under this evolving model, derived largely from existing literature, the lungs play a predominant role in establishing the high plasma levels of curcumin reported in our work. At an intuitive level, this assumption seems justified in light of the massive surface area available for drug transport, with the surface area of human lungs estimated at an astonishing 70-140 m².^(1071, 1072) Functionally, the lungs can be subdivided into two distinct systems, the conductive airways (trachea, bronchi, and bronchioles) and the regions of gas exchange (alveoli). In more detail, the conducting zone consists of the first 16 generations of airways comprised of the trachea (generation 0), which bifurcates into the two main stem bronchi (generation 1).⁽¹⁰⁷³⁾ This structure subsequently subdivides into progressively smaller diameter bronchi and bronchioles. In comparison, the respiratory zone consists of all structures that participate in gas exchange and begins with the respiratory bronchioles.⁽¹⁰⁷⁴⁾ Predictably, the epithelial morphology of each region reflects its physiological role. For this reason, the distinction between conductive and respiratory airways is of significance in the context of pulmonic drug delivery. Put simply, the pseudostratified epithelia that constitute the barrier to absorption into the bloodstream are markedly different in the airways and alveoli of the lungs. The conductive airways are composed of a gradually thinning columnar epithelium, with the bronchial epithelium of 3–

5mm and bronchiolar epithelium of 0.5–1mm in thickness.^(1074, 1075) While this represents an adequate barrier with respect to drug delivery in and of itself, it is significantly strengthened in the tracheobronchial region the epithelium by a mucus layer. Within this region, any deposited particle is promptly transported out of the lung via mucociliary clearance. Under these conditions, drug absorption becomes practically negligible. On the other hand, the alveoli have only a thin, single cell layer comprised principally of Type I and II pneumocytes. Here, the distance from the alveolar lumen to the capillary blood flow is less than 400 nm. Coupled with the large surface area already discussed, this makes the gas exchange tissues of the lung highly amenable to the delivery of pharmaceuticals into systemic circulation.⁽¹⁰⁷⁶⁾ Our work supports this theory, as an inhaled 5 mg/kg dose of the curcumin analog FMeC1 achieved similar concentrations in the brain as those reached via I.V. injection. Fortunately, our longitudinal analysis of plasma curcumin content achieved following I.V., P.O., or inhalation delivery routes sheds some light on this finding. Here, the data reveals that while I.V. injection of curcumin produces an unrivaled peak in plasma curcumin concentration, these elevated levels are rapidly fleeting. As a result, the bioavailability of this technique is far from the pharmacokinetic ideal. By comparison, pulmonic uptake of curcumin results in an attenuated (relative to I.V. injection) but sustained increase in curcumin plasma levels which, over the extended course of delivery, results in a greater than two-fold increase in peripheral bioavailability. In truth, this data might prove sufficient in addressing the underlying mechanism by which nebulized drug delivery achieves therapeutically relevant concentrations of curcumin in the brain. However, the finding that curcumin content in the hippocampus is statistically elevated in nebulized 5XFAD mice as compared to I.V. injected animals, suggests an additional route of administration. In our opinion, this second route of curcumin delivery to the brain is most likely occurring via the direct nasal pathway.

Colloquially termed “nose-to-brain delivery”, investigations conducted in human and animal models strongly support the notion that transport of exogenous materials directly from nose-to-brain is a potential route for by-passing the BBB.⁽¹⁰⁷⁷⁾ Mechanistically, this route involves the olfactory or trigeminal nerve systems, which initiate in the brain and terminate in the nasal cavity at the olfactory neuroepithelium or respiratory epithelium, respectively. As the only externally exposed portions of the CNS, these structures are uniquely positioned to provide the most direct method of non-invasive entry into the brain. In order to understand how increased FMeC1 signal in the hippocampus of nebulized animals as compared to I.V. injected animals relates to this pathway, an anatomical overview is required. Beginning with

the fundamentals, in man, the olfactory epithelium is located high in the nasal cavity. In more detail, it partly overlies the cribriform plate, a bony structure that contains many pores that allow the passage of neuronal bundles from the olfactory epithelium to pass into the CNS. As depicted in Figure 10-16, the olfactory epithelial tissues predominantly contain three cell types: the olfactory neural cells, the sustentacular cells, and the basal cells. Beneath this epithelial cell layer lies the *lamina propria* of the olfactory epithelium, in which the axons of olfactory neurons taper together and become ensheathed by glial cells. These processes are called *filia olfactoria* and are unique features in the mammalian body in that around twenty axons are partitioned by the Schwann cell into fascicles. The significance of this structural organization to CNS drug delivery is that it generates 10–15 nm sized spaces between axons that can facilitate peri-neuronal transport of molecules to the brain (Figure 10-17).⁽¹⁰⁷⁸⁾ This is because the schwann-sheathed axonal bundles pass through the porous cribriform plate before synapsing on mitral cells contained within the glomeruli of the olfactory bulb. Moreover, the presence of pores in the *filia olfactoria*, termed mesaxons, also allow passage of extracellular fluid into the neuronal bundle and vice versa.⁽¹⁰⁷⁹⁾ Admittedly, the size restrictions placed on peri-neuronal transport of pharmaceuticals has proven limiting for the majority of macro-molecules. However, this pathway remains viable for small molecule A β aggregation inhibitors such as curcumin. Moreover, theoretically, transcellular transport of particles up to 200nm in diameter is possible via retrograde transport of drugs from the nasal mucosa to the olfactory bulb.^(1080, 1081) With respect to the endocytic process underlying this transcellular transport, overall clathrin-dependent endocytosis is currently the most-well characterized mechanism. In truth however this constituent of the nose-to-brain transport phenomenon remains largely uncharacterized and debate still exists over how exactly exogenous particles initiate this event.⁽¹⁰⁸²⁾ Regardless of whether transported via transcellular or peri-neuronal transport, from the olfactory bulb third-order neuronal projections pass to the amygdala, pre-pyriform cortex, the anterior olfactory nucleus, entorhinal cortex, and most relevantly to our work the hippocampus.⁽¹⁰⁸³⁾ Thus, in congruence with the most up-to-date models, we envision that the enhanced curcumin deposition observed in our studies might be attributable to retrograde transport of compounds from the nasal mucosa, to the olfactory bulb, and ultimately to the hippocampus. Importantly, the feasibility of this pathway has already been demonstrated in studies employing large proteins and nanoparticles.^(1084, 1085)

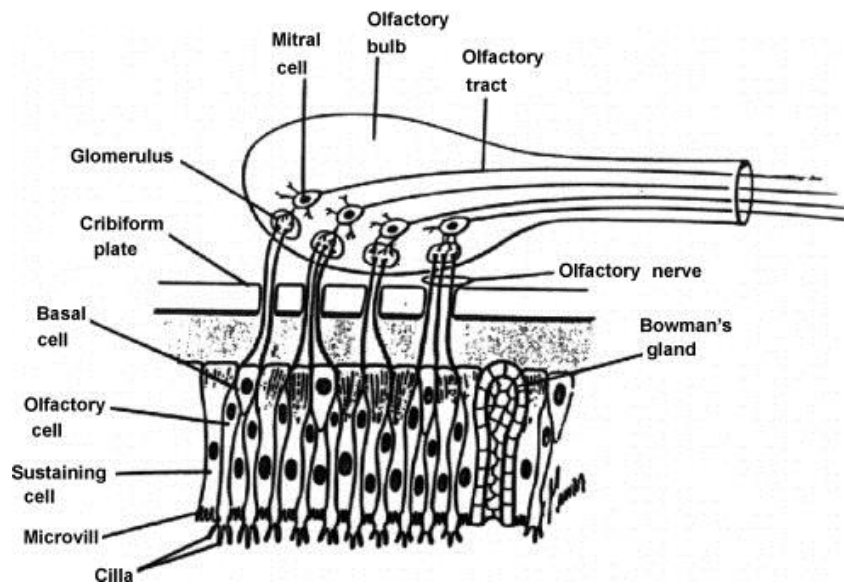


Figure 10-16. Anatomical Diagram of the Olfactory Epithelium, Bulb, and Tract.

Note the presence of three principal cell types contained in the olfactory epithelium: (i) basal cell, (ii) sustentacular cell (sustaining cell), and (iii) olfactory neuron. Reproduced with Permissions from the International Journal of Pharmaceutics.⁽¹⁰⁷⁹⁾

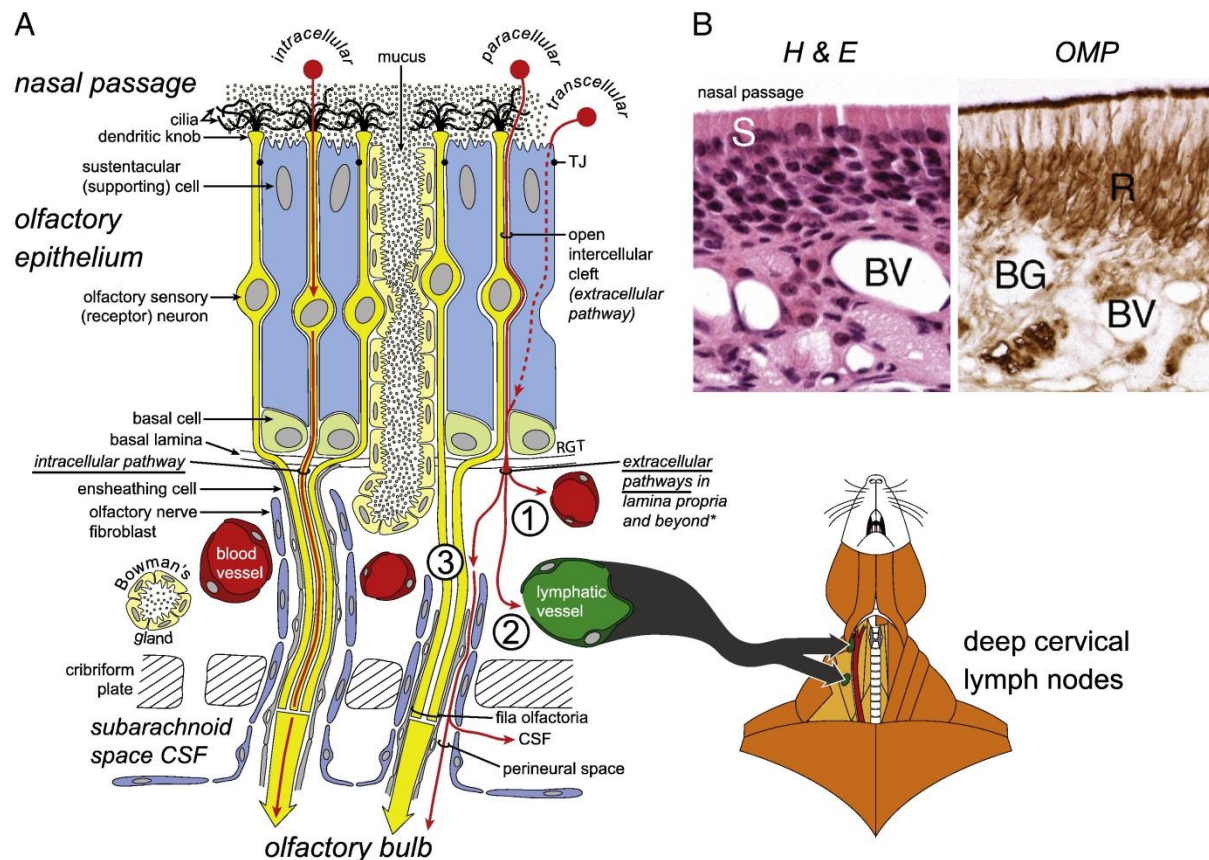


Figure 10-17. General organization of the olfactory region.

(A) The olfactory mucosa includes the olfactory epithelium and its underlying lamina propria. Axonal processes of olfactory sensory neurons converge into bundles (filia olfactoria), surrounded by ensheathing cells and fibroblasts, before projecting to the olfactory bulb. Potential pathways for drug delivery across the olfactory epithelium following intranasal administration are shown in red. Some substances may be transported by an *intracellular* pathway from the olfactory epithelium to the olfactory bulb within olfactory sensory neurons following adsorptive, receptor-mediated or non-specific fluid phase endocytosis. Other substances may cross the olfactory epithelial barrier by *paracellular* or *transcellular* transport to reach the lamina propria, where a number of different *extracellular* pathways for distribution are possible, as indicated: (1) absorption into olfactory blood vessels and entry into the general circulation; (2) absorption into olfactory lymphatic vessels draining to the deep cervical lymph nodes of the neck; and (3) extracellular diffusion or convection in compartments associated with olfactory nerve bundles and entry into the cranial compartment. Transport within the perineural space bounded by olfactory nerve fibroblasts is indicated but other possibilities exist, e.g. transport within the filia olfactoria compartment contained by ensheathing cells, transport within the perivascular spaces of blood vessels traversing the cribriform plate with olfactory nerves (not shown) or transport within lymphatics traversing the cribriform plate with olfactory nerves (not shown). Possible pathways for distribution of substances from the perineural space into the olfactory subarachnoid space cerebrospinal fluid (CSF) or into the olfactory bulb are shown. (B) Sections through the rodent olfactory mucosa stained with hematoxylin and eosin (H & E) or immunostained using an antibody to olfactory marker protein (OMP), a protein present only in mature olfactory sensory neurons and not sustentacular or basal cells. The sections show the layers of the olfactory epithelium, positions of the sustentacular (S) cells, olfactory sensory (receptor, R) neurons and the numerous blood vessels (BV) and Bowman's glands (BG) within the lamina propria. Reproduced with Permissions from Advanced Drug Delivery Reviews.⁽¹⁰⁸⁶⁾

While this theoretical model of pulmonary absorption and the direct nasal pathway help explain the first three advantages of an atomized curcumin delivery approach, (i) effective delivery of the compound to pathologically relevant regions of the brain such as the hippocampus; (ii) avoidance of the glucuronidation and biotransformation attributable to the first-pass effect, and (iii) circumvention of the low bioavailability of curcumin associated with its poor absorption/metabolism in the gut, with respect to the practicality of implanting this technique, our data highlighting the non-toxic nature of this administration is most exciting. Notably, none of the animals exhibited any signs of toxicity or discomfort during the atomization procedure, a finding that is consistent with studies of intranasal drug administration.⁽¹⁰⁸⁷⁾ In contrast, severe respiratory distress and tachycardia were apparent in all animals following bolus I.V. injection. Without question, the findings described in this work raise a myriad of opportunities for future discovery. Clearly, additional work to confirm the relative contributions of the direct nasal pathway versus pulmonic absorption might inform future clinical translation of this technique. Regardless of the outcome of such studies however, our work highlights the potential utility of aerosolized FMeC1 for the longitudinal assessment of A β plaque burden in AD. To confirm this potential, the perfluoro characteristics of FMeC1 should be leveraged via ¹⁹F-NMR imaging to detect the distribution of the compound non-invasively in targeted regions such as hippocampus and cortex of 5XFAD mice. Moreover, there remain a few important caveats which need to be confirmed before FMeC1 can be considered a theranostic agent, such as the therapeutic efficacy of FMeC1 in comparison to that of curcumin. Assuming these two compounds have a similar inhibitory effect on A β aggregation, does inhibition of plaque aggregation lead to cognitive improvement in AD? To directly address this question, we attempted to recapitulate the therapeutic efficacy demonstrated for curcumin in preclinical mouse models of AD using a nebulizer-based administration method.

10.4.2 Significance and Discussion of Prophylactic Curcumin Trial

As we learn more about the complex nature of AD pathophysiology, it becomes increasingly clear that a multi-targeted therapy, one that modulates more than just the A β -burden in the brain, may be necessary in order to efficaciously alter disease course. For this reason, rivaling or even exceeding its diagnostic potential, many in the field of AD argue that curcumin represents the most comprehensive therapeutic avenue to the prevention, management, or reversal of AD pathology discovered to date. The literature supporting this assertion is remarkably robust and emphasizes curcumin's ability to (i) perturb the aggregation of A β peptides, (ii) scavenge A β -produced free radicals, (iii) attenuate the neuro-

inflammatory response and (iv) promote neuron survival among its many other biological activities. Not surprisingly, compounds exhibiting even a fraction of curcumin's therapeutically relevant biological activities are extremely rare. For this reason, curcumin's robust potency in each of these therapeutic domains is all the more astonishing and likely only possible secondary to its uniquely pleiotropic nature. Supporting this statement, in one study evaluating the therapeutic potential of 214 known antioxidant compounds, curcumin had the strongest inhibitor effect on the formation of A β fibrils.⁽¹⁰⁸⁸⁾ In fact, a more in depth investigation of curcumin's inhibitory effect on A β aggregation reveals its ability to not only inhibit the formation of fibrils at physiologically relevant concentrations (EC50 = .8 μ M), but also disaggregate pre-formed fibrillary A β assemblies (EC50 = 1 μ M).⁽¹⁰³⁹⁾ The results of our in vitro studies (Sensolyte assay) strongly agree with this assessment. Moreover, our studies employing aerosol-mediated delivery of FMeC1 confirmed our ability to deliver curcumin in a clinically applicable manner. Together, these findings provided the impetus for us to test the hypothesis that aerosol-mediated delivery of curcumin could reduce A β burden and improve performance in behavioral measures of working and spatial memory.

Taken as a whole, the results presented in this work clearly demonstrate the profound therapeutic impact inhaled curcumin has on AD pathology in the 5XFAD mouse model. Addressing first the assertion that curcumin can modulate A β plaque levels. We characterized the therapeutic effect of prophylactic aerosol-mediated delivery of a 5 mg/kg dose of curcumin delivered three times a week over the course of 18 weeks on 1.5-month old-5XFAD mice. As detailed, this therapeutic paradigm reduced A β plaque burden in the hippocampus, subiculum, and neocortex by 90.72%, 79.48%, and 68.75% respectively. Importantly, secondary to our unique quantitative approach to analysis, a greater mechanistic understanding of these results is interpretable. Briefly, the reductions in A β plaque numbers observed across all regions analyzed is attributable, at least in part, to the ability of curcumin to inhibit the formation of A β peptide aggregation. Support for this mechanism lies in the fact that the average A β plaques contained in the brains of curcumin treated mice were significantly smaller in comparison to non-treated littermates. Additionally, the largest plaque diameters observed in the non-treated cohort were significantly greater than those observed in the treated group, suggesting that A β plaque size was restricted secondary to curcumin's inhibitory influence on A β aggregation.

While an impressive result in and of itself, cognizant of the literature we knew these reductions in A β burden would not necessarily correlate with behavioral improvements; the ultimate therapeutic goal of our study. Thus, we sought to characterize the therapeutic impact curcumin mediated clearance of A β plaques had at the level of the neurite. In

congruence with the literature, the CA3 brain region of non-treated 5XFAD mice was riddled with dystrophic neurites. By comparison, ultrastructural characterization of curcumin treated 5XFAD mice via transmission electron microscopy revealed a stunning absence of dystrophic neurites in this region of pathological relevance. As the morphology of dystrophic neurites arises secondary to an abundance of autophagic vesicles containing dense amorphous or multi-lamellar cellular debris in the lumen, the absence of these pathological features in prophylactically treated mice strongly suggests the multi-faceted nature of curcumin therapy opposes the pathophysiologic processes of AD. Importantly, although the exact mechanism surrounding A β -mediated toxicity is only partially understood, a large proportion of the literature suggests that oxidative stress is closely involved in the initiation of its toxicity.⁽¹⁴⁰⁾ Indeed, the role of oxidative stress in AD pathogenesis is well established, with substantial evidence demonstrating ROS-mediated injury and free radical damage to key intracellular targets such as DNA or mitochondria in AD brains. Moreover, this mechanism makes sense physiologically, as neurons are particularly susceptible to oxidative damage as a consequence of their i) high content of readily oxidized polyunsaturated fatty acids in the membrane, ii) low levels of natural anti-oxidant component (i.e. glutathione and vitamin E) and anti-oxidant enzymes (glutathione peroxidase, catalase and superoxide dismutase), iii) the high consumption of oxygen required for brain metabolism, iv) high content of lipid peroxidation metals (i.e. iron and ascorbate), and v) inability to replicate. Thus, the absence of dystrophic neurites in the curcumin treated cohort may be as much attributable to curcumin's anti-oxidant properties as much as its ability to perturb A β assemblies. Regardless of the dominant mechanism, the absence of dystrophic neurites in prophylactically treated mice strongly implies a robust therapeutic benefit attributable to inhaled curcumin. Moreover, the finding that markers of chronic neuro-inflammation (COX-2) are reduced in curcumin treated 5XFAD mice compared to non-treated littermates suggests this therapeutic effect is multi-factorial in nature. Interestingly, this attenuation in COX-2 transcription is a well published effect of curcumin and may involve its ability to modulate the protein kinase C signal transduction pathway.⁽¹⁰⁸⁹⁾ Thus, at a minimum, our data supports the conclusion that aerosol-mediated delivery of curcumin largely prevents the development of three, inter-related, cardinal features of AD pathology: (i) A β plaque accumulation, (ii) synaptic dysfunction, and (iii) neuro-inflammation.

Having thus characterized the multi-factorial therapeutic effect of prophylactically inhaled curcumin, the ultimate goal of our study, to demonstrate improvements in cognitive function, became experimentally reasonable. As discussed,

two variations of the Y-maze behavioral assay were employed to independently evaluate working and spatial memory. In both behavioral paradigms, memory function was preserved in 5XFAD mice treated with inhaled curcumin, as this group demonstrating no statistically significant difference in performance compared to a cohort of wild type mice. In contrast, and in a manner which highlights the robust therapeutic effect inhaled curcumin must have in order to produce this observation, working and spatial memory in non-treated 5XFAD mice is severely impaired by 6-months of age. Of note, while previous studies have noted behavioral improvements associated with curcumin treatment, the magnitude of our measured therapeutic effect in comparison to these studies, especially with respect to A β plaque clearance, likely highlights the advantages of the prophylactic treatment approach employed in our study. Confident in this assertion, we provide a preliminary assessment of inhaled curcumin's toxicity profile in order to insure chronic administration of this compound does not elicit toxicity of sufficient severity to exclude its prophylactic use. Fortuitously, in mice dosed with aerosolized curcumin three times a week for approximately 15% of their lifespan, no toxic effect on the respiratory tissues could be noted. Furthermore, our succinct analysis of systemic toxicity revealed no appreciable concerns; a finding in congruence with the published literature.^(1045, 1070) Integrating all of these findings, in conclusion, we accept the hypothesis that aerosol-mediated delivery of curcumin can be applied to efficaciously leverage the multi-factorial therapeutic profile of curcumin for the prevention of AD.

The significance of this conclusion is far-reaching, as the lack of a clinically applicable administration method has severely stunted the therapeutic impact of this promising disease-modifying agent until now. Prior to our work, investigators have only aggressively attempted to leverage traditional dosing paradigms and unfortunately, these approaches have proven woefully inadequate. Of course, intravenous administration represents the best means of introducing a substance into the blood stream. However, curcumin exhibits abysmal solubility in biologically compatible solvents such as phosphate buffered saline (< .1 mg/ml), making this approach clinically impractical. Beyond the notable absence of this administration technique in human clinical trials, the limitations imposed by curcumin's poor aqueous solubility are best exemplified by studies conducted in mouse models. Here, a common guideline is that the volume of I.V. injection is best restricted to less than 200 μ L.⁽¹⁰⁹⁰⁾ Therefore, to safely deliver a single 5 mg/kg dose of curcumin by I.V. injection, a roughly 1.7 milliM solution is required. Put another way, measures would need to be taken to enhance curcumin's aqueous solubility by more than a factor of 6 (.625 mg/mL required). Until such a breakthrough, intravenous administration of curcumin for the treatment of AD is highly unlikely. Furthermore, secondary to its invasive nature, I.V.

dosing represents a poor candidate administration method when placed in the context of a prophylactic therapy. Partially because it somewhat addresses this concern, I.P administration of curcumin has been thoroughly investigated in mice. From these studies, it is known that within 15 minutes of I.P. administration of curcumin (0.1 g/kg), plasma levels may peak as high as 2.25 µg/mL. In one particular study, one hour after administration curcumin levels in the intestines, spleen, liver, and kidneys had reached 177.04, 26.06, 26.90, and 7.51 µg/g, respectively. Disappointingly though, only trace levels of curcumin (0.41 µg/g) were noted in the brain.⁽¹⁰⁹¹⁾ To summarize these arguments, the clinical applicability of both I.V. and I.P. injections are negatively impacted by the poor solubility of curcumin in biological solvents. In the case of I.V. administration, curcumin's poor solubility necessitates the use of highly viscous solvent formulations which carry considerable toxicity. As evidence, nearly 50% of the mice injected receiving a single 5 mg/kg dose of curcumin in our work suffered lethal toxicity from the intervention. This argument is generally applicable to I.P. administration as well, but in this case, toxicity is less of a concern and the inability to reach therapeutically relevant concentrations in the brain appears to be a more relevant limitation.

Having thus exhausted the traditional repertoire of drug administration routes, investigators have unfortunately turned to oral administration for the therapeutic delivery of curcumin. Notably, this approach is highly compatible with prophylactic interventions, exhibits minimal toxicity, and is cost-effective; making it a seemingly ideal choice for human clinical trials. However, as demonstrated by the data in this work, this administration method is of negligible utility when applied to the systemic delivery of curcumin because of (i) poor intestinal absorption, (ii) a robust first-pass effect. Compounding these issues, curcumin also undergoes extensive enterohepatic recirculation, resulting in its rapid elimination in the bile and urine. Interestingly, the metabolic processing of curcumin is an area of continued research and may involve two distinct pathways. On the one hand, successive reductions, which transform curcumin to hexahydrocurcuminol and hexahydrocurcumin, have been reported. On the other hand, rapid molecular modification by conjugation, mostly in the liver, to glucuronide, sulfate and glucuronide-sulfate forms is also widely reported.⁽¹⁰⁹¹⁾ Regardless of the dominant mechanism, the main curcumin metabolites remain controversial with some authors favoring dihydrocurcumin and tetrahydrocurcumin,⁽¹⁰⁶¹⁾ while others propose that curcumin glucuronide and curcumin sulfate are predominant.⁽¹⁰⁹²⁾ Notably this issue is of therapeutic significance as each metabolite likely carries a distinct subset of curcumin's therapeutic abilities, particularly with respect to its anti-oxidant properties. This issue aside, the inability of oral administration to achieve measureable concentrations of curcumin in the blood should exclude this approach from

clinical implementation. Disappointingly, to date, at least 9 human studies evaluating the therapeutic efficacy of orally administered curcumin have been initiated. Predictably, in an effort to overcome the poor suitability of this administration method for the systemic delivery of curcumin, exceedingly high doses of up to 6 grams per day have been employed in some studies.^(1032, 1052, 1053, 1093) Despite this adaptation, all published studies to date have failed to demonstrate a therapeutically meaningful influence on cognitive function. While many investigators rightfully point to the fact that these studies are severely underpowered, with sample sizes ranging from 3 to 36 individuals, in truth these negative results simply highlight what we already know; P.O. administration fails to deliver therapeutically relevant doses of curcumin in the brain. Indeed, in those studies which measured this highly relevant variable, plasma levels of curcumin failed to reach detectable levels.⁽¹⁰⁵³⁾ In summary, the danger of these studies is that in their admirable fervor to translate curcumin to the clinic, they may potentially undermine that very same goal by inappropriately evaluating its therapeutic efficacy secondary to a reliance on an unsuitable drug delivery method. Thus, in an error similar to that committed by clinical trials evaluating amyloid-centric therapies as a whole, these studies may undermine a potentially efficacious therapy as a consequence of their failure to appropriately test the underlying hypothesis. In other words, curcumin has not failed as a therapeutic agent for AD. Instead, the field has failed to justly characterize its therapeutic profile in AD.

As reviewed, traditional administration methods have proven insufficient to achieve this aim and thus, novel drug delivery technologies must be employed. In congruence with this rationale, seemingly countless attempts to increase the oral bioavailability of curcumin have been made. These include the use of liposomal curcumin⁽¹⁰⁹⁴⁾, nanoparticles of curcumin⁽¹⁰⁹⁵⁾, and synthetic analogues of curcumin.⁽¹⁰⁹⁶⁾ Disappointingly however, despite markedly increasing curcumin delivery, these strategies have failed to overcome the inherent limitations imposed by oral biodistribution pathways. Moreover, these modified formulations have not been shown to recapitulate the therapeutic benefits of I.V. injected curcumin in a preclinical mouse model of AD. Therefore, our aerosol-mediated approach to curcumin delivery stands alone in its ability to achieve therapeutically relevant concentrations of curcumin in the brain, as evidenced by its prevention of AD pathology and memory deficits in the 5XFAD mouse model. Importantly, by overcoming the confound of poor bioavailability, our inhaled curcumin method paves the way for the construction of human clinical trials of appropriate design to appropriately evaluate the therapeutic efficacy of curcumin in AD.

In conclusion, the work described herein provides sufficient evidence to support the conclusion that generating aerosolized curcumin for inhalation-assisted delivery to the brain is a promising alternative to the field-dominant I.V. injection administration method. Recently, there is a large body of literature show optimistic results of curcumin in reversing the pathogenesis of AD in small animal models ⁽¹⁰⁷⁰⁾, we hope our work will eventually help to facilitate the translation of that knowledge into human applications. In this way, this work achieves our aim of advancing the field of AD towards the development of the first, clinically applicable, disease-modifying therapeutic for AD.

CHAPTER 11 THESIS AIM 3

11.1 AIM 3: DIAGNOSTIC READOUTS FOR THE EVALUATION OF THERAPEUTIC RESPONSE

To summarize the emerging consensus in the field, the first successful treatment of AD is predicted to include three integral components. These include some aspect of prophylactic intervention, the use of currently approved medications to provide symptomatic treatment, and the development of medications to slow and eventually halt disease progression. As repeatedly stated, the impetus behind the work presented to this point lies in our deep-seated desire to contribute to the development and clinical implementation of a disease-modifying therapeutic agent for AD. For this reason, our work with curcumin leverages a prophylactic treatment paradigm as opposed to trying to reverse accrued deficits. Still, in order for these discoveries to have their desired clinical impact, the foundation for validating AD therapeutics via randomized control clinical trials must be improved. Sub-optimally, and largely secondary to the lack of robust early detection methods, AD clinical trials recruit patients with mild to moderately progressed disease.⁽¹⁷⁴⁾ However as repeatedly mentioned, modern models of AD pathogenesis posit that disease progression becomes independent of A β burden beyond an undefined pathophysiologic threshold.⁽⁵⁵³⁾ Therefore, until such a time that this tipping-point is identified, the interpretation of clinical trials evaluating the therapeutic efficacy of A β -targeted therapies will remain hopelessly confounded.

Representing perhaps the field's greatest accomplishment over the last couple of decades, AI is beginning to emerge as a relatively sensitive and specific means of identifying those individuals with signs of mild cognitive impairment which will progress to AD.⁽⁷⁸⁸⁾ Moreover, this method has already been utilized to monitor treatment response in humans receiving a variety of A β -targeted therapies.⁽¹⁰⁹⁷⁾ However, as discussed at length in the introductory chapters, to date these methodologies have yet to reach sufficient reliability such that they can be leveraged to organize cohorts of preclinical AD patients required to test prophylactic interventions.⁽¹⁴⁴⁾ Moreover, it is becoming increasingly recognized that characterization of A β burden alone is an insufficient reporter of therapeutic effect. Instead, the field is rightly pushing towards the development of a diagnostic panel of biomarkers for AD. Such a panel of course includes an A β -specific component, likely AI imaging in the short-term, but also importantly incorporates alternative biomarkers for

equally relevant pathological processes such as tau dysregulation and neuroinflammation. Perhaps intuitively, the barriers and limitations to the development of such alternative biomarkers are highly similar to those discussed for amyloid and thus here we identified another avenue of research to which our expertise could be applied.

Highlighting the exhaustive nature of our efforts, we explored the diagnostic utility of three distinct approaches. By way of introduction, the first of these approaches sought to leverage a novel PET-precursor for cyclooxygenase 2 (COX-2), 2-Methyl-3-((4-methylthiazol-2-yl) methyl) azulene-1-yl (4-nitrophenyl) methanone, to serve as an alternative biomarker for neuro-inflammation in AD. Significantly, this compound was originally developed and radio-labeled by our lab and later successfully characterized in a breast cancer xenograft mouse model.⁽¹⁰²⁷⁾ Thus, our team can be considered the world's foremost experts in the application of this particular PET-probe to disease models of inflammation. Elaborating on the rationale of measuring COX-2 levels in AD a little further, prostaglandin endoperoxide synthase, commonly referred to as cyclooxygenase (COX), is the key enzyme required for the conversion of arachidonic acid to its biological mediators of inflammation.⁽¹⁰⁹⁸⁾ Two isoforms of the COX enzyme are recognized, COX-1 and COX-2, with each of these enzymes exhibiting a unique pattern of tissue expression.⁽¹⁰⁹⁹⁾ Briefly, COX-1 is expressed under basal conditions in almost all tissues and is particularly important to the maintenance of gastric mucosal integrity, renal function, and hemostasis.⁽¹⁰⁹⁹⁾ In comparison, COX-2 is undetectable in most normal tissues under physiological conditions yet is highly inducible in cells which mediate the body's inflammatory response.^(1100, 1101) As discussed at length in the introductory chapters, today the field recognizes neuroinflammation as one of the earliest and most potent mediators of AD pathogenesis. However, it wasn't until the discovery that non-steroidal anti-inflammatory drugs (NSAIDs) might modulate the relative risk of developing AD that COX-2 became of central interest to the field. Highlighting only a fraction of the available lines of evidence, a number of cross-sectional and longitudinal epidemiologic surveys have indicated that use of NSAIDs is associated with delayed onset and/or slowed cognitive decline in AD.⁽¹¹⁰²⁻¹¹⁰⁴⁾ Similarly, among twin and sibling pairs, prior use of NSAIDs has been associated with delayed clinical expression of AD.^(1105, 1106) While these studies are in no way conclusive, with systematic biases being particularly problematic in epidemiologic studies of this nature, the large number of reports supporting a protective effect of NSAIDs in AD has nevertheless been persuasive. However, shortly after these studies were published the initial enthusiasm behind the clinical application of traditional NSAIDs for the treatment of AD was tempered by the negative findings of randomized controlled trials. This

was largely due to the fact that daily use of traditional NSAIDs is associated with adverse effects, particularly on the gastrointestinal tract of elderly subjects. To provide an example of the impact of this unfavorable side-effect profile can have, in the six-month study of indomethacin for AD, 42% of patients in the active drug group withdrew because of adverse effects.⁽¹¹⁰⁷⁾ Critically, the side effects just described are known to be the result of COX-1 inhibition.^(1099, 1108) Therefore, investigators turned to COX-2 specific inhibitors in the hope that the same therapeutic benefit could be achieved without the detrimental effects associated with COX-1 inhibition. While a consensus on the clinical efficacy of COX-2 specific inhibitors has yet to be reached, a consequence of this movement is that the expression pattern and pathological contributions of COX-2 in AD have been extensively characterized.⁽¹¹⁰⁹⁾ Most relevantly to our work seeking to leverage COX-2 as a biomarker for AD, a large body of literature supports the theory that COX-2 is involved in the pathophysiology of AD.⁽¹¹¹⁰⁻¹¹¹²⁾ In fact, evidence suggests that COX-2 expression at the level of both mRNA and protein is upregulated in AD brains compared with controls.⁽¹¹¹³⁾ Furthermore, this increased level of COX-2 expression in AD has been found to correlate well with the degree of A β burden in humans and animal models.^(1049, 1112) This background considered, we hypothesized that PET-mediated imaging of COX-2 levels in the brain might serve as a complimentary biomarker for the longitudinal assessment of AD treatment response.

Continuing with our theme of imaging alternative biomarkers relevant to the pathogenesis of AD in the brain, the second complimentary biomarker we envisioned applying to AD was a novel PET-ligand for the insulin-like growth factor 1 receptor (IGF1R). Speaking generally, this receptor is an essential signal transducer of the insulin/IGF-1-like signaling pathway, which is mechanistically linked to longevity, protein homeostasis, and perhaps most relevantly to AD, learning and memory.⁽¹¹¹⁴⁾ In the mammalian brain, the IGF1R is a 2α - 2β -subunit tyrosine kinase receptor that is highly expressed in the central nervous system and is thus well positioned to modulate AD pathogenesis.^(1114, 1115) At its core, the intra-molecular signaling cascade which defines the insulin/IGF-1-like signaling pathway begins predictably with the binding of insulin and insulin-like growth factors to insulin receptors (IR) and/or IGF1R. Upon ligand binding, the activated IRs and IGF1Rs undergo auto-phosphorylation and initiate signaling networks that share many similarities and critical nodes of signal divergence and regulation. Touching on this briefly, insulin/IGF-1-like signaling is believed to contain at least three critical nodes of signal divergence and regulation at the level of insulin receptor substrates 1-4 (IRS 1-4), phosphoinositide 3-kinase (PI3K), and protein kinase B (PKB or Akt).⁽¹¹¹⁶⁾ Structurally, these IRS proteins are 60 to

180 kDa and are characterized by a pleckstrin homology (PH) domain, a phosphotyrosine binding (PTB) domain, which account for their high affinity for the IR, and up to 20 potential tyrosine phosphorylation sites spread throughout the molecule.⁽¹¹¹⁷⁾ Of the numerous signal transduction pathways participated in by IRS1/2, the activation of PI3K is held among these proteins' most pertinent functions with respect to AD pathogenesis. This is because PI3K activates Akt, which in turn phosphorylates a plethora of target proteins including GSK3 β (glycogen synthase kinase 3 β), mTOR (mammalian target of rapamycin), and p70/S6 kinase. In addition, Akt also inactivates the FOXO (forkhead box O) forkhead family of transcription factors.^(1118, 1119) Significantly, these and other downstream protein networks targeted by Akt regulate a diverse array of biological processes of high relevance to AD. These include neuron survival, inflammatory responses/stress resistance, protein translation, synaptic plasticity, autophagy, cell cycle, protein transport/trafficking, metabolism, myelination, and the afore mentioned learning and memory.⁽¹¹²⁰⁾ However, beyond the pathophysiological relevance of all of these downstream effectors of IR/IGF1R, there is growing evidence that perturbations in the insulin/IGF-1-like signaling pathway may be among the primary signaling mechanisms that become defective in AD such that normal proteostasis of A β and tau is pushed beyond the pathological threshold.^(1121, 1122) Supporting this model, the insulin/IGF-1-like signaling pathway is aberrantly over-activated in the brains of AD patients at the level of increased Akt activation and its downstream targets like mammalian target of rapamycin (mTOR).⁽¹¹¹⁸⁾ In addition, feedback inhibition of normal insulin/IGF activation also occurs in AD due to inactivation of IRS-1 and decreased IRS-1/2 levels.⁽¹¹²²⁾ Interestingly this phenomenon may be compounded by the ability of pathogenic forms of A β to induce aberrant and sustained activation of the PI3K/Akt signaling pathway, thus rendering IR and IGF1Rs incapable of initiating their homeostasis-maintaining signaling cascades.⁽¹¹¹⁸⁾ In support of this model, reducing IIS activity in AD animal models by decreasing IGF-1R levels or inhibiting mTOR activity alters A β and tau protein homeostasis towards less toxic protein conformations, improves cognitive function, and extends healthy lifespan.⁽⁶²⁹⁾ As a consequence of these findings, we predicted that PET-mediated measurement of IGF1R levels in the brains of 5XFAD mice would be significantly lower than those observed in wild type littermates. If proven a valid prediction, this would confirm that the [18F] BMS-754807 PET-probe might serve as a complimentary prognostic biomarker to AI for the evaluation of disease-modifying treatments for AD.

Significantly, while the two putative biomarkers discussed thus far are attractive from a pathophysiological perspective, the practical application of PET-mediated imaging for any AD biomarker is far from straightforward when placed in the context of the disease's astonishingly high prevalence. Indeed, as supported by the NIA-AA guidelines on the incorporation of biomarker technologies into the diagnosis of AD, all current diagnostic methodologies for AD are really only suitable for research studies.⁽²⁷³⁾ Being cautious not to undersell the magnitude of this contribution, this is a reasonable milestone and of supreme importance to the field, as the validation of novel disease modifying therapeutics will of course require randomized control trials which will largely rely on these biomarkers as a reporter of therapeutic efficacy. Still, as our prophylactic treatment trial with inhaled curcumin demonstrates, the most effective disease-modifying treatments will be those initiated before the onset of AD signs and symptoms. Put bluntly, current diagnostic methodologies are not a viable AD screening approach at the community level. In the case of PET-mediated imaging, the technical nature of this approach is cost-prohibitive and its associated exposure to ionizing radiation poses a significant health risk. Still, the health risk is even greater when considering CSF-based measurements of AD biomarkers. Thus, while a diagnostic panel based on PET-mediated imaging of amyloid, tau, COX-2, IGF1R, and any other number of potential biomarkers is attractive from a research perspective, the clinical applicability of these methods leaves much to be desired. Others in the field have too noted this shortcoming and for this reason, have investigated the development of fluid-based biomarkers for AD. Exemplifying the small minority of studies seeking to leverage this method, some groups have argued that plasma levels of clusterin, an apolipoprotein associated with the clearance of cellular debris and apoptosis, is a useful biomarker for AD. In support of this hypothesis, plasma clusterin levels were significantly associated with baseline prevalence and severity of AD. However in this same study, plasma clusterin levels were not related to the risk of incident AD during total follow-up (adjusted HR, 1.00; 95% CI, 0.85-1.17; P for trend = .77) or within 3 years of baseline (adjusted HR, 1.09; 95% CI, 0.84-1.42; P for trend = .65), leading the investigators and others to ultimately conclude this method may not be well-suited for the early-detection of AD.^(1123, 1124) While other groups have published similar reports for transthyretin, apolipoprotein A1, matrix metalloproteinase, and other blood proteins, predictably A β -targeted approaches dominate the field of fluid-based diagnostics for AD.⁽¹¹²⁵⁻¹¹²⁷⁾ Importantly, the discovery of mechanisms such as RAGE mediated influx of A β across the blood-brain barrier have lent credibility to the hypothesis that an equilibrium may exist between plasma A β and the CSF/interstitial fluid of the brain.⁽⁹⁰⁰⁻⁹⁰³⁾ Disappointingly however, many studies that have compared plasma A β levels with their CSF counterparts⁽⁹¹⁸⁻⁹²¹⁾ or the

binding of PET A β radiotracers^(919, 922) have reported an absence or exceedingly low correlations. On the other hand, meta-analyses of plasma A β studies confidently affirm the utility of plasma-based measurements of A β .^(1128, 1129) These studies go on to note that the predominant factor limiting the clinical utility of plasma A β measurements are a series of confounding variables. It is generally agreed that the most prevalent of these confounds are methodological in nature, secondary to the numerous technical pitfalls associated with this method. For example, when plasma samples are kept at room temperature for just 24 hours, a considerable 20% loss in A β pools has been reported.^(920, 930-932) Moreover, similar losses in sample A β can be introduced secondary to storage at -20⁰C instead of -80⁰C, with storage at 4⁰C keeping samples viable for only a matter of hours.⁽¹¹³⁰⁾ Less conspicuous methodological adaptations have also been identified, such as the use of polypropylene sample vials in lieu of glass or polystyrene collection tubes, as reports suggest A β peptides stick to these latter mentioned surfaces.⁽¹¹³¹⁾ Recognizing the potential utility of plasma A β measurements to screen therapeutic response in our own work, we set out to develop a reliable protocol for assessing this biomarker in the 5XFAD mouse model. Once successful, we leveraged this approach to monitor plasma A β levels before and after treatment with a novel A β -aggregation inhibitor discovered in Aim 1 of our work, PMZ. We hypothesized that PMZ's therapeutic ability to dissociate A β assemblies would result in an increase in the brain's soluble pool of A β . No longer confined to the brain, we predicted a detectable fraction of this solubilized A β would be cleared to the blood and thus produce a significant increase in plasma A β levels.

11.2 AIM 3 EXPERIMENTAL METHODS

Positron Emission Tomography Imaging & Analysis

Positron emission tomography imaging was performed using the micro-PET Focus220 (Siemens Pre-clinical, Knoxville, TN, USA) in a dynamic acquisition mode for 60 minutes following injection of either probe (150–200 μCi , 100–130 μL) into awake, non-fasted, eight-month-old 5XFAD and age-matched wild-type mice ($N = 2\text{--}3$ per group). Dosing was performed via tail vein injection to avoid non-specific signal artifacts typical of retro-orbital administration. To obtain scans of the brain and anterior anatomy of the animal, mice were anesthetized with isoflurane and placed in the supine position. The data were acquired in a 3-D mode with an axial span of approximately 8 cm. During the scanning, the mice remained under isoflurane-induced anesthesia and their core body temperature was maintained at 30°C using a pad connected to a circulating warm water bath. To obtain anatomical data, after PET imaging, a CT image was acquired using the micro-CATII (Siemens Pre-clinical, Knoxville, TN, USA) using the same animal holder with the subjects maintained under anesthesia throughout the procedure. Upon completion of the CT scan the mice were immediately perfused with 20 mL of normal saline and sacrificed to facilitate radiation dosimetry analysis of the probe's biodistribution. PET images were reconstructed using the iterative MAP reconstruction algorithm with 18 iterations and a beta smoothing value of 0.001 into $128 \times 128 \times 95$ slices with a voxel size of $0.475 \text{ mm} \times 0.475 \text{ mm} \times 0.796 \text{ mm}$. The PET and CT images were co-registered and analyzed using the AMIDE software package.⁽¹¹³²⁾ Mean radioactivity values were obtained from manually drawn three-dimensional regions of interest. These included the whole brain, hippocampus, cerebellum, skeletal muscle, and heart. Standardized uptake values (SUV), defined as the decay corrected brain radioactivity concentration, normalized to injected dose and body weight, were calculated for all regions. No correction for partial volume was applied to the PET data.

Autoradiography

Immediately upon completion of the CT scan, mice ($N=2$ per group) were sacrificed and perfused with 20 mL of ice cold normal saline as previously described to remove PET-ligand from the brain's microvasculature. Once perfusion was

complete, the animals were decapitated using surgical scissors and their brains removed. To facilitate immediate coronal sectioning of the hippocampus, the brains were placed into a mold which facilitated guided isolation of the midbrain. This tissue was then immediately embedded in Cryo-OCT compound and sectioned (Fisher Scientific). To generate a representative sample set of each animal's midbrain, two 12 μm sections were sectioned and mounted. Next, 48 μm were sectioned and discarded. Finally, two more 12 μm sections were sectioned and mounted. This process was repeated until four to six 12 μm coronal sections were mounted onto a single slide. All slides were then imaged for 5 hours using a digital autoradiography system (BetaIMAGER, Biospace Lab). To help estimate the exposure time, a Geiger counter (CRC-15W, Capintec, Ramsey, NJ, USA) was used to detect the relative amount of radioactivity in the sample set. Once image acquisition was completed, co-registration of auto-radiographic images with fluorescence imaging performed on consecutive slides immune-stained with anti-amyloid antibodies (A3981, Sigma Aldrich, St. Louis MO) was performed to confirm the regional deposition of the probe.

SensoLyte Assay

To investigate the ability of PMZ to perturb $\text{A}\beta$ monomer aggregation, a commercially available thioflavin T-based aggregation kit with colorimetric readout was employed (AnaSpec). Of the two commercially available versions, the 96-well plate-based assay employing synthetic $\text{A}\beta_{42}$ was chosen due to the increased relevance of this isoform to AD pathogenesis. Generally speaking, all operations were performed in congruence with the protocol provided by the manufacture. Briefly, 1 mL of the proprietary assay buffer, chilled to 4 $^{\circ}\text{C}$, was added to .5 mg of $\text{A}\beta_{42}$ peptide. Following hydration of the peptide sample (3 minutes), the reconstituted $\text{A}\beta$ peptide was sonicated for 5 minutes at 4 $^{\circ}\text{C}$ to completely dissolve the peptide and insure that monomerized $\text{A}\beta$ species predominated in solution. Next, this sample was spun at 10,000 rpm for 5 minutes at 4 $^{\circ}\text{C}$ to remove any precipitated material. With the $\text{A}\beta$ sample prepared, 10 μL of 2 mM thioflavin was added into each well. Subsequently, 5 μL of curcumin was added to achieve a final concentration in solution of 200 μM . Lastly, 85 μL of $\text{A}\beta_{42}$ -containing assay buffer was added to each reaction vessel. Immediately upon mixing (Time = 0), fluorescence at 485 nm (excitation 440 nm) was measured. Following this baseline measurement, the 96-well plate was transferred to a 37 $^{\circ}\text{C}$ incubator to expedite $\text{A}\beta$ fibrillation. Subsequently, fluorescence for each well was measured in 10 minute intervals for 90 minutes. In addition to wells containing test compounds, several control

conditions were also included. For example, wells containing only 100 μ L of assay buffer served as “blank” controls. “Vehicle controls” were also included in congruence with the manufacture’s protocol and were comprised of 85 μ L of A β -containing assay buffer, 10 μ L of thioflavin, and 5 μ L of a 20% DMSO solution.

Western Blot

Treated & Non-treated mice were anesthetized before undergoing brain perfusion with ice cold 1X PBS containing a protease inhibitor cocktail (Roche, Indianapolis, IN) in accordance with previously described methods. Following perfusion, the brain tissue was removed and homogenized in 2 mL of tissue lysate buffer containing protease inhibitor (Sigma-Aldrich, Saint Louis, MO). Brain homogenates were normalized for protein content using BCA assay (Pierce, Rockford, IL) and 20 μ g of protein was run on 4-12% Tris-HCL SDS-PAGE gels (Bio-Rad, Hercules, CA). After transfer to polyvinylidene difluoride membrane, blots were incubated with 4G8 anti-A β monoclonal antibodies (Covance, Princeton, NJ) at 1:1000 overnight at 20^oC. Peroxidase conjugated secondary antibodies (Pierce, Rockford, IL) were applied and immunoblot signals were detected by enhanced chemiluminescence and quantified using the Xenogen IVIS 200 bioluminescent and fluorescent imaging system.

Plasma A β ₄₀ and A β ₄₂ ELISA Sample Collection

Whole blood samples (100-250 μ L) were obtained from untreated and PMZ treated 6-month old 5XFAD or wild type mice via the facial vein. Blood was collected in chilled 1.5 mL Eppendorf tubes (polypropylene) pre-coated with 20 μ L of 4^oC EDTA with 1x protease inhibitor (1 Roche cOmplete protease inhibitor tablet per 4 mL EDTA). Immediately after collection, each sample was briefly spun (< 5 seconds) at 5,000 RPM (BioRad Model 16k) to collect all blood droplets adhered to the side of the collection vial. The samples were then immediately stored on ice for no more than 20 minutes before further processing. All samples were next centrifuged at 2000 G for 10 minutes to remove cellular constituents. The resulting plasma was then aliquoted into clean polypropylene Eppendorf tubes for use in the ELISA. In parallel with this procedure, each plasma sample was assayed for protein content using a commercially available BCA protein assay

kit. (Pierce Biotechnology, Rockford, IL, USA). All unused plasma was flash frozen and stored at -80°C for no more than 1 week.

Y-Maze Behavioral Assay

Y-maze study: In an effort to quantitatively assess the effect of chronic PMZ injection on spatial-dependent and working memory in a pre-clinical mouse model of AD, the Y-maze behavioral assay was employed. Briefly, 6-week old 5XFAD mice (N=8) were chronically administered a 25 mg/kg dose of PMZ three times a week for 8 weeks. Two cohorts consisting of a group of age matched 5XFAD and a group of wild type mice (N= 10 per group) which remained in their home caging and were untreated throughout the study served as controls. Following a one week habituation period in the behavioral testing facility to decrease experimental confounds attributable to the animals' stress, working memory and spatial memory were assessed via Y-maze. All behavioral assays were run during the night cycle and all mice were allowed to habituate to the experimental environment for 3 hours prior to testing.

Working Memory Y-maze Paradigm: In this behavioral assay, spontaneous alteration was tested in a Y-shaped maze with three opaque plastic arms at a 120° angle from each other. In an effort to make each arm distinguishable to the animal, laminated sheets of uniquely patterned paper were fastened to the outside of the maze. These patterns included a "black arm" surrounded completely with black background while a "dotted arm" consisted of alternating black and white vertical bars with a 2.5 cm width. Lastly, the third arm or "dotted arm" contained white circles with a 2 cm diameter on a black background. Prior to behavioral testing, rigorous controls were run on a naïve cohort of animals to insure no intrinsic preference for a particular arm existed. The entire maze was cleaned and dried thoroughly with ethanol both before and after each trial to insure standardized maze conditions. After introduction of the mouse into a standardized arm of the maze, the animal was allowed to freely explore the three arms for 6 minutes with the sequence of arm entries being recorded. The number of arm entries and the number of correct triads were recorded using ANY-maze behavior tracking software in conjunction with a CCD video camera system. Arm entries were logged when all four limbs of the animal crossed a line arbitrarily placed 50% down each of the three maze arms. A quantitative evaluation of working memory performance was made by calculating the percent spontaneous alteration for each animal.

Possible confounds associated with differences in locomotion between cohorts were controlled for via comparison of the total number of arm entries.

Spatial-Memory dependent Y-maze Behavioral Assay: One week following completion of the working memory Y-maze behavioral assay, all animal cohorts were then tested in the spatial memory paradigm. To directly assess hippocampal function at the behavioral level, a two-phase Y-maze paradigm was employed. As in the working memory task, each arm of the Y-maze was decorated with spatial cues to increase the salience of each arm. Notably, quantification of the mean number of entries and seconds exploring each arm of the maze in a naïve cohort of animals confirmed no innate preference for any of the arms. Additionally, no differences in the initiative to explore were noted between any of the cohorts suggesting that any observed differences in behavior truly reflect alterations in spatial memory. During the first phase of this paradigm, the mouse was allowed to freely explore 2 of the three arms of the Y-maze for a 6 minute period. The arm which was blocked during this first phase was randomized between animals, and designated as the "novel" arm in the secondary phase of the study. Following the first period of exploration, each mouse was returned to its home cage and left undisturbed for a 30 minute period. Following this period of rest, each mouse was placed into a randomized arm of the maze and allowed to freely explore all three arms of the Y-maze for a 5 minute time interval. To quantitatively assess spatial memory, the proportion of time spent exploring the previously blocked "novel arm" arm was quantified and plotted as the fraction of overall time spent exploring. All arms of the maze were cleaned with 70% ethanol both prior to and after each trial to insure standardized maze conditions between animals.

Plasma A β ₄₀ and A β ₄₂ ELISA

Measurements of plasma A β ₄₀ and A β ₄₂ were conducted largely in accordance with the manufacturers protocol with the exception noted here. First lyophilized 1 μ g A β ₄₀ and A β ₄₂ peptide standards were reconstituted with 1 ml of peptide standard reconstitution buffer and allowed to hydrate for ten minutes. Each sample was next thoroughly mixed by repeated inversion of the polypropylene tube. The resulting 1,000,000 pg/mL standards were then serially diluted with sample buffer to generate protein standards at concentrations of 10,000, 250, 125, 62.5, 31.25, 15.625, 7.8125, and 3.91 pg/mL. Next, the assays detection antibody was diluted to a working concentration of .5 μ g/mL. 100 μ L of each A β

peptide protein standard was then added to the provided monoclonal anti-A β coated plates (A β ₄₀ and A β ₄₂). Similarly, 100 μ L of each plasma sample (1:5 dilution) were added. All samples were loaded in duplicate fashion. To each well, 50 μ L of detection antibody solution was added. The plate was protected from light, agitated for 20 minutes at 4⁰C, and subsequently left to incubate overnight in the refrigerator. Following incubation, each well was washed 7 times with 350 μ L of wash buffer via multi-channel pipette. 100 μ L of 3, 3', 5, 5'-Tetramethylbenzidine (TMB) liquid substrate was then added to each well and protected from light. After a 20 minute incubation period at room temperature and under constant agitation, 50 μ L of 1M HCL was added to halt the colorimetric reaction. Absorbance was read at 450 nm using a microplate reader within 5 minutes of adding the stop solution. Determination of plasma sample A β ₄₀ and A β ₄₂ content was then assessed by averaging the samples absorbance readings and comparing this value to a calibration curve generated using the peptide standard wells using linear regression curve-fit. All plasma levels of A β were normalized to plasma protein content as assessed by BCA assay. The reading for the highest standard concentration (250 pg/ml) was excluded from the curve due to its robust signal intensity (Figure 11-1).

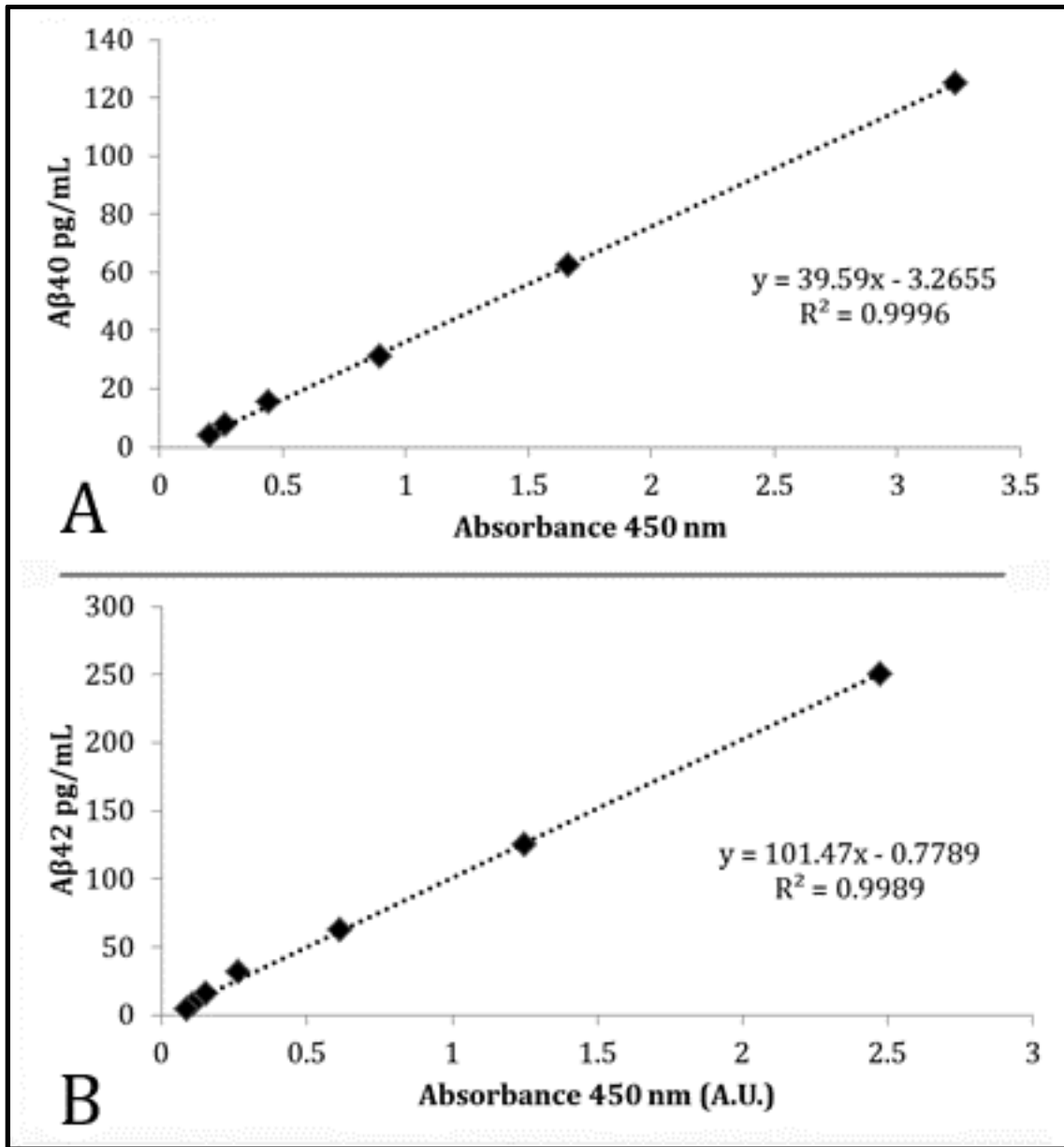


Figure 11-1. Calibration Curve for Quantification of Plasma Aβ₄₀ (A) and Aβ₄₂ (B) by ELISA.

Lyophilized 1 μg Aβ₄₀ and Aβ₄₂ peptide standards were reconstituted with 1 ml of a proprietary peptide standard reconstitution buffer and allowed to hydrate for ten minutes. Each sample was thoroughly mixed in a polypropylene tube by repeated inversion. The resulting 1,000,000 pg/mL standards were then serially diluted with sample buffer to generate protein standards at concentrations of 10,000, 250, 125, 62.5, 31.25, 15.625, 7.8125, and 3.91 pg/mL. The results demonstrate a strong linear relationship between protein concentration and absorbance up to a detection limit of 4 pg/mL.

11.3 AIM 3 EXPERIMENTAL RESULTS

11.3.1 Result: ¹⁸F-labeled COX2 Probe Does Not Penetrate the BBB

As a preliminary assessment of the hypothesis that PET-mediated imaging of COX2 levels in the brain can as a complimentary biomarker for the longitudinal assessment of AD treatment response, eight-month-old 5XFAD (N = 3) and age-matched wild-type controls (N = 2) were dosed with 150-200 µCi of radiolabeled compound via tail-vein injection. Immediately after dosing, dynamic PET (3D-mode with 8 cm axial span) imaging was employed to monitor probe uptake and retention in the brain. To provide topographical information of probe retention in the brain, the resulting PET data was co-registered with corresponding CT images (Figure 11-12). This data was then used to evaluate probe pharmacokinetics by facilitating comparison of initial brain uptake (% dose/gram 10 min post I.V. injection) and retention (% dose/gram 60 minutes post injection) between 5XFAD and wild-type cohorts. Disappointingly, such an analysis proved unwarranted as less than .02% of the initial dose per cubic centimeter (%ID/cc) of tissue was taken up in the brain at any time point. As depicted by Figure 11-12, the vast majority of the probe was retained in the liver (< 80% ID/cc). These trends hold true for both 5XFAD and wild type mice imaged with the COX2 probe. Taken together, this profile of distribution suggests radiolabeled 2-Methyl-3-((4-methylthiazol-2-yl) methyl) azulene-1-yl (4-nitrophenyl) methanone probe is not capable of penetrating the BBB and thus is not suitable for the application of biomarker imaging in AD.

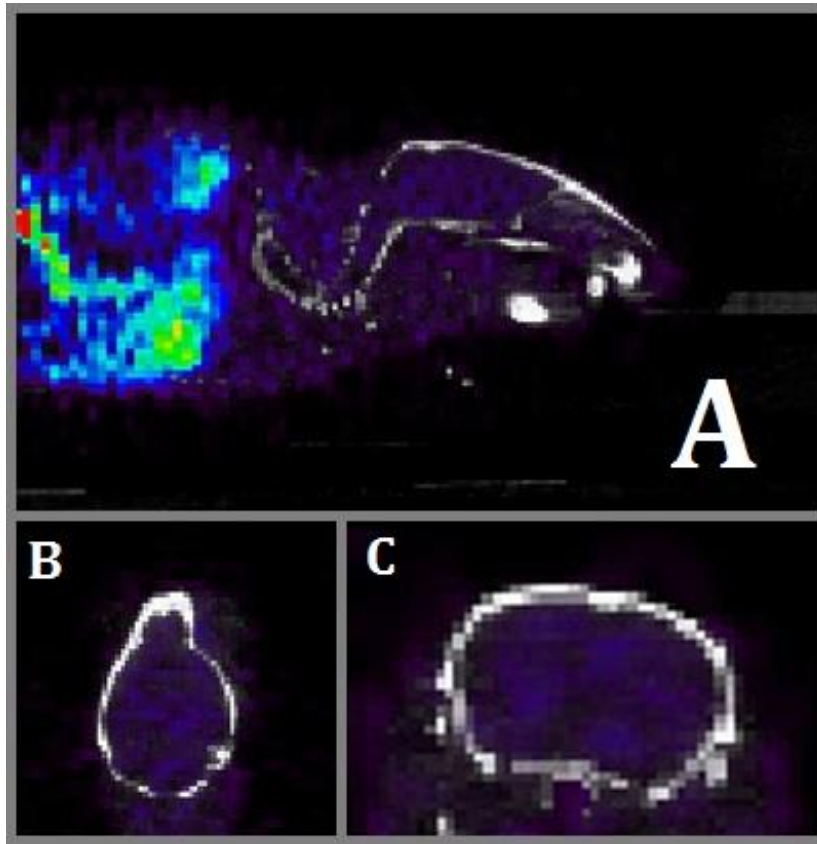


Figure 11-2. PET Imaging of COX-2 in 5XFAD Mice.

Representative (A) sagittal, (B) coronal, and (C) transverse images of PET-mediated COX-2 imaging in the brains of 8 month-old 5XFAD mice. Dynamic PET imaging was employed to monitor probe uptake and retention in the brain following a 150-200 μ Ci dose of radiolabeled compound via tail-vein injection. Qualitatively, the images strongly suggest that the COX-2 specific PET-ligand failed to robustly penetrate the blood brain barrier. This is best evidenced by the signal in the brain failing to rise above background in the images presented. Subsequent quantitative analysis revealed that less than .02% of the initial dose per cubic centimeter (%ID/cc) of tissue was taken up in the brain at any time point. Cumulatively, the results strongly suggested this particular COX-2-targeted ligand is unsuited for imaging neuro-inflammation in AD.

11.3.2 Result: ¹⁸F-labeled IGF1R Probe Does Not Penetrate the BBB

Aware of the vast literature strongly supporting the existence of AD-induced disturbances in insulin/IGF1 signaling, we chose to investigate whether expression of IGF1R in the brain differed between wild type and demented mice. Leveraging a specific PET-compatible ligand for IGF1R, we imaged the brains of 8-month old wild type (N = 2) and 5XFAD (N = 3) mice. In a manner identical to our COX2 PET study, immediately after tail-vein injection of the IGF1R probe dynamic PET imaging (3D-mode with 8 cm axial span) was employed to monitor probe uptake and retention in the brain. In congruence with standards in the field, the resulting PET images were then co-registered with CT images to provide topographical information of probe retention in the brain. A representative image of the data obtained at the 60 minute time point from a wild type mouse is provided in Figure 11-3C. In Figure 11-3B, a similar representative image is provided for the 5XFAD cohort. Once again, we were disappointed to note a complete absence of signal in the brains of either set of animals, reflecting an inability of the IGF1R-targeted PET-probe to cross the BBB (<.01% ID/cc). This conclusion is confirmed by the representative time activity curves presented in Figure 11-3A. Interpreting these graphs, seconds after injection, a brief peak in positron emission in the brain and hippocampus is detected. Unfortunately, a brief spike of this nature is typical of all radio-active ligands and represents the passage of the initial I.V. bolus through the brain's circulatory system as opposed to passage through the BBB. This is confirmed by the steep and sustained drop-off in SUV noted in the time activity curves generated for the hippocampus and whole brain. Significantly, the time activity curve presented for skeletal muscle is markedly different. For this analysis, regions of interest were manually drawn to include the triceps and biceps brachii of the anterior limb of the mouse. Within this region of interest, SUV dramatically rose and remained elevated throughout the 60 minute imaging session; a result strongly suggestive of the fact that the IGF1R targeted probe was specifically retained in these tissues. Notably, this result is in congruence with the literature, which is unanimous in its opinion of the significance of IGF1R-mediated signaling in the growth and differentiation of skeletal muscle.^(1114, 1133, 1134) Relating this finding back to our goal of imaging disturbances in insulin/IGF1 signaling within the brain, the retention of PET-ligand in skeletal muscle confirms that penetration of the BBB is the key barrier in this study as opposed to a lack of target specificity.

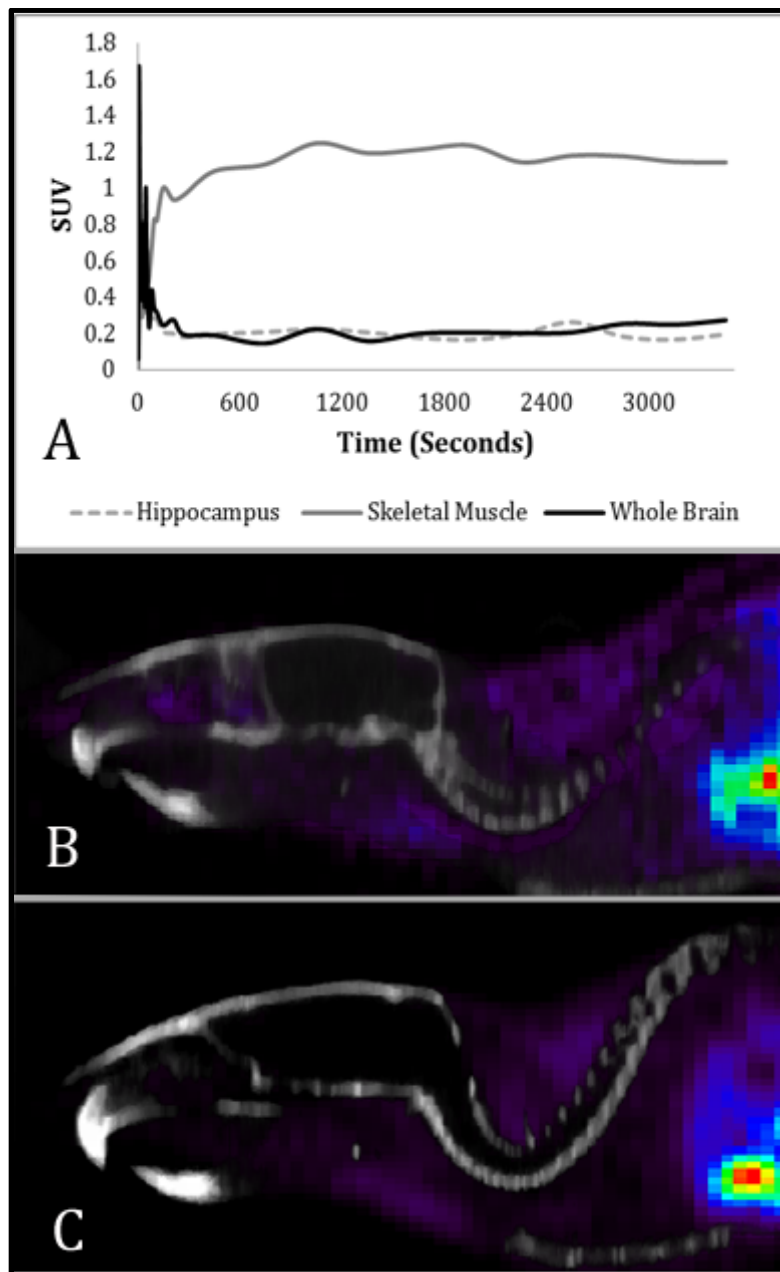


Figure 11-3. PET-mediated Imaging of IGF-1R Impaired by Poor Blood Brain Barrier Penetration.

(A) Representative time activity curves obtained from 8-month-old 5XFAD mice dosed with 150-200 μ Ci of radiolabeled compound via tail-vein injection. Results indicate negligible probe retention in the brain and hippocampus indicating this particular PET-ligand is incapable of crossing the BBB. However, probe specificity is very good, with IGF-1R expressing tissues such as skeletal muscle exhibiting robust radioactivity throughout the course of imaging. (B) Representative sagittal image of 5XFAD mouse at the 60 minute time point. (C) Representative image of an age-matched wild type mouse at the 60 minute time point.

11.3.3 *Results: Plasma A β Measurements in Non-treated 5XFAD and Wild Type Mice*

After several failed trials, we successfully adapted two independent and commercially available ELISA kits for quantification of plasma A β_{40} and A β_{42} . Importantly, a major advantage of this approach is that these kits have already been evaluated for sensitivity (2 pg/mL), cross reactivity with other A β species (< 1.2%), and intra-assay variation (CV < 7.7%). Before examining the effect of A β -aggregation inhibitors on plasma A β using this technique however, it was necessary to establish a baseline for our mouse model. Additionally, as a preliminary evaluation of whether plasma A β levels reflect A β burden in the brain, we sought to demonstrate differences in plasma A β levels between 6-month-old 5XFAD and wild type mice (N = 6 per group). To achieve both of these experimental goals, measurements of A β_{40} and A β_{42} levels in the plasma of non-treated 6-month-old 5XFAD and wild type mice were conducted via our adapted ELISA protocol. In congruence with our hypothesis that plasma A β levels reflect A β burden in the brain, measurements of both plasma A β_{40} and A β_{42} levels were significantly different between cohorts (P < .001). Moreover, plasma levels of each of peptide in the 5XFAD mouse model were remarkably consistent, ranging from 22-30 pg/mL and 6-14 pg/mL for A β_{40} and A β_{42} , respectively. Interestingly, mean A β_{40} levels in the plasma of wild type mice (60-80 pg/mL) were significantly increased in comparison to age-matched 5XFAD animals at baseline (P < .01). In a manner fitting their genotype, A β_{42} levels in the plasma of non-transgenic mice remained below the detection limit of our assay (< 2 pg/mL). Taken together, these data provide strong support for our hypothesis that plasma levels of A β peptide are modulated by A β burden in the brain. Moreover, we confirm the ability of our ELISA based approach to reliably measure A β_{40} and A β_{42} levels in the plasma of 5XFAD mice. With these key experimental requirements demonstrated, we next sought to lend mechanistic support to PMZ's ability to disrupt A β aggregation in vivo by demonstrating changes in plasma A β_{40} and A β_{42} levels in 5XFAD mice treated with this putative therapeutic agent.

11.3.4 Results: PMZ Perturbs A β ₄₂ Aggregation In-vitro

Having confirmed our ability to reliably measure A β peptide in the plasma, we next wanted to characterize the ability of A β aggregation inhibitors to modulate this biomarker. Seeking to build on our previous findings in Aim 1, we chose to evaluate PMZ's effect on plasma A β levels. Importantly, the data presented on this molecule thus far confirms its ability robustly cross the BBB. Moreover, because this compound was discovered via HTS mediated by the HATCO assay, which leverages a *in vivo* derived amyloid source, we could be confident this molecule interacts with A β assemblies present in the brains of 5XFAD mice. Before testing this compound's effect on plasma A β levels however it was necessary to demonstrate its ability to perturb A β fibrillation. To do this, a commercially available assay (SensoLyte) providing a colorimetric readout of A β ₄₂ fibrillation was leveraged. Notably, various derivations of this assay represent the gold-standard employed in the field when evaluating the therapeutic potential of A β -binding molecules. For this reason, this approach represents the ideal method to characterize the inhibitory effects of PMZ on A β -aggregation. In principal, the SensoLyte assay operates by correlating the intensity of thioflavin fluorescence at 485 nm to A β ₄₂ fibril formation. Mechanistically, this approach is viable because thioflavin binds specifically to A β -fibrils, exhibiting no modulation of fluorescence magnitude or wavelength in the presence of lower-order A β -species. Therefore, in stark contrast to 5XFAD lysate, numerous precautions are undertaken to insure the amyloid source used in the SensoLyte assay begins in a completely monomerized state. Leveraging the combination of thioflavin and A β monomers to establish a fluorescence baseline, the sample is then allowed to undergo fibrillation. Thus, when interpreting the results of this assay, an increase in thioflavin fluorescence over time is interpreted as an increase in A β fibril density. Translating this readout to an evaluation of candidate A β -aggregation inhibitors, compounds which significantly decrease the magnitude of fluorescence compared to vehicle treated samples are considered to harbor anti-A β aggregation properties.

As detailed in the appropriately titled methods section, the SensoLyte assay was used to longitudinally monitor the fibrillation kinetics of synthetic A β ₄₂ monomers in the presence and absence of PMZ. In order to demonstrate a dose dependent effect, PMZ was added to the assay at 50 μ M and 200 μ M concentrations. All other inhibitors were added at 200 μ M concentrations. As demonstrated by Figure 11-4, in the presence of only buffer, thioflavin fluorescence grows steadily as a function of time as A β fibrillation proceeds. At the 40 minute time point, an equilibrium between monomeric and higher-order A β species is reached, resulting in the observed plateau in thioflavin fluorescence. Illustrating the effect

of known A β aggregation inhibitors, the fluorescence curves produced by thioflavin and A β_{42} mixtures in the presence of Morin, phenol red, and resveratrol are markedly altered in comparison to the buffer condition. Most significantly, the plateau in thioflavin fluorescence is dramatically reduced under these conditions as compared to the buffer control. At the 100 minute time point for example, Morin, phenol red, and resveratrol reduce thioflavin fluorescence relative to the buffer condition by 58.10%, 60.93%, and 70.93%, respectively. In a manner suggesting PMZ robustly inhibits A β aggregation, a similar yet more robust trend is observed in both PMZ conditions. In more detail, the fluorescent signal measured from the 50 μ M PMZ condition was reduced by 70.89% in comparison to the positive controls. Moreover, the 200 μ M condition exhibiting just 4.88% of the positive control's fluorescent signal, inhibiting 95.11% of A β aggregation. Interpreted as a whole, the results strongly suggest that PMZ perturbs A β aggregation and thus might modulate A β levels in the brain when leveraged as a disease-modifying therapeutic.

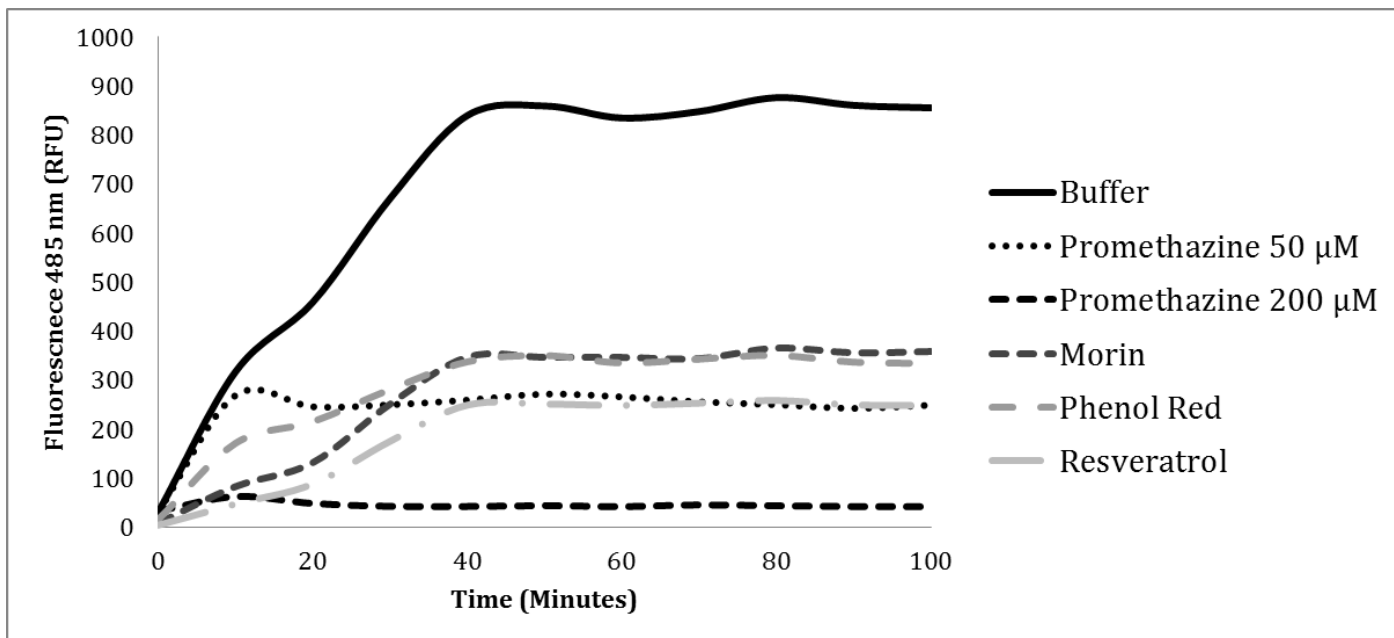


Figure 11-4. PMZ Inhibits Aggregation of A β ₄₂ Monomers In-vitro.

A colorimetric assay facilitating the identification of A β aggregation inhibitor activity was used to investigate the ability of PMZ to perturb A β monomer aggregation. Briefly, thioflavin and monomerized A β ₄₂ peptide were incubated in the presence and absence of known (200 μ M) and putative A β -aggregation inhibitors (50 μ M and 200 μ M). Thioflavin fluorescence at 485 nm served as a reporter of A β fibrillation, with increasing fluorescent signal representing an increased availability of A β fibrils in solution. As illustrated, in the presence of 50 μ M PMZ, A β -fibril induced increases in thioflavin fluorescence only reached 29.10% of that measured from the positive control condition (buffer only). Further, PMZ perturbed A β fibrillation in a dose-dependent manner, with 200 μ M PMZ reducing thioflavin fluorescence by greater than 95%. Interpreting this finding, the data strongly suggests that curcumin perturbs A β aggregation.

11.3.5 Results: Chronic I.V. Administration of PMZ Reduces A β Plaque Burden in 5XFAD Mice

Confident in our *in vitro* characterization of PMZ's ability to perturb A β aggregation, we next needed to validate that chronic therapy with this compound could modulate A β plaque levels *in vivo*. To facilitate this work, A β -plaque burden was assessed in the brains of two distinct cohorts of 6-month-old 5XFAD mice. Constituents of the treated cohort (N=5) received a 25 mg/kg dose of PMZ three times a week by tail-vein injection for 8 weeks beginning at 4 months of age. Non-treated transgenic littermates (N=3) served as controls. To quantitatively assess the effect of chronic PMZ therapy on A β plaque burden, sagittal sections (n=30 per group) isolated from treated and non-treated 5XFAD mice and were stained with 1% thioflavin as described and quantified using a custom plaque segmentation algorithm designed in Matlab. As in our previous work, three pathologically relevant regions of interest were selected for analysis. In support of our hypothesis that PMZ can perturb A β plaque assembly, quantitative analysis of the data reveals that A β plaque burden in the cortex of treated 5XFAD mice is just 36.91% that of non-treated age-matched littermates ($P < .01$). Similarly, plaque numbers in the hippocampus and subiculum were significantly reduced by 58.75% and 61.12%, respectively ($P < .01$). Importantly, no alterations in APP levels, the holoprotein from which the A β peptide fragment is derived were noted when assessed via Western blot (Figure 11-6). Moreover, qualitative assessment of COX-2 expression revealed a robust reduction in the expression of this particular marker of neuro-inflammation following a chronic regiment of PMZ injections in 5XFAD mice. Interpreted as a whole, the data support a role for PMZ in the reduction of A β peptide and its associated neuro-inflammatory effect. Additionally, PMZ inability to modulate APP expression suggests that that the observed reductions in brain A β as assessed by IHC are the result of increased clearance and not decreased production.

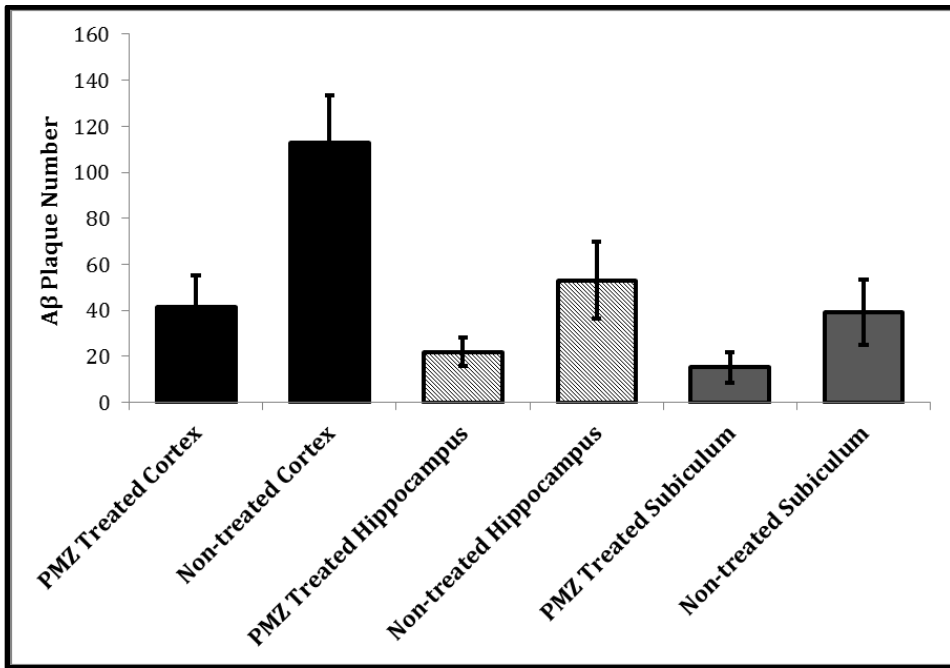


Figure 11-5. Chronic Treatment with Promethazine Reduces Amyloid Plaque Burden.

4-month-old 5XFAD mice were treated for 8 weeks with 25 mg/kg doses of PMZ delivered via tail-vein injection (N = 5). By the end of the therapeutic trial, the treated 5XFAD mice, now 6 months of age, were sacrificed in order to facilitate quantification of A β plaque burden via histochemical staining with thioflavin. Plaque numbers were quantified in the cortex, hippocampus, and subiculum both manually by a blinded reviewer and via an automated algorithm generated in MATLAB. Non-treated age-matched littermates of the 5XFAD genotype served as controls (N = 3). In each region of interest, A β burden was significantly modulated by PMZ treatment (P < .01). In the cortex, the total number of amyloid plaques in the treated cohort was reduced by 63.09% as compared to controls. Similarly, plaque numbers in the hippocampus and subiculum were significantly reduced by 58.75% and 61.12%, respectively (P < .01).

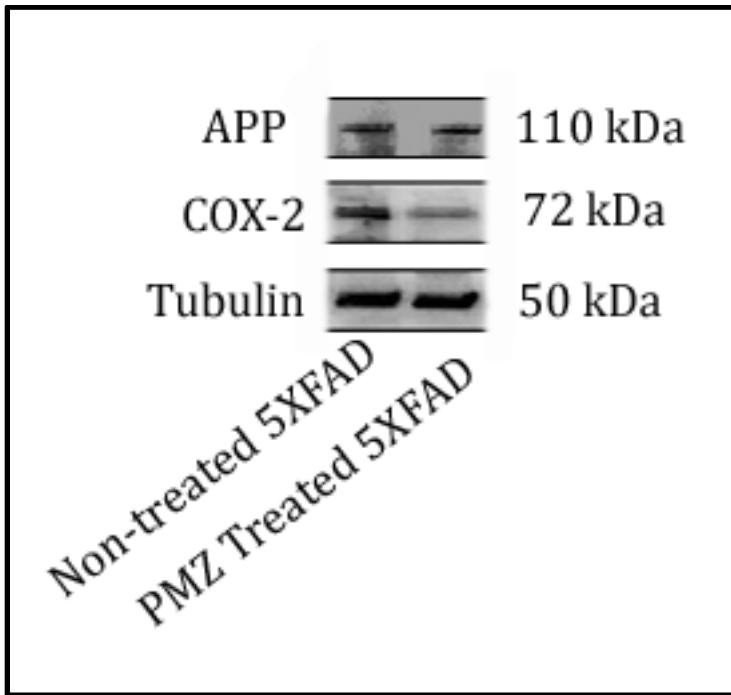


Figure 11-6. Promethazine Attenuates A β -mediated Neuro-inflammation without Effecting APP Expression.

Western blot mediated analysis of APP and COX-2 expression in homogenized hemi-sections obtained from treated (N = 3) and non-treated 5XFAD mice (N = 2). 4-month-old 5XFAD mice were treated for 8 weeks with 25 mg/kg doses of PMZ delivered via tail-vein injection. Comparison of APP expression between cohorts reveals that chronic administration of PMZ does not modulate A β burden by affecting the levels of its precursor. This data suggests that the reductions in A β plaque burden observed via fluorescence microscopy are more likely due to an increase in clearance of A β peptide, as a mechanism in which A β peptide production is somehow attenuated should affect APP levels. Regardless of the mechanism by which PMZ reduces A β burden in the brain however, it is clear from the data that this effect also attenuates the neuro-inflammatory cascade initiated by amyloid deposition. This is best evidenced by the clear reduction in COX-2 levels in treated 5XFAD animals as compared to non-treated littermates.

11.3.6 Results: Chronic I.V. Administration of PMZ Improves Working & Spatial Memory in 5XFAD Mice

Although histological analysis of PMZ treated 5XFAD mouse brains revealed a reduction in A β plaque burden, it was unclear whether this therapeutic intervention was sufficient to impact cognitive function. To investigate this question, the effect of chronic PMZ therapy on spatial and working memory was probed using two distinct versions of the Y-maze behavioral assay. Briefly, 4 month old 5XFAD mice (N=8) were administered a 25 mg/kg dose of PMZ three times a week for 8 weeks via tail-vein injection. Two cohorts consisting of a group of age matched 5XFAD and a group of wild type mice (N= 10 per group) were left untreated throughout the study and thus served as controls. Following a one week habituation period in the behavioral testing facility to decrease experimental confounds attributable to stress, working memory and spatial memory were assessed via two variations of the Y-maze behavioral paradigm. In the working memory paradigm, spontaneous alteration was quantified over a 6 minute trial and reported as percent spontaneous alternation. Importantly, this variable denotes the percentage of time the animal correctly entered all three arms in sequence over the total number of choices made. Thus, the greater the percent spontaneous alteration (%SA), the higher functioning the animal is with respect to working memory. As graphically illustrated in Figure 11-7, statistical comparison of working memory performance in non-treated 5XFAD mice reveals a mean reduction in performance of 27.53% relative (Mean = 54.43% SA) to wild type controls (Mean = 75.10% SA). Importantly this result demonstrates that without therapeutic intervention, the working memory of 5XFAD mice becomes significantly perturbed by 6 months of age when compared to non-amyloid bearing mice ($P < .001$). In stark contrast to the non-treated 5XFAD cohort, working memory function in 5XFAD mice treated with PMZ is largely persevered, with a mean %SA of 69.61%. This constitutes a 20.22% improvement over the age-matched non-treated cohort of 5XFAD mice and confirms a statistically significant therapeutic benefit for PMZ on working memory ($P < .01$). In fact, PMZ therapeutic impact was so robust that the %SA measured in the treated 5XFAD cohort did not significantly differ ($P > .05$) from wild type controls (Mean = 69.61% and 75.10%, respectively). Just as in the behavioral studies previously described, confounds attributable to differences in locomotion, motivation to explore, or arm preference were excluded. Taken as a whole, this data strongly supports the conclusion that PMZ administration prevents the acquisition of working memory deficits on the 5XFAD mouse model by inhibiting A β retention in the brain.

To directly assess hippocampal function at the behavioral level a two-phase Y-maze paradigm designed to probe spatial memory was employed one week after assessment of working memory. Summarizing the experimental design, the mouse was first allowed to freely explore two of the three Y-maze arms for a 6 minute period. The arm which was blocked during this first phase was randomized between animals and designated as the "novel" arm in the secondary phase of the study. Following the first period of exploration, each mouse was returned to its home cage and left undisturbed for a 30 minute period. Next, each mouse was placed into a randomized arm of the maze and allowed to freely explore all three arms for a 5 minute time interval. To quantitatively assess spatial memory, the proportion of time spent exploring the previously blocked "novel arm" arm was quantified and plotted as the percentage of overall time spent exploring. Under this experimental paradigm, mice with intact hippocampal function should remember exploring the original two arms during the first trial and are thus predicted to spend a majority of their time exploring the novel arm. As presented in Figure 11-7, the performance of wild type mice is congruent with this prediction, as these animals spend the majority of their time (54.20%) exploring the previously blocked arm. In contrast to this cohort, animals with impaired spatial memory function are expected to spend equal amounts of time exploring each arm; as they do not recall their previous 6 minute exploration of this environment. Again, the behavioral data is consistent with this prediction. Untreated 5XFAD mice appeared incapable of recognizing the spatial cues of the maze and thus demonstrated no discernible preference for the novel arm, spending just 25.24% of their time exploring this region of the maze. Corroborating our working memory data which suggests that PMZ-induced reductions in A β are of therapeutic significance at the behavioral level, PMZ-treated 5XFAD mice exhibited a robust and significant 18.23% improvement in spatial memory (Mean time spent exploring novel arm = 43.47%) when compared to non-treated 5XFAD littermates ($P < .01$). Importantly however, despite dramatically attenuating the progressive loss of hippocampal function typical of the 5XFAD phenotype, therapeutic intervention with PMZ did not completely rescue spatial memory. Instead, a statically significant 10.73% difference in spatial memory function persisted between wild type and PMZ treated 5XFAD mice ($P = .03$). Notably, quantification of the mean number of seconds exploring each arm of the maze in a naïve cohort of animals confirmed no innate preference for any of the arms (data not shown). Additionally, no differences in the amount of time spent actively exploring were noted between groups, indicating that the initiative to explore was similar between animals and confirming that observed differences in behavior truly reflect alterations in spatial memory (data not shown). Taken as a whole, the data strongly

supports the conclusion that PMZ-mediated reductions in A β plaque load elicit a profound therapeutic impact on memory function in the 5XFAD mouse model.

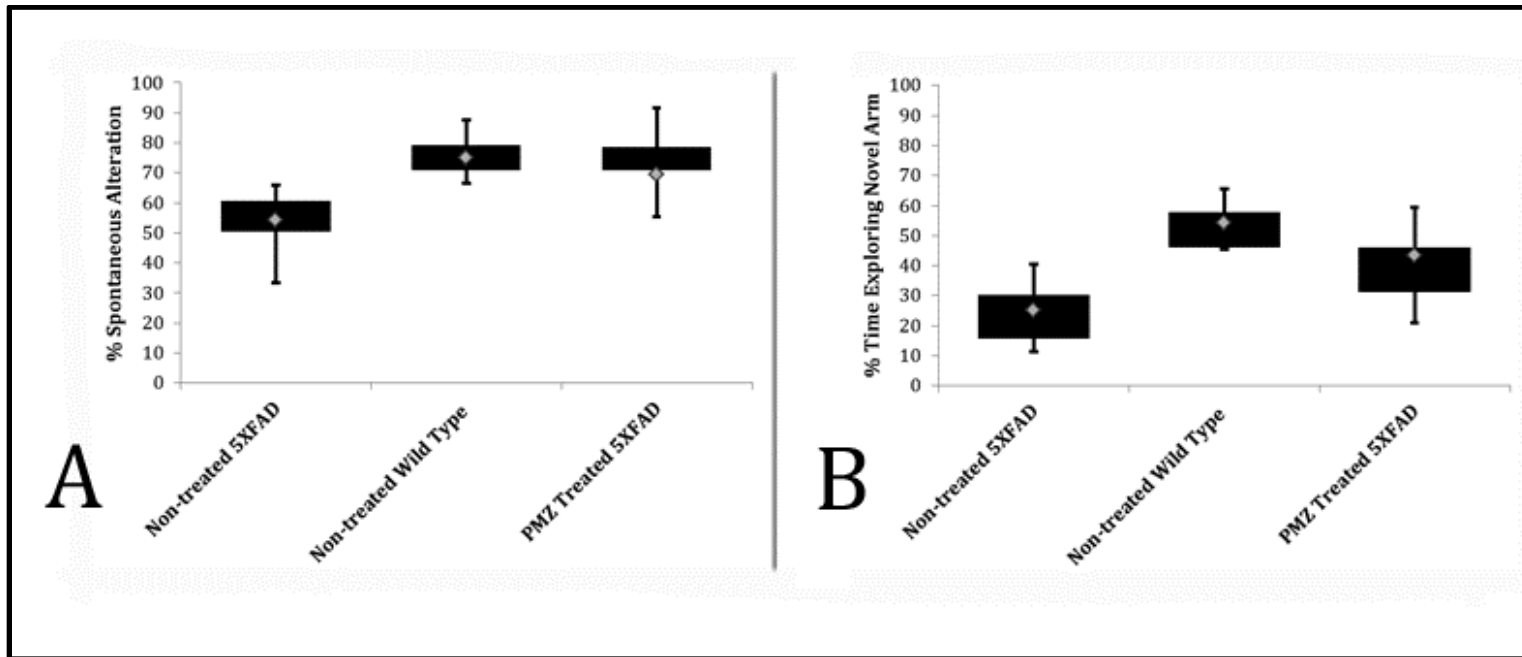


Figure 11-7. 2 Month PMZ Treatment Opposes the Development of Memory Deficits in 5XFAD mice:

(A) Box-whisker plot of percent spontaneous alternation (%SA) in the Y-maze behavioral paradigm of working memory. Spontaneous alternation in the Y-maze paradigm was evaluated in 6 month-old PMZ treated and non-treated 5XFAD cohorts as well as in non-treated wild type controls (N = 8-10 per cohort). A 25 mg/kg dose of PMZ was administered three times a week via I.V. injection beginning at 4 months of age and continued for 2 months. Following a two week non-treatment period included to alleviate stress confounds associated with routine treatment, working memory was probed during a 6 minute Y-maze trial. Statistical comparison of spontaneous alternation performance in the Y-maze paradigm reveals a mean reduction in performance of 27.53% in non-treated 5XFAD mice (Mean = 54.43%) when compared to wild type controls (Mean = 75.10%). This result confirms that without therapeutic intervention, the working memory of 5XFAD mice becomes significantly perturbed when compared to non-amyloid bearing mice ($P < .001$). In stark contrast to the non-treated 5XFAD cohort, working memory in 5XFAD mice treated with PMZ appear protected from amyloid-induced neurodegeneration. As evidence, 5XFAD mice treated with PMZ exhibit a %SA of 69.61% in the Y-maze paradigm. This constitutes a 20.22% improvement over the age-matched non-treated cohort of 5XFAD mice and confirms a statistically significant therapeutic benefit on working memory ($P < .01$). (B) Box-whisker plot reporting the time spent exploring the novel arm as a percentage of total exploration time. As an extension of our investigation into the therapeutic efficacy of PMZ, spatial memory was probed using a two-trial Y-maze behavioral assay. Briefly, during the first trial, a randomized arm of the maze was blocked and the mice were allowed to freely explore the remaining two arms of the Y-maze for 6 minutes. Following the first trial, the animals were returned to their home cage for 30 minutes. During the second trial, spatial memory was probed by recording the percentage of time the animal spent exploring each arm within a 5 minute period. Mice exhibiting normal spatial memory are expected to spend a higher percentage of time exploring the "novel" previously blocked arm while animals with impaired spatially memory are expected to spend equal amounts of time exploring each arm. Within this Y-maze paradigm, wild type mice exhibited profound recognition of Y-maze arms, spending 54.20% in the previously blocked arm. In contrast, untreated 5XFAD mice appeared incapable of recognizing the spatial cues of the maze and thus demonstrated no discernible preference for the "novel arm", spending 25.24% of their time exploring the previously blocked arm. Corroborating the immunohistochemical findings indicating a reduced plaque load in curcumin nebulized 5XFAD mice, this cohort exhibits a significant 18.23% improvement in spatial memory (Mean = 47.95%) when compared to non-treated 5XFAD littermates ($P < .01$). Notably, these findings confirm that PMZ administration improves hippocampal function as assessed by a spatial-memory dependent behavioral assay. Taken as a whole, this data strongly supports the conclusion that PMZ opposes the acquisition of memory deficits on the 5XFAD mouse model

11.3.7 Results: Promethazine Therapy Transiently Shifts A β Peptide Levels in Plasma Specimens

At this point, a myriad of converging lines of evidence strongly supported the hypothesis that PMZ is capable of attenuating A β plaque load in the brain via its inhibition of A β peptide aggregation. Moreover, this therapeutic effect was proven sufficiently robust to rescue memory performance in two iterations of the Y-maze behavioral paradigm. Given our proposed mechanism of action underlying PMZ's therapeutic effect, we predicted that A β peptides which were prevented from aggregating into A β plaques would be cleared from the brain and as a consequence transiently increase levels of A β_{40} and A β_{42} in the plasma. To test this hypothesis, measurements of these two A β species in the plasma were made in two cohorts of mice. Animals comprising the first cohort (5XFAD treated) were given a 25 mg/kg dose of PMZ for 5 consecutive days via tail-vein injection (N = 5). In the second cohort of animals (Wild type treated), age-matched wild type mice were treated with PMZ using similar dosing parameters (N = 4). In a manner consistent with our earlier work, mean plasma levels of A β_{40} and A β_{42} in wild type mice prior to treatment were 76.46 pg/mL and < 2 pg/mL, respectively. As predicted, these levels were not significantly impacted by the 5 day course of PMZ therapy (P > .05). In more detail, mean plasma levels of A β_{40} remained stable at a mean of 76 pg/mL while A β_{42} levels remained under the detection threshold. Significantly, these results confirm that treatment with PMZ does not alter plasma A β levels by modulating the production/release of A β from other sources or enhancing its clearance by the liver. With this potential confound sufficiently addressed, we are thus able to attribute any deviation in plasma A β level observed in the 5XFAD cohort to its ability to perturb A β plaque formation in the CNS. To reiterate, our hypothesis holds that in the presence of PMZ, A β peptide aggregation in the brain is observed resulting in a larger pool of soluble A β peptides which can be cleared from the brain and thus influence plasma levels. In support of this hypothesis, treatment with PMZ significantly increases levels of A β_{40} and A β_{42} peptide in the plasma of 5XFAD mice by a factor of 8.22 and 1.76, respectively (P < .001 for both peptides). Prior to treatment, plasma levels of the A β_{40} peptide in the 5XFAD treated cohort were measured at 7.16 pg/mL. Notably, this value falls within the predicted range of our previous experiments characterizing these values in non-treated 5XFAD mice. Similarly, A β_{42} peptide levels under baseline conditions were measured to be 30.32 pg per mL of plasma. However, after a 5 day treatment with PMZ, plasma levels of the A β_{40} peptide in the treated cohort rose steeply to a mean of 58.84 pg/mL while average levels of the A β_{42} peptide increased to 55.81 pg/mL. Cumulatively, these trends lead to interesting changes in the calculated ratio of A β_{42} to A β_{40} . Under baseline conditions, the propensity of the 5XFAD

genotype to overproduce $A\beta_{42}$ relative to $A\beta_{40}$ is clearly observable. However, upon treatment with PMZ, plasma levels of $A\beta_{40}$ increase more so than does the corresponding concentration of $A\beta_{42}$ and as a consequence, the $A\beta_{42}$ to $A\beta_{40}$ ratio is significantly reduced across all animals measured ($P < .001$).

Table 11-1. Pre- and Post-Treatment $A\beta$ Peptide Levels in 5XFAD Plasma

Pre- and Post-Treatment $A\beta$ Peptide Levels in 5XFAD Plasma			
	AB42	AB40	AB42/40 Ratio
Pre-test	30.32	7.16	4.24
Post-test	53.45	58.84	0.91

11.4 DISCUSSION & SIGNIFICANCE OF WORK

As emphasized at multiple points in this work, AD is a pathologically complex neurological disease characterized by a markedly heterogeneous phenotype. As a consequence, the diagnostic accuracy for AD when based uniquely on clinical presentation is lower than is required given this disease's prevalence, impact on global health, and socioeconomic cost. Therefore, in parallel with the development of disease-modifying therapeutics, the discovery of sensitive and specific biomarkers for AD has remained among the top scientific breakthroughs sought after by modern medicine. As highlighted in the introductory chapters, once identified, biomarkers for AD may be leveraged in three distinct applications: (i) as a diagnostic marker to aid in the early diagnosis of AD in clinically representative populations, (ii) as a classificatory marker capable of distinguishing AD from dementia subtypes that have similar clinical presentations, and (iii) as a prognostic marker capable of predicting disease progression with or without therapeutic intervention.⁽⁷⁸⁵⁾ Regardless of the application however, biomarkers used for screening or diagnosis also often represent surrogate manifestations of the disease, and thus can contribute to the elucidation of the disease's natural history. This has certainly held true for AD, as the predominant biomarkers used in research today, A β and tau proteins, are considered central-mediators of the neurodegeneration observed in this disease. Secondary in part to the paucity of biomarkers validated in AD clinical populations, to date, the current repertoire of imaging- and fluid-based biomarkers have necessarily been adapted to each of the three unique applications listed above. Predictably, given the differential in biomarker characteristics required for each individual application, this has been done to varying degrees of success.

Considering first the application of fluid-based or imaging-mediated measurements of A β load as a diagnostic biomarker for AD (i), these technologies appear well suited for the early-detection of disease. In support of this assertion, the literature confirms the existence of statistically significant deviations in A β burden in the brains and CSF of AD patients up to 20 years prior to symptom onset.⁽²⁵¹⁻²⁵³⁾ In contrast, alterations in CSF-tau levels and signs of neurodegeneration as assessed by structural MRI appear much later in the disease course. In one study for example, changes in CSF levels of A β ₄₂, tau, and phosphorylated-tau were assessed in individuals with MCI who either rapidly converted to AD (0-5 years) or who were better described as slowly converting (5-10 years). In a manner which supports the application of A β biomarkers for the early detection of AD, baseline CSF A β ₄₂ levels were equally reduced in patients

who converted to AD within 0 to 5 years compared with those who converted between 5 and 10 years. In comparison, CSF measurements of tau and phospho-tau were significantly higher in both early converters vs late converters.⁽¹¹³⁵⁾ Synthesized into a unified model, these results suggests that A β accumulation in the brain rises and plateaus decades before the development of symptoms whereas the occurrence of statistically significant elevations in tau biomarkers coincide more or less with the development of cognitive deficits and increase as a function of time.^(123, 1135) In these ways, the temporal dynamics of A β and tau accumulation in the brains and CSF of AD patients are markedly different and thus provide complimentary information. Exemplifying the synergistic relationship of these two biomarkers with respect to diagnostic gains, the use of A β and tau biomarkers in one study of 137 patients with MCI predicted the development of AD within 9.2 years with a sensitivity of 88%, specificity of 90%, positive predictive value of 91%, and negative predictive value of 86%.⁽¹¹³⁵⁾ Lending credibility to this result, an independent study reported very similar findings, suggesting a sensitivity of 81% and specificity of 95% when the ratio of A β_{42} to phospho-tau was used as a diagnostic predictor of MCI conversion to AD.⁽¹¹³⁶⁾ These numbers are quite impressive; even more so when considered in the context of AD's phenotypic heterogeneity. However, a major limitation of these studies is that a population of patients with MCI does not truly constitute the ideal "clinically representative population". This is because in order for newly developed interventions to elicit their maximum therapeutic benefit, it will be necessary to identify and treat patients in the preclinical stages of AD, or those individuals without discernable cognitive impairment. Therefore, considerable diagnostic gains may be garnered if complimentary biomarkers can be identified and validated.

Favorably for the current generation of AD biomarkers, the requirement to identify disease-specific pathology early is not a requirement of classificatory biomarkers (ii). Instead, biomarkers leveraged for this application need only be capable of distinguishing established AD from other dementia subtypes which have similar clinical presentations. However, as highlighted in the introductory chapters, this is no easy task, as the differential diagnosis of AD is quite broad. Overviewing only the most relevant points, although AD is by far the most likely cause of dementia, representing between 60-80% of cases, a number of alternative forms of dementia including vascular dementia (VaD), dementia with lewy bodies (DLB), fronto-temporal dementia (FTD), and dementia secondary to Creutzfeldt-Jakob disease or normal pressure hydrocephalus may closely mimic the presentation of AD.⁽²⁹⁰⁾ While this is a considerable array of diseases for current AD biomarkers to exclude in and of itself, in real-world applications the major limitation of A β and tau

biomarkers has proven to be the vast degree of pathological overlap between AD and these various neurological conditions. To appreciate the validity of this assertion, one need only to review the data produced by studies investigating the diagnostic utility of CSF tau and A β ₄₂ levels in pure AD cohorts versus in populations contained a mix of AD and non-AD dementias. In the first scenario, differentiating AD from non-demented controls, A β and tau biomarkers perform strongly, with high reports of sensitivity (50–94%) and specificity (83–100%) dominating the literature.⁽¹¹³⁷⁾ By comparison, when these same biomarkers are leveraged in an attempt to accurately differentiate between AD and VaD, current CSF-based biomarkers perform with a reported specificity of only 48%.⁽¹¹³⁸⁾ A similar short-coming in diagnostic utility is observed when A β and tau biomarkers are applied to mixed cohorts of AD and DLB, with a reported specificity of just 67% under these conditions.⁽¹¹³⁸⁾ A closer look at the data from which these statistics were generated reveals the underlying reason why the diagnostic performance of these biomarkers is markedly reduced in mixed dementia cohorts; changes in neither biomarker are completely specific to AD. For example, the reduction in CSF A β ₄₂ observed in individuals with AD is also seen in patients with DLB. Similarly, patients with VaD exhibit increases in CSF-tau levels.⁽¹¹³⁸⁾ This second finding is perhaps not surprising, as tau is widely accepted as a non-specific marker of axonal degeneration and thus wouldn't be expected to be uniquely elevated in just AD. On the other hand, many investigators in the field were likely less prepared by the revelation that A β is also imbalanced in non-AD dementias. Notably, some investigators argue that the limitations imposed by these findings can be largely overcome by characterizing the magnitude of deviation from baseline caused by AD as opposed to non-AD causes of dementia. This in fact may be true for some of the diseases included in the differential of AD, with CJD being a prime example. In this disease, CSF tau levels are dramatically enhanced, exceeding 3000 pg/mL. In comparison, the typical threshold for CSF tau levels when assigning the diagnosis of AD is nearer to 600 pg/mL. Given this large differential, few would argue the plausibility of successfully leveraging CSF measurements of tau to differentiate between AD and CJD. However, such a large differential in CSF levels is not observed between AD and other causes of dementia, raising the concern that this biomarker may be ill-suited for application as a classificatory biomarker in isolation. This is not to say that CSF-tau levels do not display a unique trend. To the contrary, the median effect size of tau level in multiple AD studies was 429 pg/mL whereas in dementia-due-to-other-causes studies it was 69 pg/mL. Thus, at the population level, statistically significant differences in CSF tau exist between cohorts of AD and non-AD dementia patients. Indeed, the limitation of this biomarker only becomes apparent when looking at the reported range for CSF tau in these studies. In cohorts of AD

patients, CSF tau levels range broadly from a minimum of 32 pg/mL to a maximum of 910 pg/mL. Comparing this to dementia-due-to-other causes (range 53 pg/mL – 518 pg/mL), it is clear that CSF tau interpretation at the individual level is muddled by inter-subject variability. Thus, while A β and tau measurements certainly exhibit potential as classificatory biomarkers, few would argue against the need to identify complimentary biomarkers to fill the remaining diagnostic gaps.

Disappointingly, the diagnostic gaps just identified when leveraging A β and tau levels as classificatory biomarkers are far from the only short-comings in the field. In fact, upon review of the data, these biomarkers are probably best suited to this application. Instead, where the field has historically struggled is in the identification of prognostic biomarkers, those capable of predicting disease progression with or without therapeutic intervention. At a minimum, such a biomarker would be expected to correlate with symptom severity. As implied, this has not proven the case for fluid- or imaging-based measurement of A β and tau. While the literature is of course mixed, multiple studies have failed to demonstrate correlations between CSF-A β_{42} level and duration or severity of dementia regardless of the modality employed.^(1139, 1140) Notably, this finding is consistent with data suggesting that A β plaque burden fails to robustly correlate with cognitive deficits when assessed via immunohistochemistry. If we continue to extrapolate the results of histological studies in this manner, then we would expect CSF tau burden to correlate better with disease severity and duration than similar measurements of A β . This is indeed the case for some AD populations, with a high proportion of studies indicating that measures of CSF tau significantly correlate with assessments of cognitive function.⁽⁹³⁵⁾ From these findings, we can conclude that assessment of tau levels likely harbors more potential as a prognostic biomarker than do A β biomarkers. On the other hand, studies longitudinally assessing CSF tau levels over shorter time periods and in mild to moderately demented AD patients have not noted changes in tau levels despite significant changes in clinical measures of disease progression.⁽¹¹⁴¹⁾ When considering these studies as a group, it appears neither A β nor tau abundance is particularly adept at predicting the severity or rate of AD progression. Thus, at best, the literature is mixed as to whether A β and tau biomarkers might be suitable for prognostic applications in AD. Summarizing the predominant opinion in the field today, assessment of A β and tau levels via imaging or fluid analysis will only optimally impact clinical care once integrated into a larger diagnostic, classificatory, or prognostic panels. Towards this end, a number of groups have attempted to identify complimentary biomarkers for AD. The majority have not strayed far from the traditional hallmark lesions of AD, investigating the diagnostic utility of A β_{42} antibodies, levels of β -secretase in the CSF, or kinases

associated with tau hyper-phosphorylation such as glycogen synthase kinase-3, cyclin-dependent kinase 5, and microtubule affinity-regulating kinase for example.⁽¹¹⁴²⁾ Other researchers, including our group, have investigated the utility of inflammatory markers for diagnostic applications in AD.

Beginning first with the discovery of microglia activation and expression of pro-inflammatory cytokines in association with A β plaques, for decades science has been aware that neuro-inflammatory processes occur in the brains of AD patients. Moreover, as reviewed, an abundance of research suggests this pro-inflammatory phenotype contributes significantly to the pathogenic mechanisms underlying neuronal dysfunction in AD. More generally, both in the brain and in peripheral tissues, unchecked or chronic inflammation becomes deleterious, leading to progressive tissue damage in degenerative diseases. At the origin of these investigative efforts, early reports on patients treated chronically with anti-inflammatory drugs for rheumatoid arthritis or leprosy found that a 2-year treatment with NSAIDs reduced significantly the risk of AD later in life and that clinical benefit increased with longer periods of treatment.⁽¹¹⁴³⁻¹¹⁴⁵⁾ Not surprisingly, the data from such observational studies encouraged the search for molecular mechanisms that could explain the positive effects of NSAIDs in delaying/preventing AD. Logically, initial investigations analyzed the role of COX1 and COX2 in the classical AD pathological cascade. Exemplifying this work, treatment of APP overexpressing mice with NSAIDs induced a significant reduction in cortical amyloid plaque load along with reduced microglial activation.⁽¹¹⁴⁶⁾ Later, this model would be refined, with reports of improved synaptic plasticity and memory formation in AD transgenic mice treated with COX-2- but not COX-1-selective inhibitors.⁽¹¹⁰⁹⁾ Beyond identifying COX-2 as the major cyclooxygenase isoform of interest in AD, this work also demonstrated that the beneficial effects of COX-2 inhibitor therapy on memory did not depend upon lowered levels of A β ₄₂ or the inflammatory cytokines, tumor necrosis factor α (TNF- α) and interleukin 1 β (IL-1 β). Instead, improved memory function was inversely related to prostaglandin E2 (PGE2) levels. In support of this PGE2 being a key mediator of neuro-inflammatory insult in AD, administration of exogenous PGE2 to treated AD mice prevented the restorative effects of COX-2 inhibitors on LTP. Together, this data indicates that the inhibition of COX-2 blocks A β -mediated suppression of LTP and memory function, and that this block occurs independently of reductions in A β ₄₂ or decreases in inflammation.⁽¹¹⁰⁹⁾ While this work is certainly interesting from a therapeutic perspective in that it highlights the multi-factorial nature of COX-2 mediated inhibition of AD pathology, it also conveys the point that measurements of COX-2 in the brains of AD patients may reveal diagnostically exploitable

profiles. In an attempt to test this hypothesis, we probed the brains of 5XFAD and wild type mice with a PET compatible radio-ligand with previously demonstrated specificity for COX-2.⁽¹⁰²⁷⁾ Considering the data, we conclude that this particular COX-2 probe cannot be applied to neuroimaging of inflammation in AD as a consequence of its inability to cross the BBB. Importantly, this negative finding only highlights the validity of our assertion that BBB penetration represents one of the largest barriers to AD theranostic development. Still, this is a disappointing finding as the literature strongly suggests that COX-2 imaging would contribute significantly to overcoming the difficulties associated with early-detection of AD. For example, this enzyme has been shown to be elevated robustly in pre-clinical mouse models of AD, including the 5XFAD mouse model.⁽¹¹⁴⁷⁾ Of course, COX-2 is not unique in this regard. Instead, several inflammatory mediators including tumor necrosis factor-alpha (TNF- α), interleukin (IL) 6, and IL-1 β are all increased in AD patients.⁽¹¹⁴⁸⁾ In fact, these molecules may even represent better imaging targets for AD, as accumulating evidence suggests that these cellular effectors influence the development of defective brain insulin signaling in AD.

As alluded to in the introduction of this aim, disturbances in homeostatic insulin/IGF-1-like signaling are increasingly becoming recognized as a pathological signature of AD. However, the molecular events and pathways leading to disrupted brain insulin signaling in AD have only recently begun to be unraveled. As reviewed, physiological activation of insulin receptors stimulates tyrosine phosphorylation of IRS to initiate intracellular signaling pathways. Evidence of how this signaling cascade is perturbed by inflammation was first recognized in type 2 diabetes, where elevated TNF- α levels trigger serine phosphorylation of IRS-1 by stress kinases, thereby interfering with its ability to engage in IR signaling.^(1116, 1149-1151) In the brain, TNF- α is secreted mainly by microglial cells in response to trauma, infection, or in the case of AD, abnormal accumulation of protein aggregates.⁽¹¹⁵²⁾ Initial evidence that impaired neuronal insulin signaling in AD is linked to pro-inflammatory signaling came from the finding that soluble oligomers of the A β peptide cause IRS-1 inhibition through TNF- α activation. This mechanism was confirmed experimentally in part via the demonstration that the triggering of IRS-1 phosphoserine by A β oligomers in hippocampal neurons is blocked by infliximab, a TNF- α neutralizing antibody.⁽¹¹⁵³⁾ In subsequent studies, A β oligomers have been shown to instigate removal of IRs from the membranes of neuronal processes and to cause defective insulin signaling in postmortem AD brains and in several experimental models of AD.^(1121, 1122, 1154) As discussed, the significance of this is that insulin signaling in the CNS promotes neuronal survival and regulates key processes underlying learning and memory, including synapse density,

dendritic plasticity, and circuit function.⁽¹¹¹⁷⁾ Thus, the induction of pro-inflammatory pathways and ensuing defective insulin signaling instigated by A β oligomers are thought to be linked to neuronal dysfunction in AD. As we were unable to image neuro-inflammation secondary to the low BBB penetrance of our probe, we hypothesized that downregulation of IGF1R might be a promising diagnostic biomarker for AD. Unfortunately, this approach again proved limited by the formidable obstacle that is the BBB. Nevertheless, the rationale behind this hypothesis is solid and further probe development will hopefully see IGF1R validated as a biomarker for AD.

Having experienced firsthand the low probability of success when attempting to apply radio-ligands optimized for peripheral targets for diagnostic use in the CNS, in our last set of experiments we abandoned this approach and instead focused on improving existing fluid-based diagnostics. To date, three biomarkers have been well-established and validated internationally to diagnose AD in CSF with ELISAs: A β ₄₂, total tau and phospho-tau-181. In congruence with our hypothesis that biomarker panels will be necessary to reliably diagnosis AD at the community level, there is now more or less a consensus that only the combination of these three CSF biomarkers significantly increases the diagnostic validity for sporadic AD. Together, these three measurements yield a combined sensitivity of >95% and a specificity of >85% for AD, however in isolation, each fail to meaningfully improve diagnostic accuracy over clinical examination.^(151, 1097, 1155) Where opinions still diverge however is in the clinical feasibility of CSF-based biomarkers, as this approach carries considerable risk to the patient. Most commonly, up to 40% of patients develop orthostatic headache lasting 1 week or less in duration after lumbar puncture. Other complications, including headaches lasting from 8 days to 1 year, cranial neuropathies, prolonged backache, nerve root injury, and meningitis, are more rare, but still worth consideration in the context of AD screening, following perhaps 0.3 % of lumbar punctures.⁽¹¹⁵⁶⁾ Moreover, increasing numbers of hemorrhages into the epidural or spinal space have been reported in patients using anticoagulants such warfarin and low-molecular weight heparins as well as factor X and thrombin inhibitors. In a world where clinical practice was congruent with expert recommendation, 50-70% of the elderly population, that at highest risk for AD, would be placed on these medications and would thus be at increased risk for bleeding complications.⁽¹¹⁵⁷⁾ However, perhaps the most practical limitation to CSF biomarkers is that the prospect of a lumbar puncture seems to cause an inordinate amount of fear and anxiety in patients. In addition to these patient risks, a number of potential factors that may influence or interfere with the analytical outcome must also be considered before a CSF biomarker can be introduced into clinical routine. These

include: concentration gradients of the protein along the spinal cord, influence of LP hemorrhage, presence of the protein in plasma and passage over the blood-brain barrier, and degradation or loss of the protein *in vitro* after the CSF tap.⁽¹¹⁵⁶⁾ All factors considered, in a 2003 report, the U.S. Preventative Services Task Force (USPSTF) did not endorse routine screening for AD. Although the report raised a number of concerns regarding screening for AD, including insufficient evidence for the accuracy of screening tests, low accuracy of screening tests for mild dementia, and biases for age, education, and ethnicity, the primary rationale for not endorsing screening is that until studies demonstrate that screening provides better outcomes for patients with AD, endorsement is premature.⁽¹¹⁵⁸⁾

Here, our group notes one of the fundamental issues with CSF-based biomarkers for AD, the technical difficulty associated with implementing these techniques in preclinical mouse models. To elaborate, national authorities like the USPSTF explicitly state that in order for CSF-based diagnostics to be successfully leveraged clinically, early-detection must demonstrate an advantage to the patient. However, without disease-modifying therapeutics, which the field agrees will be most efficacious when applied early in the disease course, this criteria is unlikely to be met. Therefore, before diagnostic screening for AD becomes clinically feasible, the biomarkers these approaches employ must be leveraged to help develop therapeutic agents which augment AD pathology. Inarguably, the preferred animal model to test putative therapeutics has been and will continue to be mouse models of AD. However, translation of serial CSF measurements of A β , tau, and phospho-tau to mice is riddled with methodological pitfalls and has yet to be validated. At the most basic level, using the only published technique allowing serial collections of CSF in mice, only 3-7 μ L of fluid can be obtained; a volume incompatible with commercially available ELISA-based assessment of all three clinically employed biomarkers.⁽¹¹⁵⁹⁾ In addition, to date longitudinal assessment of CSF biomarker levels for AD have only been performed in 2-3 month intervals, a lengthy time frame when considering the accelerated rate of pathology typical of most AD mouse models. Lastly, more so than in humans, serial CSF-collection in mice is a highly invasive procedure requiring gross dissection of the *m. biventer cervicis* and *m. rectus capitis dorsalis major* as well as penetration of the cisterna magna with a 1 mm needle.⁽¹¹⁵⁹⁾ Given the apparent role of neuro-inflammation in AD pathology, it is difficult to accept that such an invasive procedure will not influence pathology. Even less likely is that this repeated surgical intervention will prove compatible with behavioral assessment of cognitive function; inarguably a litmus test for putative therapeutic agents.

To overcome the intrinsic limitations of CSF biomarkers just discussed, we tested the feasibility of leveraging plasma measurements of A β to longitudinally monitor treatment response in the 5XFAD mouse model. As demonstrated by the data, our work suggests that baseline differences in A β_{42} and A β_{40} peptide levels exist in the blood of 5XFAD and wild type mice. Moreover, under stringent experimental conditions, this biomarker displays remarkable intra-cohort consistency with levels ranging from 22-30 pg/mL and 6-14 pg/mL for A β_{40} and A β_{42} , respectively in the 5XFAD cohort. By comparison, mean A β_{40} levels in the plasma of wild type mice were significantly increased, with reported levels of 60-80 pg of A β_{40} per milliliter of plasma noted in our preliminary experiments ($P < .01$). Two comments need to be made on this data. First, the reduced levels of A β_{40} in the plasma of 5XFAD mice as compared to wild type animals is consistent with predictions that would be made given the genotype of the two cohorts. To understand this point, it is necessary to understand that the 5XFAD mouse model is a double transgenic mouse model of AD harboring mutations in both APP and PSEN1 and thus is best characterized as a model of FAD. In more detail, 5XFAD mice overexpress mutant human APP with the Swedish (K670N, M671L), Florida (I716V), and London (V717I) Familial Alzheimer's Disease mutations along with human PS1 harboring two FAD mutations, M146L and L286V.⁽⁶⁷⁰⁾ The significance of these mutations is that they all bias the cleavage of APP towards the amyloid-ogenic pathway and as a consequence, APP is almost exclusively metabolized to A β_{42} peptide. Impressively, this trend is reflected in our data, as A β_{42} peptide only reaches detectable levels in 5XFAD mice and remains below the 2 pg/mL detection limit in wild type mice. Our data is congruent with theoretical predictions in that A β_{40} expression is higher in wild type mice, where the physiological processing of APP to this peptide isoform is not perturbed. Put another way, the reduction in plasma A β_{40} levels in 5XFAD mice are in congruence with the theory that the majority of APP is shunted towards amyloid-ogenic processing in these mice. One alternative or perhaps contributory explanation for this result is that the excess of A β_{42} present in the brains of 5XFAD serves to trap A β_{40} peptides in a manner which perturbs their physiological clearance to the plasma. A second note to be made on this data is that it is largely supported by independent investigations in the field. While published plasma measurements of A β peptide isoforms in the 5XFAD mouse model are exceedingly rare,^(1160, 1161) in general the literature agrees that reduced A β_{40} levels still exceed A β_{42} despite their increase in AD transgenic mouse models. In addition, most groups also report that C57BL6 mice, the genetic background of the 5XFAD mouse model, almost exclusively produce A β_{40} .⁽¹¹⁶²⁾ Interestingly, we and others in the field interpret the former finding to reflect the propensity of A β_{42} to be trapped in the brain's parenchyma, where it is unable to be cleared to the plasma despite its pathological overabundance.

In the context of this model, we predicted that therapeutic intervention with PMZ would result in an increase in plasma A β levels reflecting an improved ability to clear A β species from the brain. Importantly, the results from our in vitro assay support the use of PMZ as a potent amyloid aggregation inhibitor and we have already confirmed the ability of PMZ to cross the BBB and localize to regions of the brain most laden with A β assemblies in the first aim of our work.⁽⁹⁷⁰⁾ A further strength of utilizing PMZ in this work is that in comparison to other A β aggregation inhibitors, such as curcumin, it does not influence AD pathology via non-amyloid-centric mechanisms. Therefore, the finding that A β plaque load and cognitive deficits are reduced via chronic treatment with PMZ can only be interpreted as a confirmation of the therapeutic benefit of A β -targeted therapies. To clarify this point, in contrast to our work with pleiotropic molecules like curcumin, it is highly unlikely that an off-target effect of PMZ underlies the cognitive improvement observed in PMZ treated mice. What is more unique about this work however is that by measuring plasma A β biomarkers throughout the course of treatment, we are able to provide strong support for a mechanism of action underlying PMZ's therapeutic effect. To reiterate, our hypothesis holds that in the presence of PMZ, A β peptide aggregation in the brain is inhibited resulting in a larger pool of soluble A β peptides which can be cleared from the brain and thus influence plasma levels. In support of this hypothesis, treatment with PMZ significantly increased levels of A β_{40} and A β_{42} peptide in the plasma of 5XFAD mice by a factor of 8.22 and 1.76, respectively. In our opinion, the trend in the data for A β_{42} is most congruent with the conclusion that PMZ binds to, and perturbs the aggregation of, this peptide isoform resulting in its increased homeostatic clearance from the brain to plasma. On the other hand, we believe two equally plausible mechanisms for the results gathered for A β_{40} are supported by the literature. The first suggests that in disrupting existing A β plaques, PMZ frees A β_{40} and facilitates its increased clearance from the brain. Alternatively, by partially attenuating the aggregation of A β peptides, PMZ administration may prevent A β_{40} from being incorporated into amyloid assemblies in the brain. No longer restricted to the brain, A β_{40} concentration would be expected to increase towards physiological baseline; as it does in our data. At this point, our results are not sufficient to attribute full credit for the therapeutic benefits observed following PMZ treatment to either of these models. More than likely, both contribute to the sparing of cognitive function observed in PMZ treated 5XFAD mice. Regardless of the relative contribution of each mechanism, either of these models of PMZ's therapeutic effect are supported in the literature. Most fundamentally, immunohistochemical analysis of A β plaques has demonstrated that these pathologic inclusions mature over time. Early in the disease process, the more aggregation-prone A β_{42} peptides deposit in the brain to form diffuse plaques.⁽¹¹⁶³⁾ Subsequently, peptides not prone to self-aggregation such

as A β ₄₀, become increasingly incorporated into the diffuse plaque structure to form dense compact and neuritic plaques which are posited to rank among the more pathogenic amyloid assemblies.⁽¹¹⁶⁴⁾ Highlighting the pathological significance of A β plaque enrichment with A β ₄₀, it is noteworthy that in contrast to *in vitro* studies where A β ₄₂ is demonstrated to be more fibrillogenic and aggregate faster than A β ₄₀, *in vivo* studies in rodents point otherwise. For example, synthetic soluble A β ₁₋₄₀, but not A β ₁₋₄₂, when injected in rat brain, form fibrillar congophilic amyloid deposits and transgenic mice overexpressing mutant APP and PS1, deposit predominantly A β ₄₀ and not A β ₄₂ in parenchymal congophilic compact plaques.^(1165, 1166) Similarly, in amyloid plaques of AD and DS patients, A β ₄₀ is the predominant constituent, especially within the congophilic core.⁽¹¹⁶⁷⁾ Taken together, these findings may help explain why plasma A β ₄₀ levels increase more so than concentrations of A β ₄₂ following treatment with A β aggregation inhibitors like PMZ.

Most significantly, the work reviewed here provides convincing evidence in support of the therapeutic efficacy of A β -targeted pharmaceutical agents. With respect to the future translation of PMZ for therapeutic applications in AD, of course a discovery of this magnitude requires further characterization. At a minimum, the dosing regimen necessary to achieve therapeutic efficacy needs to be more clearly defined, as our approach utilizes a high-dose of the agent likely unsuitable for human applications. Without question, the ability to track therapeutic response with plasma measurements of A β will be a critical asset in this future endeavor. As discussed, the major advantages to this technique over CSF-based measurements include a reduced patient risk and feasibility in both humans and rodent models of AD. However, a number of groups have attempted to employ measurements of plasma A β to diagnostic applications in humans with mixed results.⁽⁹³⁰⁾ In interpreting these results, it is critical to realize there are several reasons why plasma levels of A β ₄₂ are unstable: (i) A β expression is influenced by medications; (ii) A β binds to other proteins; (iii) A β levels in blood fluctuate over time and among individuals, and might differ in mild, early and late AD; and (iv) blood platelets contain high amounts of A β , which directly affects plasma levels. In completing this work, we were careful to address each of these issues in our experimental design and as demonstrated by our success, we agree that elimination of methodological confounds will likely lead to the consensus that this biomarker is compatible with a subset of diagnostic applications in AD; especially intra-subject longitudinal assessment of treatment response. This is because serial plasma draws offer the ability to control for the confounding effects of between-subject variability. Importantly, this trait could have a profound impact on clinical trials. For example, in human clinical studies, baseline measurements of plasma A β can assist to

compose a more uniform population at study start, and terminal follow-up measurements might allow for detecting subtle therapeutic effects at the level of individual subjects. Thus, given the tremendous advantages of plasma-based biomarkers for AD, we believe further research is necessary to facilitate the clinical translation of this diagnostic approach. Considered as a whole, this work is unique in that it not only highlights the utility of a novel disease-modifying therapeutic agent for AD, but also proposes a method by which to monitor treatment response in a longitudinal manner. Importantly, should these discoveries prove translatable to humans; it would mark a major milestone in our group's cumulative effort towards alleviating disease burden associated with this devastating neurodegenerative disorder.

REFERENCES

1. Scoville WB, Milner B. Loss of recent memory after bilateral hippocampal lesions. *Journal of neurology, neurosurgery, and psychiatry*. 1957;20(1):11-21. PubMed PMID: 13406589; PubMed Central PMCID: PMC497229.
2. Squire LR, Zola SM. Structure and function of declarative and nondeclarative memory systems. *Proceedings of the National Academy of Sciences of the United States of America*. 1996;93(24):13515-22. PubMed PMID: 8942965; PubMed Central PMCID: PMC33639.
3. Teng E, Squire LR. Memory for places learned long ago is intact after hippocampal damage. *Nature*. 1999;400(6745):675-7. doi: 10.1038/23276. PubMed PMID: 10458163.
4. Nadel L, Hubbach A, Gomez R, Newman-Smith K. Memory formation, consolidation and transformation. *Neuroscience and biobehavioral reviews*. 2012;36(7):1640-5. doi: 10.1016/j.neubiorev.2012.03.001. PubMed PMID: 22465050.
5. Reed JM, Squire LR. Retrograde amnesia for facts and events: findings from four new cases. *The Journal of neuroscience : the official journal of the Society for Neuroscience*. 1998;18(10):3943-54. PubMed PMID: 9570821.
6. Warrington EK. Studies of retrograde memory: a long-term view. *Proceedings of the National Academy of Sciences of the United States of America*. 1996;93(24):13523-6. PubMed PMID: 8942966; PubMed Central PMCID: PMC33640.
7. Cohen NJ, Squire LR. Preserved learning and retention of pattern-analyzing skill in amnesia: dissociation of knowing how and knowing that. *Science*. 1980;210(4466):207-10. PubMed PMID: 7414331.
8. Salmon DP, Butters N. Neurobiology of skill and habit learning. *Current opinion in neurobiology*. 1995;5(2):184-90. PubMed PMID: 7620306.
9. Bloedel JR, Ebner TJ, Wise SP. *The acquisition of motor behavior in vertebrates*. Cambridge, Mass.: MIT Press; 1996. vii, 440 p. p.
10. Vallar G, Shallice T, Consiglio nazionale delle ricerche (Italy). *Neuropsychological impairments of short-term memory*. Cambridge ; New York: Cambridge University Press; 1990. xiii, 524 p. p.
11. Burwell RD, Amaral DG. Cortical afferents of the perirhinal, postrhinal, and entorhinal cortices of the rat. *The Journal of comparative neurology*. 1998;398(2):179-205. PubMed PMID: 9700566.
12. Suzuki WA, Amaral DG. Perirhinal and parahippocampal cortices of the macaque monkey: cortical afferents. *The Journal of comparative neurology*. 1994;350(4):497-533. doi: 10.1002/cne.903500402. PubMed PMID: 7890828.
13. Suzuki WA, Amaral DG. Functional neuroanatomy of the medial temporal lobe memory system. *Cortex; a journal devoted to the study of the nervous system and behavior*. 2004;40(1):220-2. PubMed PMID: 15070014.
14. Burwell RD, Witter MP, Amaral DG. Perirhinal and postrhinal cortices of the rat: a review of the neuroanatomical literature and comparison with findings from the monkey brain. *Hippocampus*. 1995;5(5):390-408. doi: 10.1002/hipo.450050503. PubMed PMID: 8773253.
15. Vago DR, Kesner RP. Disruption of the direct perforant path input to the CA1 subregion of the dorsal hippocampus interferes with spatial working memory and novelty detection. *Behavioural brain research*. 2008;189(2):273-83. doi: 10.1016/j.bbr.2008.01.002. PubMed PMID: 18313770; PubMed Central PMCID: PMC2421012.
16. Morrison JH, Hof PR. Life and death of neurons in the aging cerebral cortex. *International review of neurobiology*. 2007;81:41-57. doi: 10.1016/S0074-7742(06)81004-4. PubMed PMID: 17433917.
17. Witter MP, Naber PA, van Haeften T, Machielsen WC, Rombouts SA, Barkhof F, Scheltens P, Lopes da Silva FH. Cortico-hippocampal communication by way of parallel parahippocampal-subicular pathways. *Hippocampus*. 2000;10(4):398-410. doi: 10.1002/1098-1063(2000)10:4<398::AID-HIPO6>3.0.CO;2-K. PubMed PMID: 10985279.
18. Smith CN. Retrograde memory for public events in mild cognitive impairment and its relationship to anterograde memory and neuroanatomy. *Neuropsychology*. 2014;28(6):959-72. doi: 10.1037/neu0000117. PubMed PMID: 25068664; PubMed Central PMCID: PMC4227913.

19. Remondes M, Schuman EM. Role for a cortical input to hippocampal area CA1 in the consolidation of a long-term memory. *Nature*. 2004;431(7009):699-703. doi: 10.1038/nature02965. PubMed PMID: 15470431.
20. Sandler R, Smith AD. Coexistence of GABA and glutamate in mossy fiber terminals of the primate hippocampus: an ultrastructural study. *The Journal of comparative neurology*. 1991;303(2):177-92. doi: 10.1002/cne.903030202. PubMed PMID: 1672874.
21. Bliss TV, Collingridge GL. A synaptic model of memory: long-term potentiation in the hippocampus. *Nature*. 1993;361(6407):31-9. doi: 10.1038/361031a0. PubMed PMID: 8421494.
22. Amaral DG, Witter MP. The three-dimensional organization of the hippocampal formation: a review of anatomical data. *Neuroscience*. 1989;31(3):571-91. PubMed PMID: 2687721.
23. Neves G, Cooke SF, Bliss TV. Synaptic plasticity, memory and the hippocampus: a neural network approach to causality. *Nature reviews Neuroscience*. 2008;9(1):65-75. doi: 10.1038/nrn2303. PubMed PMID: 18094707.
24. Dekaban AS. Changes in brain weights during the span of human life: relation of brain weights to body heights and body weights. *Annals of neurology*. 1978;4(4):345-56. doi: 10.1002/ana.410040410. PubMed PMID: 727739.
25. Skullerud K. Variations in the size of the human brain. Influence of age, sex, body length, body mass index, alcoholism, Alzheimer changes, and cerebral atherosclerosis. *Acta neurologica Scandinavica Supplementum*. 1985;102:1-94. PubMed PMID: 3887832.
26. Uylings HB, de Brabander JM. Neuronal changes in normal human aging and Alzheimer's disease. *Brain and cognition*. 2002;49(3):268-76. PubMed PMID: 12139954.
27. Scahill RI, Frost C, Jenkins R, Whitwell JL, Rossor MN, Fox NC. A longitudinal study of brain volume changes in normal aging using serial registered magnetic resonance imaging. *Archives of neurology*. 2003;60(7):989-94. doi: 10.1001/archneur.60.7.989. PubMed PMID: 12873856.
28. Svennerholm L, Bostrom K, Jungbjer B. Changes in weight and compositions of major membrane components of human brain during the span of adult human life of Swedes. *Acta neuropathologica*. 1997;94(4):345-52. PubMed PMID: 9341935.
29. Brody H. Organization of the cerebral cortex. III. A study of aging in the human cerebral cortex. *The Journal of comparative neurology*. 1955;102(2):511-6. PubMed PMID: 14381544.
30. Anderson JM, Hubbard BM, Coghill GR, Slidders W. The effect of advanced old age on the neurone content of the cerebral cortex. Observations with an automatic image analyser point counting method. *Journal of the neurological sciences*. 1983;58(2):235-46. PubMed PMID: 6834079.
31. Henderson G, Tomlinson BE, Gibson PH. Cell counts in human cerebral cortex in normal adults throughout life using an image analysing computer. *Journal of the neurological sciences*. 1980;46(1):113-36. PubMed PMID: 7373341.
32. Coleman PD, Flood DG. Neuron numbers and dendritic extent in normal aging and Alzheimer's disease. *Neurobiology of aging*. 1987;8(6):521-45. PubMed PMID: 3323927.
33. Mann DM, Yates PO, Marcyniuk B. Changes in Alzheimer's disease in the magnocellular neurones of the supraoptic and paraventricular nuclei of the hypothalamus and their relationship to the noradrenergic deficit. *Clinical neuropathology*. 1985;4(3):127-34. PubMed PMID: 3160517.
34. Shefer VF. Absolute number of neurons and thickness of the cerebral cortex during aging, senile and vascular dementia, and Pick's and Alzheimer's diseases. *Neuroscience and behavioral physiology*. 1973;6(4):319-24. PubMed PMID: 4781784.
35. Blumenthal HT. *The Regulatory role of the nervous system in aging*. Basel, New York,: S. Karger; 1970. 122 p. p.
36. Ball MJ. Neuronal loss, neurofibrillary tangles and granulovacuolar degeneration in the hippocampus with ageing and dementia. A quantitative study. *Acta neuropathologica*. 1977;37(2):111-8. PubMed PMID: 848276.
37. Morrison JH, Hof PR. Life and death of neurons in the aging brain. *Science*. 1997;278(5337):412-9. PubMed PMID: 9334292.
38. Pakkenberg B, Gundersen HJ. Neocortical neuron number in humans: effect of sex and age. *The Journal of comparative neurology*. 1997;384(2):312-20. PubMed PMID: 9215725.
39. West MJ, Coleman PD, Flood DG, Troncoso JC. Differences in the pattern of hippocampal neuronal loss in normal ageing and Alzheimer's disease. *Lancet*. 1994;344(8925):769-72. PubMed PMID: 7916070.
40. Merrill DA, Roberts JA, Tuszynski MH. Conservation of neuron number and size in entorhinal cortex layers II, III, and V/VI of aged primates. *The Journal of comparative neurology*. 2000;422(3):396-401. PubMed PMID: 10861515.

41. Peters A, Leahu D, Moss MB, McNally KJ. The effects of aging on area 46 of the frontal cortex of the rhesus monkey. *Cerebral cortex*. 1994;4(6):621-35. PubMed PMID: 7703688.
42. Merrill DA, Chiba AA, Tuszynski MH. Conservation of neuronal number and size in the entorhinal cortex of behaviorally characterized aged rats. *The Journal of comparative neurology*. 2001;438(4):445-56. PubMed PMID: 11559900.
43. Rasmussen T, Schliemann T, Sorensen JC, Zimmer J, West MJ. Memory impaired aged rats: no loss of principal hippocampal and subicular neurons. *Neurobiology of aging*. 1996;17(1):143-7. PubMed PMID: 8786797.
44. Smith DE, Rapp PR, McKay HM, Roberts JA, Tuszynski MH. Memory impairment in aged primates is associated with focal death of cortical neurons and atrophy of subcortical neurons. *The Journal of neuroscience : the official journal of the Society for Neuroscience*. 2004;24(18):4373-81. doi: 10.1523/JNEUROSCI.4289-03.2004. PubMed PMID: 15128851.
45. Scheibel ME, Lindsay RD, Tomiyasu U, Scheibel AB. Progressive dendritic changes in the aging human limbic system. *Experimental neurology*. 1976;53(2):420-30. PubMed PMID: 976409.
46. Scheibel AB. The hippocampus: organizational patterns in health and senescence. *Mechanisms of ageing and development*. 1979;9(1-2):89-102. PubMed PMID: 439952.
47. Buell SJ, Coleman PD. Quantitative evidence for selective dendritic growth in normal human aging but not in senile dementia. *Brain research*. 1981;214(1):23-41. PubMed PMID: 7237164.
48. Buell SJ, Coleman PD. Dendritic growth in the aged human brain and failure of growth in senile dementia. *Science*. 1979;206(4420):854-6. PubMed PMID: 493989.
49. Flood DG, Buell SJ, Horwitz GJ, Coleman PD. Dendritic extent in human dentate gyrus granule cells in normal aging and senile dementia. *Brain research*. 1987;402(2):205-16. PubMed PMID: 3828793.
50. Flood DG, Guarnaccia M, Coleman PD. Dendritic extent in human CA2-3 hippocampal pyramidal neurons in normal aging and senile dementia. *Brain research*. 1987;409(1):88-96. PubMed PMID: 3580872.
51. Hanks SD, Flood DG. Region-specific stability of dendritic extent in normal human aging and regression in Alzheimer's disease. I. CA1 of hippocampus. *Brain research*. 1991;540(1-2):63-82. PubMed PMID: 2054634.
52. Flood DG. Region-specific stability of dendritic extent in normal human aging and regression in Alzheimer's disease. II. Subiculum. *Brain research*. 1991;540(1-2):83-95. PubMed PMID: 2054635.
53. Turner DA, Deupree DL. Functional elongation of CA1 hippocampal neurons with aging in Fischer 344 rats. *Neurobiology of aging*. 1991;12(3):201-10. PubMed PMID: 1876226.
54. Pyapali GK, Turner DA. Increased dendritic extent in hippocampal CA1 neurons from aged F344 rats. *Neurobiology of aging*. 1996;17(4):601-11. PubMed PMID: 8832635.
55. Markham JA, McKian KP, Stroup TS, Juraska JM. Sexually dimorphic aging of dendritic morphology in CA1 of hippocampus. *Hippocampus*. 2005;15(1):97-103. doi: 10.1002/hipo.20034. PubMed PMID: 15390161.
56. Grill JD, Riddle DR. Age-related and laminar-specific dendritic changes in the medial frontal cortex of the rat. *Brain research*. 2002;937(1-2):8-21. PubMed PMID: 12020857.
57. de Brabander JM, Kramers RJ, Uylings HB. Layer-specific dendritic regression of pyramidal cells with ageing in the human prefrontal cortex. *The European journal of neuroscience*. 1998;10(4):1261-9. PubMed PMID: 9749780.
58. Williams RS, Matthyse S. Age-related changes in Down syndrome brain and the cellular pathology of Alzheimer disease. *Progress in brain research*. 1986;70:49-67. PubMed PMID: 2953042.
59. Curcio CA, Hinds JW. Stability of synaptic density and spine volume in dentate gyrus of aged rats. *Neurobiology of aging*. 1983;4(1):77-87. PubMed PMID: 6877491.
60. Uemura E. Age-related changes in the subiculum of *Macaca mulatta*: synaptic density. *Experimental neurology*. 1985;87(3):403-11. PubMed PMID: 3972044.
61. Spencer WD, Raz N. Differential effects of aging on memory for content and context: a meta-analysis. *Psychology and aging*. 1995;10(4):527-39. PubMed PMID: 8749580.
62. McIntyre JS, Craik FI. Age differences in memory for item and source information. *Canadian journal of psychology*. 1987;41(2):175-92. PubMed PMID: 3502895.
63. Lyons-Warren A, Lillie R, Hershey T. Short- and long-term spatial delayed response performance across the lifespan. *Developmental neuropsychology*. 2004;26(3):661-78. doi: 10.1207/s15326942dn2603_1. PubMed PMID: 15525563.

64. Dunnett SB, Evenden JL, Iversen SD. Delay-dependent short-term memory deficits in aged rats. *Psychopharmacology*. 1988;96(2):174-80. PubMed PMID: 3148143.
65. Rapp PR, Amaral DG. Evidence for task-dependent memory dysfunction in the aged monkey. *The Journal of neuroscience : the official journal of the Society for Neuroscience*. 1989;9(10):3568-76. PubMed PMID: 2795141.
66. Moss MB, Killiany RJ, Lai ZC, Rosene DL, Herndon JG. Recognition memory span in rhesus monkeys of advanced age. *Neurobiology of aging*. 1997;18(1):13-9. PubMed PMID: 8983028.
67. Rhodes MG. Age-related differences in performance on the Wisconsin card sorting test: a meta-analytic review. *Psychology and aging*. 2004;19(3):482-94. doi: 10.1037/0882-7974.19.3.482. PubMed PMID: 15382998.
68. Moore TL, Killiany RJ, Herndon JG, Rosene DL, Moss MB. Impairment in abstraction and set shifting in aged rhesus monkeys. *Neurobiology of aging*. 2003;24(1):125-34. PubMed PMID: 12493558.
69. Ichihara-Takeda S, Funahashi S. Activity of primate orbitofrontal and dorsolateral prefrontal neurons: effect of reward schedule on task-related activity. *Journal of cognitive neuroscience*. 2008;20(4):563-79. doi: 10.1162/jocn.2008.20047. PubMed PMID: 18052781.
70. Mair RG, Burk JA, Porter MC. Lesions of the frontal cortex, hippocampus, and intralaminar thalamic nuclei have distinct effects on remembering in rats. *Behavioral neuroscience*. 1998;112(4):772-92. PubMed PMID: 9733186.
71. Godefroy O, Cabaret M, Petit-Chenal V, Pruvo JP, Rousseaux M. Control functions of the frontal lobes. Modularity of the central-supervisory system? *Cortex; a journal devoted to the study of the nervous system and behavior*. 1999;35(1):1-20. PubMed PMID: 10213531.
72. Wilkniss SM, Jones MG, Korol DL, Gold PE, Manning CA. Age-related differences in an ecologically based study of route learning. *Psychology and aging*. 1997;12(2):372-5. PubMed PMID: 9189997.
73. Lai ZC, Moss MB, Killiany RJ, Rosene DL, Herndon JG. Executive system dysfunction in the aged monkey: spatial and object reversal learning. *Neurobiology of aging*. 1995;16(6):947-54. PubMed PMID: 8622786.
74. Rapp PR, Kansky MT, Roberts JA. Impaired spatial information processing in aged monkeys with preserved recognition memory. *Neuroreport*. 1997;8(8):1923-8. PubMed PMID: 9223078.
75. Head E, Mehta R, Hartley J, Kameka M, Cummings BJ, Cotman CW, Ruehl WW, Milgram NW. Spatial learning and memory as a function of age in the dog. *Behavioral neuroscience*. 1995;109(5):851-8. PubMed PMID: 8554710.
76. Christie LA, Studzinski CM, Araujo JA, Leung CS, Ikeda-Douglas CJ, Head E, Cotman CW, Milgram NW. A comparison of egocentric and allocentric age-dependent spatial learning in the beagle dog. *Progress in neuro-psychopharmacology & biological psychiatry*. 2005;29(3):361-9. doi: 10.1016/j.pnpbp.2004.12.002. PubMed PMID: 15795044.
77. Olton DS, Markowska A, Breckler SJ, Wenk GL, Pang KC, Koliatsos V. Individual differences in aging: behavioral and neural analyses. *Biomedical and environmental sciences : BES*. 1991;4(1-2):166-72. PubMed PMID: 1910593.
78. Gallagher M, Rapp PR. The use of animal models to study the effects of aging on cognition. *Annual review of psychology*. 1997;48:339-70. doi: 10.1146/annurev.psych.48.1.339. PubMed PMID: 9046563.
79. Bach ME, Barad M, Son H, Zhuo M, Lu YF, Shih R, Mansuy I, Hawkins RD, Kandel ER. Age-related defects in spatial memory are correlated with defects in the late phase of hippocampal long-term potentiation in vitro and are attenuated by drugs that enhance the cAMP signaling pathway. *Proceedings of the National Academy of Sciences of the United States of America*. 1999;96(9):5280-5. PubMed PMID: 10220457; PubMed Central PMCID: PMC21855.
80. Bondareff W, Geinisman Y. Loss of synapses in the dentate gyrus of the senescent rat. *The American journal of anatomy*. 1976;145(1):129-36. doi: 10.1002/aja.1001450110. PubMed PMID: 1246966.
81. Geinisman Y, Bondareff W, Dodge JT. Partial deafferentation of neurons in the dentate gyrus of the senescent rat. *Brain research*. 1977;134(3):541-5. PubMed PMID: 902113.
82. Geinisman Y, deToledo-Morrell L, Morrell F, Persina IS, Rossi M. Age-related loss of axospinous synapses formed by two afferent systems in the rat dentate gyrus as revealed by the unbiased stereological disector technique. *Hippocampus*. 1992;2(4):437-44. doi: 10.1002/hipo.450020411. PubMed PMID: 1308200.
83. Geinisman Y, de Toledo-Morrell L, Morrell F. Loss of perforated synapses in the dentate gyrus: morphological substrate of memory deficit in aged rats. *Proceedings of the National Academy of Sciences of the United States of America*. 1986;83(9):3027-31. PubMed PMID: 3458260; PubMed Central PMCID: PMC323440.

84. Geinisman Y, Ganeshina O, Yoshida R, Berry RW, Disterhoft JF, Gallagher M. Aging, spatial learning, and total synapse number in the rat CA1 stratum radiatum. *Neurobiology of aging*. 2004;25(3):407-16. doi: 10.1016/j.neurobiolaging.2003.12.001. PubMed PMID: 15123345.
85. Thibault O, Landfield PW. Increase in single L-type calcium channels in hippocampal neurons during aging. *Science*. 1996;272(5264):1017-20. PubMed PMID: 8638124.
86. Clayton DF. The genomic action potential. *Neurobiology of learning and memory*. 2000;74(3):185-216. doi: 10.1006/nlme.2000.3967. PubMed PMID: 11031127.
87. Platenik J, Kuramoto N, Yoneda Y. Molecular mechanisms associated with long-term consolidation of the NMDA signals. *Life sciences*. 2000;67(4):335-64. PubMed PMID: 11003045.
88. Lanahan A, Lyford G, Stevenson GS, Worley PF, Barnes CA. Selective alteration of long-term potentiation-induced transcriptional response in hippocampus of aged, memory-impaired rats. *The Journal of neuroscience : the official journal of the Society for Neuroscience*. 1997;17(8):2876-85. PubMed PMID: 9092609.
89. Chang YM, Rosene DL, Killiany RJ, Mangiamele LA, Luebke JI. Increased action potential firing rates of layer 2/3 pyramidal cells in the prefrontal cortex are significantly related to cognitive performance in aged monkeys. *Cerebral cortex*. 2005;15(4):409-18. doi: 10.1093/cercor/bhh144. PubMed PMID: 15749985.
90. Drachman DA. If we live long enough, will we all be demented? *Neurology*. 1994;44(9):1563-5. PubMed PMID: 7936273.
91. West MJ. Regionally specific loss of neurons in the aging human hippocampus. *Neurobiology of aging*. 1993;14(4):287-93. PubMed PMID: 8367010.
92. Du AT, Schuff N, Kramer JH, Ganzer S, Zhu XP, Jagust WJ, Miller BL, Reed BR, Mungas D, Yaffe K, Chui HC, Weiner MW. Higher atrophy rate of entorhinal cortex than hippocampus in AD. *Neurology*. 2004;62(3):422-7. PubMed PMID: 14872024; PubMed Central PMCID: PMC1820859.
93. Du AT, Schuff N, Zhu XP, Jagust WJ, Miller BL, Reed BR, Kramer JH, Mungas D, Yaffe K, Chui HC, Weiner MW. Atrophy rates of entorhinal cortex in AD and normal aging. *Neurology*. 2003;60(3):481-6. PubMed PMID: 12578931; PubMed Central PMCID: PMC1851672.
94. Simic G, Kostovic I, Winblad B, Bogdanovic N. Volume and number of neurons of the human hippocampal formation in normal aging and Alzheimer's disease. *The Journal of comparative neurology*. 1997;379(4):482-94. PubMed PMID: 9067838.
95. Kril JJ, Patel S, Harding AJ, Halliday GM. Neuron loss from the hippocampus of Alzheimer's disease exceeds extracellular neurofibrillary tangle formation. *Acta neuropathologica*. 2002;103(4):370-6. doi: 10.1007/s00401-001-0477-5. PubMed PMID: 11904757.
96. Rossler M, Zarski R, Bohl J, Ohm TG. Stage-dependent and sector-specific neuronal loss in hippocampus during Alzheimer's disease. *Acta neuropathologica*. 2002;103(4):363-9. doi: 10.1007/s00401-001-0475-7. PubMed PMID: 11904756.
97. West MJ, Kawas CH, Stewart WF, Rudow GL, Troncoso JC. Hippocampal neurons in pre-clinical Alzheimer's disease. *Neurobiology of aging*. 2004;25(9):1205-12. doi: 10.1016/j.neurobiolaging.2003.12.005. PubMed PMID: 15312966.
98. Gomez-Isla T, Price JL, McKeel DW, Jr., Morris JC, Growdon JH, Hyman BT. Profound loss of layer II entorhinal cortex neurons occurs in very mild Alzheimer's disease. *The Journal of neuroscience : the official journal of the Society for Neuroscience*. 1996;16(14):4491-500. PubMed PMID: 8699259.
99. Cullen KM, Halliday GM, Double KL, Brooks WS, Creasey H, Broe GA. Cell loss in the nucleus basalis is related to regional cortical atrophy in Alzheimer's disease. *Neuroscience*. 1997;78(3):641-52. PubMed PMID: 9153647.
100. Mufson EJ, Ma SY, Cochran EJ, Bennett DA, Beckett LA, Jaffar S, Saragovi HU, Kordower JH. Loss of nucleus basalis neurons containing trkA immunoreactivity in individuals with mild cognitive impairment and early Alzheimer's disease. *The Journal of comparative neurology*. 2000;427(1):19-30. PubMed PMID: 11042589.
101. Gomez-Isla T, Hollister R, West H, Mui S, Growdon JH, Petersen RC, Parisi JE, Hyman BT. Neuronal loss correlates with but exceeds neurofibrillary tangles in Alzheimer's disease. *Annals of neurology*. 1997;41(1):17-24. doi: 10.1002/ana.410410106. PubMed PMID: 9005861.
102. Bussiere T, Giannakopoulos P, Bouras C, Perl DP, Morrison JH, Hof PR. Progressive degeneration of nonphosphorylated neurofilament protein-enriched pyramidal neurons predicts cognitive impairment in Alzheimer's

- disease: stereologic analysis of prefrontal cortex area 9. *The Journal of comparative neurology*. 2003;463(3):281-302. doi: 10.1002/cne.10760. PubMed PMID: 12820162.
103. Kempainen N, Roytta M, Collan Y, Ma SY, Hinkka S, Rinne JO. Unbiased morphological measurements show no neuronal loss in the substantia nigra in Alzheimer's disease. *Acta neuropathologica*. 2002;103(1):43-7. PubMed PMID: 11837746.
104. Vereecken TH, Vogels OJ, Nieuwenhuys R. Neuron loss and shrinkage in the amygdala in Alzheimer's disease. *Neurobiology of aging*. 1994;15(1):45-54. PubMed PMID: 8159262.
105. Scinto LF, Frosch M, Wu CK, Daffner KR, Gedi N, Geula C. Selective cell loss in Edinger-Westphal in asymptomatic elders and Alzheimer's patients. *Neurobiology of aging*. 2001;22(5):729-36. PubMed PMID: 11705632.
106. Anderson AJ, Su JH, Cotman CW. DNA damage and apoptosis in Alzheimer's disease: colocalization with c-Jun immunoreactivity, relationship to brain area, and effect of postmortem delay. *The Journal of neuroscience : the official journal of the Society for Neuroscience*. 1996;16(5):1710-9. PubMed PMID: 8774439.
107. Lassmann H, Bancher C, Breitschopf H, Wegiel J, Bobinski M, Jellinger K, Wisniewski HM. Cell death in Alzheimer's disease evaluated by DNA fragmentation in situ. *Acta neuropathologica*. 1995;89(1):35-41. PubMed PMID: 7709729.
108. Vitek MP, Bhattacharya K, Glendening JM, Stopa E, Vlassara H, Bucala R, Manogue K, Cerami A. Advanced glycation end products contribute to amyloidosis in Alzheimer disease. *Proceedings of the National Academy of Sciences of the United States of America*. 1994;91(11):4766-70. PubMed PMID: 8197133; PubMed Central PMCID: PMC43869.
109. Giannakopoulos P, Hof PR, Mottier S, Michel JP, Bouras C. Neuropathological changes in the cerebral cortex of 1258 cases from a geriatric hospital: retrospective clinicopathological evaluation of a 10-year autopsy population. *Acta neuropathologica*. 1994;87(5):456-68. PubMed PMID: 8059598.
110. Braak H, Braak E. Neuropathological staging of Alzheimer-related changes. *Acta neuropathologica*. 1991;82(4):239-59. PubMed PMID: 1759558.
111. Bancher C, Leitner H, Jellinger K, Eder H, Setinek U, Fischer P, Wegiel J, Wisniewski HM. On the relationship between measles virus and Alzheimer neurofibrillary tangles in subacute sclerosing panencephalitis. *Neurobiology of aging*. 1996;17(4):527-33. PubMed PMID: 8832626.
112. Tabaton M, Mandybur TI, Perry G, Onorato M, Autilio-Gambetti L, Gambetti P. The widespread alteration of neurites in Alzheimer's disease may be unrelated to amyloid deposition. *Annals of neurology*. 1989;26(6):771-8. doi: 10.1002/ana.410260614. PubMed PMID: 2557796.
113. Wang XF, Dong CF, Zhang J, Wan YZ, Li F, Huang YX, Han L, Shan B, Gao C, Han J, Dong XP. Human tau protein forms complex with PrP and some GSS- and fCJD-related PrP mutants possess stronger binding activities with tau in vitro. *Molecular and cellular biochemistry*. 2008;310(1-2):49-55. doi: 10.1007/s11010-007-9664-6. PubMed PMID: 18038270.
114. Cairns NJ, Bigio EH, Mackenzie IR, Neumann M, Lee VM, Hatanpaa KJ, White CL, 3rd, Schneider JA, Grinberg LT, Halliday G, Duyckaerts C, Lowe JS, Holm IE, Tolnay M, Okamoto K, Yokoo H, Murayama S, Woulfe J, Munoz DG, Dickson DW, Ince PG, Trojanowski JQ, Mann DM, Consortium for Frontotemporal Lobar D. Neuropathologic diagnostic and nosologic criteria for frontotemporal lobar degeneration: consensus of the Consortium for Frontotemporal Lobar Degeneration. *Acta neuropathologica*. 2007;114(1):5-22. doi: 10.1007/s00401-007-0237-2. PubMed PMID: 17579875; PubMed Central PMCID: PMC2827877.
115. Burns A, Tomlinson BE, Mann DM. Observations on the brains of demented old people. B.E. Tomlinson, G. Blessed and M. Roth, *Journal of the Neurological Sciences* (1970) 11, 205-242 and Observations on the brains of non-demented old people. B.E. Tomlinson, G. Blessed and M. Roth, *Journal of Neurological Sciences* (1968) 7, 331-356. *International journal of geriatric psychiatry*. 1997;12(8):785-90. PubMed PMID: 9283922.
116. Braak H, Del Tredici K. The pathological process underlying Alzheimer's disease in individuals under thirty. *Acta neuropathologica*. 2011;121(2):171-81. doi: 10.1007/s00401-010-0789-4. PubMed PMID: 21170538.
117. Bouras C, Hof PR, Giannakopoulos P, Michel JP, Morrison JH. Regional distribution of neurofibrillary tangles and senile plaques in the cerebral cortex of elderly patients: a quantitative evaluation of a one-year autopsy population from a geriatric hospital. *Cerebral cortex*. 1994;4(2):138-50. PubMed PMID: 8038565.

118. Braak H, Thal DR, Ghebremedhin E, Del Tredici K. Stages of the pathologic process in Alzheimer disease: age categories from 1 to 100 years. *Journal of neuropathology and experimental neurology*. 2011;70(11):960-9. doi: 10.1097/NEN.0b013e318232a379. PubMed PMID: 22002422.
119. Duyckaerts C, Hauw JJ. Prevalence, incidence and duration of Braak's stages in the general population: can we know? *Neurobiology of aging*. 1997;18(4):362-9; discussion 89-92. PubMed PMID: 9380250.
120. Sabbagh MN, Cooper K, DeLange J, Stoehr JD, Thind K, Lahti T, Reisberg B, Sue L, Vedders L, Fleming SR, Beach TG. Functional, global and cognitive decline correlates to accumulation of Alzheimer's pathology in MCI and AD. *Current Alzheimer research*. 2010;7(4):280-6. PubMed PMID: 19715548; PubMed Central PMCID: PMC3138789.
121. Lewis DA, Campbell MJ, Terry RD, Morrison JH. Laminar and regional distributions of neurofibrillary tangles and neuritic plaques in Alzheimer's disease: a quantitative study of visual and auditory cortices. *The Journal of neuroscience : the official journal of the Society for Neuroscience*. 1987;7(6):1799-808. PubMed PMID: 2439665.
122. Bobinski M, Wegiel J, Tarnawski M, Bobinski M, Reisberg B, de Leon MJ, Miller DC, Wisniewski HM. Relationships between regional neuronal loss and neurofibrillary changes in the hippocampal formation and duration and severity of Alzheimer disease. *Journal of neuropathology and experimental neurology*. 1997;56(4):414-20. PubMed PMID: 9100672.
123. Abner EL, Kryscio RJ, Schmitt FA, Santacruz KS, Jicha GA, Lin Y, Neltner JM, Smith CD, Van Eldik LJ, Nelson PT. "End-stage" neurofibrillary tangle pathology in preclinical Alzheimer's disease: fact or fiction? *Journal of Alzheimer's disease : JAD*. 2011;25(3):445-53. doi: 10.3233/JAD-2011-101980. PubMed PMID: 21471646; PubMed Central PMCID: PMC3171001.
124. Nelson PT, Braak H, Markesbery WR. Neuropathology and cognitive impairment in Alzheimer disease: a complex but coherent relationship. *Journal of neuropathology and experimental neurology*. 2009;68(1):1-14. doi: 10.1097/NEN.0b013e3181919a48. PubMed PMID: 19104448; PubMed Central PMCID: PMC2692822.
125. Hyman BT, Phelps CH, Beach TG, Bigio EH, Cairns NJ, Carrillo MC, Dickson DW, Duyckaerts C, Frosch MP, Masliah E, Mirra SS, Nelson PT, Schneider JA, Thal DR, Thies B, Trojanowski JQ, Vinters HV, Montine TJ. National Institute on Aging-Alzheimer's Association guidelines for the neuropathologic assessment of Alzheimer's disease. *Alzheimer's & dementia : the journal of the Alzheimer's Association*. 2012;8(1):1-13. doi: 10.1016/j.jalz.2011.10.007. PubMed PMID: 22265587; PubMed Central PMCID: PMC3266529.
126. Thal DR, Del Tredici K, Ludolph AC, Hoozemans JJ, Rozemuller AJ, Braak H, Knippschild U. Stages of granulovacuolar degeneration: their relation to Alzheimer's disease and chronic stress response. *Acta neuropathologica*. 2011;122(5):577-89. doi: 10.1007/s00401-011-0871-6. PubMed PMID: 21935637.
127. Ho GJ, Drego R, Hakimian E, Masliah E. Mechanisms of cell signaling and inflammation in Alzheimer's disease. *Current drug targets Inflammation and allergy*. 2005;4(2):247-56. PubMed PMID: 15853747.
128. Scheff SW, Price DA. Alzheimer's disease-related alterations in synaptic density: neocortex and hippocampus. *Journal of Alzheimer's disease : JAD*. 2006;9(3 Suppl):101-15. PubMed PMID: 16914849.
129. D'Andrea MR, Nagele RG. Morphologically distinct types of amyloid plaques point the way to a better understanding of Alzheimer's disease pathogenesis. *Biotechnic & histochemistry : official publication of the Biological Stain Commission*. 2010;85(2):133-47. doi: 10.3109/10520290903389445. PubMed PMID: 20121465.
130. Masliah E, Mallory M, Deerinck T, DeTeresa R, Lamont S, Miller A, Terry RD, Carragher B, Ellisman M. Re-evaluation of the structural organization of neuritic plaques in Alzheimer's disease. *Journal of neuropathology and experimental neurology*. 1993;52(6):619-32. PubMed PMID: 8229081.
131. Terry RD, Masliah E, Salmon DP, Butters N, DeTeresa R, Hill R, Hansen LA, Katzman R. Physical basis of cognitive alterations in Alzheimer's disease: synapse loss is the major correlate of cognitive impairment. *Annals of neurology*. 1991;30(4):572-80. doi: 10.1002/ana.410300410. PubMed PMID: 1789684.
132. Masliah E, Terry RD, Mallory M, Alford M, Hansen LA. Diffuse plaques do not accentuate synapse loss in Alzheimer's disease. *The American journal of pathology*. 1990;137(6):1293-7. PubMed PMID: 2124413; PubMed Central PMCID: PMC1877714.
133. Dickson TC, Vickers JC. The morphological phenotype of beta-amyloid plaques and associated neuritic changes in Alzheimer's disease. *Neuroscience*. 2001;105(1):99-107. PubMed PMID: 11483304.
134. Bertram L, Lill CM, Tanzi RE. The genetics of Alzheimer disease: back to the future. *Neuron*. 2010;68(2):270-81. doi: 10.1016/j.neuron.2010.10.013. PubMed PMID: 20955934.

135. Gatz M, Reynolds CA, Fratiglioni L, Johansson B, Mortimer JA, Berg S, Fiske A, Pedersen NL. Role of genes and environments for explaining Alzheimer disease. *Archives of general psychiatry*. 2006;63(2):168-74. doi: 10.1001/archpsyc.63.2.168. PubMed PMID: 16461860.
136. Thal DR, Rub U, Orantes M, Braak H. Phases of A beta-deposition in the human brain and its relevance for the development of AD. *Neurology*. 2002;58(12):1791-800. PubMed PMID: 12084879.
137. Pearson RC, Esiri MM, Hiorns RW, Wilcock GK, Powell TP. Anatomical correlates of the distribution of the pathological changes in the neocortex in Alzheimer disease. *Proceedings of the National Academy of Sciences of the United States of America*. 1985;82(13):4531-4. PubMed PMID: 3859874; PubMed Central PMCID: PMC391136.
138. Braak H, Braak E, Kalus P. Alzheimer's disease: areal and laminar pathology in the occipital isocortex. *Acta neuropathologica*. 1989;77(5):494-506. PubMed PMID: 2566255.
139. Castellani RJ, Lee HG, Zhu X, Perry G, Smith MA. Alzheimer disease pathology as a host response. *Journal of neuropathology and experimental neurology*. 2008;67(6):523-31. doi: 10.1097/NEN.0b013e318177eaf4. PubMed PMID: 18520771; PubMed Central PMCID: PMC2763411.
140. Lee HG, Castellani RJ, Zhu X, Perry G, Smith MA. Amyloid-beta in Alzheimer's disease: the horse or the cart? Pathogenic or protective? *International journal of experimental pathology*. 2005;86(3):133-8. doi: 10.1111/j.0959-9673.2005.00429.x. PubMed PMID: 15910547; PubMed Central PMCID: PMC2517413.
141. Whitehouse PJ, George DR, D'Alton S. Describing the dying days of "Alzheimer's disease". *Journal of Alzheimer's disease : JAD*. 2011;24(1):11-3. doi: 10.3233/JAD-2010-101639. PubMed PMID: 21187588.
142. Chen M, Maleski JJ, Sawmiller DR. Scientific truth or false hope? Understanding Alzheimer's disease from an aging perspective. *Journal of Alzheimer's disease : JAD*. 2011;24(1):3-10. doi: 10.3233/JAD-2010-101638. PubMed PMID: 21178284.
143. Nelson PT, Alafuzoff I, Bigio EH, Bouras C, Braak H, Cairns NJ, Castellani RJ, Crain BJ, Davies P, Del Tredici K, Duyckaerts C, Frosch MP, Haroutunian V, Hof PR, Hulette CM, Hyman BT, Iwatsubo T, Jellinger KA, Jicha GA, Kovari E, Kukull WA, Leverenz JB, Love S, Mackenzie IR, Mann DM, Masliah E, McKee AC, Montine TJ, Morris JC, Schneider JA, Sonnen JA, Thal DR, Trojanowski JQ, Troncoso JC, Wisniewski T, Woltjer RL, Beach TG. Correlation of Alzheimer disease neuropathologic changes with cognitive status: a review of the literature. *Journal of neuropathology and experimental neurology*. 2012;71(5):362-81. doi: 10.1097/NEN.0b013e31825018f7. PubMed PMID: 22487856; PubMed Central PMCID: PMC3560290.
144. McKhann GM, Knopman DS, Chertkow H, Hyman BT, Jack CR, Jr., Kawas CH, Klunk WE, Koroshetz WJ, Manly JJ, Mayeux R, Mohs RC, Morris JC, Rossor MN, Scheltens P, Carrillo MC, Thies B, Weintraub S, Phelps CH. The diagnosis of dementia due to Alzheimer's disease: recommendations from the National Institute on Aging-Alzheimer's Association workgroups on diagnostic guidelines for Alzheimer's disease. *Alzheimer's & dementia : the journal of the Alzheimer's Association*. 2011;7(3):263-9. doi: 10.1016/j.jalz.2011.03.005. PubMed PMID: 21514250; PubMed Central PMCID: PMC3312024.
145. Nelson PT, Jicha GA, Schmitt FA, Liu H, Davis DG, Mendiondo MS, Abner EL, Markesbery WR. Clinicopathologic correlations in a large Alzheimer disease center autopsy cohort: neuritic plaques and neurofibrillary tangles "do count" when staging disease severity. *Journal of neuropathology and experimental neurology*. 2007;66(12):1136-46. doi: 10.1097/nen.0b013e31815c5efb. PubMed PMID: 18090922; PubMed Central PMCID: PMC3034246.
146. Campion D, Dumanchin C, Hannequin D, Dubois B, Belliard S, Puel M, Thomas-Anterion C, Michon A, Martin C, Charbonnier F, Raux G, Camuzat A, Penet C, Mesnage V, Martinez M, Clerget-Darpoux F, Brice A, Frebourg T. Early-onset autosomal dominant Alzheimer disease: prevalence, genetic heterogeneity, and mutation spectrum. *American journal of human genetics*. 1999;65(3):664-70. doi: 10.1086/302553. PubMed PMID: 10441572; PubMed Central PMCID: PMC1377972.
147. de la Torre JC. Three postulates to help identify the cause of Alzheimer's disease. *Journal of Alzheimer's disease : JAD*. 2011;24(4):657-68. doi: 10.3233/JAD-2011-101884. PubMed PMID: 21321392.
148. Trojanowski JQ, Lee VM. Phosphorylation of paired helical filament tau in Alzheimer's disease neurofibrillary lesions: focusing on phosphatases. *FASEB journal : official publication of the Federation of American Societies for Experimental Biology*. 1995;9(15):1570-6. PubMed PMID: 8529836.

149. Glass CK, Saijo K, Winner B, Marchetto MC, Gage FH. Mechanisms underlying inflammation in neurodegeneration. *Cell*. 2010;140(6):918-34. doi: 10.1016/j.cell.2010.02.016. PubMed PMID: 20303880; PubMed Central PMCID: PMC2873093.
150. Hardy J, Selkoe DJ. The amyloid hypothesis of Alzheimer's disease: progress and problems on the road to therapeutics. *Science*. 2002;297(5580):353-6. doi: 10.1126/science.1072994. PubMed PMID: 12130773.
151. Blennow K, Mattsson N, Scholl M, Hansson O, Zetterberg H. Amyloid biomarkers in Alzheimer's disease. *Trends in pharmacological sciences*. 2015;36(5):297-309. doi: 10.1016/j.tips.2015.03.002. PubMed PMID: 25840462.
152. Wu L, Rosa-Neto P, Hsiung GY, Sadovnick AD, Masellis M, Black SE, Jia J, Gauthier S. Early-onset familial Alzheimer's disease (EOFAD). *The Canadian journal of neurological sciences Le journal canadien des sciences neurologiques*. 2012;39(4):436-45. PubMed PMID: 22728850.
153. Helzner EP, Scarmeas N, Cosentino S, Tang MX, Schupf N, Stern Y. Survival in Alzheimer disease: a multiethnic, population-based study of incident cases. *Neurology*. 2008;71(19):1489-95. doi: 10.1212/01.wnl.0000334278.11022.42. PubMed PMID: 18981370; PubMed Central PMCID: PMC2843528.
154. Boddaert J, Verny M. [Survival after initial diagnosis of Alzheimer disease]. *Psychologie & neuropsychiatrie du vieillissement*. 2005;3(2):136-7. PubMed PMID: 16044487.
155. Larson EB, Shadlen MF, Wang L, McCormick WC, Bowen JD, Teri L, Kukull WA. Survival after initial diagnosis of Alzheimer disease. *Annals of internal medicine*. 2004;140(7):501-9. PubMed PMID: 15068977.
156. Brookmeyer R, Corrada MM, Curriero FC, Kawas C. Survival following a diagnosis of Alzheimer disease. *Archives of neurology*. 2002;59(11):1764-7. PubMed PMID: 12433264.
157. Wolfson C, Wolfson DB, Asgharian M, M'Lan CE, Ostbye T, Rockwood K, Hogan DB, Clinical Progression of Dementia Study G. A reevaluation of the duration of survival after the onset of dementia. *The New England journal of medicine*. 2001;344(15):1111-6. doi: 10.1056/NEJM200104123441501. PubMed PMID: 11297701.
158. Schacter DL, Gilbert DT, Wegner DM. *Psychology*. 2nd ed. New York, NY: Worth Publishers; 2011.
159. Schacter DL, Gilbert DT, Wegner DM. *Introducing psychology*. 2nd ed. New York, NY: Worth Publishers; 2013.
160. Markowitsch HJ, Staniloiu A. Amnesic disorders. *Lancet*. 2012;380(9851):1429-40. doi: 10.1016/S0140-6736(11)61304-4. PubMed PMID: 22503117.
161. Tulving E. *Elements of episodic memory*. Oxford Oxfordshire

New York: Clarendon Press ;

Oxford University Press; 1983. xi, 351 p. p.

162. Tulving E. Multiple memory systems and consciousness. *Human neurobiology*. 1987;6(2):67-80. PubMed PMID: 3305441.
163. Tulving E. Episodic memory: from mind to brain. *Annual review of psychology*. 2002;53:1-25. doi: 10.1146/annurev.psych.53.100901.135114. PubMed PMID: 11752477.
164. Squire LR, Zola-Morgan S. Conscious and Unconscious Memory Systems. *Cold Spring Harbor perspectives in biology*. 2015;7(3). doi: 10.1101/cshperspect.a021667. PubMed PMID: 25731765.
165. Scoville WB, Milner B. Loss of recent memory after bilateral hippocampal lesions. 1957. *The Journal of neuropsychiatry and clinical neurosciences*. 2000;12(1):103-13. PubMed PMID: 10678523.
166. Zola-Morgan S, Squire LR, Amaral DG. Human amnesia and the medial temporal region: enduring memory impairment following a bilateral lesion limited to field CA1 of the hippocampus. *The Journal of neuroscience : the official journal of the Society for Neuroscience*. 1986;6(10):2950-67. PubMed PMID: 3760943.
167. Peters F, Collette F, Degueldre C, Sterpenich V, Majerus S, Salmon E. The neural correlates of verbal short-term memory in Alzheimer's disease: an fMRI study. *Brain : a journal of neurology*. 2009;132(Pt 7):1833-46. doi: 10.1093/brain/awp075. PubMed PMID: 19433442.
168. Cowan N. What are the differences between long-term, short-term, and working memory? *Progress in brain research*. 2008;169:323-38. doi: 10.1016/S0079-6123(07)00020-9. PubMed PMID: 18394484; PubMed Central PMCID: PMC2657600.
169. Nourhashemi F, Ousset PJ, Gillette-Guyonnet S, Cantet C, Andrieu S, Vellas B, cohort RF. A 2-year follow-up of 233 very mild (CDR 0.5) Alzheimer's disease patients (REAL.FR cohort). *International journal of geriatric psychiatry*. 2008;23(5):460-5. doi: 10.1002/gps.1904. PubMed PMID: 17894422.

170. Han L, Cole M, Bellavance F, McCusker J, Primeau F. Tracking cognitive decline in Alzheimer's disease using the mini-mental state examination: a meta-analysis. *International psychogeriatrics / IPA*. 2000;12(2):231-47. PubMed PMID: 10937543.
171. Adak S, Illouz K, Gorman W, Tandon R, Zimmerman EA, Guariglia R, Moore MM, Kaye JA. Predicting the rate of cognitive decline in aging and early Alzheimer disease. *Neurology*. 2004;63(1):108-14. PubMed PMID: 15249619.
172. Clark CM, Sheppard L, Fillenbaum GG, Galasko D, Morris JC, Koss E, Mohs R, Heyman A. Variability in annual Mini-Mental State Examination score in patients with probable Alzheimer disease: a clinical perspective of data from the Consortium to Establish a Registry for Alzheimer's Disease. *Archives of neurology*. 1999;56(7):857-62. PubMed PMID: 10404988.
173. Schmidt C, Wolff M, Weitz M, Bartlau T, Korth C, Zerr I. Rapidly progressive Alzheimer disease. *Archives of neurology*. 2011;68(9):1124-30. doi: 10.1001/archneurol.2011.189. PubMed PMID: 21911694.
174. Bernick C, Cummings J, Raman R, Sun X, Aisen P. Age and rate of cognitive decline in Alzheimer disease: implications for clinical trials. *Archives of neurology*. 2012;69(7):901-5. doi: 10.1001/archneurol.2011.3758. PubMed PMID: 22431834.
175. Peters ME, Schwartz S, Han D, Rabins PV, Steinberg M, Tschanz JT, Lyketsos CG. Neuropsychiatric Symptoms as Predictors of Progression to Severe Alzheimer's Dementia and Death: The Cache County Dementia Progression Study. *The American journal of psychiatry*. 2015:appiajp201414040480. doi: 10.1176/appi.ajp.2014.14040480. PubMed PMID: 25585033.
176. Gorno-Tempini ML, Dronkers NF, Rankin KP, Ogar JM, Phengrasamy L, Rosen HJ, Johnson JK, Weiner MW, Miller BL. Cognition and anatomy in three variants of primary progressive aphasia. *Annals of neurology*. 2004;55(3):335-46. doi: 10.1002/ana.10825. PubMed PMID: 14991811; PubMed Central PMCID: PMC2362399.
177. Canning SJ, Leach L, Stuss D, Ngo L, Black SE. Diagnostic utility of abbreviated fluency measures in Alzheimer disease and vascular dementia. *Neurology*. 2004;62(4):556-62. PubMed PMID: 14981170.
178. Marczinski CA, Kertesz A. Category and letter fluency in semantic dementia, primary progressive aphasia, and Alzheimer's disease. *Brain and language*. 2006;97(3):258-65. doi: 10.1016/j.bandl.2005.11.001. PubMed PMID: 16325251.
179. Cerhan JH, Ivnik RJ, Smith GE, Tangalos EC, Petersen RC, Boeve BF. Diagnostic utility of letter fluency, category fluency, and fluency difference scores in Alzheimer's disease. *The Clinical neuropsychologist*. 2002;16(1):35-42. doi: 10.1076/clin.16.1.35.8326. PubMed PMID: 11992224.
180. Hamilton L, Fay S, Rockwood K. Misplacing objects in mild to moderate Alzheimer's disease: a descriptive analysis from the VISTA clinical trial. *Journal of neurology, neurosurgery, and psychiatry*. 2009;80(9):960-5. doi: 10.1136/jnnp.2008.166801. PubMed PMID: 19293172.
181. Guerin F, Belleville S, Ska B. Characterization of visuoconstructional disabilities in patients with probable dementia of Alzheimer's type. *Journal of clinical and experimental neuropsychology*. 2002;24(1):1-17. doi: 10.1076/jcen.24.1.1.963. PubMed PMID: 11935419.
182. Mendez MF, Mendez MA, Martin R, Smyth KA, Whitehouse PJ. Complex visual disturbances in Alzheimer's disease. *Neurology*. 1990;40(3 Pt 1):439-43. PubMed PMID: 2314585.
183. Meguro K, Shimada M, Someya K, Horikawa A, Yamadori A. Hemispatial visual-searching impairment correlated with decreased contralateral parietal blood flow in Alzheimer disease. *Neuropsychiatry, neuropsychology, and behavioral neurology*. 2001;14(4):213-8. PubMed PMID: 11725214.
184. Mendez MF, Cherrier MM, Cymerman JS. Hemispatial neglect on visual search tasks in Alzheimer's disease. *Neuropsychiatry, neuropsychology, and behavioral neurology*. 1997;10(3):203-8. PubMed PMID: 9297714.
185. Stokholm J, Vogel A, Gade A, Waldemar G. Heterogeneity in executive impairment in patients with very mild Alzheimer's disease. *Dementia and geriatric cognitive disorders*. 2006;22(1):54-9. doi: 10.1159/000093262. PubMed PMID: 16682794.
186. Harwood DG, Sultzer DL, Wheatley MV. Impaired insight in Alzheimer disease: association with cognitive deficits, psychiatric symptoms, and behavioral disturbances. *Neuropsychiatry, neuropsychology, and behavioral neurology*. 2000;13(2):83-8. PubMed PMID: 10780626.

187. Starkstein SE, Mizrahi R, Power BD. Depression in Alzheimer's disease: phenomenology, clinical correlates and treatment. *International review of psychiatry*. 2008;20(4):382-8. doi: 10.1080/09540260802094480. PubMed PMID: 18925487.
188. Mizrahi R, Starkstein SE, Jorge R, Robinson RG. Phenomenology and clinical correlates of delusions in Alzheimer disease. *The American journal of geriatric psychiatry : official journal of the American Association for Geriatric Psychiatry*. 2006;14(7):573-81. doi: 10.1097/01.JGP.0000214559.61700.1c. PubMed PMID: 16816010.
189. Peters KR, Rockwood K, Black SE, Bouchard R, Gauthier S, Hogan D, Kertesz A, Loy-English I, Beattie BL, Sadovnick AD, Feldman HH. Characterizing neuropsychiatric symptoms in subjects referred to dementia clinics. *Neurology*. 2006;66(4):523-8. doi: 10.1212/01.wnl.0000198255.84842.06. PubMed PMID: 16505306.
190. Scarmeas N, Brandt J, Blacker D, Albert M, Hadjigeorgiou G, Dubois B, Devanand D, Honig L, Stern Y. Disruptive behavior as a predictor in Alzheimer disease. *Archives of neurology*. 2007;64(12):1755-61. doi: 10.1001/archneur.64.12.1755. PubMed PMID: 18071039; PubMed Central PMCID: PMC2690610.
191. Lyketsos CG, Steinberg M, Tschanz JT, Norton MC, Steffens DC, Breitner JC. Mental and behavioral disturbances in dementia: findings from the Cache County Study on Memory in Aging. *The American journal of psychiatry*. 2000;157(5):708-14. PubMed PMID: 10784462.
192. Lyketsos CG, Lopez O, Jones B, Fitzpatrick AL, Breitner J, DeKosky S. Prevalence of neuropsychiatric symptoms in dementia and mild cognitive impairment: results from the cardiovascular health study. *Jama*. 2002;288(12):1475-83. PubMed PMID: 12243634.
193. Mega MS, Cummings JL, Fiorello T, Gornbein J. The spectrum of behavioral changes in Alzheimer's disease. *Neurology*. 1996;46(1):130-5. PubMed PMID: 8559361.
194. Sink KM, Covinsky KE, Newcomer R, Yaffe K. Ethnic differences in the prevalence and pattern of dementia-related behaviors. *Journal of the American Geriatrics Society*. 2004;52(8):1277-83. doi: 10.1111/j.1532-5415.2004.52356.x. PubMed PMID: 15271114.
195. Merriam AE, Aronson MK, Gaston P, Wey SL, Katz I. The psychiatric symptoms of Alzheimer's disease. *Journal of the American Geriatrics Society*. 1988;36(1):7-12. PubMed PMID: 3335733.
196. Cummings JL, Miller B, Hill MA, Neshkes R. Neuropsychiatric aspects of multi-infarct dementia and dementia of the Alzheimer type. *Archives of neurology*. 1987;44(4):389-93. PubMed PMID: 3827694.
197. Deschenes CL, McCurry SM. Current treatments for sleep disturbances in individuals with dementia. *Current psychiatry reports*. 2009;11(1):20-6. PubMed PMID: 19187704; PubMed Central PMCID: PMC2649672.
198. McCurry SM, Logsdon RG, Teri L, Gibbons LE, Kukull WA, Bowen JD, McCormick WC, Larson EB. Characteristics of sleep disturbance in community-dwelling Alzheimer's disease patients. *Journal of geriatric psychiatry and neurology*. 1999;12(2):53-9. PubMed PMID: 10483925.
199. Little JT, Satlin A, Sunderland T, Volicer L. Sundown syndrome in severely demented patients with probable Alzheimer's disease. *Journal of geriatric psychiatry and neurology*. 1995;8(2):103-6. PubMed PMID: 7794472.
200. Khachiyants N, Trinkle D, Son SJ, Kim KY. Sundown syndrome in persons with dementia: an update. *Psychiatry investigation*. 2011;8(4):275-87. doi: 10.4306/pi.2011.8.4.275. PubMed PMID: 22216036; PubMed Central PMCID: PMC3246134.
201. Chen JC, Borson S, Scanlan JM. Stage-specific prevalence of behavioral symptoms in Alzheimer's disease in a multi-ethnic community sample. *The American journal of geriatric psychiatry : official journal of the American Association for Geriatric Psychiatry*. 2000;8(2):123-33. PubMed PMID: 10804073.
202. Scarmeas N, Brandt J, Albert M, Hadjigeorgiou G, Papadimitriou A, Dubois B, Sarazin M, Devanand D, Honig L, Marder K, Bell K, Wegesin D, Blacker D, Stern Y. Delusions and hallucinations are associated with worse outcome in Alzheimer disease. *Archives of neurology*. 2005;62(10):1601-8. doi: 10.1001/archneur.62.10.1601. PubMed PMID: 16216946; PubMed Central PMCID: PMC3028538.
203. Steele C, Rovner B, Chase GA, Folstein M. Psychiatric symptoms and nursing home placement of patients with Alzheimer's disease. *The American journal of psychiatry*. 1990;147(8):1049-51. PubMed PMID: 2375439.
204. Gallagher-Thompson D, Brooks JO, 3rd, Bliwise D, Leader J, Yesavage JA. The relations among caregiver stress, "sundowning" symptoms, and cognitive decline in Alzheimer's disease. *Journal of the American Geriatrics Society*. 1992;40(8):807-10. PubMed PMID: 1634724.

205. Morriss RK, Rovner BW, Folstein MF, German PS. Delusions in newly admitted residents of nursing homes. *The American journal of psychiatry*. 1990;147(3):299-302. PubMed PMID: 2309945.
206. O'Donnell BF, Drachman DA, Barnes HJ, Peterson KE, Swearer JM, Lew RA. Incontinence and troublesome behaviors predict institutionalization in dementia. *Journal of geriatric psychiatry and neurology*. 1992;5(1):45-52. PubMed PMID: 1571074.
207. Alagiakrishnan K, Lim D, Brahim A, Wong A, Wood A, Senthilselvan A, Chimich WT, Kagan L. Sexually inappropriate behaviour in demented elderly people. *Postgraduate medical journal*. 2005;81(957):463-6. doi: 10.1136/pgmj.2004.028043. PubMed PMID: 15998824; PubMed Central PMCID: PMC1743300.
208. Tsai SJ, Hwang JP, Yang CH, Liu KM, Lirng JF. Inappropriate sexual behaviors in dementia: a preliminary report. *Alzheimer disease and associated disorders*. 1999;13(1):60-2. PubMed PMID: 10192644.
209. Phillips VL, Diwan S, Egner A. Development of a tool for assessment and care planning for dementia-related problem behaviors in home and community-based services programs: the Problem Behavior Inventory. *Home health care services quarterly*. 2002;21(1):29-45. doi: 10.1300/J027v21n01_02. PubMed PMID: 12196933.
210. Zeiss AM, Davies HD, Tinklenberg JR. An observational study of sexual behavior in demented male patients. *The journals of gerontology Series A, Biological sciences and medical sciences*. 1996;51(6):M325-9. PubMed PMID: 8914506.
211. Sarazin M, Stern Y, Berr C, Riba A, Albert M, Brandt J, Dubois B. Neuropsychological predictors of dependency in patients with Alzheimer disease. *Neurology*. 2005;64(6):1027-31. doi: 10.1212/01.WNL.0000154529.53488.30. PubMed PMID: 15781821.
212. Parakh R, Roy E, Koo E, Black S. Pantomime and imitation of limb gestures in relation to the severity of Alzheimer's disease. *Brain and cognition*. 2004;55(2):272-4. doi: 10.1016/j.bandc.2004.02.049. PubMed PMID: 15177793.
213. Kato M, Meguro K, Sato M, Shimada Y, Yamazaki H, Saito H, Yamaguchi S, Yamadori A. Ideomotor apraxia in patients with Alzheimer disease: why do they use their body parts as objects? *Neuropsychiatry, neuropsychology, and behavioral neurology*. 2001;14(1):45-52. PubMed PMID: 11234908.
214. Giannakopoulos P, Duc M, Gold G, Hof PR, Michel JP, Bouras C. Pathologic correlates of apraxia in Alzheimer disease. *Archives of neurology*. 1998;55(5):689-95. PubMed PMID: 9605726.
215. Hauser WA, Morris ML, Heston LL, Anderson VE. Seizures and myoclonus in patients with Alzheimer's disease. *Neurology*. 1986;36(9):1226-30. PubMed PMID: 3092131.
216. McAreavey MJ, Ballinger BR, Fenton GW. Epileptic seizures in elderly patients with dementia. *Epilepsia*. 1992;33(4):657-60. PubMed PMID: 1628580.
217. Romanelli MF, Morris JC, Ashkin K, Coben LA. Advanced Alzheimer's disease is a risk factor for late-onset seizures. *Archives of neurology*. 1990;47(8):847-50. PubMed PMID: 2375689.
218. Scarmeas N, Honig LS, Choi H, Cantero J, Brandt J, Blacker D, Albert M, Amatniek JC, Marder K, Bell K, Hauser WA, Stern Y. Seizures in Alzheimer disease: who, when, and how common? *Archives of neurology*. 2009;66(8):992-7. doi: 10.1001/archneurol.2009.130. PubMed PMID: 19667221; PubMed Central PMCID: PMC2768279.
219. Irizarry MC, Jin S, He F, Emond JA, Raman R, Thomas RG, Sano M, Quinn JF, Tariot PN, Galasko DR, Ishihara LS, Weil JG, Aisen PS. Incidence of new-onset seizures in mild to moderate Alzheimer disease. *Archives of neurology*. 2012;69(3):368-72. doi: 10.1001/archneurol.2011.830. PubMed PMID: 22410444; PubMed Central PMCID: PMC3622046.
220. McKhann G, Drachman D, Folstein M, Katzman R, Price D, Stadlan EM. Clinical diagnosis of Alzheimer's disease: report of the NINCDS-ADRDA Work Group under the auspices of Department of Health and Human Services Task Force on Alzheimer's Disease. *Neurology*. 1984;34(7):939-44. PubMed PMID: 6610841.
221. Galton CJ, Patterson K, Xuereb JH, Hodges JR. Atypical and typical presentations of Alzheimer's disease: a clinical, neuropsychological, neuroimaging and pathological study of 13 cases. *Brain : a journal of neurology*. 2000;123 Pt 3:484-98. PubMed PMID: 10686172.
222. Ross SJ, Graham N, Stuart-Green L, Prins M, Xuereb J, Patterson K, Hodges JR. Progressive biparietal atrophy: an atypical presentation of Alzheimer's disease. *Journal of neurology, neurosurgery, and psychiatry*. 1996;61(4):388-95. PubMed PMID: 8890778; PubMed Central PMCID: PMC486580.

223. Bokde AL, Pietrini P, Ibanez V, Furey ML, Alexander GE, Graff-Radford NR, Rapoport SI, Schapiro MB, Horwitz B. The effect of brain atrophy on cerebral hypometabolism in the visual variant of Alzheimer disease. *Archives of neurology*. 2001;58(3):480-6. PubMed PMID: 11255453.
224. Renner JA, Burns JM, Hou CE, McKeel DW, Jr., Storandt M, Morris JC. Progressive posterior cortical dysfunction: a clinicopathologic series. *Neurology*. 2004;63(7):1175-80. PubMed PMID: 15477534.
225. Andrade K, Kas A, Valabregue R, Samri D, Sarazin M, Habert MO, Dubois B, Bartolomeo P. Visuospatial deficits in posterior cortical atrophy: structural and functional correlates. *Journal of neurology, neurosurgery, and psychiatry*. 2012;83(9):860-3. doi: 10.1136/jnnp-2012-302278. PubMed PMID: 22645257.
226. Andrade K, Kas A, Samri D, Sarazin M, Dubois B, Habert MO, Bartolomeo P. Visuospatial deficits and hemispheric perfusion asymmetries in posterior cortical atrophy. *Cortex; a journal devoted to the study of the nervous system and behavior*. 2013;49(4):940-7. doi: 10.1016/j.cortex.2012.03.010. PubMed PMID: 22513341.
227. Crutch SJ, Lehmann M, Schott JM, Rabinovici GD, Rossor MN, Fox NC. Posterior cortical atrophy. *The Lancet Neurology*. 2012;11(2):170-8. doi: 10.1016/S1474-4422(11)70289-7. PubMed PMID: 22265212; PubMed Central PMCID: PMC3740271.
228. Levine DN, Lee JM, Fisher CM. The visual variant of Alzheimer's disease: a clinicopathologic case study. *Neurology*. 1993;43(2):305-13. PubMed PMID: 8437694.
229. Migliaccio R, Agosta F, Rascovsky K, Karydas A, Bonasera S, Rabinovici GD, Miller BL, Gorno-Tempini ML. Clinical syndromes associated with posterior atrophy: early age at onset AD spectrum. *Neurology*. 2009;73(19):1571-8. doi: 10.1212/WNL.0b013e3181c0d427. PubMed PMID: 19901249; PubMed Central PMCID: PMC2777069.
230. Tang-Wai DF, Graff-Radford NR, Boeve BF, Dickson DW, Parisi JE, Crook R, Caselli RJ, Knopman DS, Petersen RC. Clinical, genetic, and neuropathologic characteristics of posterior cortical atrophy. *Neurology*. 2004;63(7):1168-74. PubMed PMID: 15477533.
231. Hof PR, Bouras C, Constantinidis J, Morrison JH. Selective disconnection of specific visual association pathways in cases of Alzheimer's disease presenting with Balint's syndrome. *Journal of neuropathology and experimental neurology*. 1990;49(2):168-84. PubMed PMID: 2307982.
232. Cogan DG. Visual disturbances with focal progressive dementing disease. *American journal of ophthalmology*. 1985;100(1):68-72. PubMed PMID: 3893141.
233. Dickerson BC, Wolk DA, Alzheimer's Disease Neuroimaging I. Dysexecutive versus amnesic phenotypes of very mild Alzheimer's disease are associated with distinct clinical, genetic and cortical thinning characteristics. *Journal of neurology, neurosurgery, and psychiatry*. 2011;82(1):45-51. doi: 10.1136/jnnp.2009.199505. PubMed PMID: 20562467; PubMed Central PMCID: PMC3023235.
234. Blennerhassett R, Lillo P, Halliday GM, Hodges JR, Kril JJ. Distribution of pathology in frontal variant Alzheimer's disease. *Journal of Alzheimer's disease : JAD*. 2014;39(1):63-70. doi: 10.3233/JAD-131241. PubMed PMID: 24121962.
235. Neuropathology Group. Medical Research Council Cognitive F, Aging S. Pathological correlates of late-onset dementia in a multicentre, community-based population in England and Wales. *Neuropathology Group of the Medical Research Council Cognitive Function and Ageing Study (MRC CFAS)*. *Lancet*. 2001;357(9251):169-75. PubMed PMID: 11213093.
236. Kalaria RN, Ballard C. Overlap between pathology of Alzheimer disease and vascular dementia. *Alzheimer disease and associated disorders*. 1999;13 Suppl 3:S115-23. PubMed PMID: 10609690.
237. Staekenborg SS, van der Flier WM, van Straaten EC, Lane R, Barkhof F, Scheltens P. Neurological signs in relation to type of cerebrovascular disease in vascular dementia. *Stroke; a journal of cerebral circulation*. 2008;39(2):317-22. doi: 10.1161/STROKEAHA.107.493353. PubMed PMID: 18096841.
238. Staekenborg SS, Su T, van Straaten EC, Lane R, Scheltens P, Barkhof F, van der Flier WM. Behavioural and psychological symptoms in vascular dementia; differences between small- and large-vessel disease. *Journal of neurology, neurosurgery, and psychiatry*. 2010;81(5):547-51. doi: 10.1136/jnnp.2009.187500. PubMed PMID: 19965852.
239. Jokinen H, Kalska H, Mantyla R, Pohjasvaara T, Ylikoski R, Hietanen M, Salonen O, Kaste M, Erkinjuntti T. Cognitive profile of subcortical ischaemic vascular disease. *Journal of neurology, neurosurgery, and psychiatry*. 2006;77(1):28-33. doi: 10.1136/jnnp.2005.069120. PubMed PMID: 16361588; PubMed Central PMCID: PMC2117424.

240. Mesulam M, Wicklund A, Johnson N, Rogalski E, Leger GC, Rademaker A, Weintraub S, Bigio EH. Alzheimer and frontotemporal pathology in subsets of primary progressive aphasia. *Annals of neurology*. 2008;63(6):709-19. doi: 10.1002/ana.21388. PubMed PMID: 18412267; PubMed Central PMCID: PMC2858311.
241. Knibb JA, Xuereb JH, Patterson K, Hodges JR. Clinical and pathological characterization of progressive aphasia. *Annals of neurology*. 2006;59(1):156-65. doi: 10.1002/ana.20700. PubMed PMID: 16374817.
242. Josephs KA, Whitwell JL, Duffy JR, Vanvoorst WA, Strand EA, Hu WT, Boeve BF, Graff-Radford NR, Parisi JE, Knopman DS, Dickson DW, Jack CR, Jr., Petersen RC. Progressive aphasia secondary to Alzheimer disease vs FTL D pathology. *Neurology*. 2008;70(1):25-34. doi: 10.1212/01.wnl.0000287073.12737.35. PubMed PMID: 18166704; PubMed Central PMCID: PMC2749307.
243. Alladi S, Xuereb J, Bak T, Nestor P, Knibb J, Patterson K, Hodges JR. Focal cortical presentations of Alzheimer's disease. *Brain : a journal of neurology*. 2007;130(Pt 10):2636-45. doi: 10.1093/brain/awm213. PubMed PMID: 17898010.
244. Hu WT, McMillan C, Libon D, Leight S, Forman M, Lee VM, Trojanowski JQ, Grossman M. Multimodal predictors for Alzheimer disease in nonfluent primary progressive aphasia. *Neurology*. 2010;75(7):595-602. doi: 10.1212/WNL.0b013e3181ed9c52. PubMed PMID: 20713948; PubMed Central PMCID: PMC2931765.
245. Deramecourt V, Lebert F, Debachy B, Mackowiak-Cordoliani MA, Bombois S, Kerdraon O, Buee L, Mauraige CA, Pasquier F. Prediction of pathology in primary progressive language and speech disorders. *Neurology*. 2010;74(1):42-9. doi: 10.1212/WNL.0b013e3181c7198e. PubMed PMID: 19940270.
246. Rabinovici GD, Jagust WJ, Furst AJ, Ogar JM, Racine CA, Mormino EC, O'Neil JP, Lal RA, Dronkers NF, Miller BL, Gorno-Tempini ML. Abeta amyloid and glucose metabolism in three variants of primary progressive aphasia. *Annals of neurology*. 2008;64(4):388-401. doi: 10.1002/ana.21451. PubMed PMID: 18991338; PubMed Central PMCID: PMC2648510.
247. Galasko D, Hansen LA, Katzman R, Wiederholt W, Masliah E, Terry R, Hill LR, Lessin P, Thal LJ. Clinical-neuropathological correlations in Alzheimer's disease and related dementias. *Archives of neurology*. 1994;51(9):888-95. PubMed PMID: 8080388.
248. Hyman BT, Trojanowski JQ. Consensus recommendations for the postmortem diagnosis of Alzheimer disease from the National Institute on Aging and the Reagan Institute Working Group on diagnostic criteria for the neuropathological assessment of Alzheimer disease. *Journal of neuropathology and experimental neurology*. 1997;56(10):1095-7. PubMed PMID: 9329452.
249. Knopman DS, DeKosky ST, Cummings JL, Chui H, Corey-Bloom J, Relkin N, Small GW, Miller B, Stevens JC. Practice parameter: diagnosis of dementia (an evidence-based review). Report of the Quality Standards Subcommittee of the American Academy of Neurology. *Neurology*. 2001;56(9):1143-53. PubMed PMID: 11342678.
250. Hebert LE, Beckett LA, Scherr PA, Evans DA. Annual incidence of Alzheimer disease in the United States projected to the years 2000 through 2050. *Alzheimer disease and associated disorders*. 2001;15(4):169-73. PubMed PMID: 11723367.
251. Villemagne VL, Burnham S, Bourgeat P, Brown B, Ellis KA, Salvado O, Szoek C, Macaulay SL, Martins R, Maruff P, Ames D, Rowe CC, Masters CL, Australian Imaging B, Lifestyle Research G. Amyloid beta deposition, neurodegeneration, and cognitive decline in sporadic Alzheimer's disease: a prospective cohort study. *The Lancet Neurology*. 2013;12(4):357-67. doi: 10.1016/S1474-4422(13)70044-9. PubMed PMID: 23477989.
252. Reiman EM, Quiroz YT, Fleisher AS, Chen K, Velez-Pardo C, Jimenez-Del-Rio M, Fagan AM, Shah AR, Alvarez S, Arbelaez A, Giraldo M, Acosta-Baena N, Sperling RA, Dickerson B, Stern CE, Tirado V, Munoz C, Reiman RA, Huentelman MJ, Alexander GE, Langbaum JB, Kosik KS, Tariot PN, Lopera F. Brain imaging and fluid biomarker analysis in young adults at genetic risk for autosomal dominant Alzheimer's disease in the presenilin 1 E280A kindred: a case-control study. *The Lancet Neurology*. 2012;11(12):1048-56. doi: 10.1016/S1474-4422(12)70228-4. PubMed PMID: 23137948; PubMed Central PMCID: PMC4181671.
253. Jack CR, Jr., Lowe VJ, Weigand SD, Wiste HJ, Senjem ML, Knopman DS, Shiung MM, Gunter JL, Boeve BF, Kemp BJ, Weiner M, Petersen RC. Alzheimer's Disease Neuroimaging I. Serial PIB and MRI in normal, mild cognitive impairment and Alzheimer's disease: implications for sequence of pathological events in Alzheimer's disease. *Brain : a journal of neurology*. 2009;132(Pt 5):1355-65. doi: 10.1093/brain/awp062. PubMed PMID: 19339253; PubMed Central PMCID: PMC2677798.

254. Petersen RC, Smith GE, Waring SC, Ivnik RJ, Tangalos EG, Kokmen E. Mild cognitive impairment: clinical characterization and outcome. *Archives of neurology*. 1999;56(3):303-8. PubMed PMID: 10190820.
255. Manly JJ, Tang MX, Schupf N, Stern Y, Vonsattel JP, Mayeux R. Frequency and course of mild cognitive impairment in a multiethnic community. *Annals of neurology*. 2008;63(4):494-506. doi: 10.1002/ana.21326. PubMed PMID: 18300306; PubMed Central PMCID: PMC2375143.
256. McKeith IG, Dickson DW, Lowe J, Emre M, O'Brien JT, Feldman H, Cummings J, Duda JE, Lippa C, Perry EK, Aarsland D, Arai H, Ballard CG, Boeve B, Burn DJ, Costa D, Del Ser T, Dubois B, Galasko D, Gauthier S, Goetz CG, Gomez-Tortosa E, Halliday G, Hansen LA, Hardy J, Iwatsubo T, Kalaria RN, Kaufer D, Kenny RA, Korczyn A, Kosaka K, Lee VM, Lees A, Litvan I, Londos E, Lopez OL, Minoshima S, Mizuno Y, Molina JA, Mukaetova-Ladinska EB, Pasquier F, Perry RH, Schulz JB, Trojanowski JQ, Yamada M, Consortium on DLB. Diagnosis and management of dementia with Lewy bodies: third report of the DLB Consortium. *Neurology*. 2005;65(12):1863-72. doi: 10.1212/01.wnl.0000187889.17253.b1. PubMed PMID: 16237129.
257. Roman GC. Vascular dementia: distinguishing characteristics, treatment, and prevention. *Journal of the American Geriatrics Society*. 2003;51(5 Suppl Dementia):S296-304. doi: 10.1046/j.1532-5415.5155.x. PubMed PMID: 12801386.
258. Roman GC. Vascular dementia revisited: diagnosis, pathogenesis, treatment, and prevention. *The Medical clinics of North America*. 2002;86(3):477-99. PubMed PMID: 12168556.
259. Rascovsky K, Hodges JR, Kipps CM, Johnson JK, Seeley WW, Mendez MF, Knopman D, Kertesz A, Mesulam M, Salmon DP, Galasko D, Chow TW, Decarli C, Hillis A, Josephs K, Kramer JH, Weintraub S, Grossman M, Gorno-Tempini ML, Miller BM. Diagnostic criteria for the behavioral variant of frontotemporal dementia (bvFTD): current limitations and future directions. *Alzheimer disease and associated disorders*. 2007;21(4):S14-8. doi: 10.1097/WAD.0b013e31815c3445. PubMed PMID: 18090417.
260. Gorno-Tempini ML, Hillis AE, Weintraub S, Kertesz A, Mendez M, Cappa SF, Ogar JM, Rohrer JD, Black S, Boeve BF, Manes F, Dronkers NF, Vandenberghe R, Rascovsky K, Patterson K, Miller BL, Knopman DS, Hodges JR, Mesulam MM, Grossman M. Classification of primary progressive aphasia and its variants. *Neurology*. 2011;76(11):1006-14. doi: 10.1212/WNL.0b013e31821103e6. PubMed PMID: 21325651; PubMed Central PMCID: PMC3059138.
261. Dubois B, Feldman HH, Jacova C, Cummings JL, Dekosky ST, Barberger-Gateau P, Delacourte A, Frisoni G, Fox NC, Galasko D, Gauthier S, Hampel H, Jicha GA, Meguro K, O'Brien J, Pasquier F, Robert P, Rossor M, Salloway S, Sarazin M, de Souza LC, Stern Y, Visser PJ, Scheltens P. Revising the definition of Alzheimer's disease: a new lexicon. *The Lancet Neurology*. 2010;9(11):1118-27. doi: 10.1016/S1474-4422(10)70223-4. PubMed PMID: 20934914.
262. Dubois B, Feldman HH, Jacova C, Hampel H, Molinuevo JL, Blennow K, DeKosky ST, Gauthier S, Selkoe D, Bateman R, Cappa S, Crutch S, Engelborghs S, Frisoni GB, Fox NC, Galasko D, Habert MO, Jicha GA, Nordberg A, Pasquier F, Rabinovici G, Robert P, Rowe C, Salloway S, Sarazin M, Epelbaum S, de Souza LC, Vellas B, Visser PJ, Schneider L, Stern Y, Scheltens P, Cummings JL. Advancing research diagnostic criteria for Alzheimer's disease: the IWG-2 criteria. *The Lancet Neurology*. 2014;13(6):614-29. doi: 10.1016/S1474-4422(14)70090-0. PubMed PMID: 24849862.
263. Albert MS, DeKosky ST, Dickson D, Dubois B, Feldman HH, Fox NC, Gamst A, Holtzman DM, Jagust WJ, Petersen RC, Snyder PJ, Carrillo MC, Thies B, Phelps CH. The diagnosis of mild cognitive impairment due to Alzheimer's disease: recommendations from the National Institute on Aging-Alzheimer's Association workgroups on diagnostic guidelines for Alzheimer's disease. *Alzheimer's & dementia : the journal of the Alzheimer's Association*. 2011;7(3):270-9. doi: 10.1016/j.jalz.2011.03.008. PubMed PMID: 21514249; PubMed Central PMCID: PMC3312027.
264. Forsell Y, Fratiglioni L, Grut M, Viitanen M, Winblad B. Clinical staging of dementia in a population survey: comparison of DSM-III-R and the Washington University Clinical Dementia Rating Scale. *Acta psychiatrica Scandinavica*. 1992;86(1):49-54. PubMed PMID: 1414400.
265. Fratiglioni L, Grut M, Forsell Y, Viitanen M, Winblad B. Clinical diagnosis of Alzheimer's disease and other dementias in a population survey. Agreement and causes of disagreement in applying Diagnostic and Statistical Manual of Mental Disorders, Revised Third Edition, Criteria. *Archives of neurology*. 1992;49(9):927-32. PubMed PMID: 1520083.
266. Larson EB, McCurry SM, Graves AB, Bowen JD, Rice MM, McCormick WC, Zee N, Homma A, Imai Y, White L, Masaki K, Petrovitch H, Ross W, Yamada M, Mimori Y, Sasaki H. Standardization of the clinical diagnosis of the dementia syndrome and its subtypes in a cross-national study: the Ni-Hon-Sea experience. *The journals of gerontology Series A, Biological sciences and medical sciences*. 1998;53(4):M313-9. PubMed PMID: 18314572.

267. Graham JE, Rockwood K, Beattie BL, McDowell I, Eastwood R, Gauthier S. Standardization of the diagnosis of dementia in the Canadian Study of Health and Aging. *Neuroepidemiology*. 1996;15(5):246-56. PubMed PMID: 8878077.
268. Canadian study of health and aging: study methods and prevalence of dementia. *CMAJ : Canadian Medical Association journal = journal de l'Association medicale canadienne*. 1994;150(6):899-913. PubMed PMID: 8131123; PubMed Central PMCID: PMC1486712.
269. Jobst KA, Barnetson LP, Shepstone BJ. Accurate prediction of histologically confirmed Alzheimer's disease and the differential diagnosis of dementia: the use of NINCDS-ADRDA and DSM-III-R criteria, SPECT, X-ray CT, and Apo E4 in medial temporal lobe dementias. *Oxford Project to Investigate Memory and Aging. International psychogeriatrics / IPA*. 1998;10(3):271-302. PubMed PMID: 9785148.
270. Kukull WA, Larson EB, Reifler BV, Lampe TH, Yerby MS, Hughes JP. The validity of 3 clinical diagnostic criteria for Alzheimer's disease. *Neurology*. 1990;40(9):1364-9. PubMed PMID: 2392219.
271. Bouwman FH, Verwey NA, Klein M, Kok A, Blankenstein MA, Sluimer JD, Barkhof F, van der Flier WM, Scheltens P. New research criteria for the diagnosis of Alzheimer's disease applied in a memory clinic population. *Dementia and geriatric cognitive disorders*. 2010;30(1):1-7. doi: 10.1159/000315542. PubMed PMID: 20606438.
272. de Jager CA, Honey TE, Birks J, Wilcock GK. Retrospective evaluation of revised criteria for the diagnosis of Alzheimer's disease using a cohort with post-mortem diagnosis. *International journal of geriatric psychiatry*. 2010;25(10):988-97. doi: 10.1002/gps.2448. PubMed PMID: 20217711.
273. Jack CR, Jr., Albert MS, Knopman DS, McKhann GM, Sperling RA, Carrillo MC, Thies B, Phelps CH. Introduction to the recommendations from the National Institute on Aging-Alzheimer's Association workgroups on diagnostic guidelines for Alzheimer's disease. *Alzheimer's & dementia : the journal of the Alzheimer's Association*. 2011;7(3):257-62. doi: 10.1016/j.jalz.2011.03.004. PubMed PMID: 21514247; PubMed Central PMCID: PMC3096735.
274. Harris JM, Thompson JC, Gall C, Richardson AM, Neary D, du Plessis D, Pal P, Mann DM, Snowden JS, Jones M. Do NIA-AA criteria distinguish Alzheimer's disease from frontotemporal dementia? *Alzheimer's & dementia : the journal of the Alzheimer's Association*. 2015;11(2):207-15. doi: 10.1016/j.jalz.2014.04.516. PubMed PMID: 25022535.
275. Jack CR, Jr., Knopman DS, Weigand SD, Wiste HJ, Vemuri P, Lowe V, Kantarci K, Gunter JL, Senjem ML, Ivnik RJ, Roberts RO, Rocca WA, Boeve BF, Petersen RC. An operational approach to National Institute on Aging-Alzheimer's Association criteria for preclinical Alzheimer disease. *Annals of neurology*. 2012;71(6):765-75. doi: 10.1002/ana.22628. PubMed PMID: 22488240; PubMed Central PMCID: PMC3586223.
276. Lowe VJ, Peller PJ, Weigand SD, Montoya Quintero C, Tosakulwong N, Vemuri P, Senjem ML, Jordan L, Jack CR, Jr., Knopman D, Petersen RC. Application of the National Institute on Aging-Alzheimer's Association AD criteria to ADNI. *Neurology*. 2013;80(23):2130-7. doi: 10.1212/WNL.0b013e318295d6cf. PubMed PMID: 23645596; PubMed Central PMCID: PMC3716359.
277. Tay L, Lim WS, Chan M, Ali N, Mahanum S, Chew P, Lim J, Chong MS. New DSM-V Neurocognitive Disorders Criteria and Their Impact on Diagnostic Classifications of Mild Cognitive Impairment and Dementia in a Memory Clinic Setting. *The American journal of geriatric psychiatry : official journal of the American Association for Geriatric Psychiatry*. 2015. doi: 10.1016/j.jagp.2015.01.004. PubMed PMID: 25728011.
278. Altman DG, Gardner MJ, ebrary Inc. *Statistics with confidence confidence intervals and statistical guidelines*. [Great Britain]: BMJ Books; 2000. Available from: <http://site.ebrary.com/lib/vanderbilt/Doc?id=10033071>.
279. Prestia A, Caroli A, van der Flier WM, Ossenkoppele R, Van Berckel B, Barkhof F, Teunissen CE, Wall AE, Carter SF, Scholl M, Choo IH, Nordberg A, Scheltens P, Frisoni GB. Prediction of dementia in MCI patients based on core diagnostic markers for Alzheimer disease. *Neurology*. 2013;80(11):1048-56. doi: 10.1212/WNL.0b013e3182872830. PubMed PMID: 23390179.
280. Prestia A, Caroli A, Wade SK, van der Flier WM, Ossenkoppele R, Van Berckel B, Barkhof F, Teunissen CE, Wall A, Carter SF, Scholl M, Choo IH, Nordberg A, Scheltens P, Frisoni GB. Prediction of AD dementia by biomarkers following the NIA-AA and IWG diagnostic criteria in MCI patients from three European memory clinics. *Alzheimer's & dementia : the journal of the Alzheimer's Association*. 2015. doi: 10.1016/j.jalz.2014.12.001. PubMed PMID: 25646957.
281. Galluzzi S, Geroldi C, Ghidoni R, Paghera B, Amicucci G, Bonetti M, Zanetti O, Cotelli M, Gennarelli M, Frisoni GB, Translational Outpatient Memory Clinic Working G. The new Alzheimer's criteria in a naturalistic series of patients with mild cognitive impairment. *Journal of neurology*. 2010;257(12):2004-14. doi: 10.1007/s00415-010-5650-0. PubMed PMID: 20632026.

282. Galluzzi S, Geroldi C, Amicucci G, Bocchio-Chiavetto L, Bonetti M, Bonvicini C, Cotelli M, Ghidoni R, Paghera B, Zanetti O, Frisoni GB, Translational Outpatient Memory Clinic Working G. Supporting evidence for using biomarkers in the diagnosis of MCI due to AD. *Journal of neurology*. 2013;260(2):640-50. doi: 10.1007/s00415-012-6694-0. PubMed PMID: 23070466.
283. Sperling RA, Aisen PS, Beckett LA, Bennett DA, Craft S, Fagan AM, Iwatsubo T, Jack CR, Jr., Kaye J, Montine TJ, Park DC, Reiman EM, Rowe CC, Siemers E, Stern Y, Yaffe K, Carrillo MC, Thies B, Morrison-Bogorad M, Wagster MV, Phelps CH. Toward defining the preclinical stages of Alzheimer's disease: recommendations from the National Institute on Aging-Alzheimer's Association workgroups on diagnostic guidelines for Alzheimer's disease. *Alzheimer's & dementia : the journal of the Alzheimer's Association*. 2011;7(3):280-92. doi: 10.1016/j.jalz.2011.03.003. PubMed PMID: 21514248; PubMed Central PMCID: PMC3220946.
284. Knopman DS, Jack CR, Jr., Wiste HJ, Weigand SD, Vemuri P, Lowe V, Kantarci K, Gunter JL, Senjem ML, Ivnik RJ, Roberts RO, Boeve BF, Petersen RC. Short-term clinical outcomes for stages of NIA-AA preclinical Alzheimer disease. *Neurology*. 2012;78(20):1576-82. doi: 10.1212/WNL.0b013e3182563bbe. PubMed PMID: 22551733; PubMed Central PMCID: PMC3348848.
285. Vos SJ, Xiong C, Visser PJ, Jaselecz MS, Hassenstab J, Grant EA, Cairns NJ, Morris JC, Holtzman DM, Fagan AM. Preclinical Alzheimer's disease and its outcome: a longitudinal cohort study. *The Lancet Neurology*. 2013;12(10):957-65. doi: 10.1016/S1474-4422(13)70194-7. PubMed PMID: 24012374; PubMed Central PMCID: PMC3904678.
286. Morris JC, Blennow K, Froelich L, Nordberg A, Soininen H, Waldemar G, Wahlund LO, Dubois B. Harmonized diagnostic criteria for Alzheimer's disease: recommendations. *Journal of internal medicine*. 2014;275(3):204-13. doi: 10.1111/joim.12199. PubMed PMID: 24605805.
287. Sorbi S, Hort J, Erkinjuntti T, Fladby T, Gainotti G, Gurvit H, Nacmias B, Pasquier F, Popescu BO, Rektorova I, Religa D, Rusina R, Rossor M, Schmidt R, Stefanova E, Warren JD, Scheltens P, Dementia ESPo, Cognitive N. EFNS-ENS Guidelines on the diagnosis and management of disorders associated with dementia. *European journal of neurology : the official journal of the European Federation of Neurological Societies*. 2012;19(9):1159-79. doi: 10.1111/j.1468-1331.2012.03784.x. PubMed PMID: 22891773.
288. Chertkow H, Feldman HH, Jacova C, Massoud F. Definitions of dementia and predementia states in Alzheimer's disease and vascular cognitive impairment: consensus from the Canadian conference on diagnosis of dementia. *Alzheimer's research & therapy*. 2013;5(Suppl 1):S2. doi: 10.1186/alzrt198. PubMed PMID: 24565215; PubMed Central PMCID: PMC3981054.
289. Clarfield AM. The decreasing prevalence of reversible dementias: an updated meta-analysis. *Archives of internal medicine*. 2003;163(18):2219-29. doi: 10.1001/archinte.163.18.2219. PubMed PMID: 14557220.
290. Alzheimer's A. 2014 Alzheimer's disease facts and figures. *Alzheimer's & dementia : the journal of the Alzheimer's Association*. 2014;10(2):e47-92. PubMed PMID: 24818261.
291. Lobo A, Launer LJ, Fratiglioni L, Andersen K, Di Carlo A, Breteler MM, Copeland JR, Dartigues JF, Jagger C, Martinez-Lage J, Soininen H, Hofman A. Prevalence of dementia and major subtypes in Europe: A collaborative study of population-based cohorts. *Neurologic Diseases in the Elderly Research Group. Neurology*. 2000;54(11 Suppl 5):S4-9. PubMed PMID: 10854354.
292. Fratiglioni L, Launer LJ, Andersen K, Breteler MM, Copeland JR, Dartigues JF, Lobo A, Martinez-Lage J, Soininen H, Hofman A. Incidence of dementia and major subtypes in Europe: A collaborative study of population-based cohorts. *Neurologic Diseases in the Elderly Research Group. Neurology*. 2000;54(11 Suppl 5):S10-5. PubMed PMID: 10854355.
293. Wentzel C, Rockwood K, MacKnight C, Hachinski V, Hogan DB, Feldman H, Ostbye T, Wolfson C, Gauthier S, Verreault R, McDowell I. Progression of impairment in patients with vascular cognitive impairment without dementia. *Neurology*. 2001;57(4):714-6. PubMed PMID: 11524488.
294. Hachinski VC, Bowler JV. Vascular dementia. *Neurology*. 1993;43(10):2159-60; author reply 60-1. PubMed PMID: 8414002.
295. Bowler JV, Eliasziw M, Steenhuis R, Munoz DG, Fry R, Merskey H, Hachinski VC. Comparative evolution of Alzheimer disease, vascular dementia, and mixed dementia. *Archives of neurology*. 1997;54(6):697-703. PubMed PMID: 9193204.

296. O'Brien JT. Vascular cognitive impairment. *The American journal of geriatric psychiatry : official journal of the American Association for Geriatric Psychiatry*. 2006;14(9):724-33. doi: 10.1097/01.JGP.0000231780.44684.7e. PubMed PMID: 16943169.
297. Hebert R, Brayne C. Epidemiology of vascular dementia. *Neuroepidemiology*. 1995;14(5):240-57. PubMed PMID: 7477666.
298. Smith EE, Schneider JA, Wardlaw JM, Greenberg SM. Cerebral microinfarcts: the invisible lesions. *The Lancet Neurology*. 2012;11(3):272-82. doi: 10.1016/S1474-4422(11)70307-6. PubMed PMID: 22341035; PubMed Central PMCID: PMC3359329.
299. Arvanitakis Z, Leurgans SE, Barnes LL, Bennett DA, Schneider JA. Microinfarct pathology, dementia, and cognitive systems. *Stroke; a journal of cerebral circulation*. 2011;42(3):722-7. doi: 10.1161/STROKEAHA.110.595082. PubMed PMID: 21212395; PubMed Central PMCID: PMC3042494.
300. Sacco S, Marini C, Totaro R, Russo T, Cerone D, Carolei A. A population-based study of the incidence and prognosis of lacunar stroke. *Neurology*. 2006;66(9):1335-8. doi: 10.1212/01.wnl.0000210457.89798.0e. PubMed PMID: 16682663.
301. Petty GW, Brown RD, Jr., Whisnant JP, Sicks JD, O'Fallon WM, Wiebers DO. Ischemic stroke subtypes: a population-based study of incidence and risk factors. *Stroke; a journal of cerebral circulation*. 1999;30(12):2513-6. PubMed PMID: 10582970.
302. Chamorro A, Sacco RL, Mohr JP, Foulkes MA, Kase CS, Tatemichi TK, Wolf PA, Price TR, Hier DB. Clinical-computed tomographic correlations of lacunar infarction in the Stroke Data Bank. *Stroke; a journal of cerebral circulation*. 1991;22(2):175-81. PubMed PMID: 2003281.
303. Sonnen JA, Santa Cruz K, Hemmy LS, Woltjer R, Leverenz JB, Montine KS, Jack CR, Kaye J, Lim K, Larson EB, White L, Montine TJ. Ecology of the aging human brain. *Archives of neurology*. 2011;68(8):1049-56. doi: 10.1001/archneurol.2011.157. PubMed PMID: 21825242; PubMed Central PMCID: PMC3218566.
304. Chui H. Vascular dementia, a new beginning: shifting focus from clinical phenotype to ischemic brain injury. *Neurologic clinics*. 2000;18(4):951-78. PubMed PMID: 11072269.
305. Fisher CM. Lacunar strokes and infarcts: a review. *Neurology*. 1982;32(8):871-6. PubMed PMID: 7048128.
306. Lammie GA, Brannan F, Slattery J, Warlow C. Nonhypertensive cerebral small-vessel disease. An autopsy study. *Stroke; a journal of cerebral circulation*. 1997;28(11):2222-9. PubMed PMID: 9368569.
307. Rockwood K, Ebly E, Hachinski V, Hogan D. Presence and treatment of vascular risk factors in patients with vascular cognitive impairment. *Archives of neurology*. 1997;54(1):33-9. PubMed PMID: 9006411.
308. Jick H, Zornberg GL, Jick SS, Seshadri S, Drachman DA. Statins and the risk of dementia. *Lancet*. 2000;356(9242):1627-31. PubMed PMID: 11089820.
309. Lippa CF, Duda JE, Grossman M, Hurtig HI, Aarsland D, Boeve BF, Brooks DJ, Dickson DW, Dubois B, Emre M, Fahn S, Farmer JM, Galasko D, Galvin JE, Goetz CG, Growdon JH, Gwinn-Hardy KA, Hardy J, Heutink P, Iwatsubo T, Kosaka K, Lee VM, Leverenz JB, Masliah E, McKeith IG, Nussbaum RL, Olanow CW, Ravina BM, Singleton AB, Tanner CM, Trojanowski JQ, Wszolek ZK, Group DPW. DLB and PDD boundary issues: diagnosis, treatment, molecular pathology, and biomarkers. *Neurology*. 2007;68(11):812-9. doi: 10.1212/01.wnl.0000256715.13907.d3. PubMed PMID: 17353469.
310. McKeith I. Dementia with Lewy bodies. *Dialogues in clinical neuroscience*. 2004;6(3):333-41. PubMed PMID: 22033743; PubMed Central PMCID: PMC3181810.
311. Alzheimer A, Stelzmann RA, Schnitzlein HN, Murtagh FR. An English translation of Alzheimer's 1907 paper, "Über eine eigenartige Erkrankung der Hirnrinde". *Clinical anatomy*. 1995;8(6):429-31. doi: 10.1002/ca.980080612. PubMed PMID: 8713166.
312. Johnson JK, Diehl J, Mendez MF, Neuhaus J, Shapira JS, Forman M, Chute DJ, Roberson ED, Pace-Savitsky C, Neumann M, Chow TW, Rosen HJ, Forstl H, Kurz A, Miller BL. Frontotemporal lobar degeneration: demographic characteristics of 353 patients. *Archives of neurology*. 2005;62(6):925-30. doi: 10.1001/archneur.62.6.925. PubMed PMID: 15956163.
313. Rosen HJ, Allison SC, Schauer GF, Gorno-Tempini ML, Weiner MW, Miller BL. Neuroanatomical correlates of behavioural disorders in dementia. *Brain : a journal of neurology*. 2005;128(Pt 11):2612-25. doi: 10.1093/brain/awh628. PubMed PMID: 16195246; PubMed Central PMCID: PMC1820861.

314. Rankin KP, Gorno-Tempini ML, Allison SC, Stanley CM, Glenn S, Weiner MW, Miller BL. Structural anatomy of empathy in neurodegenerative disease. *Brain : a journal of neurology*. 2006;129(Pt 11):2945-56. doi: 10.1093/brain/awl254. PubMed PMID: 17008334; PubMed Central PMCID: PMC2562652.
315. Gefen T, Gasho K, Rademaker A, Lalehzari M, Weintraub S, Rogalski E, Wieneke C, Bigio E, Geula C, Mesulam MM. Clinically concordant variations of Alzheimer pathology in aphasic versus amnesic dementia. *Brain : a journal of neurology*. 2012;135(Pt 5):1554-65. doi: 10.1093/brain/aws076. PubMed PMID: 22522938; PubMed Central PMCID: PMC3338929.
316. Roberson ED, Hesse JH, Rose KD, Slama H, Johnson JK, Yaffe K, Forman MS, Miller CA, Trojanowski JQ, Kramer JH, Miller BL. Frontotemporal dementia progresses to death faster than Alzheimer disease. *Neurology*. 2005;65(5):719-25. doi: 10.1212/01.wnl.0000173837.82820.9f. PubMed PMID: 16157905.
317. Haywood AM. Transmissible spongiform encephalopathies. *The New England journal of medicine*. 1997;337(25):1821-8. doi: 10.1056/NEJM199712183372508. PubMed PMID: 9400041.
318. Masters CL, Harris JO, Gajdusek DC, Gibbs CJ, Jr., Bernoulli C, Asher DM. Creutzfeldt-Jakob disease: patterns of worldwide occurrence and the significance of familial and sporadic clustering. *Annals of neurology*. 1979;5(2):177-88. doi: 10.1002/ana.410050212. PubMed PMID: 371520.
319. Ladogana A, Puopolo M, Croes EA, Budka H, Jarius C, Collins S, Klug GM, Sutcliffe T, Giulivi A, Alperovitch A, Delasnerie-Laupretre N, Brandel JP, Poser S, Kretzschmar H, Rietveld I, Mitrova E, Cuesta Jde P, Martinez-Martin P, Glatzel M, Aguzzi A, Knight R, Ward H, Pocchiari M, van Duijn CM, Will RG, Zerr I. Mortality from Creutzfeldt-Jakob disease and related disorders in Europe, Australia, and Canada. *Neurology*. 2005;64(9):1586-91. doi: 10.1212/01.WNL.0000160117.56690.B2. PubMed PMID: 15883321.
320. Tschampa HJ, Neumann M, Zerr I, Henkel K, Schroter A, Schulz-Schaeffer WJ, Steinhoff BJ, Kretzschmar HA, Poser S. Patients with Alzheimer's disease and dementia with Lewy bodies mistaken for Creutzfeldt-Jakob disease. *Journal of neurology, neurosurgery, and psychiatry*. 2001;71(1):33-9. PubMed PMID: 11413259; PubMed Central PMCID: PMC1737446.
321. Johnson DY, Dunkelberger DL, Henry M, Haman A, Greicius MD, Wong K, DeArmond SJ, Miller BL, Gorno-Tempini ML, Geschwind MD. Sporadic Jakob-Creutzfeldt disease presenting as primary progressive aphasia. *JAMA neurology*. 2013;70(2):254-7. doi: 10.1001/2013.jamaneurol.139. PubMed PMID: 23400721; PubMed Central PMCID: PMC4365870.
322. Brown P, Cathala F, Raubertas RF, Gajdusek DC, Castaigne P. The epidemiology of Creutzfeldt-Jakob disease: conclusion of a 15-year investigation in France and review of the world literature. *Neurology*. 1987;37(6):895-904. PubMed PMID: 3295589.
323. Monreal J, Collins GH, Masters CL, Fisher CM, Kim RC, Gibbs CJ, Jr., Gajdusek DC. Creutzfeldt-Jakob disease in an adolescent. *Journal of the neurological sciences*. 1981;52(2-3):341-50. PubMed PMID: 7031189.
324. de Silva R, Findlay C, Awad I, Harries-Jones R, Knight R, Will R. Creutzfeldt-Jakob disease in the elderly. *Postgraduate medical journal*. 1997;73(863):557-9. PubMed PMID: 9373595; PubMed Central PMCID: PMC2431436.
325. Johnson RT, Gonzalez RG, Frosch MP. Case records of the Massachusetts General Hospital. Case 27-2005. An 80-year-old man with fatigue, unsteady gait, and confusion. *The New England journal of medicine*. 2005;353(10):1042-50. doi: 10.1056/NEJMcpc059024. PubMed PMID: 16148290.
326. Heinemann U, Krasnianski A, Meissner B, Varges D, Kallenberg K, Schulz-Schaeffer WJ, Steinhoff BJ, Grasbon-Frodl EM, Kretzschmar HA, Zerr I. Creutzfeldt-Jakob disease in Germany: a prospective 12-year surveillance. *Brain : a journal of neurology*. 2007;130(Pt 5):1350-9. doi: 10.1093/brain/awm063. PubMed PMID: 17472986.
327. Pocchiari M, Puopolo M, Croes EA, Budka H, Gelpi E, Collins S, Lewis V, Sutcliffe T, Guilivi A, Delasnerie-Laupretre N, Brandel JP, Alperovitch A, Zerr I, Poser S, Kretzschmar HA, Ladogana A, Rietveld I, Mitrova E, Martinez-Martin P, de Pedro-Cuesta J, Glatzel M, Aguzzi A, Cooper S, Mackenzie J, van Duijn CM, Will RG. Predictors of survival in sporadic Creutzfeldt-Jakob disease and other human transmissible spongiform encephalopathies. *Brain : a journal of neurology*. 2004;127(Pt 10):2348-59. doi: 10.1093/brain/awh249. PubMed PMID: 15361416.
328. Bech RA, Juhler M, Waldemar G, Klinken L, Gjerris F. Frontal brain and leptomeningeal biopsy specimens correlated with cerebrospinal fluid outflow resistance and B-wave activity in patients suspected of normal-pressure hydrocephalus. *Neurosurgery*. 1997;40(3):497-502. PubMed PMID: 9055288.

329. Bech RA, Waldemar G, Gjerris F, Klinken L, Juhler M. Shunting effects in patients with idiopathic normal pressure hydrocephalus; correlation with cerebral and leptomeningeal biopsy findings. *Acta neurochirurgica*. 1999;141(6):633-9. PubMed PMID: 10929729.
330. Sudarsky L, Ronthal M. Gait disorders among elderly patients. A survey study of 50 patients. *Archives of neurology*. 1983;40(12):740-3. PubMed PMID: 6625987.
331. Temml C, Haidinger G, Schmidbauer J, Schatzl G, Madersbacher S. Urinary incontinence in both sexes: prevalence rates and impact on quality of life and sexual life. *Neurourology and urodynamics*. 2000;19(3):259-71. PubMed PMID: 10797583.
332. Klassen BT, Ahlskog JE. Normal pressure hydrocephalus: how often does the diagnosis hold water? *Neurology*. 2011;77(12):1119-25. doi: 10.1212/WNL.0b013e31822f02f5. PubMed PMID: 21849644; PubMed Central PMCID: PMC3265046.
333. Savolainen S, Paljarvi L, Vapalahti M. Prevalence of Alzheimer's disease in patients investigated for presumed normal pressure hydrocephalus: a clinical and neuropathological study. *Acta neurochirurgica*. 1999;141(8):849-53. PubMed PMID: 10536721.
334. Golomb J, Wisoff J, Miller DC, Boksay I, Kluger A, Weiner H, Salton J, Graves W. Alzheimer's disease comorbidity in normal pressure hydrocephalus: prevalence and shunt response. *Journal of neurology, neurosurgery, and psychiatry*. 2000;68(6):778-81. PubMed PMID: 10811706; PubMed Central PMCID: PMC1736969.
335. Savolainen S, Hurskainen H, Paljarvi L, Alafuzoff I, Vapalahti M. Five-year outcome of normal pressure hydrocephalus with or without a shunt: predictive value of the clinical signs, neuropsychological evaluation and infusion test. *Acta neurochirurgica*. 2002;144(6):515-23; discussion 23. doi: 10.1007/s00701-002-0936-3. PubMed PMID: 12111484.
336. Hamilton R, Patel S, Lee EB, Jackson EM, Lopinto J, Arnold SE, Clark CM, Basil A, Shaw LM, Xie SX, Grady MS, Trojanowski JQ. Lack of shunt response in suspected idiopathic normal pressure hydrocephalus with Alzheimer disease pathology. *Annals of neurology*. 2010;68(4):535-40. doi: 10.1002/ana.22015. PubMed PMID: 20687117; PubMed Central PMCID: PMC2964442.
337. Leinonen V, Koivisto AM, Savolainen S, Rummukainen J, Tamminen JN, Tillgren T, Vainikka S, Pyykko OT, Molsa J, Fraunberg M, Pirttila T, Jaaskelainen JE, Soininen H, Rinne J, Alafuzoff I. Amyloid and tau proteins in cortical brain biopsy and Alzheimer's disease. *Annals of neurology*. 2010;68(4):446-53. doi: 10.1002/ana.22100. PubMed PMID: 20976765.
338. Uttl B, Pilkenton-Taylor C. Letter cancellation performance across the adult life span. *The Clinical neuropsychologist*. 2001;15(4):521-30. doi: 10.1076/clin.15.4.521.1881. PubMed PMID: 11935454.
339. O'Donnell WE, Reynolds DM, De Soto CB. Neuropsychological impairment scale (NIS): initial validation study using trailmaking test (A & B) and WAIS digit symbol (scaled score) in a mixed grouping of psychiatric, neurological, and normal patients. *Journal of clinical psychology*. 1983;39(5):746-8. PubMed PMID: 6630550.
340. Mendez MF CJ. Mental status assessment. In: *Dementia: A Clinical Approach*. Philadelphia: Butterworth Heinemann; 2003.
341. Sprandel HZ. The psychoeducational use and interpretation of the Wechsler adult intelligence scale-revised. 2nd ed. Springfield, Ill., U.S.A.: C.C. Thomas; 1995. ix, 228 p. p.
342. Lezak MD, Lezak MD. *Neuropsychological assessment*. 4th ed. Oxford ; New York: Oxford University Press; 2004. xiv, 1016 p. p.
343. Reitan RM, Wolfson D. *The Halstead-Reitan neuropsychological test battery : theory and clinical interpretation*. Tucson, Ariz.: Neuropsychology Press; 1985. xv, 486 p. p.
344. Heaton RK, Psychological Assessment Resources Inc. *Wisconsin Card Sorting Test manual*. Rev. and expanded. ed. Odessa, Fla. (P.O. Box 998, Odessa 33556): Psychological Assessment Resources; 1993. iv, 230 p. p.
345. Dubois B, Slachevsky A, Litvan I, Pillon B. The FAB: a Frontal Assessment Battery at bedside. *Neurology*. 2000;55(11):1621-6. PubMed PMID: 11113214.
346. Folstein MF, Folstein SE, McHugh PR. "Mini-mental state". A practical method for grading the cognitive state of patients for the clinician. *Journal of psychiatric research*. 1975;12(3):189-98. PubMed PMID: 1202204.
347. Tangalos EG, Smith GE, Ivnik RJ, Petersen RC, Kokmen E, Kurland LT, Offord KP, Parisi JE. The Mini-Mental State Examination in general medical practice: clinical utility and acceptance. *Mayo Clinic proceedings*. 1996;71(9):829-37. doi: 10.1016/S0025-6196(11)63745-2. PubMed PMID: 8790257.

348. Freidl W, Schmidt R, Stronegger WJ, Irmeler A, Reinhart B, Koch M. Mini mental state examination: influence of sociodemographic, environmental and behavioral factors and vascular risk factors. *Journal of clinical epidemiology*. 1996;49(1):73-8. PubMed PMID: 8598514.
349. Crum RM, Anthony JC, Bassett SS, Folstein MF. Population-based norms for the Mini-Mental State Examination by age and educational level. *Jama*. 1993;269(18):2386-91. PubMed PMID: 8479064.
350. Hensel A, Angermeyer MC, Riedel-Heller SG. Measuring cognitive change in older adults: reliable change indices for the Mini-Mental State Examination. *Journal of neurology, neurosurgery, and psychiatry*. 2007;78(12):1298-303. doi: 10.1136/jnnp.2006.109074. PubMed PMID: 17442763; PubMed Central PMCID: PMC2095596.
351. Morris JC, Ernesto C, Schafer K, Coats M, Leon S, Sano M, Thal LJ, Woodbury P. Clinical dementia rating training and reliability in multicenter studies: the Alzheimer's Disease Cooperative Study experience. *Neurology*. 1997;48(6):1508-10. PubMed PMID: 9191756.
352. Schafer KA, Tractenberg RE, Sano M, Mackell JA, Thomas RG, Gamst A, Thal LJ, Morris JC, Alzheimer's Disease Cooperative S. Reliability of monitoring the clinical dementia rating in multicenter clinical trials. *Alzheimer disease and associated disorders*. 2004;18(4):219-22. PubMed PMID: 15592134.
353. Rockwood K, Strang D, MacKnight C, Downer R, Morris JC. Interrater reliability of the Clinical Dementia Rating in a multicenter trial. *Journal of the American Geriatrics Society*. 2000;48(5):558-9. PubMed PMID: 10811551.
354. Miller MD, Solai LK. *Geriatric psychiatry*. Oxford ; New York: Oxford University Press; 2013. xii, 387 p. p.
355. Prince M. BR, Ferri C. . The benefits of early diagnosis and intervention. . King's College London: World Alzheimer Report Institute of Psychiatry 2011.
356. Hebert LE, Weuve J, Scherr PA, Evans DA. Alzheimer disease in the United States (2010-2050) estimated using the 2010 census. *Neurology*. 2013;80(19):1778-83. doi: 10.1212/WNL.0b013e31828726f5. PubMed PMID: 23390181; PubMed Central PMCID: PMC3719424.
357. United Nations DoEaSA, Population Division. *World Population Ageing 2013*. New York: 2013.
358. Terry K. The baby boom becomes the elder boom. *Business and health*. 2002;20(1):10-7. PubMed PMID: 12534110.
359. Ives DG, Samuel P, Psaty BM, Kuller LH. Agreement between nosologist and cardiovascular health study review of deaths: implications of coding differences. *Journal of the American Geriatrics Society*. 2009;57(1):133-9. doi: 10.1111/j.1532-5415.2008.02056.x. PubMed PMID: 19016930; PubMed Central PMCID: PMC2631612.
360. Macera CA, Sun RK, Yeager KK, Brandes DA. Sensitivity and specificity of death certificate diagnoses for dementing illnesses, 1988-1990. *Journal of the American Geriatrics Society*. 1992;40(5):479-81. PubMed PMID: 1634701.
361. Olichney JM, Hofstetter CR, Galasko D, Thal LJ, Katzman R. Death certificate reporting of dementia and mortality in an Alzheimer's disease research center cohort. *Journal of the American Geriatrics Society*. 1995;43(8):890-3. PubMed PMID: 7636097.
362. Burns A, Jacoby R, Luthert P, Levy R. Cause of death in Alzheimer's disease. *Age and ageing*. 1990;19(5):341-4. PubMed PMID: 2251969.
363. Brunnstrom HR, Englund EM. Cause of death in patients with dementia disorders. *European journal of neurology : the official journal of the European Federation of Neurological Societies*. 2009;16(4):488-92. doi: 10.1111/j.1468-1331.2008.02503.x. PubMed PMID: 19170740.
364. World Health Organization. *International statistical classification of diseases and related health problems*. 10th revision, 2nd edition. ed. Geneva: World Health Organization; 2004.
365. Murphy SL, Xu J, Kochanek KD. Deaths: final data for 2010. *National vital statistics reports : from the Centers for Disease Control and Prevention, National Center for Health Statistics, National Vital Statistics System*. 2013;61(4):1-117. PubMed PMID: 24979972.
366. Weuve J, Hebert LE, Scherr PA, Evans DA. Deaths in the United States among persons with Alzheimer's disease (2010-2050). *Alzheimer's & dementia : the journal of the Alzheimer's Association*. 2014;10(2):e40-6. doi: 10.1016/j.jalz.2014.01.004. PubMed PMID: 24698031; PubMed Central PMCID: PMC3976898.
367. Arrighi HM, Neumann PJ, Lieberburg IM, Townsend RJ. Lethality of Alzheimer disease and its impact on nursing home placement. *Alzheimer disease and associated disorders*. 2010;24(1):90-5. doi: 10.1097/WAD.0b013e31819fe7d1. PubMed PMID: 19568155.

368. Murray CJ, Atkinson C, Bhalla K, Birbeck G, Burstein R, Chou D, Dellavalle R, Danaei G, Ezzati M, Fahimi A, Flaxman D, Foreman, Gabriel S, Gakidou E, Kassebaum N, Khatibzadeh S, Lim S, Lipshultz SE, London S, Lopez, MacIntyre MF, Mokdad AH, Moran A, Moran AE, Mozaffarian D, Murphy T, Naghavi M, Pope C, Roberts T, Salomon J, Schwebel DC, Shahrzaz S, Sleet DA, Murray, Abraham J, Ali MK, Atkinson C, Bartels DH, Bhalla K, Birbeck G, Burstein R, Chen H, Criqui MH, Dahodwala, Jarlais, Ding EL, Dorsey ER, Ebel BE, Ezzati M, Fahami, Flaxman S, Flaxman AD, Gonzalez-Medina D, Grant B, Hagan H, Hoffman H, Kassebaum N, Khatibzadeh S, Leasher JL, Lin J, Lipshultz SE, Lozano R, Lu Y, Mallinger L, McDermott MM, Micha R, Miller TR, Mokdad AA, Mokdad AH, Mozaffarian D, Naghavi M, Narayan KM, Omer SB, Pelizzari PM, Phillips D, Ranganathan D, Rivara FP, Roberts T, Sampson U, Sanman E, Sapkota A, Schwebel DC, Sharaz S, Shivakoti R, Singh GM, Singh D, Tavakkoli M, Towbin JA, Wilkinson JD, Zabetian A, Murray, Abraham J, Ali MK, Alvarado M, Atkinson C, Baddour LM, Benjamin EJ, Bhalla K, Birbeck G, Bolliger I, Burstein R, Carnahan E, Chou D, Chugh SS, Cohen A, Colson KE, Cooper LT, Couser W, Criqui MH, Dabhadkar KC, Dellavalle RP, Jarlais, Dicker D, Dorsey ER, Duber H, Ebel BE, Engell RE, Ezzati M, Felson DT, Finucane MM, Flaxman S, Flaxman AD, Fleming T, Foreman, Forouzanfar MH, Freedman G, Freeman MK, Gakidou E, Gillum RF, Gonzalez-Medina D, Gosselin R, Gutierrez HR, Hagan H, Havmoeller R, Hoffman H, Jacobsen KH, James SL, Jasrasaria R, Jayarman S, Johns N, Kassebaum N, Khatibzadeh S, Lan Q, Leasher JL, Lim S, Lipshultz SE, London S, Lopez, Lozano R, Lu Y, Mallinger L, Meltzer M, Mensah GA, Michaud C, Miller TR, Mock C, Moffitt TE, Mokdad AA, Mokdad AH, Moran A, Naghavi M, Narayan KM, Nelson RG, Olives C, Omer SB, Ortblad K, Ostro B, Pelizzari PM, Phillips D, Raju M, Razavi H, Ritz B, Roberts T, Sacco RL, Salomon J, Sampson U, Schwebel DC, Shahrzaz S, Shibuya K, Silberberg D, Singh JA, Steenland K, Taylor JA, Thurston GD, Vavilala MS, Vos T, Wagner GR, Weinstock MA, Weisskopf MG, Wulf S, Murray, Collaborators USBoD. The state of US health, 1990-2010: burden of diseases, injuries, and risk factors. *Jama*. 2013;310(6):591-608. doi: 10.1001/jama.2013.13805. PubMed PMID: 23842577.
369. Brody EM. "Women in the middle" and family help to older people. *The Gerontologist*. 1981;21(5):471-80. PubMed PMID: 7338304.
370. Hurd MD, Martorell P, Langa KM. Monetary costs of dementia in the United States. *The New England journal of medicine*. 2013;369(5):489-90. doi: 10.1056/NEJMc1305541. PubMed PMID: 23902508.
371. Schulz R, Mendelsohn AB, Haley WE, Mahoney D, Allen RS, Zhang S, Thompson L, Belle SH, Resources for Enhancing Alzheimer's Caregiver Health I. End-of-life care and the effects of bereavement on family caregivers of persons with dementia. *The New England journal of medicine*. 2003;349(20):1936-42. doi: 10.1056/NEJMs035373. PubMed PMID: 14614169.
372. Abdollahpour I, Nedjat S, Noroozian M, Salimi Y, Majdzadeh R. Caregiver burden: the strongest predictor of self-rated health in caregivers of patients with dementia. *Journal of geriatric psychiatry and neurology*. 2014;27(3):172-80. doi: 10.1177/0891988714524627. PubMed PMID: 24614200.
373. Marziali E, Shulman K, Damianakis T. Persistent family concerns in long-term care settings: meaning and management. *Journal of the American Medical Directors Association*. 2006;7(3):154-62. doi: 10.1016/j.jamda.2005.07.007. PubMed PMID: 16503308.
374. Alzheimer's Association Expert Advisory Workgroup on N. Changing the Trajectory of Alzheimer's Disease: How a Treatment by 2025 Saves Lives and Dollars. 2015.
375. Brauner DJ, Muir JC, Sachs GA. Treating nondementia illnesses in patients with dementia. *Jama*. 2000;283(24):3230-5. PubMed PMID: 10866871.
376. Karlawish JH, Casarett DJ, James BD, Xie SX, Kim SY. The ability of persons with Alzheimer disease (AD) to make a decision about taking an AD treatment. *Neurology*. 2005;64(9):1514-9. doi: 10.1212/01.WNL.0000160000.01742.9D. PubMed PMID: 15883310.
377. Pruchno RA, Smyer MA, Rose MS, Hartman-Stein PE, Henderson-Larabee DL. Competence of long-term care residents to participate in decisions about their medical care: a brief, objective assessment. *The Gerontologist*. 1995;35(5):622-9. PubMed PMID: 8543219.
378. Morrison RS, Siu AL. Survival in end-stage dementia following acute illness. *Jama*. 2000;284(1):47-52. PubMed PMID: 10872012.
379. Jones CK, Byun N, Bubser M. Muscarinic and nicotinic acetylcholine receptor agonists and allosteric modulators for the treatment of schizophrenia. *Neuropsychopharmacology : official publication of the American College of Neuropsychopharmacology*. 2012;37(1):16-42. doi: 10.1038/npp.2011.199. PubMed PMID: 21956443; PubMed Central PMCID: PMC3238081.

380. Bartus RT, Dean RL, 3rd, Beer B, Lippa AS. The cholinergic hypothesis of geriatric memory dysfunction. *Science*. 1982;217(4558):408-14. PubMed PMID: 7046051.
381. Mesulam MM, Mufson EJ, Levey AI, Wainer BH. Cholinergic innervation of cortex by the basal forebrain: cytochemistry and cortical connections of the septal area, diagonal band nuclei, nucleus basalis (substantia innominata), and hypothalamus in the rhesus monkey. *The Journal of comparative neurology*. 1983;214(2):170-97. doi: 10.1002/cne.902140206. PubMed PMID: 6841683.
382. Everitt BJ, Robbins TW. Central cholinergic systems and cognition. *Annual review of psychology*. 1997;48:649-84. doi: 10.1146/annurev.psych.48.1.649. PubMed PMID: 9046571.
383. Cole AE, Nicoll RA. The pharmacology of cholinergic excitatory responses in hippocampal pyramidal cells. *Brain research*. 1984;305(2):283-90. PubMed PMID: 6331600.
384. Madison DV, Nicoll RA. Control of the repetitive discharge of rat CA 1 pyramidal neurones in vitro. *The Journal of physiology*. 1984;354:319-31. PubMed PMID: 6434729; PubMed Central PMCID: PMC1193414.
385. Gil Z, Connors BW, Amitai Y. Differential regulation of neocortical synapses by neuromodulators and activity. *Neuron*. 1997;19(3):679-86. PubMed PMID: 9331357.
386. Hasselmo ME. Neuromodulation: acetylcholine and memory consolidation. *Trends in cognitive sciences*. 1999;3(9):351-9. PubMed PMID: 10461198.
387. Hasselmo ME, Bower JM. Acetylcholine and memory. *Trends in neurosciences*. 1993;16(6):218-22. PubMed PMID: 7688162.
388. Dasari S, Gullledge AT. M1 and M4 receptors modulate hippocampal pyramidal neurons. *Journal of neurophysiology*. 2011;105(2):779-92. doi: 10.1152/jn.00686.2010. PubMed PMID: 21160001; PubMed Central PMCID: PMC3059175.
389. Mrzljak L, Levey AI, Goldman-Rakic PS. Association of m1 and m2 muscarinic receptor proteins with asymmetric synapses in the primate cerebral cortex: morphological evidence for cholinergic modulation of excitatory neurotransmission. *Proceedings of the National Academy of Sciences of the United States of America*. 1993;90(11):5194-8. PubMed PMID: 8389473; PubMed Central PMCID: PMC46682.
390. Shirey JK, Xiang Z, Orton D, Brady AE, Johnson KA, Williams R, Ayala JE, Rodriguez AL, Wess J, Weaver D, Niswender CM, Conn PJ. An allosteric potentiator of M4 mAChR modulates hippocampal synaptic transmission. *Nature chemical biology*. 2008;4(1):42-50. doi: 10.1038/nchembio.2007.55. PubMed PMID: 18059262.
391. Albuquerque EX, Pereira EF, Alkondon M, Rogers SW. Mammalian nicotinic acetylcholine receptors: from structure to function. *Physiological reviews*. 2009;89(1):73-120. doi: 10.1152/physrev.00015.2008. PubMed PMID: 19126755; PubMed Central PMCID: PMC2713585.
392. Miwa JM, Freedman R, Lester HA. Neural systems governed by nicotinic acetylcholine receptors: emerging hypotheses. *Neuron*. 2011;70(1):20-33. doi: 10.1016/j.neuron.2011.03.014. PubMed PMID: 21482353.
393. Alkondon M, Pereira EF, Eisenberg HM, Albuquerque EX. Choline and selective antagonists identify two subtypes of nicotinic acetylcholine receptors that modulate GABA release from CA1 interneurons in rat hippocampal slices. *The Journal of neuroscience : the official journal of the Society for Neuroscience*. 1999;19(7):2693-705. PubMed PMID: 10087082.
394. Mike A, Pereira EF, Albuquerque EX. Ca(2+)-sensitive inhibition by Pb(2+) of alpha7-containing nicotinic acetylcholine receptors in hippocampal neurons. *Brain research*. 2000;873(1):112-23. PubMed PMID: 10915816.
395. Xu J, Zhu Y, Heinemann SF. Identification of sequence motifs that target neuronal nicotinic receptors to dendrites and axons. *The Journal of neuroscience : the official journal of the Society for Neuroscience*. 2006;26(38):9780-93. doi: 10.1523/JNEUROSCI.0840-06.2006. PubMed PMID: 16988049.
396. Gray R, Rajan AS, Radcliffe KA, Yakehiro M, Dani JA. Hippocampal synaptic transmission enhanced by low concentrations of nicotine. *Nature*. 1996;383(6602):713-6. doi: 10.1038/383713a0. PubMed PMID: 8878480.
397. Tupin JP, Shader RI, Harnett DS. *Handbook of clinical psychopharmacology*. 2nd ed. Northvale, N.J.: Aronson; 1988. x, 486 p. p.
398. Aigner TG, Mishkin M. The effects of physostigmine and scopolamine on recognition memory in monkeys. *Behavioral and neural biology*. 1986;45(1):81-7. PubMed PMID: 3954717.
399. Deutsch JA. The cholinergic synapse and the site of memory. *Science*. 1971;174(4011):788-94. PubMed PMID: 4330469.

400. Gaffan D, Murray EA. Monkeys (*Macaca fascicularis*) with rhinal cortex ablations succeed in object discrimination learning despite 24-hr intertrial intervals and fail at matching to sample despite double sample presentations. *Behavioral neuroscience*. 1992;106(1):30-8. PubMed PMID: 1554436.
401. Zola-Morgan S, Squire LR. Neuroanatomy of memory. *Annual review of neuroscience*. 1993;16:547-63. doi: 10.1146/annurev.ne.16.030193.002555. PubMed PMID: 8460903.
402. Preston GC, Brazell C, Ward C, Broks P, Traub M, Stahl SM. The scopolamine model of dementia: determination of central cholinomimetic effects of physostigmine on cognition and biochemical markers in man. *Journal of psychopharmacology*. 1988;2(2):67-79. doi: 10.1177/026988118800200202. PubMed PMID: 22155841.
403. Newman EL, Gupta K, Climer JR, Monaghan CK, Hasselmo ME. Cholinergic modulation of cognitive processing: insights drawn from computational models. *Frontiers in behavioral neuroscience*. 2012;6:24. doi: 10.3389/fnbeh.2012.00024. PubMed PMID: 22707936; PubMed Central PMCID: PMC3374475.
404. Mansvelder HD, van Aerde KI, Couey JJ, Brussaard AB. Nicotinic modulation of neuronal networks: from receptors to cognition. *Psychopharmacology*. 2006;184(3-4):292-305. doi: 10.1007/s00213-005-0070-z. PubMed PMID: 16001117.
405. Ernst M, Heishman SJ, Spurgeon L, London ED. Smoking history and nicotine effects on cognitive performance. *Neuropsychopharmacology : official publication of the American College of Neuropsychopharmacology*. 2001;25(3):313-9. doi: 10.1016/S0893-133X(01)00257-3. PubMed PMID: 11522460.
406. McGaughy J, Kaiser T, Sarter M. Behavioral vigilance following infusions of 192 IgG-saporin into the basal forebrain: selectivity of the behavioral impairment and relation to cortical AChE-positive fiber density. *Behavioral neuroscience*. 1996;110(2):247-65. PubMed PMID: 8731052.
407. Hasselmo ME, Stern CE. Mechanisms underlying working memory for novel information. *Trends in cognitive sciences*. 2006;10(11):487-93. doi: 10.1016/j.tics.2006.09.005. PubMed PMID: 17015030; PubMed Central PMCID: PMC2253490.
408. Hasselmo ME, Giocomo LM. Cholinergic modulation of cortical function. *Journal of molecular neuroscience : MN*. 2006;30(1-2):133-5. doi: 10.1385/JMN:30:1:133. PubMed PMID: 17192659.
409. Kroker KS, Rast G, Rosenbrock H. Differential effects of subtype-specific nicotinic acetylcholine receptor agonists on early and late hippocampal LTP. *European journal of pharmacology*. 2011;671(1-3):26-32. doi: 10.1016/j.ejphar.2011.09.167. PubMed PMID: 21968142.
410. Kahana MJ, Caplan JB, Sekuler R, Madsen JR. Using intracranial recordings to study theta response to J. O'Keefe and N. Burgess (1999). *Trends in cognitive sciences*. 1999;3(11):406-7. PubMed PMID: 10529793.
411. Caplan JB, Madsen JR, Raghavachari S, Kahana MJ. Distinct patterns of brain oscillations underlie two basic parameters of human maze learning. *Journal of neurophysiology*. 2001;86(1):368-80. PubMed PMID: 11431517.
412. Sederberg PB, Kahana MJ, Howard MW, Donner EJ, Madsen JR. Theta and gamma oscillations during encoding predict subsequent recall. *The Journal of neuroscience : the official journal of the Society for Neuroscience*. 2003;23(34):10809-14. PubMed PMID: 14645473.
413. Huerta PT, Lisman JE. Bidirectional synaptic plasticity induced by a single burst during cholinergic theta oscillation in CA1 in vitro. *Neuron*. 1995;15(5):1053-63. PubMed PMID: 7576649.
414. Steffenach HA, Witter M, Moser MB, Moser EI. Spatial memory in the rat requires the dorsolateral band of the entorhinal cortex. *Neuron*. 2005;45(2):301-13. doi: 10.1016/j.neuron.2004.12.044. PubMed PMID: 15664181.
415. Hafting T, Fyhn M, Molden S, Moser MB, Moser EI. Microstructure of a spatial map in the entorhinal cortex. *Nature*. 2005;436(7052):801-6. doi: 10.1038/nature03721. PubMed PMID: 15965463.
416. Brandon MP, Bogaard AR, Libby CP, Connerney MA, Gupta K, Hasselmo ME. Reduction of theta rhythm dissociates grid cell spatial periodicity from directional tuning. *Science*. 2011;332(6029):595-9. doi: 10.1126/science.1201652. PubMed PMID: 21527714; PubMed Central PMCID: PMC3252766.
417. Frotscher M, Soriano E, Leranth C. Cholinergic and GABAergic neurotransmission in the fascia dentata: electron microscopic immunocytochemical studies in rodents and primates. *Epilepsy research Supplement*. 1992;7:65-78. PubMed PMID: 1334670.
418. Toth E, Vizi ES, Lajtha A. Effect of nicotine on levels of extracellular amino acids in regions of the rat brain in vivo. *Neuropharmacology*. 1993;32(8):827-32. PubMed PMID: 8105411.

419. Murray CL, Fibiger HC. Learning and memory deficits after lesions of the nucleus basalis magnocellularis: reversal by physostigmine. *Neuroscience*. 1985;14(4):1025-32. PubMed PMID: 4000475.
420. Robbins TW, Everitt BJ, Marston HM, Wilkinson J, Jones GH, Page KJ. Comparative effects of ibotenic acid- and quisqualic acid-induced lesions of the substantia innominata on attentional function in the rat: further implications for the role of the cholinergic neurons of the nucleus basalis in cognitive processes. *Behavioural brain research*. 1989;35(3):221-40. PubMed PMID: 2688683.
421. Nordberg A. *Nicotinic receptors in the CNS : their role in synaptic transmission*. Amsterdam ; New York New York, NY, USA: Elsevier ;
- Sole distributors for the USA and Canada, Elsevier Science Pub. Co.; 1989. xiv, 366 p. p.
422. Rotter A, Birdsall NJ, Field PM, Raisman G. Muscarinic receptors in the central nervous system of the rat. II. Distribution of binding of [3H]propylbenzilylcholine mustard in the midbrain and hindbrain. *Brain research*. 1979;180(2):167-83. PubMed PMID: 519515.
423. Rotter A, Birdsall NJ, Burgen AS, Field PM, Hulme EC, Raisman G. Muscarinic receptors in the central nervous system of the rat. I. Technique for autoradiographic localization of the binding of [3H]propylbenzilylcholine mustard and its distribution in the forebrain. *Brain research*. 1979;180(2):141-65. PubMed PMID: 519514.
424. Bowen DM, Smith CB, White P, Davison AN. Neurotransmitter-related enzymes and indices of hypoxia in senile dementia and other abiotrophies. *Brain : a journal of neurology*. 1976;99(3):459-96. PubMed PMID: 11871.
425. Davies P, Maloney AJ. Selective loss of central cholinergic neurons in Alzheimer's disease. *Lancet*. 1976;2(8000):1403. PubMed PMID: 63862.
426. Perry EK, Perry RH, Blessed G, Tomlinson BE. Necropsy evidence of central cholinergic deficits in senile dementia. *Lancet*. 1977;1(8004):189. PubMed PMID: 64712.
427. Araujo DM, Lapchak PA, Collier B, Quirion R. N-[3H]methylcarbamylocholine binding sites in the rat and human brain: relationship to functional nicotinic autoreceptors and alterations in Alzheimer's disease. *Progress in brain research*. 1989;79:345-52. PubMed PMID: 2685905.
428. Zubenko GS, Moosy J, Martinez AJ, Rao GR, Kopp U, Hanin I. A brain regional analysis of morphologic and cholinergic abnormalities in Alzheimer's disease. *Archives of neurology*. 1989;46(6):634-8. PubMed PMID: 2730375.
429. Henke H, Lang W. Cholinergic enzymes in neocortex, hippocampus and basal forebrain of non-neurological and senile dementia of Alzheimer-type patients. *Brain research*. 1983;267(2):281-91. PubMed PMID: 6871677.
430. Kish SJ, Robitaille Y, el-Awar M, Deck JH, Simmons J, Schut L, Chang LJ, DiStefano L, Freedman M. Non-Alzheimer-type pattern of brain cholineacetyltransferase reduction in dominantly inherited olivopontocerebellar atrophy. *Annals of neurology*. 1989;26(3):362-7. doi: 10.1002/ana.410260309. PubMed PMID: 2802535.
431. Auld DS, Kornecook TJ, Bastianetto S, Quirion R. Alzheimer's disease and the basal forebrain cholinergic system: relations to beta-amyloid peptides, cognition, and treatment strategies. *Progress in neurobiology*. 2002;68(3):209-45. PubMed PMID: 12450488.
432. DeKosky ST, Ikonovic MD, Styren SD, Beckett L, Wisniewski S, Bennett DA, Cochran EJ, Kordower JH, Mufson EJ. Upregulation of choline acetyltransferase activity in hippocampus and frontal cortex of elderly subjects with mild cognitive impairment. *Annals of neurology*. 2002;51(2):145-55. PubMed PMID: 11835370.
433. Tuszynski MH, Thal L, Pay M, Salmon DP, U HS, Bakay R, Patel P, Blesch A, Vahlsing HL, Ho G, Tong G, Potkin SG, Fallon J, Hansen L, Mufson EJ, Kordower JH, Gall C, Conner J. A phase 1 clinical trial of nerve growth factor gene therapy for Alzheimer disease. *Nature medicine*. 2005;11(5):551-5. doi: 10.1038/nm1239. PubMed PMID: 15852017.
434. Eriksson M, Nordberg A, Amberla K, Backman L, Ebendal T, Meyerson B, Olson L, Seiger, Shigeta M, Theodorsson E, Viitanen M, Winblad B, Wahlund LO. Intracerebroventricular infusion of nerve growth factor in three patients with Alzheimer's disease. *Dementia and geriatric cognitive disorders*. 1998;9(5):246-57. PubMed PMID: 9701676.
435. Nagahara AH, Bernot T, Moseanko R, Brignolo L, Blesch A, Conner JM, Ramirez A, Gasmi M, Tuszynski MH. Long-term reversal of cholinergic neuronal decline in aged non-human primates by lentiviral NGF gene delivery. *Experimental neurology*. 2009;215(1):153-9. doi: 10.1016/j.expneurol.2008.10.004. PubMed PMID: 19013154; PubMed Central PMCID: PMC2632603.

436. Contestabile A, Ciani E, Contestabile A. The place of choline acetyltransferase activity measurement in the "cholinergic hypothesis" of neurodegenerative diseases. *Neurochemical research*. 2008;33(2):318-27. doi: 10.1007/s11064-007-9497-4. PubMed PMID: 17940885.
437. Burke SN, Barnes CA. Neural plasticity in the ageing brain. *Nature reviews Neuroscience*. 2006;7(1):30-40. doi: 10.1038/nrn1809. PubMed PMID: 16371948.
438. Coleman M. Axon degeneration mechanisms: commonality amid diversity. *Nature reviews Neuroscience*. 2005;6(11):889-98. doi: 10.1038/nrn1788. PubMed PMID: 16224497.
439. Rapp PR, Gallagher M. Preserved neuron number in the hippocampus of aged rats with spatial learning deficits. *Proceedings of the National Academy of Sciences of the United States of America*. 1996;93(18):9926-30. PubMed PMID: 8790433; PubMed Central PMCID: PMC38531.
440. Honer WG, Prohovnik I, Smith G, Lucas LR. Scopolamine reduces frontal cortex perfusion. *Journal of cerebral blood flow and metabolism : official journal of the International Society of Cerebral Blood Flow and Metabolism*. 1988;8(5):635-41. doi: 10.1038/jcbfm.1988.110. PubMed PMID: 3417793.
441. Hanin I. The AF64A model of cholinergic hypofunction: an update. *Life sciences*. 1996;58(22):1955-64. PubMed PMID: 8637424.
442. Perry EK, Blessed G, Tomlinson BE, Perry RH, Crow TJ, Cross AJ, Dockray GJ, Dimaline R, Arregui A. Neurochemical activities in human temporal lobe related to aging and Alzheimer-type changes. *Neurobiology of aging*. 1981;2(4):251-6. PubMed PMID: 6174877.
443. Mountjoy CQ, Rossor MN, Iversen LL, Roth M. Correlation of cortical cholinergic and GABA deficits with quantitative neuropathological findings in senile dementia. *Brain : a journal of neurology*. 1984;107 (Pt 2):507-18. PubMed PMID: 6722514.
444. Wilcock GK, Esiri MM, Bowen DM, Smith CC. Alzheimer's disease. Correlation of cortical choline acetyltransferase activity with the severity of dementia and histological abnormalities. *Journal of the neurological sciences*. 1982;57(2-3):407-17. PubMed PMID: 7161627.
445. Ransmayr G, Cervera P, Hirsch EC, Berger W, Fischer W, Agid Y. Alzheimer's disease: is the decrease of the cholinergic innervation of the hippocampus related to intrinsic hippocampal pathology? *Neuroscience*. 1992;47(4):843-51. PubMed PMID: 1374541.
446. Etienne P, Dastoor D, Gauthier S, Ludwick R, Collier B. Alzheimer disease: lack of effect of lecithin treatment for 3 months. *Neurology*. 1981;31(12):1552-4. PubMed PMID: 7198209.
447. Thal LJ, Rosen W, Sharpless NS, Crystal H. Choline chloride fails to improve cognition of Alzheimer's disease. *Neurobiology of aging*. 1981;2(3):205-8. PubMed PMID: 7312098.
448. Bodick NC, Offen WW, Levey AI, Cutler NR, Gauthier SG, Satlin A, Shannon HE, Tollefson GD, Rasmussen K, Bymaster FP, Hurley DJ, Potter WZ, Paul SM. Effects of xanomeline, a selective muscarinic receptor agonist, on cognitive function and behavioral symptoms in Alzheimer disease. *Archives of neurology*. 1997;54(4):465-73. PubMed PMID: 9109749.
449. Doody RS, Stevens JC, Beck C, Dubinsky RM, Kaye JA, Gwyther L, Mohs RC, Thal LJ, Whitehouse PJ, DeKosky ST, Cummings JL. Practice parameter: management of dementia (an evidence-based review). Report of the Quality Standards Subcommittee of the American Academy of Neurology. *Neurology*. 2001;56(9):1154-66. PubMed PMID: 11342679.
450. Kadoszkiewicz H, Zimmermann T, Beck-Bornholdt HP, van den Bussche H. Cholinesterase inhibitors for patients with Alzheimer's disease: systematic review of randomised clinical trials. *Bmj*. 2005;331(7512):321-7. doi: 10.1136/bmj.331.7512.321. PubMed PMID: 16081444; PubMed Central PMCID: PMC1183129.
451. Trinh NH, Hoblyn J, Mohanty S, Yaffe K. Efficacy of cholinesterase inhibitors in the treatment of neuropsychiatric symptoms and functional impairment in Alzheimer disease: a meta-analysis. *Jama*. 2003;289(2):210-6. PubMed PMID: 12517232.
452. Lanctot KL, Herrmann N, Yau KK, Khan LR, Liu BA, LouLou MM, Einarson TR. Efficacy and safety of cholinesterase inhibitors in Alzheimer's disease: a meta-analysis. *CMAJ : Canadian Medical Association journal = journal de l'Association medicale canadienne*. 2003;169(6):557-64. PubMed PMID: 12975222; PubMed Central PMCID: PMC191283.
453. Courtney C, Farrell D, Gray R, Hills R, Lynch L, Sellwood E, Edwards S, Hardyman W, Raftery J, Crome P, Lendon C, Shaw H, Bentham P, Group ADC. Long-term donepezil treatment in 565 patients with Alzheimer's disease (AD2000):

- randomised double-blind trial. *Lancet*. 2004;363(9427):2105-15. doi: 10.1016/S0140-6736(04)16499-4. PubMed PMID: 15220031.
454. Cummings JL. Use of cholinesterase inhibitors in clinical practice: evidence-based recommendations. *The American journal of geriatric psychiatry : official journal of the American Association for Geriatric Psychiatry*. 2003;11(2):131-45. PubMed PMID: 12611743.
455. Clark CM, Karlawish JH. Alzheimer disease: current concepts and emerging diagnostic and therapeutic strategies. *Annals of internal medicine*. 2003;138(5):400-10. PubMed PMID: 12614093.
456. Langa KM, Foster NL, Larson EB. Mixed dementia: emerging concepts and therapeutic implications. *Jama*. 2004;292(23):2901-8. doi: 10.1001/jama.292.23.2901. PubMed PMID: 15598922.
457. Grossberg GT, Desai AK. Management of Alzheimer's disease. *The journals of gerontology Series A, Biological sciences and medical sciences*. 2003;58(4):331-53. PubMed PMID: 12663697.
458. Holmes C, Wilkinson D, Dean C, Vethanayagam S, Olivieri S, Langley A, Pandita-Gunawardena ND, Hogg F, Clare C, Damms J. The efficacy of donepezil in the treatment of neuropsychiatric symptoms in Alzheimer disease. *Neurology*. 2004;63(2):214-9. PubMed PMID: 15277611.
459. Rainer M, Mucke HA, Kruger-Rainer C, Kraxberger E, Haushofer M, Jellinger KA. Cognitive relapse after discontinuation of drug therapy in Alzheimer's disease: cholinesterase inhibitors versus nootropics. *Journal of neural transmission*. 2001;108(11):1327-33. PubMed PMID: 11768631.
460. Tariot PN, Cummings JL, Katz IR, Mintzer J, Perdomo CA, Schwam EM, Whalen E. A randomized, double-blind, placebo-controlled study of the efficacy and safety of donepezil in patients with Alzheimer's disease in the nursing home setting. *Journal of the American Geriatrics Society*. 2001;49(12):1590-9. PubMed PMID: 11843990.
461. Black SE, Doody R, Li H, McRae T, Jambor KM, Xu Y, Sun Y, Perdomo CA, Richardson S. Donepezil preserves cognition and global function in patients with severe Alzheimer disease. *Neurology*. 2007;69(5):459-69. doi: 10.1212/01.wnl.0000266627.96040.5a. PubMed PMID: 17664405.
462. Winblad B, Kilander L, Eriksson S, Minthon L, Batsman S, Wetterholm AL, Jansson-Blixt C, Haglund A, Severe Alzheimer's Disease Study G. Donepezil in patients with severe Alzheimer's disease: double-blind, parallel-group, placebo-controlled study. *Lancet*. 2006;367(9516):1057-65. doi: 10.1016/S0140-6736(06)68350-5. PubMed PMID: 16581404.
463. Feldman H, Gauthier S, Hecker J, Vellas B, Subbiah P, Whalen E, Donepezil MSIG. A 24-week, randomized, double-blind study of donepezil in moderate to severe Alzheimer's disease. *Neurology*. 2001;57(4):613-20. PubMed PMID: 11524468.
464. Geldmacher DS, Frolich L, Doody RS, Erkinjuntti T, Vellas B, Jones RW, Banerjee S, Lin P, Sano M. Realistic expectations for treatment success in Alzheimer's disease. *The journal of nutrition, health & aging*. 2006;10(5):417-29. PubMed PMID: 17066215.
465. Kuhl DE, Minoshima S, Frey KA, Foster NL, Kilbourn MR, Koeppe RA. Limited donepezil inhibition of acetylcholinesterase measured with positron emission tomography in living Alzheimer cerebral cortex. *Annals of neurology*. 2000;48(3):391-5. PubMed PMID: 10976649.
466. Bohnen NI, Kaufer DI, Hendrickson R, Ivancov LS, Lopresti BJ, Koeppe RA, Meltzer CC, Constantine G, Davis JG, Mathis CA, Dekosky ST, Moore RY. Degree of inhibition of cortical acetylcholinesterase activity and cognitive effects by donepezil treatment in Alzheimer's disease. *Journal of neurology, neurosurgery, and psychiatry*. 2005;76(3):315-9. doi: 10.1136/jnnp.2004.038729. PubMed PMID: 15716518; PubMed Central PMCID: PMC1739536.
467. Nozawa M, Ichimiya Y, Nozawa E, Utumi Y, Sugiyama H, Murayama N, Iseki E, Arai H. Clinical effects of high oral dose of donepezil for patients with Alzheimer's disease in Japan. *Psychogeriatrics : the official journal of the Japanese Psychogeriatric Society*. 2009;9(2):50-5. doi: 10.1111/j.1479-8301.2009.00291.x. PubMed PMID: 19604325.
468. Farlow MR, Salloway S, Tariot PN, Yardley J, Moline ML, Wang Q, Brand-Schieber E, Zou H, Hsu T, Satlin A. Effectiveness and tolerability of high-dose (23 mg/d) versus standard-dose (10 mg/d) donepezil in moderate to severe Alzheimer's disease: A 24-week, randomized, double-blind study. *Clinical therapeutics*. 2010;32(7):1234-51. doi: 10.1016/j.clinthera.2010.06.019. PubMed PMID: 20678673; PubMed Central PMCID: PMC3068609.
469. Neumann PJ, Hermann RC, Kuntz KM, Araki SS, Duff SB, Leon J, Berenbaum PA, Goldman PA, Williams LW, Weinstein MC. Cost-effectiveness of donepezil in the treatment of mild or moderate Alzheimer's disease. *Neurology*. 1999;52(6):1138-45. PubMed PMID: 10214734.

470. Hauber AB, Gnanasakthy A, Mauskopf JA. Savings in the cost of caring for patients with Alzheimer's disease in Canada: an analysis of treatment with rivastigmine. *Clinical therapeutics*. 2000;22(4):439-51. PubMed PMID: 10823365.
471. Lopez-Bastida J, Hart W, Garcia-Perez L, Linertova R. Cost-effectiveness of donepezil in the treatment of mild or moderate Alzheimer's disease. *Journal of Alzheimer's disease : JAD*. 2009;16(2):399-407. doi: 10.3233/JAD-2009-0965. PubMed PMID: 19221429.
472. Hirsch C. ACP Journal Club. Review: Cholinesterase inhibitors do not prevent dementia in patients with mild cognitive impairment. *Annals of internal medicine*. 2014;160(8):JC11. doi: 10.7326/0003-4819-160-8-201404150-02011. PubMed PMID: 24733216.
473. Russ TC. Cholinesterase inhibitors should not be prescribed for mild cognitive impairment. *Evidence-based medicine*. 2014;19(3):101. doi: 10.1136/eb-2013-101687. PubMed PMID: 24482151.
474. Masoodi N. ACP Journal Club. Review: cholinesterase inhibitors do not reduce progression to dementia from mild cognitive impairment. *Annals of internal medicine*. 2013;158(4):JC3. doi: 10.7326/0003-4819-158-4-201302190-02003. PubMed PMID: 23420252.
475. Rojas-Fernandez CH. Little evidence that cholinesterase inhibitors prevent progression of mild cognitive impairment to dementia, but they are associated with adverse effects. *Evidence-based mental health*. 2013;16(2):39. doi: 10.1136/eb-2012-101087. PubMed PMID: 23299054.
476. Woodruff-Pak DS, Vogel RW, 3rd, Wenk GL. Galantamine: effect on nicotinic receptor binding, acetylcholinesterase inhibition, and learning. *Proceedings of the National Academy of Sciences of the United States of America*. 2001;98(4):2089-94. doi: 10.1073/pnas.031584398. PubMed PMID: 11172080; PubMed Central PMCID: PMC29386.
477. Karczmar AG. Brief presentation of the story and present status of studies of the vertebrate cholinergic system. *Neuropsychopharmacology : official publication of the American College of Neuropsychopharmacology*. 1993;9(3):181-99. doi: 10.1038/npp.1993.81. PubMed PMID: 8280343.
478. Erkinjuntti T, Roman G, Gauthier S, Feldman H, Rockwood K. Emerging therapies for vascular dementia and vascular cognitive impairment. *Stroke; a journal of cerebral circulation*. 2004;35(4):1010-7. doi: 10.1161/01.STR.0000120731.88236.33. PubMed PMID: 15001795.
479. Wilkinson D, Doody R, Helme R, Taubman K, Mintzer J, Kertesz A, Pratt RD, Donepezil 308 Study G. Donepezil in vascular dementia: a randomized, placebo-controlled study. *Neurology*. 2003;61(4):479-86. PubMed PMID: 12939421.
480. Aarsland D, Laake K, Larsen JP, Janvin C. Donepezil for cognitive impairment in Parkinson's disease: a randomised controlled study. *Journal of neurology, neurosurgery, and psychiatry*. 2002;72(6):708-12. PubMed PMID: 12023410; PubMed Central PMCID: PMC1737925.
481. Cubo E, Shannon KM, Tracy D, Jaglin JA, Bernard BA, Wu J, Leurgans SE. Effect of donepezil on motor and cognitive function in Huntington disease. *Neurology*. 2006;67(7):1268-71. doi: 10.1212/01.wnl.0000238106.10423.00. PubMed PMID: 17030764.
482. Kornhuber J, Weller M, Schoppmeyer K, Riederer P. Amantadine and memantine are NMDA receptor antagonists with neuroprotective properties. *Journal of neural transmission Supplementum*. 1994;43:91-104. PubMed PMID: 7884411.
483. Frankiewicz T, Parsons CG. Memantine restores long term potentiation impaired by tonic N-methyl-D-aspartate (NMDA) receptor activation following reduction of Mg²⁺ in hippocampal slices. *Neuropharmacology*. 1999;38(9):1253-9. PubMed PMID: 10471078.
484. Li L, Sengupta A, Haque N, Grundke-Iqbal I, Iqbal K. Memantine inhibits and reverses the Alzheimer type abnormal hyperphosphorylation of tau and associated neurodegeneration. *FEBS letters*. 2004;566(1-3):261-9. doi: 10.1016/j.febslet.2004.04.047. PubMed PMID: 15147906.
485. Reisberg B, Doody R, Stoffler A, Schmitt F, Ferris S, Mobius HJ, Memantine Study G. Memantine in moderate-to-severe Alzheimer's disease. *The New England journal of medicine*. 2003;348(14):1333-41. doi: 10.1056/NEJMoa013128. PubMed PMID: 12672860.
486. Howard R, McShane R, Lindesay J, Ritchie C, Baldwin A, Barber R, Burns A, Denning T, Findlay D, Holmes C, Hughes A, Jacoby R, Jones R, Jones R, McKeith I, Macharouthu A, O'Brien J, Passmore P, Sheehan B, Juszcak E, Katona C, Hills R, Knapp M, Ballard C, Brown R, Banerjee S, Onions C, Griffin M, Adams J, Gray R, Johnson T, Bentham P, Phillips P.

Donepezil and memantine for moderate-to-severe Alzheimer's disease. *The New England journal of medicine*. 2012;366(10):893-903. doi: 10.1056/NEJMoa1106668. PubMed PMID: 22397651.

487. Tariot PN. Cessation of donepezil is associated with clinical decline in patients with moderate-to-severe Alzheimer's disease compared to continuation of donepezil or addition or substitution of memantine. *Evidence-based medicine*. 2013;18(2):62-3. doi: 10.1136/eb-2012-100722. PubMed PMID: 22736656.

488. Suzuki T. Discontinuing donepezil or starting memantine for Alzheimer's disease. *The New England journal of medicine*. 2012;366(23):2227-8; author reply 8. doi: 10.1056/NEJMc1204656#SA1. PubMed PMID: 22670911.

489. Tariot PN, Farlow MR, Grossberg GT, Graham SM, McDonald S, Gergel I, Memantine Study G. Memantine treatment in patients with moderate to severe Alzheimer disease already receiving donepezil: a randomized controlled trial. *Jama*. 2004;291(3):317-24. doi: 10.1001/jama.291.3.317. PubMed PMID: 14734594.

490. Schneider LS, Dagerman KS, Higgins JP, McShane R. Lack of evidence for the efficacy of memantine in mild Alzheimer disease. *Archives of neurology*. 2011;68(8):991-8. doi: 10.1001/archneurol.2011.69. PubMed PMID: 21482915.

491. Porsteinsson AP, Grossberg GT, Mintzer J, Olin JT, Memantine MEMMDSG. Memantine treatment in patients with mild to moderate Alzheimer's disease already receiving a cholinesterase inhibitor: a randomized, double-blind, placebo-controlled trial. *Current Alzheimer research*. 2008;5(1):83-9. PubMed PMID: 18288936.

492. Cummings JL, Isaacson RS, Schmitt FA, Velting DM. A practical algorithm for managing Alzheimer's disease: what, when, and why? *Annals of clinical and translational neurology*. 2015;2(3):307-23. doi: 10.1002/acn3.166. PubMed PMID: 25815358; PubMed Central PMCID: PMC4369281.

493. Hardy JA, Higgins GA. Alzheimer's disease: the amyloid cascade hypothesis. *Science*. 1992;256(5054):184-5. PubMed PMID: 1566067.

494. Goate A, Chartier-Harlin MC, Mullan M, Brown J, Crawford F, Fidani L, Giuffra L, Haynes A, Irving N, James L, et al. Segregation of a missense mutation in the amyloid precursor protein gene with familial Alzheimer's disease. *Nature*. 1991;349(6311):704-6. doi: 10.1038/349704a0. PubMed PMID: 1671712.

495. Glenner GG, Wong CW. Alzheimer's disease and Down's syndrome: sharing of a unique cerebrovascular amyloid fibril protein. *Biochemical and biophysical research communications*. 1984;122(3):1131-5. PubMed PMID: 6236805.

496. Glenner GG, Wong CW. Alzheimer's disease: initial report of the purification and characterization of a novel cerebrovascular amyloid protein. 1984. *Biochemical and biophysical research communications*. 2012;425(3):534-9. doi: 10.1016/j.bbrc.2012.08.020. PubMed PMID: 22925670.

497. Tanzi RE, Gusella JF, Watkins PC, Bruns GA, St George-Hyslop P, Van Keuren ML, Patterson D, Pagan S, Kurnit DM, Neve RL. Amyloid beta protein gene: cDNA, mRNA distribution, and genetic linkage near the Alzheimer locus. *Science*. 1987;235(4791):880-4. PubMed PMID: 2949367.

498. Kitaguchi N, Takahashi Y, Tokushima Y, Shiojiri S, Ito H. Novel precursor of Alzheimer's disease amyloid protein shows protease inhibitory activity. *Nature*. 1988;331(6156):530-2. doi: 10.1038/331530a0. PubMed PMID: 2893291.

499. Kang J, Lemaire HG, Unterbeck A, Salbaum JM, Masters CL, Grzeschik KH, Multhaup G, Beyreuther K, Muller-Hill B. The precursor of Alzheimer's disease amyloid A4 protein resembles a cell-surface receptor. *Nature*. 1987;325(6106):733-6. doi: 10.1038/325733a0. PubMed PMID: 2881207.

500. Yoshikai S, Sasaki H, Doh-ura K, Furuya H, Sakaki Y. Genomic organization of the human-amyloid beta-protein precursor gene. *Gene*. 1991;102(2):291-2. PubMed PMID: 1908403.

501. Saitoh T, Sundsmo M, Roch JM, Kimura N, Cole G, Schubert D, Oltersdorf T, Schenk DB. Secreted form of amyloid beta protein precursor is involved in the growth regulation of fibroblasts. *Cell*. 1989;58(4):615-22. PubMed PMID: 2475254.

502. Milward EA, Papadopoulos R, Fuller SJ, Moir RD, Small D, Beyreuther K, Masters CL. The amyloid protein precursor of Alzheimer's disease is a mediator of the effects of nerve growth factor on neurite outgrowth. *Neuron*. 1992;9(1):129-37. PubMed PMID: 1632967.

503. Villa A, Latasa MJ, Pascual A. Nerve growth factor modulates the expression and secretion of beta-amyloid precursor protein through different mechanisms in PC12 cells. *Journal of neurochemistry*. 2001;77(4):1077-84. PubMed PMID: 11359873.

504. Nishimoto I, Okamoto T, Matsuura Y, Takahashi S, Okamoto T, Murayama Y, Ogata E. Alzheimer amyloid protein precursor complexes with brain GTP-binding protein G(o). *Nature*. 1993;362(6415):75-9. doi: 10.1038/362075a0. PubMed PMID: 8446172.
505. Cao X, Sudhof TC. A transcriptionally [correction of transcriptively] active complex of APP with Fe65 and histone acetyltransferase Tip60. *Science*. 2001;293(5527):115-20. doi: 10.1126/science.1058783. PubMed PMID: 11441186.
506. Lee J, Retamal C, Cuitino L, Caruano-Yzermans A, Shin JE, van Kerkhof P, Marzolo MP, Bu G. Adaptor protein sorting nexin 17 regulates amyloid precursor protein trafficking and processing in the early endosomes. *The Journal of biological chemistry*. 2008;283(17):11501-8. doi: 10.1074/jbc.M800642200. PubMed PMID: 18276590; PubMed Central PMCID: PMC2431074.
507. Jorissen E, Prox J, Bernreuther C, Weber S, Schwanbeck R, Serneels L, Snellinx A, Craessaerts K, Thathiah A, Tesseur I, Bartsch U, Weskamp G, Blobel CP, Glatzel M, De Strooper B, Saftig P. The disintegrin/metalloproteinase ADAM10 is essential for the establishment of the brain cortex. *The Journal of neuroscience : the official journal of the Society for Neuroscience*. 2010;30(14):4833-44. doi: 10.1523/JNEUROSCI.5221-09.2010. PubMed PMID: 20371803; PubMed Central PMCID: PMC2921981.
508. Sobhanifar S, Schneider B, Lohr F, Gottstein D, Ikeya T, Mlynarczyk K, Pulawski W, Ghoshdastider U, Kolinski M, Filipek S, Guntert P, Bernhard F, Dotsch V. Structural investigation of the C-terminal catalytic fragment of presenilin 1. *Proceedings of the National Academy of Sciences of the United States of America*. 2010;107(21):9644-9. doi: 10.1073/pnas.1000778107. PubMed PMID: 20445084; PubMed Central PMCID: PMC2906861.
509. Kaether C, Haass C, Steiner H. Assembly, trafficking and function of gamma-secretase. *Neuro-degenerative diseases*. 2006;3(4-5):275-83. doi: 10.1159/000095267. PubMed PMID: 17047368.
510. Selkoe DJ. The molecular pathology of Alzheimer's disease. *Neuron*. 1991;6(4):487-98. PubMed PMID: 1673054.
511. Vassar R, Bennett BD, Babu-Khan S, Kahn S, Mendiaz EA, Denis P, Teplow DB, Ross S, Amarante P, Loeloff R, Luo Y, Fisher S, Fuller J, Edenson S, Lile J, Jarosinski MA, Biere AL, Curran E, Burgess T, Louis JC, Collins F, Treanor J, Rogers G, Citron M. Beta-secretase cleavage of Alzheimer's amyloid precursor protein by the transmembrane aspartic protease BACE. *Science*. 1999;286(5440):735-41. PubMed PMID: 10531052.
512. Rocchi A, Pellegrini S, Siciliano G, Murri L. Causative and susceptibility genes for Alzheimer's disease: a review. *Brain research bulletin*. 2003;61(1):1-24. PubMed PMID: 12788204.
513. Selkoe DJ. Normal and abnormal biology of the beta-amyloid precursor protein. *Annual review of neuroscience*. 1994;17:489-517. doi: 10.1146/annurev.ne.17.030194.002421. PubMed PMID: 8210185.
514. Kuhn PH, Wang H, Dislich B, Colombo A, Zeitschel U, Ellwart JW, Kremmer E, Rossner S, Lichtenthaler SF. ADAM10 is the physiologically relevant, constitutive alpha-secretase of the amyloid precursor protein in primary neurons. *The EMBO journal*. 2010;29(17):3020-32. doi: 10.1038/emboj.2010.167. PubMed PMID: 20676056; PubMed Central PMCID: PMC2944055.
515. Alves da Costa C, Sunyach C, Pardossi-Piquard R, Sevalle J, Vincent B, Boyer N, Kawarai T, Girardot N, St George-Hyslop P, Checler F. Presenilin-dependent gamma-secretase-mediated control of p53-associated cell death in Alzheimer's disease. *The Journal of neuroscience : the official journal of the Society for Neuroscience*. 2006;26(23):6377-85. doi: 10.1523/JNEUROSCI.0651-06.2006. PubMed PMID: 16763046.
516. Madeira A, Pomet JM, Prochiantz A, Allinquant B. SET protein (TAF1beta, I2PP2A) is involved in neuronal apoptosis induced by an amyloid precursor protein cytoplasmic subdomain. *FASEB journal : official publication of the Federation of American Societies for Experimental Biology*. 2005;19(13):1905-7. doi: 10.1096/fj.05-3839fje. PubMed PMID: 16162853.
517. Muller T, Concannon CG, Ward MW, Walsh CM, Tirniceriu AL, Tribl F, Kogel D, Prehn JH, Egensperger R. Modulation of gene expression and cytoskeletal dynamics by the amyloid precursor protein intracellular domain (AICD). *Molecular biology of the cell*. 2007;18(1):201-10. doi: 10.1091/mbc.E06-04-0283. PubMed PMID: 17093061; PubMed Central PMCID: PMC1751311.
518. Dulin F, Leveille F, Ortega JB, Mornon JP, Buisson A, Callebaut I, Colloc'h N. P3 peptide, a truncated form of A beta devoid of synaptotoxic effect, does not assemble into soluble oligomers. *FEBS letters*. 2008;582(13):1865-70. doi: 10.1016/j.febslet.2008.05.002. PubMed PMID: 18474239.
519. Haass C, Selkoe DJ. Soluble protein oligomers in neurodegeneration: lessons from the Alzheimer's amyloid beta-peptide. *Nature reviews Molecular cell biology*. 2007;8(2):101-12. doi: 10.1038/nrm2101. PubMed PMID: 17245412.

520. Powers ET, Powers DL. Mechanisms of protein fibril formation: nucleated polymerization with competing off-pathway aggregation. *Biophysical journal*. 2008;94(2):379-91. doi: 10.1529/biophysj.107.117168. PubMed PMID: 17890392; PubMed Central PMCID: PMC2157252.
521. Glabe CG. Structural classification of toxic amyloid oligomers. *The Journal of biological chemistry*. 2008;283(44):29639-43. doi: 10.1074/jbc.R800016200. PubMed PMID: 18723507; PubMed Central PMCID: PMC2573087.
522. Shankar GM, Walsh DM. Alzheimer's disease: synaptic dysfunction and Aβeta. *Molecular neurodegeneration*. 2009;4:48. doi: 10.1186/1750-1326-4-48. PubMed PMID: 19930651; PubMed Central PMCID: PMC2788538.
523. Tomiyama T, Matsuyama S, Iso H, Umeda T, Takuma H, Ohnishi K, Ishibashi K, Teraoka R, Sakama N, Yamashita T, Nishitsuji K, Ito K, Shimada H, Lambert MP, Klein WL, Mori H. A mouse model of amyloid beta oligomers: their contribution to synaptic alteration, abnormal tau phosphorylation, glial activation, and neuronal loss in vivo. *The Journal of neuroscience : the official journal of the Society for Neuroscience*. 2010;30(14):4845-56. doi: 10.1523/JNEUROSCI.5825-09.2010. PubMed PMID: 20371804.
524. Lai F, Williams RS. A prospective study of Alzheimer disease in Down syndrome. *Archives of neurology*. 1989;46(8):849-53. PubMed PMID: 2527024.
525. Wisniewski KE, Wisniewski HM, Wen GY. Occurrence of neuropathological changes and dementia of Alzheimer's disease in Down's syndrome. *Annals of neurology*. 1985;17(3):278-82. doi: 10.1002/ana.410170310. PubMed PMID: 3158266.
526. Lemere CA, Blusztajn JK, Yamaguchi H, Wisniewski T, Saido TC, Selkoe DJ. Sequence of deposition of heterogeneous amyloid beta-peptides and APO E in Down syndrome: implications for initial events in amyloid plaque formation. *Neurobiology of disease*. 1996;3(1):16-32. doi: 10.1006/nbdi.1996.0003. PubMed PMID: 9173910.
527. Nelson LD, Siddarth P, Kepe V, Scheibel KE, Huang SC, Barrio JR, Small GW. Positron emission tomography of brain beta-amyloid and tau levels in adults with Down syndrome. *Archives of neurology*. 2011;68(6):768-74. doi: 10.1001/archneurol.2011.104. PubMed PMID: 21670401; PubMed Central PMCID: PMC3261613.
528. Mann DM, Yates PO, Marcyniuk B, Ravindra CR. Loss of neurones from cortical and subcortical areas in Down's syndrome patients at middle age. Quantitative comparisons with younger Down's patients and patients with Alzheimer's disease. *Journal of the neurological sciences*. 1987;80(1):79-89. PubMed PMID: 2956368.
529. Rumble B, Retallack R, Hilbich C, Simms G, Multhaup G, Martins R, Hockey A, Montgomery P, Beyreuther K, Masters CL. Amyloid A4 protein and its precursor in Down's syndrome and Alzheimer's disease. *The New England journal of medicine*. 1989;320(22):1446-52. doi: 10.1056/NEJM198906013202203. PubMed PMID: 2566117.
530. St George-Hyslop PH, Tanzi RE, Polinsky RJ, Haines JL, Nee L, Watkins PC, Myers RH, Feldman RG, Pollen D, Drachman D, et al. The genetic defect causing familial Alzheimer's disease maps on chromosome 21. *Science*. 1987;235(4791):885-90. PubMed PMID: 2880399.
531. Hyman BT, West HL, Rebeck GW, Lai F, Mann DM. Neuropathological changes in Down's syndrome hippocampal formation. Effect of age and apolipoprotein E genotype. *Archives of neurology*. 1995;52(4):373-8. PubMed PMID: 7710373.
532. Hof PR, Bouras C, Perl DP, Sparks DL, Mehta N, Morrison JH. Age-related distribution of neuropathologic changes in the cerebral cortex of patients with Down's syndrome. Quantitative regional analysis and comparison with Alzheimer's disease. *Archives of neurology*. 1995;52(4):379-91. PubMed PMID: 7710374.
533. Wilcock DM, Griffin WS. Down's syndrome, neuroinflammation, and Alzheimer neuropathogenesis. *Journal of neuroinflammation*. 2013;10:84. doi: 10.1186/1742-2094-10-84. PubMed PMID: 23866266; PubMed Central PMCID: PMC3750399.
534. Lott IT, Head E. Down syndrome and Alzheimer's disease: a link between development and aging. *Mental retardation and developmental disabilities research reviews*. 2001;7(3):172-8. doi: 10.1002/mrdd.1025. PubMed PMID: 11553933.
535. Zigman WB, Devenny DA, Krinsky-McHale SJ, Jenkins EC, Urv TK, Wegiel J, Schupf N, Silverman W. Alzheimer's Disease in Adults with Down Syndrome. *International review of research in mental retardation*. 2008;36:103-45. doi: 10.1016/S0074-7750(08)00004-9. PubMed PMID: 19633729; PubMed Central PMCID: PMC2714652.

536. Prasher VP, Farrer MJ, Kessling AM, Fisher EM, West RJ, Barber PC, Butler AC. Molecular mapping of Alzheimer-type dementia in Down's syndrome. *Annals of neurology*. 1998;43(3):380-3. doi: 10.1002/ana.410430316. PubMed PMID: 9506555.
537. Sturgeon X, Gardiner KJ. Transcript catalogs of human chromosome 21 and orthologous chimpanzee and mouse regions. *Mammalian genome : official journal of the International Mammalian Genome Society*. 2011;22(5-6):261-71. doi: 10.1007/s00335-011-9321-y. PubMed PMID: 21400203.
538. Belichenko PV, Kleschevnikov AM, Salehi A, Epstein CJ, Mobley WC. Synaptic and cognitive abnormalities in mouse models of Down syndrome: exploring genotype-phenotype relationships. *The Journal of comparative neurology*. 2007;504(4):329-45. doi: 10.1002/cne.21433. PubMed PMID: 17663443.
539. Lockrow JP, Fortress AM, Granholm AC. Age-related neurodegeneration and memory loss in down syndrome. *Current gerontology and geriatrics research*. 2012;2012:463909. doi: 10.1155/2012/463909. PubMed PMID: 22545043; PubMed Central PMCID: PMC3318235.
540. Hartley D, Blumenthal T, Carrillo M, DiPaolo G, Esralew L, Gardiner K, Granholm AC, Iqbal K, Krams M, Lemere C, Lott I, Mobley W, Ness S, Nixon R, Potter H, Reeves R, Sabbagh M, Silverman W, Tycko B, Whitten M, Wisniewski T. Down syndrome and Alzheimer's disease: Common pathways, common goals. *Alzheimer's & dementia : the journal of the Alzheimer's Association*. 2014. doi: 10.1016/j.jalz.2014.10.007. PubMed PMID: 25510383.
541. Sturgeon X, Le T, Ahmed MM, Gardiner KJ. Pathways to cognitive deficits in Down syndrome. *Progress in brain research*. 2012;197:73-100. doi: 10.1016/B978-0-444-54299-1.00005-4. PubMed PMID: 22541289.
542. Ahmed MM, Dhanasekaran AR, Tong S, Wiseman FK, Fisher EM, Tybulewicz VL, Gardiner KJ. Protein profiles in Tc1 mice implicate novel pathway perturbations in the Down syndrome brain. *Human molecular genetics*. 2013;22(9):1709-24. doi: 10.1093/hmg/ddt017. PubMed PMID: 23349361; PubMed Central PMCID: PMC3613160.
543. Jiang Y, Mullaney KA, Peterhoff CM, Che S, Schmidt SD, Boyer-Boiteau A, Ginsberg SD, Cataldo AM, Mathews PM, Nixon RA. Alzheimer's-related endosome dysfunction in Down syndrome is Abeta-independent but requires APP and is reversed by BACE-1 inhibition. *Proceedings of the National Academy of Sciences of the United States of America*. 2010;107(4):1630-5. doi: 10.1073/pnas.0908953107. PubMed PMID: 20080541; PubMed Central PMCID: PMC2824382.
544. Salehi A, Delcroix JD, Belichenko PV, Zhan K, Wu C, Valletta JS, Takimoto-Kimura R, Kleschevnikov AM, Sambamurti K, Chung PP, Xia W, Villar A, Campbell WA, Kulnane LS, Nixon RA, Lamb BT, Epstein CJ, Stokin GB, Goldstein LS, Mobley WC. Increased App expression in a mouse model of Down's syndrome disrupts NGF transport and causes cholinergic neuron degeneration. *Neuron*. 2006;51(1):29-42. doi: 10.1016/j.neuron.2006.05.022. PubMed PMID: 16815330.
545. Iulita MF, Do Carmo S, Ower AK, Fortress AM, Aguilar LF, Hanna M, Wisniewski T, Granholm AC, Buhusi M, Busciglio J, Cuellar AC. Nerve growth factor metabolic dysfunction in Down's syndrome brains. *Brain : a journal of neurology*. 2014;137(Pt 3):860-72. doi: 10.1093/brain/awt372. PubMed PMID: 24519975; PubMed Central PMCID: PMC3927704.
546. Chartier-Harlin MC, Crawford F, Houlden H, Warren A, Hughes D, Fidani L, Goate A, Rossor M, Roques P, Hardy J, et al. Early-onset Alzheimer's disease caused by mutations at codon 717 of the beta-amyloid precursor protein gene. *Nature*. 1991;353(6347):844-6. doi: 10.1038/353844a0. PubMed PMID: 1944558.
547. Levy E, Carman MD, Fernandez-Madrid IJ, Power MD, Lieberburg I, van Duinen SG, Bots GT, Luyendijk W, Frangione B. Mutation of the Alzheimer's disease amyloid gene in hereditary cerebral hemorrhage, Dutch type. *Science*. 1990;248(4959):1124-6. PubMed PMID: 2111584.
548. Haan J, Hardy JA, Roos RA. Hereditary cerebral hemorrhage with amyloidosis--Dutch type: its importance for Alzheimer research. *Trends in neurosciences*. 1991;14(6):231-4. PubMed PMID: 1716015.
549. Cruts M, Van Broeckhoven C. Molecular genetics of Alzheimer's disease. *Annals of medicine*. 1998;30(6):560-5. PubMed PMID: 9920359.
550. Tomiyama T, Nagata T, Shimada H, Teraoka R, Fukushima A, Kanemitsu H, Takuma H, Kuwano R, Imagawa M, Ataka S, Wada Y, Yoshioka E, Nishizaki T, Watanabe Y, Mori H. A new amyloid beta variant favoring oligomerization in Alzheimer's-type dementia. *Annals of neurology*. 2008;63(3):377-87. doi: 10.1002/ana.21321. PubMed PMID: 18300294.
551. Di Fede G, Catania M, Morbin M, Rossi G, Suardi S, Mazzoleni G, Merlin M, Giovagnoli AR, Prioni S, Erbetta A, Falcone C, Gobbi M, Colombo L, Bastone A, Beeg M, Manzoni C, Francescucci B, Spagnoli A, Cantu L, Del Favero E, Levy E, Salmona M, Tagliavini F. A recessive mutation in the APP gene with dominant-negative effect on amyloidogenesis.

Science. 2009;323(5920):1473-7. doi: 10.1126/science.1168979. PubMed PMID: 19286555; PubMed Central PMCID: PMC2728497.

552. Calero M, Gomez-Ramos A, Calero O, Soriano E, Avila J, Medina M. Additional mechanisms conferring genetic susceptibility to Alzheimer's disease. *Frontiers in cellular neuroscience*. 2015;9:138. doi: 10.3389/fncel.2015.00138. PubMed PMID: 25914626.

553. Armstrong RA. A critical analysis of the 'amyloid cascade hypothesis'. *Folia neuropathologica / Association of Polish Neuropathologists and Medical Research Centre, Polish Academy of Sciences*. 2014;52(3):211-25. PubMed PMID: 25310732.

554. Citron M, Oltersdorf T, Haass C, McConlogue L, Hung AY, Seubert P, Vigo-Pelfrey C, Lieberburg I, Selkoe DJ. Mutation of the beta-amyloid precursor protein in familial Alzheimer's disease increases beta-protein production. *Nature*. 1992;360(6405):672-4. doi: 10.1038/360672a0. PubMed PMID: 1465129.

555. Johnston JA, Cowburn RF, Norgren S, Wiehager B, Venizelos N, Winblad B, Vigo-Pelfrey C, Schenk D, Lannfelt L, O'Neill C. Increased beta-amyloid release and levels of amyloid precursor protein (APP) in fibroblast cell lines from family members with the Swedish Alzheimer's disease APP670/671 mutation. *FEBS letters*. 1994;354(3):274-8. PubMed PMID: 7957938.

556. Suzuki N, Cheung TT, Cai XD, Odaka A, Otvos L, Jr., Eckman C, Golde TE, Younkin SG. An increased percentage of long amyloid beta protein secreted by familial amyloid beta protein precursor (beta APP717) mutants. *Science*. 1994;264(5163):1336-40. PubMed PMID: 8191290.

557. Estus S, Golde TE, Younkin SG. Normal processing of the Alzheimer's disease amyloid beta protein precursor generates potentially amyloidogenic carboxyl-terminal derivatives. *Annals of the New York Academy of Sciences*. 1992;674:138-48. PubMed PMID: 1288359.

558. Hardy J, Allsop D. Amyloid deposition as the central event in the aetiology of Alzheimer's disease. *Trends in pharmacological sciences*. 1991;12(10):383-8. PubMed PMID: 1763432.

559. Peacock ML, Murman DL, Sima AA, Warren JT, Jr., Roses AD, Fink JK. Novel amyloid precursor protein gene mutation (codon 665Asp) in a patient with late-onset Alzheimer's disease. *Annals of neurology*. 1994;35(4):432-8. doi: 10.1002/ana.410350410. PubMed PMID: 8154870.

560. Jonsson T, Atwal JK, Steinberg S, Snaedal J, Jonsson PV, Bjornsson S, Stefansson H, Sulem P, Gudbjartsson D, Maloney J, Hoyte K, Gustafson A, Liu Y, Lu Y, Bhangale T, Graham RR, Huttenlocher J, Bjornsdottir G, Andreassen OA, Jonsson EG, Palotie A, Behrens TW, Magnusson OT, Kong A, Thorsteinsdottir U, Watts RJ, Stefansson K. A mutation in APP protects against Alzheimer's disease and age-related cognitive decline. *Nature*. 2012;488(7409):96-9. doi: 10.1038/nature11283. PubMed PMID: 22801501.

561. Wavrant-De Vrieze F, Crook R, Holmans P, Kehoe P, Owen MJ, Williams J, Roehl K, Laliiri DK, Shears S, Booth J, Wu W, Goate A, Chartier-Harlin MC, Hardy J, Perez-Tur J. Genetic variability at the amyloid-beta precursor protein locus may contribute to the risk of late-onset Alzheimer's disease. *Neuroscience letters*. 1999;269(2):67-70. PubMed PMID: 10430506.

562. Wu J, Basha MR, Zawia NH. The environment, epigenetics and amyloidogenesis. *Journal of molecular neuroscience : MN*. 2008;34(1):1-7. doi: 10.1007/s12031-007-0009-4. PubMed PMID: 18157652.

563. Van Broeckhoven C, Backhovens H, Cruts M, De Winter G, Bruylant M, Cras P, Martin JJ. Mapping of a gene predisposing to early-onset Alzheimer's disease to chromosome 14q24.3. *Nature genetics*. 1992;2(4):335-9. doi: 10.1038/ng1292-335. PubMed PMID: 1303290.

564. Sherrington R, Rogaev EI, Liang Y, Rogaeva EA, Levesque G, Ikeda M, Chi H, Lin C, Li G, Holman K, Tsuda T, Mar L, Foncin JF, Bruni AC, Montesi MP, Sorbi S, Rainero I, Pinessi L, Nee L, Chumakov I, Pollen D, Brookes A, Sanseau P, Polinsky RJ, Wasco W, Da Silva HA, Haines JL, Pericak-Vance MA, Tanzi RE, Roses AD, Fraser PE, Rommens JM, St George-Hyslop PH. Cloning of a gene bearing missense mutations in early-onset familial Alzheimer's disease. *Nature*. 1995;375(6534):754-60. doi: 10.1038/375754a0. PubMed PMID: 7596406.

565. Levy-Lahad E, Wasco W, Poorkaj P, Romano DM, Oshima J, Pettingell WH, Yu CE, Jondro PD, Schmidt SD, Wang K, et al. Candidate gene for the chromosome 1 familial Alzheimer's disease locus. *Science*. 1995;269(5226):973-7. PubMed PMID: 7638622.

566. Prihar G, Fuldner RA, Perez-Tur J, Lincoln S, Duff K, Crook R, Hardy J, Philips CA, Venter C, Talbot C, Clark RF, Goate A, Li J, Potter H, Karran E, Roberts GW, Hutton M, Adams MD. Structure and alternative splicing of the presenilin-2 gene. *Neuroreport*. 1996;7(10):1680-4. PubMed PMID: 8904781.
567. Kovacs DM, Fausett HJ, Page KJ, Kim TW, Moir RD, Merriam DE, Hollister RD, Hallmark OG, Mancini R, Felsenstein KM, Hyman BT, Tanzi RE, Wasco W. Alzheimer-associated presenilins 1 and 2: neuronal expression in brain and localization to intracellular membranes in mammalian cells. *Nature medicine*. 1996;2(2):224-9. PubMed PMID: 8574969.
568. Thinakaran G, Harris CL, Ratovitski T, Davenport F, Slunt HH, Price DL, Borchelt DR, Sisodia SS. Evidence that levels of presenilins (PS1 and PS2) are coordinately regulated by competition for limiting cellular factors. *The Journal of biological chemistry*. 1997;272(45):28415-22. PubMed PMID: 9353300.
569. Shen J, Bronson RT, Chen DF, Xia W, Selkoe DJ, Tonegawa S. Skeletal and CNS defects in Presenilin-1-deficient mice. *Cell*. 1997;89(4):629-39. PubMed PMID: 9160754.
570. Walter J, Schindzielorz A, Grunberg J, Haass C. Phosphorylation of presenilin-2 regulates its cleavage by caspases and retards progression of apoptosis. *Proceedings of the National Academy of Sciences of the United States of America*. 1999;96(4):1391-6. PubMed PMID: 9990034; PubMed Central PMCID: PMC15473.
571. Lee SF, Shah S, Yu C, Wigley WC, Li H, Lim M, Pedersen K, Han W, Thomas P, Lundkvist J, Hao YH, Yu G. A conserved GXXXG motif in APH-1 is critical for assembly and activity of the gamma-secretase complex. *The Journal of biological chemistry*. 2004;279(6):4144-52. doi: 10.1074/jbc.M309745200. PubMed PMID: 14627705.
572. Zhang YW, Luo WJ, Wang H, Lin P, Vetrivel KS, Liao F, Li F, Wong PC, Farquhar MG, Thinakaran G, Xu H. Nicastrin is critical for stability and trafficking but not association of other presenilin/gamma-secretase components. *The Journal of biological chemistry*. 2005;280(17):17020-6. doi: 10.1074/jbc.M409467200. PubMed PMID: 15711015; PubMed Central PMCID: PMC1201533.
573. Prokop S, Shirotani K, Edbauer D, Haass C, Steiner H. Requirement of PEN-2 for stabilization of the presenilin N-/C-terminal fragment heterodimer within the gamma-secretase complex. *The Journal of biological chemistry*. 2004;279(22):23255-61. doi: 10.1074/jbc.M401789200. PubMed PMID: 15039426.
574. Watanabe N, Tomita T, Sato C, Kitamura T, Morohashi Y, Iwatsubo T. Pen-2 is incorporated into the gamma-secretase complex through binding to transmembrane domain 4 of presenilin 1. *The Journal of biological chemistry*. 2005;280(51):41967-75. doi: 10.1074/jbc.M509066200. PubMed PMID: 16234244.
575. Haass C, De Strooper B. The presenilins in Alzheimer's disease--proteolysis holds the key. *Science*. 1999;286(5441):916-9. PubMed PMID: 10542139.
576. Berezovska O, Jack C, McLean P, Aster JC, Hicks C, Xia W, Wolfe MS, Weinmaster G, Selkoe DJ, Hyman BT. Rapid Notch1 nuclear translocation after ligand binding depends on presenilin-associated gamma-secretase activity. *Annals of the New York Academy of Sciences*. 2000;920:223-6. PubMed PMID: 11193154.
577. Amtul Z, Lewis PA, Piper S, Crook R, Baker M, Findlay K, Singleton A, Hogg M, Younkin L, Younkin SG, Hardy J, Hutton M, Boeve BF, Tang-Wai D, Golde TE. A presenilin 1 mutation associated with familial frontotemporal dementia inhibits gamma-secretase cleavage of APP and notch. *Neurobiology of disease*. 2002;9(2):269-73. doi: 10.1006/nbdi.2001.0473. PubMed PMID: 11895378.
578. Esler WP, Kimberly WT, Ostaszewski BL, Diehl TS, Moore CL, Tsai JY, Rahmati T, Xia W, Selkoe DJ, Wolfe MS. Transition-state analogue inhibitors of gamma-secretase bind directly to presenilin-1. *Nature cell biology*. 2000;2(7):428-34. doi: 10.1038/35017062. PubMed PMID: 10878808.
579. Yu G, Nishimura M, Arawaka S, Levitan D, Zhang L, Tandon A, Song YQ, Rogaeva E, Chen F, Kawarai T, Supala A, Levesque L, Yu H, Yang DS, Holmes E, Milman P, Liang Y, Zhang DM, Xu DH, Sato C, Rogaev E, Smith M, Janus C, Zhang Y, Aebbersold R, Farrer LS, Sorbi S, Bruni A, Fraser P, St George-Hyslop P. Nicastrin modulates presenilin-mediated notch/glp-1 signal transduction and betaAPP processing. *Nature*. 2000;407(6800):48-54. doi: 10.1038/35024009. PubMed PMID: 10993067.
580. Rogaeva EA, Fafel KC, Song YQ, Medeiros H, Sato C, Liang Y, Richard E, Rogaev EI, Frommelt P, Sadovnick AD, Meschino W, Rockwood K, Boss MA, Mayeux R, St George-Hyslop P. Screening for PS1 mutations in a referral-based series of AD cases: 21 novel mutations. *Neurology*. 2001;57(4):621-5. PubMed PMID: 11524469.
581. Janssen JC, Beck JA, Campbell TA, Dickinson A, Fox NC, Harvey RJ, Houlden H, Rossor MN, Collinge J. Early onset familial Alzheimer's disease: Mutation frequency in 31 families. *Neurology*. 2003;60(2):235-9. PubMed PMID: 12552037.

582. Cruts M, Van Broeckhoven C. Presenilin mutations in Alzheimer's disease. *Human mutation*. 1998;11(3):183-90. doi: 10.1002/(SICI)1098-1004(1998)11:3<183::AID-HUMU1>3.0.CO;2-J. PubMed PMID: 9521418.
583. Wolfe MS, Xia W, Ostaszewski BL, Diehl TS, Kimberly WT, Selkoe DJ. Two transmembrane aspartates in presenilin-1 required for presenilin endoproteolysis and gamma-secretase activity. *Nature*. 1999;398(6727):513-7. doi: 10.1038/19077. PubMed PMID: 10206644.
584. Borchelt DR, Thinakaran G, Eckman CB, Lee MK, Davenport F, Ratovitsky T, Prada CM, Kim G, Seekins S, Yager D, Slunt HH, Wang R, Seeger M, Levey AI, Gandy SE, Copeland NG, Jenkins NA, Price DL, Younkin SG, Sisodia SS. Familial Alzheimer's disease-linked presenilin 1 variants elevate Abeta1-42/1-40 ratio in vitro and in vivo. *Neuron*. 1996;17(5):1005-13. PubMed PMID: 8938131.
585. Sudoh S, Kawamura Y, Sato S, Wang R, Saido TC, Oyama F, Sakaki Y, Komano H, Yanagisawa K. Presenilin 1 mutations linked to familial Alzheimer's disease increase the intracellular levels of amyloid beta-protein 1-42 and its N-terminally truncated variant(s) which are generated at distinct sites. *Journal of neurochemistry*. 1998;71(4):1535-43. PubMed PMID: 9751187.
586. Sato T, Dohmae N, Qi Y, Kakuda N, Misonou H, Mitsumori R, Maruyama H, Koo EH, Haass C, Takio K, Morishima-Kawashima M, Ishiura S, Ihara Y. Potential link between amyloid beta-protein 42 and C-terminal fragment gamma 49-99 of beta-amyloid precursor protein. *The Journal of biological chemistry*. 2003;278(27):24294-301. doi: 10.1074/jbc.M211161200. PubMed PMID: 12707272.
587. Burdick D, Soreghan B, Kwon M, Kosmoski J, Knauer M, Henschen A, Yates J, Cotman C, Glabe C. Assembly and aggregation properties of synthetic Alzheimer's A4/beta amyloid peptide analogs. *The Journal of biological chemistry*. 1992;267(1):546-54. PubMed PMID: 1730616.
588. Duering M, Grimm MO, Grimm HS, Schroder J, Hartmann T. Mean age of onset in familial Alzheimer's disease is determined by amyloid beta 42. *Neurobiology of aging*. 2005;26(6):785-8. doi: 10.1016/j.neurobiolaging.2004.08.002. PubMed PMID: 15718035.
589. Crook R, Verkoniemi A, Perez-Tur J, Mehta N, Baker M, Houlden H, Farrer M, Hutton M, Lincoln S, Hardy J, Gwinn K, Somer M, Paetau A, Kalimo H, Ylikoski R, Poyhonen M, Kucera S, Haltia M. A variant of Alzheimer's disease with spastic paraparesis and unusual plaques due to deletion of exon 9 of presenilin 1. *Nature medicine*. 1998;4(4):452-5. PubMed PMID: 9546792.
590. Hardy J. Amyloid, the presenilins and Alzheimer's disease. *Trends in neurosciences*. 1997;20(4):154-9. PubMed PMID: 9106355.
591. Zhang Z, Hartmann H, Do VM, Abramowski D, Sturchler-Pierrat C, Staufenbiel M, Sommer B, van de Wetering M, Clevers H, Saftig P, De Strooper B, He X, Yankner BA. Destabilization of beta-catenin by mutations in presenilin-1 potentiates neuronal apoptosis. *Nature*. 1998;395(6703):698-702. doi: 10.1038/27208. PubMed PMID: 9790190.
592. Satoh J, Kuroda Y. Beta-catenin expression in human neural cell lines following exposure to cytokines and growth factors. *Neuropathology : official journal of the Japanese Society of Neuropathology*. 2000;20(2):113-23. PubMed PMID: 10935448.
593. Guerreiro RJ, Gustafson DR, Hardy J. The genetic architecture of Alzheimer's disease: beyond APP, PSENs and APOE. *Neurobiology of aging*. 2012;33(3):437-56. doi: 10.1016/j.neurobiolaging.2010.03.025. PubMed PMID: 20594621; PubMed Central PMCID: PMC2980860.
594. Utermann G, Pruin N, Steinmetz A. Polymorphism of apolipoprotein E. III. Effect of a single polymorphic gene locus on plasma lipid levels in man. *Clinical genetics*. 1979;15(1):63-72. PubMed PMID: 759055.
595. Zannis VI, Just PW, Breslow JL. Human apolipoprotein E isoprotein subclasses are genetically determined. *American journal of human genetics*. 1981;33(1):11-24. PubMed PMID: 7468588; PubMed Central PMCID: PMC1684875.
596. Lusis AJ, Heinzmann C, Sparkes RS, Scott J, Knott TJ, Geller R, Sparkes MC, Mohandas T. Regional mapping of human chromosome 19: organization of genes for plasma lipid transport (APOC1, -C2, and -E and LDLR) and the genes C3, PEPD, and GPI. *Proceedings of the National Academy of Sciences of the United States of America*. 1986;83(11):3929-33. PubMed PMID: 3459164; PubMed Central PMCID: PMC323638.
597. Raber J, Huang Y, Ashford JW. ApoE genotype accounts for the vast majority of AD risk and AD pathology. *Neurobiology of aging*. 2004;25(5):641-50. doi: 10.1016/j.neurobiolaging.2003.12.023. PubMed PMID: 15172743.

598. Corder EH, Saunders AM, Strittmatter WJ, Schmechel DE, Gaskell PC, Small GW, Roses AD, Haines JL, Pericak-Vance MA. Gene dose of apolipoprotein E type 4 allele and the risk of Alzheimer's disease in late onset families. *Science*. 1993;261(5123):921-3. PubMed PMID: 8346443.
599. Tiraboschi P, Hansen LA, Masliah E, Alford M, Thal LJ, Corey-Bloom J. Impact of APOE genotype on neuropathologic and neurochemical markers of Alzheimer disease. *Neurology*. 2004;62(11):1977-83. PubMed PMID: 15184600.
600. Reiman EM, Chen K, Liu X, Bandy D, Yu M, Lee W, Ayutyanont N, Keppler J, Reeder SA, Langbaum JB, Alexander GE, Klunk WE, Mathis CA, Price JC, Aizenstein HJ, DeKosky ST, Caselli RJ. Fibrillar amyloid-beta burden in cognitively normal people at 3 levels of genetic risk for Alzheimer's disease. *Proceedings of the National Academy of Sciences of the United States of America*. 2009;106(16):6820-5. doi: 10.1073/pnas.0900345106. PubMed PMID: 19346482; PubMed Central PMCID: PMC2665196.
601. Levy-Lahad E, Lahad A, Wijsman EM, Bird TD, Schellenberg GD. Apolipoprotein E genotypes and age of onset in early-onset familial Alzheimer's disease. *Annals of neurology*. 1995;38(4):678-80. doi: 10.1002/ana.410380420. PubMed PMID: 7574468.
602. Sorbi S, Nacmias B, Forleo P, Piacentini S, Latorraca S, Amaducci L. Epistatic effect of APP717 mutation and apolipoprotein E genotype in familial Alzheimer's disease. *Annals of neurology*. 1995;38(1):124-7. doi: 10.1002/ana.410380120. PubMed PMID: 7611715.
603. Van Broeckhoven C, Backhovens H, Cruts M, Martin JJ, Crook R, Houlden H, Hardy J. APOE genotype does not modulate age of onset in families with chromosome 14 encoded Alzheimer's disease. *Neuroscience letters*. 1994;169(1-2):179-80. PubMed PMID: 8047278.
604. Farrer LA, Cupples LA, Haines JL, Hyman B, Kukull WA, Mayeux R, Myers RH, Pericak-Vance MA, Risch N, van Duijn CM. Effects of age, sex, and ethnicity on the association between apolipoprotein E genotype and Alzheimer disease. A meta-analysis. APOE and Alzheimer Disease Meta Analysis Consortium. *Jama*. 1997;278(16):1349-56. PubMed PMID: 9343467.
605. Kalaria RN, Maestre GE, Arizaga R, Friedland RP, Galasko D, Hall K, Luchsinger JA, Ogunniyi A, Perry EK, Potocnik F, Prince M, Stewart R, Wimo A, Zhang ZX, Antuono P, World Federation of Neurology Dementia Research G. Alzheimer's disease and vascular dementia in developing countries: prevalence, management, and risk factors. *The Lancet Neurology*. 2008;7(9):812-26. doi: 10.1016/S1474-4422(08)70169-8. PubMed PMID: 18667359; PubMed Central PMCID: PMC2860610.
606. Siest G, Pillot T, Regis-Bailly A, Leininger-Muller B, Steinmetz J, Galteau MM, Visvikis S. Apolipoprotein E: an important gene and protein to follow in laboratory medicine. *Clinical chemistry*. 1995;41(8 Pt 1):1068-86. PubMed PMID: 7628082.
607. Weisgraber KH. Apolipoprotein E: structure-function relationships. *Advances in protein chemistry*. 1994;45:249-302. PubMed PMID: 8154371.
608. Herz J, Beffert U. Apolipoprotein E receptors: linking brain development and Alzheimer's disease. *Nature reviews Neuroscience*. 2000;1(1):51-8. doi: 10.1038/35036221. PubMed PMID: 11252768.
609. Rensen PC, Jong MC, van Vark LC, van der Boom H, Hendriks WL, van Berkel TJ, Biessen EA, Havekes LM. Apolipoprotein E is resistant to intracellular degradation in vitro and in vivo. Evidence for retroendocytosis. *The Journal of biological chemistry*. 2000;275(12):8564-71. PubMed PMID: 10722695.
610. Pitas RE, Boyles JK, Lee SH, Hui D, Weisgraber KH. Lipoproteins and their receptors in the central nervous system. Characterization of the lipoproteins in cerebrospinal fluid and identification of apolipoprotein B,E(LDL) receptors in the brain. *The Journal of biological chemistry*. 1987;262(29):14352-60. PubMed PMID: 3115992.
611. Fagan AM, Holtzman DM, Munson G, Mathur T, Schneider D, Chang LK, Getz GS, Reardon CA, Lukens J, Shah JA, LaDu MJ. Unique lipoproteins secreted by primary astrocytes from wild type, apoE (-/-), and human apoE transgenic mice. *The Journal of biological chemistry*. 1999;274(42):30001-7. PubMed PMID: 10514484.
612. Pfrieger FW. Outsourcing in the brain: do neurons depend on cholesterol delivery by astrocytes? *BioEssays : news and reviews in molecular, cellular and developmental biology*. 2003;25(1):72-8. doi: 10.1002/bies.10195. PubMed PMID: 12508285.
613. Mahley RW. Apolipoprotein E: cholesterol transport protein with expanding role in cell biology. *Science*. 1988;240(4852):622-30. PubMed PMID: 3283935.

614. Anderson R, Barnes JC, Bliss TV, Cain DP, Cambon K, Davies HA, Errington ML, Fellows LA, Gray RA, Hoh T, Stewart M, Large CH, Higgins GA. Behavioural, physiological and morphological analysis of a line of apolipoprotein E knockout mouse. *Neuroscience*. 1998;85(1):93-110. PubMed PMID: 9607706.
615. Vance JE, Campenot RB, Vance DE. The synthesis and transport of lipids for axonal growth and nerve regeneration. *Biochimica et biophysica acta*. 2000;1486(1):84-96. PubMed PMID: 10856715.
616. Mahley RW, Rall SC, Jr. Apolipoprotein E: far more than a lipid transport protein. *Annual review of genomics and human genetics*. 2000;1:507-37. doi: 10.1146/annurev.genom.1.1.507. PubMed PMID: 11701639.
617. Strittmatter WJ, Weisgraber KH, Huang DY, Dong LM, Salvesen GS, Pericak-Vance M, Schmechel D, Saunders AM, Goldgaber D, Roses AD. Binding of human apolipoprotein E to synthetic amyloid beta peptide: isoform-specific effects and implications for late-onset Alzheimer disease. *Proceedings of the National Academy of Sciences of the United States of America*. 1993;90(17):8098-102. PubMed PMID: 8367470; PubMed Central PMCID: PMC47295.
618. Tokuda T, Calero M, Matsubara E, Vidal R, Kumar A, Permanne B, Zlokovic B, Smith JD, Ladu MJ, Rostagno A, Frangione B, Ghiso J. Lipidation of apolipoprotein E influences its isoform-specific interaction with Alzheimer's amyloid beta peptides. *The Biochemical journal*. 2000;348 Pt 2:359-65. PubMed PMID: 10816430; PubMed Central PMCID: PMC1221074.
619. Beffert U, Poirier J. ApoE associated with lipid has a reduced capacity to inhibit beta-amyloid fibril formation. *Neuroreport*. 1998;9(14):3321-3. PubMed PMID: 9831470.
620. Webster S, Rogers J. Relative efficacies of amyloid beta peptide (A beta) binding proteins in A beta aggregation. *Journal of neuroscience research*. 1996;46(1):58-66. doi: 10.1002/(SICI)1097-4547(19961001)46:1<58::AID-JNR8>3.0.CO;2-E. PubMed PMID: 8892106.
621. Bales KR, Verina T, Dodel RC, Du Y, Altstiel L, Bender M, Hyslop P, Johnstone EM, Little SP, Cummins DJ, Piccardo P, Ghetti B, Paul SM. Lack of apolipoprotein E dramatically reduces amyloid beta-peptide deposition. *Nature genetics*. 1997;17(3):263-4. doi: 10.1038/ng1197-263. PubMed PMID: 9354781.
622. Holtzman DM, Bales KR, Tenkova T, Fagan AM, Parsadanian M, Sartorius LJ, Mackey B, Olney J, McKeel D, Wozniak D, Paul SM. Apolipoprotein E isoform-dependent amyloid deposition and neuritic degeneration in a mouse model of Alzheimer's disease. *Proceedings of the National Academy of Sciences of the United States of America*. 2000;97(6):2892-7. doi: 10.1073/pnas.050004797. PubMed PMID: 10694577; PubMed Central PMCID: PMC16026.
623. Fagan AM, Watson M, Parsadanian M, Bales KR, Paul SM, Holtzman DM. Human and murine ApoE markedly alters A beta metabolism before and after plaque formation in a mouse model of Alzheimer's disease. *Neurobiology of disease*. 2002;9(3):305-18. doi: 10.1006/nbdi.2002.0483. PubMed PMID: 11950276.
624. Irizarry MC, Cheung BS, Rebeck GW, Paul SM, Bales KR, Hyman BT. Apolipoprotein E affects the amount, form, and anatomical distribution of amyloid beta-peptide deposition in homozygous APP(V717F) transgenic mice. *Acta neuropathologica*. 2000;100(5):451-8. PubMed PMID: 11045665.
625. Buttini M, Yu GQ, Shockley K, Huang Y, Jones B, Masliah E, Mallory M, Yeo T, Longo FM, Mucke L. Modulation of Alzheimer-like synaptic and cholinergic deficits in transgenic mice by human apolipoprotein E depends on isoform, aging, and overexpression of amyloid beta peptides but not on plaque formation. *The Journal of neuroscience : the official journal of the Society for Neuroscience*. 2002;22(24):10539-48. PubMed PMID: 12486146.
626. Dolev I, Michaelson DM. A nontransgenic mouse model shows inducible amyloid-beta (Abeta) peptide deposition and elucidates the role of apolipoprotein E in the amyloid cascade. *Proceedings of the National Academy of Sciences of the United States of America*. 2004;101(38):13909-14. doi: 10.1073/pnas.0404458101. PubMed PMID: 15365176; PubMed Central PMCID: PMC518852.
627. He X, Cooley K, Chung CH, Dashti N, Tang J. Apolipoprotein receptor 2 and X11 alpha/beta mediate apolipoprotein E-induced endocytosis of amyloid-beta precursor protein and beta-secretase, leading to amyloid-beta production. *The Journal of neuroscience : the official journal of the Society for Neuroscience*. 2007;27(15):4052-60. doi: 10.1523/JNEUROSCI.3993-06.2007. PubMed PMID: 17428983.
628. Ye S, Huang Y, Mullendorff K, Dong L, Giedt G, Meng EC, Cohen FE, Kuntz ID, Weisgraber KH, Mahley RW. Apolipoprotein (apo) E4 enhances amyloid beta peptide production in cultured neuronal cells: apoE structure as a potential therapeutic target. *Proceedings of the National Academy of Sciences of the United States of America*. 2005;102(51):18700-5. doi: 10.1073/pnas.0508693102. PubMed PMID: 16344478; PubMed Central PMCID: PMC1311738.

629. Jiang Q, Lee CY, Mandrekar S, Wilkinson B, Cramer P, Zelcer N, Mann K, Lamb B, Willson TM, Collins JL, Richardson JC, Smith JD, Comery TA, Riddell D, Holtzman DM, Tontonoz P, Landreth GE. ApoE promotes the proteolytic degradation of A β . *Neuron*. 2008;58(5):681-93. doi: 10.1016/j.neuron.2008.04.010. PubMed PMID: 18549781; PubMed Central PMCID: PMC2493297.
630. Koistinaho M, Lin S, Wu X, Esterman M, Koger D, Hanson J, Higgs R, Liu F, Malkani S, Bales KR, Paul SM. Apolipoprotein E promotes astrocyte colocalization and degradation of deposited amyloid-beta peptides. *Nature medicine*. 2004;10(7):719-26. doi: 10.1038/nm1058. PubMed PMID: 15195085.
631. Nielsen HM, Veerhuis R, Holmqvist B, Janciauskiene S. Binding and uptake of A β 1-42 by primary human astrocytes in vitro. *Glia*. 2009;57(9):978-88. doi: 10.1002/glia.20822. PubMed PMID: 19062178.
632. Yamauchi K, Tozuka M, Hidaka H, Nakabayashi T, Sugano M, Katsuyama T. Isoform-specific effect of apolipoprotein E on endocytosis of beta-amyloid in cultures of neuroblastoma cells. *Annals of clinical and laboratory science*. 2002;32(1):65-74. PubMed PMID: 11848621.
633. Deane R, Sagare A, Hamm K, Parisi M, Lane S, Finn MB, Holtzman DM, Zlokovic BV. apoE isoform-specific disruption of amyloid beta peptide clearance from mouse brain. *The Journal of clinical investigation*. 2008;118(12):4002-13. doi: 10.1172/JCI36663. PubMed PMID: 19033669; PubMed Central PMCID: PMC2582453.
634. Ji Y, Permanne B, Sigurdsson EM, Holtzman DM, Wisniewski T. Amyloid beta_{40/42} clearance across the blood-brain barrier following intra-ventricular injections in wild-type, apoE knock-out and human apoE3 or E4 expressing transgenic mice. *Journal of Alzheimer's disease : JAD*. 2001;3(1):23-30. PubMed PMID: 12214069.
635. Martel CL, Mackic JB, Matsubara E, Governale S, Miguel C, Miao W, McComb JG, Frangione B, Ghiso J, Zlokovic BV. Isoform-specific effects of apolipoproteins E2, E3, and E4 on cerebral capillary sequestration and blood-brain barrier transport of circulating Alzheimer's amyloid beta. *Journal of neurochemistry*. 1997;69(5):1995-2004. PubMed PMID: 9349544.
636. Strittmatter WJ, Saunders AM, Goedert M, Weisgraber KH, Dong LM, Jakes R, Huang DY, Pericak-Vance M, Schmechel D, Roses AD. Isoform-specific interactions of apolipoprotein E with microtubule-associated protein tau: implications for Alzheimer disease. *Proceedings of the National Academy of Sciences of the United States of America*. 1994;91(23):11183-6. PubMed PMID: 7972031; PubMed Central PMCID: PMC45191.
637. DeMattos RB, Thorngate FE, Williams DL. A test of the cytosolic apolipoprotein E hypothesis fails to detect the escape of apolipoprotein E from the endocytic pathway into the cytosol and shows that direct expression of apolipoprotein E in the cytosol is cytotoxic. *The Journal of neuroscience : the official journal of the Society for Neuroscience*. 1999;19(7):2464-73. PubMed PMID: 10087061.
638. Chang S, ran Ma T, Miranda RD, Balestra ME, Mahley RW, Huang Y. Lipid- and receptor-binding regions of apolipoprotein E4 fragments act in concert to cause mitochondrial dysfunction and neurotoxicity. *Proceedings of the National Academy of Sciences of the United States of America*. 2005;102(51):18694-9. doi: 10.1073/pnas.0508254102. PubMed PMID: 16344479; PubMed Central PMCID: PMC1311737.
639. Harris FM, Brecht WJ, Xu Q, Mahley RW, Huang Y. Increased tau phosphorylation in apolipoprotein E4 transgenic mice is associated with activation of extracellular signal-regulated kinase: modulation by zinc. *The Journal of biological chemistry*. 2004;279(43):44795-801. doi: 10.1074/jbc.M408127200. PubMed PMID: 15322121.
640. Hoe HS, Harris DC, Rebeck GW. Multiple pathways of apolipoprotein E signaling in primary neurons. *Journal of neurochemistry*. 2005;93(1):145-55. doi: 10.1111/j.1471-4159.2004.03007.x. PubMed PMID: 15773914.
641. Bertrand P, Poirier J, Oda T, Finch CE, Pasinetti GM. Association of apolipoprotein E genotype with brain levels of apolipoprotein E and apolipoprotein J (clusterin) in Alzheimer disease. *Brain research Molecular brain research*. 1995;33(1):174-8. PubMed PMID: 8774959.
642. Bray NJ, Jehu L, Moskvina V, Buxbaum JD, Dracheva S, Haroutunian V, Williams J, Buckland PR, Owen MJ, O'Donovan MC. Allelic expression of APOE in human brain: effects of epsilon status and promoter haplotypes. *Human molecular genetics*. 2004;13(22):2885-92. doi: 10.1093/hmg/ddh299. PubMed PMID: 15385439.
643. Bekris LM, Millard SP, Galloway NM, Vuletic S, Albers JJ, Li G, Galasko DR, DeCarli C, Farlow MR, Clark CM, Quinn JF, Kaye JA, Schellenberg GD, Tsuang D, Peskind ER, Yu CE. Multiple SNPs within and surrounding the apolipoprotein E gene influence cerebrospinal fluid apolipoprotein E protein levels. *Journal of Alzheimer's disease : JAD*. 2008;13(3):255-66. PubMed PMID: 18430993; PubMed Central PMCID: PMC3192652.

644. Wahrle SE, Shah AR, Fagan AM, Smemo S, Kauwe JS, Grupe A, Hinrichs A, Mayo K, Jiang H, Thal LJ, Goate AM, Holtzman DM. Apolipoprotein E levels in cerebrospinal fluid and the effects of ABCA1 polymorphisms. *Molecular neurodegeneration*. 2007;2:7. doi: 10.1186/1750-1326-2-7. PubMed PMID: 17430597; PubMed Central PMCID: PMC1857699.
645. Sullivan PM, Mace BE, Maeda N, Schmechel DE. Marked regional differences of brain human apolipoprotein E expression in targeted replacement mice. *Neuroscience*. 2004;124(4):725-33. doi: 10.1016/j.neuroscience.2003.10.011. PubMed PMID: 15026113.
646. Fryer JD, Demattos RB, McCormick LM, O'Dell MA, Spinner ML, Bales KR, Paul SM, Sullivan PM, Parsadanian M, Bu G, Holtzman DM. The low density lipoprotein receptor regulates the level of central nervous system human and murine apolipoprotein E but does not modify amyloid plaque pathology in PDAPP mice. *The Journal of biological chemistry*. 2005;280(27):25754-9. doi: 10.1074/jbc.M502143200. PubMed PMID: 15888448.
647. Vitek MP, Brown CM, Colton CA. APOE genotype-specific differences in the innate immune response. *Neurobiology of aging*. 2009;30(9):1350-60. doi: 10.1016/j.neurobiolaging.2007.11.014. PubMed PMID: 18155324; PubMed Central PMCID: PMC2782461.
648. Riddell DR, Zhou H, Atchison K, Warwick HK, Atkinson PJ, Jefferson J, Xu L, Aschmies S, Kirksey Y, Hu Y, Wagner E, Parratt A, Xu J, Li Z, Zaleska MM, Jacobsen JS, Pangalos MN, Reinhart PH. Impact of apolipoprotein E (ApoE) polymorphism on brain ApoE levels. *The Journal of neuroscience : the official journal of the Society for Neuroscience*. 2008;28(45):11445-53. doi: 10.1523/JNEUROSCI.1972-08.2008. PubMed PMID: 18987181.
649. Slezak M, Pfrieder FW. New roles for astrocytes: regulation of CNS synaptogenesis. *Trends in neurosciences*. 2003;26(10):531-5. doi: 10.1016/j.tins.2003.08.005. PubMed PMID: 14522145.
650. Nathan BP, Bellosta S, Sanan DA, Weisgraber KH, Mahley RW, Pitas RE. Differential effects of apolipoproteins E3 and E4 on neuronal growth in vitro. *Science*. 1994;264(5160):850-2. PubMed PMID: 8171342.
651. White F, Nicoll JA, Roses AD, Horsburgh K. Impaired neuronal plasticity in transgenic mice expressing human apolipoprotein E4 compared to E3 in a model of entorhinal cortex lesion. *Neurobiology of disease*. 2001;8(4):611-25. doi: 10.1006/nbdi.2001.0401. PubMed PMID: 11493026.
652. Hartman RE, Wozniak DF, Nardi A, Olney JW, Sartorius L, Holtzman DM. Behavioral phenotyping of GFAP-*apoE3* and -*apoE4* transgenic mice: *apoE4* mice show profound working memory impairments in the absence of Alzheimer's-like neuropathology. *Experimental neurology*. 2001;170(2):326-44. doi: 10.1006/exnr.2001.7715. PubMed PMID: 11476599.
653. Mahley RW, Huang Y, Weisgraber KH. Detrimental effects of apolipoprotein E4: potential therapeutic targets in Alzheimer's disease. *Current Alzheimer research*. 2007;4(5):537-40. PubMed PMID: 18220516.
654. LaDu MJ, Shah JA, Reardon CA, Getz GS, Bu G, Hu J, Guo L, van Eldik LJ. Apolipoprotein E receptors mediate the effects of beta-amyloid on astrocyte cultures. *The Journal of biological chemistry*. 2000;275(43):33974-80. doi: 10.1074/jbc.M000602200. PubMed PMID: 10940295.
655. LaDu MJ, Shah JA, Reardon CA, Getz GS, Bu G, Hu J, Guo L, Van Eldik LJ. Apolipoprotein E and apolipoprotein E receptors modulate A beta-induced glial neuroinflammatory responses. *Neurochemistry international*. 2001;39(5-6):427-34. PubMed PMID: 11578778.
656. Lynch JR, Morgan D, Mance J, Matthew WD, Laskowitz DT. Apolipoprotein E modulates glial activation and the endogenous central nervous system inflammatory response. *Journal of neuroimmunology*. 2001;114(1-2):107-13. PubMed PMID: 11240021.
657. Guo L, LaDu MJ, Van Eldik LJ. A dual role for apolipoprotein e in neuroinflammation: anti- and pro-inflammatory activity. *Journal of molecular neuroscience : MN*. 2004;23(3):205-12. doi: 10.1385/JMN:23:3:205. PubMed PMID: 15181248.
658. Barger SW, Harmon AD. Microglial activation by Alzheimer amyloid precursor protein and modulation by apolipoprotein E. *Nature*. 1997;388(6645):878-81. doi: 10.1038/42257. PubMed PMID: 9278049.
659. Colton CA, Needham LK, Brown C, Cook D, Rasheed K, Burke JR, Strittmatter WJ, Schmechel DE, Vitek MP. APOE genotype-specific differences in human and mouse macrophage nitric oxide production. *Journal of neuroimmunology*. 2004;147(1-2):62-7. PubMed PMID: 14741429.

660. Lynch JR, Tang W, Wang H, Vitek MP, Bennett ER, Sullivan PM, Warner DS, Laskowitz DT. APOE genotype and an ApoE-mimetic peptide modify the systemic and central nervous system inflammatory response. *The Journal of biological chemistry*. 2003;278(49):48529-33. doi: 10.1074/jbc.M306923200. PubMed PMID: 14507923.
661. Sommer B. Alzheimer's disease and the amyloid cascade hypothesis: ten years on. *Current opinion in pharmacology*. 2002;2(1):87-92. PubMed PMID: 11786314.
662. Tanzi RE. The synaptic Abeta hypothesis of Alzheimer disease. *Nature neuroscience*. 2005;8(8):977-9. doi: 10.1038/nn0805-977. PubMed PMID: 16047022.
663. Selkoe DJ. Clearing the brain's amyloid cobwebs. *Neuron*. 2001;32(2):177-80. PubMed PMID: 11683988.
664. Zlokovic BV. The blood-brain barrier in health and chronic neurodegenerative disorders. *Neuron*. 2008;57(2):178-201. doi: 10.1016/j.neuron.2008.01.003. PubMed PMID: 18215617.
665. Games D, Adams D, Alessandrini R, Barbour R, Berthelette P, Blackwell C, Carr T, Clemens J, Donaldson T, Gillespie F, et al. Alzheimer-type neuropathology in transgenic mice overexpressing V717F beta-amyloid precursor protein. *Nature*. 1995;373(6514):523-7. doi: 10.1038/373523a0. PubMed PMID: 7845465.
666. Hsiao K, Chapman P, Nilsen S, Eckman C, Harigaya Y, Younkin S, Yang F, Cole G. Correlative memory deficits, Abeta elevation, and amyloid plaques in transgenic mice. *Science*. 1996;274(5284):99-102. PubMed PMID: 8810256.
667. Moechars D, Dewachter I, Lorent K, Reverse D, Baekelandt V, Naidu A, Tesseur I, Spittaels K, Haute CV, Checler F, Godaux E, Cordell B, Van Leuven F. Early phenotypic changes in transgenic mice that overexpress different mutants of amyloid precursor protein in brain. *The Journal of biological chemistry*. 1999;274(10):6483-92. PubMed PMID: 10037741.
668. Richardson JC, Kendal CE, Anderson R, Priest F, Gower E, Soden P, Gray R, Topps S, Howlett DR, Lavender D, Clarke NJ, Barnes JC, Haworth R, Stewart MG, Rupniak HT. Ultrastructural and behavioural changes precede amyloid deposition in a transgenic model of Alzheimer's disease. *Neuroscience*. 2003;122(1):213-28. PubMed PMID: 14596862.
669. Westerman MA, Cooper-Blacketer D, Mariash A, Kotilinek L, Kawarabayashi T, Younkin LH, Carlson GA, Younkin SG, Ashe KH. The relationship between Abeta and memory in the Tg2576 mouse model of Alzheimer's disease. *The Journal of neuroscience : the official journal of the Society for Neuroscience*. 2002;22(5):1858-67. PubMed PMID: 11880515.
670. Oakley H, Cole SL, Logan S, Maus E, Shao P, Craft J, Guillozet-Bongaarts A, Ohno M, Disterhoft J, Van Eldik L, Berry R, Vassar R. Intraneuronal beta-amyloid aggregates, neurodegeneration, and neuron loss in transgenic mice with five familial Alzheimer's disease mutations: potential factors in amyloid plaque formation. *The Journal of neuroscience : the official journal of the Society for Neuroscience*. 2006;26(40):10129-40. doi: 10.1523/JNEUROSCI.1202-06.2006. PubMed PMID: 17021169.
671. Oddo S, Caccamo A, Kitazawa M, Tseng BP, LaFerla FM. Amyloid deposition precedes tangle formation in a triple transgenic model of Alzheimer's disease. *Neurobiology of aging*. 2003;24(8):1063-70. PubMed PMID: 14643377.
672. Oddo S, Caccamo A, Shepherd JD, Murphy MP, Golde TE, Kaye R, Metherate R, Mattson MP, Akbari Y, LaFerla FM. Triple-transgenic model of Alzheimer's disease with plaques and tangles: intracellular Abeta and synaptic dysfunction. *Neuron*. 2003;39(3):409-21. PubMed PMID: 12895417.
673. Hyman BT, West HL, Rebeck GW, Buldyrev SV, Mantegna RN, Ukleja M, Havlin S, Stanley HE. Quantitative analysis of senile plaques in Alzheimer disease: observation of log-normal size distribution and molecular epidemiology of differences associated with apolipoprotein E genotype and trisomy 21 (Down syndrome). *Proceedings of the National Academy of Sciences of the United States of America*. 1995;92(8):3586-90. PubMed PMID: 7724603; PubMed Central PMCID: PMC42212.
674. Spires-Jones TL, Meyer-Luehmann M, Osetek JD, Jones PB, Stern EA, Bacskai BJ, Hyman BT. Impaired spine stability underlies plaque-related spine loss in an Alzheimer's disease mouse model. *The American journal of pathology*. 2007;171(4):1304-11. doi: 10.2353/ajpath.2007.070055. PubMed PMID: 17717139; PubMed Central PMCID: PMC1988879.
675. Koffie RM, Meyer-Luehmann M, Hashimoto T, Adams KW, Mielke ML, Garcia-Alloza M, Micheva KD, Smith SJ, Kim ML, Lee VM, Hyman BT, Spires-Jones TL. Oligomeric amyloid beta associates with postsynaptic densities and correlates with excitatory synapse loss near senile plaques. *Proceedings of the National Academy of Sciences of the United States of America*. 2009;106(10):4012-7. doi: 10.1073/pnas.0811698106. PubMed PMID: 19228947; PubMed Central PMCID: PMC2656196.

676. Walsh DM, Klyubin I, Fadeeva JV, Cullen WK, Anwyl R, Wolfe MS, Rowan MJ, Selkoe DJ. Naturally secreted oligomers of amyloid beta protein potently inhibit hippocampal long-term potentiation in vivo. *Nature*. 2002;416(6880):535-9. doi: 10.1038/416535a. PubMed PMID: 11932745.
677. Shankar GM, Leissring MA, Adame A, Sun X, Spooner E, Masliah E, Selkoe DJ, Lemere CA, Walsh DM. Biochemical and immunohistochemical analysis of an Alzheimer's disease mouse model reveals the presence of multiple cerebral Abeta assembly forms throughout life. *Neurobiology of disease*. 2009;36(2):293-302. doi: 10.1016/j.nbd.2009.07.021. PubMed PMID: 19660551; PubMed Central PMCID: PMC2782414.
678. Shankar GM, Li S, Mehta TH, Garcia-Munoz A, Shepardson NE, Smith I, Brett FM, Farrell MA, Rowan MJ, Lemere CA, Regan CM, Walsh DM, Sabatini BL, Selkoe DJ. Amyloid-beta protein dimers isolated directly from Alzheimer's brains impair synaptic plasticity and memory. *Nature medicine*. 2008;14(8):837-42. doi: 10.1038/nm1782. PubMed PMID: 18568035; PubMed Central PMCID: PMC2772133.
679. Li S, Jin M, Koeglsperger T, Shepardson NE, Shankar GM, Selkoe DJ. Soluble Abeta oligomers inhibit long-term potentiation through a mechanism involving excessive activation of extrasynaptic NR2B-containing NMDA receptors. *The Journal of neuroscience : the official journal of the Society for Neuroscience*. 2011;31(18):6627-38. doi: 10.1523/JNEUROSCI.0203-11.2011. PubMed PMID: 21543591; PubMed Central PMCID: PMC3100898.
680. Martins IC, Kuperstein I, Wilkinson H, Maes E, Vanbrabant M, Jonckheere W, Van Gelder P, Hartmann D, D'Hooge R, De Strooper B, Schymkowitz J, Rousseau F. Lipids revert inert Abeta amyloid fibrils to neurotoxic protofibrils that affect learning in mice. *The EMBO journal*. 2008;27(1):224-33. doi: 10.1038/sj.emboj.7601953. PubMed PMID: 18059472; PubMed Central PMCID: PMC2206134.
681. DeKosky ST, Scheff SW. Synapse loss in frontal cortex biopsies in Alzheimer's disease: correlation with cognitive severity. *Annals of neurology*. 1990;27(5):457-64. doi: 10.1002/ana.410270502. PubMed PMID: 2360787.
682. McLaurin J, Kierstead ME, Brown ME, Hawkes CA, Lambermon MH, Phinney AL, Darabie AA, Cousins JE, French JE, Lan MF, Chen F, Wong SS, Mount HT, Fraser PE, Westaway D, St George-Hyslop P. Cyclohexanehexol inhibitors of Abeta aggregation prevent and reverse Alzheimer phenotype in a mouse model. *Nature medicine*. 2006;12(7):801-8. doi: 10.1038/nm1423. PubMed PMID: 16767098.
683. Roberson ED, Halabisky B, Yoo JW, Yao J, Chin J, Yan F, Wu T, Hamto P, Devidze N, Yu GQ, Palop JJ, Noebels JL, Mucke L. Amyloid-beta/Fyn-induced synaptic, network, and cognitive impairments depend on tau levels in multiple mouse models of Alzheimer's disease. *The Journal of neuroscience : the official journal of the Society for Neuroscience*. 2011;31(2):700-11. doi: 10.1523/JNEUROSCI.4152-10.2011. PubMed PMID: 21228179; PubMed Central PMCID: PMC3325794.
684. Kamenetz F, Tomita T, Hsieh H, Seabrook G, Borchelt D, Iwatsubo T, Sisodia S, Malinow R. APP processing and synaptic function. *Neuron*. 2003;37(6):925-37. PubMed PMID: 12670422.
685. Hsieh H, Boehm J, Sato C, Iwatsubo T, Tomita T, Sisodia S, Malinow R. AMPAR removal underlies Abeta-induced synaptic depression and dendritic spine loss. *Neuron*. 2006;52(5):831-43. doi: 10.1016/j.neuron.2006.10.035. PubMed PMID: 17145504; PubMed Central PMCID: PMC1850952.
686. Shankar GM, Bloodgood BL, Townsend M, Walsh DM, Selkoe DJ, Sabatini BL. Natural oligomers of the Alzheimer amyloid-beta protein induce reversible synapse loss by modulating an NMDA-type glutamate receptor-dependent signaling pathway. *The Journal of neuroscience : the official journal of the Society for Neuroscience*. 2007;27(11):2866-75. doi: 10.1523/JNEUROSCI.4970-06.2007. PubMed PMID: 17360908.
687. Cirrito JR, Yamada KA, Finn MB, Sloviter RS, Bales KR, May PC, Schoepp DD, Paul SM, Mennicker S, Holtzman DM. Synaptic activity regulates interstitial fluid amyloid-beta levels in vivo. *Neuron*. 2005;48(6):913-22. doi: 10.1016/j.neuron.2005.10.028. PubMed PMID: 16364896.
688. Puzzo D, Privitera L, Leznik E, Fa M, Staniszewski A, Palmeri A, Arancio O. Picomolar amyloid-beta positively modulates synaptic plasticity and memory in hippocampus. *The Journal of neuroscience : the official journal of the Society for Neuroscience*. 2008;28(53):14537-45. doi: 10.1523/JNEUROSCI.2692-08.2008. PubMed PMID: 19118188; PubMed Central PMCID: PMC2673049.
689. Wei W, Nguyen LN, Kessels HW, Hagiwara H, Sisodia S, Malinow R. Amyloid beta from axons and dendrites reduces local spine number and plasticity. *Nature neuroscience*. 2010;13(2):190-6. doi: 10.1038/nn.2476. PubMed PMID: 20037574; PubMed Central PMCID: PMC3310198.

690. Abramov E, Dolev I, Fogel H, Ciccotosto GD, Ruff E, Slutsky I. Amyloid-beta as a positive endogenous regulator of release probability at hippocampal synapses. *Nature neuroscience*. 2009;12(12):1567-76. doi: 10.1038/nn.2433. PubMed PMID: 19935655.
691. Kullmann DM, Lamsa KP. Long-term synaptic plasticity in hippocampal interneurons. *Nature reviews Neuroscience*. 2007;8(9):687-99. doi: 10.1038/nrn2207. PubMed PMID: 17704811.
692. Mucke L, Selkoe DJ. Neurotoxicity of amyloid beta-protein: synaptic and network dysfunction. *Cold Spring Harbor perspectives in medicine*. 2012;2(7):a006338. doi: 10.1101/cshperspect.a006338. PubMed PMID: 22762015; PubMed Central PMCID: PMC3385944.
693. Snyder EM, Nong Y, Almeida CG, Paul S, Moran T, Choi EY, Nairn AC, Salter MW, Lombroso PJ, Gouras GK, Greengard P. Regulation of NMDA receptor trafficking by amyloid-beta. *Nature neuroscience*. 2005;8(8):1051-8. doi: 10.1038/nn1503. PubMed PMID: 16025111.
694. Wang Q, Walsh DM, Rowan MJ, Selkoe DJ, Anwyl R. Block of long-term potentiation by naturally secreted and synthetic amyloid beta-peptide in hippocampal slices is mediated via activation of the kinases c-Jun N-terminal kinase, cyclin-dependent kinase 5, and p38 mitogen-activated protein kinase as well as metabotropic glutamate receptor type 5. *The Journal of neuroscience : the official journal of the Society for Neuroscience*. 2004;24(13):3370-8. doi: 10.1523/JNEUROSCI.1633-03.2004. PubMed PMID: 15056716.
695. Tackenberg C, Brandt R. Divergent pathways mediate spine alterations and cell death induced by amyloid-beta, wild-type tau, and R406W tau. *The Journal of neuroscience : the official journal of the Society for Neuroscience*. 2009;29(46):14439-50. doi: 10.1523/JNEUROSCI.3590-09.2009. PubMed PMID: 19923278.
696. Thal DR, Holzer M, Rub U, Waldmann G, Gunzel S, Zedlick D, Schober R. Alzheimer-related tau-pathology in the perforant path target zone and in the hippocampal stratum oriens and radiatum correlates with onset and degree of dementia. *Experimental neurology*. 2000;163(1):98-110. doi: 10.1006/exnr.2000.7380. PubMed PMID: 10785448.
697. Gotz J, Ittner LM, Kins S. Do axonal defects in tau and amyloid precursor protein transgenic animals model axonopathy in Alzheimer's disease? *Journal of neurochemistry*. 2006;98(4):993-1006. doi: 10.1111/j.1471-4159.2006.03955.x. PubMed PMID: 16787410.
698. Ittner LM, Ke YD, Gotz J. Phosphorylated Tau interacts with c-Jun N-terminal kinase-interacting protein 1 (JIP1) in Alzheimer disease. *The Journal of biological chemistry*. 2009;284(31):20909-16. doi: 10.1074/jbc.M109.014472. PubMed PMID: 19491104; PubMed Central PMCID: PMC2742856.
699. Billingsley ML, Kincaid RL. Regulated phosphorylation and dephosphorylation of tau protein: effects on microtubule interaction, intracellular trafficking and neurodegeneration. *The Biochemical journal*. 1997;323 (Pt 3):577-91. PubMed PMID: 9169588; PubMed Central PMCID: PMC1218358.
700. Mandelkow E, von Bergen M, Biernat J, Mandelkow EM. Structural principles of tau and the paired helical filaments of Alzheimer's disease. *Brain pathology*. 2007;17(1):83-90. doi: 10.1111/j.1750-3639.2007.00053.x. PubMed PMID: 17493042.
701. Hanger DP, Byers HL, Wray S, Leung KY, Saxton MJ, Seereeram A, Reynolds CH, Ward MA, Anderton BH. Novel phosphorylation sites in tau from Alzheimer brain support a role for casein kinase 1 in disease pathogenesis. *The Journal of biological chemistry*. 2007;282(32):23645-54. doi: 10.1074/jbc.M703269200. PubMed PMID: 17562708.
702. Hanger DP, Seereeram A, Noble W. Mediators of tau phosphorylation in the pathogenesis of Alzheimer's disease. *Expert review of neurotherapeutics*. 2009;9(11):1647-66. doi: 10.1586/ern.09.104. PubMed PMID: 19903024.
703. Amniai L, Barbier P, Sillen A, Wieruszeski JM, Peyrot V, Lippens G, Landrieu I. Alzheimer disease specific phosphoepitopes of Tau interfere with assembly of tubulin but not binding to microtubules. *FASEB journal : official publication of the Federation of American Societies for Experimental Biology*. 2009;23(4):1146-52. doi: 10.1096/fj.08-121590. PubMed PMID: 19074508.
704. Cuchillo-Ibanez I, Seereeram A, Byers HL, Leung KY, Ward MA, Anderton BH, Hanger DP. Phosphorylation of tau regulates its axonal transport by controlling its binding to kinesin. *FASEB journal : official publication of the Federation of American Societies for Experimental Biology*. 2008;22(9):3186-95. doi: 10.1096/fj.08-109181. PubMed PMID: 18511549.
705. Andorfer C, Acker CM, Kress Y, Hof PR, Duff K, Davies P. Cell-cycle reentry and cell death in transgenic mice expressing nonmutant human tau isoforms. *The Journal of neuroscience : the official journal of the Society for Neuroscience*. 2005;25(22):5446-54. doi: 10.1523/JNEUROSCI.4637-04.2005. PubMed PMID: 15930395.

706. Zempel H, Thies E, Mandelkow E, Mandelkow EM. Abeta oligomers cause localized Ca(2+) elevation, missorting of endogenous Tau into dendrites, Tau phosphorylation, and destruction of microtubules and spines. *The Journal of neuroscience : the official journal of the Society for Neuroscience*. 2010;30(36):11938-50. doi: 10.1523/JNEUROSCI.2357-10.2010. PubMed PMID: 20826658.
707. Terwel D, Muyliaert D, Dewachter I, Borghgraef P, Croes S, Devijver H, Van Leuven F. Amyloid activates GSK-3beta to aggravate neuronal tauopathy in bigenic mice. *The American journal of pathology*. 2008;172(3):786-98. doi: 10.2353/ajpath.2008.070904. PubMed PMID: 18258852; PubMed Central PMCID: PMC2258274.
708. Hutton M, Perez-Tur J, Hardy J. Genetics of Alzheimer's disease. *Essays in biochemistry*. 1998;33:117-31. PubMed PMID: 10488446.
709. Ballatore C, Lee VM, Trojanowski JQ. Tau-mediated neurodegeneration in Alzheimer's disease and related disorders. *Nature reviews Neuroscience*. 2007;8(9):663-72. doi: 10.1038/nrn2194. PubMed PMID: 17684513.
710. Ferreira A, Lu Q, Orecchio L, Kosik KS. Selective phosphorylation of adult tau isoforms in mature hippocampal neurons exposed to fibrillar A beta. *Molecular and cellular neurosciences*. 1997;9(3):220-34. doi: 10.1006/mcne.1997.0615. PubMed PMID: 9245504.
711. Takashima A, Honda T, Yasutake K, Michel G, Murayama O, Murayama M, Ishiguro K, Yamaguchi H. Activation of tau protein kinase I/glycogen synthase kinase-3beta by amyloid beta peptide (25-35) enhances phosphorylation of tau in hippocampal neurons. *Neuroscience research*. 1998;31(4):317-23. PubMed PMID: 9809590.
712. Ma QL, Lim GP, Harris-White ME, Yang F, Ambegaokar SS, Ubada OJ, Glabe CG, Teter B, Frautschy SA, Cole GM. Antibodies against beta-amyloid reduce Abeta oligomers, glycogen synthase kinase-3beta activation and tau phosphorylation in vivo and in vitro. *Journal of neuroscience research*. 2006;83(3):374-84. doi: 10.1002/jnr.20734. PubMed PMID: 16385556.
713. Ma QL, Yang F, Rosario ER, Ubada OJ, Beech W, Gant DJ, Chen PP, Hudspeth B, Chen C, Zhao Y, Vinters HV, Frautschy SA, Cole GM. Beta-amyloid oligomers induce phosphorylation of tau and inactivation of insulin receptor substrate via c-Jun N-terminal kinase signaling: suppression by omega-3 fatty acids and curcumin. *The Journal of neuroscience : the official journal of the Society for Neuroscience*. 2009;29(28):9078-89. doi: 10.1523/JNEUROSCI.1071-09.2009. PubMed PMID: 19605645; PubMed Central PMCID: PMC3849615.
714. Mairet-Coello G, Courchet J, Pieraut S, Courchet V, Maximov A, Polleux F. The CAMKK2-AMPK kinase pathway mediates the synaptotoxic effects of Abeta oligomers through Tau phosphorylation. *Neuron*. 2013;78(1):94-108. doi: 10.1016/j.neuron.2013.02.003. PubMed PMID: 23583109; PubMed Central PMCID: PMC3784324.
715. Sturchler-Pierrat C, Abramowski D, Duke M, Wiederhold KH, Mistl C, Rothacher S, Ledermann B, Burki K, Frey P, Paganetti PA, Waridel C, Calhoun ME, Jucker M, Probst A, Staufenbiel M, Sommer B. Two amyloid precursor protein transgenic mouse models with Alzheimer disease-like pathology. *Proceedings of the National Academy of Sciences of the United States of America*. 1997;94(24):13287-92. PubMed PMID: 9371838; PubMed Central PMCID: PMC24301.
716. Duyckaerts C, Potier MC, Delatour B. Alzheimer disease models and human neuropathology: similarities and differences. *Acta neuropathologica*. 2008;115(1):5-38. doi: 10.1007/s00401-007-0312-8. PubMed PMID: 18038275; PubMed Central PMCID: PMC2100431.
717. Echeverria V, Ducatenzeiler A, Dowd E, Janne J, Grant SM, Szyf M, Wandosell F, Avila J, Grimm H, Dunnett SB, Hartmann T, Alhonen L, Cuelllo AC. Altered mitogen-activated protein kinase signaling, tau hyperphosphorylation and mild spatial learning dysfunction in transgenic rats expressing the beta-amyloid peptide intracellularly in hippocampal and cortical neurons. *Neuroscience*. 2004;129(3):583-92. doi: 10.1016/j.neuroscience.2004.07.036. PubMed PMID: 15541880.
718. Cohen RM, Rezai-Zadeh K, Weitz TM, Rentsendorj A, Gate D, Spivak I, Bholat Y, Vasilevko V, Glabe CG, Breunig JJ, Rakic P, Davtayan H, Agadjanyan MG, Kepe V, Barrio JR, Bannykh S, Szekely CA, Pechnick RN, Town T. A transgenic Alzheimer rat with plaques, tau pathology, behavioral impairment, oligomeric abeta, and frank neuronal loss. *The Journal of neuroscience : the official journal of the Society for Neuroscience*. 2013;33(15):6245-56. doi: 10.1523/JNEUROSCI.3672-12.2013. PubMed PMID: 23575824; PubMed Central PMCID: PMC3720142.
719. Gotz J, Chen F, van Dorpe J, Nitsch RM. Formation of neurofibrillary tangles in P301 tau transgenic mice induced by Abeta 42 fibrils. *Science*. 2001;293(5534):1491-5. doi: 10.1126/science.1062097. PubMed PMID: 11520988.

720. Braak H, Del Tredici K. Amyloid-beta may be released from non-junctional varicosities of axons generated from abnormal tau-containing brainstem nuclei in sporadic Alzheimer's disease: a hypothesis. *Acta neuropathologica*. 2013;126(2):303-6. doi: 10.1007/s00401-013-1153-2. PubMed PMID: 23824268.
721. Jack CR, Jr., Knopman DS, Jagust WJ, Shaw LM, Aisen PS, Weiner MW, Petersen RC, Trojanowski JQ. Hypothetical model of dynamic biomarkers of the Alzheimer's pathological cascade. *The Lancet Neurology*. 2010;9(1):119-28. doi: 10.1016/S1474-4422(09)70299-6. PubMed PMID: 20083042; PubMed Central PMCID: PMC2819840.
722. Musiek ES, Holtzman DM. Origins of Alzheimer's disease: reconciling cerebrospinal fluid biomarker and neuropathology data regarding the temporal sequence of amyloid-beta and tau involvement. *Current opinion in neurology*. 2012;25(6):715-20. doi: 10.1097/WCO.0b013e32835a30f4. PubMed PMID: 23041958; PubMed Central PMCID: PMC3682920.
723. Price JL, Morris JC. So what if tangles precede plaques? *Neurobiology of aging*. 2004;25(6):721-3; discussion 43-6. doi: 10.1016/j.neurobiolaging.2003.12.017. PubMed PMID: 15165694.
724. Jack CR, Jr., Knopman DS, Jagust WJ, Petersen RC, Weiner MW, Aisen PS, Shaw LM, Vemuri P, Wiste HJ, Weigand SD, Lesnick TG, Pankratz VS, Donohue MC, Trojanowski JQ. Tracking pathophysiological processes in Alzheimer's disease: an updated hypothetical model of dynamic biomarkers. *The Lancet Neurology*. 2013;12(2):207-16. doi: 10.1016/S1474-4422(12)70291-0. PubMed PMID: 23332364; PubMed Central PMCID: PMC3622225.
725. Hertel C, Terzi E, Hauser N, Jakob-Rotne R, Seelig J, Kemp JA. Inhibition of the electrostatic interaction between beta-amyloid peptide and membranes prevents beta-amyloid-induced toxicity. *Proceedings of the National Academy of Sciences of the United States of America*. 1997;94(17):9412-6. PubMed PMID: 9256496; PubMed Central PMCID: PMC23204.
726. Wang HY, Lee DH, D'Andrea MR, Peterson PA, Shank RP, Reitz AB. beta-Amyloid(1-42) binds to alpha7 nicotinic acetylcholine receptor with high affinity. Implications for Alzheimer's disease pathology. *The Journal of biological chemistry*. 2000;275(8):5626-32. PubMed PMID: 10681545.
727. Yan SD, Roher A, Chaney M, Zlokovic B, Schmidt AM, Stern D. Cellular cofactors potentiating induction of stress and cytotoxicity by amyloid beta-peptide. *Biochimica et biophysica acta*. 2000;1502(1):145-57. PubMed PMID: 10899440.
728. Lauren J, Gimbel DA, Nygaard HB, Gilbert JW, Strittmatter SM. Cellular prion protein mediates impairment of synaptic plasticity by amyloid-beta oligomers. *Nature*. 2009;457(7233):1128-32. doi: 10.1038/nature07761. PubMed PMID: 19242475; PubMed Central PMCID: PMC2748841.
729. Cisse M, Halabisky B, Harris J, Devidze N, Dubal DB, Sun B, Orr A, Lotz G, Kim DH, Hamto P, Ho K, Yu GQ, Mucke L. Reversing EphB2 depletion rescues cognitive functions in Alzheimer model. *Nature*. 2011;469(7328):47-52. doi: 10.1038/nature09635. PubMed PMID: 21113149; PubMed Central PMCID: PMC3030448.
730. Kim T, Vidal GS, Djurisic M, William CM, Birnbaum ME, Garcia KC, Hyman BT, Shatz CJ. Human LILRB2 is a beta-amyloid receptor and its murine homolog PirB regulates synaptic plasticity in an Alzheimer's model. *Science*. 2013;341(6152):1399-404. doi: 10.1126/science.1242077. PubMed PMID: 24052308; PubMed Central PMCID: PMC3853120.
731. Shipton OA, Leitz JR, Dworzak J, Acton CE, Tunbridge EM, Denk F, Dawson HN, Vitek MP, Wade-Martins R, Paulsen O, Vargas-Caballero M. Tau protein is required for amyloid {beta}-induced impairment of hippocampal long-term potentiation. *The Journal of neuroscience : the official journal of the Society for Neuroscience*. 2011;31(5):1688-92. doi: 10.1523/JNEUROSCI.2610-10.2011. PubMed PMID: 21289177; PubMed Central PMCID: PMC3836238.
732. Stancu IC, Vasconcelos B, Terwel D, Dewachter I. Models of beta-amyloid induced Tau-pathology: the long and "folded" road to understand the mechanism. *Molecular neurodegeneration*. 2014;9:51. doi: 10.1186/1750-1326-9-51. PubMed PMID: 25407337; PubMed Central PMCID: PMC4255655.
733. Ghosh S, Wu MD, Shaftel SS, Kyrkanides S, LaFerla FM, Olschowka JA, O'Banion MK. Sustained interleukin-1beta overexpression exacerbates tau pathology despite reduced amyloid burden in an Alzheimer's mouse model. *The Journal of neuroscience : the official journal of the Society for Neuroscience*. 2013;33(11):5053-64. doi: 10.1523/JNEUROSCI.4361-12.2013. PubMed PMID: 23486975; PubMed Central PMCID: PMC3637949.
734. Kitazawa M, Cheng D, Tsukamoto MR, Koike MA, Wes PD, Vasilevko V, Cribbs DH, LaFerla FM. Blocking IL-1 signaling rescues cognition, attenuates tau pathology, and restores neuronal beta-catenin pathway function in an

Alzheimer's disease model. *Journal of immunology*. 2011;187(12):6539-49. doi: 10.4049/jimmunol.1100620. PubMed PMID: 22095718; PubMed Central PMCID: PMC4072218.

735. Li Y, Liu L, Barger SW, Griffin WS. Interleukin-1 mediates pathological effects of microglia on tau phosphorylation and on synaptophysin synthesis in cortical neurons through a p38-MAPK pathway. *The Journal of neuroscience : the official journal of the Society for Neuroscience*. 2003;23(5):1605-11. PubMed PMID: 12629164; PubMed Central PMCID: PMC3833596.

736. Garwood CJ, Pooler AM, Atherton J, Hanger DP, Noble W. Astrocytes are important mediators of Abeta-induced neurotoxicity and tau phosphorylation in primary culture. *Cell death & disease*. 2011;2:e167. doi: 10.1038/cddis.2011.50. PubMed PMID: 21633390; PubMed Central PMCID: PMC3168992.

737. Jucker M, Walker LC. Self-propagation of pathogenic protein aggregates in neurodegenerative diseases. *Nature*. 2013;501(7465):45-51. doi: 10.1038/nature12481. PubMed PMID: 24005412; PubMed Central PMCID: PMC3963807.

738. Soto C, Estrada L, Castilla J. Amyloids, prions and the inherent infectious nature of misfolded protein aggregates. *Trends in biochemical sciences*. 2006;31(3):150-5. doi: 10.1016/j.tibs.2006.01.002. PubMed PMID: 16473510.

739. Clavaguera F, Bolmont T, Crowther RA, Abramowski D, Frank S, Probst A, Fraser G, Stalder AK, Beibel M, Staufenbiel M, Jucker M, Goedert M, Tolnay M. Transmission and spreading of tauopathy in transgenic mouse brain. *Nature cell biology*. 2009;11(7):909-13. doi: 10.1038/ncb1901. PubMed PMID: 19503072; PubMed Central PMCID: PMC2726961.

740. Iba M, Guo JL, McBride JD, Zhang B, Trojanowski JQ, Lee VM. Synthetic tau fibrils mediate transmission of neurofibrillary tangles in a transgenic mouse model of Alzheimer's-like tauopathy. *The Journal of neuroscience : the official journal of the Society for Neuroscience*. 2013;33(3):1024-37. doi: 10.1523/JNEUROSCI.2642-12.2013. PubMed PMID: 23325240; PubMed Central PMCID: PMC3575082.

741. Clavaguera F, Akatsu H, Fraser G, Crowther RA, Frank S, Hench J, Probst A, Winkler DT, Reichwald J, Staufenbiel M, Ghetti B, Goedert M, Tolnay M. Brain homogenates from human tauopathies induce tau inclusions in mouse brain. *Proceedings of the National Academy of Sciences of the United States of America*. 2013;110(23):9535-40. doi: 10.1073/pnas.1301175110. PubMed PMID: 23690619; PubMed Central PMCID: PMC3677441.

742. Guo JP, Arai T, Miklossy J, McGeer PL. Abeta and tau form soluble complexes that may promote self aggregation of both into the insoluble forms observed in Alzheimer's disease. *Proceedings of the National Academy of Sciences of the United States of America*. 2006;103(6):1953-8. doi: 10.1073/pnas.0509386103. PubMed PMID: 16446437; PubMed Central PMCID: PMC1413647.

743. Bolmont T, Clavaguera F, Meyer-Luehmann M, Herzog MC, Radde R, Staufenbiel M, Lewis J, Hutton M, Tolnay M, Jucker M. Induction of tau pathology by intracerebral infusion of amyloid-beta -containing brain extract and by amyloid-beta deposition in APP x Tau transgenic mice. *The American journal of pathology*. 2007;171(6):2012-20. doi: 10.2353/ajpath.2007.070403. PubMed PMID: 18055549; PubMed Central PMCID: PMC2111123.

744. Kuret J, Chirita CN, Congdon EE, Kannanayakal T, Li G, Necula M, Yin H, Zhong Q. Pathways of tau fibrillization. *Biochimica et biophysica acta*. 2005;1739(2-3):167-78. doi: 10.1016/j.bbadis.2004.06.016. PubMed PMID: 15615636.

745. Kuret J, Congdon EE, Li G, Yin H, Yu X, Zhong Q. Evaluating triggers and enhancers of tau fibrillization. *Microscopy research and technique*. 2005;67(3-4):141-55. doi: 10.1002/jemt.20187. PubMed PMID: 16103995.

746. Ross CA, Poirier MA. Protein aggregation and neurodegenerative disease. *Nature medicine*. 2004;10 Suppl:S10-7. doi: 10.1038/nm1066. PubMed PMID: 15272267.

747. Galvan M, David JP, Delacourte A, Luna J, Mena R. Sequence of neurofibrillary changes in aging and Alzheimer's disease: A confocal study with phospho-tau antibody, AD2. *Journal of Alzheimer's disease : JAD*. 2001;3(4):417-25. PubMed PMID: 12214046.

748. Maeda S, Sahara N, Saito Y, Murayama M, Yoshiike Y, Kim H, Miyasaka T, Murayama S, Ikai A, Takashima A. Granular tau oligomers as intermediates of tau filaments. *Biochemistry*. 2007;46(12):3856-61. doi: 10.1021/bi061359o. PubMed PMID: 17338548.

749. Mitchell TW, Nissanov J, Han LY, Mufson EJ, Schneider JA, Cochran EJ, Bennett DA, Lee VM, Trojanowski JQ, Arnold SE. Novel method to quantify neuropil threads in brains from elders with or without cognitive impairment. *The journal of histochemistry and cytochemistry : official journal of the Histochemistry Society*. 2000;48(12):1627-38. PubMed PMID: 11101631.

750. Ishihara T, Hong M, Zhang B, Nakagawa Y, Lee MK, Trojanowski JQ, Lee VM. Age-dependent emergence and progression of a tauopathy in transgenic mice overexpressing the shortest human tau isoform. *Neuron*. 1999;24(3):751-62. PubMed PMID: 10595524.
751. Zhang B, Maiti A, Shively S, Lakhani F, McDonald-Jones G, Bruce J, Lee EB, Xie SX, Joyce S, Li C, Toleikis PM, Lee VM, Trojanowski JQ. Microtubule-binding drugs offset tau sequestration by stabilizing microtubules and reversing fast axonal transport deficits in a tauopathy model. *Proceedings of the National Academy of Sciences of the United States of America*. 2005;102(1):227-31. doi: 10.1073/pnas.0406361102. PubMed PMID: 15615853; PubMed Central PMCID: PMC544048.
752. Arriagada PV, Growdon JH, Hedley-Whyte ET, Hyman BT. Neurofibrillary tangles but not senile plaques parallel duration and severity of Alzheimer's disease. *Neurology*. 1992;42(3 Pt 1):631-9. PubMed PMID: 1549228.
753. Lee G, Newman ST, Gard DL, Band H, Panchamoorthy G. Tau interacts with src-family non-receptor tyrosine kinases. *Journal of cell science*. 1998;111 (Pt 21):3167-77. PubMed PMID: 9763511.
754. Nakazawa T, Komai S, Tezuka T, Hisatsune C, Umemori H, Semba K, Mishina M, Manabe T, Yamamoto T. Characterization of Fyn-mediated tyrosine phosphorylation sites on GluR epsilon 2 (NR2B) subunit of the N-methyl-D-aspartate receptor. *The Journal of biological chemistry*. 2001;276(1):693-9. doi: 10.1074/jbc.M008085200. PubMed PMID: 11024032.
755. Rong Y, Lu X, Bernard A, Khrestchatskiy M, Baudry M. Tyrosine phosphorylation of ionotropic glutamate receptors by Fyn or Src differentially modulates their susceptibility to calpain and enhances their binding to spectrin and PSD-95. *Journal of neurochemistry*. 2001;79(2):382-90. PubMed PMID: 11677266.
756. Tezuka T, Umemori H, Akiyama T, Nakanishi S, Yamamoto T. PSD-95 promotes Fyn-mediated tyrosine phosphorylation of the N-methyl-D-aspartate receptor subunit NR2A. *Proceedings of the National Academy of Sciences of the United States of America*. 1999;96(2):435-40. PubMed PMID: 9892651; PubMed Central PMCID: PMC15154.
757. Aarts M, Liu Y, Liu L, Besshoh S, Arundine M, Gurd JW, Wang YT, Salter MW, Tymianski M. Treatment of ischemic brain damage by perturbing NMDA receptor- PSD-95 protein interactions. *Science*. 2002;298(5594):846-50. doi: 10.1126/science.1072873. PubMed PMID: 12399596.
758. Ittner LM, Ke YD, Delerue F, Bi M, Gladbach A, van Eersel J, Wolfing H, Chieng BC, Christie MJ, Napier IA, Eckert A, Staufenbiel M, Hardeman E, Gotz J. Dendritic function of tau mediates amyloid-beta toxicity in Alzheimer's disease mouse models. *Cell*. 2010;142(3):387-97. doi: 10.1016/j.cell.2010.06.036. PubMed PMID: 20655099.
759. Chin J, Palop JJ, Yu GQ, Kojima N, Masliah E, Mucke L. Fyn kinase modulates synaptotoxicity, but not aberrant sprouting, in human amyloid precursor protein transgenic mice. *The Journal of neuroscience : the official journal of the Society for Neuroscience*. 2004;24(19):4692-7. doi: 10.1523/JNEUROSCI.0277-04.2004. PubMed PMID: 15140940.
760. Chin J, Palop JJ, Puolivali J, Massaro C, Bien-Ly N, Gerstein H, Scarce-Levie K, Masliah E, Mucke L. Fyn kinase induces synaptic and cognitive impairments in a transgenic mouse model of Alzheimer's disease. *The Journal of neuroscience : the official journal of the Society for Neuroscience*. 2005;25(42):9694-703. doi: 10.1523/JNEUROSCI.2980-05.2005. PubMed PMID: 16237174.
761. Heneka MT, Golenbock DT, Latz E. Innate immunity in Alzheimer's disease. *Nature immunology*. 2015;16(3):229-36. doi: 10.1038/ni.3102. PubMed PMID: 25689443.
762. Hammer ND, Schmidt JC, Chapman MR. The curli nucleator protein, CsgB, contains an amyloidogenic domain that directs CsgA polymerization. *Proceedings of the National Academy of Sciences of the United States of America*. 2007;104(30):12494-9. doi: 10.1073/pnas.0703310104. PubMed PMID: 17636121; PubMed Central PMCID: PMC1941497.
763. Epstein EA, Chapman MR. Polymerizing the fibre between bacteria and host cells: the biogenesis of functional amyloid fibres. *Cellular microbiology*. 2008;10(7):1413-20. doi: 10.1111/j.1462-5822.2008.01148.x. PubMed PMID: 18373633; PubMed Central PMCID: PMC2674401.
764. Monje ML, Toda H, Palmer TD. Inflammatory blockade restores adult hippocampal neurogenesis. *Science*. 2003;302(5651):1760-5. doi: 10.1126/science.1088417. PubMed PMID: 14615545.
765. Latz E, Xiao TS, Stutz A. Activation and regulation of the inflammasomes. *Nature reviews Immunology*. 2013;13(6):397-411. doi: 10.1038/nri3452. PubMed PMID: 23702978; PubMed Central PMCID: PMC3807999.

766. Halle A, Hornung V, Petzold GC, Stewart CR, Monks BG, Reinheckel T, Fitzgerald KA, Latz E, Moore KJ, Golenbock DT. The NALP3 inflammasome is involved in the innate immune response to amyloid-beta. *Nature immunology*. 2008;9(8):857-65. doi: 10.1038/ni.1636. PubMed PMID: 18604209; PubMed Central PMCID: PMC3101478.
767. Vom Berg J, Prokop S, Miller KR, Obst J, Kalin RE, Lopategui-Cabezas I, Wegner A, Mair F, Schipke CG, Peters O, Winter Y, Becher B, Heppner FL. Inhibition of IL-12/IL-23 signaling reduces Alzheimer's disease-like pathology and cognitive decline. *Nature medicine*. 2012;18(12):1812-9. doi: 10.1038/nm.2965. PubMed PMID: 23178247.
768. Terwel D, Steffensen KR, Verghese PB, Kummer MP, Gustafsson JA, Holtzman DM, Heneka MT. Critical role of astroglial apolipoprotein E and liver X receptor-alpha expression for microglial Abeta phagocytosis. *The Journal of neuroscience : the official journal of the Society for Neuroscience*. 2011;31(19):7049-59. doi: 10.1523/JNEUROSCI.6546-10.2011. PubMed PMID: 21562267.
769. Vodovotz Y, Lucia MS, Flanders KC, Chesler L, Xie QW, Smith TW, Weidner J, Mumford R, Webber R, Nathan C, Roberts AB, Lippa CF, Sporn MB. Inducible nitric oxide synthase in tangle-bearing neurons of patients with Alzheimer's disease. *The Journal of experimental medicine*. 1996;184(4):1425-33. PubMed PMID: 8879214; PubMed Central PMCID: PMC2192831.
770. Youm YH, Grant RW, McCabe LR, Albarado DC, Nguyen KY, Ravussin A, Pistell P, Newman S, Carter R, Laque A, Munzberg H, Rosen CJ, Ingram DK, Salbaum JM, Dixit VD. Canonical Nlrp3 inflammasome links systemic low-grade inflammation to functional decline in aging. *Cell metabolism*. 2013;18(4):519-32. doi: 10.1016/j.cmet.2013.09.010. PubMed PMID: 24093676; PubMed Central PMCID: PMC4017327.
771. Paolicelli RC, Bolasco G, Pagani F, Maggi L, Scianni M, Panzanelli P, Giustetto M, Ferreira TA, Guiducci E, Dumas L, Ragozzino D, Gross CT. Synaptic pruning by microglia is necessary for normal brain development. *Science*. 2011;333(6048):1456-8. doi: 10.1126/science.1202529. PubMed PMID: 21778362.
772. Lynch MA. Neuroinflammatory changes negatively impact on LTP: A focus on IL-1beta. *Brain research*. 2014. doi: 10.1016/j.brainres.2014.08.040. PubMed PMID: 25193603.
773. Cumiskey D, Pickering M, O'Connor JJ. Interleukin-18 mediated inhibition of LTP in the rat dentate gyrus is attenuated in the presence of mGluR antagonists. *Neuroscience letters*. 2007;412(3):206-10. doi: 10.1016/j.neulet.2006.11.007. PubMed PMID: 17123727.
774. Pickering M, Cumiskey D, O'Connor JJ. Actions of TNF-alpha on glutamatergic synaptic transmission in the central nervous system. *Experimental physiology*. 2005;90(5):663-70. doi: 10.1113/expphysiol.2005.030734. PubMed PMID: 15944202.
775. Yirmiya R, Goshen I. Immune modulation of learning, memory, neural plasticity and neurogenesis. *Brain, behavior, and immunity*. 2011;25(2):181-213. doi: 10.1016/j.bbi.2010.10.015. PubMed PMID: 20970492.
776. Heneka MT, Kummer MP, Stutz A, Delekate A, Schwartz S, Vieira-Saecker A, Griep A, Axt D, Remus A, Tzeng TC, Gelpi E, Halle A, Korte M, Latz E, Golenbock DT. NLRP3 is activated in Alzheimer's disease and contributes to pathology in APP/PS1 mice. *Nature*. 2013;493(7434):674-8. doi: 10.1038/nature11729. PubMed PMID: 23254930; PubMed Central PMCID: PMC3812809.
777. Neniskyte U, Neher JJ, Brown GC. Neuronal death induced by nanomolar amyloid beta is mediated by primary phagocytosis of neurons by microglia. *The Journal of biological chemistry*. 2011;286(46):39904-13. doi: 10.1074/jbc.M111.267583. PubMed PMID: 21903584; PubMed Central PMCID: PMC3220594.
778. Fricker M, Oliva-Martin MJ, Brown GC. Primary phagocytosis of viable neurons by microglia activated with LPS or Abeta is dependent on calreticulin/LRP phagocytic signalling. *Journal of neuroinflammation*. 2012;9:196. doi: 10.1186/1742-2094-9-196. PubMed PMID: 22889139; PubMed Central PMCID: PMC3481398.
779. Stewart CR, Stuart LM, Wilkinson K, van Gils JM, Deng J, Halle A, Rayner KJ, Boyer L, Zhong R, Frazier WA, Lacy-Hulbert A, El Khoury J, Golenbock DT, Moore KJ. CD36 ligands promote sterile inflammation through assembly of a Toll-like receptor 4 and 6 heterodimer. *Nature immunology*. 2010;11(2):155-61. doi: 10.1038/ni.1836. PubMed PMID: 20037584; PubMed Central PMCID: PMC2809046.
780. Hoshino T, Murao N, Namba T, Takehara M, Adachi H, Katsuno M, Sobue G, Matsushima T, Suzuki T, Mizushima T. Suppression of Alzheimer's disease-related phenotypes by expression of heat shock protein 70 in mice. *The Journal of neuroscience : the official journal of the Society for Neuroscience*. 2011;31(14):5225-34. doi: 10.1523/JNEUROSCI.5478-10.2011. PubMed PMID: 21471357.

781. Heneka MT, Nadrigny F, Regen T, Martinez-Hernandez A, Dumitrescu-Ozimek L, Terwel D, Jardanhazi-Kurutz D, Walter J, Kirchhoff F, Hanisch UK, Kummer MP. Locus ceruleus controls Alzheimer's disease pathology by modulating microglial functions through norepinephrine. *Proceedings of the National Academy of Sciences of the United States of America*. 2010;107(13):6058-63. doi: 10.1073/pnas.0909586107. PubMed PMID: 20231476; PubMed Central PMCID: PMC2851853.
782. El Khoury J, Toft M, Hickman SE, Means TK, Terada K, Geula C, Luster AD. Ccr2 deficiency impairs microglial accumulation and accelerates progression of Alzheimer-like disease. *Nature medicine*. 2007;13(4):432-8. doi: 10.1038/nm1555. PubMed PMID: 17351623.
783. Biomarkers Definitions Working G. Biomarkers and surrogate endpoints: preferred definitions and conceptual framework. *Clinical pharmacology and therapeutics*. 2001;69(3):89-95. doi: 10.1067/mcp.2001.113989. PubMed PMID: 11240971.
784. Consensus report of the Working Group on: "Molecular and Biochemical Markers of Alzheimer's Disease". The Ronald and Nancy Reagan Research Institute of the Alzheimer's Association and the National Institute on Aging Working Group. *Neurobiology of aging*. 1998;19(2):109-16. PubMed PMID: 9558143.
785. Hampel H, Mitchell A, Blennow K, Frank RA, Brettschneider S, Weller L, Moller HJ. Core biological marker candidates of Alzheimer's disease - perspectives for diagnosis, prediction of outcome and reflection of biological activity. *Journal of neural transmission*. 2004;111(3):247-72. doi: 10.1007/s00702-003-0065-z. PubMed PMID: 14991453.
786. Bateman RJ, Xiong C, Benzinger TL, Fagan AM, Goate A, Fox NC, Marcus DS, Cairns NJ, Xie X, Blazey TM, Holtzman DM, Santacruz A, Buckles V, Oliver A, Moulder K, Aisen PS, Ghetti B, Klunk WE, McDade E, Martins RN, Masters CL, Mayeux R, Ringman JM, Rossor MN, Schofield PR, Sperling RA, Salloway S, Morris JC, Dominantly Inherited Alzheimer N. Clinical and biomarker changes in dominantly inherited Alzheimer's disease. *The New England journal of medicine*. 2012;367(9):795-804. doi: 10.1056/NEJMoa1202753. PubMed PMID: 22784036; PubMed Central PMCID: PMC3474597.
787. Klunk WE, Engler H, Nordberg A, Wang Y, Blomqvist G, Holt DP, Bergstrom M, Savitcheva I, Huang GF, Estrada S, Ausen B, Debnath ML, Barletta J, Price JC, Sandell J, Lopresti BJ, Wall A, Koivisto P, Antoni G, Mathis CA, Langstrom B. Imaging brain amyloid in Alzheimer's disease with Pittsburgh Compound-B. *Annals of neurology*. 2004;55(3):306-19. doi: 10.1002/ana.20009. PubMed PMID: 14991808.
788. Klunk WE. Amyloid imaging as a biomarker for cerebral beta-amyloidosis and risk prediction for Alzheimer dementia. *Neurobiol Aging*. 2011;32 Suppl 1:S20-36. doi: 10.1016/j.neurobiolaging.2011.09.006. PubMed PMID: 22078170; PubMed Central PMCID: PMC3233688.
789. Lockhart A, Lamb JR, Osredkar T, Sue LI, Joyce JN, Ye L, Libri V, Leppert D, Beach TG. PIB is a non-specific imaging marker of amyloid-beta (A β) peptide-related cerebral amyloidosis. *Brain : a journal of neurology*. 2007;130(Pt 10):2607-15. doi: 10.1093/brain/awm191. PubMed PMID: 17698496.
790. Ikonomic MD, Klunk WE, Abrahamson EE, Mathis CA, Price JC, Tsopelas ND, Lopresti BJ, Ziolkowski S, Bi W, Paljug WR, Debnath ML, Hope CE, Isanski BA, Hamilton RL, DeKosky ST. Post-mortem correlates of in vivo PiB-PET amyloid imaging in a typical case of Alzheimer's disease. *Brain : a journal of neurology*. 2008;131(Pt 6):1630-45. doi: 10.1093/brain/awn016. PubMed PMID: 18339640; PubMed Central PMCID: PMC2408940.
791. Bacskai BJ, Frosch MP, Freeman SH, Raymond SB, Augustinack JC, Johnson KA, Irizarry MC, Klunk WE, Mathis CA, DeKosky ST, Greenberg SM, Hyman BT, Growdon JH. Molecular imaging with Pittsburgh Compound B confirmed at autopsy: a case report. *Archives of neurology*. 2007;64(3):431-4. doi: 10.1001/archneur.64.3.431. PubMed PMID: 17353389.
792. Scholl M, Wall A, Thordardottir S, Ferreira D, Bogdanovic N, Langstrom B, Almkvist O, Graff C, Nordberg A. Low PiB PET retention in presence of pathologic CSF biomarkers in Arctic APP mutation carriers. *Neurology*. 2012;79(3):229-36. doi: 10.1212/WNL.0b013e31825fdf18. PubMed PMID: 22700814.
793. Villemagne VL, Rowe CC. Amyloid imaging. *International psychogeriatrics / IPA*. 2011;23 Suppl 2:S41-9. doi: 10.1017/S1041610211000895. PubMed PMID: 21729418.
794. Edison P, Archer HA, Hinz R, Hammers A, Pavese N, Tai YF, Hotton G, Cutler D, Fox N, Kennedy A, Rossor M, Brooks DJ. Amyloid, hypometabolism, and cognition in Alzheimer disease: an [11C]PiB and [18F]FDG PET study. *Neurology*. 2007;68(7):501-8. doi: 10.1212/01.wnl.0000244749.20056.d4. PubMed PMID: 17065593.

795. Kempainen NM, Aalto S, Wilson IA, Nagren K, Helin S, Bruck A, Oikonen V, Kailajarvi M, Scheinin M, Viitanen M, Parkkola R, Rinne JO. Voxel-based analysis of PET amyloid ligand [11C]PIB uptake in Alzheimer disease. *Neurology*. 2006;67(9):1575-80. doi: 10.1212/01.wnl.0000240117.55680.0a. PubMed PMID: 16971697.
796. Kempainen NM, Aalto S, Wilson IA, Nagren K, Helin S, Bruck A, Oikonen V, Kailajarvi M, Scheinin M, Viitanen M, Parkkola R, Rinne JO. PET amyloid ligand [11C]PIB uptake is increased in mild cognitive impairment. *Neurology*. 2007;68(19):1603-6. doi: 10.1212/01.wnl.0000260969.94695.56. PubMed PMID: 17485647.
797. Price JC, Klunk WE, Lopresti BJ, Lu X, Hoge JA, Ziolkowski SK, Holt DP, Meltzer CC, DeKosky ST, Mathis CA. Kinetic modeling of amyloid binding in humans using PET imaging and Pittsburgh Compound-B. *Journal of cerebral blood flow and metabolism : official journal of the International Society of Cerebral Blood Flow and Metabolism*. 2005;25(11):1528-47. doi: 10.1038/sj.jcbfm.9600146. PubMed PMID: 15944649.
798. Rowe CC, Ng S, Ackermann U, Gong SJ, Pike K, Savage G, Cowie TF, Dickinson KL, Maruff P, Darby D, Smith C, Woodward M, Merory J, Tochon-Danguy H, O'Keefe G, Klunk WE, Mathis CA, Price JC, Masters CL, Villemagne VL. Imaging beta-amyloid burden in aging and dementia. *Neurology*. 2007;68(20):1718-25. doi: 10.1212/01.wnl.0000261919.22630.ea. PubMed PMID: 17502554.
799. Forsberg A, Engler H, Almkvist O, Blomquist G, Hagman G, Wall A, Ringheim A, Langstrom B, Nordberg A. PET imaging of amyloid deposition in patients with mild cognitive impairment. *Neurobiology of aging*. 2008;29(10):1456-65. doi: 10.1016/j.neurobiolaging.2007.03.029. PubMed PMID: 17499392.
800. Wolk DA, Price JC, Saxton JA, Snitz BE, James JA, Lopez OL, Aizenstein HJ, Cohen AD, Weissfeld LA, Mathis CA, Klunk WE, De-Kosky ST. Amyloid imaging in mild cognitive impairment subtypes. *Annals of neurology*. 2009;65(5):557-68. doi: 10.1002/ana.21598. PubMed PMID: 19475670; PubMed Central PMCID: PMC2828870.
801. Okello A, Koivunen J, Edison P, Archer HA, Turkheimer FE, Nagren K, Bullock R, Walker Z, Kennedy A, Fox NC, Rossor MN, Rinne JO, Brooks DJ. Conversion of amyloid positive and negative MCI to AD over 3 years: an 11C-PIB PET study. *Neurology*. 2009;73(10):754-60. doi: 10.1212/WNL.0b013e3181b23564. PubMed PMID: 19587325; PubMed Central PMCID: PMC2830881.
802. Koivunen J, Verkkoniemi A, Aalto S, Paetau A, Ahonen JP, Viitanen M, Nagren K, Rokka J, Haaparanta M, Kalimo H, Rinne JO. PET amyloid ligand [11C]PIB uptake shows predominantly striatal increase in variant Alzheimer's disease. *Brain : a journal of neurology*. 2008;131(Pt 7):1845-53. doi: 10.1093/brain/awn107. PubMed PMID: 18583368.
803. Pike KE, Savage G, Villemagne VL, Ng S, Moss SA, Maruff P, Mathis CA, Klunk WE, Masters CL, Rowe CC. Beta-amyloid imaging and memory in non-demented individuals: evidence for preclinical Alzheimer's disease. *Brain : a journal of neurology*. 2007;130(Pt 11):2837-44. doi: 10.1093/brain/awm238. PubMed PMID: 17928318.
804. Mormino EC, Kluth JT, Madison CM, Rabinovici GD, Baker SL, Miller BL, Koeppe RA, Mathis CA, Weiner MW, Jagust WJ. Alzheimer's Disease Neuroimaging I. Episodic memory loss is related to hippocampal-mediated beta-amyloid deposition in elderly subjects. *Brain : a journal of neurology*. 2009;132(Pt 5):1310-23. doi: 10.1093/brain/awn320. PubMed PMID: 19042931; PubMed Central PMCID: PMC2677792.
805. Forsberg A, Almkvist O, Engler H, Wall A, Langstrom B, Nordberg A. High PIB retention in Alzheimer's disease is an early event with complex relationship with CSF biomarkers and functional parameters. *Current Alzheimer research*. 2010;7(1):56-66. PubMed PMID: 20205671.
806. Sperling RA, Laviolette PS, O'Keefe K, O'Brien J, Rentz DM, Pihlajamaki M, Marshall G, Hyman BT, Selkoe DJ, Hedden T, Buckner RL, Becker JA, Johnson KA. Amyloid deposition is associated with impaired default network function in older persons without dementia. *Neuron*. 2009;63(2):178-88. doi: 10.1016/j.neuron.2009.07.003. PubMed PMID: 19640477; PubMed Central PMCID: PMC2738994.
807. Storandt M, Mintun MA, Head D, Morris JC. Cognitive decline and brain volume loss as signatures of cerebral amyloid-beta peptide deposition identified with Pittsburgh compound B: cognitive decline associated with Abeta deposition. *Archives of neurology*. 2009;66(12):1476-81. doi: 10.1001/archneurol.2009.272. PubMed PMID: 20008651; PubMed Central PMCID: PMC2796577.
808. Furst AJ, Rabinovici GD, Rostomian AH, Steed T, Alkalay A, Racine C, Miller BL, Jagust WJ. Cognition, glucose metabolism and amyloid burden in Alzheimer's disease. *Neurobiology of aging*. 2012;33(2):215-25. doi: 10.1016/j.neurobiolaging.2010.03.011. PubMed PMID: 20417582; PubMed Central PMCID: PMC2920373.
809. Resnick SM, Sojkova J, Zhou Y, An Y, Ye W, Holt DP, Dannals RF, Mathis CA, Klunk WE, Ferrucci L, Kraut MA, Wong DF. Longitudinal cognitive decline is associated with fibrillar amyloid-beta measured by [11C]PiB. *Neurology*.

- 2010;74(10):807-15. doi: 10.1212/WNL.0b013e3181d3e3e9. PubMed PMID: 20147655; PubMed Central PMCID: PMC2839197.
810. Roe CM, Mintun MA, D'Angelo G, Xiong C, Grant EA, Morris JC. Alzheimer disease and cognitive reserve: variation of education effect with carbon 11-labeled Pittsburgh Compound B uptake. *Archives of neurology*. 2008;65(11):1467-71. doi: 10.1001/archneur.65.11.1467. PubMed PMID: 19001165; PubMed Central PMCID: PMC2752218.
811. Rentz DM, Locascio JJ, Becker JA, Moran EK, Eng E, Buckner RL, Sperling RA, Johnson KA. Cognition, reserve, and amyloid deposition in normal aging. *Annals of neurology*. 2010;67(3):353-64. doi: 10.1002/ana.21904. PubMed PMID: 20373347; PubMed Central PMCID: PMC3074985.
812. Stern Y, Gurland B, Tatemichi TK, Tang MX, Wilder D, Mayeux R. Influence of education and occupation on the incidence of Alzheimer's disease. *JAMA : the journal of the American Medical Association*. 1994;271(13):1004-10. PubMed PMID: 8139057.
813. Stern Y. Cognitive reserve. *Neuropsychologia*. 2009;47(10):2015-28. doi: 10.1016/j.neuropsychologia.2009.03.004. PubMed PMID: 19467352; PubMed Central PMCID: PMC2739591.
814. Stern Y, Albert S, Tang MX, Tsai WY. Rate of memory decline in AD is related to education and occupation: cognitive reserve? *Neurology*. 1999;53(9):1942-7. PubMed PMID: 10599762.
815. Mattsson N, Insel PS, Donohue M, Landau S, Jagust WJ, Shaw LM, Trojanowski JQ, Zetterberg H, Blennow K, Weiner MW, Alzheimer's Disease Neuroimaging I. Independent information from cerebrospinal fluid amyloid-beta and florbetapir imaging in Alzheimer's disease. *Brain : a journal of neurology*. 2015;138(Pt 3):772-83. doi: 10.1093/brain/awu367. PubMed PMID: 25541191.
816. Greenberg SM, Grabowski T, Gurol ME, Skehan ME, Nandigam RN, Becker JA, Garcia-Alloza M, Prada C, Frosch MP, Rosand J, Viswanathan A, Smith EE, Johnson KA. Detection of isolated cerebrovascular beta-amyloid with Pittsburgh compound B. *Annals of neurology*. 2008;64(5):587-91. doi: 10.1002/ana.21528. PubMed PMID: 19067370; PubMed Central PMCID: PMC2605158.
817. Ly JV, Donnan GA, Villemagne VL, Zavala JA, Ma H, O'Keefe G, Gong SJ, Gunawan RM, Saunder T, Ackerman U, Tochon-Danguy H, Churilov L, Phan TG, Rowe CC. 11C-PiB binding is increased in patients with cerebral amyloid angiopathy-related hemorrhage. *Neurology*. 2010;74(6):487-93. doi: 10.1212/WNL.0b013e3181cef7e3. PubMed PMID: 20142615.
818. Wong DF, Rosenberg PB, Zhou Y, Kumar A, Raymont V, Ravert HT, Dannals RF, Nandi A, Brasic JR, Ye W, Hilton J, Lyketsos C, Kung HF, Joshi AD, Skovronsky DM, Pontecorvo MJ. In vivo imaging of amyloid deposition in Alzheimer disease using the radioligand 18F-AV-45 (florbetapir [corrected] F 18). *Journal of nuclear medicine : official publication, Society of Nuclear Medicine*. 2010;51(6):913-20. doi: 10.2967/jnumed.109.069088. PubMed PMID: 20501908; PubMed Central PMCID: PMC3101877.
819. Nelissen N, Van Laere K, Thurfjell L, Owenius R, Vandenbulcke M, Koole M, Bormans G, Brooks DJ, Vandenberghe R. Phase 1 study of the Pittsburgh compound B derivative 18F-flutemetamol in healthy volunteers and patients with probable Alzheimer disease. *Journal of nuclear medicine : official publication, Society of Nuclear Medicine*. 2009;50(8):1251-9. doi: 10.2967/jnumed.109.063305. PubMed PMID: 19617318.
820. Rowe CC, Pejoska S, Mulligan RS, Jones G, Chan JG, Svensson S, Cselenyi Z, Masters CL, Villemagne VL. Head-to-head comparison of 11C-PiB and 18F-AZD4694 (NAV4694) for beta-amyloid imaging in aging and dementia. *Journal of nuclear medicine : official publication, Society of Nuclear Medicine*. 2013;54(6):880-6. doi: 10.2967/jnumed.112.114785. PubMed PMID: 23575995.
821. Benveniste H, Einstein G, Kim KR, Hulette C, Johnson GA. Detection of neuritic plaques in Alzheimer's disease by magnetic resonance microscopy. *Proceedings of the National Academy of Sciences of the United States of America*. 1999;96(24):14079-84. PubMed PMID: 10570201; PubMed Central PMCID: PMC24193.
822. Meadowcroft MD, Zhang S, Liu W, Park BS, Connor JR, Collins CM, Smith MB, Yang QX. Direct magnetic resonance imaging of histological tissue samples at 3.0T. *Magnetic resonance in medicine : official journal of the Society of Magnetic Resonance in Medicine / Society of Magnetic Resonance in Medicine*. 2007;57(5):835-41. doi: 10.1002/mrm.21213. PubMed PMID: 17457873; PubMed Central PMCID: PMC4040526.

823. Meadowcroft MD, Connor JR, Smith MB, Yang QX. MRI and histological analysis of beta-amyloid plaques in both human Alzheimer's disease and APP/PS1 transgenic mice. *Journal of magnetic resonance imaging : JMRI*. 2009;29(5):997-1007. doi: 10.1002/jmri.21731. PubMed PMID: 19388095; PubMed Central PMCID: PMC2723054.
824. Jack CR, Jr., Garwood M, Wengenack TM, Borowski B, Curran GL, Lin J, Adriany G, Grohn OH, Grimm R, Poduslo JF. In vivo visualization of Alzheimer's amyloid plaques by magnetic resonance imaging in transgenic mice without a contrast agent. *Magnetic resonance in medicine : official journal of the Society of Magnetic Resonance in Medicine / Society of Magnetic Resonance in Medicine*. 2004;52(6):1263-71. doi: 10.1002/mrm.20266. PubMed PMID: 15562496; PubMed Central PMCID: PMC2744889.
825. Jack CR, Jr., Wengenack TM, Reyes DA, Garwood M, Curran GL, Borowski BJ, Lin J, Preboske GM, Holasek SS, Adriany G, Poduslo JF. In vivo magnetic resonance microimaging of individual amyloid plaques in Alzheimer's transgenic mice. *The Journal of neuroscience : the official journal of the Society for Neuroscience*. 2005;25(43):10041-8. doi: 10.1523/JNEUROSCI.2588-05.2005. PubMed PMID: 16251453; PubMed Central PMCID: PMC2744887.
826. Yanagisawa D, Amatsubo T, Morikawa S, Taguchi H, Urushitani M, Shirai N, Hirao K, Shiino A, Inubushi T, Tooyama I. In vivo detection of amyloid beta deposition using (1)(9)F magnetic resonance imaging with a (1)(9)F-containing curcumin derivative in a mouse model of Alzheimer's disease. *Neuroscience*. 2011;184:120-7. doi: 10.1016/j.neuroscience.2011.03.071. PubMed PMID: 21497641.
827. Wadghiri YZ, Sigurdsson EM, Sadowski M, Elliott JI, Li Y, Scholtzova H, Tang CY, Aguinaldo G, Pappolla M, Duff K, Wisniewski T, Turnbull DH. Detection of Alzheimer's amyloid in transgenic mice using magnetic resonance microimaging. *Magnetic resonance in medicine : official journal of the Society of Magnetic Resonance in Medicine / Society of Magnetic Resonance in Medicine*. 2003;50(2):293-302. doi: 10.1002/mrm.10529. PubMed PMID: 12876705.
828. Sigurdsson EM, Wadghiri YZ, Mosconi L, Blind JA, Knudsen E, Asuni A, Scholtzova H, Tsui WH, Li Y, Sadowski M, Turnbull DH, de Leon MJ, Wisniewski T. A non-toxic ligand for voxel-based MRI analysis of plaques in AD transgenic mice. *Neurobiology of aging*. 2008;29(6):836-47. doi: 10.1016/j.neurobiolaging.2006.12.018. PubMed PMID: 17291630; PubMed Central PMCID: PMC2408732.
829. Viola KL, Sbarboro J, Sureka R, De M, Bicca MA, Wang J, Vasavada S, Satpathy S, Wu S, Joshi H, Velasco PT, MacRenaris K, Waters EA, Lu C, Phan J, Lacor P, Prasad P, Dravid VP, Klein WL. Towards non-invasive diagnostic imaging of early-stage Alzheimer's disease. *Nature nanotechnology*. 2015;10(1):91-8. doi: 10.1038/nnano.2014.254. PubMed PMID: 25531084; PubMed Central PMCID: PMC4300856.
830. Higuchi M, Iwata N, Matsuba Y, Sato K, Sasamoto K, Saido TC. 19F and 1H MRI detection of amyloid beta plaques in vivo. *Nature neuroscience*. 2005;8(4):527-33. doi: 10.1038/nn1422. PubMed PMID: 15768036.
831. Cheng KK, Chan PS, Fan S, Kwan SM, Yeung KL, Wang YX, Chow AH, Wu EX, Baum L. Curcumin-conjugated magnetic nanoparticles for detecting amyloid plaques in Alzheimer's disease mice using magnetic resonance imaging (MRI). *Biomaterials*. 2015;44:155-72. doi: 10.1016/j.biomaterials.2014.12.005. PubMed PMID: 25617135.
832. Bacskai BJ, Kajdasz ST, Christie RH, Carter C, Games D, Seubert P, Schenk D, Hyman BT. Imaging of amyloid-beta deposits in brains of living mice permits direct observation of clearance of plaques with immunotherapy. *Nature medicine*. 2001;7(3):369-72. doi: 10.1038/85525. PubMed PMID: 11231639.
833. Styren SD, Hamilton RL, Styren GC, Klunk WE. X-34, a fluorescent derivative of Congo red: a novel histochemical stain for Alzheimer's disease pathology. *The journal of histochemistry and cytochemistry : official journal of the Histochemistry Society*. 2000;48(9):1223-32. PubMed PMID: 10950879.
834. Shoghi-Jadid K, Small GW, Agdeppa ED, Kepe V, Ercoli LM, Siddarth P, Read S, Satyamurthy N, Petric A, Huang SC, Barrio JR. Localization of neurofibrillary tangles and beta-amyloid plaques in the brains of living patients with Alzheimer disease. *The American journal of geriatric psychiatry : official journal of the American Association for Geriatric Psychiatry*. 2002;10(1):24-35. PubMed PMID: 11790632.
835. Nesterov EE, Skoch J, Hyman BT, Klunk WE, Bacskai BJ, Swager TM. In vivo optical imaging of amyloid aggregates in brain: design of fluorescent markers. *Angewandte Chemie*. 2005;44(34):5452-6. doi: 10.1002/anie.200500845. PubMed PMID: 16059955.
836. Ntziachristos V, Bremer C, Weissleder R. Fluorescence imaging with near-infrared light: new technological advances that enable in vivo molecular imaging. *European radiology*. 2003;13(1):195-208. doi: 10.1007/s00330-002-1524-x. PubMed PMID: 12541130.

837. Funovics M, Weissleder R, Tung CH. Protease sensors for bioimaging. *Analytical and bioanalytical chemistry*. 2003;377(6):956-63. doi: 10.1007/s00216-003-2199-0. PubMed PMID: 12955390.
838. Hintersteiner M, Enz A, Frey P, Jatou AL, Kinzy W, Kneuer R, Neumann U, Rudin M, Staufenbiel M, Stoeckli M, Wiederhold KH, Gremlich HU. In vivo detection of amyloid-beta deposits by near-infrared imaging using an oxazine-derivative probe. *Nature biotechnology*. 2005;23(5):577-83. doi: 10.1038/nbt1085. PubMed PMID: 15834405.
839. Schmidt A, Pahnke J. Efficient near-infrared in vivo imaging of amyloid-beta deposits in Alzheimer's disease mouse models. *Journal of Alzheimer's disease : JAD*. 2012;30(3):651-64. doi: 10.3233/JAD-2012-112168. PubMed PMID: 22460331.
840. Raymond SB, Skoch J, Hills ID, Nesterov EE, Swager TM, Bacskai BJ. Smart optical probes for near-infrared fluorescence imaging of Alzheimer's disease pathology. *European journal of nuclear medicine and molecular imaging*. 2008;35 Suppl 1:S93-8. doi: 10.1007/s00259-007-0708-7. PubMed PMID: 18236039.
841. Kumar AT, Raymond SB, Boverman G, Boas DA, Bacskai BJ. Time resolved fluorescence tomography of turbid media based on lifetime contrast. *Optics express*. 2006;14(25):12255-70. PubMed PMID: 19529654; PubMed Central PMCID: PMC2700299.
842. Kumar AT, Skoch J, Bacskai BJ, Boas DA, Dunn AK. Fluorescence-lifetime-based tomography for turbid media. *Optics letters*. 2005;30(24):3347-9. PubMed PMID: 16389827.
843. Godavarty A, Sevcik-Muraca EM, Eppstein MJ. Three-dimensional fluorescence lifetime tomography. *Medical physics*. 2005;32(4):992-1000. PubMed PMID: 15895582.
844. Golde TE, Bacskai BJ. Bringing amyloid into focus. *Nature biotechnology*. 2005;23(5):552-4. doi: 10.1038/nbt0505-552. PubMed PMID: 15877070.
845. Culver JP, Siegel AM, Stott JJ, Boas DA. Volumetric diffuse optical tomography of brain activity. *Optics letters*. 2003;28(21):2061-3. PubMed PMID: 14587815.
846. Hielscher AH, Bluestone AY, Abdoulaev GS, Klose AD, Lasker J, Stewart M, Netz U, Beuthan J. Near-infrared diffuse optical tomography. *Disease markers*. 2002;18(5-6):313-37. PubMed PMID: 14646043.
847. Jack CR, Jr., Wiste HJ, Knopman DS, Vemuri P, Mielke MM, Weigand SD, Senjem ML, Gunter JL, Lowe V, Gregg BE, Pankratz VS, Petersen RC. Rates of beta-amyloid accumulation are independent of hippocampal neurodegeneration. *Neurology*. 2014;82(18):1605-12. doi: 10.1212/WNL.0000000000000386. PubMed PMID: 24706010; PubMed Central PMCID: PMC4013810.
848. Wegmann S, Jung YJ, Chinnathambi S, Mandelkow EM, Mandelkow E, Muller DJ. Human Tau isoforms assemble into ribbon-like fibrils that display polymorphic structure and stability. *The Journal of biological chemistry*. 2010;285(35):27302-13. doi: 10.1074/jbc.M110.145318. PubMed PMID: 20566652; PubMed Central PMCID: PMC2930729.
849. Chirita CN, Congdon EE, Yin H, Kuret J. Triggers of full-length tau aggregation: a role for partially folded intermediates. *Biochemistry*. 2005;44(15):5862-72. doi: 10.1021/bi0500123. PubMed PMID: 15823045.
850. Buee L, Bussiere T, Buee-Scherrer V, Delacourte A, Hof PR. Tau protein isoforms, phosphorylation and role in neurodegenerative disorders. *Brain research Brain research reviews*. 2000;33(1):95-130. PubMed PMID: 10967355.
851. Spillantini MG, Goedert M. Tau protein pathology in neurodegenerative diseases. *Trends in neurosciences*. 1998;21(10):428-33. PubMed PMID: 9786340.
852. Martin L, Latypova X, Terro F. Post-translational modifications of tau protein: implications for Alzheimer's disease. *Neurochemistry international*. 2011;58(4):458-71. doi: 10.1016/j.neuint.2010.12.023. PubMed PMID: 21215781.
853. Mukaetova-Ladinska EB, Harrington CR, Roth M, Wischik CM. Biochemical and anatomical redistribution of tau protein in Alzheimer's disease. *The American journal of pathology*. 1993;143(2):565-78. PubMed PMID: 8342603; PubMed Central PMCID: PMC1887045.
854. Naslund J, Haroutunian V, Mohs R, Davis KL, Davies P, Greengard P, Buxbaum JD. Correlation between elevated levels of amyloid beta-peptide in the brain and cognitive decline. *Jama*. 2000;283(12):1571-7. PubMed PMID: 10735393.
855. Villemagne VL, Fodero-Tavoletti MT, Masters CL, Rowe CC. Tau imaging: early progress and future directions. *The Lancet Neurology*. 2015;14(1):114-24. doi: 10.1016/S1474-4422(14)70252-2. PubMed PMID: 25496902.
856. Allan CL, Sexton CE, Welchew D, Ebmeier KP. Imaging and biomarkers for Alzheimer's disease. *Maturitas*. 2010;65(2):138-42. doi: 10.1016/j.maturitas.2009.12.006. PubMed PMID: 20060241.

857. Agdeppa ED, Kepe V, Liu J, Flores-Torres S, Satyamurthy N, Petric A, Cole GM, Small GW, Huang SC, Barrio JR. Binding characteristics of radiofluorinated 6-dialkylamino-2-naphthylethylidene derivatives as positron emission tomography imaging probes for beta-amyloid plaques in Alzheimer's disease. *The Journal of neuroscience : the official journal of the Society for Neuroscience*. 2001;21(24):RC189. PubMed PMID: 11734604.
858. Small GW, Kepe V, Ercoli LM, Siddarth P, Bookheimer SY, Miller KJ, Lavretsky H, Burggren AC, Cole GM, Vinters HV, Thompson PM, Huang SC, Satyamurthy N, Phelps ME, Barrio JR. PET of brain amyloid and tau in mild cognitive impairment. *The New England journal of medicine*. 2006;355(25):2652-63. doi: 10.1056/NEJMoa054625. PubMed PMID: 17182990.
859. Small GW, Kepe V, Siddarth P, Ercoli LM, Merrill DA, Donoghue N, Bookheimer SY, Martinez J, Omalu B, Bailes J, Barrio JR. PET scanning of brain tau in retired national football league players: preliminary findings. *The American journal of geriatric psychiatry : official journal of the American Association for Geriatric Psychiatry*. 2013;21(2):138-44. doi: 10.1016/j.jagp.2012.11.019. PubMed PMID: 23343487.
860. Kepe V, Bordelon Y, Boxer A, Huang SC, Liu J, Thiede FC, Mazziotta JC, Mendez MF, Donoghue N, Small GW, Barrio JR. PET imaging of neuropathology in tauopathies: progressive supranuclear palsy. *Journal of Alzheimer's disease : JAD*. 2013;36(1):145-53. doi: 10.3233/JAD-130032. PubMed PMID: 23579330; PubMed Central PMCID: PMC3674205.
861. Bresjanac M, Smid LM, Vovko TD, Petric A, Barrio JR, Popovic M. Molecular-imaging probe 2-(1-[6-[(2-fluoroethyl)(methyl) amino]-2-naphthyl]ethylidene) malononitrile labels prion plaques in vitro. *The Journal of neuroscience : the official journal of the Society for Neuroscience*. 2003;23(22):8029-33. PubMed PMID: 12954864.
862. Tolboom N, Yaqub M, van der Flier WM, Boellaard R, Luurtsema G, Windhorst AD, Barkhof F, Scheltens P, Lammertsma AA, van Berckel BN. Detection of Alzheimer pathology in vivo using both 11C-PIB and 18F-FDDNP PET. *Journal of nuclear medicine : official publication, Society of Nuclear Medicine*. 2009;50(2):191-7. doi: 10.2967/jnumed.108.056499. PubMed PMID: 19164243.
863. Shin J, Lee SY, Kim SH, Kim YB, Cho SJ. Multitracer PET imaging of amyloid plaques and neurofibrillary tangles in Alzheimer's disease. *NeuroImage*. 2008;43(2):236-44. doi: 10.1016/j.neuroimage.2008.07.022. PubMed PMID: 18694837.
864. Noda A, Murakami Y, Nishiyama S, Fukumoto D, Miyoshi S, Tsukada H, Nishimura S. Amyloid imaging in aged and young macaques with [11C]PIB and [18F]FDDNP. *Synapse*. 2008;62(6):472-5. doi: 10.1002/syn.20508. PubMed PMID: 18361444.
865. Velasco A, Fraser G, Delobel P, Ghetti B, Lavenir I, Goedert M. Detection of filamentous tau inclusions by the fluorescent Congo red derivative FSB [(trans,trans)-1-fluoro-2,5-bis(3-hydroxycarbonyl-4-hydroxy)styryl]benzene]. *FEBS letters*. 2008;582(6):901-6. doi: 10.1016/j.febslet.2008.02.025. PubMed PMID: 18291106; PubMed Central PMCID: PMC2726283.
866. Mohorko N, Repovs G, Popovic M, Kovacs GG, Bresjanac M. Curcumin labeling of neuronal fibrillar tau inclusions in human brain samples. *Journal of neuropathology and experimental neurology*. 2010;69(4):405-14. doi: 10.1097/NEN.0b013e3181d709eb. PubMed PMID: 20448485.
867. Braskie MN, Medina LD, Rodriguez-Agudelo Y, Geschwind DH, Macias-Islas MA, Cummings JL, Bookheimer SY, Ringman JM. Increased fMRI signal with age in familial Alzheimer's disease mutation carriers. *Neurobiology of aging*. 2012;33(2):424 e11-21. doi: 10.1016/j.neurobiolaging.2010.09.028. PubMed PMID: 21129823; PubMed Central PMCID: PMC3097258.
868. Okamura N, Suemoto T, Furumoto S, Suzuki M, Shimadzu H, Akatsu H, Yamamoto T, Fujiwara H, Nemoto M, Maruyama M, Arai H, Yanai K, Sawada T, Kudo Y. Quinoline and benzimidazole derivatives: candidate probes for in vivo imaging of tau pathology in Alzheimer's disease. *The Journal of neuroscience : the official journal of the Society for Neuroscience*. 2005;25(47):10857-62. doi: 10.1523/JNEUROSCI.1738-05.2005. PubMed PMID: 16306398.
869. Xia CF, Arteaga J, Chen G, Gangadharmath U, Gomez LF, Kasi D, Lam C, Liang Q, Liu C, Mocharla VP, Mu F, Sinha A, Su H, Szardenings AK, Walsh JC, Wang E, Yu C, Zhang W, Zhao T, Kolb HC. [(18F)T807, a novel tau positron emission tomography imaging agent for Alzheimer's disease. *Alzheimer's & dementia : the journal of the Alzheimer's Association*. 2013;9(6):666-76. doi: 10.1016/j.jalz.2012.11.008. PubMed PMID: 23411393.
870. Fodero-Tavoletti MT, Okamura N, Furumoto S, Mulligan RS, Connor AR, McLean CA, Cao D, Rigopoulos A, Cartwright GA, O'Keefe G, Gong S, Adlard PA, Barnham KJ, Rowe CC, Masters CL, Kudo Y, Cappai R, Yanai K, Vilmagne

- VL. 18F-THK523: a novel in vivo tau imaging ligand for Alzheimer's disease. *Brain : a journal of neurology*. 2011;134(Pt 4):1089-100. doi: 10.1093/brain/awr038. PubMed PMID: 21436112.
871. Villemagne VL, Furumoto S, Fodero-Tavoletti MT, Mulligan RS, Hodges J, Harada R, Yates P, Piguet O, Pejoska S, Dore V, Yanai K, Masters CL, Kudo Y, Rowe CC, Okamura N. In vivo evaluation of a novel tau imaging tracer for Alzheimer's disease. *European journal of nuclear medicine and molecular imaging*. 2014;41(5):816-26. doi: 10.1007/s00259-013-2681-7. PubMed PMID: 24514874.
872. Okamura N, Furumoto S, Fodero-Tavoletti MT, Mulligan RS, Harada R, Yates P, Pejoska S, Kudo Y, Masters CL, Yanai K, Rowe CC, Villemagne VL. Non-invasive assessment of Alzheimer's disease neurofibrillary pathology using 18F-THK5105 PET. *Brain : a journal of neurology*. 2014;137(Pt 6):1762-71. doi: 10.1093/brain/awu064. PubMed PMID: 24681664.
873. Okamura N, Furumoto S, Harada R, Tago T, Yoshikawa T, Fodero-Tavoletti M, Mulligan RS, Villemagne VL, Akatsu H, Yamamoto T, Arai H, Iwata R, Yanai K, Kudo Y. Novel 18F-labeled arylquinoline derivatives for noninvasive imaging of tau pathology in Alzheimer disease. *Journal of nuclear medicine : official publication, Society of Nuclear Medicine*. 2013;54(8):1420-7. doi: 10.2967/jnumed.112.117341. PubMed PMID: 23857514.
874. Okamura N, Harada R, Furumoto S, Arai H, Yanai K, Kudo Y. Tau PET imaging in Alzheimer's disease. *Current neurology and neuroscience reports*. 2014;14(11):500. doi: 10.1007/s11910-014-0500-6. PubMed PMID: 25239654.
875. Chien DT, Szardenings AK, Bahri S, Walsh JC, Mu F, Xia C, Shankle WR, Lerner AJ, Su MY, Elizarov A, Kolb HC. Early clinical PET imaging results with the novel PHF-tau radioligand [F18]-T808. *Journal of Alzheimer's disease : JAD*. 2014;38(1):171-84. doi: 10.3233/JAD-130098. PubMed PMID: 23948934.
876. Chien DT, Bahri S, Szardenings AK, Walsh JC, Mu F, Su MY, Shankle WR, Elizarov A, Kolb HC. Early clinical PET imaging results with the novel PHF-tau radioligand [F-18]-T807. *Journal of Alzheimer's disease : JAD*. 2013;34(2):457-68. doi: 10.3233/JAD-122059. PubMed PMID: 23234879.
877. Xia CF, Arteaga J, Chen G, Gangadharmath U, Gomez LF, Kasi D, Lam C, Liang Q, Liu C, Mocharla VP, Mu F, Sinha A, Su H, Szardenings AK, Walsh JC, Wang E, Yu C, Zhang W, Zhao T, Kolb HC. [(18)F]T807, a novel tau positron emission tomography imaging agent for Alzheimer's disease. *Alzheimer's & dementia : the journal of the Alzheimer's Association*. 2013. doi: 10.1016/j.jalz.2012.11.008. PubMed PMID: 23411393.
878. Serrano-Pozo A, Frosch MP, Masliah E, Hyman BT. Neuropathological alterations in Alzheimer disease. *Cold Spring Harbor perspectives in medicine*. 2011;1(1):a006189. doi: 10.1101/cshperspect.a006189. PubMed PMID: 22229116; PubMed Central PMCID: PMC3234452.
879. Whitwell JL, Josephs KA, Murray ME, Kantarci K, Przybelski SA, Weigand SD, Vemuri P, Senjem ML, Parisi JE, Knopman DS, Boeve BF, Petersen RC, Dickson DW, Jack CR, Jr. MRI correlates of neurofibrillary tangle pathology at autopsy: a voxel-based morphometry study. *Neurology*. 2008;71(10):743-9. doi: 10.1212/01.wnl.0000324924.91351.7d. PubMed PMID: 18765650; PubMed Central PMCID: PMC2676950.
880. Sato K, Higuchi M, Iwata N, Saido TC, Sasamoto K. Fluoro-substituted and 13C-labeled styrylbenzene derivatives for detecting brain amyloid plaques. *European journal of medicinal chemistry*. 2004;39(7):573-8. doi: 10.1016/j.ejmech.2004.02.013. PubMed PMID: 15236837.
881. Li S, He H, Cui W, Gu B, Li J, Qi Z, Zhou G, Liang CM, Feng XY. Detection of Abeta plaques by a novel specific MRI probe precursor CR-BSA-(Gd-DTPA)n in APP/PS1 transgenic mice. *Anatomical record*. 2010;293(12):2136-43. doi: 10.1002/ar.21209. PubMed PMID: 21089051.
882. Maruyama M, Shimada H, Suhara T, Shinotoh H, Ji B, Maeda J, Zhang MR, Trojanowski JQ, Lee VM, Ono M, Masamoto K, Takano H, Sahara N, Iwata N, Okamura N, Furumoto S, Kudo Y, Chang Q, Saido TC, Takashima A, Lewis J, Jang MK, Aoki I, Ito H, Higuchi M. Imaging of tau pathology in a tauopathy mouse model and in Alzheimer patients compared to normal controls. *Neuron*. 2013;79(6):1094-108. doi: 10.1016/j.neuron.2013.07.037. PubMed PMID: 24050400; PubMed Central PMCID: PMC3809845.
883. Gu J, Anumala UR, Heyny-von Haussen R, Holzer J, Goetschy-Meyer V, Mall G, Hilger I, Czech C, Schmidt B. Design, synthesis and biological evaluation of trimethine cyanine dyes as fluorescent probes for the detection of tau fibrils in Alzheimer's disease brain and olfactory epithelium. *ChemMedChem*. 2013;8(6):891-7. doi: 10.1002/cmdc.201300090. PubMed PMID: 23592568.
884. Dickson DW. Neuropathological diagnosis of Alzheimer's disease: a perspective from longitudinal clinicopathological studies. *Neurobiology of aging*. 1997;18(4 Suppl):S21-6. PubMed PMID: 9330981.

885. Iliff JJ, Wang M, Liao Y, Plogg BA, Peng W, Gundersen GA, Benveniste H, Vates GE, Deane R, Goldman SA, Nagelhus EA, Nedergaard M. A paravascular pathway facilitates CSF flow through the brain parenchyma and the clearance of interstitial solutes, including amyloid beta. *Science translational medicine*. 2012;4(147):147ra11. doi: 10.1126/scitranslmed.3003748. PubMed PMID: 22896675; PubMed Central PMCID: PMC3551275.
886. Abbott NJ. Evidence for bulk flow of brain interstitial fluid: significance for physiology and pathology. *Neurochemistry international*. 2004;45(4):545-52. doi: 10.1016/j.neuint.2003.11.006. PubMed PMID: 15186921.
887. Koh L, Zakharov A, Johnston M. Integration of the subarachnoid space and lymphatics: is it time to embrace a new concept of cerebrospinal fluid absorption? *Cerebrospinal fluid research*. 2005;2:6. doi: 10.1186/1743-8454-2-6. PubMed PMID: 16174293; PubMed Central PMCID: PMC1266390.
888. Praetorius J. Water and solute secretion by the choroid plexus. *Pflugers Archiv : European journal of physiology*. 2007;454(1):1-18. doi: 10.1007/s00424-006-0170-6. PubMed PMID: 17120021.
889. Cserr HF, Cooper DN, Suri PK, Patlak CS. Efflux of radiolabeled polyethylene glycols and albumin from rat brain. *The American journal of physiology*. 1981;240(4):F319-28. PubMed PMID: 7223889.
890. Sykova E, Nicholson C. Diffusion in brain extracellular space. *Physiological reviews*. 2008;88(4):1277-340. doi: 10.1152/physrev.00027.2007. PubMed PMID: 18923183; PubMed Central PMCID: PMC2785730.
891. Ball KK, Cruz NF, Mrak RE, Dienel GA. Trafficking of glucose, lactate, and amyloid-beta from the inferior colliculus through perivascular routes. *Journal of cerebral blood flow and metabolism : official journal of the International Society of Cerebral Blood Flow and Metabolism*. 2010;30(1):162-76. doi: 10.1038/jcbfm.2009.206. PubMed PMID: 19794399; PubMed Central PMCID: PMC2801760.
892. Tabaton M, Nunzi MG, Xue R, Usiak M, Autilio-Gambetti L, Gambetti P. Soluble amyloid beta-protein is a marker of Alzheimer amyloid in brain but not in cerebrospinal fluid. *Biochemical and biophysical research communications*. 1994;200(3):1598-603. PubMed PMID: 8185615.
893. Van Nostrand WE, Wagner SL, Shankle WR, Farrow JS, Dick M, Rozemuller JM, Kuiper MA, Wolters EC, Zimmerman J, Cotman CW, et al. Decreased levels of soluble amyloid beta-protein precursor in cerebrospinal fluid of live Alzheimer disease patients. *Proceedings of the National Academy of Sciences of the United States of America*. 1992;89(7):2551-5. PubMed PMID: 1557359; PubMed Central PMCID: PMC48699.
894. Portelius E, Westman-Brinkmalm A, Zetterberg H, Blennow K. Determination of beta-amyloid peptide signatures in cerebrospinal fluid using immunoprecipitation-mass spectrometry. *Journal of proteome research*. 2006;5(4):1010-6. doi: 10.1021/pr050475v. PubMed PMID: 16602710.
895. Motter R, Vigo-Pelfrey C, Kholodenko D, Barbour R, Johnson-Wood K, Galasko D, Chang L, Miller B, Clark C, Green R, et al. Reduction of beta-amyloid peptide42 in the cerebrospinal fluid of patients with Alzheimer's disease. *Annals of neurology*. 1995;38(4):643-8. doi: 10.1002/ana.410380413. PubMed PMID: 7574461.
896. Blennow K, Vanmechelen E. CSF markers for pathogenic processes in Alzheimer's disease: diagnostic implications and use in clinical neurochemistry. *Brain research bulletin*. 2003;61(3):235-42. PubMed PMID: 12909293.
897. Hansson O, Zetterberg H, Buchhave P, Andreasson U, Londos E, Minthon L, Blennow K. Prediction of Alzheimer's disease using the CSF Aβ42/Aβ40 ratio in patients with mild cognitive impairment. *Dementia and geriatric cognitive disorders*. 2007;23(5):316-20. doi: 10.1159/000100926. PubMed PMID: 17374949.
898. Lewczuk P, Lelental N, Spitzer P, Maler JM, Kornhuber J. Amyloid-beta 42/40 cerebrospinal fluid concentration ratio in the diagnostics of Alzheimer's disease: validation of two novel assays. *Journal of Alzheimer's disease : JAD*. 2015;43(1):183-91. doi: 10.3233/JAD-140771. PubMed PMID: 25079805.
899. Mehta PD, Pirttila T, Mehta SP, Sersen EA, Aisen PS, Wisniewski HM. Plasma and cerebrospinal fluid levels of amyloid beta proteins 1-40 and 1-42 in Alzheimer disease. *Archives of neurology*. 2000;57(1):100-5. PubMed PMID: 10634455.
900. Wiltfang J, Esselmann H, Bibl M, Hull M, Hampel H, Kessler H, Frolich L, Schroder J, Peters O, Jessen F, Luckhaus C, Perneczky R, Jahn H, Fiszer M, Maler JM, Zimmermann R, Bruckmoser R, Kornhuber J, Lewczuk P. Amyloid beta peptide ratio 42/40 but not Aβ42 correlates with phospho-Tau in patients with low- and high-CSF Aβ40 load. *Journal of neurochemistry*. 2007;101(4):1053-9. doi: 10.1111/j.1471-4159.2006.04404.x. PubMed PMID: 17254013.
901. Stroszyk D, Blennow K, White LR, Launer LJ. CSF Aβ42 levels correlate with amyloid-neuropathology in a population-based autopsy study. *Neurology*. 2003;60(4):652-6. PubMed PMID: 12601108.

902. Fagan AM, Mintun MA, Mach RH, Lee SY, Dence CS, Shah AR, LaRossa GN, Spinner ML, Klunk WE, Mathis CA, DeKosky ST, Morris JC, Holtzman DM. Inverse relation between in vivo amyloid imaging load and cerebrospinal fluid Abeta42 in humans. *Annals of neurology*. 2006;59(3):512-9. doi: 10.1002/ana.20730. PubMed PMID: 16372280.
903. Fagan AM, Mintun MA, Shah AR, Aldea P, Roe CM, Mach RH, Marcus D, Morris JC, Holtzman DM. Cerebrospinal fluid tau and ptau(181) increase with cortical amyloid deposition in cognitively normal individuals: implications for future clinical trials of Alzheimer's disease. *EMBO molecular medicine*. 2009;1(8-9):371-80. doi: 10.1002/emmm.200900048. PubMed PMID: 20049742; PubMed Central PMCID: PMC2806678.
904. Fagan AM, Roe CM, Xiong C, Mintun MA, Morris JC, Holtzman DM. Cerebrospinal fluid tau/beta-amyloid(42) ratio as a prediction of cognitive decline in nondemented older adults. *Archives of neurology*. 2007;64(3):343-9. doi: 10.1001/archneur.64.3.noc60123. PubMed PMID: 17210801.
905. Jagust WJ, Landau SM, Shaw LM, Trojanowski JQ, Koeppe RA, Reiman EM, Foster NL, Petersen RC, Weiner MW, Price JC, Mathis CA, Alzheimer's Disease Neuroimaging I. Relationships between biomarkers in aging and dementia. *Neurology*. 2009;73(15):1193-9. doi: 10.1212/WNL.0b013e3181bc010c. PubMed PMID: 19822868; PubMed Central PMCID: PMC2764726.
906. Tolboom N, van der Flier WM, Yaqub M, Boellaard R, Verwey NA, Blankenstein MA, Windhorst AD, Scheltens P, Lammertsma AA, van Berckel BN. Relationship of cerebrospinal fluid markers to 11C-PiB and 18F-FDDNP binding. *Journal of nuclear medicine : official publication, Society of Nuclear Medicine*. 2009;50(9):1464-70. doi: 10.2967/jnumed.109.064360. PubMed PMID: 19690025.
907. Degerman Gunnarsson M, Lindau M, Wall A, Blennow K, Darreh-Shori T, Basu S, Nordberg A, Larsson A, Lannfelt L, Basun H, Kilander L. Pittsburgh compound-B and Alzheimer's disease biomarkers in CSF, plasma and urine: An exploratory study. *Dementia and geriatric cognitive disorders*. 2010;29(3):204-12. doi: 10.1159/000281832. PubMed PMID: 20332638.
908. Zwan M, van Harten A, Ossenkoppele R, Bouwman F, Teunissen C, Adriaanse S, Lammertsma A, Scheltens P, van Berckel B, van der Flier W. Concordance between cerebrospinal fluid biomarkers and [11C]PiB PET in a memory clinic cohort. *Journal of Alzheimer's disease : JAD*. 2014;41(3):801-7. doi: 10.3233/JAD-132561. PubMed PMID: 24705549.
909. Landau SM, Lu M, Joshi AD, Pontecorvo M, Mintun MA, Trojanowski JQ, Shaw LM, Jagust WJ, Alzheimer's Disease Neuroimaging I. Comparing positron emission tomography imaging and cerebrospinal fluid measurements of beta-amyloid. *Annals of neurology*. 2013;74(6):826-36. doi: 10.1002/ana.23908. PubMed PMID: 23536396; PubMed Central PMCID: PMC3748164.
910. Palmqvist S, Zetterberg H, Blennow K, Vestberg S, Andreasson U, Brooks DJ, Owenius R, Hagerstrom D, Wollmer P, Minthon L, Hansson O. Accuracy of brain amyloid detection in clinical practice using cerebrospinal fluid beta-amyloid 42: a cross-validation study against amyloid positron emission tomography. *JAMA neurology*. 2014;71(10):1282-9. doi: 10.1001/jamaneurol.2014.1358. PubMed PMID: 25155658.
911. Csernansky JG, Miller JP, McKeel D, Morris JC. Relationships among cerebrospinal fluid biomarkers in dementia of the Alzheimer type. *Alzheimer disease and associated disorders*. 2002;16(3):144-9. PubMed PMID: 12218644.
912. Riemenschneider M, Schmolke M, Lautenschlager N, Guder WG, Vanderstichele H, Vanmechelen E, Kurz A. Cerebrospinal beta-amyloid ((1-42)) in early Alzheimer's disease: association with apolipoprotein E genotype and cognitive decline. *Neuroscience letters*. 2000;284(1-2):85-8. PubMed PMID: 10771168.
913. Lin YT, Cheng JT, Yao YC, Juo, Lo YK, Lin CH, Ger LP, Lu PJ. Increased total TAU but not amyloid-beta(42) in cerebrospinal fluid correlates with short-term memory impairment in Alzheimer's disease. *Journal of Alzheimer's disease : JAD*. 2009;18(4):907-18. doi: 10.3233/JAD-2009-1214. PubMed PMID: 19749420.
914. Ivanoiu A, Sindic CJ. Cerebrospinal fluid TAU protein and amyloid beta42 in mild cognitive impairment: prediction of progression to Alzheimer's disease and correlation with the neuropsychological examination. *Neurocase*. 2005;11(1):32-9. doi: 10.1080/13554790490896901. PubMed PMID: 15804922.
915. Bradbury MW, Westrop RJ. Factors influencing exit of substances from cerebrospinal fluid into deep cervical lymph of the rabbit. *The Journal of physiology*. 1983;339:519-34. PubMed PMID: 6411905; PubMed Central PMCID: PMC1199176.
916. Boulton M, Young A, Hay J, Armstrong D, Flessner M, Schwartz M, Johnston M. Drainage of CSF through lymphatic pathways and arachnoid villi in sheep: measurement of 125I-albumin clearance. *Neuropathology and applied neurobiology*. 1996;22(4):325-33. PubMed PMID: 8875467.

917. Johnston M, Zakharov A, Papaiconomou C, Salmasi G, Armstrong D. Evidence of connections between cerebrospinal fluid and nasal lymphatic vessels in humans, non-human primates and other mammalian species. *Cerebrospinal fluid research*. 2004;1(1):2. doi: 10.1186/1743-8454-1-2. PubMed PMID: 15679948; PubMed Central PMCID: PMC546409.
918. Huang Y, Potter R, Sigurdson W, Kasten T, Connors R, Morris JC, Benzinger T, Mintun M, Ashwood T, Ferm M, Budd SL, Bateman RJ. beta-amyloid dynamics in human plasma. *Archives of neurology*. 2012;69(12):1591-7. doi: 10.1001/archneurol.2012.18107. PubMed PMID: 23229043; PubMed Central PMCID: PMC3808092.
919. Toledo JB, Vanderstichele H, Figurski M, Aisen PS, Petersen RC, Weiner MW, Jack CR, Jr., Jagust W, Decarli C, Toga AW, Toledo E, Xie SX, Lee VM, Trojanowski JQ, Shaw LM, Alzheimer's Disease Neuroimaging I. Factors affecting Abeta plasma levels and their utility as biomarkers in ADNI. *Acta neuropathologica*. 2011;122(4):401-13. doi: 10.1007/s00401-011-0861-8. PubMed PMID: 21805181; PubMed Central PMCID: PMC3299300.
920. Le Bastard N, Leurs J, Blomme W, De Deyn PP, Engelborghs S. Plasma amyloid-beta forms in Alzheimer's disease and non-Alzheimer's disease patients. *Journal of Alzheimer's disease : JAD*. 2010;21(1):291-301. doi: 10.3233/JAD-2010-091501. PubMed PMID: 20421698.
921. Hansson O, Stomrud E, Vanmechelen E, Ostling S, Gustafson DR, Zetterberg H, Blennow K, Skoog I. Evaluation of plasma Abeta as predictor of Alzheimer's disease in older individuals without dementia: a population-based study. *Journal of Alzheimer's disease : JAD*. 2012;28(1):231-8. doi: 10.3233/JAD-2011-111418. PubMed PMID: 21955816.
922. Lui JK, Laws SM, Li QX, Villemagne VL, Ames D, Brown B, Bush AI, De Ruyck K, Dromey J, Ellis KA, Faux NG, Foster J, Fowler C, Gupta V, Hudson P, Laughton K, Masters CL, Pertile K, Rembach A, Rimajova M, Rodrigues M, Rowe CC, Rumble R, Szoek C, Taddei K, Taddei T, Trounson B, Ward V, Martins RN, Group AR. Plasma amyloid-beta as a biomarker in Alzheimer's disease: the AIBL study of aging. *Journal of Alzheimer's disease : JAD*. 2010;20(4):1233-42. doi: 10.3233/JAD-2010-090249. PubMed PMID: 20413897.
923. Selkoe DJ, Podlisny MB, Joachim CL, Vickers EA, Lee G, Fritz LC, Oltersdorf T. Beta-amyloid precursor protein of Alzheimer disease occurs as 110- to 135-kilodalton membrane-associated proteins in neural and nonneural tissues. *Proceedings of the National Academy of Sciences of the United States of America*. 1988;85(19):7341-5. PubMed PMID: 3140239; PubMed Central PMCID: PMC282182.
924. Roher AE, Esh CL, Kokjohn TA, Castano EM, Van Vickle GD, Kalback WM, Patton RL, Luehrs DC, Dausgs ID, Kuo YM, Emmerling MR, Soares H, Quinn JF, Kaye J, Connor DJ, Silverberg NB, Adler CH, Seward JD, Beach TG, Sabbagh MN. Amyloid beta peptides in human plasma and tissues and their significance for Alzheimer's disease. *Alzheimer's & dementia : the journal of the Alzheimer's Association*. 2009;5(1):18-29. doi: 10.1016/j.jalz.2008.10.004. PubMed PMID: 19118806; PubMed Central PMCID: PMC2663406.
925. Arai H, Lee VM, Messinger ML, Greenberg BD, Lowery DE, Trojanowski JQ. Expression patterns of beta-amyloid precursor protein (beta-APP) in neural and nonneural human tissues from Alzheimer's disease and control subjects. *Annals of neurology*. 1991;30(5):686-93. doi: 10.1002/ana.410300509. PubMed PMID: 1763893.
926. Kuo YM, Kokjohn TA, Kalback W, Luehrs D, Galasko DR, Chevallier N, Koo EH, Emmerling MR, Roher AE. Amyloid-beta peptides interact with plasma proteins and erythrocytes: implications for their quantitation in plasma. *Biochemical and biophysical research communications*. 2000;268(3):750-6. doi: 10.1006/bbrc.2000.2222. PubMed PMID: 10679277.
927. Skovronsky DM, Lee VM, Pratico D. Amyloid precursor protein and amyloid beta peptide in human platelets. Role of cyclooxygenase and protein kinase C. *The Journal of biological chemistry*. 2001;276(20):17036-43. doi: 10.1074/jbc.M006285200. PubMed PMID: 11278299.
928. Ertekin-Taner N, Graff-Radford N, Younkin LH, Eckman C, Adamson J, Schaid DJ, Blangero J, Hutton M, Younkin SG. Heritability of plasma amyloid beta in typical late-onset Alzheimer's disease pedigrees. *Genetic epidemiology*. 2001;21(1):19-30. doi: 10.1002/gepi.1015. PubMed PMID: 11443731.
929. Ibrahim-Verbaas CA, Zorkoltseva IV, Amin N, Schuur M, Coppus AM, Isaacs A, Aulchenko YS, Breteler MM, Ikram MA, Axenovich TI, Verbeek MM, van Swieten JC, Oostra BA, van Duijn CM. Linkage analysis for plasma amyloid beta levels in persons with hypertension implicates Abeta-40 levels to presenilin 2. *Human genetics*. 2012;131(12):1869-76. doi: 10.1007/s00439-012-1210-2. PubMed PMID: 22872014.
930. Bibl M, Welge V, Esselmann H, Wiltfang J. Stability of amyloid-beta peptides in plasma and serum. *Electrophoresis*. 2012;33(3):445-50. doi: 10.1002/elps.201100455. PubMed PMID: 22287174.

931. Lachno DR, Emerson JK, Vanderstichele H, Gonzales C, Martenyi F, Konrad RJ, Talbot JA, Lowe SL, Oefinger PE, Dean RA. Validation of a multiplex assay for simultaneous quantification of amyloid-beta peptide species in human plasma with utility for measurements in studies of Alzheimer's disease therapeutics. *Journal of Alzheimer's disease : JAD.* 2012;32(4):905-18. doi: 10.3233/JAD-2012-121075. PubMed PMID: 22886018.
932. Lachno DR, Evert BA, Vanderstichele H, Robertson M, Demattos RB, Konrad RJ, Talbot JA, Racke MM, Dean RA. Validation of assays for measurement of amyloid-beta peptides in cerebrospinal fluid and plasma specimens from patients with Alzheimer's disease treated with solanezumab. *Journal of Alzheimer's disease : JAD.* 2013;34(4):897-910. doi: 10.3233/JAD-122317. PubMed PMID: 23302661.
933. Arvanitakis Z, Lucas JA, Younkin LH, Younkin SG, Graff-Radford NR. Serum creatinine levels correlate with plasma amyloid Beta protein. *Alzheimer disease and associated disorders.* 2002;16(3):187-90. PubMed PMID: 12218650.
934. Chouraki V, Beiser A, Younkin L, Preis SR, Weinstein G, Hansson O, Skoog I, Lambert JC, Au R, Launer L, Wolf PA, Younkin S, Seshadri S. Plasma amyloid-beta and risk of Alzheimer's disease in the Framingham Heart Study. *Alzheimer's & dementia : the journal of the Alzheimer's Association.* 2015;11(3):249-57 e1. doi: 10.1016/j.jalz.2014.07.001. PubMed PMID: 25217292; PubMed Central PMCID: PMC4362883.
935. Sunderland T, Linker G, Mirza N, Putnam KT, Friedman DL, Kimmel LH, Bergeson J, Manetti GJ, Zimmermann M, Tang B, Bartko JJ, Cohen RM. Decreased beta-amyloid1-42 and increased tau levels in cerebrospinal fluid of patients with Alzheimer disease. *Jama.* 2003;289(16):2094-103. doi: 10.1001/jama.289.16.2094. PubMed PMID: 12709467.
936. Bloudek LM, Spackman DE, Blankenburg M, Sullivan SD. Review and meta-analysis of biomarkers and diagnostic imaging in Alzheimer's disease. *Journal of Alzheimer's disease : JAD.* 2011;26(4):627-45. doi: 10.3233/JAD-2011-110458. PubMed PMID: 21694448.
937. Mitchell AJ. CSF phosphorylated tau in the diagnosis and prognosis of mild cognitive impairment and Alzheimer's disease: a meta-analysis of 51 studies. *Journal of neurology, neurosurgery, and psychiatry.* 2009;80(9):966-75. doi: 10.1136/jnnp.2008.167791. PubMed PMID: 19465413.
938. Hutton M, Lewis J, Dickson D, Yen SH, McGowan E. Analysis of tauopathies with transgenic mice. *Trends in molecular medicine.* 2001;7(10):467-70. PubMed PMID: 11597522.
939. Crespo-Biel N, Theunis C, Van Leuven F. Protein tau: prime cause of synaptic and neuronal degeneration in Alzheimer's disease. *International journal of Alzheimer's disease.* 2012;2012:251426. doi: 10.1155/2012/251426. PubMed PMID: 22720188; PubMed Central PMCID: PMC3376502.
940. Eisenberg D, Jucker M. The amyloid state of proteins in human diseases. *Cell.* 2012;148(6):1188-203. doi: 10.1016/j.cell.2012.02.022. PubMed PMID: 22424229; PubMed Central PMCID: PMC3353745.
941. Kolarova M, Garcia-Sierra F, Bartos A, Ricny J, Ripova D. Structure and pathology of tau protein in Alzheimer disease. *International journal of Alzheimer's disease.* 2012;2012:731526. doi: 10.1155/2012/731526. PubMed PMID: 22690349; PubMed Central PMCID: PMC3368361.
942. Mudher A, Shepherd D, Newman TA, Mildren P, Jukes JP, Squire A, Mears A, Drummond JA, Berg S, MacKay D, Asuni AA, Bhat R, Lovestone S. GSK-3beta inhibition reverses axonal transport defects and behavioural phenotypes in *Drosophila*. *Molecular psychiatry.* 2004;9(5):522-30. doi: 10.1038/sj.mp.4001483. PubMed PMID: 14993907.
943. Kimura T, Yamashita S, Fukuda T, Park JM, Murayama M, Mizoroki T, Yoshiike Y, Sahara N, Takashima A. Hyperphosphorylated tau in parahippocampal cortex impairs place learning in aged mice expressing wild-type human tau. *The EMBO journal.* 2007;26(24):5143-52. doi: 10.1038/sj.emboj.7601917. PubMed PMID: 18007595; PubMed Central PMCID: PMC2140104.
944. Cowan CM, Bossing T, Page A, Shepherd D, Mudher A. Soluble hyper-phosphorylated tau causes microtubule breakdown and functionally compromises normal tau in vivo. *Acta neuropathologica.* 2010;120(5):593-604. doi: 10.1007/s00401-010-0716-8. PubMed PMID: 20617325.
945. Chee FC, Mudher A, Cuttle MF, Newman TA, MacKay D, Lovestone S, Shepherd D. Over-expression of tau results in defective synaptic transmission in *Drosophila* neuromuscular junctions. *Neurobiology of disease.* 2005;20(3):918-28. doi: 10.1016/j.nbd.2005.05.029. PubMed PMID: 16023860.
946. Mershin A, Pavlopoulos E, Fitch O, Braden BC, Nanopoulos DV, Skoulakis EM. Learning and memory deficits upon TAU accumulation in *Drosophila* mushroom body neurons. *Learning & memory.* 2004;11(3):277-87. doi: 10.1101/lm.70804. PubMed PMID: 15169857; PubMed Central PMCID: PMC419730.

947. Fox LM, William CM, Adamowicz DH, Pitstick R, Carlson GA, Spires-Jones TL, Hyman BT. Soluble tau species, not neurofibrillary aggregates, disrupt neural system integration in a tau transgenic model. *Journal of neuropathology and experimental neurology*. 2011;70(7):588-95. doi: 10.1097/NEN.0b013e318220a658. PubMed PMID: 21666499; PubMed Central PMCID: PMC3118928.
948. Tai HC, Serrano-Pozo A, Hashimoto T, Frosch MP, Spires-Jones TL, Hyman BT. The synaptic accumulation of hyperphosphorylated tau oligomers in Alzheimer disease is associated with dysfunction of the ubiquitin-proteasome system. *The American journal of pathology*. 2012;181(4):1426-35. doi: 10.1016/j.ajpath.2012.06.033. PubMed PMID: 22867711; PubMed Central PMCID: PMC3463637.
949. Cowan CM, Sealey MA, Quraishe S, Targett MT, Marcellus K, Allan D, Mudher A. Modelling tauopathies in *Drosophila*: insights from the fruit fly. *International journal of Alzheimer's disease*. 2011;2011:598157. doi: 10.4061/2011/598157. PubMed PMID: 22254145; PubMed Central PMCID: PMC3255107.
950. Lasagna-Reeves CA, Castillo-Carranza DL, Guerrero-Muoz MJ, Jackson GR, Kaye R. Preparation and characterization of neurotoxic tau oligomers. *Biochemistry*. 2010;49(47):10039-41. doi: 10.1021/bi1016233. PubMed PMID: 21047142.
951. Bian H, Van Swieten JC, Leight S, Massimo L, Wood E, Forman M, Moore P, de Koning I, Clark CM, Rosso S, Trojanowski J, Lee VM, Grossman M. CSF biomarkers in frontotemporal lobar degeneration with known pathology. *Neurology*. 2008;70(19 Pt 2):1827-35. doi: 10.1212/01.wnl.0000311445.21321.fc. PubMed PMID: 18458217; PubMed Central PMCID: PMC2707002.
952. Grossman M, Farmer J, Leight S, Work M, Moore P, Van Deerlin V, Pratico D, Clark CM, Coslett HB, Chatterjee A, Gee J, Trojanowski JQ, Lee VM. Cerebrospinal fluid profile in frontotemporal dementia and Alzheimer's disease. *Annals of neurology*. 2005;57(5):721-9. doi: 10.1002/ana.20477. PubMed PMID: 15852395.
953. Weintraub S, Wicklund AH, Salmon DP. The neuropsychological profile of Alzheimer disease. *Cold Spring Harbor perspectives in medicine*. 2012;2(4):a006171. doi: 10.1101/cshperspect.a006171. PubMed PMID: 22474609; PubMed Central PMCID: PMC3312395.
954. Flood DG, Marek GJ, Williams M. Developing predictive CSF biomarkers-a challenge critical to success in Alzheimer's disease and neuropsychiatric translational medicine. *Biochemical pharmacology*. 2011;81(12):1422-34. doi: 10.1016/j.bcp.2011.01.021. PubMed PMID: 21295552.
955. Rapoport M, Dawson HN, Binder LI, Vitek MP, Ferreira A. Tau is essential to beta -amyloid-induced neurotoxicity. *Proceedings of the National Academy of Sciences of the United States of America*. 2002;99(9):6364-9. doi: 10.1073/pnas.092136199. PubMed PMID: 11959919; PubMed Central PMCID: PMC122954.
956. Ferreira LK, Busatto GF. Neuroimaging in Alzheimer's disease: current role in clinical practice and potential future applications. *Clinics*. 2011;66 Suppl 1:19-24. PubMed PMID: 21779719; PubMed Central PMCID: PMC3118433.
957. Small GW, Bookheimer SY, Thompson PM, Cole GM, Huang SC, Kepe V, Barrio JR. Current and future uses of neuroimaging for cognitively impaired patients. *The Lancet Neurology*. 2008;7(2):161-72. doi: 10.1016/S1474-4422(08)70019-X. PubMed PMID: 18207114; PubMed Central PMCID: PMC2728702.
958. Mistur R, Mosconi L, Santi SD, Guzman M, Li Y, Tsui W, de Leon MJ. Current Challenges for the Early Detection of Alzheimer's Disease: Brain Imaging and CSF Studies. *Journal of clinical neurology*. 2009;5(4):153-66. doi: 10.3988/jcn.2009.5.4.153. PubMed PMID: 20076796; PubMed Central PMCID: PMC2806537.
959. Coimbra A, Williams DS, Hostetler ED. The role of MRI and PET/SPECT in Alzheimer's disease. *Current topics in medicinal chemistry*. 2006;6(6):629-47. PubMed PMID: 16712496.
960. Frisoni GB, Fox NC, Jack CR, Jr., Scheltens P, Thompson PM. The clinical use of structural MRI in Alzheimer disease. *Nature reviews Neurology*. 2010;6(2):67-77. doi: 10.1038/nrneurol.2009.215. PubMed PMID: 20139996; PubMed Central PMCID: PMC2938772.
961. Vemuri P, Jack CR, Jr. Role of structural MRI in Alzheimer's disease. *Alzheimer's research & therapy*. 2010;2(4):23. doi: 10.1186/alzrt47. PubMed PMID: 20807454; PubMed Central PMCID: PMC2949589.
962. Glodzik-Sobanska L, Rusinek H, Mosconi L, Li Y, Zhan J, de Santi S, Convit A, Rich K, Brys M, de Leon MJ. The role of quantitative structural imaging in the early diagnosis of Alzheimer's disease. *Neuroimaging clinics of North America*. 2005;15(4):803-26, x. doi: 10.1016/j.nic.2005.09.004. PubMed PMID: 16443492.
963. Ramani A, Jensen JH, Helpert JA. Quantitative MR imaging in Alzheimer disease. *Radiology*. 2006;241(1):26-44. doi: 10.1148/radiol.2411050628. PubMed PMID: 16990669.

964. Lehericy S, Marjanska M, Mesrob L, Sarazin M, Kinkingnehun S. Magnetic resonance imaging of Alzheimer's disease. *European radiology*. 2007;17(2):347-62. doi: 10.1007/s00330-006-0341-z. PubMed PMID: 16865367.
965. Yakushev I, Schreckenberger M, Muller MJ, Schermuly I, Cumming P, Stoeter P, Gerhard A, Fellgiebel A. Functional implications of hippocampal degeneration in early Alzheimer's disease: a combined DTI and PET study. *European journal of nuclear medicine and molecular imaging*. 2011;38(12):2219-27. doi: 10.1007/s00259-011-1882-1. PubMed PMID: 21792570.
966. Hattori T, Sato R, Aoki S, Yuasa T, Mizusawa H. Different patterns of fornix damage in idiopathic normal pressure hydrocephalus and Alzheimer disease. *AJNR American journal of neuroradiology*. 2012;33(2):274-9. doi: 10.3174/ajnr.A2780. PubMed PMID: 22081679.
967. Wu W, Small SA. Imaging the earliest stages of Alzheimer's disease. *Current Alzheimer research*. 2006;3(5):529-39. PubMed PMID: 17168652.
968. Brickman AM, Small SA, Fleisher A. Pinpointing synaptic loss caused by Alzheimer's disease with fMRI. *Behavioural neurology*. 2009;21(1):93-100. doi: 10.3233/BEN-2009-0240. PubMed PMID: 19847048; PubMed Central PMCID: PMC2857999.
969. Sperling RA, Dickerson BC, Pihlajamaki M, Vannini P, LaViolette PS, Vitolo OV, Hedden T, Becker JA, Rentz DM, Selkoe DJ, Johnson KA. Functional alterations in memory networks in early Alzheimer's disease. *Neuromolecular medicine*. 2010;12(1):27-43. doi: 10.1007/s12017-009-8109-7. PubMed PMID: 20069392; PubMed Central PMCID: PMC3036844.
970. McClure R, Chumbley C, Reyzer M, Wilson K, Caprioli R, Gore J, Pham W. Identification of promethazine as an amyloid-binding molecule using fluorescence high-throughput assay and MALDI imaging mass spectrometry *Neuroimage: Clinical*. 2013;2:620-9.
971. Karran E, Hardy J. A critique of the drug discovery and phase 3 clinical programs targeting the amyloid hypothesis for Alzheimer disease. *Annals of neurology*. 2014;76(2):185-205. doi: 10.1002/ana.24188. PubMed PMID: 24853080; PubMed Central PMCID: PMC4204160.
972. Salloway S, Sperling R, Fox NC, Blennow K, Klunk W, Raskind M, Sabbagh M, Honig LS, Porsteinsson AP, Ferris S, Reichert M, Ketter N, Nejadnik B, Guenzler V, Miloslavsky M, Wang D, Lu Y, Lull J, Tudor IC, Liu E, Grundman M, Yuen E, Black R, Brashear HR, Bapineuzumab, Clinical Trial I. Two phase 3 trials of bapineuzumab in mild-to-moderate Alzheimer's disease. *The New England journal of medicine*. 2014;370(4):322-33. doi: 10.1056/NEJMoa1304839. PubMed PMID: 24450891; PubMed Central PMCID: PMC4159618.
973. Green RC, Schneider LS, Amato DA, Beelen AP, Wilcock G, Swabb EA, Zavitz KH, Tarenflur bil Phase 3 Study G. Effect of tarenflur bil on cognitive decline and activities of daily living in patients with mild Alzheimer disease: a randomized controlled trial. *Jama*. 2009;302(23):2557-64. doi: 10.1001/jama.2009.1866. PubMed PMID: 20009055; PubMed Central PMCID: PMC2902875.
974. Toyn JH, Ahlijanian MK. Interpreting Alzheimer's disease clinical trials in light of the effects on amyloid-beta. *Alzheimer's research & therapy*. 2014;6(2):14. doi: 10.1186/alzrt244. PubMed PMID: 25031632; PubMed Central PMCID: PMC4014014.
975. Gilman S, Koller M, Black RS, Jenkins L, Griffith SG, Fox NC, Eisner L, Kirby L, Rovira MB, Forette F, Orgogozo JM, Team ANS. Clinical effects of Abeta immunization (AN1792) in patients with AD in an interrupted trial. *Neurology*. 2005;64(9):1553-62. doi: 10.1212/01.WNL.0000159740.16984.3C. PubMed PMID: 15883316.
976. Hyman BT. Amyloid-dependent and amyloid-independent stages of Alzheimer disease. *Archives of neurology*. 2011;68(8):1062-4. doi: 10.1001/archneurol.2011.70. PubMed PMID: 21482918.
977. Serpell LC. Alzheimer's amyloid fibrils: structure and assembly. *Biochimica et biophysica acta*. 2000;1502(1):16-30. PubMed PMID: 10899428.
978. Sunde M, Serpell LC, Bartlam M, Fraser PE, Pepys MB, Blake CC. Common core structure of amyloid fibrils by synchrotron X-ray diffraction. *Journal of molecular biology*. 1997;273(3):729-39. doi: 10.1006/jmbi.1997.1348. PubMed PMID: 9356260.
979. Serpell LC, Blake CC, Fraser PE. Molecular structure of a fibrillar Alzheimer's A beta fragment. *Biochemistry*. 2000;39(43):13269-75. PubMed PMID: 11052680.

980. Pike VW. PET radiotracers: crossing the blood-brain barrier and surviving metabolism. *Trends in pharmacological sciences*. 2009;30(8):431-40. doi: 10.1016/j.tips.2009.05.005. PubMed PMID: 19616318; PubMed Central PMCID: PMC2805092.
981. Pardridge WM. The blood-brain barrier: bottleneck in brain drug development. *NeuroRx : the journal of the American Society for Experimental NeuroTherapeutics*. 2005;2(1):3-14. doi: 10.1602/neurorx.2.1.3. PubMed PMID: 15717053; PubMed Central PMCID: PMC539316.
982. Pardridge WM. Drug transport across the blood-brain barrier. *Journal of cerebral blood flow and metabolism : official journal of the International Society of Cerebral Blood Flow and Metabolism*. 2012;32(11):1959-72. doi: 10.1038/jcbfm.2012.126. PubMed PMID: 22929442; PubMed Central PMCID: PMC3494002.
983. Brightman MW, Reese TS. Junctions between intimately apposed cell membranes in the vertebrate brain. *The Journal of cell biology*. 1969;40(3):648-77. PubMed PMID: 5765759; PubMed Central PMCID: PMC2107650.
984. Mukherjee J, Christian BT, Dunigan KA, Shi B, Narayanan TK, Satter M, Mantil J. Brain imaging of 18F-fallypride in normal volunteers: blood analysis, distribution, test-retest studies, and preliminary assessment of sensitivity to aging effects on dopamine D-2/D-3 receptors. *Synapse*. 2002;46(3):170-88. doi: 10.1002/syn.10128. PubMed PMID: 12325044.
985. Fujimura Y, Zoghbi SS, Simeon FG, Taku A, Pike VW, Innis RB, Fujita M. Quantification of translocator protein (18 kDa) in the human brain with PET and a novel radioligand, (18)F-PBR06. *Journal of nuclear medicine : official publication, Society of Nuclear Medicine*. 2009;50(7):1047-53. doi: 10.2967/jnumed.108.060186. PubMed PMID: 19525468; PubMed Central PMCID: PMC2786064.
986. Kropholler MA, Boellaard R, Schuitemaker A, van Berckel BN, Luurtsema G, Windhorst AD, Lammertsma AA. Development of a tracer kinetic plasma input model for (R)-[11C]PK11195 brain studies. *Journal of cerebral blood flow and metabolism : official journal of the International Society of Cerebral Blood Flow and Metabolism*. 2005;25(7):842-51. doi: 10.1038/sj.jcbfm.9600092. PubMed PMID: 15744248.
987. Pajouhesh H, Lenz GR. Medicinal chemical properties of successful central nervous system drugs. *NeuroRx : the journal of the American Society for Experimental NeuroTherapeutics*. 2005;2(4):541-53. doi: 10.1602/neurorx.2.4.541. PubMed PMID: 16489364; PubMed Central PMCID: PMC1201314.
988. van de Waterbeemd H, Camenisch G, Folkers G, Chretien JR, Raevsky OA. Estimation of blood-brain barrier crossing of drugs using molecular size and shape, and H-bonding descriptors. *Journal of drug targeting*. 1998;6(2):151-65. doi: 10.3109/10611869808997889. PubMed PMID: 9886238.
989. Waterhouse RN. Determination of lipophilicity and its use as a predictor of blood-brain barrier penetration of molecular imaging agents. *Molecular imaging and biology : MIB : the official publication of the Academy of Molecular Imaging*. 2003;5(6):376-89. PubMed PMID: 14667492.
990. Fodero-Tavoletti MT, Rowe CC, McLean CA, Leone L, Li QX, Masters CL, Cappai R, Villemagne VL. Characterization of PiB binding to white matter in Alzheimer disease and other dementias. *Journal of nuclear medicine : official publication, Society of Nuclear Medicine*. 2009;50(2):198-204. doi: 10.2967/jnumed.108.057984. PubMed PMID: 19164220.
991. Hawe A, Sutter M, Jiskoot W. Extrinsic fluorescent dyes as tools for protein characterization. *Pharmaceutical research*. 2008;25(7):1487-99. doi: 10.1007/s11095-007-9516-9. PubMed PMID: 18172579; PubMed Central PMCID: PMC2440933.
992. Bolder SG, Sagis LM, Venema P, van der Linden E. Thioflavin T and birefringence assays to determine the conversion of proteins into fibrils. *Langmuir : the ACS journal of surfaces and colloids*. 2007;23(8):4144-7. doi: 10.1021/la063048k. PubMed PMID: 17341102.
993. Biancalana M, Koide S. Molecular mechanism of Thioflavin-T binding to amyloid fibrils. *Biochimica et biophysica acta*. 2010;1804(7):1405-12. doi: 10.1016/j.bbapap.2010.04.001. PubMed PMID: 20399286; PubMed Central PMCID: PMC2880406.
994. Paravastu AK, Leapman RD, Yau WM, Tycko R. Molecular structural basis for polymorphism in Alzheimer's beta-amyloid fibrils. *Proceedings of the National Academy of Sciences of the United States of America*. 2008;105(47):18349-54. doi: 10.1073/pnas.0806270105. PubMed PMID: 19015532; PubMed Central PMCID: PMC2587602.
995. Kodali R, Williams AD, Chemuru S, Wetzel R. Abeta(1-40) forms five distinct amyloid structures whose beta-sheet contents and fibril stabilities are correlated. *Journal of molecular biology*. 2010;401(3):503-17. doi: 10.1016/j.jmb.2010.06.023. PubMed PMID: 20600131; PubMed Central PMCID: PMC2919579.

996. Petkova AT, Leapman RD, Guo Z, Yau WM, Mattson MP, Tycko R. Self-propagating, molecular-level polymorphism in Alzheimer's beta-amyloid fibrils. *Science*. 2005;307(5707):262-5. doi: 10.1126/science.1105850. PubMed PMID: 15653506.
997. Stine WB, Jr., Dahlgren KN, Krafft GA, LaDu MJ. In vitro characterization of conditions for amyloid-beta peptide oligomerization and fibrillogenesis. *The Journal of biological chemistry*. 2003;278(13):11612-22. doi: 10.1074/jbc.M210207200. PubMed PMID: 12499373.
998. Kittelberger KA, Piazza F, Tesco G, Reijmers LG. Natural amyloid-beta oligomers acutely impair the formation of a contextual fear memory in mice. *PLoS one*. 2012;7(1):e29940. doi: 10.1371/journal.pone.0029940. PubMed PMID: 22238679; PubMed Central PMCID: PMC3251597.
999. Frautschy SA, Hu W, Kim P, Miller SA, Chu T, Harris-White ME, Cole GM. Phenolic anti-inflammatory antioxidant reversal of Abeta-induced cognitive deficits and neuropathology. *Neurobiology of aging*. 2001;22(6):993-1005. PubMed PMID: 11755008.
1000. McDonald MP, Dahl EE, Overmier JB, Mantyh P, Cleary J. Effects of an exogenous beta-amyloid peptide on retention for spatial learning. *Behavioral and neural biology*. 1994;62(1):60-7. PubMed PMID: 7945146.
1001. O'Hare E, Weldon DT, Mantyh PW, Ghilardi JR, Finke MP, Kuskowski MA, Maggio JE, Shephard RA, Cleary J. Delayed behavioral effects following intrahippocampal injection of aggregated A beta (1-42). *Brain research*. 1999;815(1):1-10. PubMed PMID: 9974116.
1002. Goldsbury CS, Wirtz S, Muller SA, Sunderji S, Wicki P, Aebi U, Frey P. Studies on the in vitro assembly of a beta 1-40: implications for the search for a beta fibril formation inhibitors. *Journal of structural biology*. 2000;130(2-3):217-31. doi: 10.1006/jsbi.2000.4259. PubMed PMID: 10940227.
1003. Re F, Airoldi C, Zona C, Masserini M, La Ferla B, Quattrocchi N, Nicotra F. Beta amyloid aggregation inhibitors: small molecules as candidate drugs for therapy of Alzheimer's disease. *Current medicinal chemistry*. 2010;17(27):2990-3006. PubMed PMID: 20629631.
1004. Chen J, Armstrong AH, Koehler AN, Hecht MH. Small molecule microarrays enable the discovery of compounds that bind the Alzheimer's Abeta peptide and reduce its cytotoxicity. *J Am Chem Soc*. 2010;132(47):17015-22. Epub 2010/11/11. doi: 10.1021/ja107552s. PubMed PMID: 21062056; PubMed Central PMCID: PMC3063105.
1005. Lublin AL, Link CD. Alzheimer's disease drug discovery: in vivo screening using *Caenorhabditis elegans* as a model for beta-amyloid peptide-induced toxicity. *Drug discovery today Technologies*. 2013;10(1):e115-9. doi: 10.1016/j.ddtec.2012.02.002. PubMed PMID: 24050239.
1006. Pouplana S, Espargaro A, Galdeano C, Viayna E, Sola I, Ventura S, Munoz-Torrero D, Sabate R. Thioflavin-S staining of bacterial inclusion bodies for the fast, simple, and inexpensive screening of amyloid aggregation inhibitors. *Current medicinal chemistry*. 2014;21(9):1152-9. PubMed PMID: 24059241.
1007. Choi SH, Kim YH, Hebisch M, Sliwinski C, Lee S, D'Avanzo C, Chen H, Hooli B, Asselin C, Muffat J, Klee JB, Zhang C, Wainger BJ, Peitz M, Kovacs DM, Woolf CJ, Wagner SL, Tanzi RE, Kim DY. A three-dimensional human neural cell culture model of Alzheimer's disease. *Nature*. 2014;515(7526):274-8. doi: 10.1038/nature13800. PubMed PMID: 25307057; PubMed Central PMCID: PMC4366007.
1008. Doody RS, Thomas RG, Farlow M, Iwatsubo T, Vellas B, Joffe S, Kieburtz K, Raman R, Sun X, Aisen PS, Siemers E, Liu-Seifert H, Mohs R, Alzheimer's Disease Cooperative Study Steering C, Solanezumab Study G. Phase 3 trials of solanezumab for mild-to-moderate Alzheimer's disease. *The New England journal of medicine*. 2014;370(4):311-21. doi: 10.1056/NEJMoa1312889. PubMed PMID: 24450890.
1009. Buttini M, Masliah E, Barbour R, Grajeda H, Motter R, Johnson-Wood K, Khan K, Seubert P, Freedman S, Schenk D, Games D. Beta-amyloid immunotherapy prevents synaptic degeneration in a mouse model of Alzheimer's disease. *The Journal of neuroscience : the official journal of the Society for Neuroscience*. 2005;25(40):9096-101. doi: 10.1523/JNEUROSCI.1697-05.2005. PubMed PMID: 16207868.
1010. Blennow K, Zetterberg H, Rinne JO, Salloway S, Wei J, Black R, Grundman M, Liu E, Investigators AAB. Effect of immunotherapy with bapineuzumab on cerebrospinal fluid biomarker levels in patients with mild to moderate Alzheimer disease. *Archives of neurology*. 2012;69(8):1002-10. doi: 10.1001/archneurol.2012.90. PubMed PMID: 22473769.
1011. Salloway S, Sperling R, Brashear HR. Phase 3 trials of solanezumab and bapineuzumab for Alzheimer's disease. *The New England journal of medicine*. 2014;370(15):1460. PubMed PMID: 24724181.

1012. Burstein AH, Zhao Q, Ross J, Styren S, Landen JW, Ma WW, McCush F, Alvey C, Kupiec JW, Bednar MM. Safety and pharmacology of ponezumab (PF-04360365) after a single 10-minute intravenous infusion in subjects with mild to moderate Alzheimer disease. *Clinical neuropharmacology*. 2013;36(1):8-13. doi: 10.1097/WNF.0b013e318279bcfa. PubMed PMID: 23334069.
1013. Landen JW, Zhao Q, Cohen S, Borrie M, Woodward M, Billing CB, Jr., Bales K, Alvey C, McCush F, Yang J, Kupiec JW, Bednar MM. Safety and pharmacology of a single intravenous dose of ponezumab in subjects with mild-to-moderate Alzheimer disease: a phase I, randomized, placebo-controlled, double-blind, dose-escalation study. *Clinical neuropharmacology*. 2013;36(1):14-23. doi: 10.1097/WNF.0b013e31827db49b. PubMed PMID: 23334070.
1014. Adolfsson O, Pihlgren M, Toni N, Varisco Y, Buccarello AL, Antonello K, Lohmann S, Piorkowska K, Gafner V, Atwal JK, Maloney J, Chen M, Gogineni A, Weimer RM, Mortensen DL, Friesenhahn M, Ho C, Paul R, Pfeifer A, Muhs A, Watts RJ. An effector-reduced anti-beta-amyloid (A β) antibody with unique A β binding properties promotes neuroprotection and glial engulfment of A β . *The Journal of neuroscience : the official journal of the Society for Neuroscience*. 2012;32(28):9677-89. doi: 10.1523/JNEUROSCI.4742-11.2012. PubMed PMID: 22787053.
1015. Banks WA, Terrell B, Farr SA, Robinson SM, Nonaka N, Morley JE. Passage of amyloid beta protein antibody across the blood-brain barrier in a mouse model of Alzheimer's disease. *Peptides*. 2002;23(12):2223-6. PubMed PMID: 12535702.
1016. Boado RJ, Lu JZ, Hui EK, Sumbria RK, Pardridge WM. Pharmacokinetics and brain uptake in the rhesus monkey of a fusion protein of arylsulfatase a and a monoclonal antibody against the human insulin receptor. *Biotechnology and bioengineering*. 2013;110(5):1456-65. doi: 10.1002/bit.24795. PubMed PMID: 23192358; PubMed Central PMCID: PMC3919501.
1017. Niewoehner J, Bohrmann B, Collin L, Urich E, Sade H, Maier P, Rueger P, Stracke JO, Lau W, Tissot AC, Loetscher H, Ghosh A, Freskgard PO. Increased brain penetration and potency of a therapeutic antibody using a monovalent molecular shuttle. *Neuron*. 2014;81(1):49-60. doi: 10.1016/j.neuron.2013.10.061. PubMed PMID: 24411731.
1018. Niessen WM. Fragmentation of toxicologically relevant drugs in positive-ion liquid chromatography-tandem mass spectrometry. *Mass spectrometry reviews*. 2011;30(4):626-63. doi: 10.1002/mas.20332. PubMed PMID: 21294151.
1019. Hudson SA, Ecroyd H, Kee TW, Carver JA. The thioflavin T fluorescence assay for amyloid fibril detection can be biased by the presence of exogenous compounds. *The FEBS journal*. 2009;276(20):5960-72. doi: 10.1111/j.1742-4658.2009.07307.x. PubMed PMID: 19754881.
1020. Zhang DS, Wei GW, Kouri DJ, Hoffman DK, Gorman M, Palacios A, Gunaratne GH. Integrating the Kuramoto-Sivashinsky equation in polar coordinates: application of the distributed approximating functional approach. *Physical review E, Statistical physics, plasmas, fluids, and related interdisciplinary topics*. 1999;60(3):3353-60. PubMed PMID: 11970149.
1021. Sui Y, Wu Z. Alternative statistical parameter for high-throughput screening assay quality assessment. *Journal of biomolecular screening*. 2007;12(2):229-34. doi: 10.1177/1087057106296498. PubMed PMID: 17218666.
1022. Ghiso J, Frangione B. Amyloidosis and Alzheimer's disease. *Advanced drug delivery reviews*. 2002;54(12):1539-51. PubMed PMID: 12453671.
1023. Masters CL, Simms G, Weinman NA, Multhaup G, McDonald BL, Beyreuther K. Amyloid plaque core protein in Alzheimer disease and Down syndrome. *Proceedings of the National Academy of Sciences of the United States of America*. 1985;82(12):4245-9. PubMed PMID: 3159021; PubMed Central PMCID: PMC397973.
1024. Kumagai H, Pham W, Kataoka M, Hiwatari K, McBride J, Wilson KJ, Tachikawa H, Kimura R, Nakamura K, Liu EH, Gore JC, Sakuma S. Multifunctional nanobeacon for imaging Thomsen-Friedenreich antigen-associated colorectal cancer. *International journal of cancer Journal international du cancer*. 2013;132(9):2107-17. doi: 10.1002/ijc.27903. PubMed PMID: 23055136; PubMed Central PMCID: PMC3566327.
1025. Allender WJ, Archer AW. Liquid chromatographic analysis of promethazine and its major metabolites in human postmortem material. *Journal of forensic sciences*. 1984;29(2):515-26. PubMed PMID: 6726155.
1026. Ponder GW, Stewart JT. A liquid chromatographic method for the determination of promethazine enantiomers in human urine and serum using solid-phase extraction and fluorescence detection. *Journal of pharmaceutical and biomedical analysis*. 1995;13(9):1161-6. PubMed PMID: 8573643.

1027. Nolting DD, Nickels M, Tantawy MN, Yu JY, Xie J, Peterson TE, Crews BC, Marnett L, Gore JC, Pham W. Convergent synthesis and evaluation of (18)F-labeled azulenyl COX2 probes for cancer imaging. *Frontiers in oncology*. 2012;2:207. doi: 10.3389/fonc.2012.00207. PubMed PMID: 23316477; PubMed Central PMCID: PMC3539664.
1028. Engkvist O, Wrede P, Rester U. Prediction of CNS activity of compound libraries using substructure analysis. *Journal of chemical information and computer sciences*. 2003;43(1):155-60. doi: 10.1021/ci0102721. PubMed PMID: 12546548.
1029. Newman DJ, Cragg GM, Snader KM. Natural products as sources of new drugs over the period 1981-2002. *Journal of natural products*. 2003;66(7):1022-37. doi: 10.1021/np030096l. PubMed PMID: 12880330.
1030. Ganguli M, Chandra V, Kamboh MI, Johnston JM, Dodge HH, Thelma BK, Juyal RC, Pandav R, Belle SH, DeKosky ST. Apolipoprotein E polymorphism and Alzheimer disease: The Indo-US Cross-National Dementia Study. *Archives of neurology*. 2000;57(6):824-30. PubMed PMID: 10867779.
1031. Ng TP, Chiam PC, Lee T, Chua HC, Lim L, Kua EH. Curry consumption and cognitive function in the elderly. *American journal of epidemiology*. 2006;164(9):898-906. doi: 10.1093/aje/kwj267. PubMed PMID: 16870699.
1032. Brondino N, Re S, Boldrini A, Cuccomarino A, Lanati N, Barale F, Politi P. Curcumin as a therapeutic agent in dementia: a mini systematic review of human studies. *TheScientificWorldJournal*. 2014;2014:174282. doi: 10.1155/2014/174282. PubMed PMID: 24578620; PubMed Central PMCID: PMC3919104.
1033. Kim H, Park BS, Lee KG, Choi CY, Jang SS, Kim YH, Lee SE. Effects of naturally occurring compounds on fibril formation and oxidative stress of beta-amyloid. *Journal of agricultural and food chemistry*. 2005;53(22):8537-41. doi: 10.1021/jf051985c. PubMed PMID: 16248550.
1034. Ono K, Hasegawa K, Naiki H, Yamada M. Curcumin has potent anti-amyloidogenic effects for Alzheimer's beta-amyloid fibrils in vitro. *Journal of neuroscience research*. 2004;75(6):742-50. doi: 10.1002/jnr.20025. PubMed PMID: 14994335.
1035. Lin R, Chen X, Li W, Han Y, Liu P, Pi R. Exposure to metal ions regulates mRNA levels of APP and BACE1 in PC12 cells: blockage by curcumin. *Neuroscience letters*. 2008;440(3):344-7. doi: 10.1016/j.neulet.2008.05.070. PubMed PMID: 18583042.
1036. Park SY, Kim HS, Cho EK, Kwon BY, Phark S, Hwang KW, Sul D. Curcumin protected PC12 cells against beta-amyloid-induced toxicity through the inhibition of oxidative damage and tau hyperphosphorylation. *Food and chemical toxicology : an international journal published for the British Industrial Biological Research Association*. 2008;46(8):2881-7. doi: 10.1016/j.fct.2008.05.030. PubMed PMID: 18573304.
1037. Zhang L, Fiala M, Cashman J, Sayre J, Espinosa A, Mahanian M, Zaghi J, Badmaev V, Graves MC, Bernard G, Rosenthal M. Curcuminoids enhance amyloid-beta uptake by macrophages of Alzheimer's disease patients. *Journal of Alzheimer's disease : JAD*. 2006;10(1):1-7. PubMed PMID: 16988474.
1038. Shimmyo Y, Kihara T, Akaike A, Niidome T, Sugimoto H. Epigallocatechin-3-gallate and curcumin suppress amyloid beta-induced beta-site APP cleaving enzyme-1 upregulation. *Neuroreport*. 2008;19(13):1329-33. doi: 10.1097/WNR.0b013e32830b8ae1. PubMed PMID: 18695518.
1039. Yang F, Lim GP, Begum AN, Ubeda OJ, Simmons MR, Ambegaokar SS, Chen PP, Kaye R, Glabe CG, Frautschy SA, Cole GM. Curcumin inhibits formation of amyloid beta oligomers and fibrils, binds plaques, and reduces amyloid in vivo. *The Journal of biological chemistry*. 2005;280(7):5892-901. doi: 10.1074/jbc.M404751200. PubMed PMID: 15590663.
1040. Garcia-Alloza M, Borrelli LA, Rozkalne A, Hyman BT, Bacskai BJ. Curcumin labels amyloid pathology in vivo, disrupts existing plaques, and partially restores distorted neurites in an Alzheimer mouse model. *Journal of neurochemistry*. 2007;102(4):1095-104. doi: 10.1111/j.1471-4159.2007.04613.x. PubMed PMID: 17472706.
1041. Ryu EK, Choe YS, Lee KH, Choi Y, Kim BT. Curcumin and dehydrozingerone derivatives: synthesis, radiolabeling, and evaluation for beta-amyloid plaque imaging. *Journal of medicinal chemistry*. 2006;49(20):6111-9. doi: 10.1021/jm0607193. PubMed PMID: 17004725.
1042. McClure R, Yanagisawa D, Stec D, Abdollahian D, Koktysh D, Xhillari D, Jaeger R, Stanwood G, Chekmenev E, Tooyama I, Gore JC, Pham W. Inhalable curcumin: offering the potential for translation to imaging and treatment of Alzheimer's disease. *Journal of Alzheimer's disease : JAD*. 2015;44(1):283-95. doi: 10.3233/JAD-140798. PubMed PMID: 25227316; PubMed Central PMCID: PMC4297252.
1043. Wahlstrom B, Blennow G. A study on the fate of curcumin in the rat. *Acta pharmacologica et toxicologica*. 1978;43(2):86-92. PubMed PMID: 696348.

1044. Ravindranath V, Chandrasekhara N. Metabolism of curcumin--studies with [3H]curcumin. *Toxicology*. 1981;22(4):337-44. PubMed PMID: 7342372.
1045. Cheng AL, Hsu CH, Lin JK, Hsu MM, Ho YF, Shen TS, Ko JY, Lin JT, Lin BR, Ming-Shiang W, Yu HS, Jee SH, Chen GS, Chen TM, Chen CA, Lai MK, Pu YS, Pan MH, Wang YJ, Tsai CC, Hsieh CY. Phase I clinical trial of curcumin, a chemopreventive agent, in patients with high-risk or pre-malignant lesions. *Anticancer research*. 2001;21(4B):2895-900. PubMed PMID: 11712783.
1046. Bolte S, Cordelieres FP. A guided tour into subcellular colocalization analysis in light microscopy. *Journal of microscopy*. 2006;224(Pt 3):213-32. doi: 10.1111/j.1365-2818.2006.01706.x. PubMed PMID: 17210054.
1047. Anand P, Kunnumakkara AB, Newman RA, Aggarwal BB. Bioavailability of curcumin: problems and promises. *Molecular pharmaceutics*. 2007;4(6):807-18. doi: 10.1021/mp700113r. PubMed PMID: 17999464.
1048. Garbuzenko OB, Saad M, Pozharov VP, Reuhl KR, Mainelis G, Minko T. Inhibition of lung tumor growth by complex pulmonary delivery of drugs with oligonucleotides as suppressors of cellular resistance. *Proceedings of the National Academy of Sciences of the United States of America*. 2010;107(23):10737-42. doi: 10.1073/pnas.1004604107. PubMed PMID: 20498076; PubMed Central PMCID: PMC2890783.
1049. Eimer WA, Vassar R. Neuron loss in the 5XFAD mouse model of Alzheimer's disease correlates with intraneuronal A β 42 accumulation and Caspase-3 activation. *Molecular neurodegeneration*. 2013;8:2. doi: 10.1186/1750-1326-8-2. PubMed PMID: 23316765; PubMed Central PMCID: PMC3552866.
1050. Trujillo-Estrada L, Davila JC, Sanchez-Mejias E, Sanchez-Varo R, Gomez-Arboledas A, Vizuete M, Vitorica J, Gutierrez A. Early neuronal loss and axonal/presynaptic damage is associated with accelerated amyloid-beta accumulation in A β PP/PS1 Alzheimer's disease mice subiculum. *Journal of Alzheimer's disease : JAD*. 2014;42(2):521-41. doi: 10.3233/JAD-140495. PubMed PMID: 24927710.
1051. Kaur N, Garg T, Goyal AK, Rath G. Formulation, optimization and evaluation of curcumin-beta-cyclodextrin-loaded sponge for effective drug delivery in thermal burns chemotherapy. *Drug delivery*. 2014;1-10. doi: 10.3109/10717544.2014.963900. PubMed PMID: 25268151.
1052. Baum L, Lam CW, Cheung SK, Kwok T, Lui V, Tsoh J, Lam L, Leung V, Hui E, Ng C, Woo J, Chiu HF, Goggins WB, Zee BC, Cheng KF, Fong CY, Wong A, Mok H, Chow MS, Ho PC, Ip SP, Ho CS, Yu XW, Lai CY, Chan MH, Szeto S, Chan IH, Mok V. Six-month randomized, placebo-controlled, double-blind, pilot clinical trial of curcumin in patients with Alzheimer disease. *Journal of clinical psychopharmacology*. 2008;28(1):110-3. doi: 10.1097/jcp.0b013e318160862c. PubMed PMID: 18204357.
1053. Ringman JM, Frautschy SA, Teng E, Begum AN, Bardens J, Beigi M, Gylys KH, Badmaev V, Heath DD, Apostolova LG, Porter V, Vanek Z, Marshall GA, Hellemann G, Sugar C, Masterman DL, Montine TJ, Cummings JL, Cole GM. Oral curcumin for Alzheimer's disease: tolerability and efficacy in a 24-week randomized, double blind, placebo-controlled study. *Alzheimer's research & therapy*. 2012;4(5):43. doi: 10.1186/alzrt146. PubMed PMID: 23107780; PubMed Central PMCID: PMC3580400.
1054. Ireson CR, Jones DJ, Orr S, Coughtrie MW, Boocock DJ, Williams ML, Farmer PB, Steward WP, Gescher AJ. Metabolism of the cancer chemopreventive agent curcumin in human and rat intestine. *Cancer epidemiology, biomarkers & prevention : a publication of the American Association for Cancer Research, cosponsored by the American Society of Preventive Oncology*. 2002;11(1):105-11. PubMed PMID: 11815407.
1055. Ravindranath V, Chandrasekhara N. In vitro studies on the intestinal absorption of curcumin in rats. *Toxicology*. 1981;20(2-3):251-7. PubMed PMID: 7256789.
1056. Hassaninasab A, Hashimoto Y, Tomita-Yokotani K, Kobayashi M. Discovery of the curcumin metabolic pathway involving a unique enzyme in an intestinal microorganism. *Proceedings of the National Academy of Sciences of the United States of America*. 2011;108(16):6615-20. doi: 10.1073/pnas.1016217108. PubMed PMID: 21467222; PubMed Central PMCID: PMC3080977.
1057. Back DJ, Rogers SM. Review: first-pass metabolism by the gastrointestinal mucosa. *Alimentary pharmacology & therapeutics*. 1987;1(5):339-57. PubMed PMID: 2979678.
1058. Gibaldi M, Boyes RN, Feldman S. Influence of first-pass effect on availability of drugs on oral administration. *Journal of pharmaceutical sciences*. 1971;60(9):1338-40. PubMed PMID: 5567579.
1059. Rowland M. Influence of route of administration on drug availability. *Journal of pharmaceutical sciences*. 1972;61(1):70-4. PubMed PMID: 5019220.

1060. Holder GM, Plummer JL, Ryan AJ. The metabolism and excretion of curcumin (1,7-bis-(4-hydroxy-3-methoxyphenyl)-1,6-heptadiene-3,5-dione) in the rat. *Xenobiotica; the fate of foreign compounds in biological systems*. 1978;8(12):761-8. PubMed PMID: 726520.
1061. Ireson C, Orr S, Jones DJ, Verschoye R, Lim CK, Luo JL, Howells L, Plummer S, Jukes R, Williams M, Steward WP, Gescher A. Characterization of metabolites of the chemopreventive agent curcumin in human and rat hepatocytes and in the rat in vivo, and evaluation of their ability to inhibit phorbol ester-induced prostaglandin E2 production. *Cancer research*. 2001;61(3):1058-64. PubMed PMID: 11221833.
1062. Aggarwal BB, Deb L, Prasad S. Curcumin differs from tetrahydrocurcumin for molecular targets, signaling pathways and cellular responses. *Molecules*. 2015;20(1):185-205. doi: 10.3390/molecules20010185. PubMed PMID: 25547723.
1063. Begum AN, Jones MR, Lim GP, Morihara T, Kim P, Heath DD, Rock CL, Pruitt MA, Yang F, Hudspeth B, Hu S, Faulkner KF, Teter B, Cole GM, Frautschy SA. Curcumin structure-function, bioavailability, and efficacy in models of neuroinflammation and Alzheimer's disease. *The Journal of pharmacology and experimental therapeutics*. 2008;326(1):196-208. doi: 10.1124/jpet.108.137455. PubMed PMID: 18417733; PubMed Central PMCID: PMC2527621.
1064. Shytle RD, Tan J, Bickford PC, Rezai-Zadeh K, Hou L, Zeng J, Sanberg PR, Sanberg CD, Alberte RS, Fink RC, Roschek B, Jr. Optimized turmeric extract reduces beta-Amyloid and phosphorylated Tau protein burden in Alzheimer's transgenic mice. *Current Alzheimer research*. 2012;9(4):500-6. PubMed PMID: 21875408; PubMed Central PMCID: PMC3474959.
1065. Sasaki H, Sunagawa Y, Takahashi K, Imaizumi A, Fukuda H, Hashimoto T, Wada H, Katanasaka Y, Takeya H, Fujita M, Hasegawa K, Morimoto T. Innovative preparation of curcumin for improved oral bioavailability. *Biological & pharmaceutical bulletin*. 2011;34(5):660-5. PubMed PMID: 21532153.
1066. Cheng KK, Yeung CF, Ho SW, Chow SF, Chow AH, Baum L. Highly stabilized curcumin nanoparticles tested in an in vitro blood-brain barrier model and in Alzheimer's disease Tg2576 mice. *The AAPS journal*. 2013;15(2):324-36. doi: 10.1208/s12248-012-9444-4. PubMed PMID: 23229335; PubMed Central PMCID: PMC3675736.
1067. Anand P, Nair HB, Sung B, Kunnumakkara AB, Yadav VR, Tekmal RR, Aggarwal BB. Design of curcumin-loaded PLGA nanoparticles formulation with enhanced cellular uptake, and increased bioactivity in vitro and superior bioavailability in vivo. *Biochemical pharmacology*. 2010;79(3):330-8. doi: 10.1016/j.bcp.2009.09.003. PubMed PMID: 19735646; PubMed Central PMCID: PMC3181156.
1068. Khalil NM, do Nascimento TC, Casa DM, Dalmolin LF, de Mattos AC, Hoss I, Romano MA, Mainardes RM. Pharmacokinetics of curcumin-loaded PLGA and PLGA-PEG blend nanoparticles after oral administration in rats. *Colloids and surfaces B, Biointerfaces*. 2013;101:353-60. doi: 10.1016/j.colsurfb.2012.06.024. PubMed PMID: 23010041.
1069. Gandapu U, Chaitanya RK, Kishore G, Reddy RC, Kondapi AK. Curcumin-loaded apotransferrin nanoparticles provide efficient cellular uptake and effectively inhibit HIV-1 replication in vitro. *PloS one*. 2011;6(8):e23388. doi: 10.1371/journal.pone.0023388. PubMed PMID: 21887247; PubMed Central PMCID: PMC3161739.
1070. Goel A, Kunnumakkara AB, Aggarwal BB. Curcumin as "Curecumin": from kitchen to clinic. *Biochemical pharmacology*. 2008;75(4):787-809. doi: 10.1016/j.bcp.2007.08.016. PubMed PMID: 17900536.
1071. Gehr P, Bachofen M, Weibel ER. The normal human lung: ultrastructure and morphometric estimation of diffusion capacity. *Respiration physiology*. 1978;32(2):121-40. PubMed PMID: 644146.
1072. Groneberg DA, Witt C, Wagner U, Chung KF, Fischer A. Fundamentals of pulmonary drug delivery. *Respiratory medicine*. 2003;97(4):382-7. PubMed PMID: 12693798.
1073. Yang W, Peters JI, Williams RO, 3rd. Inhaled nanoparticles--a current review. *International journal of pharmaceutics*. 2008;356(1-2):239-47. doi: 10.1016/j.ijpharm.2008.02.011. PubMed PMID: 18358652.
1074. Weibel ER. Principles and methods for the morphometric study of the lung and other organs. *Laboratory investigation; a journal of technical methods and pathology*. 1963;12:131-55. PubMed PMID: 13999512.
1075. Patton JS, Byron PR. Inhaling medicines: delivering drugs to the body through the lungs. *Nature reviews Drug discovery*. 2007;6(1):67-74. doi: 10.1038/nrd2153. PubMed PMID: 17195033.
1076. Courrier HM, Butz N, Vandamme TF. Pulmonary drug delivery systems: recent developments and prospects. *Critical reviews in therapeutic drug carrier systems*. 2002;19(4-5):425-98. PubMed PMID: 12661699.

1077. Illum L. Transport of drugs from the nasal cavity to the central nervous system. *European journal of pharmaceutical sciences : official journal of the European Federation for Pharmaceutical Sciences*. 2000;11(1):1-18. PubMed PMID: 10913748.
1078. De Lorenzo AJ. Electron microscopy of the olfactory and gustatory pathways. *The Annals of otology, rhinology, and laryngology*. 1960;69:410-20. PubMed PMID: 13814865.
1079. Mistry A, Stolnik S, Illum L. Nanoparticles for direct nose-to-brain delivery of drugs. *International journal of pharmaceutics*. 2009;379(1):146-57. doi: 10.1016/j.ijpharm.2009.06.019. PubMed PMID: 19555750.
1080. Burd GD. Development of the olfactory nerve in the clawed frog, *Xenopus laevis*: II. Effects of hypothyroidism. *The Journal of comparative neurology*. 1992;315(3):255-63. doi: 10.1002/cne.903150302. PubMed PMID: 1740543.
1081. Matsuzaki O. Numbers of olfactory receptor cells and fine structure of olfactory nerves in various birds. *Zoological science*. 1995;12(1):117-23. PubMed PMID: 7795486.
1082. Sorkin A. Cargo recognition during clathrin-mediated endocytosis: a team effort. *Current opinion in cell biology*. 2004;16(4):392-9. doi: 10.1016/j.ceb.2004.06.001. PubMed PMID: 15261671.
1083. Lledo PM, Gheusi G, Vincent JD. Information processing in the mammalian olfactory system. *Physiological reviews*. 2005;85(1):281-317. doi: 10.1152/physrev.00008.2004. PubMed PMID: 15618482.
1084. Shipley MT. Transport of molecules from nose to brain: transneuronal anterograde and retrograde labeling in the rat olfactory system by wheat germ agglutinin-horseradish peroxidase applied to the nasal epithelium. *Brain research bulletin*. 1985;15(2):129-42. PubMed PMID: 3840049.
1085. Oberdorster G, Sharp Z, Atudorei V, Elder A, Gelein R, Kreyling W, Cox C. Translocation of inhaled ultrafine particles to the brain. *Inhalation toxicology*. 2004;16(6-7):437-45. doi: 10.1080/08958370490439597. PubMed PMID: 15204759.
1086. Lochhead JJ, Thorne RG. Intranasal delivery of biologics to the central nervous system. *Advanced drug delivery reviews*. 2012;64(7):614-28. doi: 10.1016/j.addr.2011.11.002. PubMed PMID: 22119441.
1087. Subhashini, Chauhan PS, Kumari S, Kumar JP, Chawla R, Dash D, Singh M, Singh R. Intranasal curcumin and its evaluation in murine model of asthma. *International immunopharmacology*. 2013;17(3):733-43. doi: 10.1016/j.intimp.2013.08.008. PubMed PMID: 24021755.
1088. Lee WH, Loo CY, Bebawy M, Luk F, Mason RS, Rohanizadeh R. Curcumin and its derivatives: their application in neuropharmacology and neuroscience in the 21st century. *Current neuropharmacology*. 2013;11(4):338-78. doi: 10.2174/1570159X11311040002. PubMed PMID: 24381528; PubMed Central PMCID: PMC3744901.
1089. Zhang F, Altorki NK, Mestre JR, Subbaramaiah K, Dannenberg AJ. Curcumin inhibits cyclooxygenase-2 transcription in bile acid- and phorbol ester-treated human gastrointestinal epithelial cells. *Carcinogenesis*. 1999;20(3):445-51. PubMed PMID: 10190560.
1090. Hedrich HJ, Bullock GR. *The laboratory mouse*. Amsterdam ; Boston: Elsevier Academic Press; 2004. xvi, 600 p. p.
1091. Pan MH, Huang TM, Lin JK. Biotransformation of curcumin through reduction and glucuronidation in mice. *Drug metabolism and disposition: the biological fate of chemicals*. 1999;27(4):486-94. PubMed PMID: 10101144.
1092. Vareed SK, Kakarala M, Ruffin MT, Crowell JA, Normolle DP, Djuric Z, Brenner DE. Pharmacokinetics of curcumin conjugate metabolites in healthy human subjects. *Cancer epidemiology, biomarkers & prevention : a publication of the American Association for Cancer Research, cosponsored by the American Society of Preventive Oncology*. 2008;17(6):1411-7. doi: 10.1158/1055-9965.EPI-07-2693. PubMed PMID: 18559556; PubMed Central PMCID: PMC4138955.
1093. Hishikawa N, Takahashi Y, Amakusa Y, Tanno Y, Tuji Y, Niwa H, Murakami N, Krishna UK. Effects of turmeric on Alzheimer's disease with behavioral and psychological symptoms of dementia. *Ayu*. 2012;33(4):499-504. doi: 10.4103/0974-8520.110524. PubMed PMID: 23723666; PubMed Central PMCID: PMC3665200.
1094. Takahashi M, Uechi S, Takara K, Asikin Y, Wada K. Evaluation of an oral carrier system in rats: bioavailability and antioxidant properties of liposome-encapsulated curcumin. *Journal of agricultural and food chemistry*. 2009;57(19):9141-6. doi: 10.1021/jf9013923. PubMed PMID: 19757811.
1095. Bisht S, Feldmann G, Soni S, Ravi R, Karikar C, Maitra A, Maitra A. Polymeric nanoparticle-encapsulated curcumin ("nanocurcumin"): a novel strategy for human cancer therapy. *Journal of nanobiotechnology*. 2007;5:3. doi: 10.1186/1477-3155-5-3. PubMed PMID: 17439648; PubMed Central PMCID: PMC1868037.

1096. Sun A, Shoji M, Lu YJ, Liotta DC, Snyder JP. Synthesis of EF24-tripeptide chloromethyl ketone: a novel curcumin-related anticancer drug delivery system. *Journal of medicinal chemistry*. 2006;49(11):3153-8. doi: 10.1021/jm051141k. PubMed PMID: 16722634.
1097. Blennow K. CSF biomarkers for Alzheimer's disease: use in early diagnosis and evaluation of drug treatment. *Expert review of molecular diagnostics*. 2005;5(5):661-72. doi: 10.1586/14737159.5.5.661. PubMed PMID: 16149870.
1098. Moore BC, Simmons DL. COX-2 inhibition, apoptosis, and chemoprevention by nonsteroidal anti-inflammatory drugs. *Current medicinal chemistry*. 2000;7(11):1131-44. PubMed PMID: 11032963.
1099. Dubois RN, Abramson SB, Crofford L, Gupta RA, Simon LS, Van De Putte LB, Lipsky PE. Cyclooxygenase in biology and disease. *FASEB journal : official publication of the Federation of American Societies for Experimental Biology*. 1998;12(12):1063-73. PubMed PMID: 9737710.
1100. van Ryn J, Trummelitz G, Pairet M. COX-2 selectivity and inflammatory processes. *Current medicinal chemistry*. 2000;7(11):1145-61. PubMed PMID: 11032964.
1101. Rouzer CA, Marnett LJ. Cyclooxygenases: structural and functional insights. *Journal of lipid research*. 2009;50 Suppl:S29-34. doi: 10.1194/jlr.R800042-JLR200. PubMed PMID: 18952571; PubMed Central PMCID: PMC2674713.
1102. Beard CM, Waring SC, O'Brien PC, Kurland LT, Kokmen E. Nonsteroidal anti-inflammatory drug use and Alzheimer's disease: a case-control study in Rochester, Minnesota, 1980 through 1984. *Mayo Clinic proceedings*. 1998;73(10):951-5. doi: 10.4065/73.10.951. PubMed PMID: 9787743.
1103. Andersen K, Launer LJ, Ott A, Hoes AW, Breteler MM, Hofman A. Do nonsteroidal anti-inflammatory drugs decrease the risk for Alzheimer's disease? The Rotterdam Study. *Neurology*. 1995;45(8):1441-5. PubMed PMID: 7644037.
1104. Delanty N, Vaughan C. Risk of Alzheimer's disease and duration of NSAID use. *Neurology*. 1998;51(2):652. PubMed PMID: 9710076.
1105. Breitner JC, Gau BA, Welsh KA, Plassman BL, McDonald WM, Helms MJ, Anthony JC. Inverse association of anti-inflammatory treatments and Alzheimer's disease: initial results of a co-twin control study. *Neurology*. 1994;44(2):227-32. PubMed PMID: 8309563.
1106. Breitner JC, Welsh KA, Helms MJ, Gaskell PC, Gau BA, Roses AD, Pericak-Vance MA, Saunders AM. Delayed onset of Alzheimer's disease with nonsteroidal anti-inflammatory and histamine H2 blocking drugs. *Neurobiology of aging*. 1995;16(4):523-30. PubMed PMID: 8544901.
1107. Rogers J, Kirby LC, Hempelman SR, Berry DL, McGeer PL, Kaszniak AW, Zilinski J, Cofield M, Mansukhani L, Willson P, et al. Clinical trial of indomethacin in Alzheimer's disease. *Neurology*. 1993;43(8):1609-11. PubMed PMID: 8351023.
1108. McGahan L. COX-2 inhibitors: a role in Alzheimer's disease? *Issues in emerging health technologies*. 1999(10):1-6. PubMed PMID: 11902218.
1109. Kotilinek LA, Westerman MA, Wang Q, Panizzon K, Lim GP, Simonyi A, Lesne S, Falinska A, Younkin LH, Younkin SG, Rowan M, Cleary J, Wallis RA, Sun GY, Cole G, Frautschy S, Anwyl R, Ashe KH. Cyclooxygenase-2 inhibition improves amyloid-beta-mediated suppression of memory and synaptic plasticity. *Brain : a journal of neurology*. 2008;131(Pt 3):651-64. doi: 10.1093/brain/awn008. PubMed PMID: 18292081; PubMed Central PMCID: PMC2628581.
1110. Yasojima K, Schwab C, McGeer EG, McGeer PL. Distribution of cyclooxygenase-1 and cyclooxygenase-2 mRNAs and proteins in human brain and peripheral organs. *Brain research*. 1999;830(2):226-36. PubMed PMID: 10366679.
1111. Ho L, Pieroni C, Winger D, Purohit DP, Aisen PS, Pasinetti GM. Regional distribution of cyclooxygenase-2 in the hippocampal formation in Alzheimer's disease. *Journal of neuroscience research*. 1999;57(3):295-303. PubMed PMID: 10412020.
1112. Pasinetti GM, Aisen PS. Cyclooxygenase-2 expression is increased in frontal cortex of Alzheimer's disease brain. *Neuroscience*. 1998;87(2):319-24. PubMed PMID: 9740394.
1113. O'Banion MK. COX-2 and Alzheimer's disease: potential roles in inflammation and neurodegeneration. *Expert opinion on investigational drugs*. 1999;8(10):1521-36. PubMed PMID: 11139808.
1114. Delafontaine P, Song YH, Li Y. Expression, regulation, and function of IGF-1, IGF-1R, and IGF-1 binding proteins in blood vessels. *Arteriosclerosis, thrombosis, and vascular biology*. 2004;24(3):435-44. doi: 10.1161/01.ATV.0000105902.89459.09. PubMed PMID: 14604834.

1115. Massague J, Pilch PF, Czech MP. Electrophoretic resolution of three major insulin receptor structures with unique subunit stoichiometries. *Proceedings of the National Academy of Sciences of the United States of America*. 1980;77(12):7137-41. PubMed PMID: 6938960; PubMed Central PMCID: PMC350456.
1116. Rui L, Aguirre V, Kim JK, Shulman GI, Lee A, Corbould A, Dunaif A, White MF. Insulin/IGF-1 and TNF-alpha stimulate phosphorylation of IRS-1 at inhibitory Ser307 via distinct pathways. *The Journal of clinical investigation*. 2001;107(2):181-9. doi: 10.1172/JCI10934. PubMed PMID: 11160134; PubMed Central PMCID: PMC199174.
1117. Zhao WQ, Chen H, Quon MJ, Alkon DL. Insulin and the insulin receptor in experimental models of learning and memory. *European journal of pharmacology*. 2004;490(1-3):71-81. doi: 10.1016/j.ejphar.2004.02.045. PubMed PMID: 15094074.
1118. De Felice FG. Alzheimer's disease and insulin resistance: translating basic science into clinical applications. *The Journal of clinical investigation*. 2013;123(2):531-9. doi: 10.1172/JCI64595. PubMed PMID: 23485579; PubMed Central PMCID: PMC3561831.
1119. Taniguchi CM, Emanuelli B, Kahn CR. Critical nodes in signalling pathways: insights into insulin action. *Nature reviews Molecular cell biology*. 2006;7(2):85-96. doi: 10.1038/nrm1837. PubMed PMID: 16493415.
1120. Kahn CR. The molecular mechanism of insulin action. *Annual review of medicine*. 1985;36:429-51. doi: 10.1146/annurev.me.36.020185.002241. PubMed PMID: 2986528.
1121. Craft S. Alzheimer disease: Insulin resistance and AD--extending the translational path. *Nature reviews Neurology*. 2012;8(7):360-2. doi: 10.1038/nrneurol.2012.112. PubMed PMID: 22710630.
1122. De Felice FG, Vieira MN, Bomfim TR, Decker H, Velasco PT, Lambert MP, Viola KL, Zhao WQ, Ferreira ST, Klein WL. Protection of synapses against Alzheimer's-linked toxins: insulin signaling prevents the pathogenic binding of Abeta oligomers. *Proceedings of the National Academy of Sciences of the United States of America*. 2009;106(6):1971-6. doi: 10.1073/pnas.0809158106. PubMed PMID: 19188609; PubMed Central PMCID: PMC2634809.
1123. Silajdzic E, Minthon L, Bjorkqvist M, Hansson O. No diagnostic value of plasma clusterin in Alzheimer's disease. *PloS one*. 2012;7(11):e50237. doi: 10.1371/journal.pone.0050237. PubMed PMID: 23209684; PubMed Central PMCID: PMC3509147.
1124. Schrijvers EM, Koudstaal PJ, Hofman A, Breteler MM. Plasma clusterin and the risk of Alzheimer disease. *Jama*. 2011;305(13):1322-6. doi: 10.1001/jama.2011.381. PubMed PMID: 21467285.
1125. Velayudhan L, Killick R, Hye A, Kinsey A, Guntert A, Lynham S, Ward M, Leung R, Lourdasamy A, To AW, Powell J, Lovestone S. Plasma transthyretin as a candidate marker for Alzheimer's disease. *Journal of Alzheimer's disease : JAD*. 2012;28(2):369-75. doi: 10.3233/JAD-2011-110611. PubMed PMID: 22002789.
1126. Choi J, Lee HW, Suk K. Plasma level of chitinase 3-like 1 protein increases in patients with early Alzheimer's disease. *Journal of neurology*. 2011;258(12):2181-5. doi: 10.1007/s00415-011-6087-9. PubMed PMID: 21562723.
1127. Lim NK, Villemagne VL, Soon CP, Laughton KM, Rowe CC, McLean CA, Masters CL, Evin G, Li QX. Investigation of matrix metalloproteinases, MMP-2 and MMP-9, in plasma reveals a decrease of MMP-2 in Alzheimer's disease. *Journal of Alzheimer's disease : JAD*. 2011;26(4):779-86. doi: 10.3233/JAD-2011-101974. PubMed PMID: 21694463.
1128. Koyama A, Okereke OI, Yang T, Blacker D, Selkoe DJ, Grodstein F. Plasma amyloid-beta as a predictor of dementia and cognitive decline: a systematic review and meta-analysis. *Archives of neurology*. 2012;69(7):824-31. doi: 10.1001/archneurol.2011.1841. PubMed PMID: 22451159; PubMed Central PMCID: PMC3772635.
1129. Song F, Poljak A, Valenzuela M, Mayeux R, Smythe GA, Sachdev PS. Meta-analysis of plasma amyloid-beta levels in Alzheimer's disease. *Journal of Alzheimer's disease : JAD*. 2011;26(2):365-75. doi: 10.3233/JAD-2011-101977. PubMed PMID: 21709378.
1130. Lachno DR, Vanderstichele H, De Groote G, Kostanjevecki V, De Meyer G, Siemers ER, Willey MB, Bourdage JS, Konrad RJ, Dean RA. The influence of matrix type, diurnal rhythm and sample collection and processing on the measurement of plasma beta-amyloid isoforms using the INNO-BIA plasma Abeta forms multiplex assay. *The journal of nutrition, health & aging*. 2009;13(3):220-5. PubMed PMID: 19262957.
1131. Rosa-Neto P, Hsiung GY, Masellis M, participants C. Fluid biomarkers for diagnosing dementia: rationale and the Canadian Consensus on Diagnosis and Treatment of Dementia recommendations for Canadian physicians. *Alzheimer's research & therapy*. 2013;5(Suppl 1):S8. doi: 10.1186/alzrt223. PubMed PMID: 24565514; PubMed Central PMCID: PMC3980280.

1132. Loening AM, Gambhir SS. AMIDE: a free software tool for multimodality medical image analysis. *Molecular imaging*. 2003;2(3):131-7. PubMed PMID: 14649056.
1133. Musaro A, McCullagh K, Paul A, Houghton L, Dobrowolny G, Molinaro M, Barton ER, Sweeney HL, Rosenthal N. Localized Igf-1 transgene expression sustains hypertrophy and regeneration in senescent skeletal muscle. *Nature genetics*. 2001;27(2):195-200. doi: 10.1038/84839. PubMed PMID: 11175789.
1134. Duan C, Ren H, Gao S. Insulin-like growth factors (IGFs), IGF receptors, and IGF-binding proteins: roles in skeletal muscle growth and differentiation. *General and comparative endocrinology*. 2010;167(3):344-51. doi: 10.1016/j.ygcen.2010.04.009. PubMed PMID: 20403355.
1135. Buchhave P, Minthon L, Zetterberg H, Wallin AK, Blennow K, Hansson O. Cerebrospinal fluid levels of beta-amyloid 1-42, but not of tau, are fully changed already 5 to 10 years before the onset of Alzheimer dementia. *Archives of general psychiatry*. 2012;69(1):98-106. doi: 10.1001/archgenpsychiatry.2011.155. PubMed PMID: 22213792.
1136. Parnetti L, Chiasserini D, Eusebi P, Giannandrea D, Bellomo G, De Carlo C, Padiglioni C, Mastrocola S, Lisetti V, Calabresi P. Performance of abeta1-40, abeta1-42, total tau, and phosphorylated tau as predictors of dementia in a cohort of patients with mild cognitive impairment. *Journal of Alzheimer's disease : JAD*. 2012;29(1):229-38. doi: 10.3233/JAD-2011-111349. PubMed PMID: 22232006.
1137. Verbeek MM, De Jong D, Kremer HP. Brain-specific proteins in cerebrospinal fluid for the diagnosis of neurodegenerative diseases. *Annals of clinical biochemistry*. 2003;40(Pt 1):25-40. doi: 10.1258/000456303321016141. PubMed PMID: 12542908.
1138. Andreasen N, Minthon L, Davidsson P, Vanmechelen E, Vanderstichele H, Winblad B, Blennow K. Evaluation of CSF-tau and CSF-Abeta42 as diagnostic markers for Alzheimer disease in clinical practice. *Archives of neurology*. 2001;58(3):373-9. PubMed PMID: 11255440.
1139. Andreasen N, Hesse C, Davidsson P, Minthon L, Wallin A, Winblad B, Vanderstichele H, Vanmechelen E, Blennow K. Cerebrospinal fluid beta-amyloid(1-42) in Alzheimer disease: differences between early- and late-onset Alzheimer disease and stability during the course of disease. *Archives of neurology*. 1999;56(6):673-80. PubMed PMID: 10369305.
1140. Tapiola T, Pirttila T, Mikkonen M, Mehta PD, Alafuzoff I, Koivisto K, Soininen H. Three-year follow-up of cerebrospinal fluid tau, beta-amyloid 42 and 40 concentrations in Alzheimer's disease. *Neuroscience letters*. 2000;280(2):119-22. PubMed PMID: 10686392.
1141. Sunderland T, Wolozin B, Galasko D, Levy J, Dukoff R, Bahro M, Lasser R, Motter R, Lehtimaki T, Seubert P. Longitudinal stability of CSF tau levels in Alzheimer patients. *Biological psychiatry*. 1999;46(6):750-5. PubMed PMID: 10494442.
1142. Humpel C. Identifying and validating biomarkers for Alzheimer's disease. *Trends in biotechnology*. 2011;29(1):26-32. doi: 10.1016/j.tibtech.2010.09.007. PubMed PMID: 20971518; PubMed Central PMCID: PMC3016495.
1143. Zandi PP, Anthony JC, Hayden KM, Mehta K, Mayer L, Breitner JC, Cache County Study I. Reduced incidence of AD with NSAID but not H2 receptor antagonists: the Cache County Study. *Neurology*. 2002;59(6):880-6. PubMed PMID: 12297571.
1144. in t' Veld BA, Ruitenbergh A, Hofman A, Launer LJ, van Duijn CM, Stijnen T, Breteler MM, Stricker BH. Nonsteroidal antiinflammatory drugs and the risk of Alzheimer's disease. *The New England journal of medicine*. 2001;345(21):1515-21. doi: 10.1056/NEJMoa010178. PubMed PMID: 11794217.
1145. McGeer PL, Rogers J. Anti-inflammatory agents as a therapeutic approach to Alzheimer's disease. *Neurology*. 1992;42(2):447-9. PubMed PMID: 1736183.
1146. Yan Q, Zhang J, Liu H, Babu-Khan S, Vassar R, Biere AL, Citron M, Landreth G. Anti-inflammatory drug therapy alters beta-amyloid processing and deposition in an animal model of Alzheimer's disease. *The Journal of neuroscience : the official journal of the Society for Neuroscience*. 2003;23(20):7504-9. PubMed PMID: 12930788.
1147. Hwang DY, Chae KR, Kang TS, Hwang JH, Lim CH, Kang HK, Goo JS, Lee MR, Lim HJ, Min SH, Cho JY, Hong JT, Song CW, Paik SG, Cho JS, Kim YK. Alterations in behavior, amyloid beta-42, caspase-3, and Cox-2 in mutant PS2 transgenic mouse model of Alzheimer's disease. *FASEB journal : official publication of the Federation of American Societies for Experimental Biology*. 2002;16(8):805-13. doi: 10.1096/fj.01-0732com. PubMed PMID: 12039862.
1148. Swardfager W, Lanctot K, Rothenburg L, Wong A, Cappell J, Herrmann N. A meta-analysis of cytokines in Alzheimer's disease. *Biological psychiatry*. 2010;68(10):930-41. doi: 10.1016/j.biopsych.2010.06.012. PubMed PMID: 20692646.

1149. Hotamisligil GS, Peraldi P, Budavari A, Ellis R, White MF, Spiegelman BM. IRS-1-mediated inhibition of insulin receptor tyrosine kinase activity in TNF-alpha- and obesity-induced insulin resistance. *Science*. 1996;271(5249):665-8. PubMed PMID: 8571133.
1150. Kanety H, Feinstein R, Papa MZ, Hemi R, Karasik A. Tumor necrosis factor alpha-induced phosphorylation of insulin receptor substrate-1 (IRS-1). Possible mechanism for suppression of insulin-stimulated tyrosine phosphorylation of IRS-1. *The Journal of biological chemistry*. 1995;270(40):23780-4. PubMed PMID: 7559552.
1151. Yang J, Park Y, Zhang H, Xu X, Laine GA, Dellsperger KC, Zhang C. Feed-forward signaling of TNF-alpha and NF-kappaB via IKK-beta pathway contributes to insulin resistance and coronary arteriolar dysfunction in type 2 diabetic mice. *American journal of physiology Heart and circulatory physiology*. 2009;296(6):H1850-8. doi: 10.1152/ajpheart.01199.2008. PubMed PMID: 19363130; PubMed Central PMCID: PMC2716110.
1152. Park KM, Bowers WJ. Tumor necrosis factor-alpha mediated signaling in neuronal homeostasis and dysfunction. *Cellular signalling*. 2010;22(7):977-83. doi: 10.1016/j.cellsig.2010.01.010. PubMed PMID: 20096353; PubMed Central PMCID: PMC2860549.
1153. Bomfim TR, Fornyy-Germano L, Sathler LB, Brito-Moreira J, Houzel JC, Decker H, Silverman MA, Kazi H, Melo HM, McClean PL, Holscher C, Arnold SE, Talbot K, Klein WL, Munoz DP, Ferreira ST, De Felice FG. An anti-diabetes agent protects the mouse brain from defective insulin signaling caused by Alzheimer's disease-associated Abeta oligomers. *The Journal of clinical investigation*. 2012;122(4):1339-53. doi: 10.1172/JCI57256. PubMed PMID: 22476196; PubMed Central PMCID: PMC3314445.
1154. Zhao WQ, De Felice FG, Fernandez S, Chen H, Lambert MP, Quon MJ, Krafft GA, Klein WL. Amyloid beta oligomers induce impairment of neuronal insulin receptors. *FASEB journal : official publication of the Federation of American Societies for Experimental Biology*. 2008;22(1):246-60. doi: 10.1096/fj.06-7703com. PubMed PMID: 17720802.
1155. Blennow K. CSF biomarkers for mild cognitive impairment. *Journal of internal medicine*. 2004;256(3):224-34. doi: 10.1111/j.1365-2796.2004.01368.x. PubMed PMID: 15324365.
1156. Evans RW. Complications of lumbar puncture. *Neurologic clinics*. 1998;16(1):83-105. PubMed PMID: 9421542.
1157. Stafford RS, Singer DE. National patterns of warfarin use in atrial fibrillation. *Archives of internal medicine*. 1996;156(22):2537-41. PubMed PMID: 8951296.
1158. Boustani M, Peterson B, Hanson L, Harris R, Lohr KN, Force USPST. Screening for dementia in primary care: a summary of the evidence for the U.S. Preventive Services Task Force. *Annals of internal medicine*. 2003;138(11):927-37. PubMed PMID: 12779304.
1159. Liu L, Duff K. A technique for serial collection of cerebrospinal fluid from the cisterna magna in mouse. *Journal of visualized experiments : JoVE*. 2008(21). doi: 10.3791/960. PubMed PMID: 19066529; PubMed Central PMCID: PMC2762909.
1160. Lehman EJ, Kulnane LS, Gao Y, Petriello MC, Pimpis KM, Younkin L, Dolios G, Wang R, Younkin SG, Lamb BT. Genetic background regulates beta-amyloid precursor protein processing and beta-amyloid deposition in the mouse. *Human molecular genetics*. 2003;12(22):2949-56. doi: 10.1093/hmg/ddg322. PubMed PMID: 14506131.
1161. Zhu H, Wang X, Wallack M, Li H, Carreras I, Dedeoglu A, Hur JY, Zheng H, Li H, Fine R, Mwamburi M, Sun X, Kowall N, Stern RA, Qiu WQ. Intraperitoneal injection of the pancreatic peptide amylin potently reduces behavioral impairment and brain amyloid pathology in murine models of Alzheimer's disease. *Molecular psychiatry*. 2015;20(2):252-62. doi: 10.1038/mp.2014.17. PubMed PMID: 24614496; PubMed Central PMCID: PMC4161670.
1162. Takechi R, Galloway S, Pallegage-Gamarallage MM, Lam V, Dhaliwal SS, Mamo JC. Probucol prevents blood-brain barrier dysfunction in wild-type mice induced by saturated fat or cholesterol feeding. *Clinical and experimental pharmacology & physiology*. 2013;40(1):45-52. doi: 10.1111/1440-1681.12032. PubMed PMID: 23167559.
1163. Dickson DW. The pathogenesis of senile plaques. *Journal of neuropathology and experimental neurology*. 1997;56(4):321-39. PubMed PMID: 9100663.
1164. Iwatsubo T, Mann DM, Odaka A, Suzuki N, Ihara Y. Amyloid beta protein (A beta) deposition: A beta 42(43) precedes A beta 40 in Down syndrome. *Annals of neurology*. 1995;37(3):294-9. doi: 10.1002/ana.410370305. PubMed PMID: 7695229.
1165. Shin RW, Ogino K, Kondo A, Saido TC, Trojanowski JQ, Kitamoto T, Tateishi J. Amyloid beta-protein (Abeta) 1-40 but not Abeta1-42 contributes to the experimental formation of Alzheimer disease amyloid fibrils in rat brain. *The*

Journal of neuroscience : the official journal of the Society for Neuroscience. 1997;17(21):8187-93. PubMed PMID: 9334394.

1166. McGowan E, Sanders S, Iwatsubo T, Takeuchi A, Saido T, Zehr C, Yu X, Uljon S, Wang R, Mann D, Dickson D, Duff K. Amyloid phenotype characterization of transgenic mice overexpressing both mutant amyloid precursor protein and mutant presenilin 1 transgenes. *Neurobiology of disease*. 1999;6(4):231-44. doi: 10.1006/nbdi.1999.0243. PubMed PMID: 10448051.

1167. Iwatsubo T, Odaka A, Suzuki N, Mizusawa H, Nukina N, Ihara Y. Visualization of A beta 42(43) and A beta 40 in senile plaques with end-specific A beta monoclonals: evidence that an initially deposited species is A beta 42(43). *Neuron*. 1994;13(1):45-53. PubMed PMID: 8043280.